Reactivity of Electron Deficient Arenes Upon Coordination to the Tungsten Dearomatization Agent {WTp(NO)(PMe_3)}

Spenser Simpson
Zionsville, Indiana

B.S., Chemistry, Tulane University, 2016

A dissertation presented to the Graduate Faculty of
the University of Virginia in Candidacy for the Degree
of Doctor of Philosophy

Department of Chemistry

University of Virginia
July 2021

Abstract

Chapter 1 presents the concept of chemical space and the current issues with lead identification due to the limits of traditional synthetic methods that support the screened small-molecule libraries. Important factors for biologically successful molecules are discussed, such as three-dimensional shape. An argument for the need for new synthetic methodologies to introduce more three-dimensional nature is presented, along with a solution that involves using alkene reactivity on aromatic molecules. The chapter concludes with a presentation of typical aromatic reactivity and the benefits of using aromatic molecules as starting materials in lieu of their stability and reluctance to undergo addition reactions.

Chapter 2 offers a solution to the stability challenge of aromatic molecules through the process of dearomatization. A discussion of the pros and cons of radical, photochemical, enzymatic, and transition metal-mediated dearomatization processes is included.

In Chapter 3, the exceptionally π-basic metal fragments {MoTp(NO)(DMAP)} and {WTp(NO)(PMe_3)} (Tp = tris(pyrazolyl)-borate; DMAP = 4-(N,N-dimethylamino)pyridine) ability to form thermally stable η^2-coordinated complexes with a variety of electron-deficient arenes is explored. The tolerance of substituted arenes with fluorine-containing electron-withdrawing groups (EWG; −F, $-CF_3$, $-SF_5$) is examined for tungsten systems. When the EWG contains a π bond (nitriles, aldehydes, ketones, ester), η^2-coordination occurs predominantly on the nonaromatic functional group. However, complexation of the tungsten complex with trimethyl orthobenzoate ($PhC(OMe)_3$) followed by hydrolysis allows access to an η^2-coordinated arene with an ester substituent. In general, the tungsten system tolerates sulfur-based withdrawing groups well (e.g., $PhSO_2Ph$, $MeSO_2Ph$), and the integration of multiple electron-withdrawing groups on a benzene ring further enhances the π-backbonding interaction between the metal and aromatic ligand. A quick comparison to the study with the molybdenum system is included.

Chapter 4 presents the synthesis of sulfone functionalized trisubstituted cyclohexenes. These compounds are prepared from two sequential tandem protonation/nucleophilic additions to a phenyl

sulfone ($PhSO_2R$; R = Me, Ph, NC_4H_8) dihapto-coordinated to the tungsten complex {$WTp(NO)(PMe_3)$}. Such coordination renders the aryl ring susceptible to protonation at a carbon ortho to the sulfone group. The resulting arenium species readily reacts with the first nucleophile to form a dihapto-coordinated diene complex. The protonation/nucleophilic addition process can be repeated for the diene complex, rendering trisubstituted cyclohexenes. Nucleophiles employed include masked enolates, cyanide, and hydride, with all three additions occurring on the same face of the ring, anti to the metal. Structural assignments are supported with six crystal structures, DFT studies, and full 2D NMR analysis.

Chapter 5 examines an example of sulfone elimination upon exposure to silica. A novel process is described for the synthesis of cyclohexenes bearing up to three substituents. These compounds are prepared from three independent nucleophilic addition reactions to the phenyl sulfone systems presented in Chapter 4. In some instances, the protonation/nucleophilic addition process for the diene complex renders an allyl sulfone species. The allyl sulfone, in turn, can undergo a process in which a third nucleophile replaces the sulfone. Nucleophiles employed include masked enolates, cyanide, amines, and hydride, with all three additions occurring on the same face of the ring, anti to the metal. Of the nine novel functionalized cyclohexenes prepared as examples of this methodology, six compounds meet five independent criteria for evaluating drug likeliness. Structural assignments are supported with one crystal structure, DFT studies, and full 2D NMR analysis.

Chapter 6 focuses on the reactivity of η^2-phenyl sulfones with amine nucleophiles. The successful addition of secondary and aromatic amines as first nucleophiles is shown. An intramolecular cyclization reaction is described using an acetal as the first nucleophile and a primary amine as the second to yield bicyclic lactam products. Upon formation of the lactam, the sulfone eliminates, and a range of third nucleophilic additions are shown for the bicyclic system.

Copyright Information

Acknowledgments

Much like my former Harmanites, I have put off writing my acknowledgments till the night before my final thesis submission is due. If anyone truly knows the Harman lab, this is considered normal when one realizes that most of our group meeting presentations are made the night before or the morning of group meeting. As I start to think back on all the people who have helped me along my academic career, I want to make a very rough analogy. My family and friends know my love for having a good time by sharing a drink, whether it be at a bar, sporting event, or just hanging out at the pool on the weekend. Currently, I am drinking a glass of Blanton's bourbon. This bourbon has become my family's go-to drink ever since I discovered it while trying to find the perfect 21st birthday gift for my brother Austin. Most know any type of whiskey is aged for multiple years to achieve the desired taste that many enjoy. This sums up the relationships that I have built up over the last 28 years. From the ones that were there from the start to the friendships I have formed in the past 5 years, these relationships have and will continue to grow in strength, just like whiskey tastes better with age. For this, I cannot thank everyone enough. There are many people to thank, and I do apologize for anyone that I miss. With that said, let us begin the thank yous, and just like many Harman group graduates, this will be long, so settle in for a read.

First and foremost, I would like to thank my mom and dad. They have been there supporting me at every moment of my life. My parents raised my brother and me to be well round human beings. They pushed us academically, socially, and athletically. Still, no matter what we did, they celebrated the wins and consoled us after the losses. I still remember the early years of my wrestling career at Zionsville Middle School. My mom had no idea what her tiny 90-pound 6th grader was getting himself into, and honestly, I don't think she had any clue what the rules were, but she was the loudest fan in the stands by a long shot. As I got into high school, I had to have a little talk with my mother about decreasing her volume so I could hear my coaches. You would have thought I just ripped her heart out when I asked this

cause all she wanted to do was be my biggest fan, and that is what she has been throughout my life. My mom and dad were at every soccer game, wrestling match, honor society induction, and academic award ceremony. They did not miss anything and still do not. I could not do any of this without their support. As I grew older, I started to realize that at certain points, three letters would follow my dad's name, or someone would address his doctor while we were out. I was so confused. My dad wasn't a medical doctor, so why would he be called a doctor. I soon realized that my dad had a Ph.D. in agronomy and started to realize the amount of work and time that he put in to get to where he is in life to support my family. He has inspired me to get to this point, and I hope I made you proud dad. You have been there for me through every step of this process. You got me through this process, all the way back to candidacy up to proofing chapters for this dissertation.

I next want to thank my brother Austin. For without him, I would not be at the University of Virginia. Headed into my last year of undergrad, I was very lost. I didn't know what I wanted to do and started to look at graduate schools. I had no idea where to begin looking. Austin encouraged me to come visit. From there, I began looking into UVA as a possible home for my graduate school experience. He has always been there for me whether I needed to complain about work or just grab a drink after a long day. According to his fiancé Maddy, I am the only phone call he will answer. We have been in each other's corners throughout the years, but like brothers, we have had our fair share of fights. To this day, though, you are the only one I cannot wake up the next day upset with. As you look to graduate from medical school next spring, I want you to know that I couldn't be prouder of who you have become over the years and all your accomplishments. I cannot wait to stand with you on Yours and Maddy's big day in March.

At this point, I feel like it will be easiest to go through these thank yous in chronological order. Let us begin with who I consider to be my family, not through blood but through the bonds we have made over the years. This group would be my Mississippi or Lake crew. The Shermans, Taylors, and

Curries have been the kind of friends that I do not deserve but love with all my heart. From 4th of Julys on Lake Chicot to Mississippi State tailgates and all the way to the kids' weddings, you guys have been there for me. The support you guys have given me was emphasized when a large group of y'all showed up at my undergraduate graduation. Thomas, you have been with me since basically day one. You have been my oldest friend and have always been there for me. I cannot wait to see where your life takes you here in the next few months as you and Lauren become parents. To Mary Elizabeth, Anne, and Laci, thank y'all for calling me out on my crap and the constant visits during my undergraduate career. I will always cherish those Mardi Gras moments and cannot wait to make more.

I would next like to thank all my teachers from elementary to High School. I would like to take a second and thank a few of them specifically. I had three teachers that exposed to me chemistry in my high school years and made me fall in love with it. I cannot thank Mary Testin, Lee Banitt, and Paulette Berger. You three nurtured me through introductory chemistry all the way through my AP test. You opened a new world to me, and I truly owe you three so much. I hope that I could make you proud, and yes, Mary, I still am combating those commies. Lastly, I want to thank Christie Clark. For the reader, Christie taught my freshman and junior honors English classes. As anyone knows, I hate English and literature. This may honestly just be because I am a horrible writer, so thank you, Christie, for not failing me. But in all seriousness, Christie was always one of my biggest inspirations. She taught me how to critically think and analyze not just prose but life. While English class was not always my favorite, her class was. She didn't let me slack off and called me out when I was just being lazy. She expected your best no matter the situation. These lessons and analysis skills have stuck with me throughout my years.

At this point, I want to thank two of my friends from high school that have stuck with me to this point. Becca Schroyer and Adam Kern have been there throughout the years since we graduated high school back in 2012. Thank y'all for being smiling faces whenever I am home and for just talking life with me. You both have been there for me no matter what happens, and I cannot thank you enough for

putting up with my stupid butt over the years. I know all our stories are still evolving, and I cannot wait to see where your lives go. I love you both.

Moving on from high school to undergrad. I attended Tulane University in New Orleans for four years (2012-2016). In New Orleans, I made many friends and forged relationships that I am so grateful to have in my life. I would like to start with a thanks to the Tulane chemistry department. You all nurtured my love for chemistry and pushed me to pursue a graduate degree. Thank you to Dr. Donahue for allowing me to do research in your lab for three years and pairing me up with Dr. Patricia Fontenot. Patricia, I cannot thank you enough for putting up with me during your graduate career. You are such a strong, smart, and amazing women who any young scientist should look up. You taught me what it took to succeed in graduate school and what was needed to be a good scientist. I owe you so much and cannot thank you enough.

Now Tulane was not all work. There was plenty of play. There are two groups that I want to thank. First, I want to thank my soccer people. You guys allowed me into your group and to begin enjoying playing soccer again. Bailey, Andrew, Joe, Anthony, and many more, thank you guys for being drinking buddies and giving me a break from school through a sport I love.

The second group is a group that has now basically become family. This group includes Calvin Gallion III, Bradley Doyle, Madison Pitre, and Amanda Doyle. From being roommates to long nights of shenanigans, you have been the best of friends. This group still communicates daily, and I can share anything with these guys. The support you all have given me is fully underserved, and I love you all. Also, a big thank you to Calvin for even coming up to Virginia for my defense.

Moving on to Charlottesville. I would like to start this section by thanking my P.I. Dean Harman. Dean, you have been the best boss that I could have asked for during my graduate career. Everything you did made me feel like you truly cared about me as a scientist and a person. You fully supported me through times of great progress and, more importantly, encouraged me through the roadblocks. With all

the issues my colleagues would have with their P.I.'s, I was always thankful that I never had those with you. You are truly there for all your students. I am indebted to you for giving me a chance and sticking with me over the last 5 years. I will miss learning from you and cannot wait to see the direction of the lab in the years to come. They are in good hands with you.

To the older Harmanites, thank you for training me and teaching me the ways of the lab. I want to thank Dr. Jeff Myers for his instillment of lab safety and of giving back to the chemistry community through outreach. Next, I owe a lot to Dr. Katy Wilson. Thank you for training me as a lonely first year and setting up the electron-withdrawing group chemistry. I miss our drinking nights and spikeball games. Thank you for being a confidant as well as a mentor. The next Harmanite is Dr. Steven Dakermanji. Thank you for just being my friend. You overcame a lot throughout your graduate career, and I am so proud of you. I miss our brewery adventures and cannot wait to get to visit you in your new city of Philadelphia. Our next lab members are Dr. Jacob Smith and Dr. Justin Wilde. You guys are inspirations. You both have great work ethics and pushed our group to new heights. Thank you both for the mentorship and science discussions. To Jacob and Katy, I greatly miss our Dirty Nelly's adventures and our seven degrees of Kevin Bacon games. I want to wish the best of luck to our rising fourth years Jacob Weatherford-Pratt and Jonathan Dabbs. You guys are great chemists, and I am super excited to see how y'all's dissertations turn out. To our rising third-year, Mary Shingler, keep your head up. You have had roadblock after roadblock, and you have broken through each block with hard work. Keep pushing forward, and you will do great things. To our youngest lab members Paolo Siano and Megan Ericson, you both are set up very well to bring this group to new heights. You both bring many talents and new tools that the lab has not seen in years. You both have work ethics that will carry you both through your graduate years. I am very excited to see where both of your careers take you. The final Harmanite that I want to thank is one from a previous generation. Dr. Kevin Welch graduated back in the 2000s but came to UVA to teach when I began my graduate career. Kevin has been a rock for me. I

taught for him for 3 years and basically came to him with all my research issues. Kevin was always there to talk science, listen to lab issues, and give general advice. I could not have gotten through the last 5 years without your help and mentorship.

I would like to thank all my friends that I made in the department. Thank you, Philip Hahn and Asa Nichols, for being roommates, beer buddies, and supportive friends. Kevin Mayer and Anthony Ciancone have been my soccer friends throughout the years. I will miss skipping work for Champions League games and EPL Sundays at Random Row. We all got to watch our teams lift the champions league trophy while we were together, which is rather lucky now that I think about it. My last thank you in this group goes out to Tiffany Layne. You have been my best friend here. You are always there for me, and I cannot thank you enough for everything. You are going to kick some butt at the FBI!

A quick thanks needs to go out to my hockey and soccer teams. You guys and gals have given me an escape from grad school in a productive manner. Without you all, I do not know if I would be able to have kept my sanity.

The final thank you is reserved for my girlfriend, Taylor Sealy. She has been with me throughout most of this graduate school experience. She now has seen the lows of candidacy and now the highs of a successful defense. Thank you for dealing with my crazy work schedules and bring me snacks during my late-night experiments. I appreciate you listening to all my issues with lab and allowing me to talk through research with a smile on your face even though I probably wasn't making sense at all. You were an escape from work and coming home to a loving embrace every day meant the world to me. Thank you for putting up with me through quarantine. You are smart, amazing, and beautiful, and I cannot wait to see what the world has in store for us. I love you with all my heart and could not have done this without you. We did it, baby. We finally did it.

Table of Contents

List of Abbreviations

Å	Angstrom
aq	Aqueous
br	Broad
CAN	Cerin ammonium nitrate
Cdr	Coordination diastereomer ration
COSY	Correlation Spectroscopy
CV	Cyclic Voltammetry
DBU	1,8-Diazabicyclo[5.4.0]undec-7-ene
DDQ	2,3-dichloro-5,6-dicyanoquinone
DCM	Dichloromethane
DDQ	2,3-dichloro-5,6-dicyanoquinone
DFT	Density functional theory
DiPAT	Diisopropylammonium triflate
DMA	*N,N*-Dimethylacetamide
DMAP	4-Dimehtylaminopyridine
DME	1,2-Dimethoxyethane
DMF	*N,N*-Dimethylformamide
DMM	Dimethyl malonate
DMSO	Dimethyl sulfoxide
DPhAT	Diphenylammonium triflate
EA	Elemental Analysis
EDG	Electron donating group
Ee	Enantiomeric excess

Et_3N	Triethylamine
Et_2O	Diethyl ether
EtOAc	Ethyl Acetate
EVK	Ethyl vinyl Ketone
EWG	Electron withdrawing group
HATR	Horizontal Attenuated Total Reflectance
HMBC	Heteronuclear Multiple Bond Coherence Spectroscopy
HRMS	High-Resolution Mass Spectroscopy
HSQC	Heteronuclear Sing Quantum Correlation Spectroscopy
Hz	Hertz
IR	Infrared
KHMDS	Potassium bis(trimethylsilyl)amide
L	Ancillary ligand
LAH/$LiALH_4$	Lithium Aluminum Hydride
LiDMM	Lithium dimethyl malonate
LUMO	Lowest unoccupied molecular orbital
mCPBA	m-Chloroperbenzoic acid
MeCN	Acetonitrile
MeIm	N-Methylimidazole
MTAD	4-Phenyl-1,2,4-triazoline-3,5-dione
MTDA/MMTP	1-methoxy-2-methyl-1-trimethylsiloxypropene
MVK	Methyl vinyl ketone
NHE	Normal Hydrogen Electrode
NMR	Nuclear Magnetic Resonance

NOE	Nuclear Overhauser Effect
NOESY	Nuclear Overhauser Effect Spectroscopy
$NOPF_6$	Nitrosonium hexafluorophosphate
ORTEP	Oak Ridge Thermal Ellipsoid Program
OTf	Trifluoromethanesulfonate or triflate
PMe_3	Trimethylphosphine
Ppm	Parts Per Million
Pz	Tp pyrazole ring
SAR	Structure-activity relationship
SOMO	Single Occupied Molecular Orbital
TBAB	Tetrabutylammonium borohydride
TBAH	Tetrabutylammonium hexafluorophosphate
TFT	α,α,α-Trifluorotoluene
THF	Tetrahydrofuran
TLC	Thin Layer Chromatography
TMS	Tetramethylsilane
Tp	Hydridotris(pyrazolyl)borate
UV	Ultraviolet

List of Figures

List of Schemes

List of Tables

Chapter 1

Introduction: Aromatic Molecules as Starting Materials for Medicinal Chemistry

1.1 Introduction

Over recent years, high-throughput screening of small molecule libraries has increased the efficiency of identifying promising pharmaceutical leads. This is due to the ability of high-throughput screening to rapidly conduct millions of tests to identify active compounds, genes, or antibodies that play a role in targeted biological processes. With the ability to test millions of compounds quickly, the number of pharmaceutical leads has increased, but the success rate of a lead becoming a drug has decreased to about 5%.[1,2] A potential contributing factor to this low success rate is chemists focusing on maximizing the number of compounds in these small-molecule libraries versus focusing on making more topologically diverse molecules.[3-5]

In order to maximize the number of molecules in medical chemistry libraries, chemists have shown the tendency to revert to traditional synthetic methods that produce relatively easy to access molecules.[6] To emphasize this, none of the most commonly used synthetic methods were discovered within the last 20 years.[6] Such methods include C-C coupling processes like the Suzuki-Miyaura, SnAr, and Heck reactions that yield substitution products and are good at introducing functional groups but create complexes that are predominantly "flat" and lack stereocenters.[6,7] Overutilization of these methods leads to a lack of structural diversity in small-molecule libraries.[5] This limits the chemical space that can be explored, which inhibits the efficiency of the high throughput screening process.

The previously mentioned methodology is in direct contrast with recent pushes to explore biologically active natural products that are more structurally complex. One of the key features of natural products is the number of stereocenters that they contain. Lovering et al. showed that the incorporation of chiral centers and a high fraction of sp^3 carbons in a molecule significantly correlates to a compound successfully being developed into a drug.[2,7-9] The more three-dimensional nature that chiral centers and sp^3 carbons give to a molecule is believed to aid in specificity in favorable receptor-ligand interactions.[2,3,9,10] Thus, the limitations of current small molecule libraries can be overcome with a new

synthetic approach that focuses on diversity-oriented synthesis to produce a more diverse range of complexes containing the three-dimensional features of successful natural products.[7,8,11-14] This more diverse synthetic approach allows for the exploration of new chemical space, increases the diversity of compound libraries, and increases the efficacy in SAR studies.[2,14] In order to accomplish this, new synthetic methodologies will need to be developed in order to access novel structures and aid in the demand for innovative synthetic tools for medicinal chemistry.[4,6,15]

With the desire to form complexes with stereocenters and 3-dimensional nature, new strategies need to be developed. One strategy is to utilize the reactivity of alkenes. Alkene chemistry has been comprehensively studied to the point that their reactivity is commonly taught in introductory organic chemistry courses. Reactions like epoxidations, halogenations, and hydrogenations that transform two sp^2 carbons into two sp^3 carbons are well researched and commonly used (**Scheme 1.1**). The question then becomes how to utilize these reactions to help add stereocenters to more complex systems.

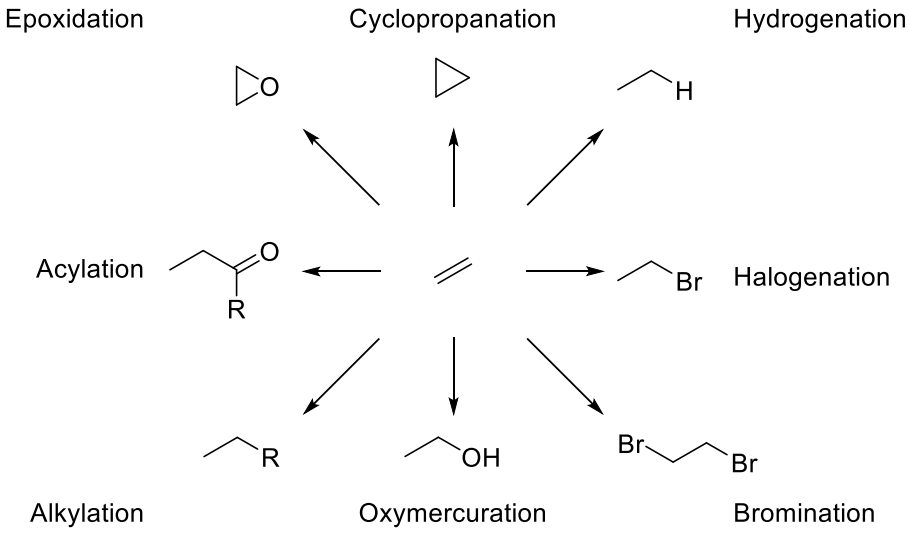

Scheme 1.1: Sampling of olefin reactivity

A common group of molecules that contain multiple alkene bonds is aromatic molecules. If we utilize a common aromatic molecule like benzene as an example, we can see that it is a six-member carbon ring with three alternating double bonds. If these double bonds could be functionalized through known reactions, then we can rapidly form alicyclic complexes. For example, if this could be done, benzene could

go from containing six sp^2 carbons to being made up of six sp^3 carbons efficiently (**Figure 1.1**). However, aromatics have an inherent stability that inhibits their ability to undergo addition reactions under most conditions.

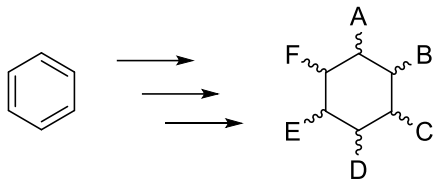

Figure 1.1: Functionalization of benzene

1.2 Aromaticity

Aromatic compounds are defined through Hückel's rule, which states that a planar ring molecule is aromatic when it has a cyclic array of π electrons equal to 4n + 1 (n = 0, 1, 2, …).[16] This cyclic array of π electrons gives rise to multiple resonance structures in an aromatic molecule which aids in its stabilization. Benzene has a delocalized π electron structure, so instead of three localized double bonds, the electron density is spread equally between all six carbons. Evidence of this can be seen through benzene's bond lengths. The bond length for each carbon-carbon bond in benzene is 1.39 Å, which is longer than the expected carbon-carbon double bond (1.34 Å) and shorter than a carbon-carbon single bond (1.47 Å).[16]

Another demonstration of aromatic stability comes from $\Delta H_{Hydrogenation}$ comparisons between cyclohexene, 1,3-cyclohexadiene, and benzene. Experimental hydrogenation of cyclohexene was shown to release 28.6 kcal/mol. If a second double bond is added to form 1,3-cyclohexadiene, we would expect hydrogenation to release 57.2 kcal/mol in energy. If a third double bond is added to form cyclohexatriene, one could expect a release of 85.8 kcal/mol in energy upon hydrogenation. However, these hypothetical values do not match with experimental findings. Hydrogenation of 1,3-cyclohexadiene is 2 kcal/mol less than the hypothetical amount, while benzene releases a remarkable 36 kcal/mol less than the hypothetical value. The energy difference is attributed to aromatic stabilization and can be seen through all aromatic compounds.[17]

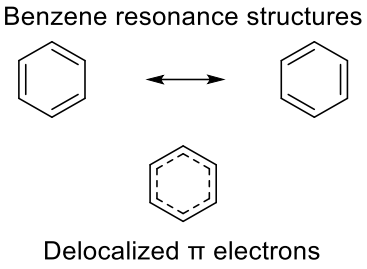

Figure 1.2: Resonance stabilization of benzene

1.3 Classical Aromatic Reactivity

The stability that a compound gains by being aromatic heavily influences its reactivity. Instead of forming sp^3 carbons from sp^2 carbons through functionalization like in traditional alkene chemistry, traditional aromatic reactivity favors substitution reactions where sp^2 carbons remain sp^2 carbons. This is due to the stability incentive to restore aromaticity after functionalization. Typical substitution reactions include Friedel-Crafts acylation and alkylation, halogenation, nitration, and sulfonylation. Another family of useful reactions for the functionalization of aromatic complexes is palladium-catalyzed cross-coupling reactions. These coupling reactions include the Suzuki, Heck, Negishi, and Sonogashira reactions that form carbon-carbon bonds and the Buchwald-Hartwig amination that forms a carbon-nitrogen bond.[18,19] While these substitution and coupling reactions are great tools to introduce functionality, none lead to the formation of sp^3 carbons, and the compounds retain their aromaticity.

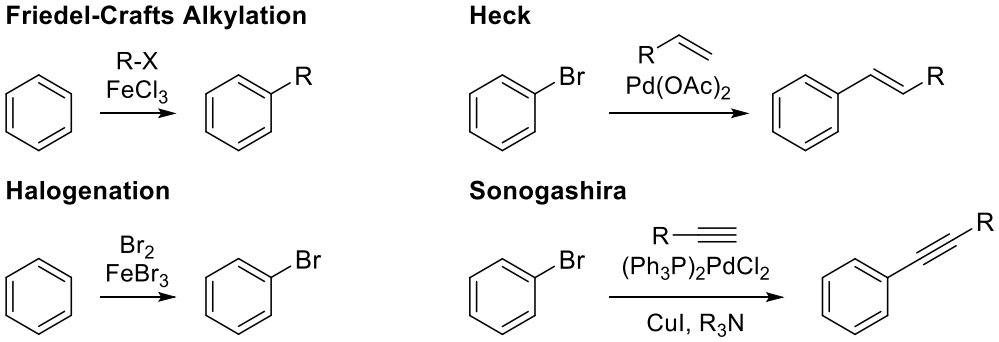

Scheme 1.2: Examples of electrophilic aromatic substitution and coupling reactions

1.4 Aromatics as Starting Materials

With the issues of stability and limitations in traditional reactivity, the question of why aromatics should still be utilized as potential starting materials for the synthesis of molecules with more complex three-dimensional structures needs to be addressed. To begin this argument, aromatics are readily available in nature and come at a low cost. Benzene is a component of crude oil, phenolic moieties are commonly found in naturally occurring steroids, and fused benzenes like naphthalene are components of crude oil and wood tars. Aromatics can also have built-in biologically relevant atoms and functional groups. Such atoms include oxygen, nitrogen, sulfur, and fluorine, while functional groups can include fluoride, trifluoromethyl, sulfonyl, or sulfonamide groups. The ability to start with a built-in biologically active site and build complexity around it would allow for an alternative to "late-stage" functionalization.[20,21]

As stated before, aromatics are attractive targets for functionalization with their many sites of unsaturation. Generalized strategies to overcome the stability of aromatics that would allow for functionalization through addition reactions can be widely classified as "dearomatization." Dearomatization would allow for the formation of multiple sp^3 carbons in a regio- and stereoselective manner. This would ideally lead to new cyclic products with limited rotatable bonds, increased saturation (fraction of sp^3 carbons), and new stereocenters. All these characteristics have been correlated with an increased chance of success in pharmaceutical trials when compared to more "flat" or two-dimensional molecules.[2,7,8]

Aromatics have the potential to be functionalized into more topologically diverse complexes that would add diversity to small-molecule libraries. However, the inherent stability of these aromatic molecules will need to be overcome to access addition reactions versus the more typical substitution reactions. A broad range of dearomatization processes has been explored, which give access to alicyclic compounds. These methods will be further explored in chapter 2.

References

(1) Takebe, T.; Imai, R.; Ono, S. *Clin Transl Sci* **2018**, *11*, 597.

(2) Clemons, P. A.; Bodycombe, N. E.; Carrinski, H. A.; Wilson, J. A.; Shamji, A. F.; Wagner, B. K.; Koehler, A. N.; Schreiber, S. L. *Proceedings of the National Academy of Sciences* **2010**, *107*, 18787.

(3) Reymond, J.-L.; Awale, M. *ACS Chemical Neuroscience* **2012**, *3*, 649.

(4) Blakemore, D. C.; Castro, L.; Churcher, I.; Rees, D. C.; Thomas, A. W.; Wilson, D. M.; Wood, A. *Nature Chemistry* **2018**, *10*, 383.

(5) Cooper, T. W. J.; Campbell, I. B.; Macdonald, S. J. F. *Angewandte Chemie International Edition* **2010**, *49*, 8082.

(6) Brown, D. G.; Boström, J. *Journal of Medicinal Chemistry* **2016**, *59*, 4443.

(7) Lovering, F.; Bikker, J.; Humblet, C. *Journal of Medicinal Chemistry* **2009**, *52*, 6752.

(8) Lovering, F. *MedChemComm* **2013**, *4*, 515.

(9) Ishikawa, M.; Hashimoto, Y. *Journal of Medicinal Chemistry* **2011**, *54*, 1539.

(10) Yang, Y.; Chen, H.; Nilsson, I.; Muresan, S.; Engkvist, O. *Journal of Medicinal Chemistry* **2010**, *53*, 7709.

(11) Arya, P.; Joseph, R.; Gan, Z.; Rakic, B. *Chemistry & Biology* **2005**, *12*, 163.

(12) Burke, M. D.; Schreiber, S. L. *Angewandte Chemie International Edition* **2004**, *43*, 46.

(13) Schreiber, S. L. *Science* **2000**, *287*, 1964.

(14) Tan, D. S. *Nature Chemical Biology* **2005**, *1*, 74.

(15) Marson, C. M. *Chemical Society Reviews* **2011**, *40*, 5514.

(16) Schleyer, P. v. R. *Chemical Reviews* **2001**, *101*, 1115.

(17) Good, W. D.; Smith, N. K. *Journal of Chemical & Engineering Data* **1969**, *14*, 102.

(18) Miyaura, N.; Suzuki, A. *Chemical Reviews* **1995**, *95*, 2457.

(19) Hartwig, J. F. *Angewandte Chemie International Edition* **1998**, *37*, 2046.

(20) Campbell, M. G.; Ritter, T. *Organic Process Research & Development* **2014**, *18*, 474.

(21) Yerien, D. E.; Bonesi, S.; Postigo, A. *Organic & Biomolecular Chemistry* **2016**, *14*, 8398.

Chapter 2

Introduction: Dearomatization of Aromatic Molecules

2.1 Introduction

In the previous chapter, we discussed the need for new synthetic methodologies that can produce more diverse molecules. One overarching methodology would be to utilize known alkene reactivity and apply it to aromatic complexes. However, due to the stability of aromatic compounds, this can be difficult. Fortunately, a broad range of dearomatization methods has been explored, which break the stability afforded to a molecule by being aromatic and allows access to alicyclic systems. Dearomatization methods include radical, photochemical, enzymatic, and transition metal-mediated dearomatization.

2.2 Radical Dearomatization

The Birch reduction is an effective process to convert benzenes into dienes.[1] The aromatic stability of benzene is overcome to yield a 1,4-cyclohexadiene product by treating benzene with either sodium or lithium dissolved in liquid ammonia followed by a protic solvent like methanol or isopropanol (**Scheme 2.1**). Due to the harsh conditions of the classic Birch reduction found over 70 years ago, researchers are still finding modifications to the process.[2,3] A recent example allows the replacement of sodium dissolved in liquid ammonia with sodium dissolved in various crown ethers in anhydrous THF.[4] This process yields electride salts, which promote the reduction without the need for lithium or liquid ammonia. However, due to the use of strong reducing agents, functional group tolerance is limited. Even in the cases where substituted benzenes are tolerated, no new stereocenters are formed.

The Stannane-mediated addition utilizes a radical process to add aryl iodides to benzene using catalytic benzeneselenol. This method also produces 1,4-cyclohexadienes; however, they can then undergo an intramolecular cyclization with ortho-substituted aryl rings (**Scheme 2.1**). This process was utilized to synthesize phenanthridinone derivatives, one of which is a key intermediate in Danishefsky's synthesis of (±)-pancratistatin.[5]

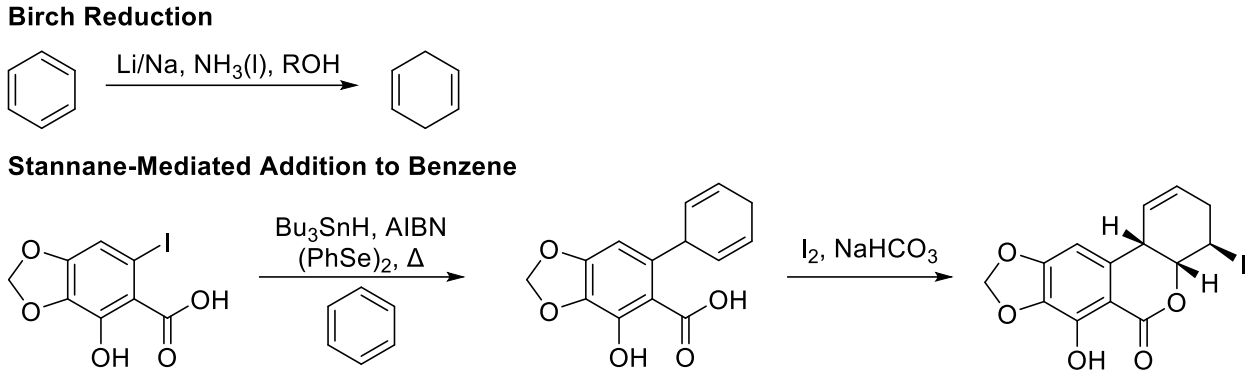

Scheme 2.1: Radical dearomatization of benzene

2.3 Photochemical Cycloaddition Dearomatization

Benzene rings should be primed to undergo a thermal [4+2] cycloaddition, but few examples have been shown due to aromatic stability. Activated dienes and elevated temperatures are required for this type of addition to occur with benzene.[6] More success has been seen with the use of ultraviolet light; however, the high energy required to push the transformation forward can lead to degradation of the organic product.[7-9] Recently, the Sarlah group at the University of Illinois at Urbana-Champaign has demonstrated the ability to conduct [4+2] cycloadditions with a class of arenophiles activated by visible light.[10-13] This process was utilized to synthesize (+)-pancratistatin through a dearomative photoaddition to benzene.[12] Activation of 4-phenyl-1,2,4-triazoline-3,5-dione (MTAD) with visible light results in a high energy species whose SOMO can add to the LUMO group orbitals of the benzene (**Scheme 2.2**). This results in a bicyclic 1,4-cyclohexadiene. Coordination of the resulting cycloadduct to a Ni-catalyst with chiral bidentate ligands generates a catalytic and enantioselective trans-carboamination. The resulting desymmetrized diene was taken onto (+)-pancratistatin in 5 steps with an er of 98:2.[12]

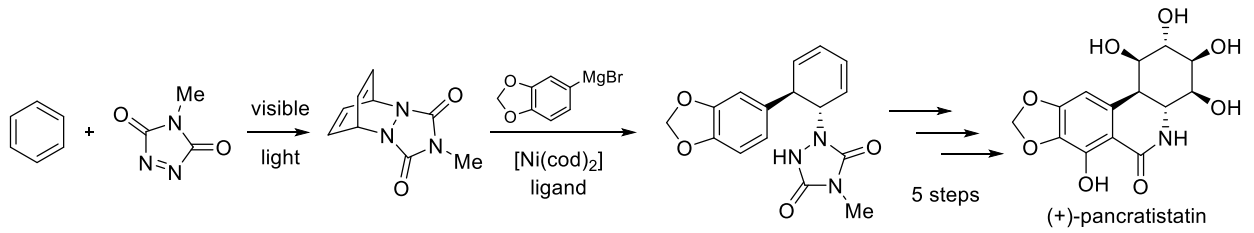

Scheme 2.2: Photochemical dearomatization of benzene

2.4 Enzymatic Dearomatization

Enzymes like *Pseudomonas putida* have been used as dearomatization agents to yield chiral diol dienes.[14-17] Specifically, utilization of *Pseudomonas putida* by Hudlicky and coworkers has led to the synthesis of the natural products (+)-lycoricidine, (+)-kifunensine (19), and L-threosphingosine (**Scheme 2.3** top).[18,19] Myers et al. demonstrated that they could synthesize 6-deoxytetracycline antibiotics from benzoic acid using the bacterial dioxygenase *Alcaligenes eutrophus* (**Scheme 2.3** bottom).[16]

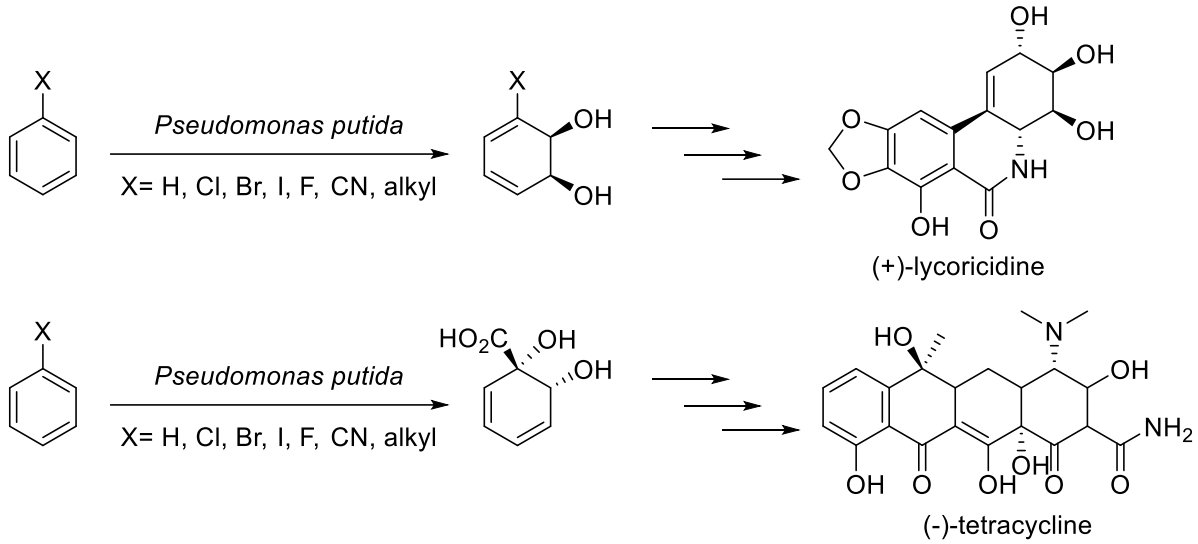

Scheme 2.3: Enzymatic dearomatization of benzene

2.5 Transition Metal-Mediated Dearomatization

The next and last type of dearomatization that will be discussed is transition metal-mediated dearomatization. This widely researched field has shown that aromatic reactivity can be heavily influenced through coordination to a transition metal.[20,21] There are two families of transition metals that coordinate to aromatic molecules: electron-deficient metals and electron-rich metals. Electron-deficient metal systems like $\{Cr(CO)_3\}$ activate aromatic molecules to nucleophilic addition through hexahapto-coordination (η^6) (**Figure 2.1** left).[21] Electron-rich metal systems like $\{Os(NH_3)_5\}^{2+}$ activate aromatics to electrophilic addition at an uncoordinated carbon through dihapto coordination (η^2) (**Figure 2.1** right).[21-23]

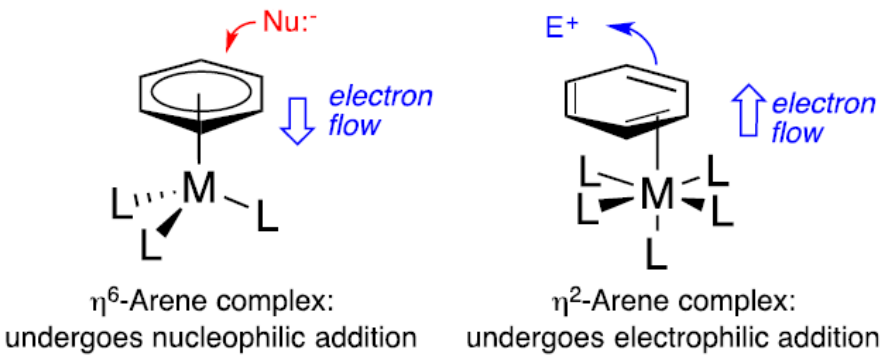

Figure 2.1: Electron-rich and electron-deficient transition metal dearomatization

2.6 Effects of Electron-Deficient Metal Complexes on Aromatic Reactivity

$\{Cr(CO)_3\}$, $\{Mo(CO)_3\}$, $\{Mn(CO)_3\}^+$, $\{Mn(CO)_2(NO)\}^{2+}$, and $\{FeCp\}^+$ are commonly used electron-deficient transition metal complexes.[20,21,24-26] These complexes are often coordinated to strong π-acceptor ligands such as carbonyl or nitrosyl ligands and are cationic. These properties cause the metal to be exceptionally electron-deficient, allowing for η^6-coordination to the arene where donation of electron density from the aromatic's π-cloud to the electron-deficient metal center stabilizes the complex.

The η^6-coordination of an aromatic molecule to the electron-deficient metal activates the aromatic molecule to nucleophilic addition. Arenes coordinated to $\{Cr(CO)_3\}$ have been shown to undergo additions with a range of nucleophiles, but many give access to substituted arenes due to the restoration of aromaticity upon isolation of the product.[27,28] Dearomatization and the formation of alicyclic products can also be achieved through the use of a strong nucleophile like an organolithium or Grignard reagent followed by an electrophile (**Scheme 2.4**).[29] The nucleophile adds anti to the metal center to form an anionic chromium-supported cyclohexadienyl species. This anionic species can then react with acid to generate a 1,3-cyclohexadiene product with a new stereocenter.[20,29] Alternatively, when a carbon electrophile is used, the addition occurs syn to the metal due to the electrophile initial attacking the metal center and being delivered endo to the cyclohexadienyl ligand (**Scheme 2.4**).[20,29] During this process, the

electrophile can insert into the carbonyl, which leads to the trans addition of a ketone across one of the double bonds.

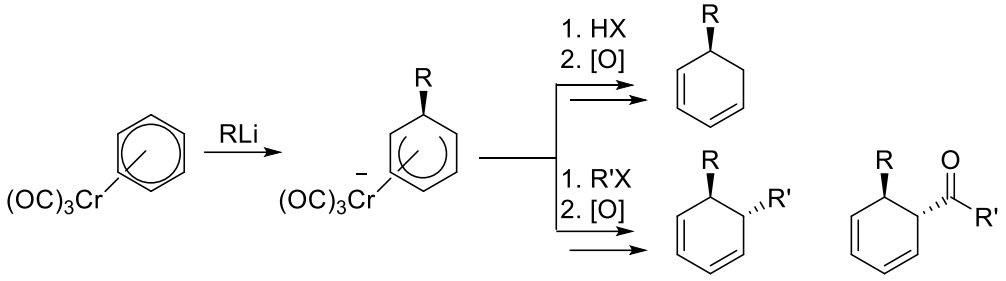

RLi= MeLi, PhLi, CH_2CHLi, $NCCH_2Li$, ect R'X= prim. and sec. alkyl iodides, prim. alkyl bromides, mesylates, triflates allyl- benzyl- and propargyl bromides

Scheme 2.4: $\{Cr(CO)_3\}$ dearomatization of benzene

$\{Mn(CO)_3\}^+$ is a cationic metal fragment that is more electrophilic compared to the neutral chromium complex. The increased π acidity of the manganese system allows for a larger range of initial nucleophiles such as Grignard reagents, ketone enolates, malonates, and hydrides. Due to the complex resulting from the nucleophilic addition being neutral, a subsequent electrophile cannot be added. This leads to rearomatization upon decomplexation from the metal. However, a second nucleophile can be added to yield either cis or trans-1,3-cyclohexadienes (**Scheme 2.5**).[20,21]

Cis-1,3-cyclohexadienes result from the use of a very reactive second nucleophile where the nucleophile adds anti to the metal system. They can also result from a substitution of a CO ligand on the metal complex with a NO^+ ligand followed by a nucleophile (**Scheme 2.5**). The initial ligand substitution results in the formation of a cationic species, which can be treated with a broader range of nucleophiles such as phosphorous and nitrogen nucleophiles, hydrides, enolates, Grignards, and organolithium reagents. In the cases of phenyl and methyl organolithium reagents, nucleophilic attack can occur at one of the two remaining CO ligands. Insertion of the resulting acyl group into the cyclohexadienyl ligand yields trans 1,3-cyclohexadiene products (**Scheme 2.5**).[20,21]

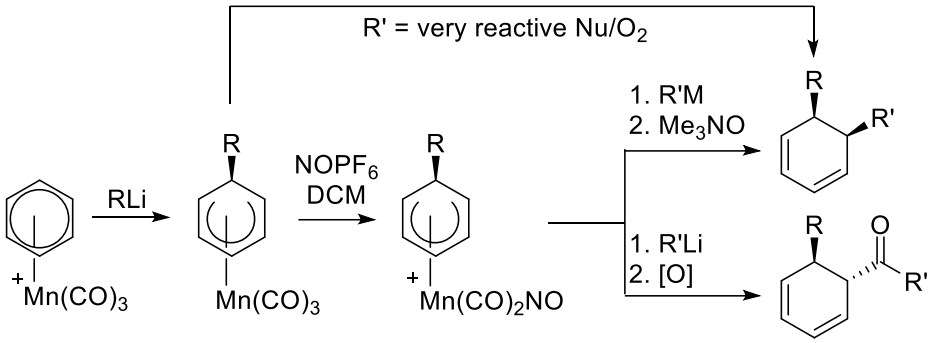

Scheme 2.5: $\{Mn(CO)_3\}^+$ dearomatization of benzene

While the activation of aromatic molecules towards nucleophilic addition can be a powerful tool in accessing dearomatized products, there are limitations to this process. One is the use of strong and/or harsh nucleophiles. Another is that the metal fragment only influences the functionalization of a single alkene bond and only yields 1,3-cyclohexadienes. Lastly, to access enantioenriched products, chiral auxiliaries are necessary.[20,21,30]

2.7 Effects of Electron-Rich Metal Complexes on Aromatic Reactivity

The second family of transition metal dearomatization agents exploits π-basic d^6 $18e^-$ metal fragments. This family of electron-rich metal fragments coordinates to an aromatic molecule through only two carbons (η^2).[21-23] This coordination is possible through the phenomenon of π-backdonation. π-backdonation occurs in this type of system when the metal uses a filled dπ-orbital to donate into a symmetry-appropriate anti-bonding orbital of the aromatic ligand (**Figure 2.2**). Through this process, the electron-rich metal fragment can dearomatize the arene upon coordination. This differs from the η^6-coordinated system where a nucleophilic addition must occur for the arene to be dearomatized. Support for the dearomatization of benzene occurring upon coordination can be seen in crystal structure data. The bond that the metal fragment is bound to is significantly lengthened compared to free benzene (1.46 vs. 1.40 A), and the unbound alkenes shorten in length.[31] This leads to the previously aromatic structure resembling a diene (**Figure 2.2**). The donating of electron density from the metal into the disrupted π-

system of an arene activates the arene towards electrophilic additions that can be followed up with various nucleophiles.

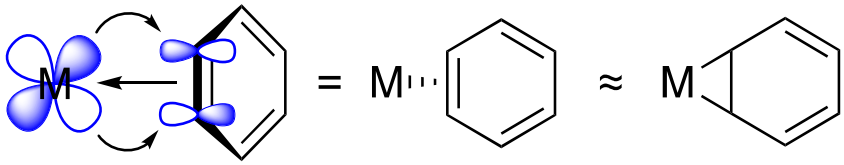

Figure 2.2: π-backbonding from metal to aromatic ligand

This coordination chemistry was originally seen with the pentaamineosmium(II) system.[32] It was found that reducing $(NH_3)_5Os(OTf)_3$ in the presence of benzene made the resulting osmium(II) species electron-rich enough to engage the benzene in an η^2-coordination mode. Further investigation saw that the Os(II) fragment could coordinate aniline, anisole, phenol, naphthalene, and pyrroles.[33-37] Once coordinated to the Os(II) fragment, benzene was able to undergo electrophilic addition with a range of carbon electrophiles, including Michael acceptors and acetals.[38] A nucleophilic addition to the newly formed allyl species could occur with masked enolates and alkyl lithium compounds to yield 1,4-cyclohexadiene species (**Scheme 2.6**). In this case, both the electrophile and nucleophile add to the face of the aromatic anti to the metal.

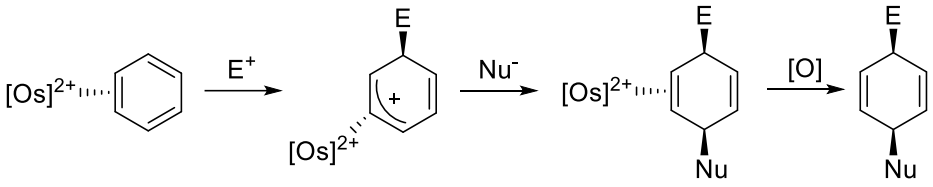

Scheme 2.6: Os(II) promoted dearomatization of benzene

Despite the ability to activate arenes, an alternative was needed to the Os(II) fragment due to the substantial cost, toxicity, and achiral nature of the system. This led to an investigation where the metal's d^5/d^6 reduction potential was identified as a key factor in developing suitable alternatives. It was found that a reduction potential of approximately 0.00 V (NHE) is required to coordinate aromatics in a dihapto fashion (**Figure 2.3**).[22,39,40] Further work resulted in the development of the π-basic fragment {ReTp(MeIm)(CO)}.[31,41] This fragment is a stronger π-base than the Os(II) system and establishes chirality.

A notable feature of the Re(I) fragment is the use of the trispyrazolylborate (Tp) ligand developed by Trofimenko.[42] The tridentate scorpionate ligand fortifies the octahedral geometry of the metal complex through suppression of a seven-coordinate system that would result from an oxidative addition.

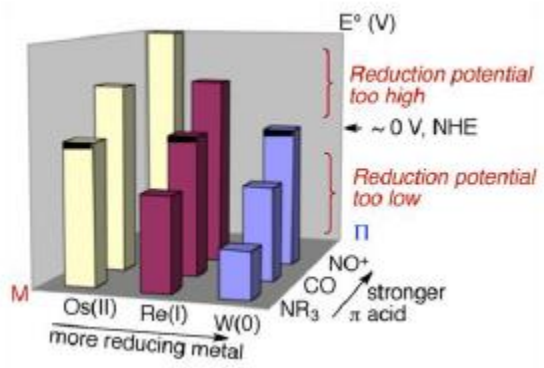

Figure 2.3: Metal and ligand comparison to allow for desired reduction potential of 0.00 V (NHE)

The Re(I) fragment could coordinate a similar range of aromatics compared to the Os(II) fragment while also coordinating pyridine derivatives.[22,23] Dearomatization of benzene with the Re(I) fragment allows for a Diels-Alder reaction with NMM giving a bicylco[2.2.2]octene core.[41] The Re(I) dearomatization agent also allows for a tandem electrophilic/nucleophilic addition similar to that of the Os(II) system yielding cis-disubstituted 1,4-cyclohexadiene products.[43] Yields for the organic transformation allowed by the Re(I) system were high compared to the Os(II) system.

Issues in preparation and scalability of the {ReTp(MeIm)(CO)} led to the development of dearomatization agents based off of Group 6 metals in the forms of {TpW(NO)(PMe_3)} and {TpMo(NO)(DMAP)} fragments (**Figure 2.4**). Akin to the development of the Re(I) system, the ligands of Group 6 dearomatization fragments were chosen to match the electrochemical parameters needed for dihapto coordination to an aromatic molecule resulting in the use of a NO ligand versus the previously used CO.[22,23] The W(0) fragment is the most π-basic of the four dearomatization agents developed in the Harman lab. This has led to the coordination of a wide range of aromatics, including benzene, arenes, heterocycles, and polycyclic aromatic hydrocarbons.[22,23,44,45] The Mo(0) fragment is a significantly weaker π-base compared to the W(0) fragment. This has led to a limited range of aromatics that can bind to the

Mo(0) fragment to yield stable complexes. Recent efforts, however, have led to the isolation of TpMo(NO)(DMAP)(η^2-benzene) and TpMo(NO)(DMAP)(η^2-PhCF$_3$).[46]

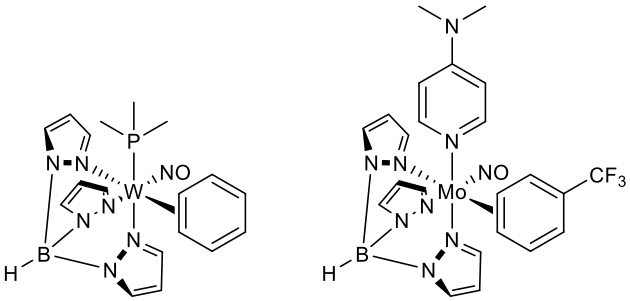

Figure 2.4: Group 6 dearomatization agents

2.8 Chemistry of Electron-Deficient Arenes Coordinated to Electron-Rich Metal Complexes

Although the reactivity of the benzene system and electron-rich aromatics has been thoroughly explored (**Scheme 2.7**),[36,37,47-52] the ability of the tungsten and molybdenum systems to promote reactivity on electron-deficient benzenes is relatively unexplored. Of note, η^2-arene complexes are exceedingly rare. Before the trifluorotoluene complexes of the tungsten and molybdenum systems,[53,54] the only other examples of thermally stable η^2-benzene with an electron-withdrawing group are pentaammineosmium(II) complexes of trifluorotoluene, benzophenone, and pivalophenone.[55]

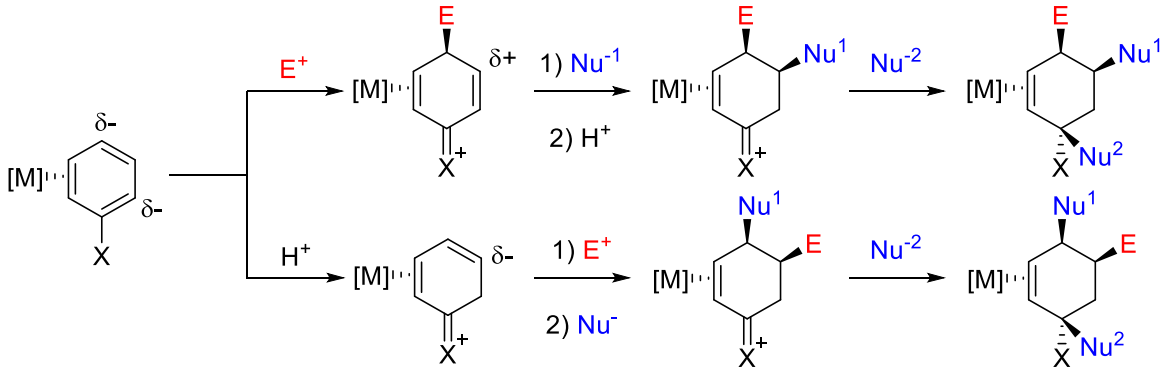

Scheme 2.7: Reactivity of electron-rich aromatics upon η^2-coordination to a π-basic metal fragment

More recent work from the Harman lab has demonstrated that when α,α,α-trifluorotoluene is bound to {WTp(NO)(PMe$_3$)} in a dihapto fashion, the electron-withdrawing CF$_3$ group polarizes the arene in such a way that protonation occurs selectively at an ortho carbon.[56] Nucleophiles are then selectively

directed to the adjacent carbon of the corresponding η^2-arenium complex anti to the face of the arene bound to the metal. The resulting diene is electronically complementary to η^2-diene complexes prepared from electron-rich arenes and can be elaborated further into novel trisubstituted cyclohexenes (**Scheme 2.8**).[56]

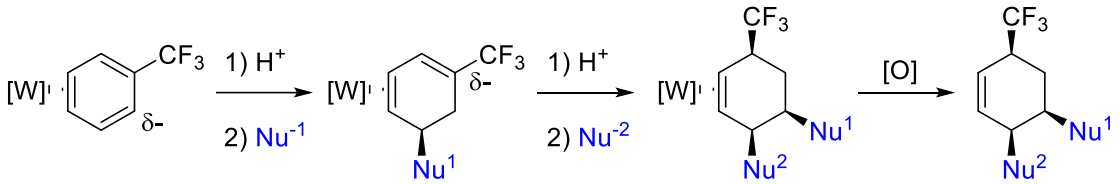

Scheme 2.8: Reactivity of TpW(NO)(PMe_3)(η^2-$PhCF_3$)

The expansion of electron-deficient benzenes that can be coordinated to the {WTp(NO)(PMe_3)} fragment and the subsequent organic manipulations to these complexes will be the focus of this dissertation. An investigation of what electron-deficient arenes can bind in a dihapto fashion to the metal fragment {TpW(NO)(PMe_3)} is presented in Chapter 3. Consecutive tandem electrophilic/nucleophilic additions to a family of phenyl sulfones to yield trisubstituted cyclohexenes in a similar pattern to the WTp(NO)(PMe_3)(η^2-TFT) will be the focus of Chapter 4. Sulfones have been demonstrated as leaving groups for nucleophilic substitution and elimination reactions.[57-64] Chapter 5 investigates the replacement of the sulfone functional groups to expand the diversity of anticipated trisubstituted cyclohexene products. Finally, Chapter 6 describes the phenyl sulfone family's ability to tolerate the addition of amines and bicyclic complexes resulting from lactam formation after the amine addition.

References

(1) Hook, J. M.; Mander, L. N. *Natural Product Reports* **1986**, *3*, 35.

(2) Rabideau, P. W.; Marcinow, Z. *Organic Reactions* **2004**, 1.

(3) Birch, A. J. *Journal of the Chemical Society (Resumed)* **1944**, 430.

(4) Lei, P.; Ding, Y.; Zhang, X.; Adijiang, A.; Li, H.; Ling, Y.; An, J. *Organic Letters* **2018**, *20*, 3439.

(5) Crich, D.; Hwang, J.-T. *The Journal of Organic Chemistry* **1998**, *63*, 2765.

(6) Ciganek, E. *Tetrahedron Letters* **1967**, *8*, 3321.

(7) Wender, P. A.; Dore, T. M.; deLong, M. A. *Tetrahedron Letters* **1996**, *37*, 7687.

(8) Remy, R.; Bochet, C. G. *Chemical Reviews* **2016**, *116*, 9816.

(9) Hamrock, S. J.; Sheridan, R. S. *Journal of the American Chemical Society* **1989**, *111*, 9247.

(10) Southgate, E. H.; Pospech, J.; Fu, J.; Holycross, D. R.; Sarlah, D. *Nature Chemistry* **2016**, *8*, 922.

(11) Wertjes, W. C.; Southgate, E. H.; Sarlah, D. *Chemical Society Reviews* **2018**, *47*, 7996.

(12) Hernandez, L. W.; Pospech, J.; Klöckner, U.; Bingham, T. W.; Sarlah, D. *Journal of the American Chemical Society* **2017**, *139*, 15656.

(13) Okumura, M.; Sarlah, D. *European Journal of Organic Chemistry* **2020**, *2020*, 1259.

(14) Hudlicky, T. *Chemical Reviews* **1996**, *96*, 3.

(15) Hudlicky, T.; Olivo, H. F. *Journal of the American Chemical Society* **1992**, *114*, 9694.

(16) Charest, M. G.; Lerner, C. D.; Brubaker, J. D.; Siegel, D. R.; Myers, A. G. *Science* **2005**, *308*, 395.

(17) Carless, H. A. J.; Malik, S. S. *Tetrahedron: Asymmetry* **1992**, *3*, 1135.

(18) Hudlicky, T. *Pure and Applied Chemistry* **1994**, *66*, 2067.

(19) Hudlicky, T.; Reed, J. W. *Synlett* **2009**, *2009*, 685.

(20) Kundig, E. P. *Transition Metal Arene Complexes in Organic Synthesis and Catalysis*; Springer: Berlin, 2004; Vol. 7.

(21) Pape, A. R.; Kaliappan, K. P.; Kündig, E. P. *Chemical Reviews* **2000**, *100*, 2917.

(22) Keane, J. M.; Harman, W. D. *Organometallics* **2005**, *24*, 1786.

(23) Liebov, B. K.; Harman, W. D. *Chemical Reviews* **2017**, *117*, 13721.

(24) Kündig, E. P.; Fabritius, C.-H.; Grossheimann, G.; Romanens, P.; Butenschön, H.; Wey, H. G. *Organometallics* **2004**, *23*, 3741.

(25) Kündig, E. P.; Cannas, R.; Fabritius, C.-H.; Grossheimann, G.; Kondratenko, M.; Laxmisha, M.; Pache, S.; Ratni, H.; Robvieux, F.; Romanens, P.; Tchertchian, S. *Pure and Applied Chemistry* **2004**, *76*, 689.

(26) Semmelhack, M. F. *Comprehensive Organometallic Chemistry II: A Review of the Literature 1982-1994*; Pergamon: Oxford, UK, 1995; Vol. 12.

(27) Semmelhack, M. F.; Hall, H. T.; Farina, R.; Yoshifuji, M.; Clark, G.; Bargar, T.; Hirotsu, K.; Clardy, J. *Journal of the American Chemical Society* **1979**, *101*, 3535.

(28) Semmelhack, M. F.; Clark, G. R.; Farina, R.; Saeman, M. *Journal of the American Chemical Society* **1979**, *101*, 217.

(29) Kündig, E. P.; Cunningham Jr., A. F.; Paglia, P.; Simmons, D. P.; Bernardinelli, G. *Helvetica Chimica Acta* **1990**, *73*, 386.

(30) Amurrio, D.; Khan, K.; Kündig, E. P. *The Journal of Organic Chemistry* **1996**, *61*, 2258.

(31) Meiere, S. H.; Brooks, B. C.; Gunnoe, T. B.; Carrig, E. H.; Sabat, M.; Harman, W. D. *Organometallics* **2001**, *20*, 3661.

(32) Harman, W. D.; Taube, H. *Journal of the American Chemical Society* **1987**, *109*, 1883.

(33) Kolis, S. P.; Gonzalez, J.; Bright, L. M.; Harman, W. D. *Organometallics* **1996**, *15*, 245.

(34) Cordone, R.; Harman, W. D.; Taube, H. *Journal of the American Chemical Society* **1989**, *111*, 5969.

(35) Myers, W. H.; Koontz, J. I.; Harman, W. D. *Journal of the American Chemical Society* **1992**, *114*, 5684.

(36) Kopach, M. E.; Harman, W. D. *Journal of the American Chemical Society* **1994**, *116*, 6581.

(37) Kolis, S. P.; Kopach, M. E.; Liu, R.; Harman, W. D. *The Journal of Organic Chemistry* **1997**, *62*, 130.

(38) Ding, F.; Kopach, M. E.; Sabat, M.; Harman, W. D. *Journal of the American Chemical Society* **2002**, *124*, 13080.

(39) Harman, W. D. *Coordination Chemistry Reviews* **2004**, *248*, 853.

(40) Surendranath, Y.; Harman, W. D. *Dalton Transactions* **2006**, 3957.

(41) Chordia, M. D.; Smith, P. L.; Meiere, S. H.; Sabat, M.; Harman, W. D. *Journal of the American Chemical Society* **2001**, *123*, 10756.

(42) Trofimenko, S. *Journal of the American Chemical Society* **1966**, *88*, 1842.

(43) Ding, F.; Harman, W. D. *Journal of the American Chemical Society* **2004**, *126*, 13752.

(44) Graham, P. M.; Meiere, S. H.; Sabat, M.; Harman, W. D. *Organometallics* **2003**, *22*, 4364.

(45) Welch, K. D.; Harrison, D. P.; Lis, E. C.; Liu, W.; Salomon, R. J.; Harman, W. D.; Myers, W. H. *Organometallics* **2007**, *26*, 2791.

(46) Myers, J. T.; Smith, J. A.; Dakermanji, S. J.; Wilde, J. H.; Wilson, K. B.; Shivokevich, P. J.; Harman, W. D. *Journal of the American Chemical Society* **2017**, *139*, 11392.

(47) Lis, E. C.; Salomon, R. J.; Sabat, M.; Myers, W. H.; Harman, W. D. *Journal of the American Chemical Society* **2008**, *130*, 12472.

(48) Kopach, M. E.; Gonzalez, J.; Harman, W. D. *Journal of the American Chemical Society* **1991**, *113*, 8972.

(49) Todd, M. A.; Grachan, M. L.; Sabat, M.; Myers, W. H.; Harman, W. D. *Organometallics* **2006**, *25*, 3948.

(50) Todd, M. A.; Sabat, M.; Myers, W. H.; Smith, T. M.; Harman, W. D. *Journal of the American Chemical Society* **2008**, *130*, 6906.

(51) Gonzalez, J.; Sabat, M.; Harman, W. D. *Journal of the American Chemical Society* **1993**, *115*, 8857.

(52) Salomon, R. J.; Todd, M. A.; Sabat, M.; Myers, W. H.; Harman, W. D. *Organometallics* **2010**, *29*, 707.

(53) Myers, J. T.; Smith, J. A.; Dakermanji, S. J.; Wilde, J. H.; Wilson, K. B.; Shivokevich, P. J.; Harman, W. D. *J. Am. Chem. Soc.* **2017**, *139*, 11392.

(54) Wilson, K. B.; Myers, J. T.; Nedzbala, H. S.; Combee, L. A.; Sabat, M.; Harman, W. D. *J. Am. Chem. Soc.* **2017**, *139*, 11401.

(55) Harman, W. D.; Sekine, M.; Taube, H. *Journal of the American Chemical Society* **1988**, *110*, 5725.

(56) Wilson, K. B.; Myers, J. T.; Nedzbala, H. S.; Combee, L. A.; Sabat, M.; Harman, W. D. *Journal of the American Chemical Society* **2017**, *139*, 11401.

(57) Wallace, T. J.; Hofmann, J. E.; Schriesheim, A. *Journal of the American Chemical Society* **1963**, *85*, 2739.

(58) Cubbage, J. W.; Vos, B. W.; Jenks, W. S. *Journal of the American Chemical Society* **2000**, *122*, 4968.

(59) Guan, Y.; Wang, C.; Wang, D.; Dang, G.; Chen, C.; Zhou, H.; Zhao, X. *RSC Advances* **2015**, *5*, 12821.

(60) Sakakibara, T.; Suganuma, T.; Kajihara, Y. *Chemical Communications* **2007**, 3568.

(61) Ochiai, M.; Ukita, T.; Fujita, E. *Journal of the Chemical Society, Chemical Communications* **1983**, 619.

(62) Trost, B. M. *Chemistry: a European journal* **2019**, *25*, 11193.

(63) Brown, D. S.; Ley, S. V.; Vile, S. *Tetrahedron Letters* **1988**, *29*, 4873.

(64) Brown, D. S.; Charreau, P.; Hansson, T.; Ley, S. V. *Tetrahedron* **1991**, *47*, 1311.

Chapter 3

η^2-Coordination of Electron-Deficient Arenes with Group 6 Dearomatization Agents

3.1 Introduction

The binding of aromatic molecules to a transition metal can enable a wide array of chemical transformations, often inaccessible by other means. Over the past several decades, the Harman lab has endeavored to explore how transition-metal complexes can activate aromatic molecules toward novel organic transformations through their coordination to just two carbons (η^2).[1-3] Studies concerning the η^2-coordination of substituted benzenes to a transition metal have focused on anisoles,[4-6] phenols,[7-9] anilines,[7,10,11] and other arenes bearing a single π-donor group. In these systems, the metal and heteroatom substituent act together to render the arene susceptible to protonation and electrophilic addition (**Scheme 3.1**). However, the organic chemistry derived from the dihapto-coordinated of electron-deficient arenes to a transition metal is largely underexplored.

Until recently, it was thought that although arenes with electron-withdrawing groups (EWGs) are better π-acids, they would be inferior as η^2-aromatic substrates for organic reactions since this type of substituent and the electron-donating metal are at cross-purposes. Despite the opposing electronic effects, we recently showed that when bound to {WTp(NO)(PMe_3)}, α,α,α-trifluorotoluene was capable of being protonated by strong acid.[12] The electron-withdrawing -CF_3 group polarizes the arene so that protonation occurs selectively at an ortho carbon. Nucleophiles are then selectively directed to the adjacent carbon of the corresponding η^2-arenium complex. The resulting diene is electronically complementary to η^2-diene complexes prepared from electron-rich arenes and can be elaborated further into novel trisubstituted cyclohexenes (**Scheme 3.1**).[12]

Of note, η^2-arene complexes are exceedingly rare, owing to the loss of aromatic stability upon coordination. Besides the trifluorotoluene complexes of the tungsten and molybdenum systems,[12,13] the only other examples of thermally stable η^2-benzene with an electron-withdrawing group are pentaammineosmium(II) complexes of trifluorotoluene, benzophenone, and pivalophenone.[14] The potential for organic transformations of η^2-arenes with electron-withdrawing substituents has prompted

us to evaluate the scope and binding selectivity of arenes that can be coordinated by the {WTp(NO)(PMe_3)} and {MoTp(NO)(DMAP)} systems, particularly where the substituent is relevant to pharmaceutical design (e.g., nitriles,[15] esters,[16] sulfones,[17] fluorines[18]). This chapter will focus on the tungsten system {WTp(NO)(PMe_3)} with a few comparisons to the molybdenum system {MoTp(NO)(DMAP)}.

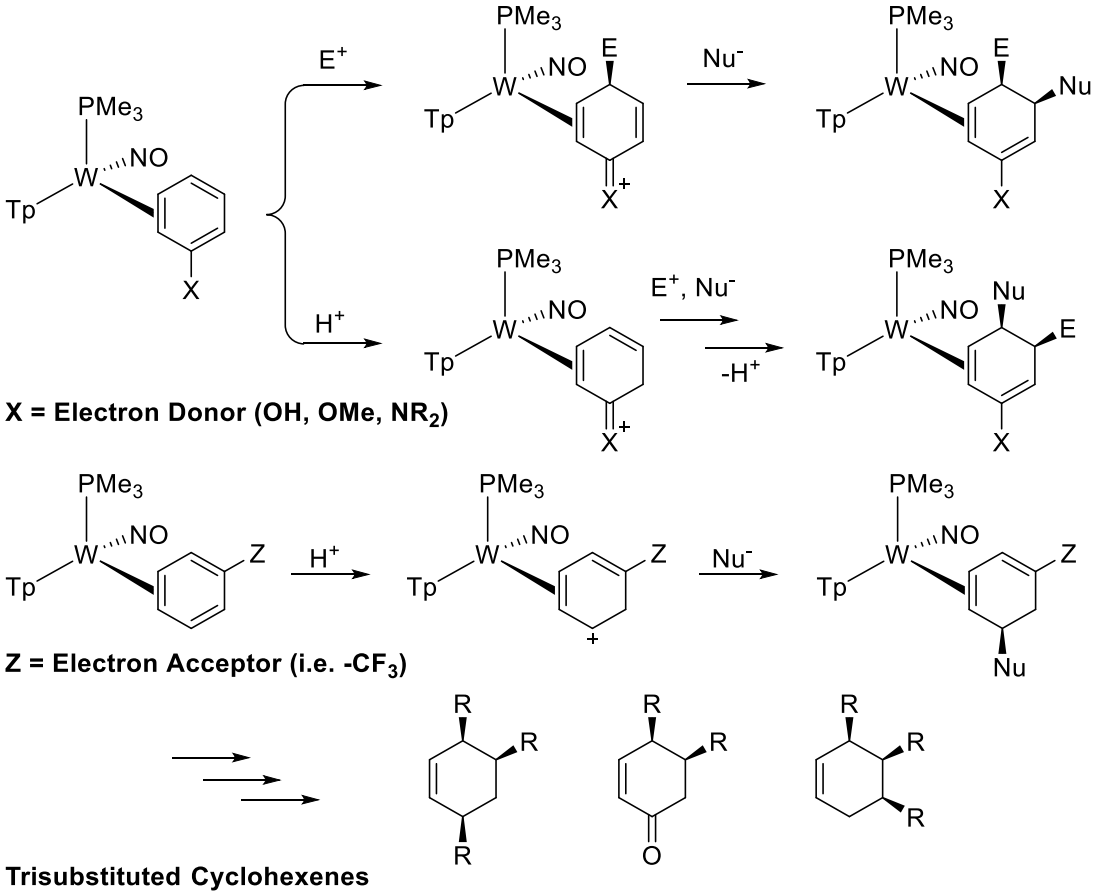

Scheme 3.1: Incorporation of functional groups into cyclohexenes via an η^2-benzene complex precursor

3.2 Studies of Electron-Withdrawing Groups on Benzenes and Tungsten Fragments

Various benzenes bearing a single electron-withdrawing group (Z) were surveyed for their potential coordination to either {MoTp(DMAP)(NO)} or {WTp(PMe_3)(NO)} fragments. The complexes WTp(PMe_3)(NO)(benzene) (**1**) and MoTp(DMAP)(NO)(TFT) serve as synthons to these fragments.[13,19] In many cases, the EWG itself often proved to be a superior position for coordination. DFT calculations (M06;

hybrid LANL2DZ, 6-31G(d,p) basis set; in vacuum) done by Jacob Smith and Karl Westendorff support this notion (**Table 3.1**). For benzaldehyde, benzonitrile, methyl benzoate, and even the bulky ketone 2,2-dimethylpropiophenone, calculations indicate that binding at the substituent is heavily favored over coordination in the arene. Thus, formation of a purported ring-bound complex for these arenes relies on the kinetic trapping of such an isomer.

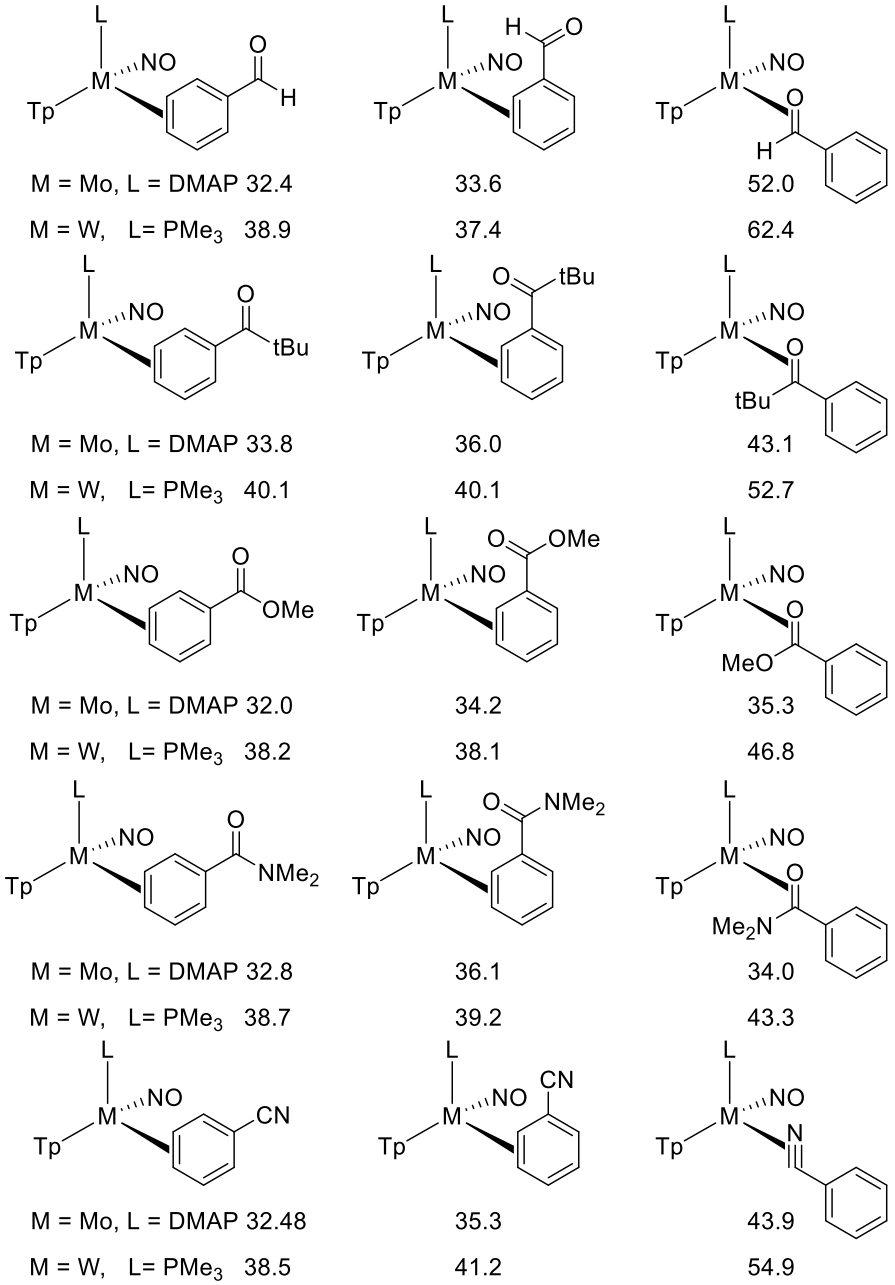

Table 3.1: DFT calculations of relative binding energies for electron-deficient benzenes (Gibbs free energy; kcal/mol)

For example, benzonitrile appears to form a complex with {MoTp(NO)(DMAP)} in which only the nitrile is coordinated.[20,21] Yet, when benzonitrile was allowed to react with the more substitution-inert tungsten precursor, at least seven tungsten complexes were present in the crude reaction mixture, judging from ^{31}P NMR data. Of these, the major species (−9.39 ppm, η^2-nitrile) has a chemical shift and ^{183}W–^{31}P coupling constant (313 Hz) outside the ranges expected for a κ-N species or an η^2-arene.[22] This species is tentatively ascribed to a C,N-η^2-nitrile complex.[21] The two most downfield (−9.39, −13.05 ppm) signals, accounting for roughly 60% of the reaction mixture, are absent after silica chromatography.

After elution through a silica column, an analytically pure sample of five dihapto-coordinate isomers in the form of WTp(NO)(PMe_3)(PhCN) (**2A-E**) were recovered (27% yield, **Scheme 3.2**). All five isomers feature the tungsten bound to two of the aromatic carbons. Of these five species, the two major species show resonances consistent with η^2-arene formation where the metal is bound to the 3,4-carbons. The major isomer shows five ring resonances at 7.74, 6.88, 5.67, 4.00, and 2.14 ppm, which favorably compare with the known complex WTp(NO)(PMe_3)(η^2-3,4-$PhCF_3$) (cf., 7.50, 6.87, 6.03, 3.95, and 2.30 ppm).[23,24] Two of the minor isomers were found to be bound by the tungsten through the 2,3-carbons. The fifth and final isomer is observed to be a rare example of where the tungsten is bound in a dihapto-fashion to the 1,2-carbons, where the -CN group is located on the carbon distal to the phosphine ligand and is directed toward the TpA and TpC ligands. All five nitrile isomers (**2A-2E**) are considerably more stable in acetone solution than their η^2-benzene counterpart. No dissociation of the benzonitrile ligand or isomerization to the purported CN isomer was observed over a period of 4 days.

While the low equilibrium concentrations and considerable overlap of ^{1}H NMR signals for several of these η^2-arene complexes make their conclusive identification challenging, NOESY data revealed a complex set of chemical exchange processes that occur under ambient conditions. The NOESY data thus allowed for characterization of the minor isomers through their relationship to the major isomers. A summary of the data is shown in **Scheme 3.2**. NOESY spin-saturation exchange indicates that at room

temperature in acetonitrile, **2B** and **2D** can readily isomerize, while **2A** and **2C** can also readily isomerize. There is no evidence of isomerization between **2B** and **2A,** nor is there any exchange between **2D** and **2C** under ambient conditions.

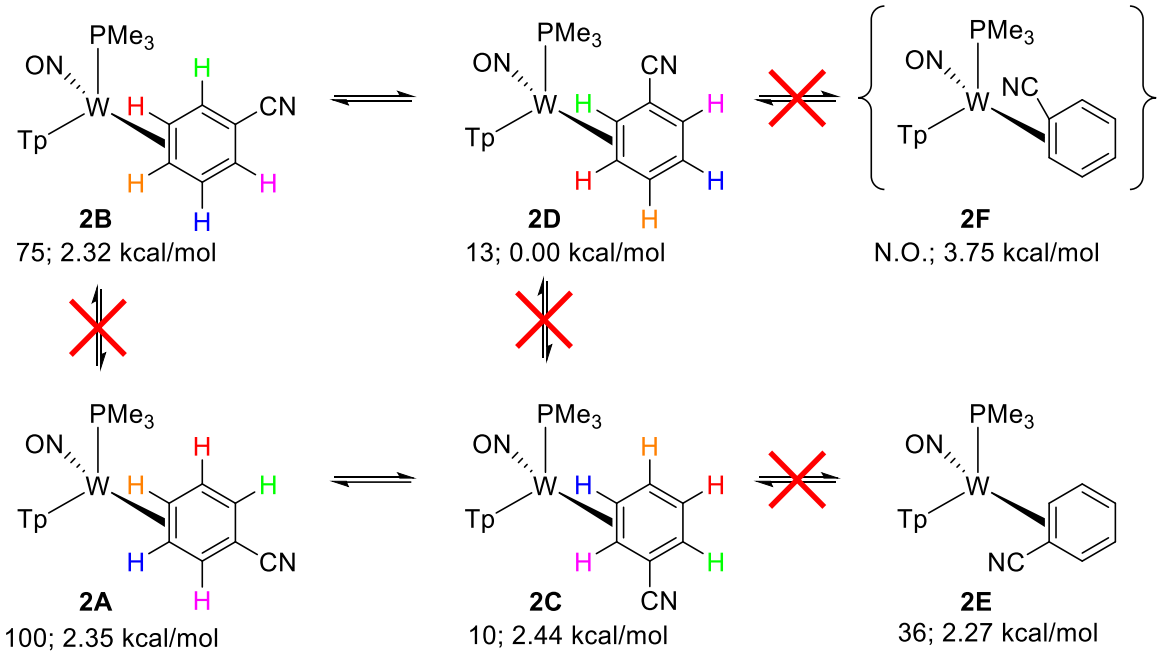

Scheme 3.2: Isomerization of η^2-coordinated benzonitrile (ratio; calculated Gibbs free energy)

NOESY data for η^2-benzonitrile is shown with red peaks indicating through-space NOE interactions, while blue off-diagonal peaks indicate spin-exchange peaks. The H5 proton of the 3,4-η^2-isomer **2B** (blue H) undergoes chemical exchange exclusively with that same position of the minor 2,3-η^2 isomer **2D** (**Figure 3.1**). The doublet of doublets shifts from 7.01 to 5.73 during isomerization, indicating that the proton has become more shielded, a characteristic seen of protons at the beta position to the bound carbon.

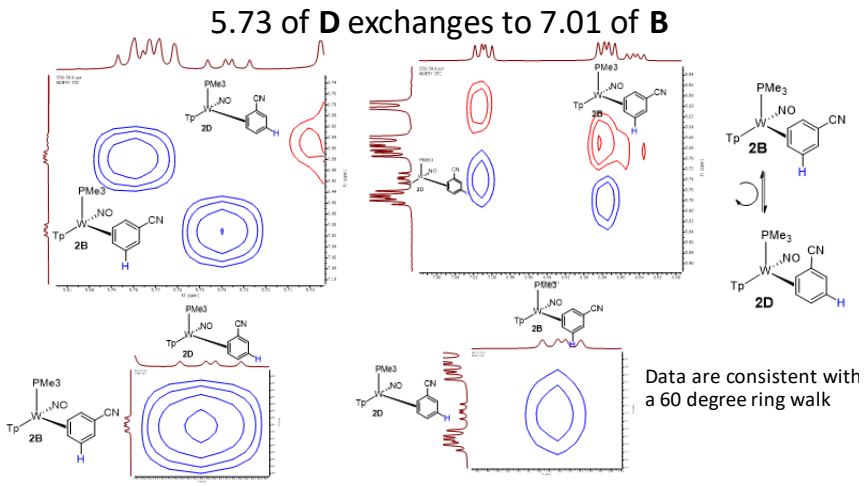

Figure 3.1: Spin-saturation exchange between H5 of **2B** and **2D**

Additionally, a spin-exchange is exclusively seen between H2 of **2B** (green H) and H2 of the minor isomer **2D**. The spin-saturation exchange seen here indicates that upon isomerization, the H2 alkene proton of **2B** at 7.62 ppm is shifted upfield to become the H2 proton of **2D** at 4.16 ppm, which is the proton of the bound carbon proximal to the PMe_3 ligand (**Figure 3.2**). An interesting feature that can be seen is the alkene doublet becoming a doublet of doublets due to the bound proton's coupling with the PMe_3 ligand upon isomerization. The reverse exchange can be seen between H4 of **2B** (orange H) and H4 of **2D**. The proton of **2B** at 2.17 ppm exhibits a spin-saturation exchange with the more downfield proton of **2D** at 7.38 ppm (**Figure 3.2**). This indicates that the proton of the bound carbon distal to the PMe_3 ligand becomes an alkene proton upon isomerization.

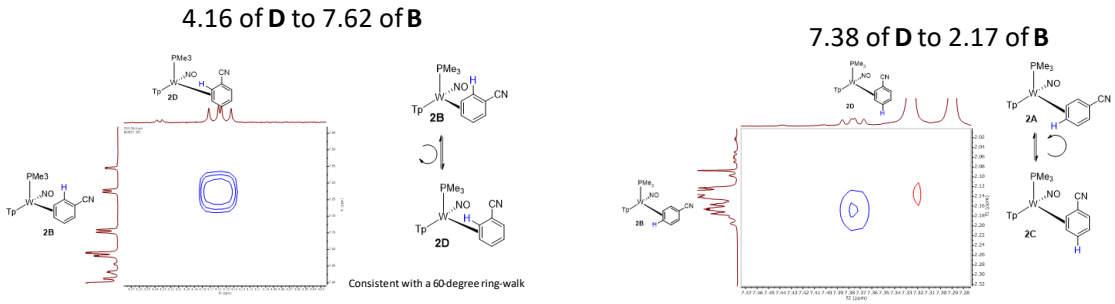

Figure 3.2: Spin-saturation exchange of H2 and H4 upon isomerization of **2B** to **2D**

The next two spin-saturation exchanges seen are not as drastic as the previous two shifts but still demonstrate an exchange with an adjacent proton, thus indicating an isomerization represented by a

rotation of the benzene ring of 60° about the C6 axis. A blue signal between H3 of **2B** 3.75 ppm (red H) and H3 of **2D** at 2.06 ppm indicates an exchange between the proton on the bound carbon proximal to the PMe_3 ligand of **2B** and the proton on the bound carbon distal to the PMe_3 ligand of **2D** (**Figure 3.3**). The second spin-saturation exchange shown below between the H6 proton of **2B** at 5.60 ppm (purple H) and the 6H proton of **2D** at 6.54 ppm simply demonstrates that the 6H proton becomes more proximal to the PMe_3 ligand upon isomerization from **2B** to **2D**.

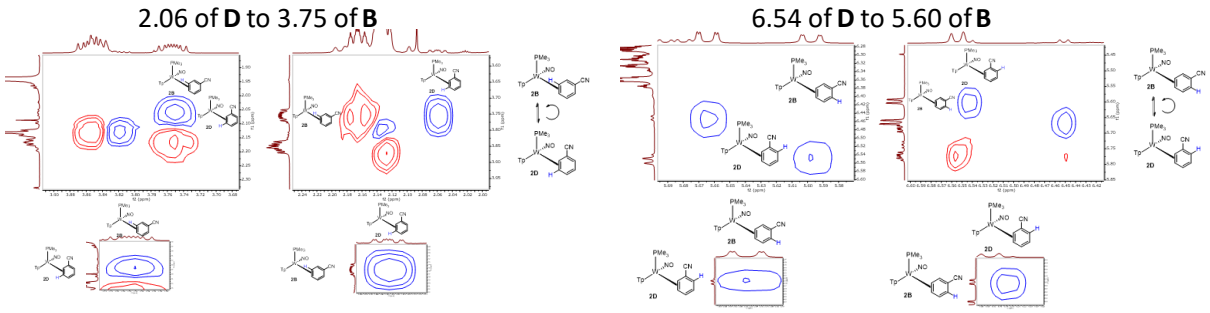

Figure 3.3: Spin-saturation exchange of H3 and H6 upon isomerization of **2B** to **2D**

While we were able to find spin-saturation correlations between all 5 protons of **2B** and **2D**, only 4 protons were correlated between **2A** and **2C**. The exchanges are as follows. H5 (red H) of **2A** at 6.88 ppm undergoes chemical exchange exclusively with H5 of **2C** at 5.78 ppm (**Figure 3.4**). As seen previously, the doublet of doublets experiences an up-field shift upon isomerization to the less prevalent isomer, indicating that the proton has become more shielded, which is a characteristic seen of protons at the beta position to the bound carbon.

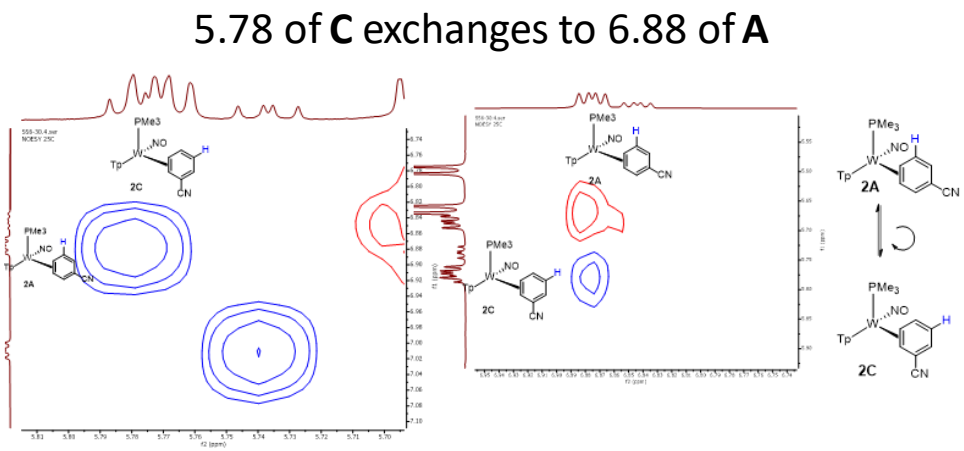

Figure 3.4: Spin-saturation exchange of H5 upon isomerization of **2A** to **2C**

Additionally, a spin-exchange is exclusively seen between H2 of **2A** (purple H) and the H2 of the minor isomer **2C**. The spin-saturation exchange seen here indicates that upon isomerization, the doublet H2 alkene proton of **2A** at 7.74 ppm is shifted upfield to become the doublet H2 proton of **2C** at 2.19 ppm, which is the proton of the bound carbon distal to the PMe_3 ligand (**Figure 3.5**). The reverse exchange can be seen between H4 of **2A** (orange H) and H4 of **2C**. The proton of **2A** at 3.85 ppm exhibits a spin-saturation exchange with the more downfield proton of **2C** at 7.19 ppm (**Figure 3.5**). This indicates that the proton of the bound carbon proximal to the PMe_3 ligand becomes an alkene proton upon isomerization.

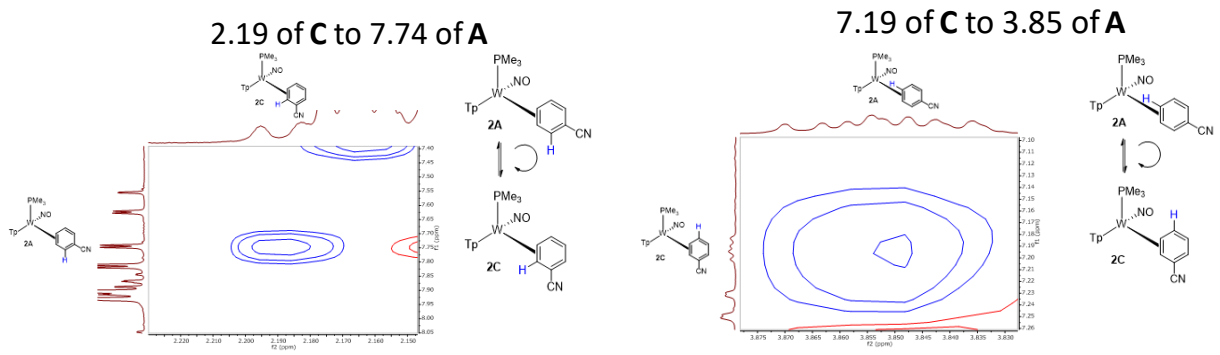

Figure 3.5: Spin-saturation exchange of H2 and H4 upon isomerization of **2A** to **2C**

The last spin-saturation exchange seen is once again not as drastic as the previous two shifts but helps confirm a 60° rotation about the C6 axis as the isomerization. A blue signal between H6 of **2A** at 5.67 ppm (pink H) and H6 of **2C** at 6.45 ppm simply demonstrates that the 6H proton becomes more proximal to the PMe_3 ligand upon isomerization from **2A** to **2C**.

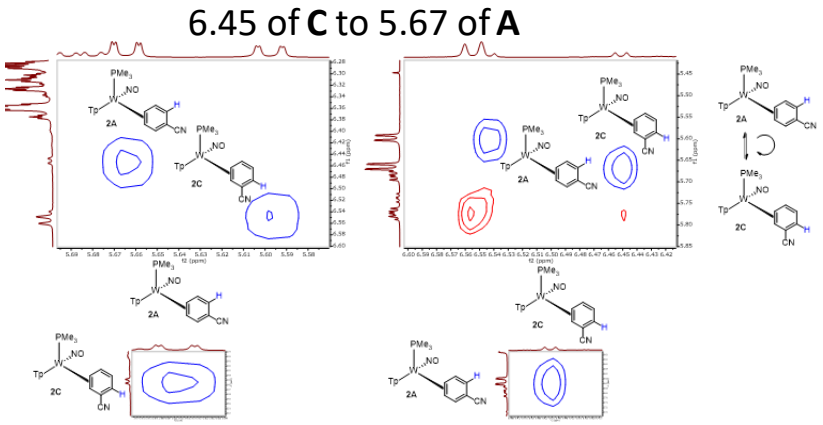

Figure 3.6: Spin-saturation exchange of H6 upon isomerization of **2A** to **2C**

The spin-saturation exchanges shown above are exclusively between the selected protons. They show no other spin-saturation exchanges with other protons. As stated above, there is no observable exchange between **2A** and **2B** on the NMR timescale at room temperature, while **2E** does not undergo any exchange with any of the observable isomers under these conditions. These observations indicate not only that the 2,3-η^2 ↔ 3,4-η^2 isomerization is facile under ambient conditions, but also that it occurs via a ring-slip mechanism, to the exclusion of any other mechanism (i.e., a face-flip, or oxidative addition)[25] under these NOESY conditions.

3.3 Benzene Substituents without Covalent π-Bonds

Given the large energetic preferences for coordination to the nitrile or carbonyl group (**Table 3.1**), we decided to explore benzenes with an EWG without covalent π bonds (**Scheme 3.3**). Stirring a solution of benzene complex **1** and an excess of the target arene resulted in the formation of several new η^2-coordinated arene complexes of the form WTp(NO)(PMe_3)(η^2-arene), where arene = trimethyl o-benzoate (**4**), methyl phenyl sulfone (**6**) (see appendix for crystal struture), diphenyl sulfone (**5**), phenyl sulfonyl pyrrolidine (**7**), and pentafluorosulfanyl benzene (**8**).

Despite the strongly electron-withdrawing substituents, these complexes were formed with minimal oxidative decomposition. In most cases, the metal complex was isolated as an ~1:1 mixture of two coordination diastereomers in which the metal was 3,4-η^2 bound, analogous to the case for **2A** and **2B**. While DFT calculations (**Table 3.1**) suggested that in some cases, the 2,3-η^2 arene isomers were energetically competitive, only in complex **2** were they conclusively identified. Judging from IR and electrochemical data, the sulfur analogs (SO_2Ph; **5**, SO_2Me; **6**, SF_5; **8**) appear to have a stronger metal-arene back bonding interaction for **5**, **6**, and **7** compared to **2**, **3**, or **4**. An increase in $E_{p,a}$ for W(0) -> W(I)) (100 mV/s), and an increase in NO stretch frequency in the infrared absorption spectrum further support this notion (**Table 3.2**).

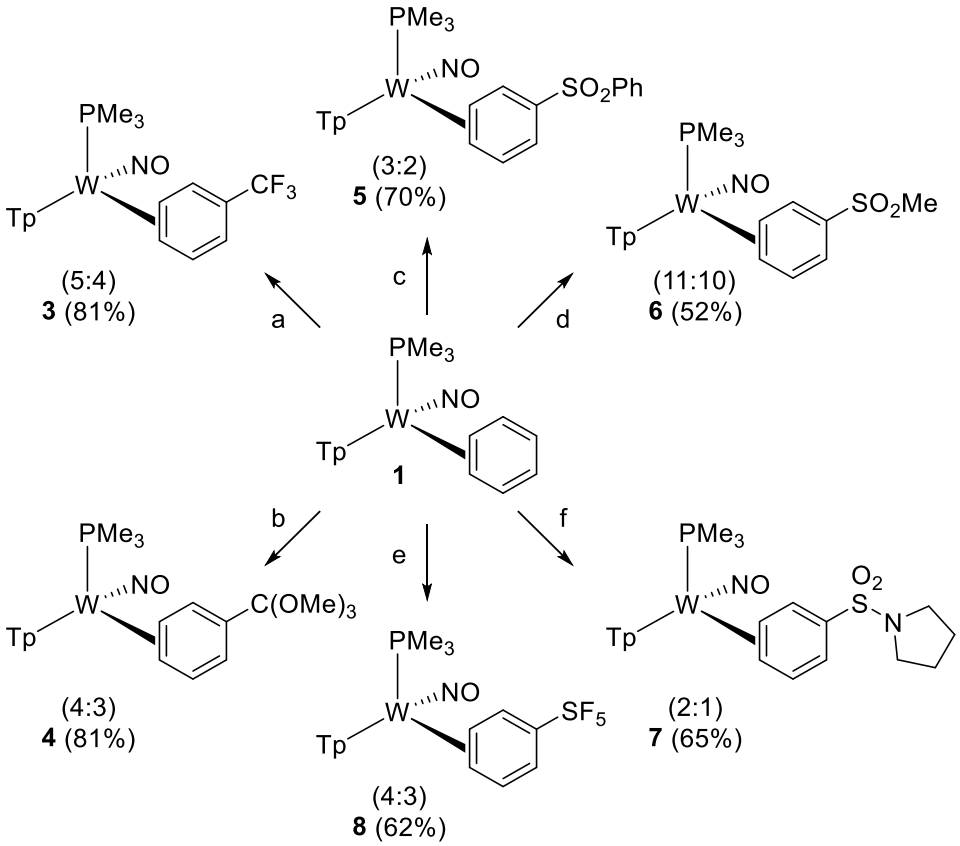

Legend: (a) neat $PhCF_3$, 20 h, ambient temperature; (b) neat $PhC(OMe)_3$, 16 h, ambient temperature; (c) $PhSO_2Ph$ dissolved in dimethoxyethane (DME), 48 h, ambient temperature; (d) $PhSO_2Me$ dissolved in THF, 16 h, ambient temperature; (e) neat $PhSF_5$, 24 h, ambient temperature; (F) $PhSO_2(NC_4H_8)$ dissolved in dimethoxyethane (DME), 48 h, ambient temperature. Only one of the two coordination diastereomers is shown, with ratios given in parentheses.

Scheme 3.3: Benzene complexes with a single EWG

3.4 Tungsten Hydrides

The reaction mixture resulting from the methyl phenyl sulfone exchange contained three species in a ratio of 2.7: 2.5: 1. We tentatively assign this third species as the sulfonylmethyl hydride **6H**. Key features in the 1H NMR spectrum include a diastereotopic methylene group at 3.14 and 1.88 ppm and a matching hydride signal at 9.03 ppm with a large J_{PH} = 114.9 Hz and tungsten-183 satellites (J_{WH} = 9.3 Hz). To further support the assignment of **6H** as an alkyl hydride, the benzene complex **1** was also combined with dimethyl sulfone and 4-(methylsulfonyl)toluene to yield **9** and **10** (**Scheme 3.4**), respectively. In both cases, the only complex formed was the expected sulfonylmethyl hydride, the net product of a tungsten

insertion into the methyl CH bond. ^{1}H NMR data shows diastereotopic methylene and hydride peaks similar to those observed for the methyl phenyl sulfone derivative (**6H**). Previously, the {WTp(NO)(PMe$_3$)} system has been observed to insert into N-H, O-H, C-H, and C-F bonds, but to our knowledge, this is the first example involving an sp^3 carbon with this tungsten fragment. It should be noted, however, that seminal work by the Legzdins group includes many such examples for the {WCp*(NO)} system.[26,27]

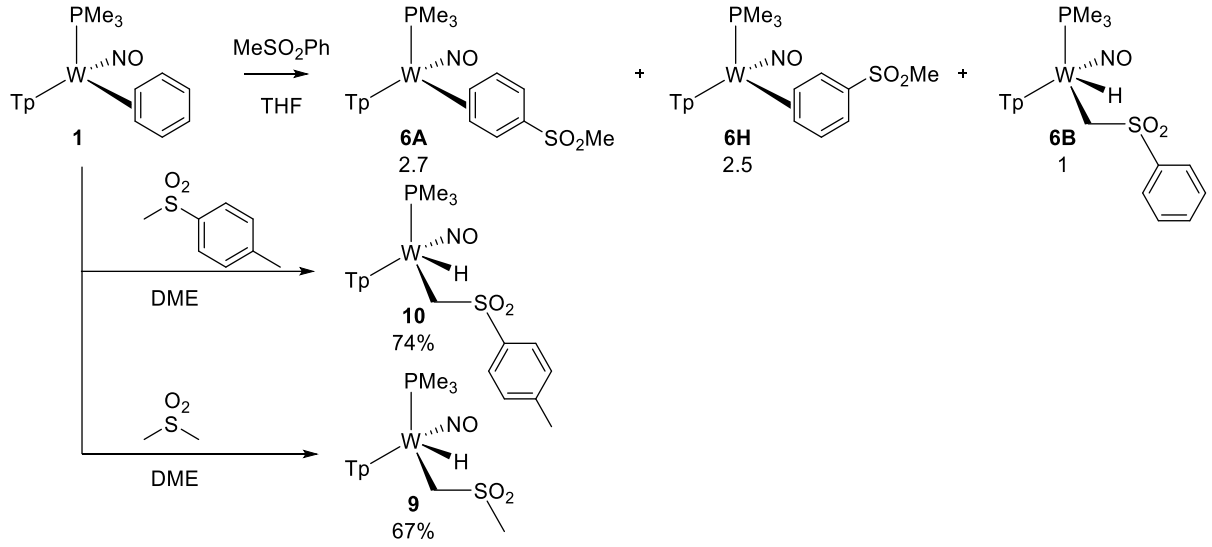

Scheme 3.4: Formation of sulfonylmethyl hydride complexes of {WTp(NO)(PMe$_3$)}

3.5 η2-Arenes Functionalized with EWGs that Possess π-Bonds

During our attempts to purify the *o*-benzoate complex **4**, it was found that hydrolysis would occur on a silica column. The resulting C,C-η^2-benzoate ester, **11A** and **11B**, was recovered in a 45% yield. This provided a rare example of an η^2-coordinated arene with a carbonyl group (**Scheme 3.5**). In most aspects, compound **11** is similar to the other monosubstituted arene complexes **3**-**8**, where the 3,4-η^2 isomers dominate. It should be noted that DFT calculations predict that η^2-coordination to the ester is thermodynamically favored by roughly 8 kcal/mol relative to the η^2 coordination of the arene (**Table 3.1**). This is noteworthy due to the observation that a purported carbonyl bound complex is not observed in solution after 24 hours (further time points were not investigated). This indicates that the arene to ester isomerization rate is sufficiently slow, implying that the barrier to isomerization is sufficiently high. This is

comparable with the observation from **section 3.2,** which demonstrated no isomerization from the η^2-arene form of the benzonitrile to the η^2-nitrile form over a period of days. These data points testify to the remarkable kinetic stability of the η^2-arene isomers when compared to η^2-benzene.

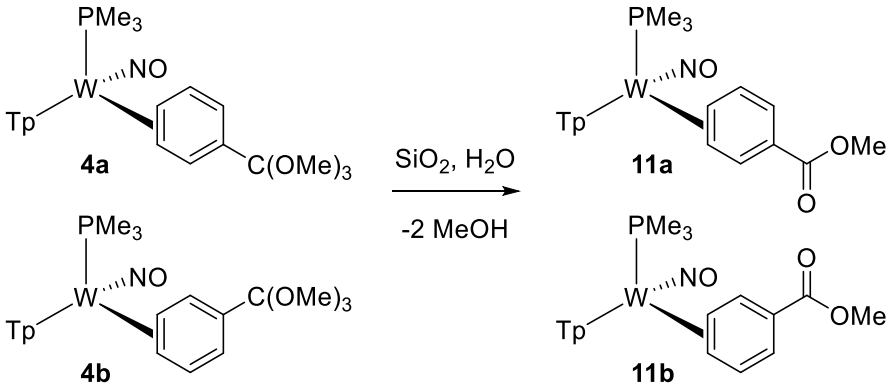

Scheme 3.5: Formation of an arene-bound benzoate complex

3.6 Substituted Trifluoromethylated Benzenes

We next considered how an η^2-benzene complex bearing an EWG would be influenced by an additional benzene substituent (**Scheme 3.6**). Thus, we examined a family of trifluorotoluene derivatives with a methoxy (**12**), dimethylamino (**13**), or trifluoromethyl (**15**) group at the 3-position. In addition, we examined one case of a 1,2-disubstituted arene (**14**). For example, where the second substituent was a π-donor (**12**, **13**), the metal was directed exclusively to the 5,6-positions. For both **12** and **13**, the complex was isolated as a mixture of two different coordination diastereomers. Similarly, introducing a second -CF_3 withdrawing group in the 3 position also yielded a mixture of two isomers (**15**). Isolation of 1,2-bis(trifluoromethyl)benzene yielded a single isomer bound to the 3,4-carbons.

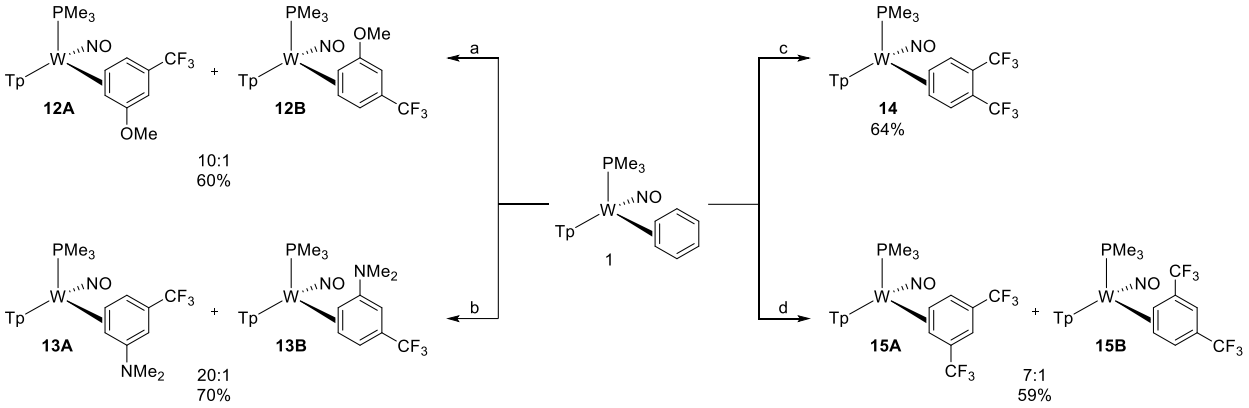

Legend: (a) 3-trifluoromethylanisole and DME cosolvent, 48 h, ambient temperature; (b) neat 3-trifluoromethyl-N,N-dimethylaniline, 16 h, ambient temperature; (c) neat 1,2-bis(trifluoromethyl)benzene, 16 h, ambient temperature: (d) neat 1,3-bis(trifluoromethyl)benzene, 18 h, ambient temperature.

Scheme 3.6: Regioselective formation of substituted trifluorotoluene complexes

As an example, combining **1** and 3-(trifluoromethyl)-N,N-dimethylaniline, which was prepared by a modified literature procedure,[28] resulted in the synthesis of **13**. The robust nature of this compound stands in contrast to that observed for the N,N-dimethylaniline analog, which is too thermally sensitive to isolate. In the latter case, the aniline ligand must be stabilized as an η^2-2H-anilinium complex (**Scheme 3.7**) by the action of a weak acid.[11] The ability to isolate **13** in its neutral form demonstrates the ability of a single $-CF_3$ group to stabilize arenes functionalized with π-donor groups. The trifluoromethylated aniline complex **13** can still be selectively protonated at the C2 ring carbon, but a stronger acid is required (e.g., diphenylammonium triflate (DPhAT); $pK_a \approx 0$). The resulting 2H-anilinium compound (**16**) has spectroscopic features similar to those reported for {W(PMe$_3$)(NO)(η^2-N,Ndimethyl-2H-anilinium)}OTf (**Scheme 3.7**).[11]

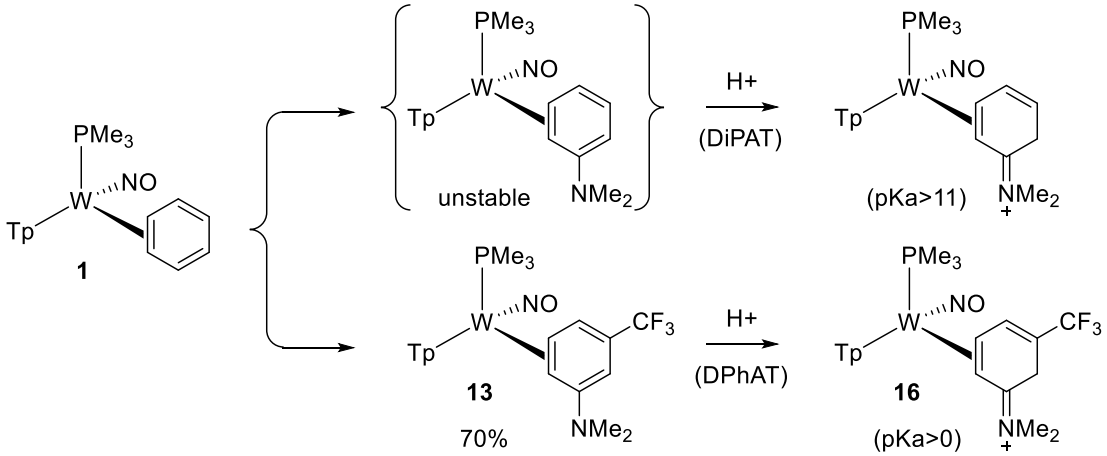

Scheme 3.7: Preparation of complex **13** and its protonation to give the anilinium (**16**) as a single isomer

3.7 Arenes Bearing EWGs that do not Bind to the {WTp(NO)(PMe_3)} Synthon

When the {WTp(NO)(PMe_3)} synthon **1** was dissolved in a DME solution of nitrobenzene, oxidation of the metal rapidly occurred, resulting in free benzene and uncharacterized paramagnetic materials. Cationic benzene derivatives such as N,N,N-trimethylanilinium iodide and trityl triflate, when they are combined with **1**, resulted in reaction mixtures that showed encouraging signs of η^2-coordination, with resonances in their ^{1}H NMR spectra resembling those associated with the previously reported tungsten-$PhCF_3$ complex **3**. However, difficulties in purification and low yields of the desired products dissuaded us from pursuing these complexes further, as η^2-coordination of these cationic complexes was accompanied by large amounts of decomposition. Other arenes bearing electron-withdrawing groups that did not give promising indications of complex formation included $PhOCF_3$, $PhCCl_3$, and $PhSCF_3$. A summary of recent η^2-arene complexes for the {WTp(NO)(PMe_3)} system appears in **Table 3.2**.

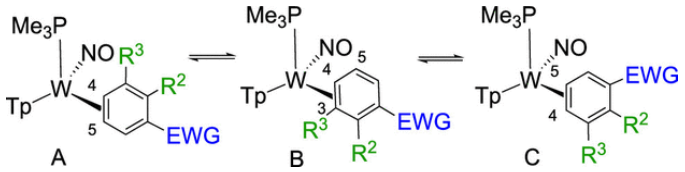

Cpd	EWG	R2	R3	cdr (A:B:C)	vNO (cm^{-1})	CV ($E_{p,a}$) (V, NHE)
1	H	H	H	Na:Na:Na	1564	-0.13
3	CF_3	H	H	Na:5:4	1575	0.06
4	$C(OMe)_3$	H	H	Na:4:3	1580	-0.08
5	SO_2Ph	H	H	Na:3:2	1564	0.07
6	SO_2Me	H	H	Na:11:10	1568	0.07
8	SF_5	H	H	Na:4:3	1573	0.14
12	CF_3	H	OMe	1:Na:10	1573	0.07
13	CF_3	H	NMe_2	1:NA:>20	1570	-0.16
14	CF_3	CF_3	H	20:1:1	1592	0.45
15	CF_3	H	CF_3	1:Na:7	1582	0.42

Table 3.2: Coordination diastereomer ratios and infrared and electrochemical data for **1** and **3**–**15**

3.8 Comparisons to the {MoTp(NO)(DMAP)} Systems

Compared to tungsten compounds **12**, **14**, and **15**, the corresponding molybdenum complexes have NO stretching features consistently 3 to 5 cm^{-1} higher and anodic peak currents ($E_{p,a}$) roughly 400 mV more negative. Reactions of MoTp(NO)(DMAP)(TFT) with $Ph(OMe)_3$, $PhSF_5$, and 3-(trifluoromethyl)-N,N-dimethylaniline were all unsuccessful.

The ability of the tungsten complex {$WTp(NO)(PMe_3)$} to form complexes with aryl halides of any type has been largely unsuccessful. Reactions with iodobenzene, bromobenzene, and chlorobenzene all result in intractable mixtures of paramagnetic materials. Only in the case of fluorinated arenes have well-defined reactions been observed. For fluorobenzene itself, a clean oxidative addition product, $WTp(NO)(PMe_3)(F)(Ph)$, was produced from **1** in neat PhF with a ligand exchange half-life of 3.3 h at 298 K.[29] Even in the presence of a CF_3 group, C−F insertion occurs with 3-fluorotrifluorotoluene at ambient temperature. In contrast, stable η^2-arene complexes were realized for tungsten with 1-fluoronaphthalene, as well as hexafluorobenzene.[29] Jacob Smith investigated if the molybdenum fragment {MoTp(NO)(DMAP)}, which is more tempered in its π basicity than its tungsten analog, might allow for a stable η^2-coordinated arene complex. Dr. Smith found that in contrast to its heavy-metal congener, the {MoTp(DMAP)(NO)} fragment successfully binds fluorobenzene, *o*-, *m*-, and *p*-difluorobenzene, and various tetrafluorotoluenes in an η^2 fashion.[30]

3.9 Conclusion

Arenes with electron-withdrawing groups that contain π bonds have an unfortunate tendency to form η^2-adducts with the substituent itself to allow the arene to retain its aromaticity. To avoid this coordination mode, we needed to utilize electron-withdrawing groups that did not contain π bonds. To this extent, we successfully prepared a series of tungsten complexes of dihapto-coordinated benzenes bearing electron-withdrawing substituents that lack π bonds. A notable exception is the complexation of

trimethyl ortho-benzoate ($PhC(OMe)_3$) by tungsten and subsequent hydrolysis to provide a benzoate ester bound through the arene. To accomplish this feat, we first had to bind the orthobenzoate and rely on the stability of the dihapto arene bond in order to avoid isomerization to the newly formed carbonyl after hydrolysis. The following chapters explore the organic chemistry available to these newly found systems.

Experimental Section

General Methods. NMR spectra were obtained on 500, 600, or 800 MHz spectrometers. Chemical shifts are referenced to tetramethylsilane (TMS) utilizing residual ^{1}H signals of the deuterated solvents as internal standards. Chemical shifts are reported in ppm, and coupling constants (J) are reported in hertz (Hz). Chemical shifts for ^{19}F and ^{31}P spectra are reported relative to standards of hexafluorobenzene (164.9 ppm) and triphenylphosphine (−6.00 ppm) or triphenyl phosphate (−16.58 ppm). Infrared spectra (IR) were recorded as a solid on a spectrometer with an ATR crystal accessory, and peaks are reported in cm^{-1}. Electrochemical experiments were performed under a nitrogen atmosphere. Most cyclic voltammetric data were recorded at ambient temperature at 100 mV/s, unless otherwise noted, with a standard three-electrode cell from +1.8 to −1.8 V with a platinum working electrode, acetonitrile or dimethylacetamide (DMA) solvent, and tetrabutylammonium (TBAH) electrolyte (∼1.0 M). All potentials are reported versus the normal hydrogen electrode (NHE) using cobaltocenium hexafluorophosphate ($E_{1/2}$ = −0.78 V, −1.75 V) or ferrocene ($E_{1/2}$ = 0.55 V) as an internal standard. The peak separation of all reversible couples was less than 100 mV. All synthetic reactions were performed in a glovebox under a dry nitrogen atmosphere unless otherwise noted. All solvents were purged with nitrogen prior to use. Deuterated solvents were used as received from Cambridge Isotopes and were purged with nitrogen under an inert atmosphere. When possible, pyrazole protons of the tris(pyrazolyl)borate (Tp) ligand were uniquely assigned (e.g., “Tp3B”) using two-dimensional NMR data. If unambiguous assignments were not possible, Tp protons were labeled as “Tp3/5 or Tp4”. All J values for Tp protons are 2(±0.4) Hz.

WTp(NO)(PMe_3)(η^2-benzene) (1) (Large-Scale Procedure).

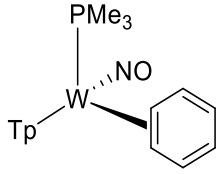

Anhydrous benzene (4.0 L) was added to a 4 L Erlenmeyer flask containing a stir bar. WTp(NO)(PMe_3)(Br) (50.0 g, 85.8 mmol) followed by an excess of 35 wt % sodium dispersion in toluene (48.0 g, 731 mmol) were then added to the flask. The resulting heterogeneous green reaction mixture was stirred rapidly for 14 h. Subsequently, the dark golden brown reaction mixture was filtered through a slurry of Celite (200 mL) and anhydrous benzene (100 mL) in a 600 mL medium-porosity fritted funnel. The filtrate was collected and set aside. A slurry of silica (450 mL) and Et_2O (1.5 L) was prepared and transferred to a 2 L large capacity pressure filter funnel. The Et_2O was allowed to drain until the solvent surface was 4 cm from the top of the silica, and then benzene (500 mL) was carefully added. The solvent was allowed to drain until the surface was 4 cm from the top of the silica, and then the reaction mixture filtrate was added until the funnel was full. Using nitrogen pressure, the filtrate was loaded onto the column. The funnel was refilled with filtrate as necessary until all of the filtrate had been loaded. At this point, a green band was ∼1 cm from the bottom of the column. The green band was eluted with 4/1 benzene/Et_2O (600 mL) using nitrogen pressure. When the green band had eluted, and the solvent level was within 2 cm of the top of the silica, Et_2O was added to fill the funnel. Nitrogen pressure was used to elute a vivid yellow band, which was collected. Additional Et_2O was placed in the funnel, and the elution was continued until the filtrate became colorless (after ∼2 L of total Et_2O). The golden yellow eluent was evaporated under vacuum until the volume was approximately 500 mL. Hexanes (400 mL) were added to the concentrated solution, and the resulting solution was evaporated under vacuum to a final volume of 400 mL. The solid which had precipitated was isolated on a 150 mL medium-porosity fritted funnel, washed with hexanes (3 × 75 mL), and desiccated under dynamic vacuum to yield **1** as a vivid yellow solid (22.7 g, 45.5%). The complex has been previously reported.

WTp(NO)(PMe$_3$)(η^2-benzonitrile) (2A-E)

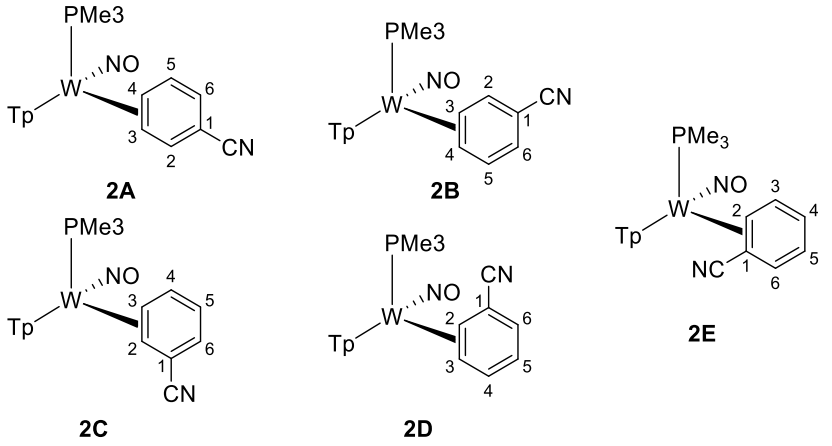

A 4-dram vial was charged with WTp(NO)(PMe$_3$)(η^2-2,3-anisole) complex (1.00 g, 1.64 mmol) and a stir pea. To this vial was added benzonitrile (7.00 mL, 67.9 mmol).This yellow heterogenous solution was allowed to stir at room temperature. After 48 h, the reaction had turned to a black homogenous mixture. A 60 mL course porosity fritted disc was filled 2/3 full of silica and set in diethyl ether. The reaction mixture was added to the column and hexanes (200 mL) were eluted through the column. An orange band could be seen beginning eluting down the column. Next diethyl ether (500 mL) was used to elute the orange band. The resulting orange filtrate was evaporated to dryness under vacuum, pick up in a minimal amount of DCM, and added to a solution of stirring pentane (50 mL). An orange solid was isolated on a 15 mL fine porosity fritted disc. The resulting solid was desiccated overnight yielding **2** (0.271 g, 27.0 % yield). CV (DMA) $E_{p,a}$= +0.09 (NHE). IR: ν(BH)= 2493 cm^{-1}, ν(CN)= 2189 cm^{-1}, ν(NO)= 1550 cm^{-1}. ^{1}H-NMR (d$_3$-MeCN, δ, 25 ^{o}C): 8.20 (1H, Tp3/5**E**), 8.11 (1H, Tp3/5**B**), 8.10 (1H, Tp3/5**C**), 8.06 (1H, Tp/5**A**), 8.05 (1H, Tp3/5**D**), 7.93 (6H, Tp3/5**A** 2**B** 2**D E**), 7.91 (7H, Tp3/5 2**A B** 2**C** 2**E**), 7.89 (1H, Tp3/5**E**), 7.87 (3H, Tp3/5 2**C D**), 7.84 (1H, Tp3/5**D**), 7.82 (1H, Tp3/5**B**), 7.81 (1H, Tp3/5**A**), 7.74 (1H, d J= 6.3, H2**A**), 7.62 (1H, d J= 5.7, H2**B**), 7.55 (1H, Tp3/5**E**), 7.38 (1H, dd J= 8.6, 6.3, H4**D**), 7.33 (1H, Tp3/5**A**), 7.29 (1H, Tp3/5**B**), 7.25 (1H, Tp3/5**C**), 7.23 (1H, Tp3/5**D**), 7.19 (1H, dd J= 9.0, 5.6, H4**C**), 7.01 (1H, dd J= 9.2, 6.0, H5**B**), 6.88 (1H, dd J= 8.1, 5.4, H5**A**), 6.84 (1H, dd J= 9.3, 5.6, H3**E**), 6.55 (1H, d J= 9.1, H6**E**), 6.54 (1H, d J= 7.4, H6**D**), 6.45 (1H, d J = 6.3, H6**C**), 6.33

(15H, Tp3**A B C D E**), 5.77 (2H, m, H5**C** H5**E**), 5.74 (1H, dd J= 8.4, 6.4, H5**D**), 5.69 (1H, dd J= 9.0, 6.0, H4**E**), 5.67 (1H, dd J= 9.2, 1.4, H6**A**), 5.60 (1H, dd J= 9.2, 1.2, H6**B**), 4.16 (1H, dd J= 13.3, 9.9, H2**D**), 3.85 (2H, m, H4**A** H2**E**), 3.82 (1H, dd J= 8.8, 5.4, H3**C**), 3.75 (1H, m, H3**B**), 2.17 (2H, m, H4**B** H2**C**), 2.14 (1H, m, H3**A**), 2.06 (1H, ddd J= 10.0, 6.2, 1.5, H3**D**), 1.29 (9H, d J= 8.7, PMe_3**C**), 1.23 (18H, d J= 8.7, PMe_3**B E**), 1.22 (18H, d J= 8.7, PMe_3**A D**). ^{13}C-NMR (d_3-MeCN, δ, 25 °C): 150.7 (1C, C2**A**), 147.6 (1C, d J= 3.7, C2**B**), 145.5 (1C, Tp3/5**A**), 145.2 (2C, Tp3/5**B E**), 143.3 (1C, Tp3/5**A**), 143.2 (1C, Tp3/5**E**), 142.2 (1C, Tp3/5**B**), 142.0 (1C, Tp3/5**A**), 142.0 (1C, Tp3/5**B**), 141.9 (1C, Tp3/5**E**), 138.2 (2C, Tp3/5**A E**), 138.1 (1C, Tp3/5**B**), 137.6 (1C, Tp3/5**E**), 137.5 (1C, Tp3/5**A**), 137.5 (1C, Tp3/5**B**), 137.4 (1C, Tp3/5**E**), 137.1 (1C, Tp3/5**A**), 137.1 (1C, Tp3/5**B**), 136.5 (1C, C4**B**), 134.6 (1C, d J= 3.2, C4**A**), 133.6 (1C, d J= 3.5, C3**E**), 128.4 (1C, C6**E**), 126.0 (1C, CN**E**), 121.8 (1C, CN**A**), 121.7 (1C, CN**B**), 117.3 (1C, C4**E**), 116.9 (1C, C5**E**), 114.8 (1C, C6**A**), 113.1 (1C, C6**B**), 107.7 (1C, Tp4**E**), 107.6 (1C, Tp4**A**), 107.6 (1C, Tp4**B**), 107.3 (2C, Tp4**A B**), 107.3 (1C, Tp4**E**), 107.1 (1C, Tp4**A**), 107.1 (1C, Tp4**E**), 106.8 (1C, Tp4**B**), 100.3 (1C, C1**B**), 98.4 (1C, C1**A**), 66.9 (1C, d J= 10.1, C2**E**), 64.9 (1C, d J= 9.0, C4**A**), 63.5 (1C, d J= 7.5, C3**B**), 63.1 (1C, C4**B**), 61.9 (1C, C3**A**), 13.2 (3C, d J= 28.3, PMe_3**B**), 13.2 (3C, d J= 29.1, PMe_3**A**), 13.0 (3C, d J= 30.1, PMe_3**E**). Anal. Calcd for $C_{19}H_{24}BN_8OPW$ and 1/2 DCM molecule: C, 36.11; H, 3.89; N, 17.28. Found: C, 36.44; H, 3.90; N, 17.19.

WTp(NO)(PMe_3)(3,4-η^2-(trimethylorthobenzoate)) (4)

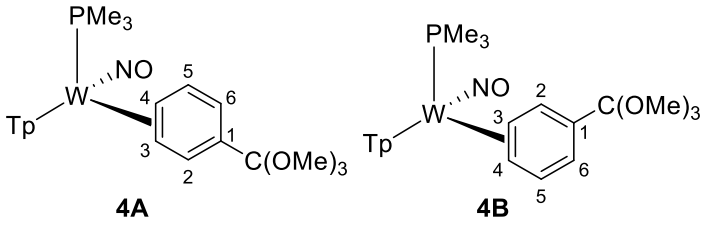

An oven-dried 4-dram vial was charged with **1** (0.092 g, 0.158 mmol) and trimethyl orthobenzoate (1.00 g, 5.49 mmol). The heterogeneous yellow reaction mixture was allowed to stir with a small stir bar. Over time the reaction mixture turns to a homogeneous brown reaction mixture and after 16 h the reaction

mixture was added to 15 mL of stirring pentane that had been chilled to -30 °C. Upon addition, a light-yellow solid precipitates from solution. The solid was then filtered through a 15 mL medium porosity fritted disc and washed with pentane (2 x 5 mL) before the light tan powder was allowed to desiccate under active vacuum for 2 h and a mass taken (0.040 g, 37.0 % yield). CV (DMA): $E_{p,a}$ = - 0.08 V (NHE). IR: ν(BH) = 2496 cm^{-1}, ν(NO) = 1580 cm^{-1}. Characterization of **4A** 1H NMR (acetone-*d6*, δ, 0 °C): 8.35 (1H, d, Tp3A), 8.00 (1H, d, Tp3/5), 7.95 (1H, d, Tp3B), 7.87 (1H, d, Tp5), 7.49 (1H, d, Tp3C), 7.31 (1H, d, *J* = 5.9, H2), 7.05 (1H, dd, *J* = 5.6, 9.1, H5), 6.36 (2H, t, overlapping Tp4), 6.35 (1H, t, Tp4A), 6.32 (2H, t, overlapping Tp4), 6.31 (1H, t, Tp4C), 5.74 (1H, d, *J* = 9.2, H6), 3.90 (1H, m, H3), 3.14 (9H, overlapping s, (OMe)), 2.28 (1H, m, H4), 1.37 (9H, d, J_{PH} = 8.2, PMe3). ^{31}P NMR (acetone-*d6*, δ, 25 °C): -12.15 (J_{WP} = 310.3). ^{13}C {1H} NMR (acetone-*d6*, δ, 25 °C): 137.7/136.3 (C1 for **A** or **B**), 136.4 (C2), 134.9 (C5), 114.9 (C6), 115.8 (overlapping with **A**, ipso C-$(OR)_3$), 63.5 (C3, d, J_{PC} = 7.0), 62.3 (C4), 49.7/49.6 (OMe groups for **A** or **B**), 13.6 (PMe_3, d, J_{PC} = 28.3). ^{13}C {1H} NMR (acetone-*d6*, δ, 25 °C): Tp resonances for **A** and **B**. 145.0 (Tp3/5), 144.4 (Tp3/5), 142.4 (Tp3/5), 142.4 (Tp3/5), 141.8 (Tp3/5), 141.5 (Tp3/5), 137.7 (Tp3/5), 137.7 (Tp3/5), 137.6 (Tp3/5), 136.8 (Tp3/5), 136.7 (Tp3/5), 136.5(Tp3/5), 136.3 (Tp3/5), 107.0 (Tp4), 106.9 (Tp4), 106.8 (Tp4), 106.7 (Tp4), 106.5 (Tp4), 106.4 (Tp4). Characterization of **4B** 1H NMR (acetone-*d6*, δ, 0 °C): 8.25 (1H, d, Tp3A), 8.01 (1H, d, Tp5C), 7.93 (1H, d, Tp3B), 7.89 (1H, d, Tp3/5), 7.40 (1H, d, Tp3C), 7.39 (1H, buried, H2), 6.84 (1H, dd, *J* = 4.9, 9.4, H5), 6.36 (1H, t, overlapping Tp4), 6.35 (1H, t, Tp4A), 6.32 (2H, t, overlapping Tp4), 6.31 (1H, t, Tp4C), 5.84 (1H, d, *J* = 9.7, H6), 4.13 (1H, m, H4), 3.14 (9H, overlapping s, (OMe)), 2.17 (1H, t, *J* = 7.90, H3), 1.37 (9H, d, *J*PH = 8.2, PMe3). 31P NMR (acetone-*d6*, δ, 25 °C): -12.79 (J_{WP} = 310). 137.7/136.3 (C1 for **A** or **B**), 137.5 (C2), 133.4 (C5), 116.4 (C6), 115.8 (overlapping with **A**, ipso C-$(OR)_3$), 63.9 (C4, d, J_{PC} = 7.7), 62.3 (C3), 49.7/49.6 (OMe groups for **A** or **B**), 12.9 (PMe_3, d, J_{PC} = 27.7). Attempts to purify **4** for elemental analysis by chromatography led to the generation of **11**.

WTp(NO)(PMe_3)(3,4-η^2-diphenyl sulfone) (5)

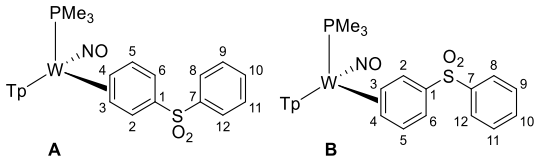

A 4-dram bottle was charged with WTp(NO)(PMe_3)(η^2-2,3-anisole) (5 grams, 8.18 mmol), diphenyl sulfone (5.35 g, 24.5 mmol), and a stir pea. 20 mL of 1,2-dimethoxyethane was charged to the vial along with a stir bar. This yellow heterogeneous mixture was stirred for 48 hours, until the reaction became a bright orange heterogenous mixture. The orange precipitate was collected on a 30 mL fine porosity fritted disc. The product was washed with 2 x 20 mL of ether to remove any leftover ligand, then followed by washing with 4 x 20 mL of hexanes. The product was desiccated overnight, yielding **5A** and **B** (4.13 g, 5.73 mmol, 70% yield). CV (DMA) $E_{p,a}$= +0.07 V (NHE). IR: *v*(BH)= 2482 cm^{-1}, *v*(NO)= 1564 cm^{-1}, *v*(SO)= 14074 cm^{-1}. ^{1}H-NMR (d_3-MeCN, δ, 25 ^{o}C): 8.13 (1H, d, Tp3/5**B**), 8.00 (1H, dd J= 6.5, 1.4, H2**A**), 7.95 (4H, m, H8/12**A B**), 7.90 (6H, m, 3Tp3/5**A**, H2**B**, 2Tp3/5**B**), 7.85 (1H, d, Tp3/5**B**), 7.82 (2H, d, 2Tp3/5**A**), 7.80 (1H, d, Tp3/5**B**), 7.56 (1H, m, H10**B**), 7.52 (3H, m, H10**A**, H11/9**B**), 7.48 (2H, m, H11/9**A**), 7.30 (1H, d, Tp3/5**B**), 7.27 (1H, d, Tp3/5**A**), 7.07 (1H, dd J= 9.5, 5.9, H5**B**), 6.91 (1H, dd J= 9.3, 5.2, H5**A**), 6.36 (1H, t, Tp4**A**), 6.33 (2H, t, Tp4**A B**), 6.29 (1H, t, Tp4**B**), 6.28 (2H, t, Tp4**A B**), 5.93 (1H, dd J= 9.5, 1.8, H6**A**), 5.82 (1H, dd J= 9.3, 1.5, H6**B**), 3.85 (1H, m, H4**A**), 3.70 (1H, m, H3**B**), 2.10 (2H, m, H3**A**, H4**B**), 1.27 (9H, d J= 8.4, PMe_3**B**), 1.20 (9H, d J= 8.4, PMe_3**A**). ^{13}C-NMR (d_3-MeCN, δ, 25 ^{o}C): 147.3 (1C, C2**A**), 145.3 (1C, Tp3/5**B**), 144.8 (1C, C7**A**), 144.6 (1C, C7**B**), 143.7 (1C, d J = 3.2, C2**B**), 143.2 (2C, Tp3/5**B**), 142.4 (1C, Tp3/5**B**), 142.1 (1C, Tp3/5**B**), 141.9 (1C, Tp3/5**A**), 138.2 (1C, Tp3/5**B**), 138.1 (1C, Tp3/5**A**), 137.6 (1C, Tp3/5**A**), 137.4 (1C, Tp3/5**B**), 137.4 (1C, Tp3/5**A**), 137.1 (1C, C5**B**), 137.0 (1C, Tp3/5**B**), 135.2 (1C, d J= 3.9, C5**A**), 133.4 (1C, C10**B**), 133.2 (1C, C10**A**), 129.9 (1C, C1**B**), 129.8 (4C, C11/9**A B**), 128.3 (1C, C1**A**), 128.2 (4C, C12/8**A B**), 111.9 (1C, C6**A**), 110.2 (1C, C6**B**), 107.6 (1C, Tp4**A**), 107.5 (1C, Tp4**B**), 107.3 (1C, Tp4**A**), 107.2 (1C, Tp4**B**), 107.2 (1C, Tp4**A**), 106.9 (1C, Tp4**B**), 65.4 (1C, d J= 9.1, H4**A**), 63.4 (1C, C4**B**), 63.1 (1C, d J= 7.5, H3**B**), 61.6 (1C, C3**A**), 13.4 (3C, d J= 29.0,

PMe_3**B**), 13.2 (3C, d J= 28.8, PMe_3**A**) Anal. Calcd for $C_{24}H_{29}BN_7O_3PSW$: C, 39.97; H, 4.05; N, 13.59. Found: C, 40.13; H, 4.03; N, 13.42.

WTp(NO)(PMe_3)(3,4-η^2-methyl phenyl sulfone) (6)

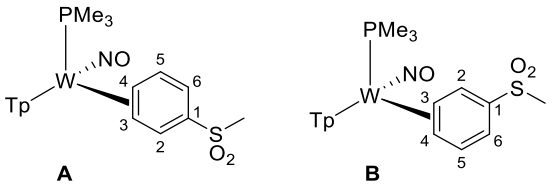

A 4-dram vial was charged with WTp(NO)(PMe_3)(η^2-2,3-anisole) (5.00 g, 8.60 mmol), methyl phenyl sulfone (2.42 g, 15.5 mmol), and a stir pea. 8 mL of THF were added to the vial. This heterogenous mixture was stirred at room temperature for 16 hrs. During this time the reaction became homogenous, before an orange solid had precipitated out of the solution. The orange product was collected on a 30 mL fine porosity fritted disc, washed with ether (4 x 20 ml) and desiccated overnight, yielding **6A** and **B** (2.95 g, 4.48 mmol, 52% yield). CV (DMA) $E_{p,a}$= +0.07 V (NHE). IR: *ν*(BH)= 2487 cm^{-1}, *ν*(NO)= 1568 cm^{-1}, *ν*(SO)= 1407 cm^{-1}. ^{1}H-NMR (d_3-Acetone, δ, 25 °C): 8.23 (1H, d, TpA3**B**), 8.10 (1H, d, TpA3**A**), 8.03 (4H, Tp5**A B**), 7.99 (1H, d, TpB3**B**), 7.96 (1H, d, TpB3**A**), 7.92 (1H, d J=6.2, H2**A**), 7.90 (1H, d, Tp5**A**), 7.89 (1H, d, Tp5**B**), 7.77 (1H, d J= 5.5, H2**B**), 7.53 (1H, d, TpC3**A**), 7.51 (1H, d, TpC3**B**), 7.13 (1H, dd J=9.5, 5.9, H5**B**), 6.98 (1H, dd J= 9.3, 5.3, H5**A**), 6.39 (3H, t, TpA4**A**, TpB4**B**, Tp4**B**), 6.35 (3H, t, TpB4**A**, TpC4**A**, Tp4**B**), 6.02 (1H, dd J= 9.2, 1.6, H6**A**), 5.95 (1H, dd J= 9.1, 1.6, H6**B**), 4.00 (1H, m, H4**A**), 3.83 (1H, m, H3**B**), 2.97 (3H, s, S-CH_3**A**), 2.93 (3H, s, S-CH_3**B**), 2.26 (1H, m, H4**B**), 2.17 (1H, m, H3**A**), 1.36 (9H, d J=8.4, PMe_3**B**), 1.32 (9H, d J= 8.4, PMe_3**A**). ^{13}C-NMR (d_3-Acetonitrile, δ, 25 °C): 145.4 (1C, Tp 3/5), 145.4 (1C, Tp 3/5), 145.0 (1C, C2**A**), 143.1 (1C, Tp 3/5), 142.3 (1C, Tp 3/5), 142.1 (1C, Tp 3/5), 142.0 (1C, Tp 3/5), 142.0 (1C, d J= 3.4, C2**B**), 138.2 (2C, Tp 3/5), 137.6 (1C, Tp 3/5), 137.5 (1C, Tp 3/5), 137.2 (1C, Tp 3/5), 137.1 (1C, Tp 3/5), 137.0 (1C, C5**B**), 135.0 (1C, d J= 3.0, C5**A**), 129.5 (1C, C1**B**), 127.3 (1C, C1**A**), 112.0 (1C, C6**A**), 110.3 (1C, C6**B**), 107.6 (1C, Tp 4), 107.6 (1C, Tp 4), 107.4 (1C, Tp 4), 107.3 (1C, Tp 4), 107.2 (1C, Tp 4), 106.9 (1C, Tp 4), 46.7 (1C, S-Me**B**), 46.6 (1C, S-

Me**A**), 65.4 (1C, d J= 9.2, C4**A**), 63.6 (1C, C4**B**), 62.3 (1C, d J= 7.7, C5**B**), 60.5 (1C, C3**A**), 13.3 (6C, d $J_{P,C}$= 29.0 Hz, PMe_3). Anal. Calcd for $C_{19}H_{27}BN_7O_3PSW$ and 1 THF molecule: C, 37.78; H, 4.82; N, 13.41. Found: C, 37.70; H, 4.62; N, 13.60.

WTp(NO)(PMe_3)(3,4-η^2-phenyl sulfonyl pyrrolidine) (7)

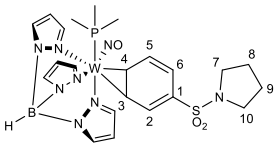

A

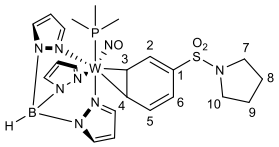

B

A 4-dram vial was charged with WTp(NO)(PMe_3)(η^2-2,3-anisole) (1.00 g, 1.64 mmol), phenylsulfonyl pyrrolidine (1.04 g, 4.92 mmol), a stir pea, and 5 mL of DME. The yellow heterogenous mixture was stirred at room temperature for 72 hrs. The reaction remained heterogeneous throughout the course of the 72 hours. The precipitant underwent an observable color change of a dull gold to a light orange. The orange product was collected on a 30 mL fine porosity fritted disc, washed with ether (5 x 20 ml), and desiccated overnight, yielding **7A** and **B** (0.760 g, 1.06 mmol, 65% yield). CV (DMA): $E_{p,a}$= + 0.10 V (NHE). IR: *ν*(SO) 1405 cm^{-1}, *ν*(NO) 1563 cm^{-1}, *ν*(BH) 2504 cm^{-1}. ^{1}H-NMR (d_3-MeCN, δ, 25 °C): 8.16 (1H, d, Tp3/5**B**), 8.15 (1H, d, Tp3/5**A**), 7.94 (1H, d, Tp3/5**A**), 7.93 (1H, d, Tp3/5**B**), 7.91 (3H, 2Tp3/5**A**, Tp3/5**B**), 7.89 (1H, d, Tp3/5**B**), 7.82 (2H, Tp3/5**A**, Tp3/5**B**), 7.80 (1H, d J = 6.6, H2**A**), 7.64 (1H, d J = 6.1, H2**B**), 7.30 (2H, Tp3/5**A**, Tp3/5**B**), 7.08 (1H, dd J = 9.6, 5.9, H5**B**), 6.93 (1H, dd J = 9.4, 5.1, H5**A**), 6.36 (3H, m, 2Tp4**A**, Tp4**B**), 6.33 (1H, t, Tp4**B**), 6.29 (2H, t, Tp4**A**, Tp4**B**), 6.28 (1H, t, Tp4**B**), 5.95 (1H, dd J = 9.4, 1.8, H6**A**), 5.88 (1H, dd J = 9.3, 1.7, H6**B**), 3.87 (1H, m, H4**A**), 3.79 (1H, m, H3**B**), 3.22 (8H, m, H10**A**, H10**B**, H7**A**, H7**B**), 2.16 (2H, m, H3**A**, H4**B**), 1.75 (4H, m, H9**B**, H8**B**), 1.72 (4H, m, H9**A**, H8**A**), 1.25 (9H, d J = 8.4, PMe_3**B**), 1.23 (9H, d J = 8.5, PMe_3**A**). ^{13}C-NMR (d_3-MeCN, δ, 25 °C): 145.3 (1C, Tp3**A**), 145.2 (1C, Tp3**B**), 145.1 (1C, C2**A**), 142.8 (1C, Tp3**A**), 142.3 (1C, Tp3**B**), 142.0 (2C, Tp3**A**, Tp3**B**), 142.2 (1C, C2**B**), 138.2 (2C, Tp5**A**, Tp5**B**), 137.5 (1C, Tp5**A**), 137.4 (1C, Tp5**B**), 137.1 (1C, Tp5**A**), 137.0 (1C, Tp5**B**), 136.6 (1C, C5**B**), 134.8 (1C, C5**A**), 126.0 (1C,

C1**B**), 123.4 (1C, C1**A**), 113.7 (1C, C6**A**), 112.1 (1C, C6**B**), 107.6 (1C, Tp4**A**), 107.6 (1C, Tp4**B**), 107.3 (1C, Tp4**A**), 107.3 (1C, Tp4**B**), 107.1 (1C, Tp4**A**), 106.9 (1C, Tp4**B**), 65.1 (1C, d J = 8.6, C4**A**), 63.2 (1C, C4**B**), 62.5 (1C, d J = 8.2, C3**B**), 61.0 (1C, C3**A**), 48.6 (1C, C10/7**A**), 48.6 (1C, C10/7**B**), 25.7 (2C, C9**B**, C8**B**), 25.6 (2C, C9**A**, C8**A**), 13.6 (3C, d J = 28.6, PMe_3**B**), 13.0 (3C, d J = 28.8, PMe_3**A**). Anal. Calcd for $C_{22}H_{32}BN_8O_3PSW \cdot 1/10DCM$: C, 36.73; H, 4.49; N, 15.50. Found: C, 36.33; H, 4.53; N, 15.90.

WTp(NO)(PMe_3)(3,4-η²-pentafluorosulfanyl benzene) (8)

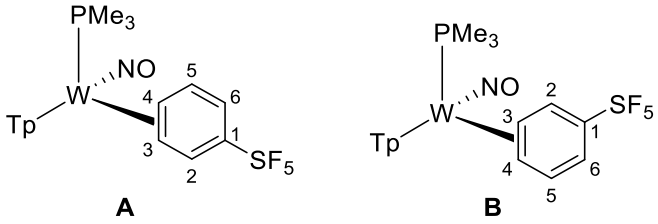

An oven-dried 4-dram vial was charged with **1** (0.411 g, 0.707 mmol), pentafluorosulfanyl benzene (2.21 g, 10.8 mmol), and the heterogeneous yellow reaction mixture was allowed to stir. Over time, the reaction mixture turns to a homogeneous red solution, and after 24 h, the reaction mixture was added to stirring pentane (50 mL), and upon addition, a light tan solid precipitates from the solution. The solid was then filtered through a fine porosity 15 mL fritted disc and washed with pentane (3 x 10 mL) before the light tan powder was allowed to desiccate under active vacuum for 3 h, and a mass was taken (0.311 g, 62.2 %). The filtrate was collected, and the pentane was distilled to re-collect the excess pentafluorosulfanyl benzene. The recovered aromatic ligand was used in similar reaction procedures without noticeable inhibition of yield.

Characterization of **8A**: CV (DMA): $E_{p,a}$ = + 0.14 V (NHE). IR: ν(BH) = 2496 cm^{-1}, ν(NO) = 1573 cm^{-1}. ^{1}H NMR (acetone-*d6*, δ, 25 °C): 8.22 (1H, d, Tp3A), 8.08 (1H, d, Tp3/5), 7.98 (1H, d, Tp3/5), 7.87 (1H, d, Tp3/5), 7.51 (1H, d, *J* = 5.9, H2), 7.02 (1H, m, H5), 6.48 (1H, t, Tp4), 6.37 (2H, t, overlapping Tp4), 6.34 (2H, t, overlapping

Tp4), 5.89 (1H, dd, *J* = 2.2, 9.6, H6), 3.83 (1H, m, H3), 2.15 (1H, t, *J* = 7.78, H4), 1.34 (9H, d, J_{PH} = 8.56, PMe3). ^{19}F NMR (acetone-*d6*, δ, 25 °C): 91.53 (-SF_5 (1F), overlapping diastereomers q, J_{FF} = 148.6), 64.12 (SF (4F), J_{FF} = 148.6). ^{31}P NMR {1H} (acetone-*d6*, δ, 25 °C): -13.54 (buried J_{WP}). Characterization of **8B**: ^{1}H NMR (acetone-*d6*, δ, 25 °C): 8.21 (1H, d, Tp3A), 8.08 (1H, d, Tp3/5), 7.98 (1H, d, Tp3/5), 7.96 (1H, d, Tp3/5), 7.89 (1H, d, Tp3/5), 7.60 (1H, d, *J* = 6.90, H2), 7.47 (1H, t, Tp3A), 6.86 (1H, m, H5), 6.48 (2H, t, overlapping Tp4), 6.37 (1H, t, Tp4) 6.34 (2H, t, overlapping Tp4), 5.96 (1H, dd, *J* = 2.21, 5.89, H6), 3.93 (1H, m, H4), 2.11 (1H, buried, H4), 1.32 (9H, d, J_{PH} = 8.20, PMe3). ^{19}F NMR (acetone-*d6*, δ, 25 °C): 85.10 (-SF_5 (1F), overlapping diastereomers q, J_{FF} = 147.3), 64.52 (-SF_5 (4F), J_{FF} = 147.3). ^{31}P {^{1}H} NMR (acetone- *d6*, δ, 25 °C): -12.88 (buried J_{WP}). Combined ^{13}C {^{1}H} data for Diastereomers **A** and **B**. When possible, distinction between the isomers is made. ^{13}C NMR (acetone-*d6*, δ, 25 °C): 146.0 (C-SF_5, identified by HMBC interactions, **A**), 145.2 (overlapping 2C, Tp3/5s), 146.0 (C-SF_5, identified by HMBC interactions, **B**), 142.6 (Tp3/5), 142.2 (Tp3/5), 142.6 (Tp3/5), 141.9 (Tp3/5), 141.8 (Tp3/5), 139.1 (C2 for **B**), 137.9 (Tp3/5), 137.9 (Tp3/5), 137.8 (Tp3/5), 137.2 (Tp3/5), 137.1 (Tp3/5), 136.8 (C2 for **A**), 136.7 (Tp3/5), 136.6 (Tp3/5), 135.9 (C2 for **A**), 134.0 (C5 for **B**), 113.3 (C6 for **B**), 111.6 (C6 for **A**), 107.3 (Tp4), 107.2 (2C, overlapping Tp4s), 107.1 (Tp4), 106.8 (Tp4), 106.5 (Tp4), 63.5 (C4 for **B**, d, J_{PC} = 9.5), 62.0 (C4 for **A**), 61.2 (C3 for **A**, d, J_{PC} = 8.5), 59.8 (C3 for **B**), 13.4 (PMe_3 for **A**, d, J_{PC} = 28.0), 13.3 (PMe_3 for **B**, d, J_{PC} = 28.5).

WTp(NO)(PMe_3)(H)(-CH_2SO_2Me) (9)

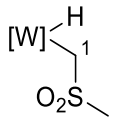

A 4-dram vial was charged with WTp(NO)(PMe_3)(η^2-2,3-anisole) (0.200 g, 0.327 mmol), dimethyl sulfone (0.090 g, 0.956 mmol), a stir pea, and 4 mL of DME. This yellow heterogenous mixture was stirred at room temperature for 72 h. The reaction began heterogeneous but turned homogeneous after 24 h. After 72 h, a light grey precipitant was observed to have crashed out of solution. The light grey product was collected

on a 15 mL fine porosity fritted disc, washed with ether (2 x 10 ml) and desiccated overnight, yielding **9** (0.131 g, 0.219 mmol, 67% yield). CV (DMA): $E_{p,a}$= + 1.10 V (NHE). IR: *v*(SO) 1406 cm^{-1}, *v*(NO) 1578 cm^{-1}, *v*(BH) 2508 cm^{-1}. ^{1}H-NMR (d3-MeCN, δ, 25 °C): 9.04 (1H, dt J = 112.9, 10.2, W-H), 8.04 (1H, d, TpC3), 8.03 (1H, d, TpB3), 7.97 (1H, d, TpA3), 7.92 (1H, d, TpB5), 7.84 (1H, d, TpC5), 7.70 (1H, d, TpA5), 6.39 (1H, t, TpB4), 6.30 (1H, t, TpC4), 6.26 (1H, t, TpA4), 2.95 (3H, s, SO2Me), 2.93 (1H, d J = 12.4, H1a), 1.88 (1H, d J = 12.5, H1b), 1.43 (9H, d J = 9.9, PMe3). ^{13}C-NMR (d3-MeCN, δ, 25 °C): 146.6 (1C, TpC3), 146.1 (1C, d J = 3.7, Tp B3), 144.0 (1C, TpA3). 138.8 (1C, TpB5), 137.6 (1C, TpC5), 137.0 (1C, TpA5), 107.6 (1C, TpB4), 107.1 (2C, TpA4, TpC4), 55.2 (1C, d J = 4.1, C1), 43.7 (1C, SO_2Me), 17.2 (3C, d J = 34.7, PMe_3). Anal. Calcd for $C_{14}H_{25}BN_7O_3PSW \cdot 1/4DME$ (present in 1H NMR): C, 28.87; H, 4.52; N, 15.71. Found: C, 28.58; H, 4.38; N, 15.85.

WTp(NO)(PMe_3)(H)(-CH_2SO_2PhMe) (10)

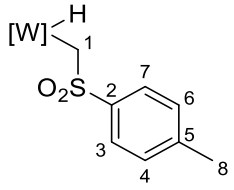

A 4-dram vial was charged with WTp(NO)(PMe_3)(η^2-2,3-anisole) (0.200 g, 0.327 mmol), methyl p-tolyl sulfone (0.170 g, 0.998 mmol), a stir pea, and 4 mL of DME. This heterogenous mixture was stirred at room temperature for 72 h. The reaction became homogeneous after 24 h. After 72 h, the reaction was then evaporated to dryness. A 30 mL medium porosity medium frit was filled . full with silica and set in ether. The reaction was loaded on the column using minimal acetone. The remaining methyl p-tolyl sulfone was eluted off the column with 50 mL of ether. 100 mL of THF was used to elute off a brown band. The brown band was evaporated to dryness, picked up in minimal DCM, and added to 10 mL of stirring pentane. A light grey solid precipitated out of the pentane and was collected on a 15 mL fine porosity fritted disc, washed with diethyl ether (2 x 10 mL) and hexanes (2 x 10 mL), then desiccated overnight to yield **10**

(0.163 g, 0.242 mmol, 74%). CV (DMA): $E_{p,a}$= + 1.11 V (NHE). IR: *ν*(SO) 1404 cm^{-1}, *ν*(NO) 1580 cm^{-1}, *ν*(BH) 2477 cm^{-1}. ^{1}HNMR (d3-MeCN, δ, 25 °C): 9.14 (1H, d J = 113.0, W-H), 8.17 (1H, d, TpC3), 8.02 (1H, d, TpB3), 7.91 (1H, d, TpB5), 7.88 (1H, d, TpA3), 7.84 (1H, d, TpC5), 7.74 (2H, m, H7, H3), 7.66 (1H, d, TpA5), 7.30 (2H, dm J = 7.8, H6, H4), 6.38 (1H, t, TpB4), 6.31 (1H, t, TpC4), 6.18 (1H, t, TpA4), 3.02 (1H, dt J = 12.1, 1.3, H1), 2.38 (3H, s, H8), 1.88 (1H, dt J = 12.1, 1.1, H1), 1.43 (9H, d J = 10.0, PMe3). ^{13}C-NMR (d3-MeCN, δ, 25 °C): 146.7 (1C, TpC3), 146.0 (1C, d J = 3.6, TpB3), 144.3 (1C, C5), 143.8 (1C, TpA3), 142.8 (1C, C2), 138.7 (1C, TpB5), 137.6 (1C, TpC5), 136.9 (1C, TpA5), 130.2 (2C, C6, C4), 127.4 (2C, C7, C3), 107.6 (1C, TpB4), 107.1 (1C, Tp4), 107.1 (1C, Tp4), 56.3 (1C, C1), 21.4 (1C, C8), 17.2 (3C, d J = 36.1, PMe3). Repeated attempts to purify this compound by chromatography or recrystallization were unsuccessful.

WTp(NO)(PMe$_3$)(η^2-1,2-methyl benzoate) (11)

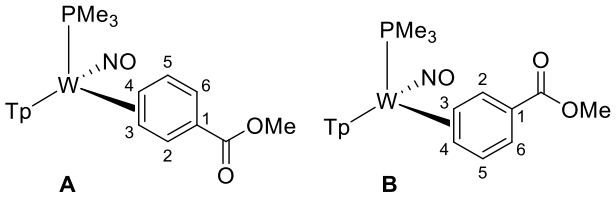

A 4-dram vial was charged with **1** (1.00 g, 1.72 mmol) and trimethylorthobenzoate (0.940 g, 5.16 mmol). 3 mL of THF were added to the vial. This homogenous mixture was stirred at room temperature for 16 hours. The resulting solution turned black. A 150 mL course porosity fritted disc was filled 2/3 full with silica. The silica was set in ether. The reaction solution was then loaded onto a silica column. A green band was first eluted with ether. This green band was followed by a yellow band, which turned orange halfway down the silica column. The orange band was isolated with 700 mL of ether. Orange band evaporated to dryness under vacuum. Resulting orange film was picked up in minimal DCM and precipitated into 100 mL of stirring pentane. The resulting orange precipitant was collected on a 30 mL fine porosity fritted disc and washed with hexanes (4 x 15mL). The resulting solid was desiccated overnight, yielding **11A** and **B** (0.495 g, 0.775 mmol, 45% yield). CV (DMA) $E_{p,a}$= -0.03 V (NHE). IR: ν(BH)= 2480 cm^{-1}, ν(CO)= 1688 cm^{-1},

ν(NO)= 1568 cm^{-1}. ^{1}H-NMR (d_3-MeCN, δ, 25 °C): 8.18 (1H, d, TpA5**B**), 8.13 (1H, d J = 6.3, H2**A**), 8.06 (1H, d, TpA5**A**), 7.99 (1H, d J = 5.5, H2**B**), 7.91 (2H, d, TpB5**A**, TpB5**B**), 7.90 (2H, d, TpC5**A**, TpC5**B**), 7.87 (1H, d, TpB3**A**), 7.86 (1H, d, TpB3**B**), 7.81 (2H, d, TpA3**A**, TpA3**B**), 7.35 (1H, d, TpC3**A**), 7.34 (1H, d, TpC3**B**), 6.96 (1H, dd J = 9.8, 5.9, H5**B**), 6.82 (1H, dd J= 9.6, 5.0, H5**A**), 6.35 (1H, t, TpA4**A**), 6.34 (1H, t, TpB4**A**), 6.33 (1H, t, TpA4**B**), 6.31 (1H, t, TpB4**B**), 6.29 (1H, t, TpC4**A**), 6.28 (1H, t, TpC4**B**), 6.14 (1H, dd J = 9.6, 1.5, H6**A**), 6.07 (1H, dd J = 9.3, 1.3, H6**B**), 4.02 (1H, m, H4**A**), 3.87 (1H, m, H3**B**), 3.76 (3H, s, OMe**A**), 3.75 (3H, s, OMe**B**), 2.29 (1H, m, H4**B**), 2.23 (1H, m, H3**A**), 1.26 (9H, d J = 8.5, PMe_3**B**), 1.24 (9H, d, J = 8.5, PMe_3**A**). ^{13}C-NMR (d_3-MeCN, δ, 25 °C): 167.9 (1C, C7**B**), 167.7 (1C, C7**A**), 147.7 (2C, Tp3/5**A B**), 145.4 (1C, Tp3/5**A**), 145.2 (1C, Tp3/5**B**), 144.4 (1C, d J = 2.8, C2**B**), 143.3 (2C, Tp3/5**A B**), 142.1 (1C, Tp3/5**A**), 142.1 (1C, Tp3/5**B**), 142.0 (1C, C2**A**), 138.1 (1C, Tp3/5**A**), 137.4 (1C, Tp3/5**B**), 137.0 (1C, Tp3/5**A**), 136.9 (1C, Tp3/5**B**), 134.4 (1C, C5**B**), 132.9 (1C, d J = 2.6, C5**A**), 129.9 (1C, C1**A**), 129.2 (1C, C1**B**), 115.5 (1C, C6**A**), 113.9 (1C, C6**B**), 107.5 (1C, Tp4**A**), 107.4 (1C, Tp4**B**), 107.3 (1C, Tp4**A**), 107.2 (1C, Tp4**B**), 107.0 (1C, Tp**A**), 106.7 (1C, Tp4**B**), 66.3 (1C, d J = 8.5, C4**A**), 64.6 (1C, C4**B**), 634.0 (1C, d J = 7.0, C3**B**), 62.4 (1C, C3**A**), 51.5 (1C, OMe**B**), 51.5 (1C, OMe**A**), 13.4 (3C, d J = 28.9, PMe_3**B**), 13.33 (3C, d J = 28.7, PMe_3**A**). Anal. Calcd for $C_{20}H_{27}BN_7O_3PW$: C, 37.59; H, 4.26; N, 15.34. Found: C, 37.39; H, 4.05; N, 15.25.

WTp(NO)(PMe_3)(5,6-η^2-(3-trifluoromethylanisole)) (12)

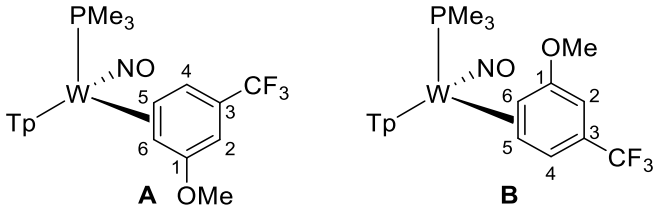

A 4-dram vial was charged with WTp(NO)(PMe_3)(η^2-2,3-anisole) (0.519 g, 0.404 mmol), 3-(trifluoromethyl)anisole (2.15 g, 23.8 mmol), DME (2 mL) and a stir pea. This yellow, heterogeneous mixture was stirred over 48 hours. Over this period, the mixture became dark brown and homogenous. Next a medium 30 mL fritted disc was filled with silica (~ 3 cm) and set in diethyl ether. The reaction

mixture was loaded onto the column and subsequently eluted with diethyl ether. Upon elution a golden yellow band developed and was eluted with diethyl ether (100 mL). The resulting homogeneous, yellow solution was evaporated in vacuo until product began to precipitate from solution. Next pentane (50 mL) was added to induce further precipitation. The resulting gold precipitate was collected on a fine porosity 15 mL fritted disc (0.154 g, 59.5%). CV (DMA): $E_{p,a}$= +0.07. IR: ν(NO) = 1573 cm^{-1}. Characterization of **12A:** ^{1}H NMR (MeCN-*d3*, δ, 0 °C): 7.98 (1H, d, Tp3/5), 7.91 (1H, d, Tp3/5), 7.90 (1H, d, Tp3/5), 7.86 (1H, d, Tp3/5), 7.80 (1H, d, Tp3/5), 7.26 (1H, d, Tp3/5), 7.09 (1H, d, *J* = 5.6, H4), 6.34 (1H, t, Tp4), 6.30 (1H, t, Tp4), 6.27 (1H, t, 1H), 5.18 (1H, s, H2), 3.88 (1H, dd, *J* = 13.7, 12.8, H5),3.75 (3H, s, -OMe), 2.05 (1H, m, H6), 1.20 (9H, d, J_{PH} = 8.7, PMe3). ^{13}C {1H} NMR (MeCN-*d3*, δ, 25 °C): 165.9 (C2), 145.0 (Tp3/5), 142.4 (Tp3/5), 141.7 (Tp3/5), 137.9 (Tp3/5), 137.3 (Tp3/5), 137.0 (Tp3/5), 129.2 (d, J_{PC} = 6.0, C4), 126.1 (q, J_{CF} =270, C8), 118.2 (buried, C3), 107.5 (Tp4), 107.0 (Tp4), 106.8 (Tp4), 85.6 (C2), 60.7 (C6), 58.7 (d, J_{PC} = 10.3, C5), 54.9 (-OMe), 13.6 (d, J_{PC} = 29.7, PMe_3). ^{31}P NMR (MeCN-*d3*, δ, 25 °C): -1.51 (J_{WP} =304, PMe_3). ^{19}F {1H} NMR (MeCN-*d3*, δ, 25 °C): - 64.58 (CF_3). A SC-XRD study confirms the identify of this compound (SI). Although a minor isomer (**B**) with features of the isomer below were observed along with a C-H activated adduct unambiguous assignment of the carbon resonances was precluded by the low intensity of signals (~ 10% of major isomer) and significant overlap with Tp resonances of **12A**. Partial Characterization of **12B** 1H-NMR (MeCN-*d3*, δ, 0 °C): 6.86 (1H, broad d, H4), 4.94 (1H, broad s, H2), 4.03 (1H, dd, *J* = 10.8, 12.8, H6), 3.66 (3H, s, -OMe), 2.16 (1H, dd, *J* = 5.9, 10.8), 1.21 (9H, buried, PMe_3).

WTp(NO)(PMe_3)(η^2-5,6-(3-trifluoromethyl-N,N-dimethylaniline)) (13)

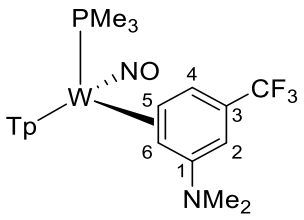

An oven-dried 4-dram vial was charged with **1** (0.817 g, 1.41 mmol) and 3-trifluoromethyl-N,N-dimethylaniline (3.89 g, 20.6 mmol), and the heterogeneous yellow reaction mixture was allowed to stir. After 16 h the reaction mixture had retained its heterogeneous golden-colored consistency but analysis by ^{31}P NMR confirmed the absence of **1** and the generation of a new species. The heterogeneous yellow reaction mixture was added to a solution of stirring pentane (50 mL) to precipitate out a light yellow solid. The solid was then filtered through a 30 mL fine porosity fritted disc and washed with pentane (3 x 20 mL) before the light tan powder was allowed to desiccate under active vacuum and a mass taken of the vibrant yellow solid (0.680 g**,** 70.0 %). The filtrate was collected and the pentane was distilled to re-collect the excess 3-trifluoromethyl-N,N-dimethylaniline and the recovered aromatic ligand was used in similar reaction procedures without noticeable inhibition of yield. CV (DMA): $E_{p,a}$= - 0.16 V (NHE). IR: ν(BH) = 2483 cm^{-1}, ν(NO) = 1570 cm^{-1}. ^{1}H NMR (acetone-*d6*, δ, 25 °C): 8.03 (1H, d, Tp5C), 7.96 (1H, d, Tp3/5), 7.92 (1H, d, Tp3B), 7.90 (1H, d, Tp3A), 7.88 (1H, d, Tp3/5), 7.48 (1H, d, Tp3C), 6.50 (1H, d, *J* = 5.2, H4), 6.38 (1H, t, Tp4C), 6.33 (1H, t, Tp4), 6.23 (1H, t, Tp4), 4.54 (1H, s, H2), 4.07 (1H, m, H5), 2.47 (6H, broad s, NMe_2), 2.23 (1H, d, *J* = 10.9, H6), 1.33 (9H, d, J_{PH} = 8.2, PMe_3). ^{13}C {1H} NMR (acetone-*d6*, δ, 25 oC): 157.8 (C1), 144.5 (Tp3/5), 142.4 (Tp3/5), 142.1 (Tp3/5), 140.8 (Tp3/5), 136.7 (Tp3/5), 136.5 (Tp3/5), 126.5 (-CF3, q, J_{CF} = 270.6), 121.5 (C3, q, J_{CF} = 28.9), 118.2 (C4), 105.8 (overlap 2Cs, Tp4), 105.3 (Tp4), 82.6 (C2), 61.0 (C5, d, J_{PC} = 8.5), 56.3 (C6), 39.1 (NMe_2), 13.2 (d, J_{CP} = 28.7, PMe_3). ^{19}F {1H} NMR (acetone-*d6*, δ, 25 °C): -61.68 (s, -CF_3). ^{31}P {1H} NMR (acetone-*d6*, δ, 25 °C): - 12.43 (J_{WP} = 308). HRMS ESI-MS (m/z, calculated (rel. intensity, %), observed (rel. intensity, %), ppm, (M + H)+: 691.1812 (84.71), 691.1819 (87.15), 692.1837 (80.03), 692.1844 (83.95), 693. 1835 (100), 693.1845 (100), 694.1877 (42.5), 694.1880 (46.17), 695.1868 (84.18), 695.1875 (87.58).

WTp(NO)(PMe_3)(4,5-η^2-(1,2-bistrifluoromethylbenzene)) (14)

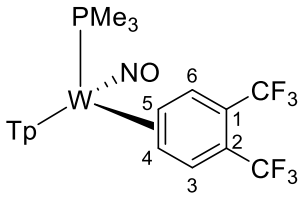

An oven-dried 4-dram vial was charged with **1** (0.608 g, 1.05 mmol) and 1,2-bis-trifluoromethylbenzene (3.02 g, 14.1 mmol), and the heterogeneous yellow reaction mixture was allowed to stir. After 16 h the reaction mixture had retained its heterogeneous golden-colored consistency but analysis by 31P NMR confirmed the absence of **1** and the generation of a new species. The heterogeneous yellow reaction mixture was added to 50 mL of stirring pentane to precipitate out a vibrant yellow solid. The solid was then filtered through a 30 mL fine porosity fritted disc and washed with pentane (3 x 20 mL) before the yellow powder was allowed to desiccate under active vacuum and a mass taken of the vibrant yellow solid (0.477 g**,** 64.0 % yield). CV (DMA): $E_{p,a}$ = +0.45 V (NHE). IR: ν(BH) = 2482 cm^{-1}, ν(NO) = 1592 cm^{-1}. ^{1}H NMR (acetone-*d6*, δ, 25 °C): 8.04 (3H, d, overlapping Tp3/5), 8.00 (1H, d, Tp3/5), 7.90 (1H, d, Tp3/5), 7.68 (1H, d, *J* = 6.9, H3), 7.55 (1H, d, *J* = 5.5, H6), 7.53 (1H, d, Tp3C), 6.40 (1H, t, Tp4A), 6.38 (1H, t, Tp4B), 6.37 (1H, t, Tp4C), 3.80 (1H, m, H5), 2.15 (1H, t, *J* = 7.6, H4), 1.71 (9H, d, J_{PC} = 8.5, PMe_3). ^{31}P {1H} NMR (acetone-*d6*, δ, 25 °C): -13.57 (J_{WP} = 302). ^{19}F {1H} NMR (acetone-*d6*, δ, 25°C): -56.6 (3F, q, $^5J_{FF}$ = 12.5, CF_3), -56.7 (3F, q, $^5J_{FF}$ = 12.5, CF_3). ^{13}C {1H} NMR (acetone-*d6*, δ, 25 °C): 144.5 (Tp3/5), 141.7 (Tp3/5), 141.3 (C3), 141.0 (Tp3/5), 138.5 (C6), 137.2 (Tp3/5), 136.5 (Tp3/5), 136.0 (Tp3/5), 124.1 (overlapping CF_3, q, J_{CF} = 273.4), 113.3 (C1/C2, q, J_{CF} = 30.1), 111.0 (C1/C2, q, J_{CF} = 31.2), 106.5 (Tp4), 106.4 (Tp4), 106.0 (Tp4), 60.7 (C5, d, J_{PC} = 9.5), 58.2 (C4), 13.6 (PMe_3, d, J_{PC} = 28.7). A SC-XRD study confirms the identify of this compound (SI).

WTp(NO)(PMe$_3$)(4,5-η^2-(1,3-bistrifluoromethylbenzene)) (15)

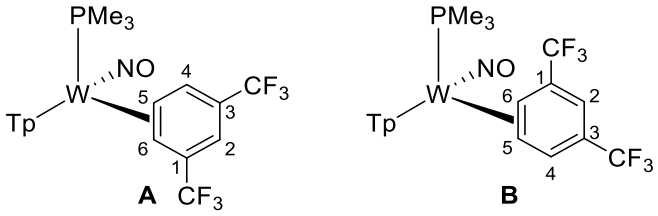

A 4-dram vial was charged with **1** (0.097 g, 0.167 mmol) and neat 1,3-bis(trifluoromethyl)benzene (3.17 g, 14.8 mmol) and the initially heterogeneous yellow reaction mixture was allowed to stir. After 18 h the reaction mixture was still a heterogeneous yellow but no starting material was detected by cyclic voltammetry. This mixture was then slowly added a solution of stirring hexanes (20 mL) that had been cooled to – 30 oC to generate a yellow precipitate. The precipitate was then isolated on a 15mL fine porosity fritted disc, washed with hexanes (3x 10 mL) and desiccated to yield **5**. A yellow solid was obtained (0.041 g, 34%). The filtrate was collected and the pentane was distilled to re-collect the excess aromatic ligand which was used in similar reaction procedures without noticeable inhibition of yield. This complex is isolated in an approximate 7:1 ratio of A:B. CV (DMA): $E_{p,a}$= + 0.42 V (NHE). IR: ν(BH) = 2493 cm^{-1}, ν(NO) = 1582 cm^{-1}. Characterization for **21A** ^{1}H NMR (acetone-*d6*, δ, 25 °C): 8.06 (1H, d, Tp5C), 8.00 (1H, d, Tp5B), 7.95 (1H, d, Tp3B), 7.88 (1H, d, Tp3/5A), 7.71 (1H, d, Tp3/5A), 7.57 (1H, d, *J* = 5.0, H6), 7.50 (1H, d, Tp3C), 6.39 (1H, t, Tp4C), 6.36 (1H, t, Tp4B), 6.27 (1H, t, Tp4A), 6.25 (1H, broad s, H2), 3.91 (1H, m, H5), 2.30 (1H, d, *J* = 9.3, H4), 1.36 (9H, d, *J* = 8.4, PMe$_3$). ^{13}C {1H} NMR (acetone-*d6*, δ, 25 °C): 145.3 (Tp3/5A), 142.5 (Tp3/5A), 141.7 (Tp3C), 138.5 (C6), 138.0 (Tp3/5), 137.5 (Tp5B), 137.2 (Tp3/5), 128.8 (C1/C3, q, J_{CF} = 31.5), 126.3 (CF$_3$, q, J_{CF} = 272.1), 125.7 (CF$_3$, q, J_{CF} = 272.7), 116.8 (C1/C3, q, J_{CF} = 32.1), 107.5 (Tp4), 107.3 (Tp4), 106.2 (Tp4), 106.5 (H2), 62.1 (H5), 60.7 (H4, *J* = 25.0), 12.95 (d, J_{PC} = 28.7, PMe$_3$). ^{31}P {1H} NMR (acetone-*d6*, δ, 25 °C): -14.46 (J_{WP} = 289). Partial characterization for **15B** 7.70 (1H, buried, H4), 6.49 (1H, broad s, H2), 4.33 (1H, dd, *J* = 9.3, 12.4, H4), 2.19 (1H, broad t, *J* = 9.3, H5), 1.14 (9H, d, J_{PH} = 8.5, PMe$_3$). ^{31}P NMR (acetone-*d6*, δ, 25 °C): -12.17. Partial characterization for **15H**: 1H NMR (acetone-*d6*, δ, 25 °C): 9.23 (1H, m, J_{PH} =102.1 J_{WH} = 30.8, W-H resonance), 6.01 (1H, t, Tp4). ^{31}P {1H} NMR (acetone-*d6*, δ,

25 °C): -2.84 (J_{WP} = 172). ^{19}F {1H} NMR resonances for all isomers (acetone-*d6*, δ, 25 °C): -56.9, -59.7 for **15A**, -60.0 for **15A**, -60.8 , - 61.8, -62.4. Elemental Analysis for $C_{20}H_{23}BF_6N_7OPW$: Calculated: C, 33.50; H, 3.23; N, 13.67. Found: C, 33.50; H, 3.09; N, 13.54.

WTp(NO)(PMe$_3$)(5,6-η^2-(3-trifluoromethyl-N,N-dimethyl-anilinium)]OTf (16)

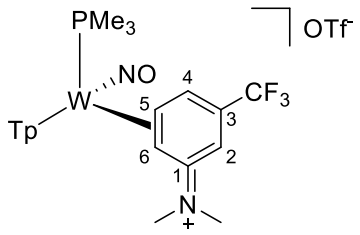

To an oven dried 4-dram vials added **15** (0.096 g, 0.139 mmol) and along with MeOH (~ 2 mL) to generate a heterogeneous yellow reaction mixture. This solution was allowed to cool in a -30 °C freezer over a course of 30 min before DPhAT (0.072 g, 0.225 mmol) was added to the reaction mixture at reduced temperature. After 1.5 h the reaction mixture was added to a stirring solution of diethyl ether (30 mL) to precipitate out a yellow solid and the isolated solid was washed with pentane (3 x 10 mL) after isolation on a fine 15 mL fritted disc and allowed to desiccate for 3 h (0.096 g, 82.1%). CV (DMA): $E_{p,a}$= + 1.34 V (NHE), $E_{p,c}$ = - 1.54 V (NHE). IR: ν(BH) = 2519 cm^{-1}, ν(NO) = 1602 cm^{-1}, ν(CN iminium) = 1581 cm^{-1}. ^{1}H NMR (acetone-*d6*, δ, 25 °C): 8.22 (1H, d, Tp3/5C), 8.16 (1H, d, Tp5B), 8.07 (2H overlapping, d, Tp5A and Tp3/5), 8.03 (1H, d, Tp3C), 7.49 (1H, d, Tp3A), 7.27 (1H, broad s, Tp3/5C), 6.55 (1H, t, Tp4C), 6.49 (1H, t, Tp4B), 6.47 (1H, t, Tp4A), 4.00 (1H, m, H5), 3.80 (3H, s, NMeA), 3.74 (1H, d, *J* = 22.4, H2), 3.47 (1H, d, *J*= 22.4, H2'), 2.67 (1H, m, H6), 2.58 (3H, s, NMeB), 1.41 (9H, d, J_{PH} = 9.2, PMe$_3$). ^{13}C NMR (acetone-*d6*, δ, 25 °C): 181.7 (C1), 145.9 (Tp3/5C), 143.1 (Tp3/5), 142.7 (Tp3/5), 142.6 (Tp3C), 139.2 (Tp5B), 138.8 (Tp3/5), 133.6 (C4), 122.3 (CF3, q, J_{CF} = 322.2), 113.0 (C3, q, J_{CF} = 31.6), 108.4 (Tp4), 108.3 (Tp4), 107.8 (Tp4), 61.2 (C5, J_{PC} = 12.3), 55.3 (C6), 28.6 (C2), 43.1 (NMeA), 41.8 (NMeB) 28.5 (C3, buried) 13.5 (PMe$_3$, d, J_{CP} = 31.7). ^{19}F NMR (acetone-*d6*, δ, 25 °C): -78.28 (s, CF$_3$). ^{31}P NMR (acetone-*d6*, δ, 25 °C): -11.16 (J_{WP} = 281)

References

(1) Liebov, B. K.; Harman, W. D. *Chem. Rev.* **2017**, *117*, 13721.

(2) Keane, J. M.; Harman, W. D. *Organometallics* **2005**, *24*, 1786.

(3) Harman, W. D. *Chem. Rev.* **1997**, *97*, 1953.

(4) Lis, E. C.; Salomon, R. J.; Sabat, M.; Myers, W. H.; Harman, W. D. *J. Am. Chem. Soc.* **2008**, *130*, 12472.

(5) Kolis, S. P.; Kopach, M. E.; Liu, R.; Harman, W. D. *J. Org. Chem.* **1997**, *62*, 130.

(6) Kopach, M. E.; Harman, W. D. *J. Org. Chem.* **1994**, *59*, 6506.

(7) Kopach, M. E.; Gonzalez, J.; Harman, W. D. *J. Am. Chem. Soc.* **1991**, *113*, 8972.

(8) Todd, M. A.; Grachan, M. L.; Sabat, M.; Myers, W. H.; Harman, W. D. *Organometallics* **2006**, *25*, 3948.

(9) Todd, M. A.; Sabat, M.; Myers, W. H.; Smith, T. M.; Harman, W. D. *J. Am. Chem. Soc.* **2008**, *130*, 6906.

(10) Gonzalez, J.; Sabat, M.; Harman, W. D. *J. Am. Chem. Soc.* **1993**, *115*, 8857.

(11) Salomon, R. J.; Todd, M. A.; Sabat, M.; Myers, W. H.; Harman, W. D. *Organometallics* **2010**, *29*, 707.

(12) Wilson, K. B.; Myers, J. T.; Nedzbala, H. S.; Combee, L. A.; Sabat, M.; Harman, W. D. *J. Am. Chem. Soc.* **2017**, *139*, 11401.

(13) Myers, J. T.; Smith, J. A.; Dakermanji, S. J.; Wilde, J. H.; Wilson, K. B.; Shivokevich, P. J.; Harman, W. D. *J. Am. Chem. Soc.* **2017**, *139*, 11392.

(14) Harman, W. D.; Sekine, M.; Taube, H. *J. Am. Chem. Soc.* **1988**, *110*, 5725.

(15) Fleming, F. F.; Yao, L.; Ravikumar, P. C.; Funk, L.; Shook, B. C. *J. Med. Chem.* **2010**, *53*, 7902.

(16) Beaumont, K.; Webster, R.; Gardner, I.; Dack, K. *Curr. Drug Metab.* **2003**, *4*, 461.

(17) Chen, X.; Hussain, S.; Parveen, S.; Zhang, S.; Yang, Y.; Zhu, C. *Curr. Med. Chem.* **2012**, *19*, 3578.

(18) Zhou, Y.; Wang, J.; Gu, Z.; Wang, S.; Zhu, W.; Aceña, J. L.; Soloshonok, V. A.; Izawa, K.; Liu, H. *Chem. Rev.* **2016**, *116*, 422.

(19) Graham, P. M.; Meiere, S. H.; Sabat, M.; Harman, W. D. *Organometallics* **2003**, *22*, 4364.

(20) Shivokevich, P. J.; Myers, J. T.; Smith, J. A.; Pienkos, J. A.; Dakermanji, S. J.; Pert, E. K.; Welch, K. D.; Trindle, C. O.; Harman, W. D. *Organometallics* **2018**, *37*, 4446.

(21) Lis, E. C.; Delafuente, D. A.; Lin, Y.; Mocella, C. J.; Todd, M. A.; Liu, W.; Sabat, M.; Myers, W. H.; Harman, W. D. *Organometallics* **2006**, *25*, 5051.

(22) Welch, K. D.; Harrison, D. P.; Lis, E. C.; Liu, W.; Salomon, R. J.; Harman, W. D.; Myers, W. H. *Organometallics* **2007**, *26*, 2791.

(23) Wilson, K. B.; Myers, J. T.; Nedzbala, H. S.; Combee, L. A.; Sabat, M.; Harman, W. D. *Journal of the American Chemical Society* **2017**, *139*, 11401.

(24) Welch, K. D.; Harrison, D. P.; Lis, E. C.; Liu, W.; Salomon, R. J.; Harman, W. D.; Myers, W. H. *Organometallics* **2007**, *26*, 2791.

(25) Smith, J. A.; Schouten, A.; Wilde, J. H.; Westendorff, K. S.; Dickie, D. A.; Ess, D. H.; Harman, W. D. *Journal of the American Chemical Society* **2020**, *142*, 16437.

(26) Shree, M. V.; Fabulyak, D.; Baillie, R. A.; Lefèvre, G. P.; Dettelbach, K.; Béthegnies, A.; Patrick, B. O.; Legzdins, P.; Rosenfeld, D. C. *Organometallics* **2017**, *36*, 2714.

(27) Baillie, R. A.; Patrick, B. O.; Legzdins, P.; Rosenfeld, D. C. *Organometallics* **2017**, *36*, 26.

(28) Sheppard, W. A. *Org. Synth.* **1969**, *49*, 111.

(29) Liu, W.; Welch, K.; Trindle, C. O.; Sabat, M.; Myers, W. H.; Harman, W. D. *Organometallics* **2007**, *26*, 2589.

(30) Smith, J. A.; Simpson, S. R.; Westendorff, K. S.; Weatherford-Pratt, J.; Myers, J. T.; Wilde, J. H.; Dickie, D. A.; Harman, W. D. *Organometallics* **2020**, *39*, 2493.

Chapter 4

Phenyl Sulfones: A Route to a Trisubstituted, Sulfone Functionalized Cyclohexenes

4.1 Introduction

While we have conducted several studies on arenes bearing π-donor groups,[1-10] it was not until recently that organic manipulations of electron-deficient η^2-benzene complexes were explored.[11-13] As shown in Chapter 3, most functional groups that are electron-withdrawing (e.g., benzoates, benzonitrile, phenones) have π-bonds that compete with the aromatic ring for metal coordination.[14,15] However, in the complexes MoTp(NO)(DMAP)(η^2-trifluorotoluene) and WTp(NO)(PMe_3)(η^2-trifluorotoluene),[11,12,16] the metal binds exclusively to the benzene ring. Despite the electron-withdrawing nature of the CF_3 group, protonation of the η^2-trifluorotoluene ligand can be achieved, ortho to the CF_3 group. The resulting η^2-benzenium complex then undergoes nucleophilic addition at an adjacent ring carbon, resulting in a 1,5-disubstituted η^2-1,3-cyclohexadiene complex (**Scheme 4.1**). The η^2-diene complex can then undergo another protonation/nucleophilic addition sequence to provide a trisubstituted cyclohexene containing up to three new stereocenters (**Scheme 4.1**).[11]

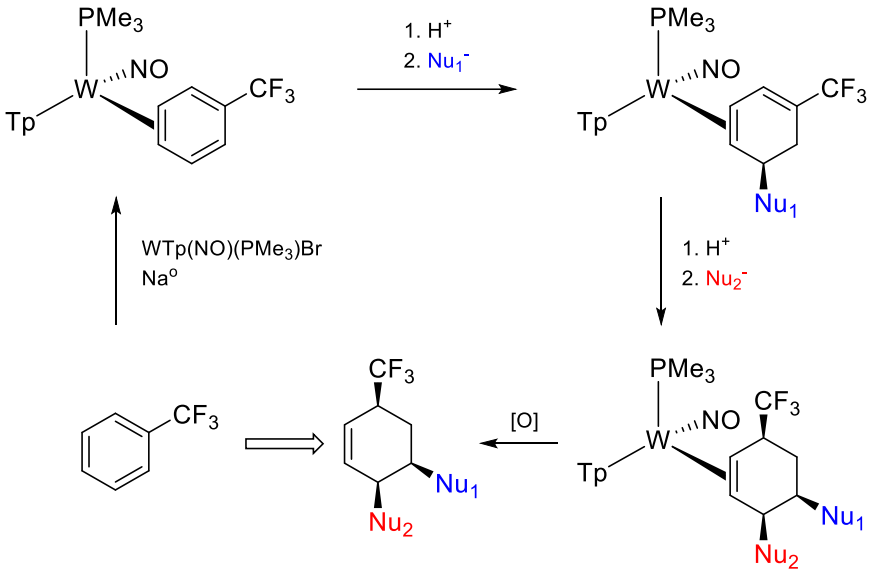

Scheme 4.1: Reactivity pattern of a dihapto-coordinated trifluorotoluene complex

Chapter 3 evaluated the scope and binding selectivity of complexes prepared from other electron-deficient arenes.[13] That investigation revealed that sulfones were well-tolerated by the {WTp(NO)(PMe_3)} fragment. Sulfones and sulfonamides are attractive functional groups to leverage in the dearomatization

of benzene. Sulfur is the third most common heteroatom in marketed pharmaceuticals behind nitrogen and oxygen.[17,18] Further, sulfones and sulfonamides are prevalent in various antibiotics, cancer therapeutics, COX-2 inhibitors, diuretics, and ulcer preventatives.[17,19] We postulated that the reactivity of η^2-phenyl sulfone complexes would follow a reaction pattern similar to their trifluorotoluene analog.

4.2 Review of η^2-Sulfone Complexes

Complexes of the form WTp(NO)(PMe_3)(3,4-η^2-$PhSO_2R$) (R= -Me (**2**), -Ph (**3**), -N(C_4H_8) (**4**)) were prepared by ligand exchange from the precursor complex WTp(NO)(PMe_3)(η^2-anisole) **(1; Scheme 4.2)**.[16] The diphenyl sulfone complex **3** exists in solution as an equilibrium ratio of coordination diastereomers (cdr = 2 : 1), differing by which face of the ring is coordinated. The sulfonamide derivative **4** similarly equilibrates in solution, with a cdr of 1.7 : 1. However, the methyl phenyl sulfone ligand exchange reaction yielded three isomers of **2** in a ratio of 2.7 : 2.5 : 1. The minor complex was determined to be a tungsten hydride species formed as a result of the metal inserting into the methyl C-H bond. To further support the assignment of **2c** as an alkyl hydride, the anisole complex **1** was also combined with dimethyl sulfone and 4-(methylsulfonyl)toluene. In both cases, the only complex formed was the expected sulfonylmethyl hydride, the net product of a tungsten insertion into the methyl CH bond, as shown in chapter 3.

4.3 Reactivity of η^2-Phenyl Sulfones

Previous work with the WTp(NO)(PMe_3)(η^2-trifluorotoluene) complex demonstrated that even though η^2-arene complexes with electron-deficient benzenes exhibit poor coordination diastereoselectivity, protonation of the isomeric mixture at -30 °C followed by treatment with a nucleophile such as a cyanide ion (NaCN) results in the formation of a *single* diastereomer of an η^2-diene complex.[11] Initial attempts to replicate this with the methyl phenyl sulfone system that contains the hydride led to consistent failures with protonation and nucleophilic addition. ^{1}H NMR observed multiple

allylic isomers at 0 °C after exposure to triflic acid leveled in MeCN at -30 °C. Nucleophilic addition was attempted even in the presence of multiple isomers in the hope that chromatography would clean up the final product. However, neither NaCN nor MTDA appeared to lead to the formation of a clean complex when used as the nucleophile at -60 °C, -40 °C, -30 °C, -10 °C, nor 0 °C. Fortunately, it was found that the ring-bound isomers **2a** and **2b** selectively precipitate out of the reaction mixture in an isolated yield of 52% if the ligand exchange is conducted using THF as the solvent.[13]

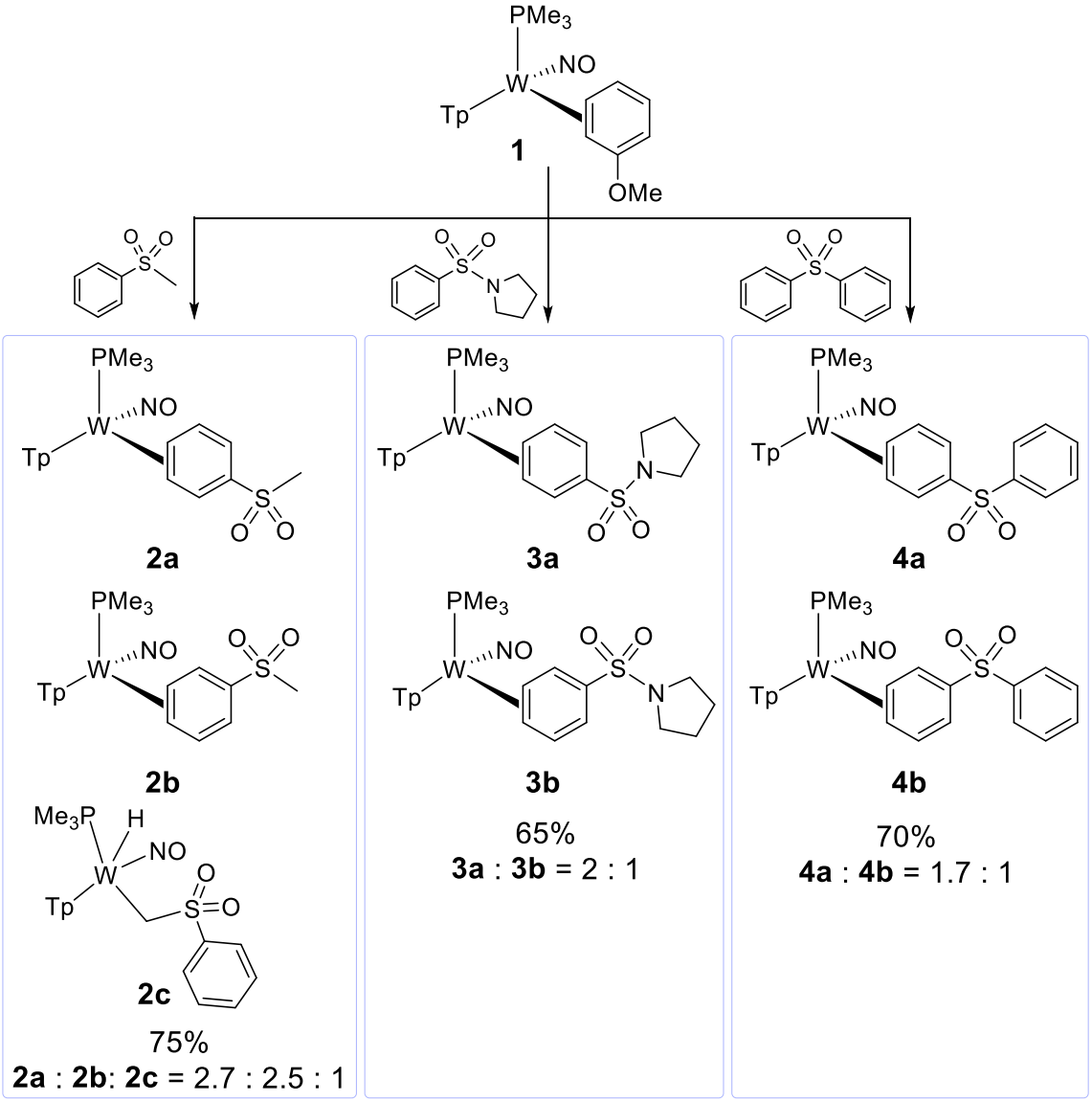

Scheme 4.2: Preparation of dihapto-coordinated phenyl sulfone complexes of {WTp(NO)(PMe_3)}

Separation of the η^2 isomers from the hydride led to successful protonation followed by nucleophilic addition of NaCN to **2**. Disappointingly, when the methyl phenyl sulfone complex mixture of **2a a**nd **2b** was protonated with triflic acid (HOTf/CH_3CN) and then treated with NaCN at -30 °C, two products (**16a**, **16b**) were formed in roughly a 1 : 2 ratio instead of a single compound seen with the trifluorotoluene system. Repeating this reaction at room temperature destroyed the complex. However, when the reaction was performed at 0 °C, a single dominant product (**16b**, dr > 20 : 1; later referred to as **16**) was formed. When the nucleophile was changed from NaCN to MTDA, the ratio of the diene complex **10b** to **10a** at -30 °C was roughly 1.75 : 1 for the addition to the methyl sulfone complex **2**, but this again improved to > 20 : 1 at 0 °C.

When a ^{1}H NMR spectrum was taken after the addition of acid to **2** at 0 °C, one dominant complex (**5b**) was observed. Key features from the ^{1}H NMR spectrum that support the formation of an η^2-arenium complex (**5b**) include a diastereotopic methylene group at δ 4.30 and 4.10, a single unbound alkene resonance at δ 7.11, and three π allylic protons at δ 7.29, 5.12, and 4.34. These spectroscopic features were similar to those reported for the "η^2-arenium" species $[WTp(NO)(PMe_3)(\eta^2\text{-}HC_6H_5CF_3)]^+$, derived from α,α,α-trifluorotoluene.[11]

Taken together, this data suggests that two different η^2-arenium diastereomers evolve upon protonation of **2** at -30 °C, each derived from a different stereoisomer of the initial arene complex. Presumably, these arenium species then react with the nucleophile to give two different diene products (*vide infra*). The warmer reaction temperature of 0 °C apparently facilitates the isomerization of the arene complex **2a** to **2b** prior to its protonation. Repeating the cyanide addition with the other two sulfone derivatives (**3**, **4**) resulted in similar results, providing diene complexes **15** and **16,** respectively. These results are summarized in **Table 4.1**.

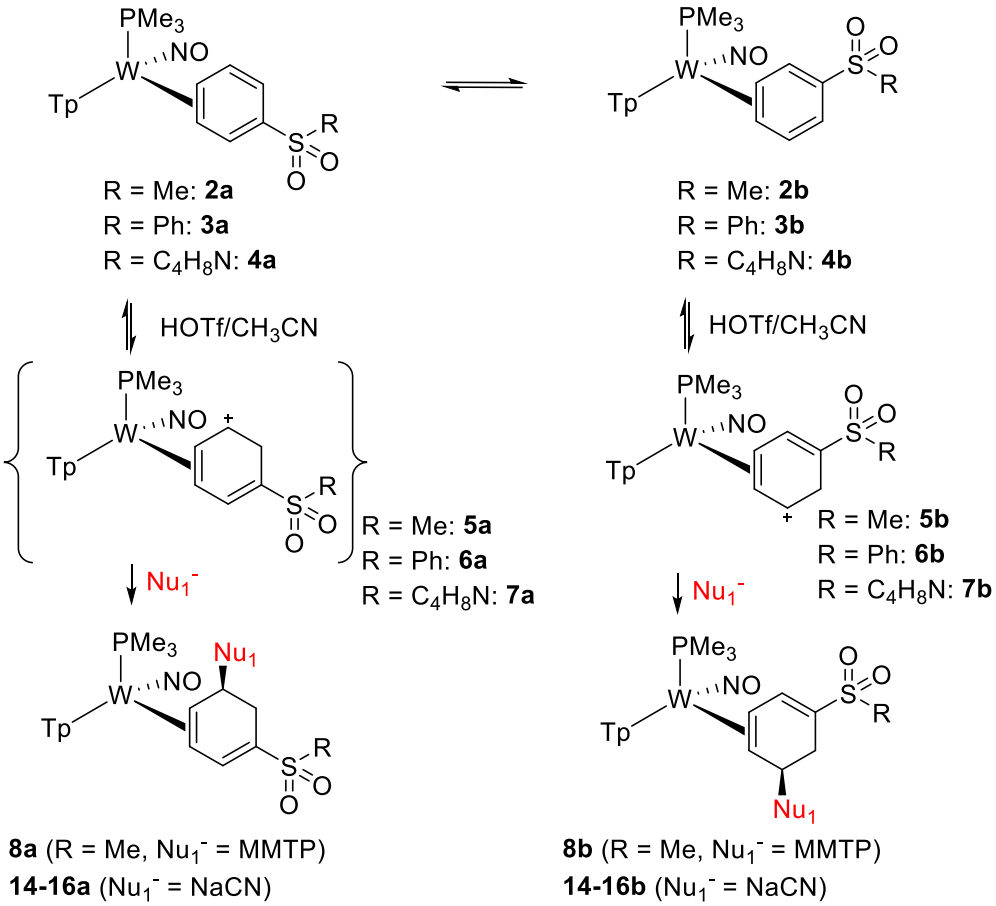

Nu	R	Temperature (°C)	Ratio (b:a)
MMTP	Me (**8**)	-30 0	1.7:1 >20:1
NaCN	Me (**14**)	-30 0	2:1 >20:1
NaCN	Ph (**15**)	-30 0	1:1 >20:1
NaCN	C_4H_8N (**16**)	-30 0	2:1 >20:1

Table 4.1: Protonation of dihapto-coordinated phenyl sulfone ligands followed by nucleophilic addition

2D NMR techniques were used to characterize the diene complexes (**8b**, **14**-**16b**), and in all three cases, NOE correlations between the protons of the pyrazole ring trans to the PMe_3 ligand and the methine proton of C5 support the conclusion that the nucleophile added adjacent to the site of arene protonation, and to the face of the bound carbocycle anti to metal coordination. In a similar fashion, other nucleophiles could be selectively added to the η^2-arenium intermediates **5b**-**7b,** including MMTP, lithium dimethyl malonate (LiDMM), and tetrabutylammonium borohydride (TBAB), all of which cleanly react

with the η^2-arenium complexes **5b**-**7b** (prepared in situ) to form 1-sulfonyl-1,3-diene complexes with high levels of regio- and stereocontrol (**Table 4.2**; 43%-68%). Single-crystal X-ray diffraction (SC-XRD) studies provided molecular structures of the diene complexes **8**, **9**, **11**-**13**, and **17**, all of which support the assigned stereochemistries (see appendix for crystal strutures).[13] We posit that the high diastereoselectivity observed for these diene complexes (**Table 4.2**, **8**-**18**) is the result of the reversible isomerization for the η^2-arene coordination diastereomers (**Table 4.1**, **a** and **b**) coupled with a faster rate of formation for the thermodynamically favored arenium isomer **5b**, compared to that of **5a**.

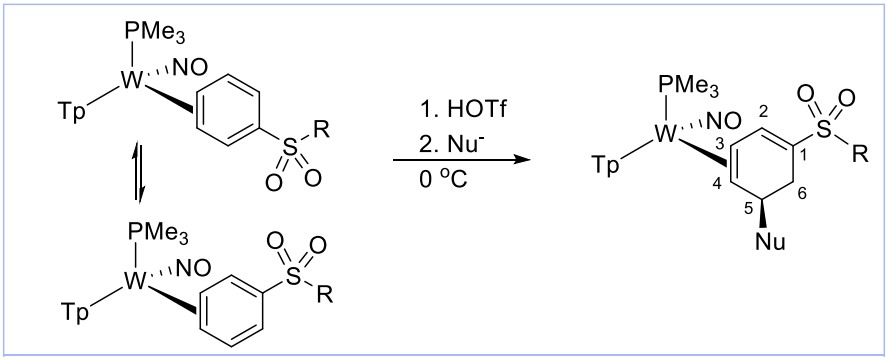

Reagent (Nu^-)	R	Product	Yield
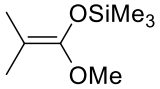	Me (**8**) Ph (**9**) C_4H_8N (**10**)	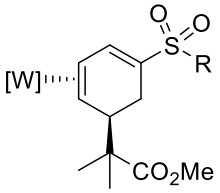	54% 67% 53%
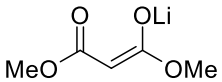	Me (**11**) Ph (**12**) C_4H_8N (**13**)	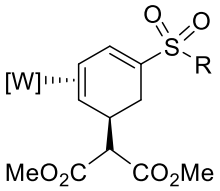	65% 61% 62%
NaCN	Me (**14**) Ph (**15**) C_4H_8N (**16**)	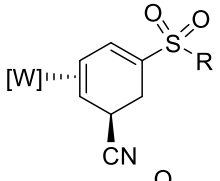	56% 31% 50%
tBu_4NBH_4	Me (**17**) Ph (**18**)	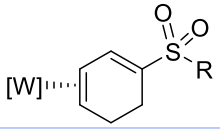	62% 68%

[W] = $WTp(NO)(PMe_3)$

Table 4.2: Tandem protonation/nucleophilic addition to the phenyl sulfone complex (T = 0 °C)

4.4 Protonation of Sulfone Functionalized η^2-Dienes

The products resulting from the 1,2-addition reactions of the η^2-phenyl sulfones are rare examples of conjugated dienes in which a metal binds only two carbons. The uncoordinated double bond is still in conjugation with the tungsten, and as seen previously in the η^2-trifluorotoluene and η^2-benzene systems, is expected to have a basic carbon at the terminus of the diene.[11,12] Protonation of **8**, **9**, and **10** at -30 °C yields single products (**19**-**21**) in all three cases according to proton NMR data (20 °C).

The hyper distorted η^2-allyl complex[20] resulting from the protonation of the η^2-1,3-cyclohexadiene species **8** was confirmed to be predominantly **19b** (**Scheme 5**) according to 2D NMR data. This type of allyl distortion, in which only two of the three allyl carbons are strongly coordinated by the metal, is typical for allyl complexes of the form $[WTp(NO)(PMe_3)(\pi\text{-allyl})]^+$ (*vide infra*).[20] Further, calculations indicate that having the weakly coordinated carbon (indicated as a carbocation in **Scheme 5**) distal to the PMe_3 is favored by 3-4 kcal/mol over the proximal allyl conformer (**a**) for the parent cyclohexadienium species (SI).[20] This inherent preference also avoids placing the carbocation-like allyl carbon next to the electron-withdrawing SO_2R group (**a** in **Scheme 5**). NOE correlations between the doublet at 6.00 ppm corresponding to C4 and the pyrazole ring trans to the PMe_3 indicate that the "cationic" carbon is distal to the PMe_3, as expected.

The addition of diethyl ether to the reaction mixture precipitates the complex **22b** as its triflate salt (81%). Protonation of **9** or **10** at -30 °C followed by ether-induced precipitation generates predominantly **20b** and **21b** in a similar manner (76-79%). NOE correlations between the methine group bound to the sulfone and the PMe_3 group, along with stereochemical determinations of subsequently derived products (vide infra) support the notion that the sulfone group is oriented trans to tungsten. NMR data for **19** and **20** are consistent with their trifluorotoluene-derived analogs.[11] As seen with the latter,[11] we suspect that initial protonation of the η^2-diene complex likely occurs anti to the metal (**a** in **Scheme 5**),[21,22] but such an action creates a steric interaction between the sulfone and the PMe_3 and NO ligands.

Subsequent epimerization of this stereocenter would provide the observed stereochemistry in which the sulfone group is anti to the metal.

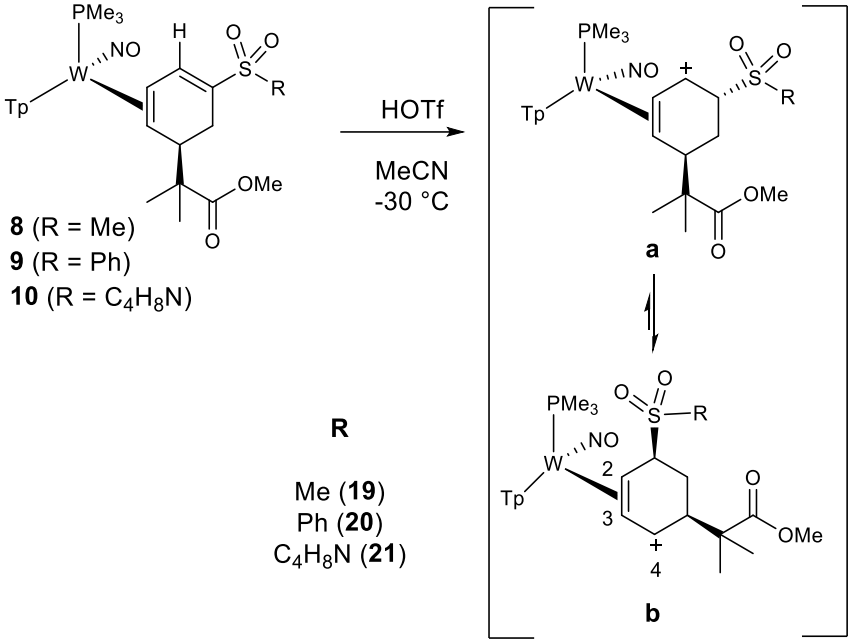

Scheme 4.3: Protonation of η^2-(1-sulfonyl-1,3-diene) complexes, conformational change ("allyl shift"), and epimerization of the resulting η^2-allyl complex

4.5 Second Nucleophilic Additions

Once we confirmed that protonation of all three sulfone substituted η^2-1,3-cyclohexadiene complexes (**8**-**10**) resulted in the clean formation of η^2-allyl complexes, η^2-diene **8** was protonated with HOTf in CH_3CN at -30 °C, and the resulting solution was then treated with a methanol solution of NaCN. A white precipitate formed overnight in the reaction vial. Full 2D NMR analysis of the isolated solid confirmed the formation of the desired trisubstituted η^2-cyclohexene complex (**23**; 65%). Repeating this reaction at -60 °C increased the yield of the precipitate (**23**) to 82%. NOE and COSY data indicate that the CN^- adds to what was initially the para carbon of the phenyl sulfone, anti to the metal. This 1,4-addition pattern is consistent with that observed for the η^2-trifluorotoluene complex.[11] Eluting the filtrate down silica yielded a second product, **22**, determined to be an η^2-1,3-cyclohexadiene complex, with the ester and nitrile substituents still intact, but not the sulfone group. Repeating this process with the η^2-diene **9**

resulted in a similar white precipitate that was found to be the desired trisubstituted η^2-cyclohexene complex (**24**, 72%). Elution of the filtrate through silica also yielded the η^2-cyclohexadiene complex **22**. Unfortunately, the tandem protonation/CN^- addition to the η^2-diene **10** did not yield a precipitate. Efforts to isolate the reaction via silica chromatography or aqueous extraction yielded the η^2-cyclohexadiene complex **22**. An X-ray crystal structure determination confirms the identity of **22** as that shown in **Scheme 4.4** (see appendix for crystal struture)**.** Further exploration of the sulfone elimination will be discussed in the following chapter.

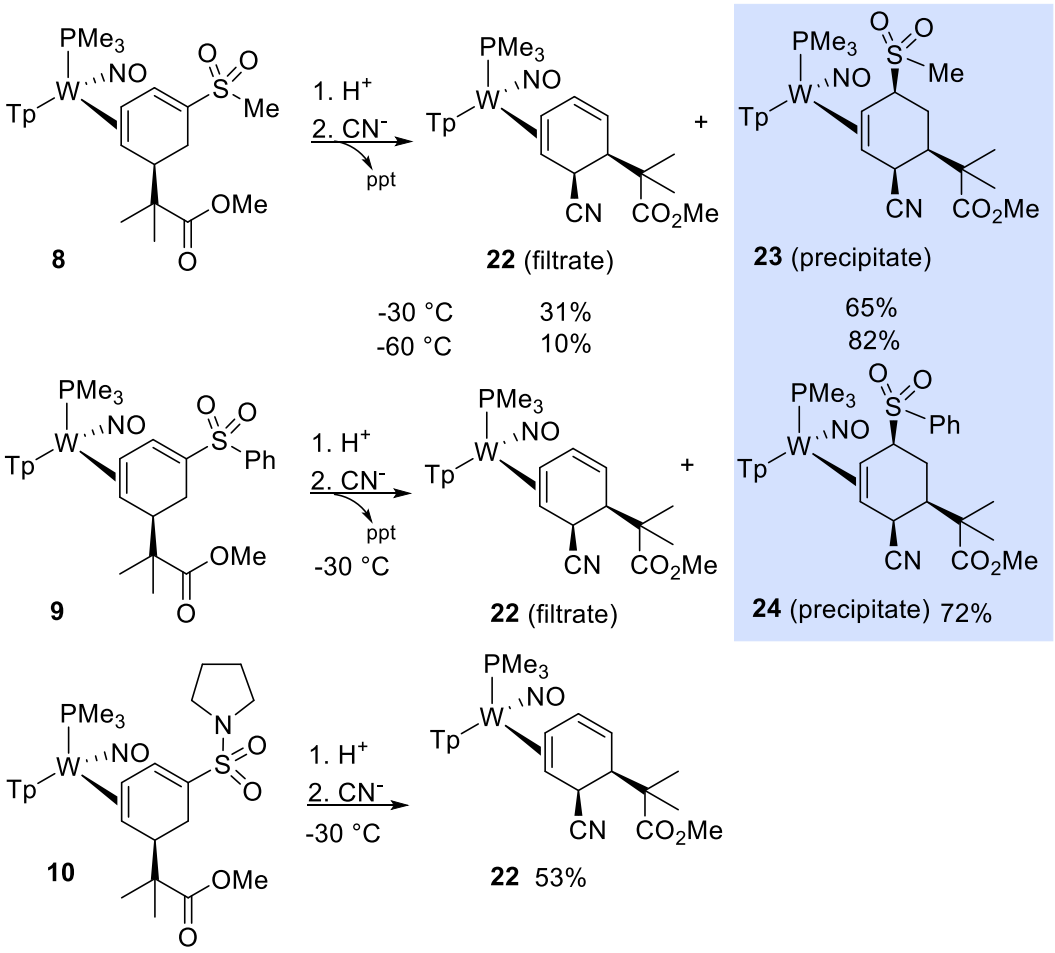

Scheme 4.4: Second protonation/nucleophilic addition of cyanide to the arene ring.

4.6 Liberation of Organics from Metal

Previous studies have shown that cyclohexenes can be liberated from the {WTp(NO)(PMe_3)} system using a variety of different oxidants, including Ag+, [$FeCp_2$] +, DDQ, $NOPF_6$, CAN, and even O_2. These cyclohexenes were liberated from the metal through oxidation with $NOPF_6$ in yields ranging from 64 to 76% (**Scheme 4.5**).

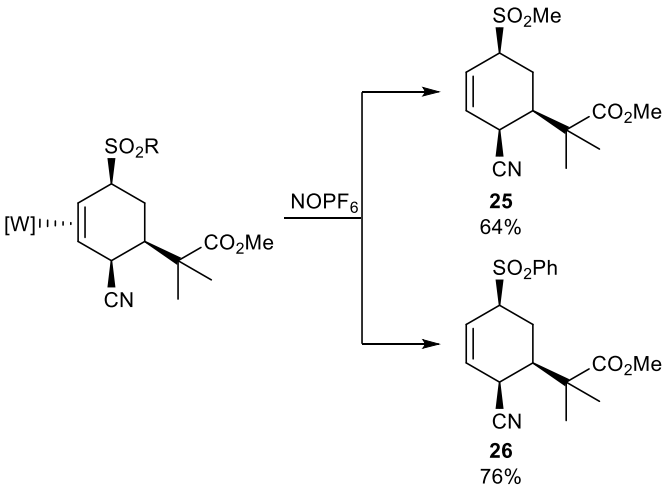

Scheme 4.5: Decomplexation of sulfone functionalized cyclohexenes

4.7 Conclusion

The coordination of methyl phenyl sulfone, diphenyl sulfone, and phenylsulfonyl pyrrolidine by the π-base {WTp(NO)(PMe_3)} increases the electron density of the phenyl ring, which enables the selective protonation of the carbon ortho to the sulfone group. The resulting η^2-arenium complexes undergo nucleophilic addition with a range of nucleophiles to yield conjugated η^2-diene species. In turn, these diene complexes are susceptible to a second protonation and nucleophilic addition, leading to trisubstituted cyclohexenes, which are liberated from the metal through oxidative decomplexation. Given that WTp(NO)(PMe_3)(η^2-benzene) and its derivatives can be prepared in enantioenriched form,[23] the compounds reported herein should be accessible as single enantiomers.[11,24] Further discussion of the sulfone elimination product follows in the next chapter.

Experimental

General Methods. NMR spectra were obtained on 500, 600, or 800 MHz spectrometers. Chemical shifts are referenced to tetramethylsilane (TMS) utilizing residual ^{1}H signals of the deuterated solvents as internal standards. Chemical shifts are reported in ppm, and coupling constants (J) are reported in hertz (Hz). Chemical shifts for ^{19}F and ^{31}P spectra are reported relative to standards of hexafluorobenzene (164.9 ppm) and triphenylphosphine (−6.00 ppm) or triphenyl phosphate (−16.58 ppm). Infrared spectra (IR) were recorded as a solid on a spectrometer with an ATR crystal accessory, and peaks are reported in cm^{-1}. Electrochemical experiments were performed under a nitrogen atmosphere. Most cyclic voltammetric data were recorded at ambient temperature at 100 mV/s, unless otherwise noted, with a standard three-electrode cell from +1.8 to −1.8 V with a platinum working electrode, acetonitrile or dimethylacetamide (DMA) solvent, and tetrabutylammonium (TBAH) electrolyte (∼1.0 M). All potentials are reported versus the normal hydrogen electrode (NHE) using cobaltocenium hexafluorophosphate ($E_{1/2}$ = −0.78 V, −1.75 V) or ferrocene ($E_{1/2}$ = 0.55 V) as an internal standard. The peak separation of all reversible couples was less than 100 mV. All synthetic reactions were performed in a glovebox under a dry nitrogen atmosphere unless otherwise noted. All solvents were purged with nitrogen prior to use. Deuterated solvents were used as received from Cambridge Isotopes and were purged with nitrogen under an inert atmosphere. When possible, pyrazole protons of the tris(pyrazolyl)borate (Tp) ligand were uniquely assigned (e.g., “Tp3B”) using two-dimensional NMR data. If unambiguous assignments were not possible, Tp protons were labeled as “Tp3/5 or Tp4”. All J values for Tp protons are 2(±0.4) Hz.

Compound 5

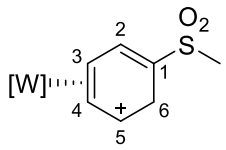

This species is thermally unstable and cannot be isolated. *in situ* ^{1}H-NMR data (d^{3}-MeCN, δ, 25 °C): 8.34 (1H, d, Tp3/5), 8.05 (1H, d, Tp3/5), 8.04 (1H, d, Tp3/5), 8.00 (1H, d, Tp3/5), 7.82 (1H, d, Tp3/5), 7.29 (1H, m, H5), 7.11 (1H, m, H2), 6.58 (1H, t, Tp4), 6.51 (1H, t, Tp4), 6.34 (1H, t, Tp4), 5.12 (1H, t J = 7.3, H3), 4.34 (1H, m, H4), 4.30 (1H, dm J = 25.7, H6a), 4.10 (1H, dm J = 25.5, H6b), 3.05 (3H, s, SO_2Me), 1.24 (9H, d J = 9.9, PMe_3).

Compound 8

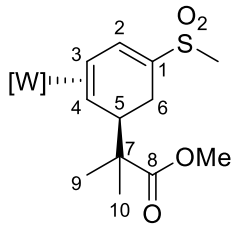

Compound **2** (1.50 g, 2.27 mmol) and MeCN were combined in a test tube to form an orange heterogeneous solution. The heterogeneous mixture was cooled to 0 °C for 15 min. A 1M HOTf/MeCN solution (4.32 mL, 4.32 mmol, −30 °C) was added to the reaction via syringe. Upon addition, the reaction became a dark red, homogeneous mixture. After 2 min, 1-methoxy-2-methyl-1- (trimethylsiloxy)propene (1.98 g, 2.31 mL, 11.4 mmol, −30 °C) was added to the reaction mixture. The reaction mixture was stirred for 16 h at 0 °C. Et_3N (2.30 g, 3.17 mL, 22.7 mmol, −30 °C) was then added to the reaction mixture. The reaction was removed from the box and evaporated to dryness to form a dark brown oil. A 60 mL medium-porosity fine frit was filled three-fourths full with silica and set in ether. Minimal acetone was used to pick the reaction oil up and loaded onto the column. Hexanes (100 mL) was eluted through the column, followed by diethyl ether (200 mL) and by ethyl acetate (250 mL). The ethyl acetate eluted a light brown

band, which was evaporated to dryness, redissolved in minimal DCM, then added to 30 mL of stirred pentane. An off-white solid precipitated out of the pentane and was collected on a 30 mL fine-porosity fitted disk, washed with diethyl ether (2 × 10 mL) and hexanes (2 × 15 mL), and then desiccated overnight to yield **8** (0.935 g, 1.23 mmol, 54.0%). CV (DMA): Ep,a = +0.74 V (NHE). IR: ν(NO) 1551 cm^{-1}, ν(SO) 1409 cm^{-1}. ^{1}H NMR (MeCN-d3, δ, 25 °C): 8.07 (1H, d, Tp3A), 8.04 (1H, d, Tp3B), 7.86 (2H, m, Tp5B, Tp5C), 7.80 (1H, d, Tp5A), 7.57 (1H, dd, J = 5.3, 2.8, H2), 7.50 (1H, d, Tp3C), 6.36 (1H, t, Tp4B), 6.32 (1H, t, Tp4A), 6.31 (1H, t, Tp4C), 3.49 (1H, d, J = 8.9, H5), 3.24 (3H, s, H9), 3.01 (1H, m, H3), 2.89 (3H, s, H12), 2.80 (1H, dd, J = 17.4, 9.3, H6y), 2.39 (1H, d, J = 17.4, H6x), 1.25 (3H, s, H10/H11), 1.21 (9H, d, J_{PH} = 8.6, PMe3), 1.09 (3H, s, H10/ H11), 0.97 (1H, d, J = 9.9, H4). ^{13}C NMR (MeCN-d3, δ, 25 °C): 179.2 (C8), 145.0 (d, J_{PC} = 2.5, C2), 144.5 (Tp3A), 142.3 (Tp3B), 142.1 (Tp3C), 138.1 (Tp5), 137.5 (Tp5A), 137.4 (Tp5), 127.7 (C1), 107.6 (Tp4B), 107.3 (Tp4C), 106.7 (Tp4A), 55.0 (C4), 52.3 (C7), 51.6 (C9), 50.0 (d, J_{PC} = 8.8, C3), 44.8 (C12), 43.3 (C5), 23.8 (C10/11), 22.9 (C6), 21.9 (C10/C11), 13.6 (3C, d, J_{PC} = 29.2, PMe_3) Anal. Calcd for $C_{24}H_{37}BN_7O_5PSW$: C, 37.87; H, 4.90; N, 12.88. Found: C, 38.11; H, 4.79; N, 12.92.

Compound 9

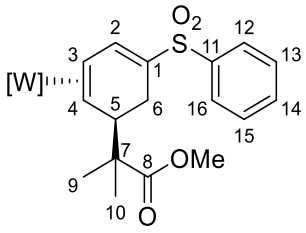

Compound **4** (2.00 g, 2.77 mmol) and MeCN were combined in a test tube to form an orange heterogenous solution. The heterogenous mixture was cooled to 0 °C for 15 min. 1M HOTf/MeCN (5.27 mL, 5.27 mmol, -30 °C) was added to the reaction. Upon addition, the reaction became a dark red, homogeneous mixture. After 15 min, 1-methoxy-2-methyl-1-(trimethylsiloxy)propene (2.42 g, 2.82 mL, 13.9 mmol, -30 °C) was added to the reaction mixture. The reaction was stirred for 16 hours at 0 °C. Et_3N (2.81 g, 3.86 mL, 27.7

mmol, -30 °C) was then added to the reaction. The reaction was removed from the glove box and evaporated to dryness to form a dark brown oil. A 150 mL medium porosity medium frit was filled ¾ full with silica and set in ether. Minimal acetone was used to pick the reaction oil up and load it onto the column. 300 mL of hexanes were eluted through the column, followed by 400 mL of ether, and finally 400 mL of ethyl acetate. The ethyl acetate eluted a light brown band, which was evaporated to dryness, redissolved in minimal DCM, then added dropwise to 30 mL of stirring pentane. An off-white solid precipitated out of the pentane and was collected on a 30 mL fine porosity fritted disc, washed with diethyl ether (2 x 10 mL) and hexanes (2 x 15 mL), and desiccated overnight to yield **9** (1.53 g, 1.86 mmol, 67%). CV (DMA): $E_{p,a}$= + 0.73 V (NHE). IR: *ν*(SO) 1405 cm^{-1}, *ν*(NO) 1563 cm^{-1}, *ν*(CO) 1721 cm^{-1}, *ν*(BH) 2473 cm^{-1}. ^{1}H-NMR (d_3-MeCN, δ, 25 °C): 8.03 (1H, d, TpA3), 8.00 (1H, d, TpB3), 7.88 (2H, m, H16, H12), 7.85 (1H, d, TpC5), 7.84 (1H, d, TpB5), 7.82 (1H, dd J = 5.9, 2.6, H2), 7.76 (1H, d, TpA5), 7.57 (1H, m, H14), 7.51 (3H, m, TpC3, H15, H13), 6.35 (1H, t, TpB4), 6.30 (1H, t, TpC4), 6.28 (1H, t, TpA4), 3.45 (1H, d J = 8.8, H5), 3.14 (3H, s, OMe), 2.98 (1H, m, H3), 2.66 (1H, dd J = 17.7, 9.1, H6b), 2.19 (1H, d J = 17.7, H6a), 1.24 (9H, d J = 8.6, PMe_3), 1.02 (3H, s, H10/9), 0.89 (1H, d J = 9.1, H4), 0.84 (3H, s, H10/9). ^{13}C-NMR (d_3-MeCN, δ, 25 °C): 179.1 (1C, C8), 146.8 (1C, d J = 2.8, C2), 144.4 (1C, TpB3), 143.3 (1C, C11), 142.4 (1C, TpA3), 142.1 (1C, TpC3), 138.1 (1C, TpC5), 137.5 (1C, TpB5), 137.4 (1C, TpA5), 133.3 (1C, C14), 129.8 (2C, C15/13), 128.6 (2C, C16, C12), 127.9 (1C, C1), 107.5 (1C, TpB4), 107.3 (1C, TpC4), 106.6 (1C, TpA4), 55.3 (1C, C4), 52.1 (1C, C7), 51.5 (1C, OMe), 50.7 (1C, d J = 8.1, C3), 43.3 (1C, C5), 28.8 (1C, C10/9), 22.5 (1C, C6), 21.1 (1C, C10/9), 13.9 (3C, d J = 29.3, PMe_3). Anal. Calcd for $C_{29}H_{39}BN_7O_5PSW \cdot H_2O$: C, 41.74; H, 4.73; N, 11.67 Found: C, 41.81; H, 4.73; N, 11.68.

Compound 10

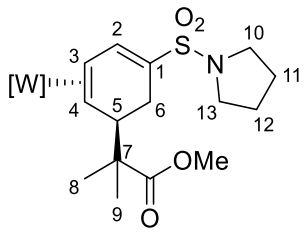

Compound **3** (0.100 g, 0.140 mmol) and MeCN were combined in a test tube to form an orange heterogenous solution. The heterogenous mixture was cooled to 0 °C for 15 min. 1M HOTf/MeCN (0.26 mL, 0.263 mmol, 0 °C) was added to the reaction via syringe. Upon addition, the reaction became a dark red, homogeneous mixture. After 30 min, 1-methoxy-2-methyl-1-(trimethylsiloxy)propene (0.11 g, 2.130 mL, 0.630 mmol, 0 °C) was added to the reaction mixture. The reaction was stirred for 16 hours at 0°C. Et_3N (0.127 g, 0.167 mL, 1.26 mmol) was then added to the reaction. The reaction was removed from the glove box and evaporated to dryness to form a dark brown oil. A 30 mL medium porosity fine frit was filled ¾ full with silica and set in ether. Minimal acetone was used to pick the reaction oil up and loaded onto the column. 50 mL of Hexanes were eluted through the column, followed by 100 mL of ethyl acetate. The ethyl acetate eluted a light brown band, which was evaporated to dryness, redissolved in minimal DCM, then added to 10 mL stirring pentane. An off-white solid precipitated out of the pentane and was collected on a 15 mL fine porosity fitted disc, washed with hexanes (3 x 15 mL), and desiccated overnight to yield **10** (0.060 g, 0.074 mmol, 53%). CV (DMA): $E_{p,a}$= + 0.72 V (NHE). IR: *ν*(SO) 1406 cm^{-1}, *ν*(NO) 1549 cm^{-1}, *ν*(CO) 1724 cm^{-1}, *ν*(BH) 2503 cm^{-1}. ^{1}H-NMR (d_3-MeCN, δ, 25 °C): 8.05 (1H, d, TpA3), 8.03 (1H, d, TpB3), 7.86 (2H, m, TpB5, TpC5). 7.79 (1H, d, TpA5), 7.51 (1H, d, TpC3), 7.48 (1H, dd J = 6.1, 2.8, H2), 6.36 (1H, t, TpB4), 6.31 (2H, m, TpA4, TpC4), 3.44 (1H, d J = 8.5, H5), 3.28 (2H, m, H13/10), 3.20 (2H, m, H13/10), 3.16 (3H, s, OMe), 3.00 (1H, m, H3), 2.71 (1H, ddm J = 16.9, 8.8, H6b), 2.42 (1H, d J = 16.6, H6a), 1.79 (4H, m, H12, H11), 1.26 (3H, s, H9/8), 1.20 (9H, d J = 8.6, PMe_3), 1.10 (3H, s, H9/8), 0.86 (1H, d J = 9.4, H4). ^{13}C-NMR (d_3-MeCN, δ, 25 °C): 179.3 (1C, C=O), 144.9 (1C, d J = 3.0, C2), 144.3 (1C, TpC3), 142.3 (1C, Tp3), 142.0 (1C,

Tp3), 138.1 (1C, Tp5), 137.5 (1C, Tp5), 137.4 (1C, Tp5), 126.0 (1C, C1), 107.6 (1C, TpB4), 107.3 (1C, Tp4), 106.7 (1C, Tp4), 55.1 (1C, C4), 52.3 (1C, C7), 51.5 (1C, OMe), 50.2 (1C, d J = 8.7, C3), 48.4 (2C, C13, C10), 43.4 (1C, C5), 26.2 (2C, C12, C11), 24.2 (1C, C9/8), 23.4 (1C, C6), 21.4 (1C, C9/8), 14.1 (3C, d J = 28.9, PMe_3). Anal. Calcd for $C_{27}H_{42}BN_8O_5PSW \cdot DCM$: C, 37.31; H, 4.92; N, 12.43 Found: C, 37.47; H, 4.79; N, 13.03.

Compound 11

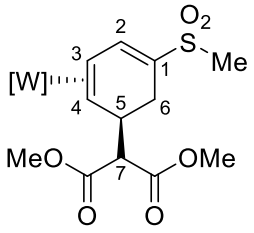

Compound **2** (0.100 g, 0.152 mmol) and MeCN were combined in a test tube to form an orange heterogeneous solution. Lithium dimethyl malonate (0.125 g, 0.910 mmol) and MeCN were combined in a second test tube to form a clear solution. Both solutions were cooled to 0 °C for 15 min. 1M HOTf/MeCN (0.30 mL, 0.303 mmol, -30 °C) was added to the reaction via syringe. Upon addition, the reaction became a dark red, homogeneous mixture. After 5 minutes, the cold bath was reduced to -30 °C. The protonated solution was added slowly to the lithium dimethyl malonate solution. The first test tube was rinsed with 0.5 mL of MeCN, which was added to the reaction. The reaction was stirred for 18 hrs. The test tube was removed from the glove box and evaporated to dryness. The resulting oil was purified by Combiflash flash chromatography on a 12 g silica column using a gradient elution of 0-100% ethyl acetate in hexanes. The fractions of 100% ethyl acetate containing the product were evaporated to dryness, picked up in minimal DCM, and precipitated into 10 mL of pentane yielding a light brown solid. The light brown precipitant was collected on a 15 mL fine porosity fitted disc, washed with hexanes (3 x 10 ml), and desiccated overnight to yield **11** (0.078 g, 0.099 mmol, 65%). CV (DMA): $E_{p,a}$= + 0.81 V (NHE). IR: *ν*(SO) 1406 cm^{-1}, *ν*(NO) 1556 cm^{-1}, *ν*(CO) 1726 cm^{-1}, *ν*(BH) 2489 cm^{-1}. ^{1}H-NMR (d_3-MeCN, δ, 25 °C): 8.05 (1H, d, TpB3), 7.98 (1H, d, TpA3),

7.88 (2H, d, TpB5, TpC5), 7.80 (1H, d, TpA5), 7.67 (1H, dd J = 5.7, 2.6, H2), 7.40 (1H, d, TpC3), 6.38 (1H, t, TpB4), 6.35 (1H, t, TpA4), 6.30 (1H, t, TpC4), 3.68 (3H, s, CO_2Me), 3.52 (2H, m, H5, H7). 3.44 (3H, s, CO_2Me), 2.91 (1H, m, H3), 2.90 (3H, s, SO_2Me), 2.86 (1H, ddm J = 17.1, 6.1, H6B), 2.27 (1H, d J = 16.8, H6A), 1.22 (9H, d J = 8.8, PMe_3), 1.11 (1H, d J = 9.2, H4). ^{13}C-NMR (d_3-MeCN, δ, 25 °C): 170.7 (1C, C=O), 170.3 (1C, C=O), 145.6 (1C, d J = 3.0, C2), 144.5 (1C, TpB3), 142.9 (1C, TpA3), 141.9 (1C, TpC3), 138.3 (1C, Tp5), 137.7 (1C, Tp5), 137.3 (1C, TpA5), 126.4 (1C, C1), 107.7 (1C, Tp4), 107.5 (1C, Tp4), 107.0 (1C, Tp4), 60.9 (1C, C7), 59.0 (1C, C4), 52.9 (1C, OMe), 52.6 (1C, OMe), 48.0 (1C, d J = 8.9, C3), 45.1 (1C, SO_2Me), 38.3 (1C, C5), 26.3 (1C, C6), 13.6 (3C, J = 30.2, PMe_3). Anal. Calcd for $C_{24}H_{35}BN_7O_7PSW \cdot H_2O$: C, 35.62; H, 4.61; N, 12.12. Found: C, 35.37; H, 4.55; N, 12.46.

Compound 12

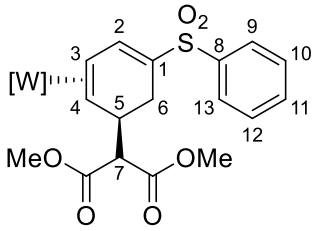

Compound **4** (0.100 g, 0.138 mmol) and MeCN were combined in a test tube to form an orange heterogeneous solution. Lithium dimethyl malonate (0.114 g, 0.832 mmol) and MeCN were combined in a second test tube to form a clear solution. Both solutions were cooled to 0 °C for 15 min. 1M HOTf/MeCN (0.277 mL, 0.277 mmol, -30 °C) was added to the reaction. Upon addition, the reaction became a dark red, homogeneous mixture. After 15 minutes, the cold bath was reduced to -30 °C. The protonated solution was added slowly to the lithium dimethyl malonate solution. The first test tube was rinsed with 0.5 mL of MeCN, which was added to the reaction. The reaction was stirred for 18 hrs. The test tube was removed from the box and evaporated to dryness. The resulting oil was purified by Combiflash flash chromatography on a 12 g silica column using a gradient elution of 0-100% ethyl acetate in hexanes. The

fractions of 100% ethyl acetate contains the product were evaporated to dryness, picked up in minimal DCM, and precipitated into 10 mL of pentane yielding an off white solid. The off-white precipitant was collected on a 15 mL fine porosity fitted disc, washed with hexanes (3 x 10 ml), and desiccated overnight to yield **12** (0.072 g, 0.084 mmol, 61%). CV (DMA): $E_{p,a}$= + 0.82 V (NHE). IR: *ν*(SO) 1406 cm^{-1}, *ν*(NO) 1555 cm^{-1}, *ν*(CO) 1728 cm^{-1}, *ν*(BH) 2525 cm^{-1}. ^{1}H-NMR (d_3-MeCN, δ, 25 °C): 8.01 (1H, d, TpB3), 7.92 (1H, d, TpA3), 7.91 (1H, m, H2), 7.87 (1H, d, TpB5), 7.86 (1H, d, TpC5), 7.83 (2H, m, H9, H13), 7.76 (1H, d, TpA5), 7.58 (1H, m, H11), 7.52 (2H, m, H10, H12), 7.40 (1H, d, TpC3), 6.37 (1H, t, TpC4), 6.30 (1H, t, TpA4), 6.28 (1H, t, TpB4), 3.46 (3H, s, OMe), 3.40 (1H, m, H5), 3.35 (3H, s, OMe), 3.07 (1H, d J = 10.4, H7), 2.90 (1H, m, H3), 2.77 (1H, , J = 17.3, 6.5, H6b), 2.07 (1H, d J = 16.9, H6a), 1.24 (9H, d J = 8.7, PMe_3), 0.90 (1H, d J = 9.1, H4). ^{13}C-NMR (d_3-MeCN, δ, 25 °C): 170.3 (1C, C=O), 170.2 (1C, C=O), 147.1 (1C, d J = 2.7, C2), 144.5 (1C, TpB3), 143.2 (1C, C8), 142.8 (1C, TpA3), 141.7 (1C, TpC3), 138.3 (1C, Tp5), 137.7 (1C, Tp5), 137.2 (1C, TpA5), 133.3 (1C, C11), 129.9 (2C, C10, C12), 128.3 (2C, C9, C13), 126.5 (1C, C1), 107.7 (1C, Tp4), 107.4 (1C, Tp4), 107.0 (1C, TpB4), 59.9 (1C, C7), 58.4 (1C, C4), 52.9 (1C, OMe), 52.4 (1C, OMe), 48.4 (1C, d J = 8.6, C3), 37.9 (1C, C5), 26.3 (1C, C6), 13.4 (3C, d J = 28.8, PMe_3). Anal. Calcd for $C_{29}H_{37}BN_7O_7PSW \cdot 1/3DCM$: C, 39.96; H, 4.31; N, 11.12. Found: C, 39.66; H, 4.33; N, 10.99.

Compound 13

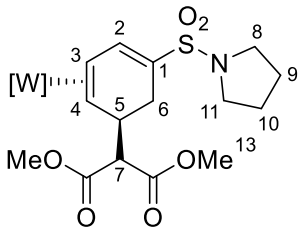

Compound **3** (0.110 g, 0.154 mmol) and MeCN were combined in a test tube to form an orange heterogeneous solution. Lithium dimethyl malonate (0.127 g, 0.924 mmol) and MeCN were combined in a second test tube to form a clear solution. Both solutions were cooled to 0 °C for 15 min. 1M HOTf/MeCN

(0.30 mL, 0.300 mmol, -30 °C) was added to the reaction. Upon addition, the reaction became a dark red, homogeneous mixture. After 15 minutes, the cold bath was reduced to -30 °C. The protonated solution was added slowly to the lithium dimethyl malonate solution. The first test tube was rinsed with 0.5 mL of MeCN, which was added to the reaction. The reaction was stirred for 18 hrs. The test tube was removed from the box and evaporated to dryness. The resulting oil was purified by Combiflash flash chromatography on a 12 g silica column using a gradient elution of 0-100% ethyl acetate in hexanes. The fractions of 100% ethyl acetate contains the product were evaporated to dryness, picked up in minimal DCM, and precipitated into 10 mL of pentane yielding off white solid. The off-white precipitant was collected on a 15 mL fine porosity fitted disc, washed with hexanes (3 x 10 ml), and desiccated overnight to yield **13** (0.081 g, 0.096 mmol, 62%). CV (DMA): $E_{p,a}$= + 0.79 V (NHE). IR: *v*(SO) 1406 cm^{-1}, *v*(NO) 1559 cm^{-1}, *v*(CO) 1736 cm^{-1}, *v*(BH) 2505 cm^{-1}. ^{1}H-NMR (d_3-MeCN, δ, 25 °C): 8.04 (1H, d, TpB3), 7.95 (1H, d, TpA3), 7.89 (1H, d, Tp5), 7.88 (1H, d, Tp5), 7.79 (1H, d, TpA5), 7.56 (1H, dd J = 5.9, 2.5, H2), 7.40 (1H, d, TpC3), 6.39 1H , t, TpB4), 6.34 (1H, t, TpA4), 6.30 (1H, t, TpC4), 3.67 (3H, s, OMe), 3.48 (1H, d J = 10.3, H7), 3.47 (1H, m, H5), 3.40 (3H, s, OMe), 3.19 (4H, m, H11, H8), 2.19 (1H, m, H3), 2.78 (1H, dd J = 16.5, 5.8, H6a), 2.30 (1H, d J = 16.5, H6b), 1.79 (4H, H10, H9), 1.21 (9H, d J = 8.6, PMe_3), 0.93 (1H, d J = 9.4, H4). ^{13}C-NMR (d_3-MeCN, δ, 25 °C): 170.6 (1C, C=O), 170.4 (1C, C=O), 145.0 (1C, d J = 2.2, C2), 144.3 (1C, TpB3), 142.9 (1C, TpA3), 141.7 (1C, TpC3), 138.3 (1C, Tp5), 137.7 (1C, Tp5), 137.3 (1C, TpA5), 124.1 (1C, C1), 107.7 (1C, TpB4), 107.5 (1C, TpC4), 107.0 (1C, TpA4), 60.4 (1C, C7), 58.4 (1C, C4), 52.9 (1C, OMe), 52.5 (1C, OMe), 48.3 (2C, C11, C8), 48.0 (1C, d J = 9.1, C3), 38.2 (1C, C5), 27.2 (1C, C6), 26.0 (2C, C10, C9), 13.9 (3C, d J = 29.1, PMe_3). Anal. Calcd for $C_{27}H_{40}BN_8O_7PSW \cdot 2/3LiOTf$: C, 34.97; H, 4.24; N, 11.79. Found: C, 35.03; H, 4.42; N, 11.54.

Compound 14

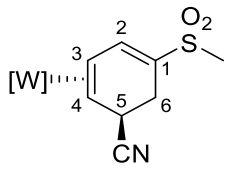

Compound **2** (0.100 g, 0.152 mmol) and MeCN were combined in a test tube to form an orange heterogeneous solution. NaCN (0.037 g, 0.760 mmol) and MeOH were combined in a second test tube to form a clear solution. Both solutions were cooled to 0 °C for 15 min. 1M HOTf/MeCN (0.230 mL, 0.230 mmol, -30 °C) was added to the reaction via syringe. Upon addition, the reaction became a dark red, homogeneous mixture. After 5 minutes, the protonated solution was added slowly to the NaCN solution. The first test tube was rinsed with 0.5 mL of MeCN, which was added to the reaction. The reaction was stirred for 15 hrs. The test tube was removed from the box and evaporated to dryness. The resulting oil was purified by Combiflash flash chromatography on a 12 g silica column using a gradient elution of 0-100% ethyl acetate in hexanes. The fractions of 100% ethyl acetate containing the product were evaporated to dryness, picked up in minimal DCM, and precipitated into 10 mL of pentane yielding white solid. The white precipitant was collected on a 15 mL fine porosity fitted disc, washed with hexanes (3 x 10 ml), and desiccated overnight to yield **14** (0.059 g, 0.085 mmol, 56%). CV (DMA): $E_{p,a}$= + 0.97 V (NHE). IR: *ν*(SO) 1405 cm^{-1}, *ν*(NO) 1571 cm^{-1}, *ν*(CN) 2225 cm^{-1}, *ν*(BH) 2502 cm^{-1}. ^{1}H-NMR (d_3-MeCN, δ, 25 °C): 8.05 (1H, d, TpB3), 7.89 (2H, d, TpA5, TpB5), 7.81 (1H, d, TpA3), 7.80 (1H, d, TpC5), 7.79 (1H, dd J = 5.7, 2.5, H2), 7.49 (1H, d, TpC3), 6.39 (1H, t, TpB4), 6.33 (2H, t, TpA4, TpC4), 3.91 (1H, m, H5), 3.03 (1H, m, H3), 2.94 (3H, s, SO_2Me), 2.87 (1H, ddm J = 16.8, 6.7, H6a), 2.67 (1H, d J = 16.8, H6b), 1.53 (1H, d J = 9.1, H4), 1.25 (9H, d J = 9.0, PMe_3). ^{13}C-NMR (d_3-MeCN, δ, 25 °C): 146.0 (1C, C2), 144.6 (1C, TpB3), 142.7 (1C, TpA3), 142.2 (TpC3), 138.4 (1C, Tp5), 138.0 (1C, Tp5), 137.5 (1C, TpC5), 127.5 (1C, CN), 125.9 (1C, C1), 107.8 (1C, Tp4), 107.6 (1C, Tp4), 107.4 (1C, Tp4), 57.67 (1C, d J = 2.5, C4), 47.0 (1C, d J = 9.3, C3), 45.1 (1C, SO_2Me),

30.0 (1C, C5), 26.9 (1C, C6), 13.6 (3C, d J = 30.1, PMe_3). Anal. Calcd for $C_{20}H_{28}BN_8O_3PSW \cdot 1/3DCM$: C, 34.18; H, 4.04; N, 15.68. Found: C, 34.22; H, 4.19; N, 15.75.

Compound 15

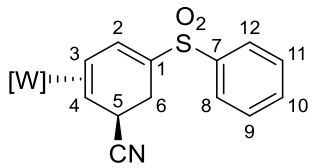

Compound **4** (0.100 g, 0.138 mmol) and MeCN were combined in a test tube to form an orange heterogeneous solution. NaCN (0.034 g, 0.690 mmol) and MeOH were combined in a second test tube to form a clear solution. Both solutions were cooled to 0 °C for 15 min. 1M HOTf/MeCN (0.21 mL, 0.210 mmol, -30 °C) was added to the reaction via syringe. Upon addition, the reaction became a dark red, homogeneous mixture. After 15 minutes, the protonated solution was added slowly to the NaCN solution. The first test tube was rinsed with 0.5 mL of MeCN, which was added to the reaction. The reaction was stirred for 16 hrs. A white precipitant was found to have crashed out of solution overnight. The white precipitant was collected on a 15 mL fine porosity fitted disc, washed with hexanes (3 x 10 ml), and desiccated overnight to yield **15** (0.052 g, 0.069 mmol, 50%). CV (DMA): $E_{p,a}$= + 0.99 V (NHE). IR: *ν*(SO) 1406 cm^{-1}, *ν*(NO) 1547 cm^{-1}, *ν*(CN) 2350 cm^{-1}, *ν*(BH) 2488 cm^{-1}. ^{1}H-NMR (d_3-MeCN, δ, 25 °C): 8.02 (1H, dd J = 6.0, 2.5, H2), 7.99 (1H, d, TpB3), 7.90 (2H, m, H12, H8), 7.87 (1H, d, TpC5), 7.86 (1H, d, TpB5), 7.77 (1H, d, TpA5), 7.75 (1H, d, TpA3), 7.58 (1H, m, H10), 7.52 (2H, m, H11, H9), 7.50 (1H, d, TpC3), 6.37 (1H, t, TpB4), 6.32 (1H, t, TpC4), 6.29 (1H, t, TpA4), 3.83 (1H, m, H5), 3.01 (1H, m, H3), 2.76 (1H, ddm J = 16.6, 6.8, H6b), 2.50 (1H, d J = 16.5, H6a), 1.49 (1H, d J = 9.3, H4), 1.26 (9H, d J = 8.8, PMe_3). ^{13}C-NMR (d_3-MeCN, δ, 25 °C): 147.6 (1C, d J = 2.8, C2), 144.6 (1C, TpB3), 143.4 (1C, C7), 142.7 (1C, TpA3), 142.2 (1C, TpC3), 138.4 (1C, TpB5), 138.0 (1C, TpC5), 137.5 (1C, TpA5), 133.5 (1C, C10), 129.9 (2C, C11, C9), 128.5 (2C, C12, C8), 127.2 (1C, CN), 126.2 (1C, C1), 107.9 (1C, TpB4), 107.6 (1C, TpC4), 107.4 (1C, TpA4), 57.9 (1C, C4), 47.7

(1C, d J = 9.3, C3), 30.1 (1C, C5), 26.9 (1C, C6), 14.0 (3C, d J = 29.6, PMe_3). Anal. Calcd for $C_{25}H_{30}BN_8O_3PSW$ ·1/2DCM: C, 38.73; H, 3.95; N, 14.17. Found: C, 38.47; H, 4.05; N, 14.16.

Compound 16

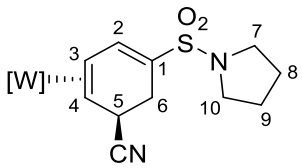

Compound **3** (0.100 g, 0.140 mmol) and MeCN were combined in a test tube to form an orange heterogeneous solution. NaCN (0.034 g, 0.700 mmol) and MeOH were combined in a second test tube to form a clear solution. Both solutions were cooled to 0 °C for 15 min. 1M HOTf/MeCN (0.210 mL, 0.210 mmol, -30 °C) was added to the reaction via syringe. Upon addition, the reaction became a dark red, homogeneous mixture. After 15 minutes, the protonated solution was added slowly to the NaCN solution. The first test tube was rinsed with 0.5 mL of MeCN, which was added to the reaction. The reaction was stirred for 16 hrs. A white precipitant was found to have crashed out of solution overnight. The white precipitant was collected on a 15 mL fine porosity fitted disc, washed with hexanes (3 x 10 ml), and desiccated overnight to yield **16** (0.043 g, 0.059 mmol, 42%). CV (DMA): $E_{p,a}$= + 0.93 V (NHE). IR: *ν*(SO) 1406 cm^{-1}, *ν*(NO) 1559 cm^{-1}, *ν*(CN) 2361 cm^{-1}, *ν*(BH) 2512 cm^{-1}. ^{1}H-NMR (d_3-MeCN, δ, 25 °C): 8.04 (1H, d, TpB3), 7.89 (2H, d, TpB5, TpC5), 7.80 (1H, d, TpA5), 7.79 (1H, TpA3), 7.67 (1H, dd J = 6.1, 2.7, H2), 7.50 (1H, d, TpC3), 6.39 (1H, t, TpB4), 6.33 (1H, t, TpC4), 6.32 (1H, t, TpA4), 3.83 (1H, m, H5), 3.27 (4H, m, H10, H7), 3.01 (1H, m, H3), 2.81 (1H, ddm J = 16.8, 6.7, H6b), 2.63 (1H, d J = 16.3, H6a), 1.83 (4H, m, H9, H8), 1.44 (1H, d J = 9.5, H4), 1.23 (9H, d J = 8.7, PMe_3). ^{13}C-NMR (d_3-MeCN, δ, 25 °C): 145.4 (1C, d J = 2.9, C2), 144.4 (1C, TpB3), 142.6 (1C, TpA3), 142.1 (1C, TpC3), 138.4 (1C, Tp5), 137.9 (1C, Tp5), 137.5 (1C, TpA5), 127.6 (1C, CN), 123.5 (1C, C1), 107.8 (1C, TpB4), 107.6 (1C, Tp4), 107.4 (1C, Tp4), 57.4 (1C, C4), 48.5 (2C,

C10, C7), 47.1 (1C, d J = 9.6, C3), 30.0 (1C, C5), 27.8 (1C, C6), 26.1 (2C, C9, C8), 13.9 (3C, d J = 28.8, PMe_3). Anal. Calcd for $C_{23}H_{33}BN_9O_3PSW \cdot 1/3NaOTf$: C, 35.09; H, 4.17; N, 15.79. Found: C, 34.86; H, 4.39; N, 15.92.

Compound 17

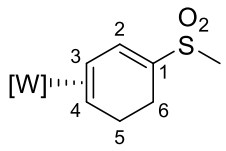

Compound **2** (0.100 g, 0.152 mmol) and MeCN were combined in a test tube to form an orange heterogeneous solution. Tetrabutylammonium borohydride (0.117 g, 0.455 mmol) and MeCN were combined in a second test tube to form a clear solution. Both solutions were cooled to 0 °C for 15 min. 1M HOTf/MeCN (0.167 mL, 0.167 mmol, -30 °C) was added to the reaction. Upon addition, the reaction became a dark red, homogeneous mixture. After 5 minutes, the protonated solution was added slowly to the tetrabutylammonium borohydride solution. The first test tube was rinsed with 0.5 mL of MeCN, which was added to the reaction. Reaction may turn blue. The reaction was stirred for 18 hrs. The reaction was warmed to room temperature and removed from the glovebox. H_2O (13 mL) was added slowly to the stirring solution to induce precipitation of a white solid. The white solid was collected on a 15 mL fine porosity fritted disc, wash with ether (2 x 10 mL) and hexanes (3 x 10 mL), then desiccated overnight to yield **17** (0.062 g, 0.094 mmol, 62%). CV (DMA): $E_{p,a}$= + 0.72 V (NHE). IR: *ν*(SO) 1401 cm^{-1}, *ν*(NO) 1551 cm^{-1}, *ν*(BH) 2485 cm^{-1}. ^{1}H-NMR (d_3-MeCN, δ, 25 °C): 8.04 (1H, d, TpB3), 7.97 (1H, d, TpA3), 7.87 (1H, d, TpB5), 7.86 (1H, d, TpC5), 7.78 (1H, d, TpA5), 7.67 (1H, dd J = 5.8, 2.4, H2), 7.45 (1H, d, TpC3), 6.37 (1H, t, TpB4), 6.31 (1H, t, TpA4), 6.29 (1H, t, TpC4), 3.45 (1H, m, H5a), 2.94 (1H, m, H3), 2.90 (3H, s, SO_2Me), 2.82 (1H, ddm J = 14.2, 7.1, H5b), 2.56 (1H, m, H6b), 2.34 (1H, dd J = 15.9, 6.3, H6a), 1.36 (1H, m, H4), 1.25 (9H, d J = 8.6, PMe_3). ^{13}C-NMR (d_3-MeCN, δ, 25 °C): 145.7 (1C, d J = 2.7, C2), 144.4 (1C, TpB3), 142.7 (1C, TpA3), 142.0 (1C, TpC3), 138.1 (1C, TpC5), 137.5 (1C, TpB5), 137.1 (1C, TpA5), 129.1 (1C, C1), 107.6 (1C, TpB4),

107.3 (1C, TpC4), 107.0 (1C, TpA4), 57.1 (1C, C4), 48.9 (1C, d J = 8.5, C3), 45.1 (1C, SO_2Me), 27.0 (1C, C5), 23.0 (1C, C6), 13.8 (3C, d J = 28.7, PMe_3). Anal. Calcd for $C_{19}H_{29}BN_7O_3PSW$: C, 34.53; H, 4.42; N, 14.83. Found: C, 34.35; H, 4.27; N, 14.49.

Compound 18

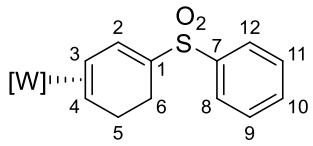

Compound **4** (0.100 g, 0.138 mmol) and MeCN were combined in a test tube to form an orange heterogeneous solution. Sodium borohydride (0.013 g, 0.344 mmol) and MeCN were combined in a second test tube to form a clear solution. Both solutions were cooled to 0 °C for 15 min. 1M HOTf/MeCN (0.150 mL, 0.150 mmol, -30 °C) was added to the reaction. Upon addition, the reaction became a dark red, homogeneous mixture. After 5 minutes, the protonated solution was added slowly to the sodium borohydride solution. The first test tube was rinsed with 0.5 mL of MeCN, which was added to the reaction. Reaction may turn blue. The reaction was stirred for 16 hrs. The reaction was warmed to room temperature and removed from the glovebox. H_2O (13 mL) was added slowly to the stirring solution to induce precipitation of a white solid. The white solid was collected on a 15 mL fine porosity fritted disc, wash with ether (2 x 10 mL) and hexanes (3 x 10 mL), then desiccated overnight to yield **18** (0.068 g, 0.094 mmol, 68%). CV (DMA): $E_{p,a}$= + 0.72 V (NHE). IR: *ν*(SO) 1405 cm^{-1}, *ν*(NO) 1557 cm^{-1}, *ν*(BH) 2474 cm^{-1}. ^{1}H-NMR (d_3-MeCN, δ, 25 °C): 7.98 (1H, d, TpB3), 7.93 (1H, dd J = 6.0, 2.5, H2), 7.91 (1H, d, TpA3), 7.87 (2H, m, H12, H8), 7.84 (2H, d, TpB5, TpC5), 7.75 (1H, d, TpA5), 7.55 (1H, m, H10), 7.49 (2H, m, H11, H9), 7.46 (1H, d, TpC3), 6.35 (1H, t, TpB4), 6.28 (1H, t, TpC4), 6.26 (1H, t, TpA4), 3.25 (1H, m, H5a), 2.91 (1H, m, H3), 2.75 (1H, m, H5b), 2.41 (1H, m, H6b), 2.14 (1H, dd J = 16.2, 5.8, H6a), 1.32 (1H, d J = 10.0, H4), 1.26 (9H, d J = 8.6, PMe_3). ^{13}C-NMR (d_3-MeCN, δ, 25 °C): 147.7 (1C, d J = 2.7, C2), 144.3 (1C, TpB3), 143.9 (1C, C7), 142.6 (1C, TpA3), 142.0 (1C, TpC3), 138.1 (1C, Tp5), 137.5 (1C, Tp5), 137.1 (1C, Tp5), 133.1 (1C, C10), 129.7 (2C,

C11, C9), 129.0 (1C, C1), 128.3 (2C, C12, C8), 107.4 (1C, TpB4), 107.3 (1C, TpC4), 106.9 (1C, TpA4), 57.3 (1C, C4), 49.5 (1C, d J = 8.6, C3), 27.3 (1C, C5), 22.9 (1C, C6), 14.1 (3C, d J = 29.4, PMe_3). Anal. Calcd for $C_{24}H_{31}BN_7O_3PSW \cdot 1/4NaOTf$: C, 38.01; H, 4.08; N, 12.80. Found: C, 38.18; H, 4.26; N, 13.10.

Compound 19

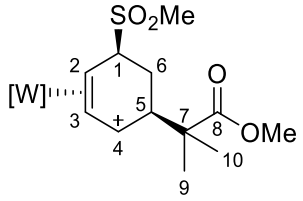

Complex is unstable in solution. Partial characterization ^{1}H-NMR (d^3-MeCN, δ, 25 °C): 8.35 (1H, d, Tp3/5), 8.04 (1H, d, Tp3/5), 8.02 (1H, d, Tp3/5), 7.99 (1H, d, Tp3/5), 7.95 (1H, d, Tp3/5), 7.84, (1H, d, Tp3/5), 6.55 (1H, t, Tp4), 6.52 (1H, t, Tp4), 6.36 (1H, t, Tp4), 6.08 (1H, d J = 8.1, H4), 5.52 (1H, tm J = 7.8, H3), 4.61 (1H, ddm J = 15.5, 6.9, H2), 4.13 (1H, t J = 8.9, H1), 3.94 (1H, t J = 8.4, H5), 3.74 (3H, s, OMe), 3.01 (3H, s, SO_2Me), 1.35 (1H, s, H10/9), 1.33 (3H, s, H10/9), 1.22 (9H, d J = 9.3, PMe_3).

Compound 20

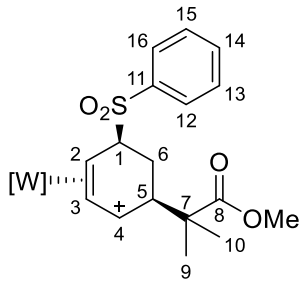

Complex is unstable in solution. Partial Characterization ^{1}H-NMR (d^3-MeCN, δ, 25 °C): 8.34 (1H, d, Tp3/5), 8.05 (1H, d, Tp3/5), 8.00 (1H, d, Tp3/5), 7.99 (2H, m, H16, H12), 7.97 (1H, d, Tp3/5), 7.96 (1H, d, Tp3/5), 7.83 (1H, d, Tp3/5), 7.82 (1H, m, H14), 7.72 (2H, m, H15, H13), 6.58 (1H, t, Tp4), 6.52 (1H, t, Tp4), 6.34 (1H, t, Tp4), 6.00 (1H, d J = 8.2, H4), 5.50 (1H, tm J = 7.8, H3), 4.77 (1H, dd J = 15.7, 6.7, H2), 4.18

(1H, t J = 8.2, H1), 3.78 (1H, t J = 8.61, H5), 3.63 (3H, s, OMe), 3.01 (3H, s, SO_2Me), 1.26 (9H, d J = 9.8, PMe_3), 1.20 (3H, s, H10/9), 1.16 (3H, s, H10/9).

Compound 22

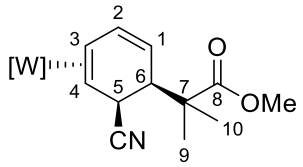

Compound **23** (0.400 g, 0.507 mmol) and 15 mL of THF were combined in a 4-dram vial with a stir pea. The heterogenous cloudy mixture was stirred for an hour. A 150 mL medium porosity fritted disc was filled ¾ full of silica and set in ether. The heterogenous reaction was loaded onto the silica column and eluted with 250 mL of ethyl acetate. No bands visible to the eye were observed to have eluted. All eluant was combined and evaporated to dryness. The resulting oil was picked up in minimal DCM and precipitated into 20 mL of stirring pentane to yield a white solid. The white precipitant was collected on a 15 mL fine porosity fritted disc, was with hexanes (3 x 10 mL), and desiccated overnight to yield **22** (0.214 g, 0.302 mmol, 60%). CV (DMA): $E_{p,a}$= + 0.73 V (NHE). IR: *ν*(NO) 1575 cm^{-1}, *ν*(CO) 1718 cm^{-1}, *ν*(CN) 2359 cm^{-1}, *ν*(BH) 2503 cm^{-1}. ^{1}H-NMR (d_3-MeCN, δ, 25 °C): 8.03 (1H, d, TpB5), 7.87 (1H, d, TpB3), 7.85 (1H, d, TpC3), 7.79 (2H, TpA5, TpA3), 7.43 (1H, d, TpC5), 6.66 (1H, m, H2), 6.37 (1H, t, TpB4), 6.34 (1H, t, TpA4), 6.29 (1H, t, TpC4), 5.02 (1H, d J = 10.4, H1), 3.74 (3H, s, OMe), 3.34 (1H, m, H5), 3.16 (1H, m, H6), 3.01 (1H, m, H3), 1.37 (3H, s, H10/9), 1.32 (3H, s, H10/9), 1.24 (9H, d J = 8.7, PMe_3), 1.21 (1H, d J = 9.6, H4). ^{13}C-NMR (d_3-MeCN, δ, 25 °C): 178.5 (1C, C8), 144.4 (1C, TpB5), 142.4 (1C, TpA5), 141.8 (1C, TpC5), 138.0 (1C, TpC3), 137.6 (1C, TpB3), 137.1 (1C, TpA3), 133.9 (1C, C2), 127.4 (1C, CN), 116.8 (1C, C1), 107.5 (1C, Tp4), 107.4 (1C, Tp4), 107.3 (1C, Tp4), 59.2 (1C, C4), 52.4 (1C, OMe), 48.6 (1C, d J = 10.9, C3), 45.4 (1C, C7), 43.5 (1C, C6), 31.7 (1C, C5), 27.2 (1C, C10/9), 20.7 (1C, C10/9), 13.7 (3C, d J = 28.9, PMe_3). Anal. Calcd for $C_{24}H_{34}BN_8O_3PW$: C, 40.70; H, 4.84; N, 15.82. Found: C, 40.85; H, 4.76; N, 15.55.

Compound 23

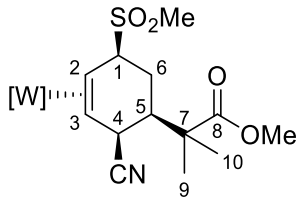

Compound **8** (0.700 g, 0.919 mmol) and MeCN were combined in a test tube. NaCN (0.135 g, 2.757 mmol), MeOH, and a stir pea were combined in a second test tube. Both solutions were cooled to -30 °C for 15 min. 1M HOTf/MeCN (1.10 mL, 1.10 mmol, -30 °C) was added to the solution of **8** and MeCN via syringe. The reaction turned a dark brown upon addition of the acid. After 15 min, the reaction was added to the solution of NaCN and MeOH. 2 mL of MeCN were used to rinse the first test tube and added to the reaction solution. The reaction was stirred for 24 hrs. A white precipitant formed in the solution overnight. The white solid was collected on a 30 mL fine porosity fritted disc and washed with ether (3 x 15 mL) and desiccated overnight yielding **23** (0.470 g, 0.596 mmol, 65%). CV (DMA): $E_{p,a}$= + 0.69 V (NHE). IR: *ν*(SO) 1405 cm^{-1}, *ν*(NO) 1542 cm^{-1}, *ν*(CO) 1719 cm^{-1}, *ν*(CN) 2215 cm^{-1}, *ν*(BH) 2517 cm^{-1}. ^{1}H-NMR (d_3-MeCN, δ, 25 ^{o}C): 8.05 (1H, d, TpB3), 7.87 (1H, d, TpC5), 7.86 (1H, d, TpB5), 7.78 (1H, d, TpA5), 7.66 (1H, d, TpA3), 7.36 (1H, d, TpC3), 6.36 (1H, t, TpB4), 6.31 (2H, m, TpA4, TpC4), 4.45 (1H, m, H1), 3.71 (3H, s, OMe), 3.39 (1H, bs, H4), 3.06 (3H, s, SO_2Me), 2.93 (1H, m, H2), 2.62 (1H, dt J = 13.2, 3.0, H5), 2.07 (1H, m, H6b), 1.87 (1H, m, H6a), 1.35 (3H, s, H10/9), 1.34 (3H, s, H10/9), 1.22 (9H, d J = 8.9, PMe_3), 1.20 (1H, d J = 11.3, H3). ^{13}C-NMR (d_3-MeCN, δ, 25 ^{o}C): 178.1 (1C, C=O), 145.2 (1C, TpB3), 143.9 (1C, TpA3), 142.4 (1H, TpC3), 138.2 (1H, Tp5), 138.0 (1C, Tp5), 137.9 (1C, Tp5), 127.0 (1C, CN), 107.6 (1C, TpB4), 107.4 (1C, Tp4), 107.3 (1C, Tp4), 64.5 (1C, C1), 59.1 (1C, C3), 52.3 (1C, OMe), 46.1 (1C, C7), 39.7 (1C, C5), 37.8 (1C, d J = 11.7, C2), 37.0 (1C, SO_2Me), 32.1 (1C, C4), 25.8 (1C, C10/9), 25.4 (1C, C6), 21.1 (1C, C10/9), 13.5 (3C, d J = 29.0, PMe_3). Anal. Calcd for $C_{25}H_{38}BN_8O_5PSW \cdot 1/4NaOTf$: C, 36.48; H, 4.61; N, 13.48. Found: C, 36.83; H, 4.78; N, 13.69.

Compound 24

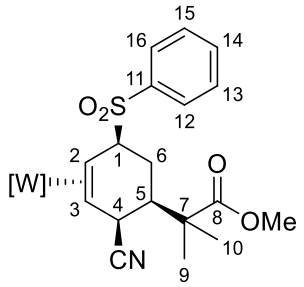

Compound **9** (0.200 g, 0.243 mmol) and MeCN were combined in a test tube. NaCN (0.038 g, 0.729 mmol), MeOH, and a stir pea were combined in a second test tube. Both solutions were cooled to -30 °C for 15 min. 1M HOTf/MeCN (0.29 mL, 0.29 mmol, -30 °C) was added to the solution of **9** and MeCN via syringe. The reaction turned a dark brown upon addition of the acid. After 15 min, the reaction was added to the solution of NaCN and MeOH. 1 mL of MeCN were used to rinse the first test tube and added to the reaction solution. The reaction was stirred for 24 hrs. A white precipitant formed in the solution overnight. The white solid was collected on a 15 mL fine porosity fritted disc and washed with ether (3 x 10 mL) and desiccated overnight yielding **24** (0.15 g, 0.176 mmol, 72%). CV (MeCN): $E_{p,a}$= + 0.78 V (NHE). IR: *v*(SO) 1405 cm^{-1}, *v*(NO) 1541 cm^{-1}, *v*(CO) 1714 cm^{-1}, *v*(CN) 2336 cm^{-1}, *v*(BH) 2520 cm^{-1}. ^{1}H-NMR (d_3-MeCN, δ, 25 ^{o}C): 8.05 (1H, d, TpB3), 8.01 (2H, dm J = 8.3, H16, H12), 7.88 (1H, d, TpC5), 7.86 (1H, d, TpB5), 7.78 (1H, d, TpA5), 7.76 (1H, tt J = 7.5, 1.1, H14), 7.69 (2H, t J = 8.1, H15, H13), 7.60 (1H, d, TpA3), 7.38 (1H, d, TpC3), 6.36 (1H, t, TpB4), 6.34 (1H, t, TpC4), 6.29 (1H, t, Tp A4), 4.58 (1H, m, H1), 3.62 (3H, s, OMe), 3.34 (1H, bs, H4), 3.15 (1H, m, H2), 2.41 (1H, dt J = 13.2, 2.9, H5), 1.76 (1H, q J = 13.2, H6a), 1.47 (1H, ddt J = 13.2, 6.9, 1.9, H6b), 1.32 (9H, d J = 9.0, PMe_3), 1.19 (3H, s, C10/9), 1.14 (3H, s, C10/9), 1.11 (1H, d J = 11.3, H3). ^{13}C-NMR (d_3-MeCN, δ, 25 ^{o}C): 177.8 (1C, C=O), 145.2 (1C, TpB3), 143.8 (1C, TpA3), 142.3 (1H, TpC3), 138.8 (1C, C11), 138.2 (1H, Tp5), 138.0 (1C, Tp5), 137.9 (1C, Tp5), 134.9 (1H, C14), 130.4 (2C, C15, C13), 130.1 (2C, C16, C12), 126.2 (1C, CN), 107.6 (1C, TpB4), 107.5 (1C, Tp4), 107.4 (1C, Tp4), 65.8 (1C, C1), 59.0 (1C, C3), 52.5 (1C, OMe), 45.8 (1C, C7), 39.7 (1C, C5), 37.7 (1C, d J = 11.6, C2), 31.9 (1C, C4), 26.1 (1C, C6), 25.3 (1C,

C10/9), 21.4 (1C, C10/9), 13.6 (3C, d J = 29.0, PMe_3). Anal. Calcd for $C_{30}H_{40}BN_8O_5PSW \cdot 1/4NaOTf$: C, 40.67; H, 4.51; N, 12.54. Found: C, 40.43; H, 4.74; N, 12.37.

Compound 25

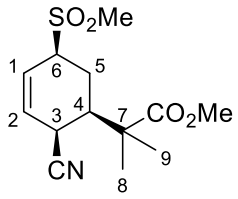

Outside of the glovebox, **23** (0.100 g, 0.126 mmol) and acetone were combined in a 4-dram vial. A stir pea and $NOPF_6$ (0.035 g, 0.202 mmol) were added to a separate 4-dram vial. The solution of **23** in acetone was then added to the vial with the stir pea and $NOPF_6$ while stirring. The initial solution was black and became a golden yellow as it stirred overnight. The golden solution was evaporated to dryness, picked up in minimal DCM, and added to 20 mL of stirring pentane. A green precipitant formed and was collected on a 15 mL medium porosity fritted disc and washed with hexanes (2 x 10 mL). The resulting filtrate was evaporated to dryness. The resulting oil was washed with 25 mL of hexanes followed by 25 mL of ether. The remaining oil was dissolved in ethyl acetate and ran through 30 mL of silica. The silica was washed with 60 mL of ethyl acetate. The filtrate was evaporated to dryness yielding **25** (0.023 g, 0.081 mmol, 64%). ^{1}H-NMR (d_3-MeCN, δ, 25 ^{o}C): 6.14 (1H, ddd J = 9.9, 5.9, 2.48 Hz, H2), 6.07 (1H, dm J = 9.9 Hz, H1), 3.91 (1H, m, H6), 3.67 (3H, s, OMe), 3.48 (1H, m, H1), 2.87 (3H, s, SO_2Me), 2.26 (1H, dm J = 13.1, H5), 2.13 (1H, dd J = 4.3, 2.0 Hz, H4), 1.88 (1H, m, H5), 1.32 (6H, s, H9, H8). ^{13}C-NMR (d_3-MeCN, δ, 25 ^{o}C): 177.2 (1C, C=O), 130.0 (1C, C2), 124.2 (1C, C1), 119.4 (1C, CN), 62.9 (1C, C6), 52.7 (1C, OMe), 45.4 (1C, C7), 42.6 (1C, C4), 37.9 (1C, SO_2Me), 28.6 (1C, C3), 23.2 (1C, C5), 23.0 (1C, C9/8), 22.9 (1C, C9/8). HRMS (ESI-TOF) *m*/*z*: $[M+Na]^+$ calcd for 308.0927; found 308.0927.

Compound 26

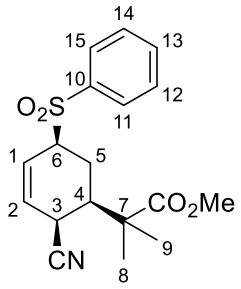

Outside of the glovebox, **24** (0.105 g, 0.123 mmol) and acetone were combined in a 4-dram vial. A stir pea and $NOPF_6$ (0.051 g, 0.291 mmol) were added to a separate 4-dram vial. The solution of **24** in acetone was then added to the vial with the stir pea and $NOPF_6$ while stirring. The initial solution was black and became a golden yellow as it stirred overnight. The golden solution was evaporated to dryness, picked up in minimal DCM, and added to 20 mL of stirring pentane. A green precipitant formed and was collected on a 15 mL medium porosity fritted disc and washed with hexanes (2 x 10 mL). The resulting filtrate was evaporated to dryness. The resulting oil was washed with 25 mL of hexanes followed by 25 mL of ether. The remaining oil was dissolved in ethyl acetate and ran through 30 mL of silica. The silica was washed with 60 mL of ethyl acetate. The filtrate was evaporated to dryness yielding **26** (0.033 g, 0.094 mmol, 76%). ^{1}H-NMR (d_3-MeCN, δ, 25 °C): 7.88 (2H, dm J = 8.6, H15, H11), 7.75 (1H, tm J = 7.6, H13), 7.64 (2H, tm J = 7.8, H14, H12), 6.02 (2H, m, H2, H1), 4.09 (1H, m, H6), 3.61 (3H, s, OMe), 3.37 (1H, m, H3), 2.12 (1H, m, H5a), 2.03 (1H, ddd J = 12.9, 4.3, 2.0, H4), 1.70 (1H, m, H5b), 1.23 (6H, s, H9, H8). ^{13}C-NMR (d_3-MeCN, δ, 25 °C): 177.1 (1C, C=O), 137.2 (1C, C10), 135.3 (1C, C13), 130.3 (2C, C14, C12), 130.1 (2C, C15, C11), 129.9 (1C, C2), 124.4 (1C, C1), 118.9 (1C, CN), 64.1 (1C, C6), 52.6 (1C, OMe), 45.3 (1C, C7), 42.5 (1C, C4), 28.5 (1C, C3), 23.3 (1C, C5), 23.0 (1C, C9/8). 22.8 (1C, C9/8). HRMS (ESI-TOF) *m/z*: $[M+Na]^+$ calcd for 370.1083; found 370.1083.

References

(1) Pienkos, J. A.; Zottig, V. E.; Iovan, D. A.; Li, M.; Harrison, D. P.; Sabat, M.; Salomon, R. J.; Strausberg, L.; Teran, V. A.; Myers, W. H.; Harman, W. D. *Organometallics* **2013**, *32*, 691.

(2) Lis, E. C.; Salomon, R. J.; Sabat, M.; Myers, W. H.; Harman, W. D. *Journal of the American Chemical Society* **2008**, *130*, 12472.

(3) Zottig, V. E.; Todd, M. A.; Nichols-Nielander, A. C.; Harrison, D. P.; Sabat, M.; Myers, W. H.; Harman, W. D. *Organometallics* **2010**, *29*, 4793.

(4) Todd, M. A.; Sabat, M.; Myers, W. H.; Harman, W. D. *Journal of the American Chemical Society* **2007**, *129*, 11010.

(5) Todd, M. A.; Sabat, M.; Myers, W. H.; Smith, T. M.; Harman, W. D. *Journal of the American Chemical Society* **2008**, *130*, 6906.

(6) Salomon, R. J.; Todd, M. A.; Sabat, M.; Myers, W. H.; Harman, W. D. *Organometallics* **2010**, *29*, 707.

(7) Kolis, S. P.; Chordia, M. D.; Liu, R.; Kopach, M. E.; Harman, W. D. *Journal of the American Chemical Society* **1998**, *120*, 2218.

(8) Kolis, S. P.; Kopach, M. E.; Liu, R.; Harman, W. D. *Journal of the American Chemical Society* **1998**, *120*, 6205.

(9) Kopach, M. E.; Kolis, S. P.; Liu, R.; Robertson, J. W.; Chordia, M. D.; Harman, W. D. *Journal of the American Chemical Society* **1998**, *120*, 6199.

(10) Keane, J. M.; Ding, F.; Sabat, M.; Harman, W. D. *Journal of the American Chemical Society* **2004**, *126*, 785.

(11) Wilson, K. B.; Myers, J. T.; Nedzbala, H. S.; Combee, L. A.; Sabat, M.; Harman, W. D. *Journal of the American Chemical Society* **2017**, *139*, 11401.

(12) Myers, J. T.; Smith, J. A.; Dakermanji, S. J.; Wilde, J. H.; Wilson, K. B.; Shivokevich, P. J.; Harman, W. D. *Journal of the American Chemical Society* **2017**, *139*, 11392.

(13) Smith, J. A.; Simpson, S. R.; Westendorff, K. S.; Weatherford-Pratt, J.; Myers, J. T.; Wilde, J. H.; Dickie, D. A.; Harman, W. D. *Organometallics* **2020**, *39*, 2493.

(14) Graham, P. M.; Mocella, C. J.; Sabat, M.; Harman, W. D. *Organometallics* **2005**, *24*, 911.

(15) Lis, E. C.; Delafuente, D. A.; Lin, Y.; Mocella, C. J.; Todd, M. A.; Liu, W.; Sabat, M.; Myers, W. H.; Harman, W. D. *Organometallics* **2006**, *25*, 5051.

(16) Welch, K. D.; Harrison, D. P.; Lis, E. C.; Liu, W.; Salomon, R. J.; Harman, W. D.; Myers, W. H. *Organometallics* **2007**, *26*, 2791.

(17) Feng, M.; Tang, B.; Liang, S. H.; Jiang, X. *Curr Top Med Chem* **2016**, *16*, 1200.

(18) Martins, P.; Jesus, J.; Santos, S.; Raposo, L. R.; Roma-Rodrigues, C.; Baptista, P. V.; Fernandes, A. R. *Molecules (Basel, Switzerland)* **2015**, *20*, 16852.

(19) Surur, A. S.; Schulig, L.; Link, A. *Archiv der Pharmazie* **2019**, *352*, 1800248.

(20) Harrison, D. P.; Nichols-Nielander, A. C.; Zottig, V. E.; Strausberg, L.; Salomon, R. J.; Trindle, C. O.; Sabat, M.; Gunnoe, T. B.; Iovan, D. A.; Myers, W. H.; Harman, W. D. *Organometallics* **2011**, *30*, 2587.

(21) Smith, J. A.; Schouten, A.; Wilde, J. H.; Westendorff, K. S.; Dickie, D. A.; Ess, D. H.; Harman, W. D. *Journal of the American Chemical Society* **2020**, *142*, 16437.

(22) Smith, J. A.; Wilson, K. B.; Sonstrom, R. E.; Kelleher, P. J.; Welch, K. D.; Pert, E. K.; Westendorff, K. S.; Dickie, D. A.; Wang, X.; Pate, B. H.; Harman, W. D. *Nature* **2020**, *581*, 288.

(23) Lankenau, A. W.; Iovan, D. A.; Pienkos, J. A.; Salomon, R. J.; Wang, S.; Harrison, D. P.; Myers, W. H.; Harman, W. D. *Journal of the American Chemical Society* **2015**, *137*, 3649.

(24) Wilson, K. B.; Smith, J. A.; Nedzbala, H. S.; Pert, E. K.; Dakermanji, S. J.; Dickie, D. A.; Harman, W. D. *The Journal of Organic Chemistry* **2019**, *84*, 6094.

Chapter 5

Utilization of Sulfones as Leaving Groups to Yield Trisubstituted Cyclohexenes from Three Independent Nucleophilic Additions

5.1 Introduction

In chapter 3, we demonstrated the ability of the π-base {WTp(NO)(PMe_3)} to coordinate methyl phenyl sulfone, diphenyl sulfone, and phenylsulfonyl pyrrolidine, thus increasing the electron density of the phenyl ring.[1] This enabled the selective protonation of the carbon ortho to the sulfone group, which allowed for the η^2-arenium complexes to undergo a nucleophilic addition with a range of nucleophiles to yield conjugated η^2-diene species as demonstrated in Chapter 4. The η^2-diene complexes that underwent addition with the nucleophile MTDA were then able to undergo a second protonation followed by nucleophilic addition of a CN^- anion, which led to sulfone-functionalized trisubstituted cyclohexenes. It should be noted that the two η^2-cyclohexene products described in Chapter four (**6**, **7**) resulted from a selective precipitation out of the reaction mixture. When the filtrate was ran through a silica column, sulfone elimination was observed to yield a new conjugated η^2-diene species (**8**). Knowing that sulfinates ($:SO_2R^-$) have been observed as leaving groups for nucleophilic substitution and elimination reactions,[2-10] we sought to explore which conditions would allow for sulfinate retention versus those that would allow for the replacement of the sulfonyl group by other substituents.

5.2 Double Nucleophilic Additions

In an effort to form other examples of sulfonyl cyclohexene complexes such as compounds **6** or **7**, solutions of diene complexes **1** and **2** were treated with either LiDMM or H^-. Protonation of either diene complex **1** or **2** followed by the addition of TBAB resulted in the monosubstituted cyclohexene complex **3**. In this case, the purported cyclohexene **D** (**Scheme 5.1**) loses sulfinate then adds the second hydride (i.e., an SN1 reaction mechanism). Analysis of compound **3** revealed that the alkyl substituent is oriented anti to the tungsten at the homoallylic carbon closer to the PMe_3. The proximal allyl conformation (**E** in **Scheme 5.1**) is calculated to be unstable with respect to the distal form (**F**) by ~2 kcal/mol similar to the parent,[11] and the hydride addition occurs with the latter conformer.

In contrast, when LiDMM was used as the nucleophile, the reactions of either **1** or **2** yielded the trialkylated η^2-cyclohexene complex **4**. Apparently, in a manner similar to the reaction with cyanide, **1** and **2** undergo the addition of the malonate but then rapidly lose the sulfinate to form allyl **B** (**Scheme 5.1**). Although for the parent cyclohexenyl allyl complex, the distal conformer is more favorable than the proximal by several kcal/mol,[11] DFT calculations show that the proximal allyl **B** has a lower free energy than its conformer **C** by 1.3 kcal/mol (CH_3CN). Reaction of this conformer leads to the 3,4,6-trisubstituted cyclohexene product **4**. Repeating this reaction with only one equivalent of LiDMM generates half an equivalent of the product and the parent allyl, respectively. This observation suggests that the rate of addition of DMM to form **A** is slower than the sequence that converts the purported sulfonyl-bearing cyclohexene (**A**) to the trialkylated cyclohexene **4**.

This tandem addition and substitution sequence from **1** to **4** occurred in less than 10 minutes. However, if the reaction is allowed to stand overnight, the product partially undergoes an isomerization to form **5** (ratio of **5:4** is 10:1 after 26 h). Apparently, epimerization of the tungsten stereocenter occurs in order to lower steric interactions for this unusually congested species. The stereochemical assignments for both **4** and **5** are supported by NOESY and COSY correlations between the five methine ring hydrogens. Further, DFT calculations determine that **5** is thermodynamically competitive with its isomer **4** (**Scheme 5.1**) (+0.6 kcal/mol in CH_3CN). Of note, if **4** is isolated, washed with hexanes, and dried before being placed into a solution of acetonitrile, then no epimerization is observed over a period of 48 h, indicating that the epimerization is catalyzed by an impurity in the initial reaction mixture.

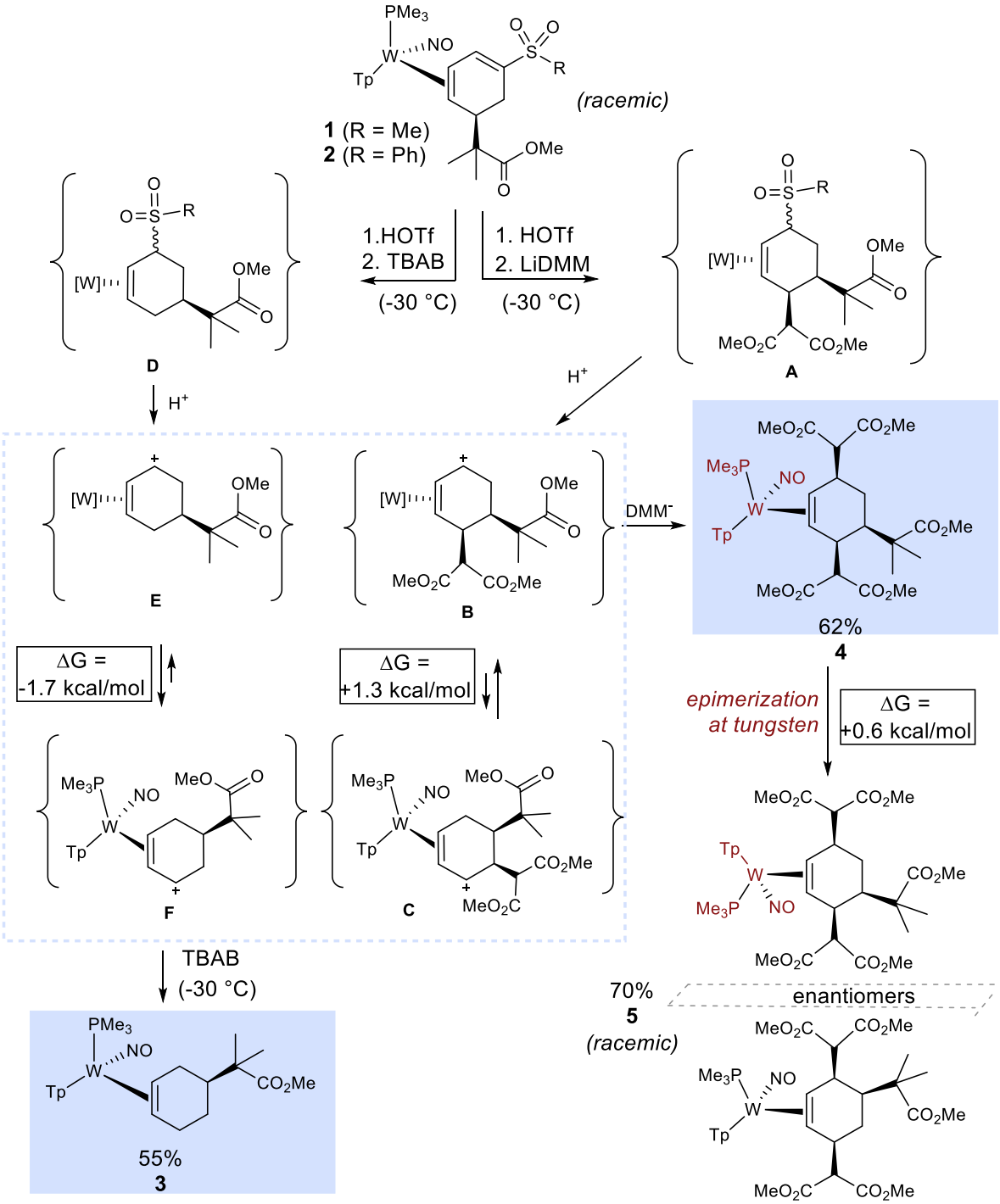

Scheme 5.1: Double nucleophilic additions to η²-1-sulfonyl-1,3-diene complexes

5.3 Elimination of the Sulfone Functionality

Given the difficulties with adding a third nucleophile through direct substitution of the sulfone, we next sought to cleanly eliminate the sulfone group in the η²-cyclohexene complex **6** to form diene **8**.

Curiously, treatment of the sulfonyl cyclohexene (**6** or **7**) with acid (HOTf/MeOH, HOTf/CH_3CN, HOTf/acetone, diphenyl ammonium triflate (DPhAT)) or base (triethylamine) alone failed to cause any reaction. However, running a solution of **6** or **7** down a silica column resulted in clean formation of **8**. Treatment of **6** or **7** directly with the nucleophilic salts LiDMM, TBAB, or NaCN resulted in cyclohexenes **9** (see appendix for crystal struture), **10**, and **11**, respectively (**Scheme 5.2**). However, the sulfone substitution did not proceed in the case of covalent nucleophiles such as methylamine, dimethylamine, or methyl trimethylsilyl dimethyl ketone acetal. Yet, if diene **8** was protonated at low temperature, the purported allyl intermediate (**8H**) reacts with imidazole to provide the trisubstituted cyclohexene **12** (**Scheme 5.2**). Compounds **9**, **10**, and **11** can also be synthesized through **8H**. As in earlier cases, the nucleophilic addition occurred at the carbon adjacent to the bound carbon, proximal to the PMe_3 ligand and to the face of the diene anti to the metal.

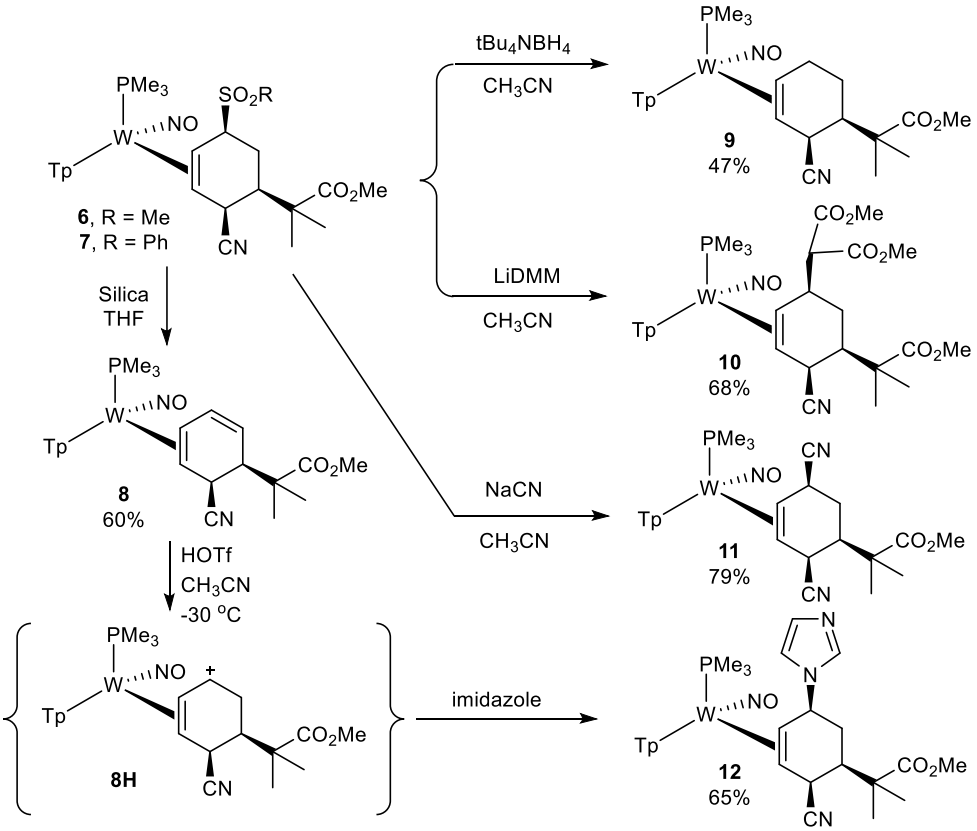

Scheme 5.2: The third nucleophilic addition to the initial aromatic ring, via replacement of the sulfone

5.4 Formation of an η^2-Trans Substituted Cyclohexene Ring

Even though exposing **6** or **7** to Brønsted acids failed to cause any reaction, treatment of **6** or **7** with a Lewis acid such as $ZnBr_2$ led to the formation of three complexes after stirring in deuterated acetonitrile for half an hour (**Scheme 5.3**). The Lewis acid is believed to interact with the sulfone ligand, thus allowing it to act as a leaving group. The sulfone functionality leaves as a sulfinate, and the electron donation from the W(0) fragment allows for the stable formation of allyl **8H** with the positive charge proximal to the PMe_3 ligand as the dominant isomer. **8H** exists in an equilibrium between the proximal (**8H**p) and distal (**8H**d) forms. Even though the **8H**p is the favored isomer, **8H**d still is present and presents the cation ortho to an acidic proton. This proton is apparently acidic enough to be easily deprotonated to yield the η^2-diene **13** (**Scheme 5.3**). Compound **13** can be reprotonated to revert to **8H** if the protonation occurs syn to the metal. However, if the proton protonates **13** on the face of the diene anti to the face bound by the metal, then a new thermodynamically competitive allyl (**14**) is formed where the two substituents are now trans to each other. If triethylamine is added to this reaction, deprotonation occurs, and **13** is exclusively formed.

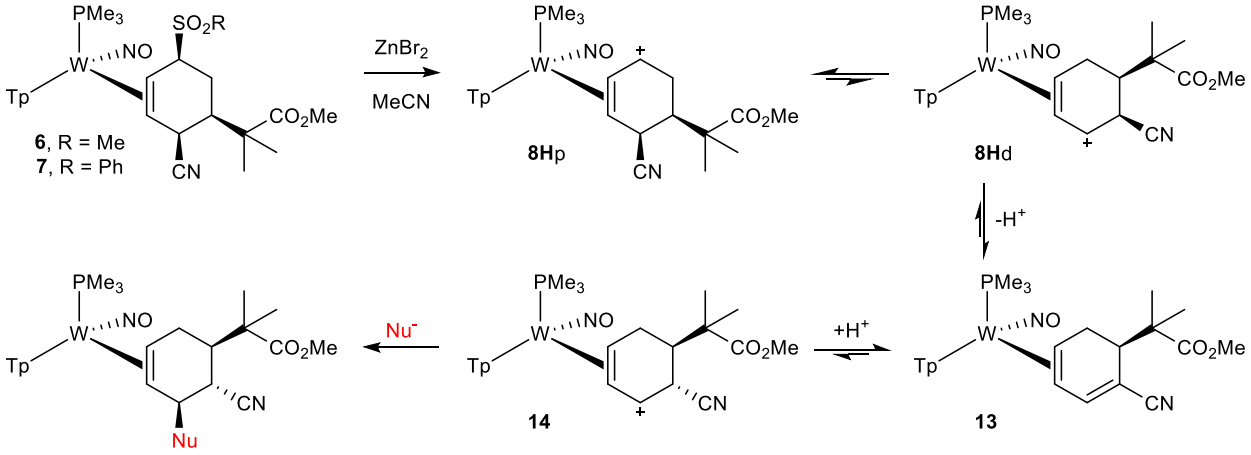

Scheme 5.3: Lewis acid promotion of sulfone elimination and subsequent allyl isomerization

Similarly, if **8** is protonated and allowed to sit in solution for a few hours, both **8H** and **14** can be observed via ^{1}H-NMR in a 1:1 ratio. However, if **13** is exposed to acid and followed by exposure to $NaBH_4$ fifteen minutes later, only complex **9** is formed, indicating that initial protonation occurs on the face of

the diene bound to the metal. When LiDMM was used as the nucleophile, only complex **10** was observed. It appears that while the trans allyl **14** is a competitive isomer to **8H**, epimerization needs to occur after the initial protonation to access **14**. Work is currently underway to find conditions that will allow for the addition of a nucleophile that yields trans substituted cyclohexenes.

5.5 Formation of 3,6-Disubstituted Cyclohexenes

Finally, we attempted to prepare 3,6-disubstituted cyclohexenes using a hydride reagent as the first nucleophile. Treatment of the diphenylsulfone complex **15** with acid followed by TBAB resulted in the diene complex **16**. When this material was subjected to acid followed by NaCN, two complexes resulted from the addition of cyanide. Presumably, the reaction occurs via an intermediate sulfonylcyclohexene **17**. Subsequent loss of the sulfinate results in an allyl complex that can react with CN with either the distal or proximal conformer of the allyl complex to generate the 3,4-dicyano (**18B**) or 3,6-dicyanocyclohexene species (**18A**), respectively (**Scheme 8**). Through a similar sequence, the 3,6-disubstituted bis malonate **20** was generated via allyl **19**.

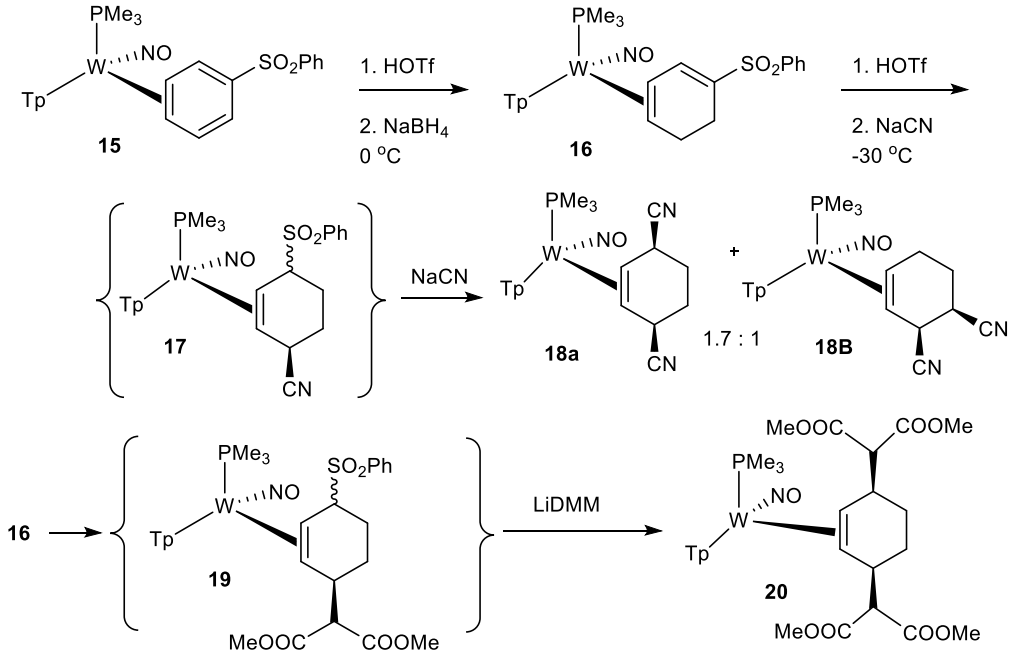

Scheme 5.4: Synthesis of 3,6-disubstituted cyclohexenes

5.6 Liberation of Organics from Metal

Previous studies have shown that cyclohexenes can be liberated from the {WTp(NO)(PMe_3)} system using a variety of different oxidants, including Ag^+, $[FeCp2]^+$, DDQ, NOPF6, CAN, and even O_2. Several additional examples are provided in **Table 3**. These cyclohexenes were liberated from the metal through oxidation with $NOPF_6$ in yields ranging from 54 to 68%.

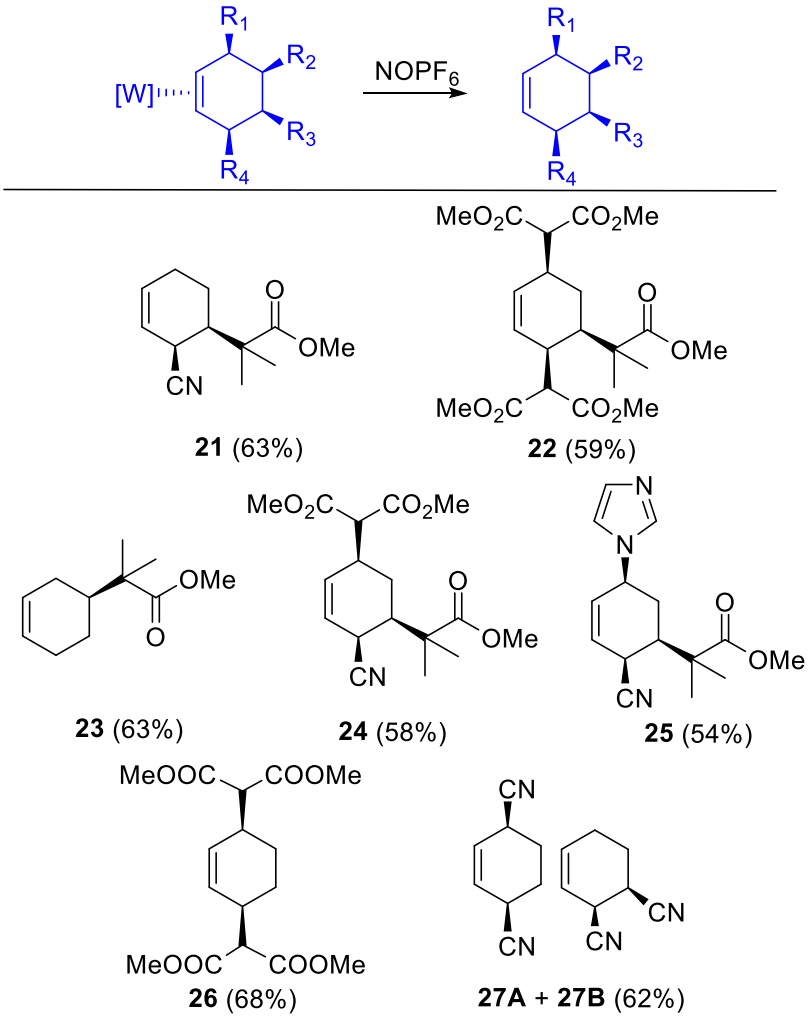

Table 5.1: Decomplexation of functionalized cyclohexenes

5.7 Position of Carbocation in η^2-allyls

The allyl complexes resulting from the protonation of dihapto-coordinated dienes are usefully described as dihapto-coordinated with one of the three allylic carbons bound only weakly by the tungsten.

This carbon takes on considerable carbocation character, as has been experimentally and theoretically documented previously.[11] Comprehensive DFT calculations (SI) reveal that each cyclohexadienium allyl exists as two ring conformations (chair and boat; **Scheme 5.5**), and any substituents (A-C) at C4-C6 can significantly influence the energy difference between distal and proximal forms (SI). Although the {WTp(NO)(PMe_3)} system typically favors the distal-boat conformer, the proximal-chair conformation becomes more competitive when an electron-withdrawing group is located at C4, or when a sterically bulky group is located at C6, trans (or cis) to the metal (SI). Consequently, these π-allyl complexes can be separated by several kcal/mol, with a kinetic barrier of roughly 6 kcal/mol.[11]

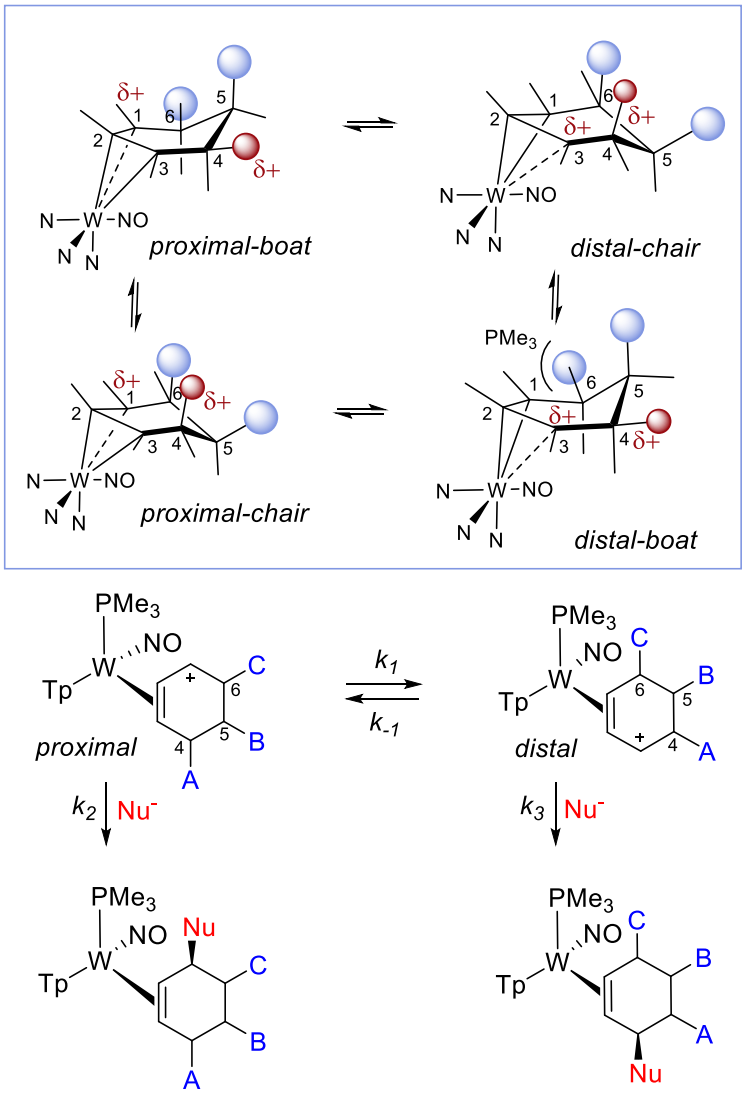

Scheme 5.5: Equilibrium of distal and proximal allyl complexes and the two ring conformations for each species

While we expect that the rates of the "allyl-shift" (**Scheme 5.5**, k1, k-1) to be much greater than those of nucleophilic addition (k2, k3), the four competing transition states for the addition will reflect the relative stabilities of the allyl conformations. Provided the transition states for nucleophilic addition proximal and distal to the PMe_3 are the same, the difference in the overall reaction barriers (reflected in the ratio of cyclohexene product isomers) is directly impacted by the free-energy difference of the competing allyl conformers (Curtin-Hammett).[12] Of course, steric interactions between the incoming nucleophile and ring substituents will also play a role in determining the location of nucleophilic addition of the second and third nucleophile. The consequence is a clear preference for a cis-3,4,6 substitution pattern of the cyclohexene ligand. When a hydride is implemented as one of the nucleophiles, this methodology gives rise to cis-3,4-, and cis-3,6- substitution patterns as well.

5.8 Significance of this Work

The revered Diels-Alder reaction, which produces a cyclohexene from an alkene and a diene, is considered one of the most important reactions in modern synthetic chemistry. This is largely because of the predominance of six-membered carbocycles in nature and the ability to create multiple stereocenters in the newly formed ring with considerable selectivity. The work described herein conceptually represents a complementary approach to cyclohexenes with multiple stereocenters, in this case, derived from simple benzene precursors and common nucleophiles.

In recent years there has been an explosion of new methods for dearomatization of benzenes[13], including catalytic hydrogenations,[14,15] enzymatic oxidations,[16] radical cyclizations,[17,18] photochemical and thermal cycloadditions,[19-23] and transition metal-mediated approaches.[24-28] Regarding the last approach, arenes can be coordinated through two, four, or six carbons, with η^2-arene complexes such as $Cr(CO)_3(\eta^6$-benzene) being the most common method.[25] In such compounds, the metal acts as an electron-withdrawing group, and the arene is activated toward nucleophilic addition reactions.

In contrast, the tungsten complex in the present study is a powerful π base and activates the arene toward electrophilic addition and protonation reactions, even in the presence of an electron withdrawing substituent such as a sulfonyl group. The resulting η^2-arenium complex can then be subjected to nucleophilic addition. Because the metal only occupies one double bond of the benzene ring, the entire process can be repeated. *The distinguishing feature of the current study is the ability of the EWG substituent to be replaced with a third independent nucleophile.*

But as demonstrated above, in addition to using the sulfone or sulfonamide as a leaving group, these medicinally relevant functional groups can be left intact.[29,30] Of the nine novel substituted cyclohexenes prepared as examples of this methodology, six meet the criteria of Lipinski's rule of five[31] for evaluating drug likeliness, as well as the criteria of Ghose,[32] Veber,[33] Egan,[34] and Muegge.[35] This indicates that these six compounds have a high probability of showing desirable biological activity.

5.9 Comparison with Previous Methods in which a Metal Mediates 3 additions to an Aromatic Ring

The dearomatization of benzene by π-basic metal fragments has been extensively investigated for arenes containing a π donor substituent such as anisoles,[36-39] phenols,[40-44] and anilines.[45-47] The closest prior example of a reaction sequence in which a metal mediates three additions to an aromatic ring was observed for an osmium anisole derivative (**Scheme 5.6**),[48] where the addition of an acetal at C4 followed by nucleophilic addition at C3 generated an alkoxydiene complex. Subsequent reduction and substitution of the alkoxy group via an allyl intermediate provided a net addition of an electrophile (E1) and two nucleophiles (Nu1, Nu2) to the benzene ring system (**Scheme 5.6**).[49]

An intramolecular example of this reaction pattern has also been documented for tungsten,[36] in which the addition of the beta carbon of acrolein (E1) followed by the addition of a cyanoalkoxide (Nu1) created an oxadecalin core. Subsequent reduction, replacement of the methoxy group with CN- (Nu2), and oxidative decomplexation provided the trisubstituted cyclohexene product. We note that methoxy

groups and halides are well known as leaving groups for η^6-benzene complexes of $Cr(CO)_3$ and $[Mn(CO)_3]^+$,[50] but to our knowledge, sulfinates have not been utilized for such purposes, even though several examples have been documented of η^6-sulfone complexes.[51-54]

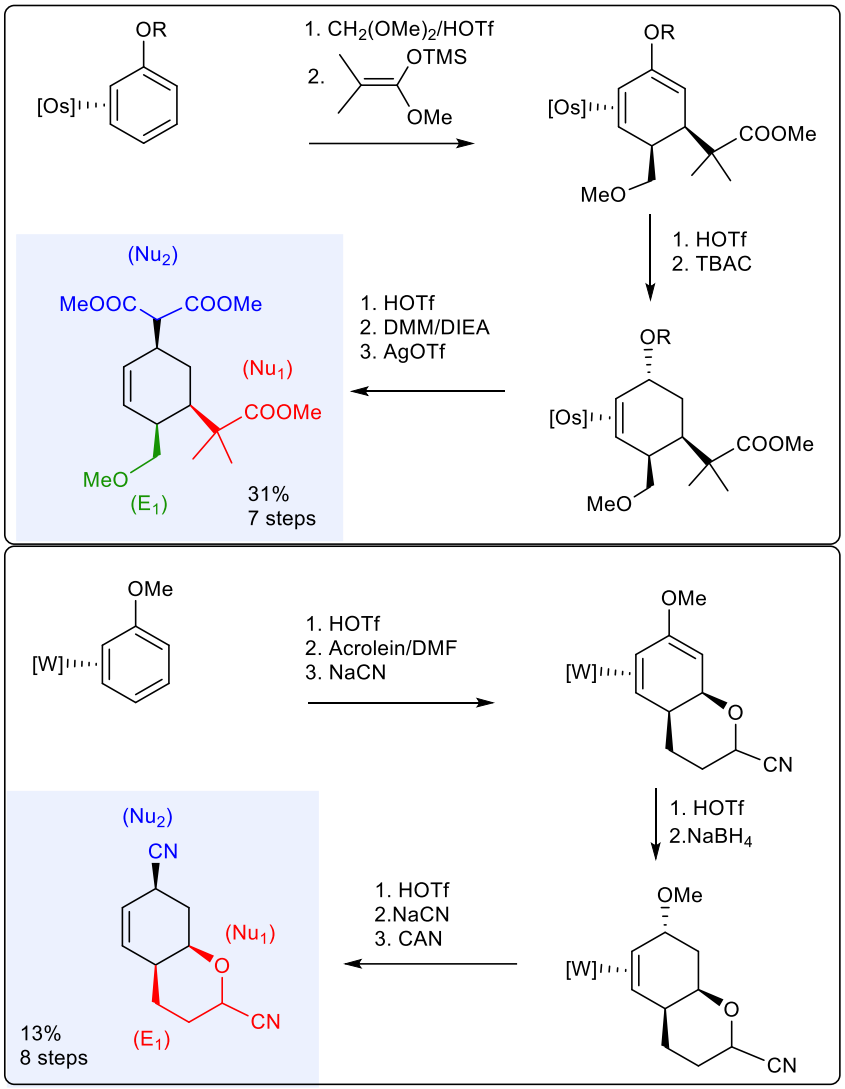

Scheme 5.6: Prior examples of triple addition reactions ($E^+/Nu^-/Nu^-$) to η^2-anisole complexes

5.10 Proposed Mechanism for Sulfone Elimination

Sulfones are generally regarded as robust functional groups, with elimination occurring only at high temperatures (ca. 500 °C) through an intramolecular process (Ei).[4] However, elimination of sulfinic acid was observed to occur on silica for a tosylated glucopyranoside in which the tosylated carbon was

attached to an oxygen.[6] Fujita et al. also demonstrated that b-tributylstannyl sulfones undergo elimination on silica to form the corresponding alkene, whereas, without the silica, refluxing xylenes was required to achieve elimination.[7] Ley et al. demonstrated that a-sulfonated cyclic ethers or cyclic amides could undergo substitution or elimination with a suitable nucleophile in the presence of a Lewis acid such as $MgBr_2$.[9,10] This behavior is similar to that observed for the tungsten allyl sulfones of the present report, where the tungsten-bound alkene moiety serves as the π-donor, facilitating loss of the sulfinate group (**Scheme 11**) in tandem with a Lewis acid. With the tungsten acting as a π donor, exposing **26** to silica, for example, promotes the elimination of the sulfinic acid and formation of **25**. It was also observed that when salts of stabilized carbanions such as NaCN or LiDMM were used, no external Lewis acid was needed (beyond the alkali metal cation). Finally, we comment that Pd(0) has been used to catalyze the allylic substitution of allylic sulfones,[55] where one can consider the metal as stabilizing both allyl and sulfonate fragments (**Scheme 11**). By contrast, $[WTp(NO)(PMe_3)(allyl)]^+$ is an 18e system and cannot stabilize the sulfinate group; thus, a Lewis acid appears to be required.

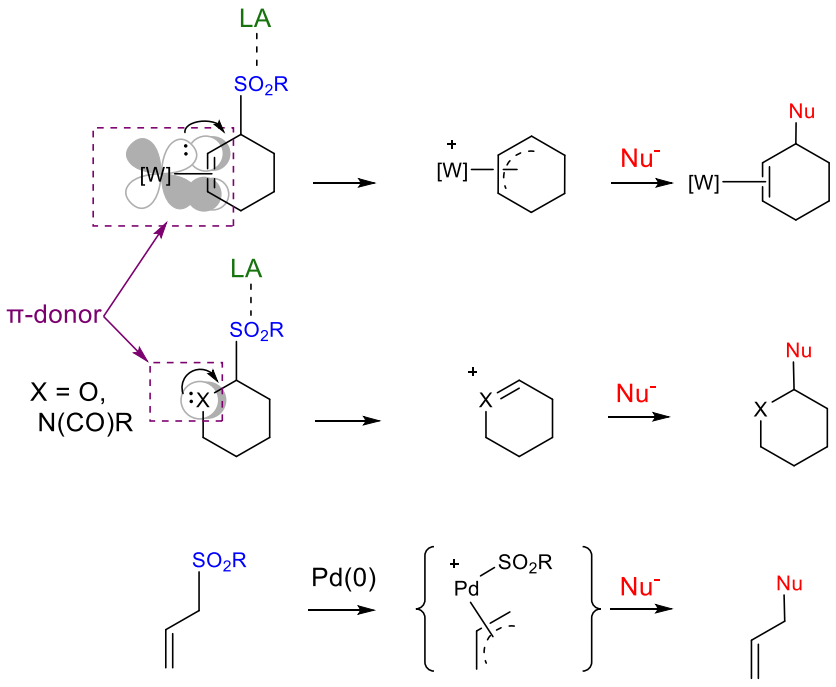

Scheme 5.7: Sulfone substitution reactions (LA = Lewis acid)

5.11 Conclusion

Previous chapters demonstrated the ability of η^2-phenyl sulfones two sequential tandem protonation/nucleophilic additions. This chapter expanded on the phenyl sulfone reactivity by demonstrating that the sulfone functional group can be substituted for a third independent nucleophile. Without exception, this reaction sequence produces a predictable regio- and stereochemical pattern for the cyclohexene ligand, which is liberated from the metal through oxidative decomplexation. Through this methodology, not only can cis, cis- 3,4,6 trisubstituted cyclohexenes be generated, but through the appropriate use of hydride, cis-3,4- and cis-3,6- disubstituted cyclohexene patterns are also achieved. Given that WTp(NO)(PMe_3)(η^2-benzene) and its derivatives can be prepared in enantioenriched form,[56] the compounds reported herein should be accessible as single enantiomers.[57,58] Work is currently underway to carry out controlled epimerizations in the cyclohexene ring via a deprotonation/ protonation sequence, in order to achieve trans- substitution patterns for the cyclohexene ring, where the influence of the metal can be leveraged still further.

Experimental

General Methods. NMR spectra were obtained on 500, 600, or 800 MHz spectrometers. Chemical shifts are referenced to tetramethylsilane (TMS) utilizing residual ^{1}H signals of the deuterated solvents as internal standards. Chemical Shifts are reported in ppm, and coupling constants (J) are reported in hertz (Hz). Infrared spectra (IR) were recorded as a solid on a spectrometer with an ATR crystal accessory, and peaks are reported in cm^{-1}. Electrochemical experiments were performed under a nitrogen atmosphere. Most cyclic voltammetric data were recorded at ambient temperature at 100 mV/ s, unless otherwise noted, with a standard three-electrode cell from +1.8 to −1.8 V with a platinum working electrode, acetonitrile or N,N-dimethylacetamide (DMA) solvent, and tetrabutylammonium (TBAH) electrolyte (∼1.0 M). All potentials are reported versus the normal hydrogen electrode (NHE) using cobaltocenium hexafluorophosphate ($E_{1/2}$ = −0.78 V, −1.75 V) or ferrocene ($E_{1/2}$ = 0.55 V) as an internal standard. The peak separation of all reversible couples was less than 100 mV. All synthetic reactions were performed in a glovebox under a dry nitrogen atmosphere unless otherwise noted. All solvents were purged with nitrogen prior to use. Deuterated solvents were used as received from Cambridge Isotopes and were purged with nitrogen under an inert atmosphere. When possible, pyrazole protons of the tris(pyrazolyl)borate (Tp) ligand were uniquely assigned (e.g., “Tp3B”) using two-dimensional NMR data. If unambiguous assignments were not possible, Tp protons were labeled as “Tp3/5 or Tp4”. All J values for Tp protons are 2(±0.4) Hz. BH peaks (around 4−5 ppm) in the ^{1}H NMR spectra are not assigned due to their quadrupole broadening; However, confirmation of the BH group is provided by IR data (ca 2500 cm^{-1}).

Compound 3

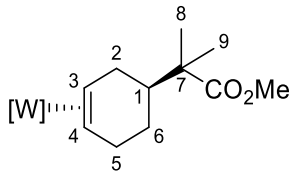

Compound **2** (0.23 g, 0.279 mmol) and MeCN were combined in a test tube. $NaBH_4$ and MeCN were combined in a second test tube along with a stir pea. Both test tubes were cooled to -40 °C for 15 min. 1M HOTf/MeCN (0.56 mL, 0.56 mmol) was then added to the test tube containing compound **2** to form a homogenous golden-brown solution. After 15 min, the reaction was added dropwise to the test tube containing $NaBH_4$. The reaction was stirred for 18 hours. The reaction was removed from the box and purified via Combiflash flash chromatography on a 12 g silica column using a gradient elution of 0-100% ethyl acetate in hexanes. A large U.V. peak was observed at 100% ethyl acetate. The resulting fractions were evaporated to dryness. The resulting oil was picked up in minimal DCM and added to 10 mL of pentane. Nitrogen gas was blown over the solution to allow for a slow precipitation of a tan solid out of solution. The tan product was collected on a 15 mL fine porosity fritted disc, washed with hexanes (3 x 10 mL), and desiccated overnight to yield **3** (0.106 g, 0.155 mmol, 55%). CV (DMA): $E_{p,a}$= + 0.31 V (NHE). IR: *ν*(NO) 1536 cm^{-1}, *ν*(CO) 1719 cm^{-1}, *ν*(BH) 2481 cm^{-1}. ^{1}H-NMR (d_3-MeCN, δ, 25 °C): 8.31 (1H, d, TpA3), 8.05 (1H, d, TpB3), 7.86 (1H, d, TpB5), 7.78 (1H, d, TpC5), 7.73 (1H, d, TpA5), 7.35 (1H, d, TpC3), 6.38 (1H, t, TpB4), 6.26 (1H, 5, TpA4), 6.20 (1H, t, TpC4), 3.61 (3H, OMe), 3.23 (1H, m, H2a), 2.97 (1H, tt J = 13.2, 4.1 Hz, H5b), 2.84 (1H, m, H5a), 2.67 (1H, m, H3, H2b), 2.09 (1H, m, H1), 1.65 (1H, m, H6a), 1.38 (1H, m, H4), 1.18 (3H, s, H9/8), 1.14 (12H, d, PMe_3, H9/8 buried), 1.09 (2H, qd J = 11.9, 3.6 Hz, H6b). ^{13}C-NMR (d_3-MeCN, δ, 25 °C): 179.4 (1C, C=O), 144.2 (1C, TpB3), 143.4 (1C, TpA3), 141.7 (1C, TpC3), 137.7 (1C, TpC5), 136.9 (1C, TpB5), 136.8 (1C, TpA5), 107.4 (1C, TpB4), 106.8 (1C, TpC4), 106.5 (1C, TpA4), 55.6 (1C, d J = 10.8 Hz, C3), 52.9 (1C, C4), 51.9 (1C, OMe), 46.6 (1C, C7), 43.1 (1C, C1), 33.3 (1C, d J = 3.6 Hz, C2), 31.7 (1C, C5),

28.9 (1C, C6), 23.4 (1C, C9/8), 22.1 (1C, C9/8), 13.5 (3C, d J = 27.7 Hz, PMe_3). Anal. Calcd for $C_{23}H_{37}BN_7O_3PW$: C, 40.32; H, 5.44; N, 14.31. Found: C, 40.59; H, 5.53; N, 14.12.

Compound 4

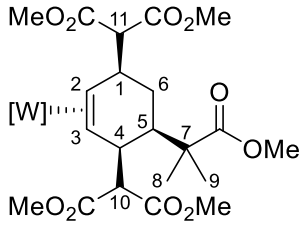

Compound **1** (0.210 g, 0.275 mmol) and MeCN were combined in a test tube. LiDMM (0.190 g, 1.38 mmol) and MeCN were combined in a second test tube along with a stir pea. Both test tubes were cooled to -40 °C for 15 min. 1M HOTf/MeCN (0.55 mL, 0.550 mmol) was then added to the test tube containing compound **1** to form a homogenous golden-brown solution. After 15 min, the reaction was added dropwise to the test tube containing LiDMM. The reaction was stirred for 30 min. The reaction was removed from the box and purified via Combiflash flash chromatography on a 12 g silica column using a gradient elution of 0-100% ethyl acetate in hexanes. A large U.V. peak was observed at 100% ethyl acetate. The resulting fractions were evaporated to dryness. The resulting oil was picked up in minimal DCM and added dropwise to 10 mL of stirring pentane yielding a white solid. The resulting white product was collected on a 15 mL fine porosity fritted disc, washed with hexanes (3 x 10 mL), and desiccated overnight to yield **4** (0.208 g, 0.216 mmol, 78%). CV (DMA): $E_{p,a}$= + 0.38 V (NHE). IR: *ν*(NO) 1544 cm^{-1}, *ν*(CO) 1716 cm^{-1}, *ν*(BH) 2474 cm^{-1}. ^{1}H-NMR (d_3-MeCN, δ, 25 °C): 8.00 (1H, d, TpB3), 7.94 (1H, d, TpA3), 7.82 (2H, m, TpC5, TpB5), 7.75 (1H, d, TpA5), 7.10 (1H, d, TpC4), 6.32 (1H, t, TpB4), 6.29 (1H, t, TpC4), 6.27 (1H, TpA4), 3.93 (1H, d J = 4.0, H11), 3.91 (3H, s, OMe), 3.88 (1H, d J = 3.8, H10), 3.72 (3H, s, OMe), 3.67 (4H, s, OMe, H4), 3.58 (1H, m, H1), 3.49 (3H, s, OMe), 3.26 (1H, s, OMe), 2.72 (1H, m, H2), 2.38 (1H, ddd J = 12.4, 3.9, 1.6, H5), 1.58 (1H, dd J = 12.9, 5.0, H6b), 1.49 (1H, q J = 12.4, H6a), 1.28 (3H, s, H9/8), 1.22 (9H, d J = 8.1, PMe_3),

1.16 (3H, s, H9/8), 0.81 (1H, d J = 11.3, H3). ^{13}C-NMR (d_3-MeCN, δ, 25 °C): 179.0 (1C, C=O), 171.2 (1C, C=O), 170.5 (2C, C=O), 170.0 (1C, C=O), 145.1 (1C, TpB3), 144.3 (1C, TpA3), 141.6 (1C, TpC3), 137.6 (1C, TpC5), 137.4 (2C, TpA5, TpB5), 107.2 (1C, TpB4), 107.0 (1C, TpC4), 106.7 (1C, TpA4), 60.1 (1C, C3), 57.7 (1C, C11), 56.5 (1C, C10), 52.9 (2C, OMe), 52.5 (1C, OMe), 52.4 (1C, OMe), 52.3 (1C, OMe), 48.6 (1C, d J = 11.1, C2), 45.6 (1C, C7), 44.7 (1C, C5), 41.31 (1C, C1), 39.5 (C1, C4), 28.3 (1C, C9/8), 24.6 (1C, C9/8), 23.1 (1C, C6), 14.9 (3C, d J = 28.1, PMe_3). Anal. Calcd for $C_{33}H_{49}BN_7O_{11}PW$: C, 41.92; H, 5.22; N, 10.37. Found: C, 41.95; H, 5.24; N, 10.45.

Compound 5

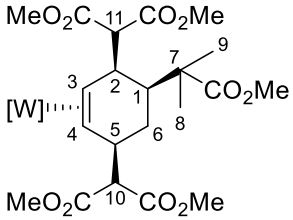

Compound **1** (0.100 g, 0.131 mmol) and MeCN were combined in a test tube. LiDMM (0.091 g, 0.657 mmol) and MeCN were combined in a second test tube along with a stir pea. Both test tubes were cooled to -40 °C for 15 min. 1M HOTf in MeCN (0.26 mL, 0.260 mmol) was then added to the test tube containing compound **1** to form a homogenous golden-brown solution. After 15 min, the reaction was added dropwise to the test tube containing LiDMM. The reaction was stirred for 24 hours. The reaction was removed from the box and purified via Combiflash flash chromatography on a 12 g silica column using a gradient elution of 0-100% ethyl acetate in hexanes. A large U.V. peak was observed at 100% ethyl acetate. The resulting fractions were evaporated to dryness. The resulting oil was picked up in minimal DCM and added dropwise to 10 mL of stirring pentane yielding a white solid. The resulting white product was collected on a 15 mL fine porosity fritted disc, washed with hexanes (3 x 10 mL), and desiccated overnight to yield **5** (0.087 g, 0.092 mmol, 70%). ^{1}H-NMR (d_3-Acetone, δ, 25 °C): 8.07 (1H, d, TpB3), 8.05 (1H, d,

TpA3), 7.94 (1H, d, TpC5), 7.90 (1H, d, TpB5), 7.84 (1H, d, TpA5), 7.23 (1H, d, TpC3), 6.37 (1H, t, TpB4), 6.36 (1H, t, TpC4), 6.25 (1H, t, TpA4), 4.13 (1H, bs, H2), 4.04 (1H, m, H5), 3.85 (1H, d J = 6.8, H11), 3.74 (3H, s, OMe), 3.72 (3H, s, OMe), 3.70 (3H, s, OMe), 3.61 (3H, s, OMe), 3.32 (3H, s, OMe), 3.24 (1H, d J = 5.9, H10), 2.62 (1H, dm J = 11.5, H1), 2.36 (1H, t J = 12.6, H3), 2.14 (1H, dd J = 13.1, 5.6, H4a), 1.49 (1H, q J = 12.0, H4b), 1.27 (3H, s, H8/7), 1.26 (10H, d J = 8.3, PMe_3, H8/7), 1.04 (1H, dt J = 11.4, 2.4, H4). ^{13}C-NMR (d_3-MeCN, δ, 25 °C): 179.3 (1C, C=O), 171.5 (1C, C=O), 171.0 (2C, C=O), 170.5 (1C, C=O), 144.0 (1C, TpB3), 143.5 (1C, TpA3), 140.9 (1C, TpC3), 138.5 (1C, TpC5), 137.9 (1C, Tp5), 137.2 (1C, Tp5), 107.4 (1C, TpB4), 107.1 (1C, TpC4), 106.7 (1C, TpA4), 58.9 (1C, C11), 56.9 (1C, d J = 10.2, C3), 56.4 (1C, C10), 53.4 (1C, OMe), 53.0 (1C, OMe), 52.9 (1C, OMe), 52.8 (1C, OMe), 51.91 (1C, OMe), 49.6 (1C, C1), 49.3 (1C, C4), 43.5 (1C, C5), 40.5 (1H, d J = 3.5, C2), 34.9 (1C, C7), 25.5 (1C, C9/8), 24.4 (1C, C6), 19.6 (1C, C9/8), 13.9 (3C, d J = 27.8, PMe_3).

Compound 8H

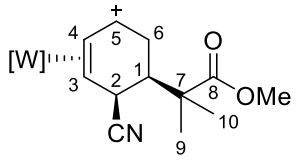

^{1}H-NMR (d_3-MeCN, δ, 25 °C): 8.22 (1H, d, TpB3), 8.08 (1H, d, TpC5), 8.05 (1H, d, TpB5), 7.95 (1H, d, TpC3), 7.92 (1H, d, TpA5), 7.53 (1H, d, TpA3), 7.12 (1H, m, H5), 6.55 (1H, t, TpB4), 6.53 (1H, t, TpC4), 6.42 (1H, t, TpA4), 5.51 (1H, m, H4), 3.71 (3H, s, OMe), 3.37 (1H, ddt J = 19.8, 10.7, 2.3, H6a), 3.30 (1H, m, H2), 3.24 (1H, m, H3), 3.02 (1H, dm J = 19.5, H6b), 2.18 (1H, m, H1), 1.40 (3H,s, H10/9), 1.34 (3H, s, H10/9), 1.12 (9H, d J = 9.7, PMe_3). ^{13}C-NMR (d_3-MeCN, δ, 25 °C): 177.4 (1C, CO), 144.4 (1C, Tp3), 144.3 (1C, Tp3), 142.6 (1C, TpA3), 140.3 (1C, Tp5), 139.7 (1C, Tp5), 139.0 (1C, Tp5), 136.6 (1C, C5), 124.71 (1C, CN), 109.5 (1C, Tp4), 109.0 (1C, Tp4), 109.4 (1C, TpA4), 93.4 (1C, C4), 73.0 (1C, C3), 52.8 (1C, OMe), 45.4 (1C, C7), 42.2 (1C, C1), 28.2 (1C, C2), 27.9 (1C, C6), 26.0 (1C, C10/9), 21.4 (1C, C10/C9), 11.9 (3C, d J = 33.9, PMe_3).

Compound 9

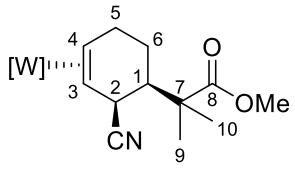

Compound **6** (0.200 g, 0.254 mmol), $NaCNBH_3$ (0.064 g, 1.02 mmol), MeCN, and a stir pea were added to a 4 dram to form a cloudy, yellow tinted solution. The reaction was allowed to stir overnight. A 60 mL course porosity fritted disc was then filled ¾ full of silica and set in ether. The reaction was evaporated to dryness, picked up in minimal DCM, and loaded onto the column. 200 mL of ethyl acetate was used to pull the product off the column. There is no colored band observed. The ethyl acetate was evaporated to dryness. The resulting oil was dissolved in minimal DCM and added dropwise to 20 mL of stirring pentane to yield a white solid. The resulting solid was collected on a 15 mL fine porosity fritted disc, washed with hexanes (2 x 10 mL), and desiccated overnight to yield **9**. (0.135 g, 0.190 mmol, 75%). CV (DMA): $E_{p,a}$= + 0.55 V (NHE). IR: *ν*(NO) 1561 cm^{-1}, *ν*(CO) 1718 cm^{-1}, *ν*(CN) 2219 cm^{-1}, *ν*(BH) 2505 cm^{-1}. ^{1}H-NMR (d_3-MeCN, δ, 25 °C): 8.02 (1H, d, TpB5), 7.85 (1H, d, TpB3), 7.82 (1H, d, TpC5), 7.81 (1H, d, TpA5), 7.78 (1H, d, TpA3), 7.33 (1H, d, TpC3), 6.36 (1H, t, TpB4), 6.35 (1H, t, TpA4), 6.26 (1H, t, TpC4), 3.71 (3H, s, OMe), 3.54 (1H, bs, H2), 3.01 (1H, m, H5), 2.82 (2H, m, H5, H4), 2.38 (1H, ddd J = 112.1, 3.7, 2.0 Hz, H1), 1.62 (1H, dm J = 13.3 Hz, H6), 1.53 (1H, m, H6), 1.29 (3H, s, H10/9), 1.28 (3H, s, H10/9), 1.20 (9H, d J = 8.1 Hz, PMe3), 1.04 (1H, d J =11.0 Hz, H3). ^{13}C-NMR (d_3-MeCN, δ, 25 °C): 178.6 (1C, C8), 144.4 (1C, TpB3), 143.5 (1C, TpA3), 141.5 (1C, TpC3), 137.8 (1C, Tp5), 137.5 (2C, Tp5), 127.8 (1C, CN), 107.5 (1C, Tp4), 107.4 (2C, Tp4), 59.1 (1C, C3), 52.3 (1C, OMe), 46.3 (1C, d J = 12.5 Hz, C4), 46.1 (1C, C7), 42.3 (1C, C1), 33.5 (1C, C2), 29.5 (1C, d J = 4.1 Hz, C5), 26.4 (1C, C10/9), 24.5 (1C, C6), 21.0 (1C, C10/9), 13.9 (3C, d J = 29.0 Hz, PMe_3). Anal. Calcd for $C_{24}H_{36}BN_8O_3PW \cdot 1DCM$: C, 37.76; H, 4.82; N, 14.09. Found: C, 37.51; H, 54.85; N, 14.37.

Compound 10

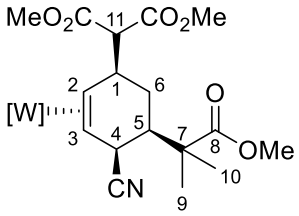

Compound **6** (0.100 g, 0.127 mmol), LiDMM (0.087 g, 0.634 mmol), MeCN, and a stir pea were added to a 4 dram to form a cloudy, yellow tinted solution. The reaction was allowed to stir overnight. A 30 mL course porosity fritted disc was then filled ¾ full of silica and set in ether. The reaction was evaporated to dryness, picked up in minimal DCM, and loaded onto the column. 200 mL of ethyl acetate was used to pull the product off the column. There is no colored band observed. The ethyl acetate was evaporated to dryness. The resulting oil was dissolved in minimal DCM and added dropwise to 20 mL of stirring pentane to yield a white solid. The resulting solid was collected on a 15 mL fine porosity fritted disc, washed with hexanes (2 x 10 mL), and desiccated overnight to yield **10** (0.072 g, 0.086 mmol, 68%). CV (DMA): $E_{p,a}$= + 0.63 V (NHE). IR: *ν*(NO) 1565 cm^{-1}, *ν*(CO) 1717 cm^{-1}, *ν*(CN) 2218 cm^{-1}, *ν*(BH) 2515 cm^{-1}. ^{1}H-NMR (d_3-MeCN, δ, 25 °C): 8.03 (1H, d, TpB3), 7.84 (2H, d, TpB5, TpC5), 7.78 (1H, d, TpA5), 7.69 (1H, d, TpA3), 7.18 (1H, d, TpC3), 6.35 (1H, t, TpB4), 6.32 (1H, t, TpA4), 6.29 (1H, t, TpC4), 4.06 (1H, d, J = 7.0 Hz, H11), 3.84 (3H, s, OMe), 3.75 (3H, s, OMe), 3.70 (3H, s, OMe), 3.65 (1H, m, H1), 3.42 (1H, bs, H4), 2.47 (1H, m, H2), 2.39 (1H, dt J = 12.6, 3.6 Hz, H5), 1.91 (1H, q J = 11.8 Hz, H6), 1.59 (1H, dd = 13.5, 5.3 Hz, H6), 1.28 (3H, s, H10/9), 1.26 (3H, s, H10/9), 1.22 (9H, d J = 8.2 Hz, PMe_3), 1.02 (1H, d J = 11.3 Hz, H3). ^{13}C-NMR (d_3-MeCN, δ, 25 °C): 178.5 (1C, C=O), 170.4 (1C, C=O), 170.1 (1C, C=O), 145.1 (1C, TpB3), 143.7 (1C, TpA3), 141.8 (1C, TpC3), 138.0 (1C, Tp5), 137.8 (1C, Tp5), 137.7 (1C, TpC5), 127.3 (1C, CN), 107.5 (1C, Tp3), 107.4 (1C, Tp3), 107.4 (1C, Tp3), 59.6 (1C, C3), 59.0 (1C, C11), 53.0 (1C, OMe), 52.9 (1C, OMe), 52.4 (1C, OMe) 47.6 (1C, d J = 12.2 Hz, C2), 46.1 (1C, C7), 41.4 (1C, C5), 40.1 (1C, C1), 32.7 (1C, C4), 26.2 (1C, C10/9), 25.7 (1C, C6), 20.9 (1C, C10/9), 14.6 (1C, d J = 31.0 Hz, PMe_3). Anal. Calcd for $C_{29}H_{42}BN_8O_7PW$: C, 41.45; H, 5.04; N, 13.33. Found: C, 41.40; H, 5.06; N, 13.32.

Compound 11

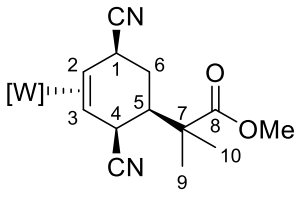

Compound **6** (0.100 g, 0.127 mmol), NaCN (0.032 g, 0.634 mmol), MeCN, and a stir pea were added to a 4 dram to form a cloudy, yellow tinted solution. The reaction was allowed to stir overnight. A white precipitant crashed out of solution overnight. The resulting solid was collected on a 15 mL fine porosity fritted disc, washed with hexanes (2 x 10 mL), and desiccated overnight to yield **11** (0.074 g, 0.100 mmol, 79%). CV (MeCN): $E_{p,a}$= + 0.95 V (NHE). IR: *ν*(NO) 1540 cm^{-1}, *ν*(CO) 1714 cm^{-1}, *ν*(CN) 2226 cm^{-} *ν*(BH) 2527 cm^{-1}. ^{1}H-NMR (d_3-MeCN, δ, 25 ^{o}C): 8.04 (1H, d, TpB3), 7.87 (1H, d, TpB5), 7.86 (1H, d, TpC5), 7.81 (1H, d, TpA5), 7.71 (1H, d, TpA3), 7.36 (1H, d, TpC3), 6.38 (1H, t, TpB4), 6.34 (1H, t, TpA4), 6.30 (1H, t, TpC4), 3.96 (1H, m, H1), 3.72 (3H, s, OMe), 3.53 (1H, bs, H4), 2.79 (1H, m, H2), 2.36 (1H, dm J = 12.4, H5), 2.09 (1H, m, H6a), 1.80 (1H, q J = 12.6, H6b), 1.32 (3H, s, H10/9), 1.30 (3H, s, H10/9), 1.25 (9H, d J = 8.3, PMe_3), 1.05 (1H, d J = 11.3, H3). ^{13}C-NMR (d_3-MeCN, δ, 25 ^{o}C): 178.0 (1C, C=O), 144.7 (1C, TpB3), 143.7 (1C, TpA3), 141.8 (1C, TpC3), 138.1 (1C, Tp5), 138.0 (1C, Tp5), 137.9 (1C, Tp5), 126.8 (2C, CN), 107.8 (1C, TpC4), 107.6 (2C, TpA4, TpB4), 57.5 (1C, C3), 52.6 (1C, OMe), 45.9 (1C, C7), 43.8 (1C, d J = 12.9, C2), 41.0 (1C, C5), 32.5 (1C. C4), 30.7 (1C, C1), 28.9 (1C, C6), 26.2 (1C, C10/9), 21.0 (1C, C10/9), 14.17 (3C, d J = 28.9, PMe_3).

Compound 12

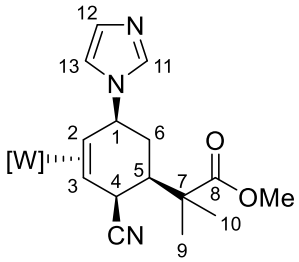

Compound **8** (0.200 g, 0.282 mmol) and MeCN were combined in a test tube. Imidazole (0.190 g, 2.79 mmol), MeCN, and a stir pea were combined in a second test tube. Both solutions were cooled to -30 °C for 15 min. 1M HOTf/MeCN (0.56 mL, 0.560 mmol, -30 °C) was added to the solution of **8** and MeCN via syringe. After 5 min the reaction mixture was added to the imidazole solution. The reaction was stirred for 19 hrs. A tan precipitant formed overnight in solution. The tan precipitant was collected on a 15 mL fine porosity fritted disc, washed with hexanes (3 x 10 mL), and desiccated overnight yielding **12** (0.143 g, 0.184 mmol, 65%). CV (MeCN): $E_{p,a}$= + 0.78 V (NHE). IR: *ν*(NO) 1575 cm^{-1}, *ν*(CO) 1712 cm^{-1}, *ν*(CN) 2358 cm^{-1}, *ν*(BH) 2508 cm^{-1}. ^{1}H-NMR (d_3-MeCN, δ, 25 °C): 8.05 (1H, d, TpB3), 7.89 (1H, s, H11), 7.87 (1H, d, TpB5), 7.85 (1H, d, TpC5), 7.82 (1H, d, TpA5), 7.76 (1H, d, TpA3), 7.51 (1H, s, H13), 7.31 (1H, d, TpC3), 7.07 (1H, s, H12), 6.39 (1H, t, TpB4), 6.36 (1H, t,TpA4), 6.28 (1H, t, TpC4), 5.54 (1H, m, H1), 3.72 (3H, s, OMe), 3.54 (1H, bs, H4), 2.84 (1H, m, H2), 2.56 (1H, dm J = 13.7, H5), 2.02 (1H, dm J = 13.6, H6a), 1.69 (1H, m, H6b), 1.30 (1H, s, H10/9), 1.27 (1H, s, H10/9), 1.23 (1H, d J = 11.5, H3), 0.90 (9H, d J = 8.6, PMe_3). ^{13}C-NMR (d_3-MeCN, δ, 25 °C): 178.2 (1C, C=O), 144.3 (1C, TpB3), 143.9 (1C, TpA3), 141.6 (1C, TpC3), 138.0 (1C, Tp5), 137.8 (2C, Tp5), 137.5 (1C, C11), 130.1 (1C, C13), 127.1 (1C, CN), 118.8 (1C, C13), 107.8 (1C, Tp4), 107.5 (2C, Tp4), 59.5 (1C, C1), 58.4 (1C, C3), 52.5 (1C, OMe), 48.8 (1C, d J = 11.8, C2), 45.9 (1C, C7), 40.6 (1C, C5), 35.7 (1C, C6), 32.8 (1C, C4), 26.4 (1C, C10/9), 20.8 (1C, C10/9), 13.6 (3C, d J = 29.0, PMe_3). Anal. Calcd for $C_{27}H_{38}BN_{10}OPW \cdot 1/3N_2C_3H_5OTf$: C, 40.08; H, 4.71; N, 17.60 Found: C, 39.98; H, 4.72; N, 17.36.

Compound 13

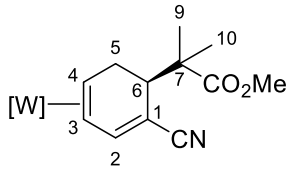

^{1}H-NMR (d_3-MeCN, δ, 25 °C): 8.10 (1H, d, Tp3/5), 8.00 (1H, d, Tp3/5), 7.90 (1H, d, Tp3/5), 7.88 (1H, d, Tp3/5), 7.74 (3H, d, Tp3/5, C2), 7.54 (1H, d, Tp3/5), 6.42 (1H, t, Tp4), 6.30 (1H, t, Tp4), 6.29 (1H, t, Tp4),

3.65 (3H, s, OMe), 3.42 (1H, m, H5a), 3.11 (1H, m, H6), 2.82 (1H, m, H4), 2.69 (1H, m, H5b), 1.66 (1H, m, H3), 1.38 (3H, s, H10/9), 1.30 (3H, s, H10/9), 1.21 (9H, d J = 8.5, PMe_3).

Compound 14

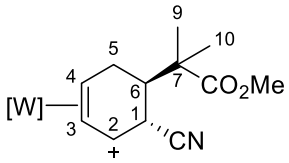

^{1}H-NMR (d_3-MeCN, δ, 25 °C): 8.45 (1H, d, Tp3/5), 8.43 (1H, d, Tp3/5), 8.02 (1H, d, Tp3/5), 7.96 (1H, d, Tp3/5), 7.89 (1H, d, Tp3/5), 7.84 (1H, d, Tp3/5), 6.55 (1H, t, Tp4), 6.54 (1H, t, Tp4), 6.41 (1H, t, Tp4), 5.96 (1H, d J = 7.7, H2), 5.23 (1H, t J = 8.6, H3), 4.82 (1H, d J = 10, H1), 4.62 (1H, m, H4), 3.69 (3H, t, OMe), 3.55 (1H, m, H5a), 2.61 (1H, dd J = 16.0, 8.4, H5b), 2.48 (1H, q J = 9.2, H6), 1.29 (3H, s, H10/9), 1.28 (3H, s, H10/9), 1.20 (9H, d J = 9.8, PMe_3). ^{13}C-NMR (d_3-MeCN, δ, 25 °C): 177.3 (1C, CO), 148.5 (1C, Tp3), 144.6 (1C, Tp3), 1423.1 (1C, Tp3), 149.8 (1C, Tp5), 139.7 (1C, Tp5), 139.6 (1C, Tp5), 122.2 (1C, CN), 117.6 (1C, C2), 109.4 (1C, Tp4), 109.2 (1C, Tp4), 108.4 (1C, Tp4), 104.6 (1C, C3), 73.0 (1C, C4), 52.8 (1C, OMe), 46.6 (1C, C7), 40.1 (1C, C6), 32.3 (1C, C1), 28.6 (1C, C5), 23.5 (1C, C10/9), 23.4 (1C, C10/C9), 12.8 (3C, d J = 34.0, PMe_3).

Compound 18a and 18b

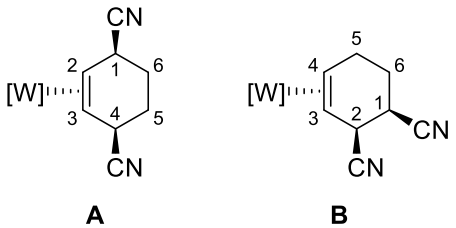

Compound **16** (0.250 g, 0.346 mmol) and MeCN were combined in a test tube. NaCN (0.051 g, 1.04 mmol), MeOH, and a stir pea were combined in a second test tube. Both solutions were cooled to -30 °C for 15

min. 1M HOTf/MeCN (0.41 mL, 0.41 mmol, -30 °C) was added to the solution of **16** and MeCN via syringe. The reaction turned a dark brown upon addition of the acid. After 15 min, the reaction was added to the solution of NaCN and MeOH. 1 mL of MeCN was used to rinse the first test tube and added to the reaction solution. The reaction was stirred for 24 hrs. After 24 hrs, the reaction was removed from the glovebox and warmed to room temperature. The reaction was evaporated to dryness to form a dark brown oil. A 60 mL medium porosity frit was filled ¾ full with silica and set in hexanes. Minimal acetone was used to pick the reaction oil up and load it onto the column. The silica plug was washed with 100 mL of hexanes, followed by 150 mL of diethyl ether, and finally by 150 mL of ethyl acetate. The ethyl acetate was then evaporated to dryness yielding a yellow oil. The oil was picked up in minimal DCM and precipitated into 20 mL of stirring pentane to yield an off white solid. The off-white solid was collected on a 15 mL fine porosity fritted disc, washed with hexanes (3 x 10 mL), and desiccated overnight yielding a combination of **18a** and **18b** (0.155 g, 0.244 mmol, 70%). CV (MeCN): $E_{p,a}$= + 0.69 V (NHE). IR: *ν*(NO) 1547cm^{-1}, *ν*(CN) 2230 cm^{-1}, *ν*(BH) 2480 cm^{-1}. ^{1}H-NMR **18a** (d_3-MeCN, δ, 25 ^{o}C): 8.06 (1H, d, TpA3), 8.03 (1H, d, TpB3), 7.89 (1H, d, TpB5), 7.87 (1H, d, TpC5), 7.82 (1H, d, TpA5), 7.43 (1H, d, TpC3), 6.40 (1H, t, TpB4), 6.33 (1H, t, TpA4), 6.29 (1H, t, TpC4), 4.03 (1H, m, H4), 3.86 (1H, t J= 5.7, H1), 2.62 (1H, td J = 11.4, 1.6, H2), 2.07 (1H, m, H5a), 2.02 (1H, m, H6a), 1.92 (1H, m, H6b), 1.82 (1H, m, H5b), 1.16 (10H, d J = 8.2, PMe_3, H3). ^{1}H-NMR **18b** (d_3-MeCN, δ, 25 ^{o}C): 8.09 (1H, d, TpA3), 8.02 (1H, d, TpB3), 7.88 (1H, d, TpB5), 7.85 (1H, d, TpC5), 7.82 (1H, d, TpA5), 7.43 (1H, d, TpC3), 6.39 (1H, t, TpB4), 6.33 (1H, t, TpA4), 6.28 (1H, t, TpC4), 4.25 (1H, t J = 3.7, H2), 3.41 (1H, m, H5a), 3.33 (1H, m, H1), 2.78 (1H, m, H5b), 2.70 (1H, m, H4), 1.94 (1H buried, H6a, H6b), 1.13z (10H, d J = 8.5, PMe_3, H3). ^{13}C-NMR (d_3-MeCN, δ, 25 ^{o}C) **18a**: 144.4 (1C, Tp3), 142.9 (1C, Tp3), 142.0 (1C, Tp3), 138.3 (1C, Tp5), 137.9 (1C, Tp5), 137.8 (1C, Tp5), 127.7 (1C, CN), 127.2 (1C, CN), 107.9 (1C, Tp4). 107.4 (1C, Tp4), 107.1 (1C, Tp4), 50.3 (1C, C3), 48.9 (1C, d J = 12.4, C2), 31.3 (1C, d J = 4.3, C1), 30.9 (1C, C4), 26.0 (2C, C5, C6), 13.42 (3C, d J = 29.3, PMe_3). ^{13}C-NMR (d_3-MeCN, δ, 25 ^{o}C) **18b**: 144.5 (1C, Tp3), 143.4 (1C, Tp3), 141.7 (1C, Tp3), 138.1 (1C, Tp5), 137.8 (1C, Tp5), 137.7 (1C, Tp5), 124.9 (1C, CN), 121.7

(1C, CN), 107.8 (1C, Tp4). 107.4 (1C, Tp4), 107.1 (1C, Tp4), 50.3 (1C, C3) 47.9 (1C, d J = 11.8, C4), 35.5 (1C, C2), 30.1 (1C, C1), 27.3 (1C, d J = 4.0, C5), 26.2 (1C, C6) 13.42 (3C, d J = 29.3, PMe_3). Anal. Calcd for $C_{20}H_{27}BN_9OPW$: C: 37.82, H: 4.29, N: 19.85. Found: C: 38.19, H: 4.49, N: 19.80.

Compound 21

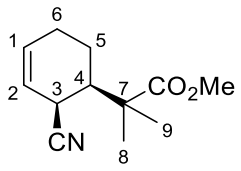

Outside of the glovebox, **9** (0.100 g, 0.140 mmol) and acetone were combined in a 4-dram vial. A stir pea and $NOPF_6$ (0.040 g, 0.228 mmol) were added to a separate 4-dram vial. The solution of **9** in acetone was then added to the vial with the stir pea and $NOPF_6$ while stirring. The initial solution was black and became a golden yellow as it stirred overnight. The golden solution was evaporated to dryness, picked up in minimal DCM, and added to 20 mL of stirring pentane. A green precipitant formed and was collected on a 15 mL medium porosity fritted disc and washed with hexanes (2 x 10 mL). The resulting filtrate was evaporated to dryness. The resulting oil was washed with 25 mL of hexanes. The remaining oil was washed with ether and ran through 30 mL of silica. The silica was washed with 60 mL of ether. The filtrate was evaporated to dryness yielding **21** (0.018 g, 0.088 mmol, 63%). ^{1}H-NMR (d_3-MeCN, δ, 25 ^{o}C): 5.92 (1H, m, H1), 5.70 (1H, m, H2), 3.65 (3H, s, OMe), 3.32 (1H, m, H3), 2.25 (1H, dt J = 18.6, 5.3, H6a), 2.12 (1H, m, H6b), 2.01 (1H, dd J = 12.7, 1.9, H4), 1.80 (1H, dd J = 13.6, 6.3, H5a), 1.60 (1H, m, H5b), 1.28 (3H, s, H9/8), 1.27 (3H, s, H9/8). ^{13}C-NMR (d_3-MeCN, δ, 25 ^{o}C): 177.8 (1C, C=O), 132.4 (1C, C1), 123.2 (1C, C2), 120.9 (1C, CN), 52.5 (1C, OMe), 45.6 (1C, C7), 44.0 (1C, 4), 28.9 (1C, C3), 27.2 (1C, 6), 23.1 (1C, 9/8), 22.7 (1C, C9/8), 22.3 (1C, C5). HRMS (ESI-TOF) *m/z*: $[M+Na]^+$ calcd for 230.1151 found 230.1154.

Compound 22

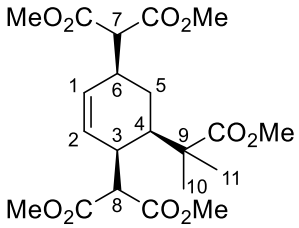

Outside of the glovebox, **10** (0.100 g, 0.106 mmol) and acetone were combined in a 4-dram vial. A stir pea and $NOPF_6$ (0.028 g, 0.160 mmol) were added to a separate 4-dram vial. The solution of **10** in acetone was then added to the vial with the stir pea and $NOPF_6$ while stirring. The initial solution was black and became a golden yellow as it stirred overnight. The golden solution was evaporated to dryness, picked up in minimal DCM, and added to 20 mL of stirring pentane. A green precipitant formed and was collected on a 15 mL medium porosity fritted disc and washed with hexanes (2 x 10 mL). The resulting filtrate was evaporated to dryness. The resulting oil was washed with 25 mL of hexanes followed by 25 mL of ether. The remaining oil was dissolved in ethyl acetate and ran through 30 mL of silica. The silica was washed with 60 mL of ethyl acetate. The filtrate was evaporated to dryness yielding **22** (0.028 g, 0.063 mmol, 59%). ^{1}H-NMR (d_3-MeCN, δ, 25 °C): 5.77 (1H, ddd J = 10.11, 5.61, 2.44 Hz, H2), 5.57 (1H, dm J = 10.12 Hz, H1), 3.37 (1H, d J = 2.89 Hz, H8), 3.71 (3H, s, OMe), 3.70 (3H, s, OMe), 3.68 (3H, s, OMe), 3.62 (6H, s, 2OMe), 3.16 (1H, d J = 9.11 Hz, H7), 3.11 (1H, bm, H3), 2.85 (1H, m, H6), 2.00 (1H, ddd J = 12.98, 4.98, 2.00 Hz, H4), 1.79 (1H, m, H5), 1.21 (1H, m, H5), 1.20 (3H, s, H11/10), 1.18 (3H, s, H11/10). ^{13}C-NMR (d_3-MeCN, δ, 25 °C): 178.28 (1C, C=O), 170.40 (1C, C=O), 169.97 (1C, C=O), 169.47 (1C, C=O), 169.46 (1C, C=O), 130.66 (1C, C2), 129.95 (1C, C1), 57.35 (1C, C8), 53.33 (1C, OMe), 53.08 (2C, 2OMe), 52.76 (1C, C7), 52.41 (1C, OMe), 52.31 (1C, OMe), 47.03 (1C, C4), 45.07 (1C, C9), 38.88 (1C, C6), 36.76 (1C, C3), 25.67 (1C, C11/10), 25.08 (1C, C5), 23.94 (1C, C11/10). HRMS (ESI-TOF) *m*/*z*: $[M+Na]^+$ calcd for 465.1731; found 465.1734.

Compound 23

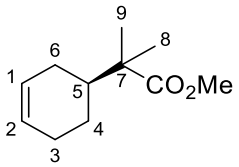

Outside of the glovebox, **3** (0.100 g, 0.156 mmol) and acetone were combined in a 4-dram vial. A stir pea and $NOPF_6$ (0.040 g, 0.228 mmol) were added to a separate 4-dram vial. The solution of **3** in acetone was then added to the vial with the stir pea and $NOPF_6$ while stirring. The initial solution was black and became a golden yellow as it stirred overnight. The golden solution was evaporated to dryness, picked up in minimal DCM, and added to 20 mL of stirring pentane. A green precipitant formed and was collected on a 15 mL medium porosity fritted disc and washed with hexanes (2 x 10 mL). The resulting filtrate was evaporated to dryness **23** (0.018 g, 0.098 mmol, 63%). ^{1}H-NMR (d_3-MeCN, δ, 25 °C): 5.65 (2H, m, H2, H1), 3.61 (3H, s, OMe), 2.08 (1H, H3a), 2.03 (1H, m, H3b), 1.88 (1H, m, H6a), 1.82 (2H, m, H6b, H5), 1.65 (1H, m, H4a), 1.19 (1H, m, H4b), 1.13 (3H, s, H9/8), 1.09 (3H, s, H9/8). ^{13}C-NMR (d_3-MeCN, δ, 25 °C): 178.8 (1C, C=O), 127.7 (1C, C2/1), 127.4 (1C, C2/1), 52.0 (1C, OMe), 45.9 (1C, C7), 42.6 (1C, C5), 27.3 (1C, C6), 27.0 (1C, C3), 24.9 (1C, C4), 22.2 (1C, C9/8), 22.1 (1C, C9/8). HRMS (ESI-TOF) *m*/*z*: $[M+H]^+$ calcd for 183.1379; found 183.1378.

Compound 25

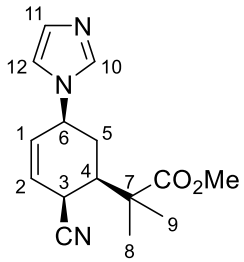

Outside of the glovebox, **12** (0.100 g, 0.129 mmol) and acetone were combined in a 4-dram vial. A stir pea and $NOPF_6$ (0.036 g, 0.206 mmol) were added to a separate 4-dram vial. The solution of **12** in acetone was

then added to the vial with the stir pea and $NOPF_6$ while stirring. The initial solution was black and became a golden yellow as it stirred overnight. The golden solution was evaporated to dryness, picked up in minimal DCM, and added to 20 mL of stirring pentane. A green precipitant formed and was collected on a 15 mL medium porosity fritted disc and washed with hexanes (2 x 10 mL). The resulting filtrate was evaporated to dryness. The resulting oil was washed with 25 mL of hexanes followed by 25 mL of ether. The remaining oil was dissolved in ethyl acetate and ran through 30 mL of basic alumina. The basic alumina was washed with 60 mL of ethyl acetate. The basic alumina was washed with 100 mL of acetone. The acetone filtrate was evaporated to dryness yielding **25** (0.019 g, 0.070 mmol, 54%) ^{1}H-NMR A (d_3-MeCN, δ, 25 ^{o}C): 7.56 (1H, bs, H10), 5.04 (1H, t J = 1.3, H11), 6.97 (1H, t J = 1.2, H12), 6.01 (1H, ddd J = 9.5, 5.5, 2.4, H2), 5.92 (1H, dm J = 9.8, H1), 4.96 (1H, m, H6), 3.67 (3H, s, OMe), 3.50 (1H, m, H3), 2.29 (2H, m, H5a, H4), 1.84 (1H, m, H5b), 1.30 (6H, s, H9, H8). ^{13}C-NMR (d_3-MeCN, δ, 25 ^{o}C): 177.3 (1C, C=O), 137.1 (1C, C10), 131.9 (1C, C1), 129.8 (1C, C11), 127.1 (C1, C2), 119.8 (C1, CN), 118.1 (1C, buried, C12), 55.6 (1C, C6), 52.6 (1C, OMe), 45.4 (1C, C7), 43.3 (1C, C4), 31.1 (1C, C5), 28.8 (1C, C3), 23.1 (1C, C9/8), 22.8 (1C, C9/8). HRMS (ESI-TOF) *m*/*z*: $[M+H]^+$ calcd for 274.1550; found 274.1552.

Compound 27 a and b

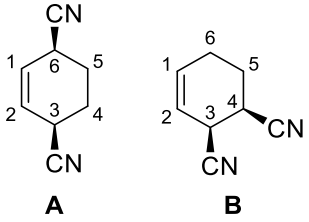

Outside of the glovebox, **18** (0.055 g, 0.086 mmol) and acetone were combined in a 4-dram vial. A stir pea and $NOPF_6$ (0.024 g, 0.1.37 mmol) were added to a separate 4-dram vial. The solution of **18** in acetone was then added to the vial with the stir pea and $NOPF_6$ while stirring. The initial solution was black and became a golden yellow as it stirred overnight. The golden solution was evaporated to dryness, picked up

in minimal DCM, and added to 20 mL of stirring pentane. A green precipitant formed and was collected on a 15 mL medium porosity fritted disc and washed with hexanes (2 x 10 mL). The resulting filtrate was evaporated to dryness. The resulting oil was washed with 25 mL of hexanes followed by 25 mL of ether. The remaining oil was dissolved in ethyl acetate and ran through 30 mL of silica. The silica was washed with 60 mL of ethyl acetate. The filtrate was evaporated to dryness yielding **27** (0.007 g, 0.053 mmol, 62%). ^{1}H-NMR **A** (d_3-MeCN, δ, 25 ^{o}C): 5.92 (2H, d J = 1.5, H2, H1), 3.42 (2H, m, H3, H6), 2.1 (4H, m, H5, H4). ^{1}H-NMR **B** (d_3-MeCN, δ, 25 ^{o}C): 6.01 (1H, m, H2), 5.65 (1H, m, H1), 3.75 (1H, m, H3), 3.28 (1H, q J = 6.1, H4), 2.27 (1H, m, H6/5), 2.01 (3H, buried, H6, H5). ^{13}C-NMR **A** (d_3-MeCN, δ, 25 ^{o}C): 126.4 (2C, C2, C1), 1221.3 (2C, CN), 26.5 (2C, C6, C3), 24.67 (2C, C5, C4). ^{13}C-NMR **B** (d_3-MeCN, δ, 25 ^{o}C): 132.3 (1C, C2), 119.7 (1C, C1), 30.3 (1C, C3), 28.9 (1C, C4), 23.9 (1C, C6/5), 23.1 (1C, C6/5).

References

(1) Smith, J. A.; Simpson, S. R.; Westendorff, K. S.; Weatherford-Pratt, J.; Myers, J. T.; Wilde, J. H.; Dickie, D. A.; Harman, W. D. *Organometallics* **2020**, *39*, 2493.

(2) Wallace, T. J.; Hofmann, J. E.; Schriesheim, A. *Journal of the American Chemical Society* **1963**, *85*, 2739.

(3) Wilson, K. B.; Myers, J. T.; Nedzbala, H. S.; Combee, L. A.; Sabat, M.; Harman, W. D. *Journal of the American Chemical Society* **2017**, *139*, 11401.

(4) Cubbage, J. W.; Vos, B. W.; Jenks, W. S. *Journal of the American Chemical Society* **2000**, *122*, 4968.

(5) Guan, Y.; Wang, C.; Wang, D.; Dang, G.; Chen, C.; Zhou, H.; Zhao, X. *RSC Advances* **2015**, *5*, 12821.

(6) Sakakibara, T.; Suganuma, T.; Kajihara, Y. *Chemical Communications* **2007**, 3568.

(7) Ochiai, M.; Ukita, T.; Fujita, E. *Journal of the Chemical Society, Chemical Communications* **1983**, 619.

(8) Trost, B. M. *Chemistry: a European journal* **2019**, *25*, 11193.

(9) Brown, D. S.; Ley, S. V.; Vile, S. *Tetrahedron Letters* **1988**, *29*, 4873.

(10) Brown, D. S.; Charreau, P.; Hansson, T.; Ley, S. V. *Tetrahedron* **1991**, *47*, 1311.

(11) Harrison, D. P.; Nichols-Nielander, A. C.; Zottig, V. E.; Strausberg, L.; Salomon, R. J.; Trindle, C. O.; Sabat, M.; Gunnoe, T. B.; Iovan, D. A.; Myers, W. H.; Harman, W. D. *Organometallics* **2011**, *30*, 2587.

(12) Seeman, J. I. *Chemical Reviews* **1983**, *83*, 83.

(13) Wertjes, W. C.; Southgate, E. H.; Sarlah, D. *Chemical Society Reviews* **2018**, *47*, 7996.

(14) Dyson, P. J. *Dalton Transactions* **2003**, 2964.

(15) **!!! INVALID CITATION !!! =**

(16) Hudlicky, T.; Entwistle, D. A.; Pitzer, K. K.; Thorpe, A. J. *Chemical Reviews* **1996**, *96*, 1195.

(17) Ohno, H.; Okumura, M.; Maeda, S.-i.; Iwasaki, H.; Wakayama, R.; Tanaka, T. *The Journal of Organic Chemistry* **2003**, *68*, 7722.

(18) Wefelscheid, U. K.; Berndt, M.; Reißig, H.-U. *European Journal of Organic Chemistry* **2008**, *2008*, 3635.

(19) Southgate, E. H.; Pospech, J.; Fu, J.; Holycross, D. R.; Sarlah, D. *Nature Chemistry* **2016**, *8*, 922.

(20) Remy, R.; Bochet, C. G. *Chemical Reviews* **2016**, *116*, 9816.

(21) Jacquemot, G.; Ménard, M.-A.; L'Homme, C.; Canesi, S. *Chemical Science* **2013**, *4*, 1287.

(22) Lee, S.; Chataigner, I.; Piettre, S. R. *Angewandte Chemie International Edition* **2011**, *50*, 472.

(23) Schmidt, Y.; Lam, J. K.; Pham, H. V.; Houk, K. N.; Vanderwal, C. D. *Journal of the American Chemical Society* **2013**, *135*, 7339.

(24) Liebov, B. K.; Harman, W. D. *Chemical Reviews* **2017**, *117*, 13721.

(25) Pape, A. R.; Kaliappan, K. P.; Kündig, E. P. *Chemical Reviews* **2000**, *100*, 2917.

(26) Harman, W. D. *Chemical Reviews* **1997**, *97*, 1953.

(27) Keane, J. M.; Harman, W. D. *Organometallics* **2005**, *24*, 1786.

(28) Kundig, E. P. *Transition Metal Arene Complexes in Organic Synthesis and Catalysis*; Springer: Berlin, 2004; Vol. 7.

(29) Feng, M.; Tang, B.; Liang, S. H.; Jiang, X. *Curr Top Med Chem* **2016**, *16*, 1200.

(30) Reitz, A. B.; Smith, G. R.; Parker, M. H. *Expert Opinion on Therapeutic Patents* **2009**, *19*, 1449.

(31) Lipinski, C. A.; Lombardo, F.; Dominy, B. W.; Feeney, P. J. *Advanced drug delivery reviews* **2001**, *46*, 3.

(32) Ghose, A. K.; Viswanadhan, V. N.; Wendoloski, J. J. *Journal of combinatorial chemistry* **1999**, *1*, 55.

(33) Veber, D. F.; Johnson, S. R.; Cheng, H. Y.; Smith, B. R.; Ward, K. W.; Kopple, K. D. *J Med Chem* **2002**, *45*, 2615.

(34) Egan, W. J.; Merz, K. M., Jr.; Baldwin, J. J. *J Med Chem* **2000**, *43*, 3867.

(35) Muegge, I.; Heald, S. L.; Brittelli, D. *J Med Chem* **2001**, *44*, 1841.

(36) Lis, E. C.; Salomon, R. J.; Sabat, M.; Myers, W. H.; Harman, W. D. *Journal of the American Chemical Society* **2008**, *130*, 12472.

(37) Kolis, S. P.; Chordia, M. D.; Liu, R.; Kopach, M. E.; Harman, W. D. *Journal of the American Chemical Society* **1998**, *120*, 2218.

(38) Smith, P. L.; Keane, J. M.; Shankman, S. E.; Chordia, M. D.; Harman, W. D. *J Am Chem Soc* **2004**, *126*, 15543.

(39) Kopach, M. E.; Harman, W. D. *The Journal of Organic Chemistry* **1994**, *59*, 6506.

(40) Kopach, M. E.; Harman, W. D. *Journal of the American Chemical Society* **1994**, *116*, 6581.

(41) Zottig, V. E.; Todd, M. A.; Nichols-Nielander, A. C.; Harrison, D. P.; Sabat, M.; Myers, W. H.; Harman, W. D. *Organometallics* **2010**, *29*, 4793.

(42) Todd, M. A.; Grachan, M. L.; Sabat, M.; Myers, W. H.; Harman, W. D. *Organometallics* **2006**, *25*, 3948.

(43) Todd, M. A.; Sabat, M.; Myers, W. H.; Harman, W. D. *Journal of the American Chemical Society* **2007**, *129*, 11010.

(44) Todd, M. A.; Sabat, M.; Myers, W. H.; Smith, T. M.; Harman, W. D. *Journal of the American Chemical Society* **2008**, *130*, 6906.

(45) Salomon, R. J.; Todd, M. A.; Sabat, M.; Myers, W. H.; Harman, W. D. *Organometallics* **2010**, *29*, 707.

(46) Gonzalez, J.; Sabat, M.; Harman, W. D. *Journal of the American Chemical Society* **1993**, *115*, 8857.

(47) Kolis, S. P.; Gonzalez, J.; Bright, L. M.; Harman, W. D. *Organometallics* **1996**, *15*, 245.

(48) Kopach, M. E.; Kolis, S. P.; Liu, R.; Robertson, J. W.; Chordia, M. D.; Harman, W. D. *Journal of the American Chemical Society* **1998**, *120*, 6199.

(49) Chordia, M. D.; Harman, W. D. *Journal of the American Chemical Society* **2000**, *122*, 2725.

(50) Rose-Munch, F.; Rose, E. *European Journal of Inorganic Chemistry* **2002**, *2002*, 1269.

(51) Gibson, S. E.; Guillo, N.; White, A. J. P.; Williams, D. J. *Journal of the Chemical Society, Perkin Transactions 1* **1996**, 2575.

(52) Zhao, Z.; Messinger, J.; Schön, U.; Wartchow, R.; Butenschön, H. *Chemical Communications* **2006**, 3007.

(53) G. Davies, S.; Loveridge, T.; Fatima C. C. Teixeira, M.; M. Clough, J. *Journal of the Chemical Society, Perkin Transactions 1* **1999**, 3405.

(54) Marcos, C. F.; Perrio, S.; Slawin, A. M. Z.; Thomas, S. E.; Willams, D. J. *Journal of the Chemical Society, Chemical Communications* **1994**, 753.

(55) Hutchins, R. O.; Learn, K. *The Journal of Organic Chemistry* **1982**, *47*, 4380.

(56) Lankenau, A. W.; Iovan, D. A.; Pienkos, J. A.; Salomon, R. J.; Wang, S.; Harrison, D. P.; Myers, W. H.; Harman, W. D. *Journal of the American Chemical Society* **2015**, *137*, 3649.

(57) Wilson, K. B.; Smith, J. A.; Nedzbala, H. S.; Pert, E. K.; Dakermanji, S. J.; Dickie, D. A.; Harman, W. D. *The Journal of Organic Chemistry* **2019**, *84*, 6094.

(58) Myers, J. T.; Smith, J. A.; Dakermanji, S. J.; Wilde, J. H.; Wilson, K. B.; Shivokevich, P. J.; Harman, W. D. *Journal of the American Chemical Society* **2017**, *139*, 11392.

Chapter 6

An Investigation of Amine Additions to the η^2-Phenyl Sulfone Family of Complexes

6.1 Introduction

While numerous methods have been developed for the addition of amines to alkenes and alkynes, similar reactions for benzene functionalization are less common and highly endergonic.[1-4] Previous work in our lab found that protonation of the W(Tp)(NO)(PMe_3)(η^2-benzene) system followed by the addition of methylamine resulted in the hydroamination of the benzene ring when kept under basic conditions and low temperatures.[5] This chapter presents the use of amines to expand the range of nucleophiles tolerable by the W(Tp)(NO)(PMe_3)(η^2-phenyl sulfone) systems. Also included is an intramolecular cyclization that results in the formation of a bicyclic compound. Recently highlighted issues of late-stage tolerance of amines and lack of methodology to synthesize or modify aliphatic nitrogen heterocycles led us to this investigation.[6-8] Also, to note, Njardarson et al. conducted a recent study that reported that 59% of unique small molecules contained a nitrogen heterocycle with piperidine being one of the most common.[6,7]

6.2 Secondary Amines as First Nucleophiles

Previous work in our lab reported the ability to introduce a proton followed by a range of amines to the cationic η^2-*N*-ethylindolinium species at room temperature with the products being isolated via basic extraction.[9] This work was applied to the η^2-trifluorotoluene tungsten system with a few modifications.[10] Due to the tendency for amines to eliminate at room temperature and reform starting material, a lower temperature (-30 °C) and base quench with a relatively strong base (tBuOK) was needed for the additions to be successful. This strategy was applied to the η^2-phenyl sulfone systems. It was shown in Chapter 4 that protonation of **1** and **2** can occur with HOTf leveled in MeCN at 0 °C to afford a distorted allyl with the positive charge localized distal to the PMe_3 ligand. The introduction of a primary amine (i.e., methyl amine) to the newly formed allyls led to what was believed to be a successful addition based on *in situ* ^{1}H and ^{31}P NMR data at low temperatures. However, attempts to work up the addition product led to the elimination of the amine and formation of the dihapto bound aromatic starting material.

Fortunately, the usage of secondary amines appeared to rectify this issue. Piperidine, morpholine, and the aromatic heterocycle imidazole were all successfully added as the first nucleophile and isolated to yield the η^2-dienes **3**, **4**, and **5** (**Scheme 6.1**). The additions of morpholine (**5**) and imidazole (**3**) were isolated as precipitates after aqueous extractions, while the addition of morpholine (**4**) crashed out of the reaction solution. As seen in Chapter 4, the nucleophiles add anti to the metal.

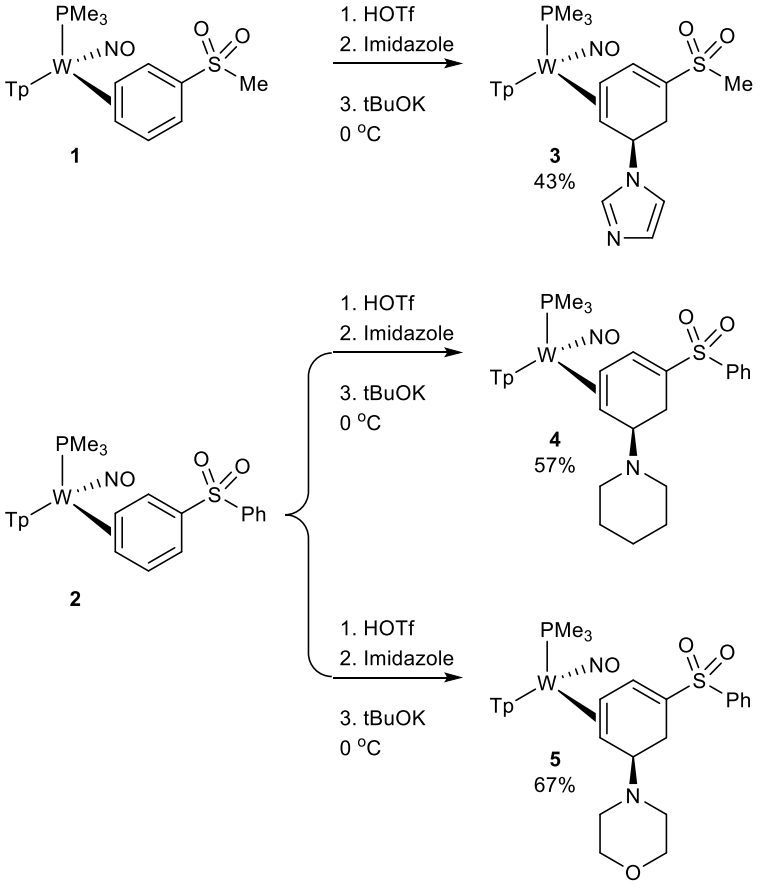

Scheme 6.1: First nucleophilic addition of secondary amines to η^2-phenyl sulfones

6.3 Intramolecular Cyclization Reaction Resulting in Lactam Formation

Previous work with the η^2-trifluorotoluene and η^2-benzene systems showed a vast range of nucleophiles that could be added following initial protonation at low temperature.[5,10] Investigation of a second tandem protonation/nucleophilic addition with a high concentration of a primary amine as the nucleophile led to an intramolecular lactamization if the first nucleophilic addition resulted in an ester.[5,10]

This process led to the formation of indoline derivatives functionalized by a -CF_3 group in the case of the η^2-trifluorotoluene system. These conditions were applied to the η^2-methyl phenyl sulfone system in the hope that the commonly seen intramolecular lactamization would occur.[11-19]

Initial protonation of complexes **6** and **7** at low temperatures was followed quickly by the introduction of ten equivalents of a variety of amines. The initial amine addition stirred overnight at -30 °C. The reaction was warmed to room temperature and allowed to stir for two days. The process was monitored by ^{31}P NMR until a single product was observed. Aqueous workups yielded lactam products **8**, **9**, **10**, and **11** (**Scheme 6.2**). Successful addition of the amine group is indicated through the primary functionality of the amine. In the case of the benzylamine nucleophile, two geminal doublets at 4.55 and 4.22 appear in the product along with corresponding aromatic features. The C5 methine proton appears downfield at 4.65 ppm compared to the typical methine protons of carbon or hydride nucleophiles. This proton exhibits a COESY correlation to the downbound at 1.29 ppm indicating the functional group adding to the carbon adjacent to the downbound carbon. This same proton exhibits NOE correlations to the TpA and TpC pyrazole rings, indicating that the proton is syn to the metal. This demonstrates that the addition occurs anti to the metal and thus a cis fused ring. An intramolecular cyclization is indicated through the loss of the methoxy peak from the starting material and the retention of the carbonyl IR frequency. HMBC correlations between the carbonyl carbon, the two proton singlets of the methyl groups H15 and H16, and the methine protons at 4.65 and 2.82 ppm also indicated cyclization. Previous carbonyls from second additions like those in Chapters 4 and 5 do not have HMBC correlations with the methines of C5. The data also matches nicely with similar lactam formations in the W(Tp)(NO)(PMe_3)(η^2-trifluorotoluene) and W(Tp)(NO)(PMe_3)(η^2-benzene) systems.[5,10]

While the products **8**, **9**, **10**, and **11** were synthesized through previously demonstrated methods, the products significantly differed from those of the W(Tp)(NO)(PMe_3)(η^2-trifluorotoluene) and W(Tp)(NO)(PMe_3)(η^2-benzene) systems. The lactam products synthesized from the η^2-methyl phenyl

sulfone system were η^2-dienes resulting from the elimination of the sulfone functionality. While the trifluorotoluene system was restricted to -CF_3 functionalization, compounds **8**, **9**, **10**, and **11** now have to ability to undergo a third tandem protonation/nucleophilic addition, as shown in Chapter 5. This process allows for the formation of a nitrogen-containing heterocycle while potentially allowing for further functionalization. Both the η^2-$PhSO_2Ph$ and η^2-$PhSO_2(NC_4H_8)$ systems yielded identical products. In no instance was the sulfone functionality retained.

Though intramolecular lactamization is not anything novel, a recent paper submitted for publication from our group demonstrated efforts to synthesize a multicyclic biologically active molecule known as γ-lycorane from lactams synthesized from the W(Tp)(NO)(PMe_3)(η^2-trifluorotoluene) and W(Tp)(NO)(PMe_3)(η^2-benzene) systems. A benefit that the lactam products resulting from the W(Tp)(NO)(PMe_3)(η^2-phenyl sulfone) systems have is the elimination of the sulfone moiety to form a diene during the reaction. This allows for a third protonation, which could allow for a potential cyclization that would be influenced by the metal center. Work is currently underway to synthesize multicyclic products from complexes such as **9** and **10.**

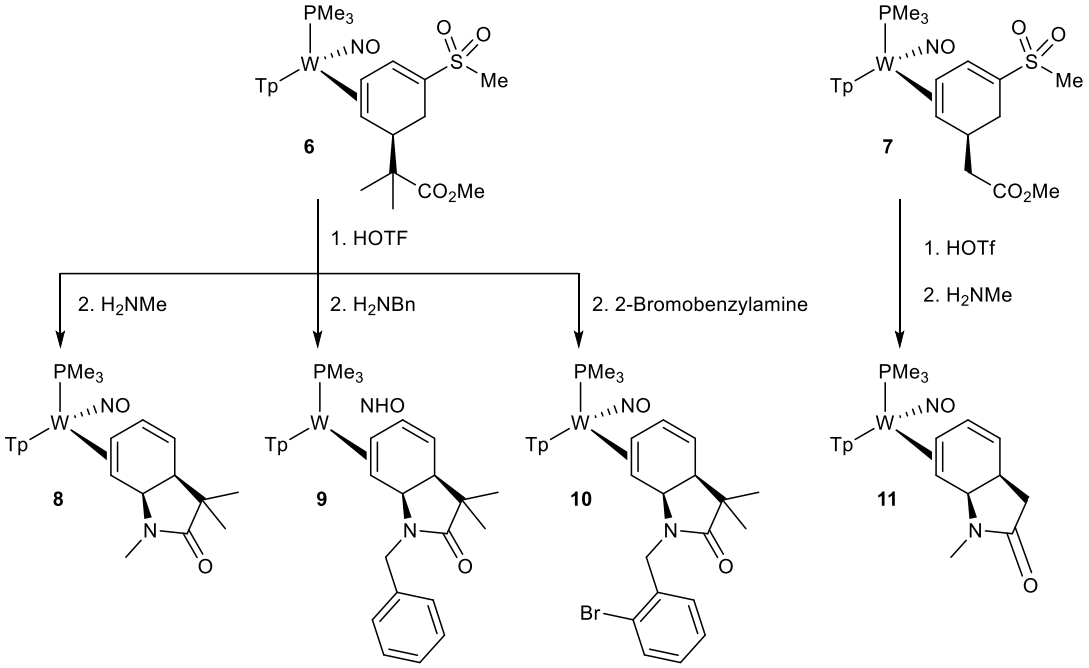

Scheme 6.2: Intramolecular cyclization reaction forming lactam products

6.4 Third Additions to Coordinated Bicyclic Lactams

With the intramolecular lactamization successful and resulting in an η^2-diene, sights were set on demonstrating the ability of the new bicyclic η^2-diene to undergo a third tandem protonation/nucleophilic addition. Compounds **8** and **11** were both successfully protonated at low temperatures and upon exposure to a hydride source, underwent addition of H^- to form **12** and **14,** respectively (**Scheme 6.3**). The hydride adds to the allyl with the cation proximal to the PMe_3 ligand compared to the allyl with the cation distal to the PMe_3 ligand in a ratio of ~10 : 1. Repeating this process with CN^- as the nucleophile led to the same result and formed complexes **13** and **15** (**Scheme 6.3**). In this instance, the nucleophile adds anti to the face of the diene bound by the metal. Current work is underway to expand the range of nucleophiles.

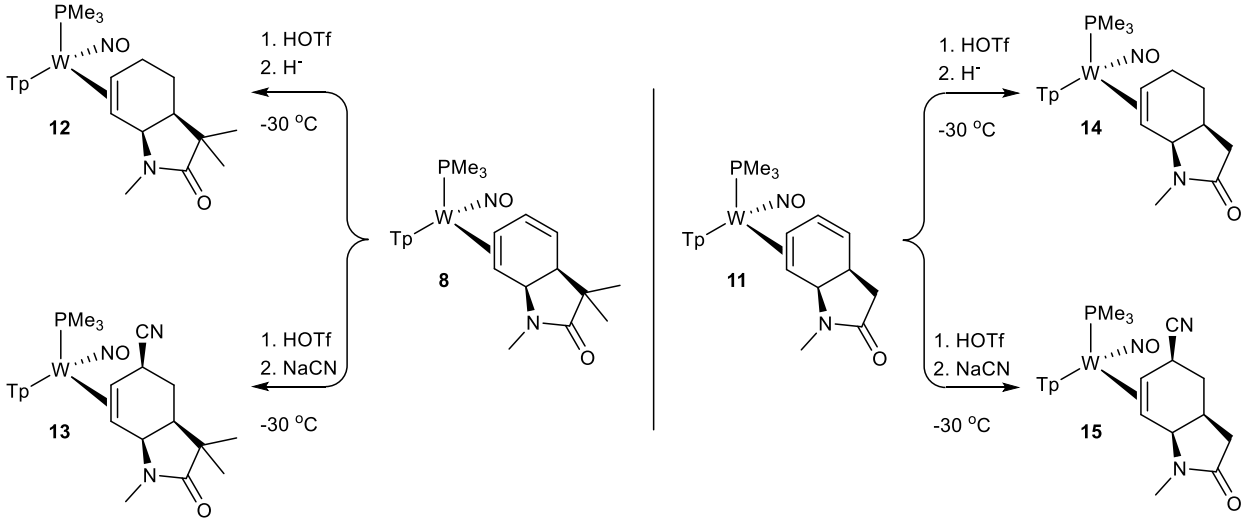

Scheme 6.3: Third tandem protonation/nucleophilic addition to dihapto bound bicyclic lactams

6.5 Conclusion

The dihapto coordinated compounds $WTp(NO)(PMe_3)(\eta^2\text{-}PhSO_2Me)$ and $WTp(NO)(PMe_3)(\eta^2\text{-}PhSO_2Ph)$ were able to successfully undergo an initial tandem protonation/nucleophilic addition utilizing secondary amines. The use of primary amines as the second nucleophile led to an intramolecular cyclization resulting in a lactam when the first nucleophile contained an ester. Finally, the resulting η^2-

dienes from the lactamization process were able to under a third tandem protonation/nucleophilic addition to yield η^2-cyclohexenes. This work hit on the overall goals laid out in the introduction. A variety of amine nucleophiles were able to be added at every step of the functionalization process. Nitrogen-containing heterocycles were able to be introduced through this tandem addition, while intramolecular cyclization also resulted in the synthesis of a nitrogen-containing heterocycle in the form of a lactam. Future work will include isolation of these organics and manipulations of the lactam products to form more complex multicyclic products.

Experimental

General Methods. NMR spectra were obtained on 500, 600, or 800 MHz spectrometers. Chemical shifts are referenced to tetramethylsilane (TMS) utilizing residual ^{1}H signals of the deuterated solvents as internal standards. Chemical shifts are reported in ppm and coupling constants (J) are reported in hertz (Hz). Chemical shifts for ^{19}F and ^{31}P spectra are reported relative to standards of hexafluorobenzene (164.9 ppm) and triphenylphosphine (−6.00 ppm) or triphenyl phosphate (−16.58 ppm). Infrared spectra (IR) were recorded as a solid on a spectrometer with an ATR crystal accessory, and peaks are reported in cm^{-1}. Electrochemical experiments were performed under a nitrogen atmosphere. Most cyclic voltammetric data were recorded at ambient temperature at 100 mV/s, unless otherwise noted, with a standard three-electrode cell from +1.8 to −1.8 V with a platinum working electrode, acetonitrile or dimethylacetamide (DMA) solvent, and tetrabutylammonium (TBAH) electrolyte (∼1.0 M). All potentials are reported versus the normal hydrogen electrode (NHE) using cobaltocenium hexafluorophosphate ($E_{1/2}$ = −0.78 V, −1.75 V) or ferrocene ($E_{1/2}$ = 0.55 V) as an internal standard. The peak separation of all reversible couples was less than 100 mV. All synthetic reactions were performed in a glovebox under a dry nitrogen atmosphere unless otherwise noted. All solvents were purged with nitrogen prior to use. Deuterated solvents were used as received from Cambridge Isotopes and were purged with nitrogen under an inert atmosphere. When possible, pyrazole protons of the tris(pyrazolyl)borate (Tp) ligand were uniquely assigned (e.g., “Tp3B”) using two-dimensional NMR data. If unambiguous assignments were not possible, Tp protons were labeled as “Tp3/5 or Tp4”. All J values for Tp protons are 2(±0.4) Hz. Characterization of products is given when available. This work demonstrates some of the most recent advancements of this project, and thus only 2-dimensional NMR has been carried out on every product at this time.

Compound 3

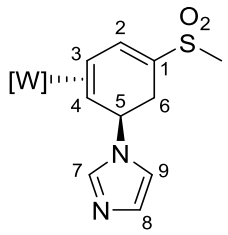

Compound **1** (0.100 g, 0.152 mmol) and MeCN were combined in a test tube to form an orange heterogeneous solution. Imidazole (0.155 g, 2.28 mmol) was added to a second test tube. Both solutions were cooled to 0 °C for 15 min. 1M HOTf/MeCN (0.227 mL, 0.227 mmol, -30 °C) was added to the reaction. Upon addition, the reaction became a dark red, homogeneous mixture. After 5 minutes, the cooled imidazole was added to the reaction. The reaction was stirred for 20 hrs. While the reaction was still in the cold probe, 1M tBuOK in tert-butanol (0.61 mL, 0.610 mmol) was added to the reaction and allowed to stir for an hour. The reaction was warmed to room temperature and removed from the glovebox. The reaction was diluted with 30 mL of H_2O and washed with 40 mL DCM. The aqueous layer was back extracted twice with DCM (25mL). The organic layers were combined and dried over $MgSO_4$ before being evaporated to dryness. The film was redissolved in MeCN and added to 15 mL of stirring H_2O. The resulting brown precipitant was collected on a 15 mL fine porosity fritted disc, washed with ether (2 x 10 mL) and hexanes (3 x 10 mL), and desiccated to yield **3** (0.048 g, 0.065 mmol, 43%). CV (DMA): $E_{p,a}$= + 0.93 V (NHE). IR: *v*(SO) 1405 cm^{-1}, *v*(NO) 1540 cm^{-1}, *v*(BH) 2488 cm^{-1}. ^{1}H-NMR (d_3-MeCN, δ, 25 °C): 8.08 (1H, d, TpA3), 8.03 (1H, d, TpB3), 7.90 (1H, d, TpA5), 7.87 (1H, d, TpC5), 7.80 (2H, m, H2, TpB5), 7.68 (1H, s, H7), 7.51 (1H, d, TpC5), 7.19 (1H, t J = 1.2, H8), 6.84 (1H, t J = 1.1, H9), 6.40 (1H, t, TpA4), 6.35 (1H, t, TpB4), 6.30 (1H, t, TpC4), 5.46 (1H, m, H5), 3.19 (2H, m, H3, H6b), 2.84 (3H, s, SO_2Me), 2.69 (1H, d J = 16.9, H6a), 1.45 (1H, d J = 9.0, H4), 1.26 (9H, d J = 8.8, PMe_3). ^{13}C-NMR (d_3-MeCN, δ, 25 °C): 145.9 (1C, d J = 2.9, C2), 144.7 (1C, TpA3), 143.0 (1C, TpB3), 142.2 (1C, TpC3), 138.3 (1C, TpC5), 137.9 (1C, TpA5), 137.5 (1C, TpB5), 136.8 (1C, C7), 128.9 (1C, C8), 126.2 (1C, C1), 119.2 (1C, C9), 107.8 (1C, TpA4), 107.5 (1C, TpC4), 107.3 (1C, TpB5),

58.2 (1C, C4), 57.2 (1C, C5), 50.0 (1C, d J = 9.2, C3), 44.7 (1C, SO_2Me), 31.2 (1C, C6), 13.7 (3C, d J = 29.6, PMe_3). Anal. Calcd for $C_{22}H_{31}BN_9O_3PSW \cdot 2H_2O$: C, 34.62; H, 4.62; N, 16.52. Found: C, 34.84; H, 4.38; N, 16.52.

Compound 4

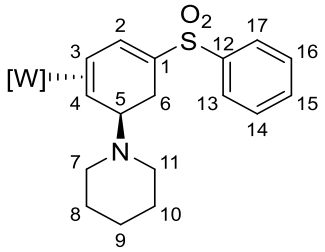

Compound **2** (0.100 g, 0.138 mmol) and MeCN were combined in a test tube to form an orange heterogeneous solution. Piperidine (0.18 mL, 0.18 g, 2.07 mmol) was added to a second test tube. Both solutions were cooled to 0 °C for 15 min. 1M HOTf/MeCN (0.21 mL, 0.210 mmol) was added to the reaction. Upon addition, the reaction became a dark red, homogeneous mixture. After 15 minutes, the reaction was added to the cooled piperidine test tube. The reaction was stirred overnight for 16 hrs. A white precipitant formed overnight. The test tube was removed from the glove box and the white solid was isolated on a 15 mL fine frit. The solid was washed with 5 mL H_2O followed by hexanes (2 x 15 mL) and dessicated overnight yielding **4** (0.063 g, 0.078 mmol, 57 %). CV (MeCN) $E_{p,a}$ = +0.71 V (NHE). IR: *v*(BH) = 2488 cm^{-1}, *v*(NO) = 1574 cm^{-1}, *v*(SO) = 1406 cm^{-1}. ^{1}H NMR (CD_3CN, δ): 8.00 (1H, d, TpB3), 7.94 (1H, d, TpA3), 7.89 (2H, m, H17, H13), 7.86 (1H, d, TpC5), 7.84 (1H, d, TpB5), 7.82 (1H, dd J = 6.0, 2.7, H2), 7.76 (1H, d, TpA3), 7.57 (1H, m, H15), 7.53 (23H, m, TpC3, H16, H14), 6.35 (1H, t, TpB4), 6.31 (1H, t, TpC4), 6.24 (1H, t, TpA4), 3.90 (1H, d J = 8.0, H5), 3.04 (1H, m, H3), 2.65 (1H, ddm J = 17.7, 8, H6a), 2.48 (4H, m, H11, H7), 2.38 (1H, d J = 17.7, H6b), 1.26 (9H, d J = 8.6, PMe_3), 1.21 (4H, m, H10, H8), 1.14 (3H, m, H9, H4). ^{13}C NMR (CD_3CN, δ): 146.7 (1C, C2), 144.6 (1C, TpB3), 143.3 (1C, C12), 142.4 (1C, TpA3), 142.1 (1C, TpC3), 138.1 (1C, TpC5), 137.5 (2C, TpA5, TpB5), 133.3 (1C, C15), 129.8 (2C, C16, C14), 138.7 (2C, C17, C13), 128.4

(1C, C1), 107.5 (1C, TpB4), 107.3 (1C, TpC4), 106.9 (1C, TpA4), 62.7 (1C, C5), 53.7 (1C, C4), 51.3 (1C, C3), 50.31 (2C, C11, C7), 27.43 (2C, C10, C8), 25.62 (1C, C9), 23.8 (1C, C6) 14.0 (3C, d J = 28.6, PMe_3). Anal. Calc'd for $C_{29}H_{40}BN_8O_3PSW \cdot H_2O$: C, 42.25; H, 5.14; N, 13.59. Found: C, 42.22; H, 4.86; N, 13.53.

Compound 5

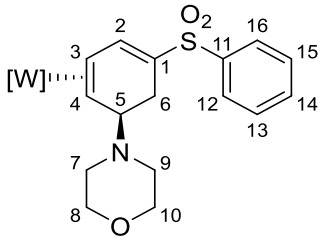

Compound **1** (0.100 g, 0.138 mmol) and MeCN were combined in a test tube to form an orange heterogeneous solution. Morpholine (0.18 mL, 0.18 g, 2.07 mmol) was added to a second test tube. Both solutions were cooled to 0 °C for 15 min. 1M HOTf/MeCN (0.21 mL, 0.210 mmol) was added to the reaction. Upon addition, the reaction became a dark red, homogeneous mixture. After 15 minutes, the reaction was added to the cooled morpholine test tube. The reaction was stirred overnight for 16 hrs. While the reaction was still in the cold probe, 1M tBuOK in tert-butanol (0.55 mL, 0.55 mmol) was added to the reaction and allowed to stir for an hour. The reaction was warmed to room temperature and removed from the glovebox. The reaction was diluted with 30 mL of H_2O and washed with 40 mL DCM. The aqueous layer was back extracted with DCM (25mL). The organic layers were combined and dried over $MgSO_4$ before being evaporated to dryness. The film was washed with hexanes and then ether. The remaining film was picked up in ethyl acetate and ran through a 30 mL basic alumina plug with 100 mL of ethyl acetate. The resulting filtrate was evaporated to dryness, pick up in minimal DCM, and crashed out into 50 mL of stirring pentane. The resulting brown precipitant was collected on a 15 mL fine porosity fritted disc, washed with ether (2 x 10 mL) and hexanes (3 x 10 mL), and desiccated to yield **5** (0.075 g, 0.093 mmol, 67%). CV (MeCN) $E_{p,a}$ = +0.77 V (NHE). IR: ν(BH) = 2484 cm^{-1}, ν(NO) = 1573 cm^{-1}, ν(SO) = 1407

cm^{-1}. ^{1}H NMR (CD_3CN, δ): 8.00 (1H, d, TpB3), 7.93 (1H, d, TpA3), 7.89 (2H, m, H16, H12), 7.86 (1H, d, TpC5), 7.85 (1H, d, TpB5), 7.84 (1H, dd J = 6.0, 2.6, H2), 7.76 (1H, d, TpA5), 7.57 (1H, m, H14), 7.53 (1H, d, TpC3), 7.52 (2H, m, H15, H13), 6.35 (1H, t, TpB4), 6.31 (1H, t, TpC4), 6.24 (1H, t, TpA4), 3.86 (1H, d J = 7.3, H5), 3.33 (4H, m, H10, H8), 3.05 (1H, m, H3), 2.69 (1H, ddm J = 17.1, 7.7, H6a), 2.50 (2H, m, H9/H7), 2.43 (1H, d J = 17.1, H6b), 2.12 (2H, m, H9/H7), 1.25 (9H, d J = 8.5, PMe_3), 1.17 (1H, d J = 9.5, H4). ^{13}C NMR (CD_3CN, δ): 146.8 (1C, C2), 144.6 (1C, TpB3), 143.3 (1C, C11), 142.5 (1C, TpA3), 142.1 (1C, TpC3), 138.2 (1C, TpC5), 137.6 (1C, TpB5), 137.5 (1C, TpA5), 133.3 (1C, C14), 129.8 (2C, C15, C13), 138.7 (2C, C15, C12), 128.0 (1C, C1), 107.6 (1C, TpB4), 107.3 (1C, TpC4), 106.9 (1C, TpA4), 68.0 (2C, C10, C8), 62.5 (1C, C5), 53.2 (1C, C4), 51.2 (1C, C3), 50.0 (2C, C9, C7), 24.4 (1C, C6), 14.9 (3C, d J = 29.0, PMe_3). Anal. Calc'd for $C_{28}H_{38}BN_8O_4PSW$: C, 41.60; H, 4.74; N, 13.86. Found: C, 41.54; H, 4.69; N, 13.66.

Compound 7

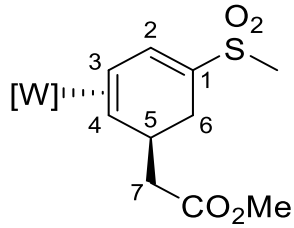

Compound **1** (0.500 g, 0.758 mmol) was added to a test a tube along with MeCN, and an orange heterogeneous solution formed. The solution was cooled at 0 °C for 15 min. Then, a 1 M HOTf/MeCN mixture (1.44 mL, 1.44 mmol, −30 °C) was added to the reaction using a syringe. Once the acid was added, the solution turned to a dark homogeneous mixture. Shortly after, 1-(*tert*-Butyldimethylsilyloxy)-1-methoxyethene (0.713 m, 0.827 mL, 3.79 mmol, −30 °C) was syringed to the reaction mixture. The solution stirred overnight. Excess Et_3N (1.1 mL, 7.58 mmol) was added to the test tube. This was removed from the box and evaporated to dryness to form a dark oil, which was washed three times with hexanes. Two scoops of silica were then added to the oil and evaporated to dryness. A 60 mL medium-porosity frit was

filled two-thirds with silica, and the previous silica mixture was placed on top. Hexanes (250 mL) was eluted through the column, followed by diethyl ether (100 mL) and by ethyl acetate (250 mL). The ethyl acetate eluted a yellow band, which was evaporated to dryness, redissolved in minimal DCM, and then added to 20 mL of stirred pentane. An off-white solid precipitated out of the pentane, which was collected on a 15 mL fine-porosity fitted disk, washed pentane (2 × 10 mL) and desiccated overnight to yield **7** (0.325 mg, 0.443 mmol, 58%). CV (MeCN) $E_{p,a}$ = +0.80 V (NHE). IR: *v*(BH) = 2503 cm^{-1}, *v*(CO) = 1732 cm^{-1}, *v*(NO) = 1558 cm^{-1}, *v*(SO) = 1407 cm^{-1}. ^{1}H NMR (CD_3CN, δ): 8.05 (1H, d, TpB3), 7.99 (1H, d, TpA3), 7.87 (2H, d, TpB5, TpC5), 7.78 (1H, d, TpA5), 7.66 (1H, dd J = 5.7, 2.5, H2) 7.41 (1H, d, TpC3), 6.37 (1H, t, TpB4), 6.33 (1H, t, TpA4), 6.29 (1H, t, TpC4), 3.52 (3H, s, OMe), 3.29 (1H, m, H5), 2.91 (1H, m, H3), 2.90 (3H, s, SO_2Me), 2.83 (1H, dd J= 16.5, 6.0, H6a), 2.57 (1H, dd J= 16.0, 7.4, H7b), 2.39 (1H, dd J = 14.5, 6.8, H7b), 2.28 (1H, d J = 16.2, H6b), 1.23 (10H, d J = 8.9, PMe_3, H2). ^{13}C NMR (CD_3CN, δ): 174.4 (1C, CO), 145.2 (1C, C2), 143.9 (1C, TpB3), 141.9 (1C, TpA3), 141.8 (1C, TpC3), 138.2 (1C, Tp5), 137.6 (1C, Tp5), 137.4 (1C, TpA5), 126.6 (1C, C1), 107.4 (1C, TpB4), 107.3 (1C, TpC4), 106.9 (1C, TpA4), 63.2 (1C, C4), 51.5 (1C, OMe), 47.5 (1C, SO_2Me), 44.8 (1C, d J= 17.5, C7), 44.7 (1C, C3), 34.2 (1C, C5), 27.6 (1C, d J= 10.0, C6), 13.7 (3C, d J= 28.9, PMe_3)

Compound 8

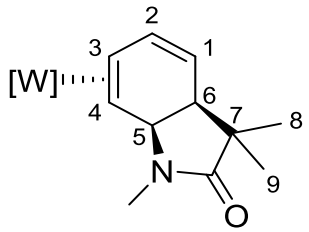

Compound **6** (1.30 g, 1.71 mmol) was added to a test tube with MeCN and stirred at -30 °C for 20 min. Then, HOTf (0.46 g, 3.07 mmol, −30 °C) leveled in MeCN was added to the reaction using a syringe, and the solution was stirred at −30 °C. Once the acid was added, the solution turned to a dark homogeneous mixture. After 30 min a 2M $MeNH_2$/THF (8.5 mL, 17.0 mmol) was syringed in the test tube, and the solution

became a red homogeneous mixture. The reaction stirred at −30 °C overnight. The resulting mixture was stirred at room temperature for 48 h. ^{31}P confirmed the presence of only one species. An extraction with DCM/H_2O was performed, and the organic layer was washed three times. This was dried over $MgSO_4$ and evaporated *in vacuo*. The resulting yellow film was dissolved in minimal DCM and added dropwise to 15 mL of stirring pentane. An off-white solid precipitated out and was collected on a 15 mL fine-porosity fitted disk, washed pentane (2 × 10 mL), and desiccated overnight to yield **8** (0.725 g, 1.06 mmol, 62%). ^1H NMR (CD_3CN, δ): 8.05 (1H, d, TpB3), 8.03 (1H, d, TpC5), 7.86 (2H, d, TpB5, TpA5), 7.78 (1H, d, TpA3), 7.49 (1H, d, TpC3), 6.41 (1H, ddd J = 10.0, 4.7, 2.3, H2), 6.37 (1H, t, TpB4), 6.31 (1H, t, TpC4), 6.29 (1H, t, TpA4), 4.72 (1H, dd J = 10.2, 2.1, H1), 4.62 (1H, d J = 6.2, H5), 2.85 (1H, m, H3), 2.82 (1H, m, H6), 2.61 (3H, s, N-Me), 1.35 (1H, d J = 9.9, H4), 1.18 (12 H, d J = 9.0, PMe_3, H9/8), 1.08 (3H, s, H9/8).

Compound 9

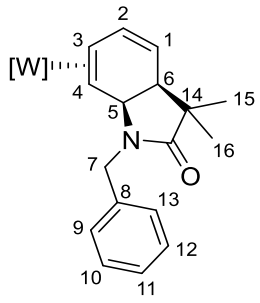

Compound **6** (0.438 g, 0.532 mmol) was added to a test tube with MeCN and stirred at -30 °C for 20 min. Then, HOTf (0.120 g, 0.800 mmol, −30 °C) levelled in MeCN was added to the reaction using a syringe, and the solution stirred at −30 °C. Once the acid was added, the solution turned to a dark homogeneous mixture. After 30 min, benzylamine (0.570 g, 0.58 mL, 5.32 mmol) was syringed in the test tube, and the solution became a red homogeneous mixture. The reaction stirred at −30 °C overnight. The resulting mixture was stirred at room temperature for 48 h. ^{31}P confirmed the presence of only one species. An extraction with DCM/H_2O was performed and the organic layer washed three times. This was dried over

$MgSO_4$ and evaporated *in vacuo*. The resulting yellow film was dissolved in minimal DCM and added dropwise to 15 mL of stirring pentane. An off-white solid precipitated out and was collected on a 15 mL fine-porosity fitted disk, washed pentane (2 × 10 mL), and desiccated overnight to yield **9** (0.220 g, 0.291 mmol, 55%). IR: *v*(BH) = 2477 cm^{-1}, *v*(CO) = 1662 cm^{-1}, *v*(NO) = 1559 cm^{-1}. ^{1}H NMR (CD_3CN, δ): 8.02 (1H, d, TpB3), 7.84 (1H, d, TpC5), 7.83 (1H, d, TpB5), 7.69 (1H, d, TpA5), 7.68 (1H, d, TpA3), 7.32 (1H, d, TpC3), 7.13 (3H, m, H10, H11, H12), 6.91 (2H, m, H13, H9), 6.40 (1H, dm J= 10.0 Hz, H2), 6.35 (1H, t, TpB4), 6.29 (1H, t, TpC4), 6.06 (1H, t, TpA4), 4.77 (1H, dd J= 10.0, 2.0 Hz, H1), 4.65 (1H, d J= 6.2 Hz, H5), 4.55 (1H, d J= 15.2 Hz, H7a), 4.22 (1H, d J= 15.3 Hz, H7b), 2.82 (1H, m, H6), 2.64 (1H, m, H3), 1.29 (1H, d J= 9.7 Hz, H4), 1.20 (3H, s, H16/15), 1.16 (9H, d J= 8.6, PMe_3), 1.15 (3H, s, H16/15). ^{13}C NMR (CD_3CN, δ): 180.3 (1C, CO), 144.5 (1C, TpB3), 143.1 (1C, TpA3), 142.0 (1C, TpC3), 139.4 (1C, C8), 137.9 (1C, TpC5), 137.3 (1C, TpB5), 137.0 (1C, TpA5), 132.2 (1C, d J= 3.5 Hz, C2), 129.1 (2C, C12, 10), 128.2 (2C, C13, C9), 127.5 (1C, C11), 115.4 (1C, C1), 107.5 (1C, TpB4), 107.1 (1C, TpC4), 106.8 (1C, TpA4), 59.2 (1C, C5), 49.9 (1C, d J= 9.8 Hz, C3), 47.8 (1C, C4), 45.0 (1C, C14), 44.0 (1C, C7), 43.8 (1C, C6), 25.1 (1C, C16/15), 20.8 (1C, C16/15), 13.6 (3C, d J= 28.8, PMe_3).

Compound 10

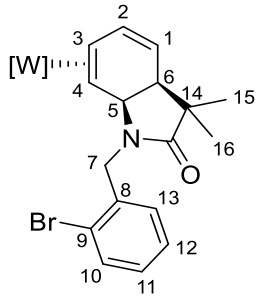

Compound **6** (0.200 g, 0.243 mmol) was added to a test tube with MeCN and stirred at -30 °C for 20 min. Then, HOTf (0.055 g, 0.366 mmol, −30 °C) levelled in MeCN was added to the reaction using a syringe, and the solution stirred at −30 °C. Once the acid was added, the solution turned to a dark homogeneous

mixture. After 30 min. 2-bromobenzylamine (0.32 g, 0.22 mL, 1.72 mmol) was syringed in the test tube, and the solution became a red homogeneous mixture. The reaction stirred at −30 °C overnight. The resulting mixture was stirred at room temperature for 48 h. ^{31}P confirmed the presence of only one species. An extraction with DCM/H_2O was performed and the organic layer washed three times. This was dried over $MgSO_4$ and evaporated *in vacuo*. The resulting yellow film was dissolved in minimal DCM and added dropwise to 15 mL of stirring pentane. An off-white solid precipitated out and was collected on a 15 mL fine-porosity fitted disk, washed pentane (2 × 10 mL), and desiccated overnight to yield **10** (0.150 g, 0.179 mmol, 74%). ^{1}H NMR (CD_3CN, δ): 8.01 (1H, d, TpB3), 7.82 (1H, d, TpB5), 7.81 (1H, d, TpC5), 7.71 (1H, d, TpA3), 7.67 (1H, d, TpA5), 7.28 (1H, dd J= 8.0, 1.0, H10), 7.23 (3H, m, TpC3, H13, H12), 7.04 (1H, m, H11), 6.43 (1H, ddd J= 10.1, 4.8, 2.6, H2), 6.34 (1H, t, TpB4), 6.24 (1H, t, TpC4), 6.05 (1H, t, TpA4), 4.80 (1H, dd J=10.0, 2.1, H1), 4.68 (1H, d J= 6.5, H5), 4.48 (1H, d J= 15.9, H7a), 4.42 (1H d J= 15.9, H7b), 2.84 (1H, m, H6), 2.58 (1H, m, H3), 1.28 (3H, d, H16/15), 1.23 (1H, d J= 9.6, H4), 1.17 (3H, s, H16/15), 1.16 (9H, d J= 8.3, PMe_3). ^{13}C NMR (CD_3CN, δ): 180.6 (1C, CO), 144.6 (1C, TpB3), 142.9 (1C, TpA3), 141.9 (1C, TpC3), 138.5 (1C, C8), 137.8 (1C, TpC5), 137.4 (1C, TpB4), 136.9 (1C, TpA5), 133.3 (1C, C10), 132.2 (1C, d J= 3.6, C2), 130.2 (1C, C13), 129.4 (1C, C11), 128.3 (1C, C12), 122.9 (1C, C9), 115.4 (1C, C1), 107.5 (1C, TpB4), 107.1 (1C, TpC4), 106.8 (1C, TpA4), 59.5 (1C, C5), 49.8 (1C, d J= 10.2, C3), 47.5 (1C, C4), 45.2 (1C, C14), 44.2 (1C, C7), 43.9 (1C, C6), 25.3 (1C, C16/15), 20.9 (1C, C16/15), 13.7 (3C, d J= 28.7, PMe_3).

Compound 11

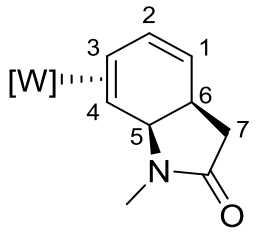

Compound **7** (0.150 g, 0.204 mmol) was added to a test tube with MeCN and stirred at -30 °C for 20 min. Then, a 1 M HOTf/MeCN mixture (0.409 mL, 0.409 mmol, −30 °C) was added to the reaction using a syringe, and the solution stirred at −30 °C. Once the acid was added, the solution turned to a dark homogeneous mixture. After 30 min a 2M $MeNH_2$/THF (1.02 mL, 2.04 mmol) was syringed in the test tube, and the solution became a red homogeneous mixture. The reaction stirred at −30 °C overnight. The resulting mixture was stirred at room temperature for 24 h. ^{31}P confirmed the presence of only one species. An extraction with DCM/H_2O was performed and the organic layer washed three times. This was dried over $MgSO_4$ and evaporated *in vacuo*. The resulting yellow film was dissolved in minimal DCM and pipetted in 15 mL of stirring pentane. An off-white solid precipitated out and was collected on a 15 mL fine-porosity fitted disk, washed pentane (2 × 10 mL), and desiccated overnight to yield **11** (0.100 g, 0.153 mmol, 75%). CV (MeCN) $E_{p,a}$ = +0.49 V (NHE). IR: ν(BH) = 2504 cm^{-1}, ν(CO) = 1664 cm^{-1}, ν(NO) = 1552 cm^{-1}. ^1H NMR (CD_3CN, δ): 8.07 (2H, d, TpB3, TpC5), 7.87 (2H, d, TpB5, TpA3), 7.77 (1H, d, TpA5), 7.49 (1H, d, TpC3), 6.43 (1H, m, H2) 6.37 (1H, t, TpA4), 6.30 (1H, t, TpB4) 6.27 (1H, t, TpC4), 4.54 (1H, d J = 6.2, H5), 4.50 (1H, d J = 9.7, H1), 3.21 (1H, m, H6), 2.81 (1H, m, H3), 2.61 (3H, s, N-Me), 2.58 (1H, dd J= 16.2, 8.9 , H7a), 1.90 (1H, d J = 16.3, H7b), 1.35 (1H, d J = 9.6, H4), 1.19 (9H, d J = 8.5, PMe_3). ^{13}C NMR (CD_3CN, δ): 175.4 (1C, CO), 144.6 (1C, Tp3), 143.7 (1C, Tp3), 141.6 (1C, TpC3), 138.1 (1C, Tp5), 137.4 (1C, Tp5), 136.8 (1C, Tp5), 136.39 (1C, TpA5), 132.0 (1C, C2), 120.3 (1C, C1), 107.6 (1C, Tp4), 107.2 (1C, Tp4), 106.9 (1C, Tp4), 64.3 (1C, C5), 49.2 (1C, C3), 48.2 (1C, C4), 40.3 (1C, C7), 33.0 (1C, C6), 27.0 (1C, N-Me), 13.7 (3C, d J= 29.3, PMe_3).

Compound 12

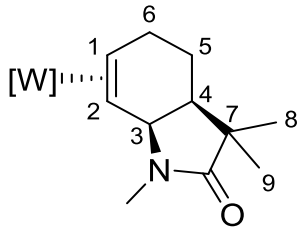

Compound **8** (0.100 g, 0.147 mmol) was added to a test tube with MeCN and cooled to −30 °C for 15 min. Then, a 1 M HOTf/MeCN mixture (0.22 mL, 0.22 mmol, −30 °C) was added to the reaction using a syringe, and the solution was stirred at −30 °C. After 15 min, a cooled solution of sodium borohydride (0.028 g, 0.74 mmol) in MeCN was added to the test tube and the solution became a dark red homogeneous mixture. The solution was stirred at -30°C overnight. The test tube was removed from the box and added to a silica plug of a 30 mL medium-porosity frit filled two-thirds with silica. A yellow band was eluted with ether (150 ml). The band was evaporated to dryness, and a brown oil formed. This was picked up in DCM and dissolved in 15 mL of stirring pentane. An off-white solid precipitated out and was collected on a 15 mL fine-porosity fitted disk, washed pentane (2 × 10 mL) desiccated overnight to yield **12** (0.072 g, 0.105 mmol, 71%). ^{1}H NMR (CD_3CN, δ): 8.29 (1H, d, TpA3), 8.05 (1H, d, TpB3), 7.87 (1H, d, TpB5), 7.84 (1H, d, TpA5), 7.81 (1H, d, TpC5), 7.45 (1H, d, TpC3), 6.38 (1H, t, TpB4), 6.28 (1H, t, TpA4), 6.27 (1H, t, TpC4), 4.93 (1H, d J = 5.2, H3), 2.78 (2H, m, H6a, H1), 2.49 (3H, s, N-Me), 2.40 (1H, m, H4), 2.01 (1H, m, H5a), 1.52 (1H, m, H5b), 1.26 (1H, d J = 10.5, H2), 1.14 (3H, s, H9/8), 1.12 (9H, d J = 8.5, PMe_3), 1.04 (3H, s, H9/10).

Compound 13

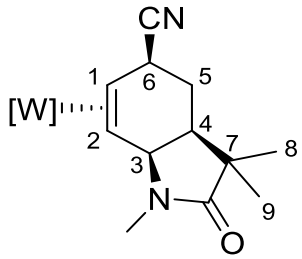

Compound **8** (0.100 g, 0.147 mmol) was added to a test tube with MeCN and cooled to −30 °C for 15 min. Then, a 1 M HOTf/MeCN mixture (0.22 mL, 0.22 mmol, −30 °C) was added to the reaction using a syringe, and the solution was stirred at −30 °C. NaCN (0.036 g, 0.735 mmol) and minimal MeOH were mixed into a separate test tube. After 15 min, the reaction mixture was added to the NaCN solution. The solution was stirred at -30°C overnight. The test tube was removed from the box and added to a silica plug of a 30 mL medium-porosity frit filled two-thirds with silica. A yellow band was eluted with ether (150 ml). The band was evaporated to dryness, and a brown oil formed. This was picked up in DCM and dissolved in 15 mL of stirring pentane. An off-white solid precipitated out and was collected on a 15 mL fine-porosity fitted disk, washed pentane (2 × 10 mL) desiccated overnight to yield **13** (0.068 g, 0.096 mmol, 65%). ^{1}H NMR (CD_3CN, δ): 8.09 (1H, d, TpA3), 8.06 (1H, d, TpB3), 7.88 (1H, d, TpB5), 7.88 (1H, d, TpC5), 7.80 (1H, d, TpA5), 7.45 (1H, d, TpC3), 6.39 (1H, t, TpB4), 6.30 (1H, t, TpC4), 6.27 (1H, t, TpA4), 4.82 (1H, d J = 5.1, H3), 3.53 (1H , m, H6), 2.77 (1H, m, H1), 2.48 (3H, s, N-Me), 2.08 (1C, dt J = 12.1, 4.5, H4), 1.92 (1H, m, H5a), 1.43 (1H, q J = 12.1, H5b), 1.21 (9H, d J = 8.2, PMe_3), 1.19 (1H, d J = 12.1, H2), 1.16 (3H, s, H9/8), 1.07 (3H, s, H9/8).

Compound 14

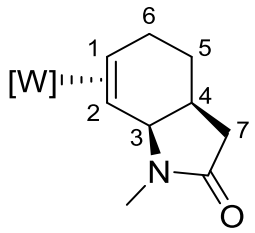

Compound **11** (0.120 g, 0.184 mmol) was added to a test tube with MeCN and cooled to −30 °C for 15 min. Then, a 1 M HOTf/MeCN mixture (0.348 mL, 0.348 mmol, −30 °C) was added to the reaction using a syringe, and the solution stirred at −30 °C. Tetrabutylammonium borohydride (0.142 g, 0.552 mmol) was added to the test tube and the solution became a dark red homogeneous mixture. The solution stirred at -30°C overnight. The resulting mixture was cloudy and produced a precipitate, which was collected on a

15 mL fine-porosity fitted disk, washed pentane (2 × 10 mL), MeCN (2 x 10 mL) and desiccated overnight to yield **14** (0.074 mg, 0.113 mmol, 62%). CV (MeCN) $E_{p,a}$ = +0.39 V (NHE). IR: *v*(BH) = 2505 cm^{-1}, *v*(CO) = 1675 cm^{-1}, *v*(NO) = 1557 cm^{-1}. ^{1}H NMR (CD_3CN, δ): 8.29 (1H, d, TpA3), 8.05 (1H, d, TpB3), 7.86 (1H, d, TpB5), 7.83 (1H, d, TpA5), 7.80 (1H, d, TpC5), 7.45 (1H, d, TpC3), 6.38 (1H, t, TpB4), 6.29 (1H, t, TpA4), 6.28 (1H, t, TpC4), 4.81 (1H, d J = 5.6, H3), 3.08 (1H, m, H6a), 2.73 (1H, m, H1), 2.51 (1H, m, H6b), 2.48 (3H, s, N-Me), 2.41 (2H, m, H4, H7a), 2.07 (1H, d J = 17.6, H7b), 1.65 (1H, m, H5a), 1.28 (1H, m, H5b), 1.16 (1H, d J = 11.3, H2), 1.13 (9H, d J = 8.7, PMe_3). ^{13}C NMR (CD_3CN, δ): 175.4 (1C, CO), 144.3 (1C, TpA5), 143.0 (1C, TpA3), 142.0 (1C, TpB3), 138.0 (1C, TpC3), 137.7 (1C, TpC5), 137.2 (1C, TpB5), 107.6 (1C, TpA4), 107.1 (1C, Tp4C) 106.5 (1C, Tp4B), 63.8 (1C, C3), 52.3 (1C, d J = 11.0, C1), 49.5 (1C, C2), 38.3 (1C, C7), 32.8 (1C, C4), 28.0 (1C, J = 4.48, C6), 27.6 (1C, C5), 27.6 (1C, N-Me), 13.20 (3C, d J= 29.1, PMe_3)

Compound 15

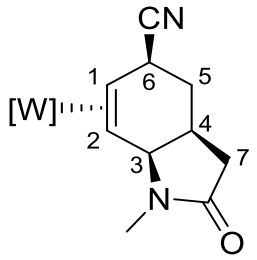

Compound **11** (0.120 g, 0.184 mmol) was added to a test tube with MeCN and cooled to −30 °C for 15 min. Then, a 1 M HOTf/MeCN mixture (0.22 mL, 0.22 mmol, −30 °C) was added to the reaction using a syringe, and the solution stirred at −30 °C. NaCN (0.027 g, 0.552 mmol) and minimal MeOH were mixed to a separate vial. The NaCN/MeOH solution was then added to the test tube and the undissolved NaCN was picked up using the reaction mixture. The solution became an orange homogeneous mixture. The solution stirred at -30°C overnight. The test tube was removed from the box and added to a silica plug of a 30 mL medium-porosity frit filled two-thirds with silica. A yellow band was eluted with ether (150 ml). The band was evaporated to dryness, and a brown oil formed. This was picked up in DCM and dissolved

in 15 mL of stirring pentane. An off-white solid precipitated out and was collected on a 15 mL fine-porosity fitted disk, washed pentane (2 × 10 mL) desiccated overnight to yield **15** (0.082 g, 0.121 mmol, 66%). CV (MeCN) $E_{p,a}$ = +0.94 V (NHE). IR: ν(BH) = 2504 cm^{-1}, ν(CO) = 1663 cm^{-1}, ν(NO) = 1556 cm^{-1}.^{1}H NMR (CD_3CN, δ): 8.13 (1H, d, TpA3), 8.06 (1H, d, TpB3), 7.89 (1H, d, TpB5), 7.88 (1H, d, TpC5), 7.81 (1H, d, TpA5), 7.48 (1H, d, TpC3), 6.38 (1H, t, TpB4), 6.30 (1H, t, TpC4), 6.27 (1H, t, TpA4), 4.72 (1H, d J = 5.8, H3), 3.65 (1H, m, H6), 2.72 (1H, m, H1), 2.56 (1H, m, H7a), 2.52 (1H, m, H4), 2.48 (3H, s, N-Me), 2.19 (1H, H7b), 2.02 (1H, m, H5a), 1.59 (1H, m, H5b), 1.18 (9H, d J = 8.8, PMe_3), 1.16 (1H, d J = 12.6, H2).^{13}C NMR (CD_3CN, δ): 175.2 (1C, CO), 144.6 (1C, TpB3), 143.6 (1C, TpA3), 142.3 (1C, TpC3), 138.3 (1C, TpA5), 138.0 (1C, TpC5), 137.7 (1C, TpB5), 127.8 (1C, CN), 107.8 (1C, TpB4), 107.3 (1C, Tp4), 106.7 (1C, Tp4), 62.6 (1C, C3), 49.6 (1C, d J = 12.6, C1), 47.3 (1C, C2), 39.3 (1C, C7), 31.2 (1C, C5), 31.0 (1C, C4), 29.7 (1H, C6), 27.5 (1C, N-Me), 13.8 (3C, d J = 29.1, PMe_3).

References

(1) Huo, J.; He, G.; Chen, W.; Hu, X.; Deng, Q.; Chen, D. *BMC Chemistry* **2019**, *13*, 89.

(2) Huang, L.; Arndt, M.; Gooßen, K.; Heydt, H.; Gooßen, L. J. *Chemical Reviews* **2015**, *115*, 2596.

(3) Zhu, S.; Niljianskul, N.; Buchwald, S. L. *Journal of the American Chemical Society* **2013**, *135*, 15746.

(4) Hultzsch, K. C. *Advanced Synthesis & Catalysis* **2005**, *347*, 367.

(5) Wilson, K. B.; Smith, J. A.; Nedzbala, H. S.; Pert, E. K.; Dakermanji, S. J.; Dickie, D. A.; Harman, W. D. *The Journal of Organic Chemistry* **2019**, *84*, 6094.

(6) Blakemore, D. C.; Castro, L.; Churcher, I.; Rees, D. C.; Thomas, A. W.; Wilson, D. M.; Wood, A. *Nature Chemistry* **2018**, *10*, 383.

(7) Vitaku, E.; Smith, D. T.; Njardarson, J. T. *Journal of Medicinal Chemistry* **2014**, *57*, 10257.

(8) Ilardi, E. A.; Vitaku, E.; Njardarson, J. T. *Journal of Medicinal Chemistry* **2014**, *57*, 2832.

(9) MacLeod, B. L.; Pienkos, J. A.; Wilson, K. B.; Sabat, M.; Myers, W. H.; Harman, W. D. *Organometallics* **2016**, *35*, 370.

(10) Wilson, K. B.; Myers, J. T.; Nedzbala, H. S.; Combee, L. A.; Sabat, M.; Harman, W. D. *Journal of the American Chemical Society* **2017**, *139*, 11401.

(11) Aurell, C.-J.; Karlsson, S.; Pontén, F.; Andersen, S. M. *Organic Process Research & Development* **2014**, *18*, 1116.

(12) Stavila, E.; Loos, K. *Tetrahedron Letters* **2013**, *54*, 370.

(13) Gutman, A. L.; Meyer, E.; Yue, X.; Abell, C. *Tetrahedron Letters* **1992**, *33*, 3943.

(14) Xu, Z.; Yan, P.; Jiang, H.; Liu, K.; Zhang, Z. C. *Chinese Journal of Chemistry* **2017**, *35*, 581.

(15) Ogiwara, Y.; Uchiyama, T.; Sakai, N. *Angewandte Chemie International Edition* **2016**, *55*, 1864.

(16) Wei, Y.; Wang, C.; Jiang, X.; Xue, D.; Li, J.; Xiao, J. *Chemical Communications* **2013**, *49*, 5408.

(17) Wei, Y.; Wang, C.; Jiang, X.; Xue, D.; Liu, Z.-T.; Xiao, J. *Green Chemistry* **2014**, *16*, 1093.

(18) Shi, Y.; Tan, X.; Gao, S.; Zhang, Y.; Wang, J.; Zhang, X.; Yin, Q. *Organic Letters* **2020**, *22*, 2707.

(19) Mourelle-Insua, Á.; Zampieri, L. A.; Lavandera, I.; Gotor-Fernández, V. *Advanced Synthesis & Catalysis* **2018**, *360*, 686.

Concluding Remarks

The backbone of this thesis may appear to be the organic manipulations that can be done to phenyl sulfones to yield alicyclic molecules. However, while these organic manipulations may be the basis of the thesis, none of it would be possible without the π-basic metal fragment {WTp(NO)(PMe_3)}. The development began back in 1987 with the publication of the first report of the {$Os(NH_3)_5$} metal fragment. Over the last thirty years, the Harman lab has developed a family of dearomatization agents based on the transition metals Re(I), W(0), and Mo(0) that have all promoted novel synthetic transformations of aromatics. The ability of these metal fragments to promote rapid and stereoselective conversions of planar aromatic molecules into complex alicyclic systems has allowed for the work presented in this thesis to be developed. For this, I must thank all the "Harmanites" that came before me.

The {WTp(NO)(PMe_3)} fragment itself has over 15 years of facilitating the formation of alicyclic compounds from aromatic precursors, including aniline, phenol, anisole, pyridines, naphthalene, furan, and pyrroles. It still baffles me that even after more than 15 years of the lab using the {WTp(NO)(PMe_3)} metal fragment, new novel reactivity is still being found. One example would be a recent report on the reactivity of benzene bound to the {WTp(NO)(PMe_3)} fragment. Previous attempts had been relatively unsuccessful when attempting to protonate the bound benzene. However, this has been overcome within the past few years, resulting in Nature and JOC papers. On this note, while multiple papers have been published on the reactivity of dihapto bound anisole, multiple projects are still ongoing years later with the dihapto-bound anisole due to the discovery of even more novel reactivity.

Now that I have bragged enough about advancements of the Harman lab. Let us get into the work presented in this thesis. While I jumped from project to project over my first couple of years in the Harman Lab at UVA, I never would have imagined that an initial screening of what electron-deficient benzenes could be bound in a dihapto fashion through the aromatic ring to the metal fragment {WTp(NO)(PMe_3)} would lead to a fully developed thesis. These initial screenings that were the basis of Chapter 3 led to fourteen novel

dearomatized complexes. Each complex gave its own mysteries, especially the binding of benzonitrile, but eventually, the phenyl sulfone system was chosen to go onto further elaboration.

The hope for the organic manipulations of the phenyl sulfone systems presented in Chapter 4 was to investigate if the same reactivity of the recent η^2-trifluorotoluene complex could be replicated. An easy one-off project in theory. Show that the reactivity of electron-deficient benzenes is the same across the board and move on to the next project. Initially, this is what we saw. The initial tandem protonation/nucleophilic addition to the phenyl sulfone systems worked well with protonation occurring ortho to the sulfone functionality and the nucleophile adding regio- and stereoselectively anti to the metal. The resulting η^2-1,3-dienes were then successfully protonated to yield allylic species that matched the data from the second protonation of the η^2-trifluorotoluene complex. Initial additions of NaCN to the allylic species yielded the same reactivity and regioselectivity as the η^2-trifluorotoluene system to yield a cis-3,4,6-cyclohexene. However, this is where the similarities ended.

As presented in Chapter 4, it was found that the NaCN addition resulted in the formation of a new η^2-diene when exposed to silica due to the elimination of the sulfone moiety. Chapter 5 further elaborates on the sulfone's ability to eliminate and the introduction of a third nucleophile of our choosing. This led to the synthesis of up to trisubstituted cyclohexenes, including cis-3,4,6-cyclohexenes, cis-3,4-cyclohexenes, and cis-3,6-cyclohexenes. This ability to add a third nucleophile selectively had only previously been seen with the Os(II) fragment in one instance. The ability of the sulfone to eliminate opened up the potential to access trans isomers through the epimerization of the allyl resulting from the system’s third protonation. While the trans-functionalized allyl has been viewed *in situ*, initial attempts to add a nucleophile to it have been unsuccessful. Due to time restrictions set by COVID, a full investigation into this phenomenon was not possible at the time of this dissertation.

Chapter 6 gives a brief overview of the ability of the η^2-phenyl sulfone system to tolerate a variety of amine nucleophiles in all three possible tandem additions. The introduction of a primary amine during the second tandem addition allows for an intramolecular cyclization resulting in the formation of an indoline

derivate. The formation of the indoline derivatives gives access to a η^2-1,3-diene through the elimination of the sulfone moiety. Further functionalization on this bound diene is possible in a stereo- and regioselective manner. Overall, this process allows for the addition of nitrogen-containing heterocycles, the intramolecular formation of nitrogen-containing heterocycles, and the addition of amines at various stages of the reaction schemes.

This work has demonstrated the ability to regio- and stereoselectively add up to three new stereocenters through three nucleophilic additions due to the ability of the sulfone to eliminate under specific conditions. The organics isolated from this methodology meet a variety of drug-likeness rules such as Lipinski's Rule of 5 as well as the criteria of Ghose, Veber, Egan, and Muegge. Future work of this system will include the investigation of creating multicyclic systems from the η^2-dienes resulting from the lactam formation and the creation of trans isomers in an effort to expand the possible selective stereochemistry that the {WTp(NO)(PMe_3)} system can afford.

As our understanding of the reactivity and regioselectivity of the WTp(NO)(PMe_3)(η^2-aromatic) systems continues to evolve with each new project, the ability to predict new reactivity and incorporate more complex reagents will increase. Predictable reactivity and regio- and stereoselective control are important features for medicinal chemists. The ability of our metal systems to provide these features along with facile introduction of a range of functional groups, will hopefully outweigh the issues of air sensitivity and quantitative use of the metal in the eyes of synthetic chemists. As demonstrated in this dissertation, the {WTp(NO)(PMe_3)} metal fragment has powerful synthetic potential, but its potential is limited by the quantity of those researching it. Thus, we must continue to bridge the gap between the range of synthetic transformations this process can achieve and what is valued in the synthetic and medicinal chemistry fields.

Appendix

Includes supporting spectroscopic data, crystal data, supporting figures, and calculations for molecules discussed throughout this work. The organization is on a per-chapter basis.

Supporting Information for Chapter 3

^{1}H NMR Spectrum of 2A 2B 2C 2D and 2E

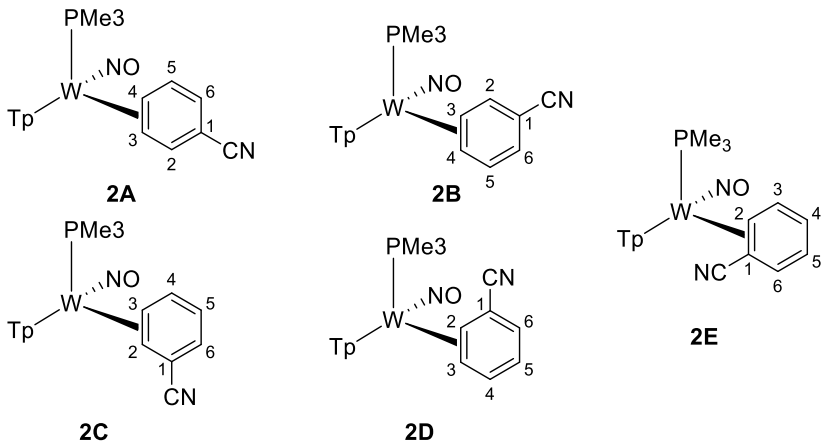

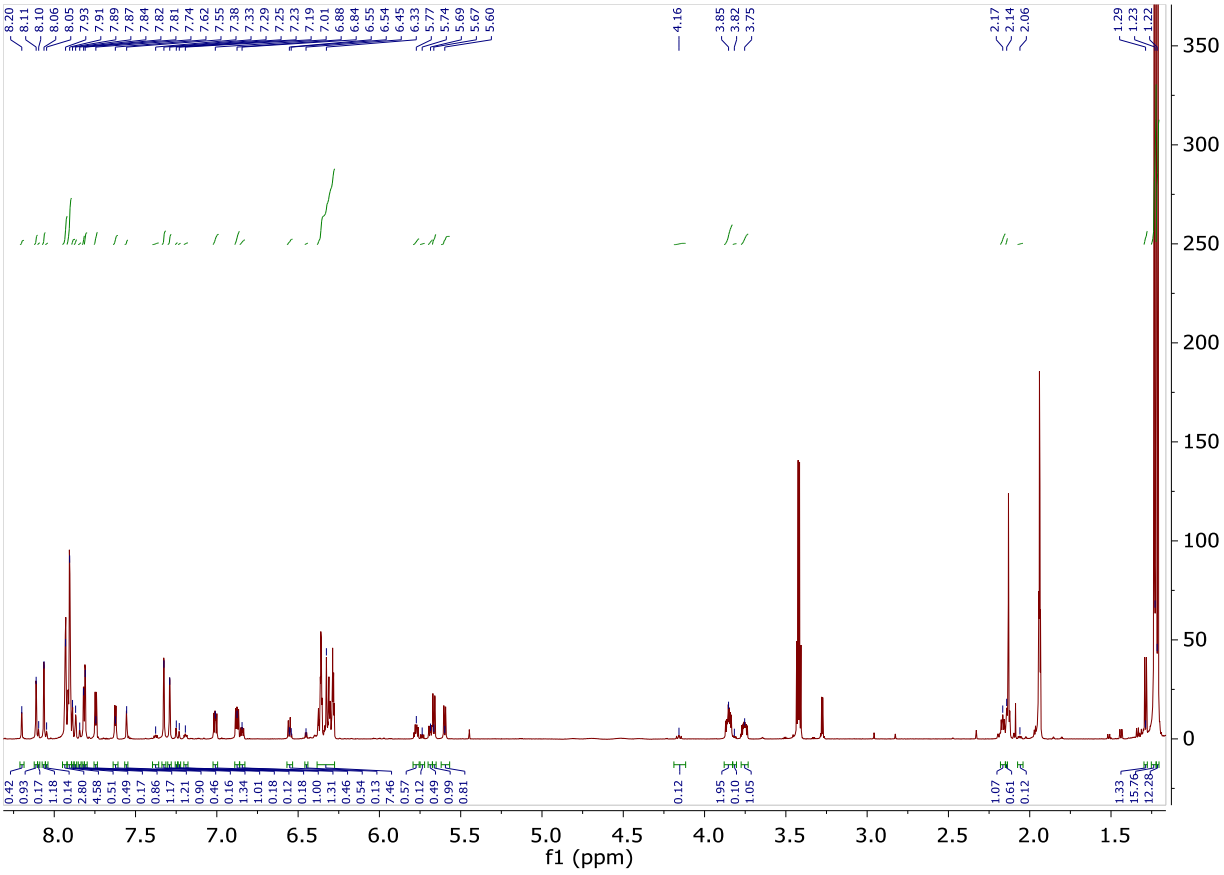

^{13}C {^{1}H} NMR Spectrum of 2A 2B 2C 2D and 2E

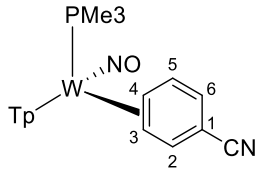

2A

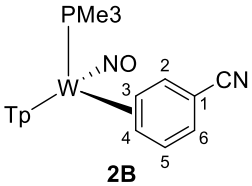

2B

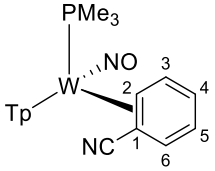

2E

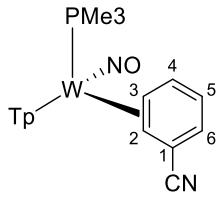

2C

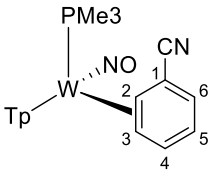

2D

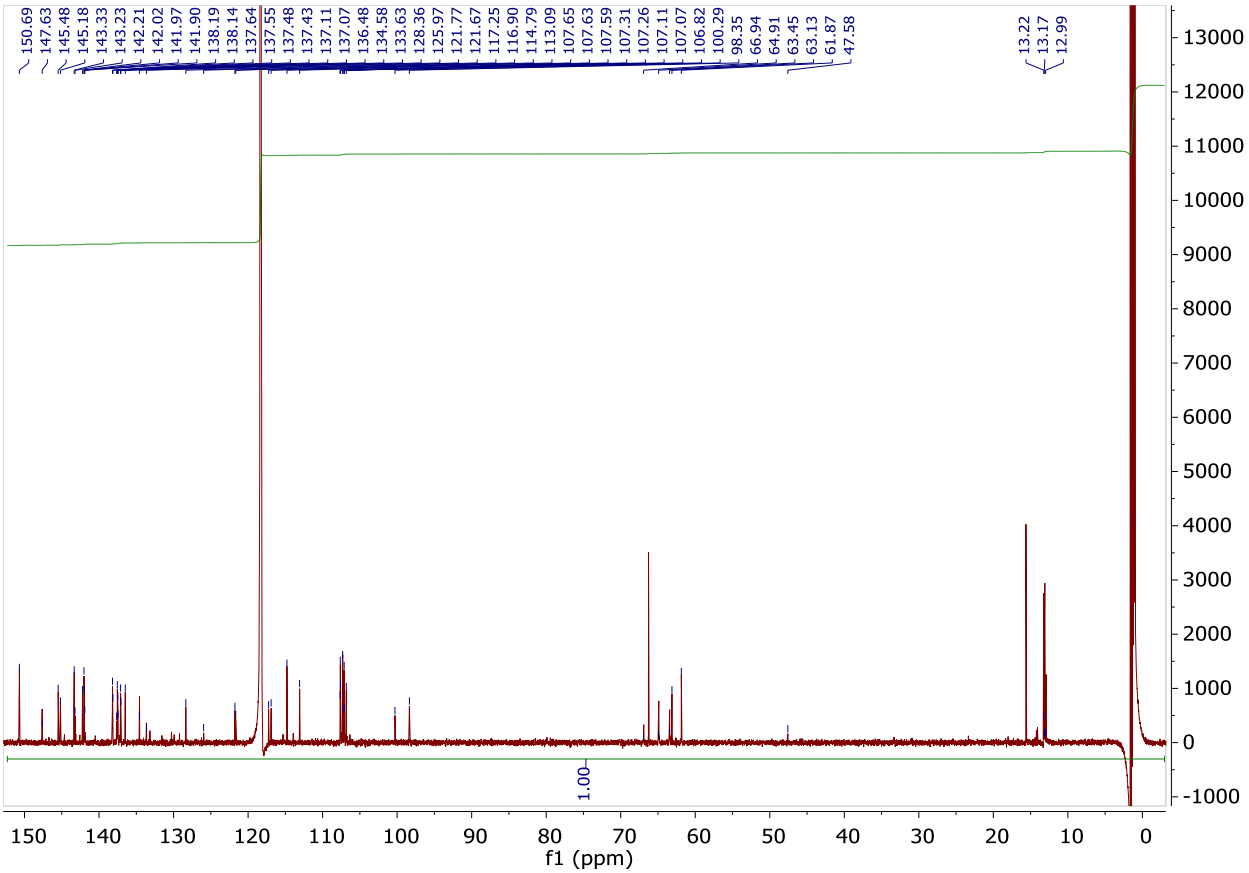

^{1}H NMR Spectrum of 4A and 4B

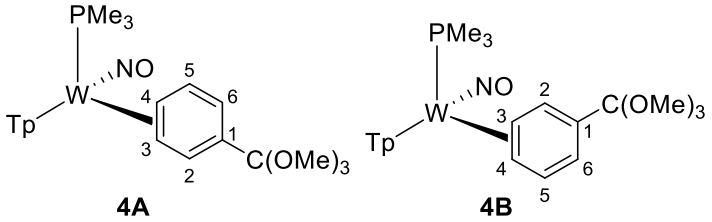

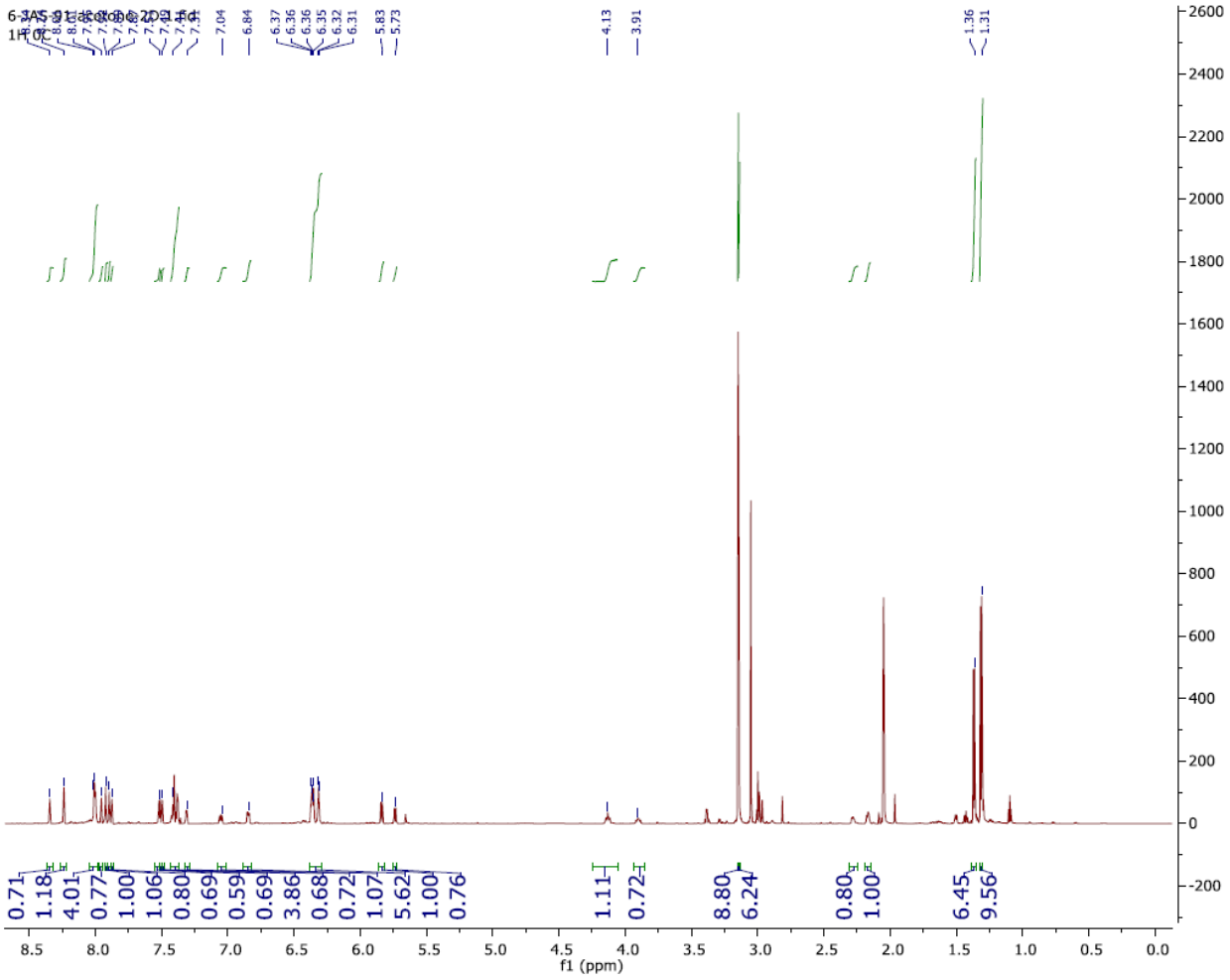

^{13}C {^{1}H} NMR Spectrum of 4A and 4B

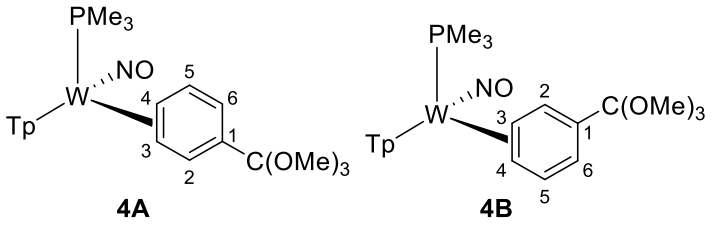

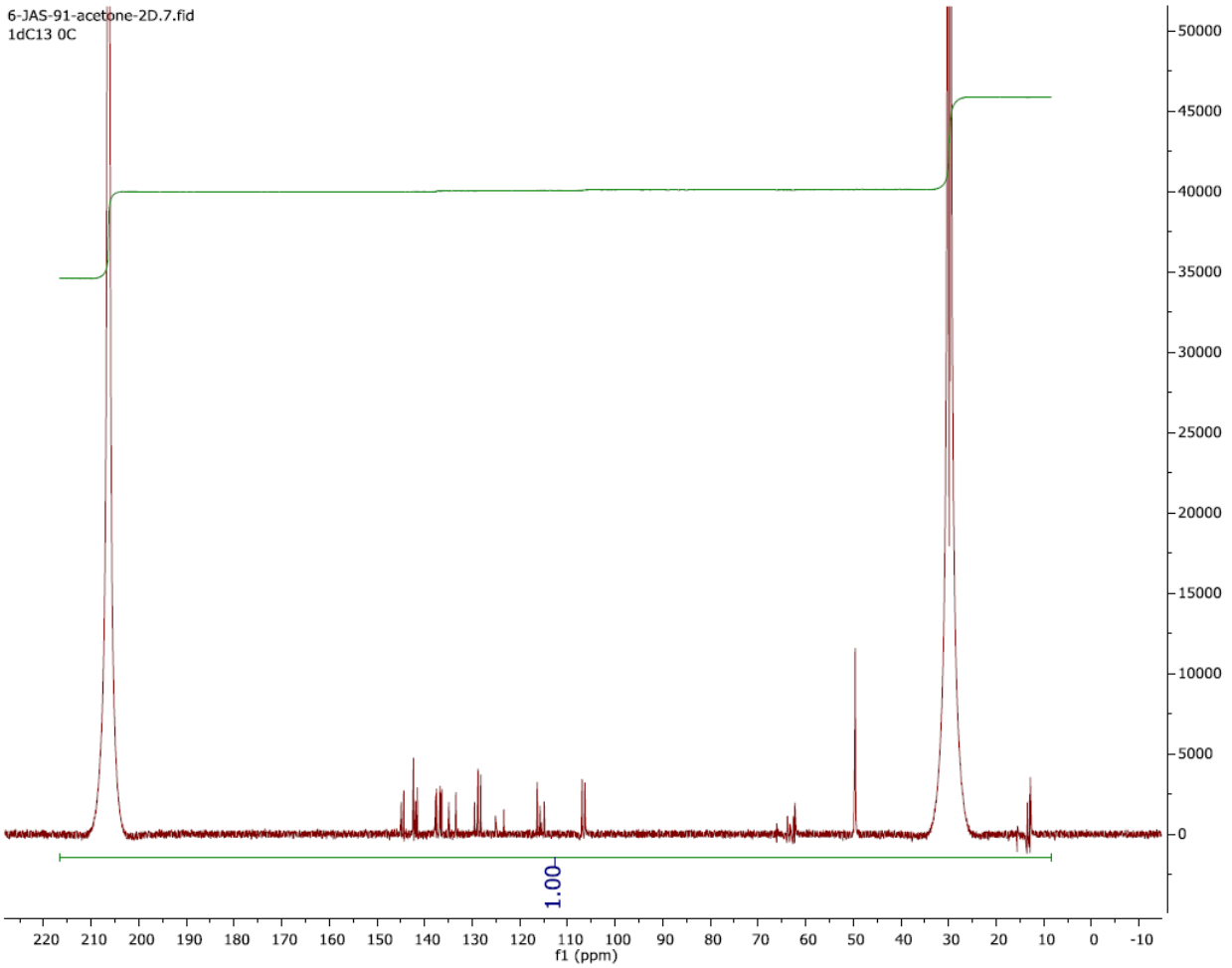

^{1}H NMR Spectrum of 5A and 5B

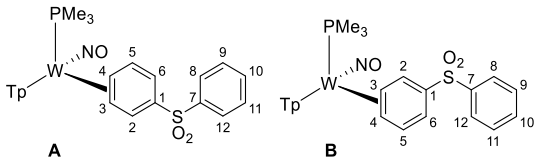

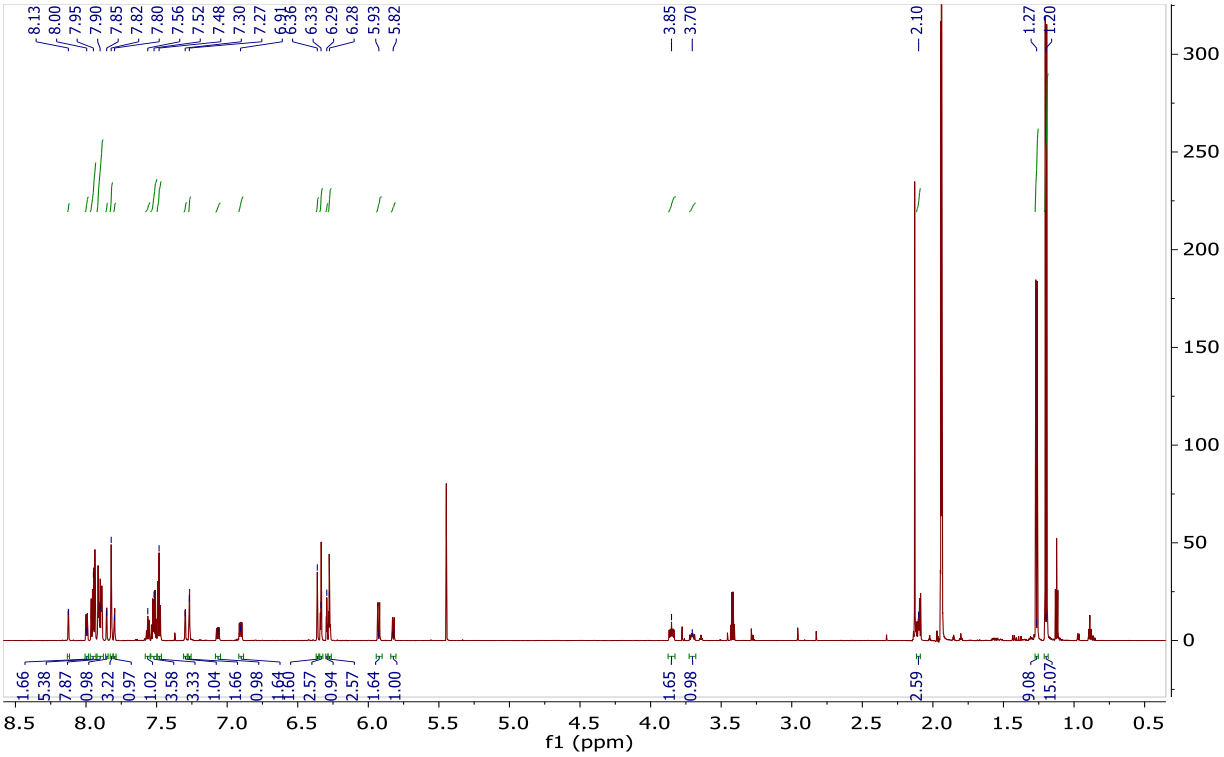

^{13}C {^{1}H} NMR Spectrum of 5A and 5B

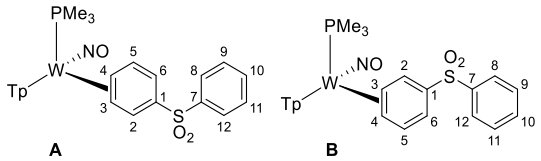

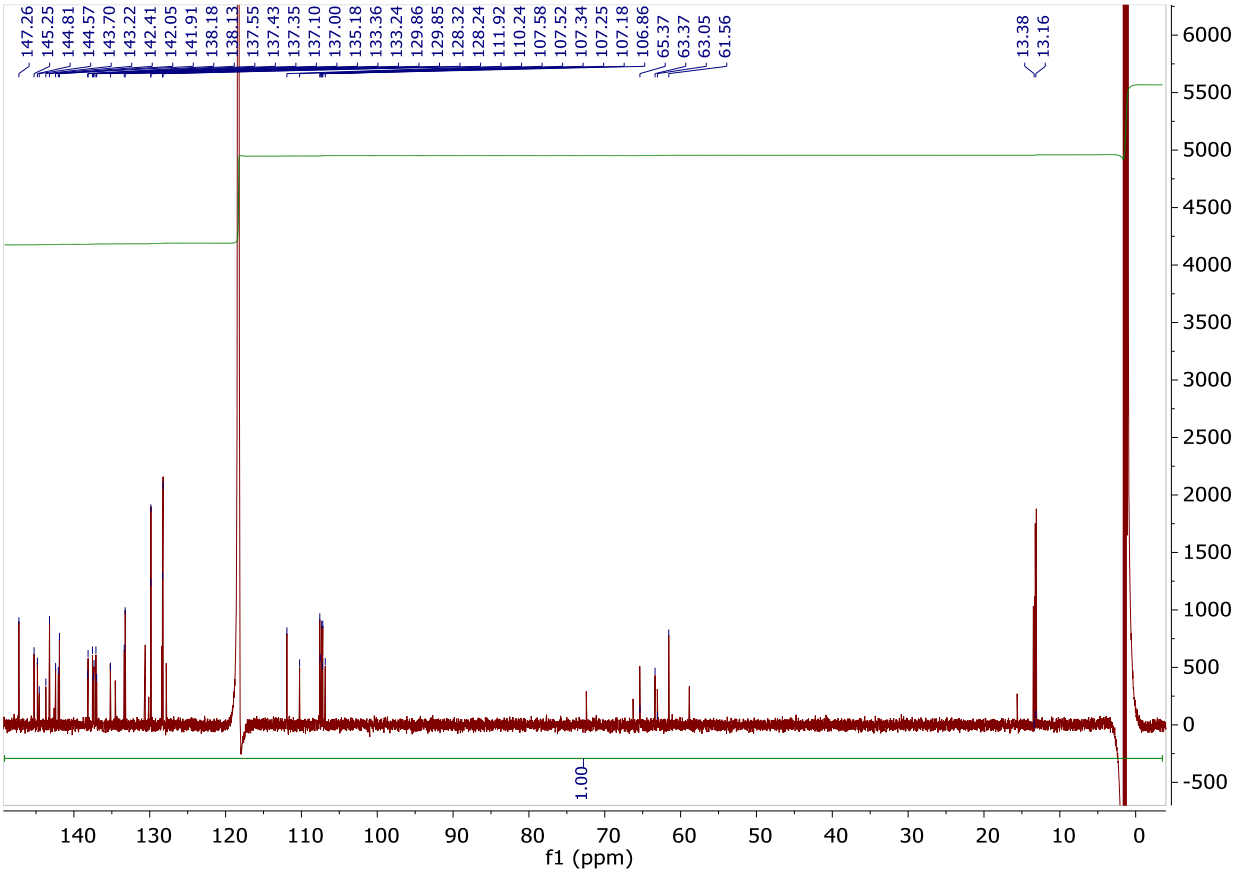

^{1}H NMR Spectrum of 6A and 6B

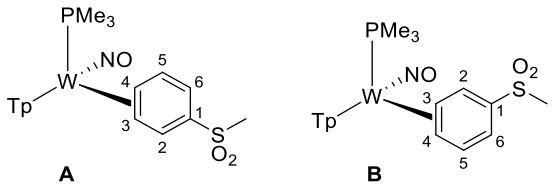

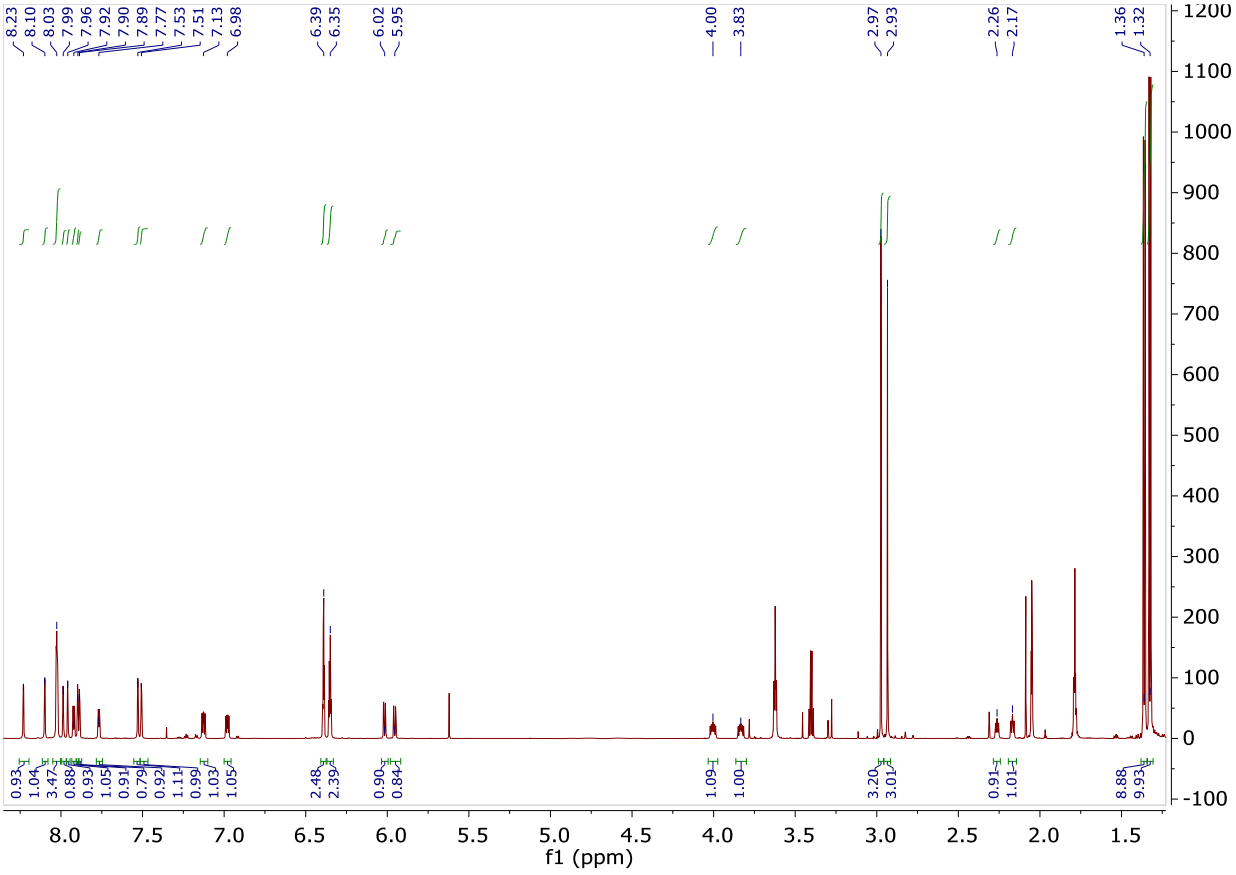

^{13}C {^{1}H} NMR Spectrum of 6A and 6B

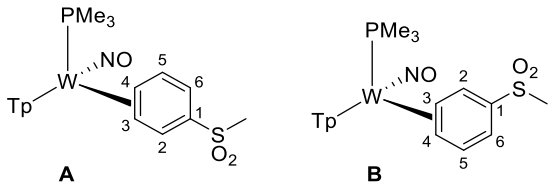

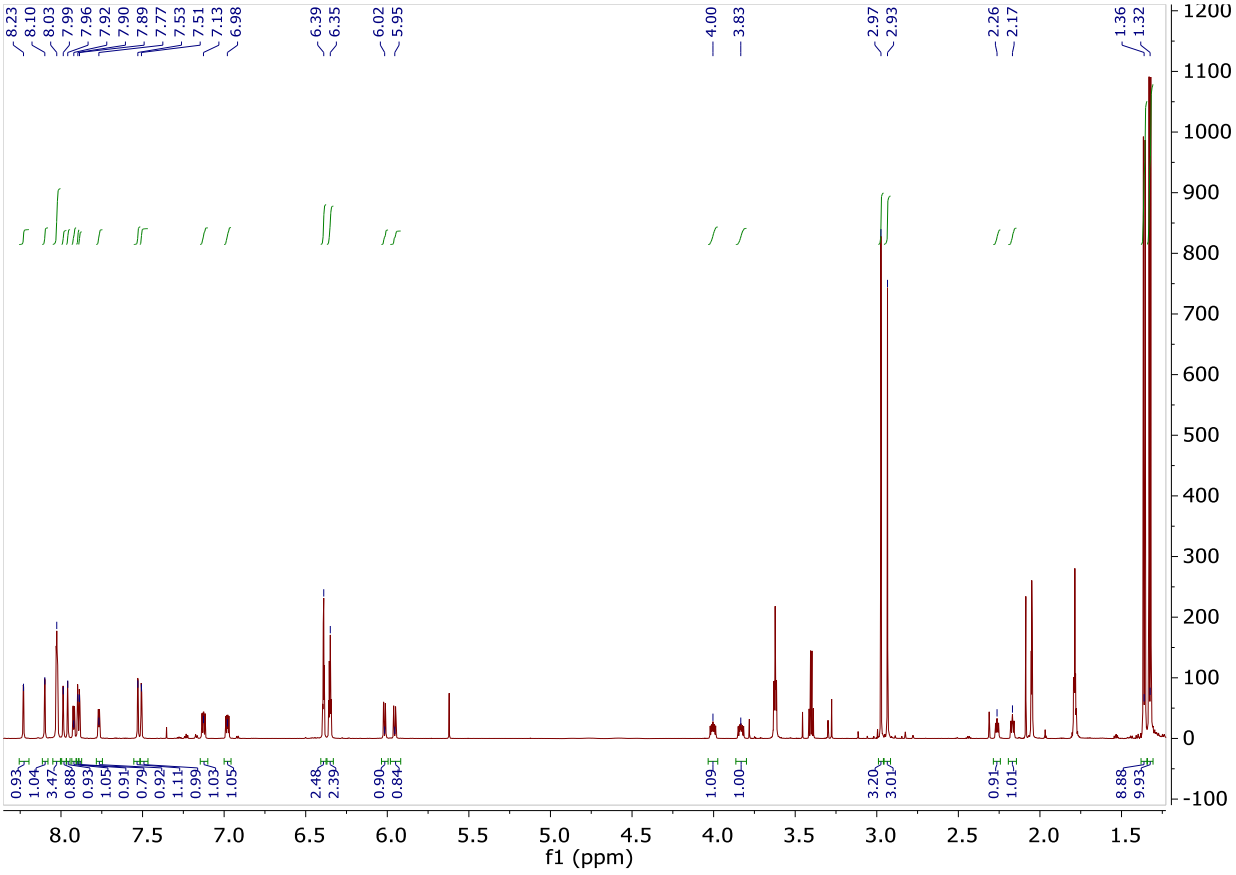

^{1}H NMR Spectrum of 7A and 7B

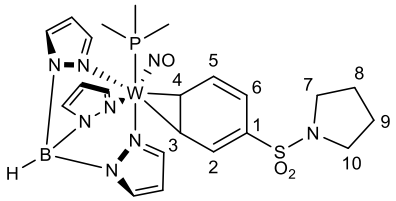

A

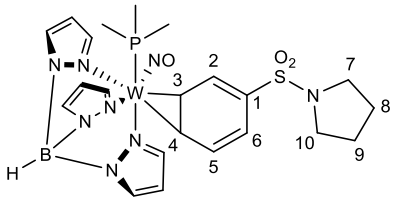

B

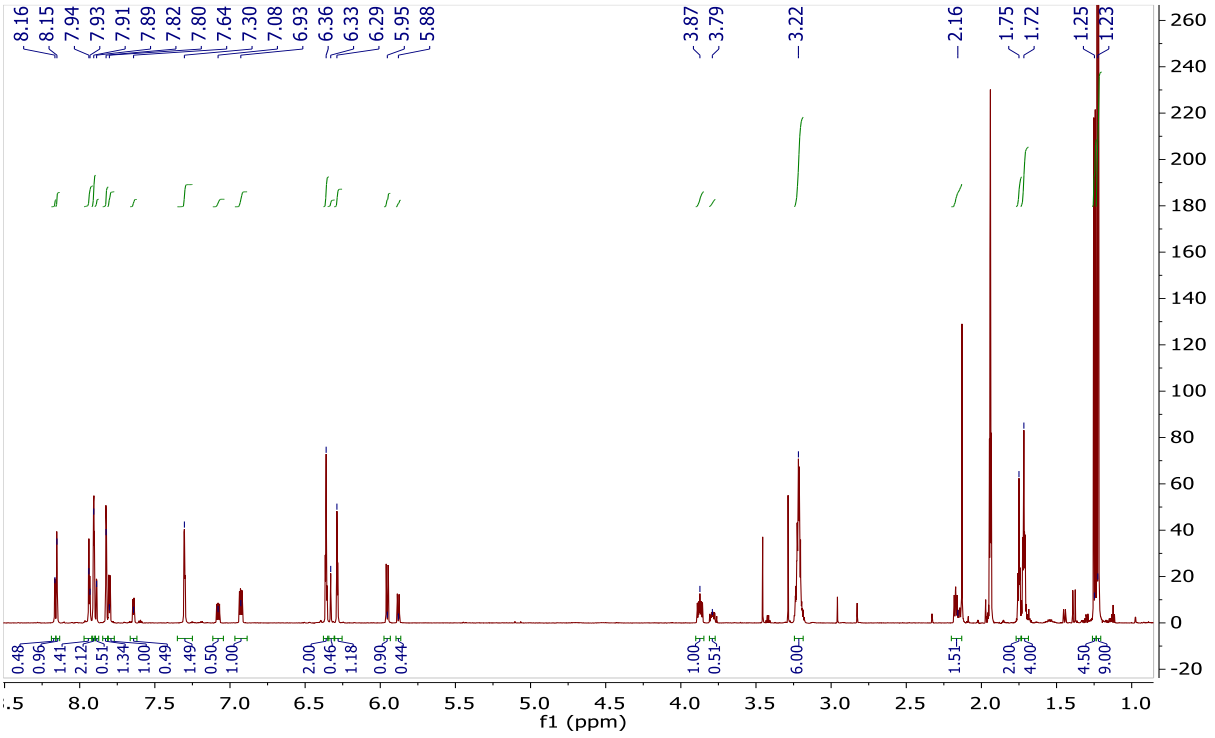

^{13}C {^{1}H} NMR Spectrum of 7A and 7B

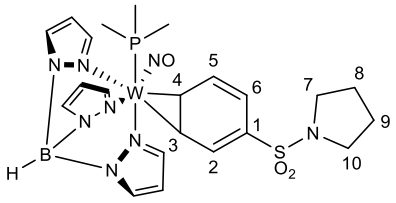

A

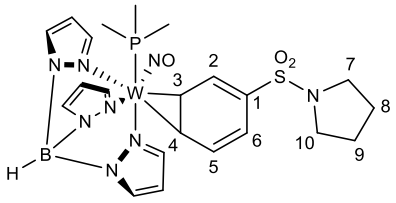

B

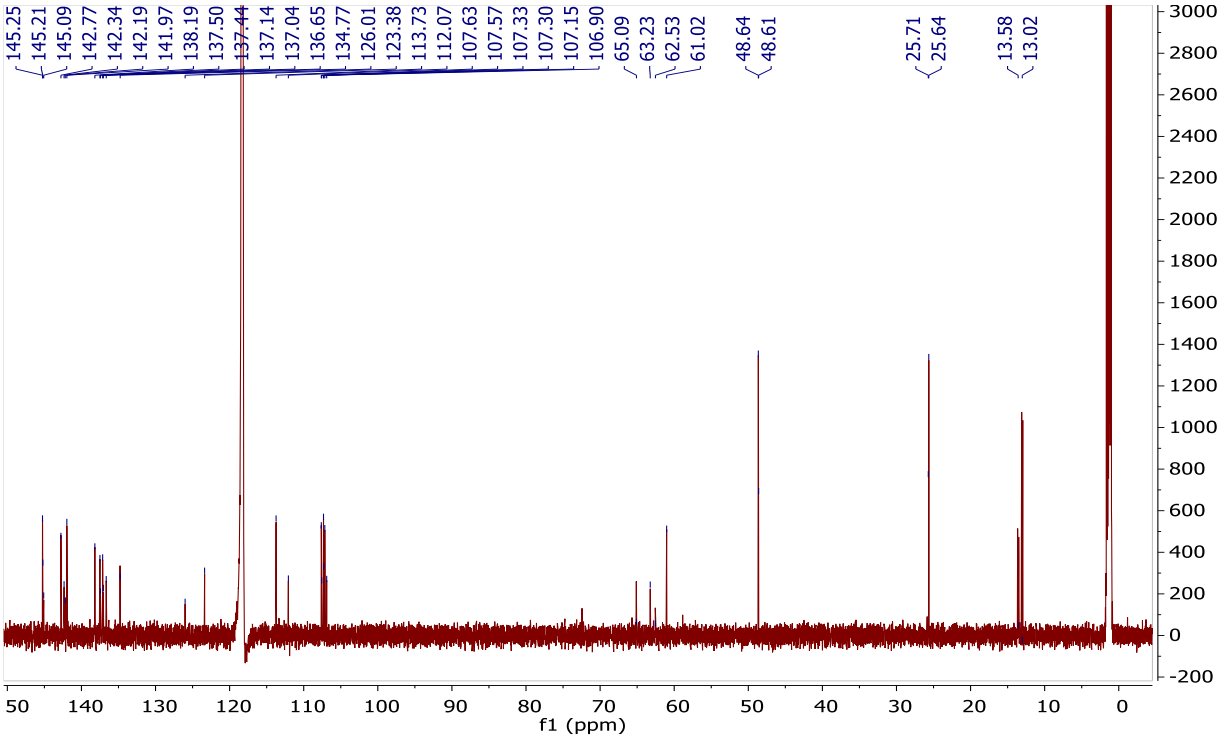

^{1}H NMR Spectrum of 8A and 8B

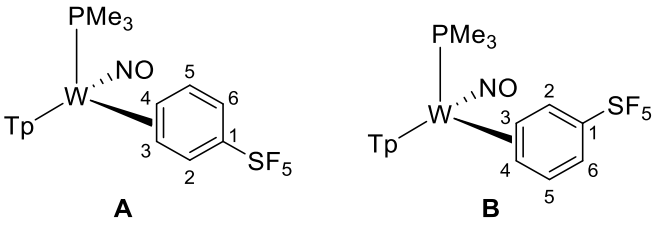

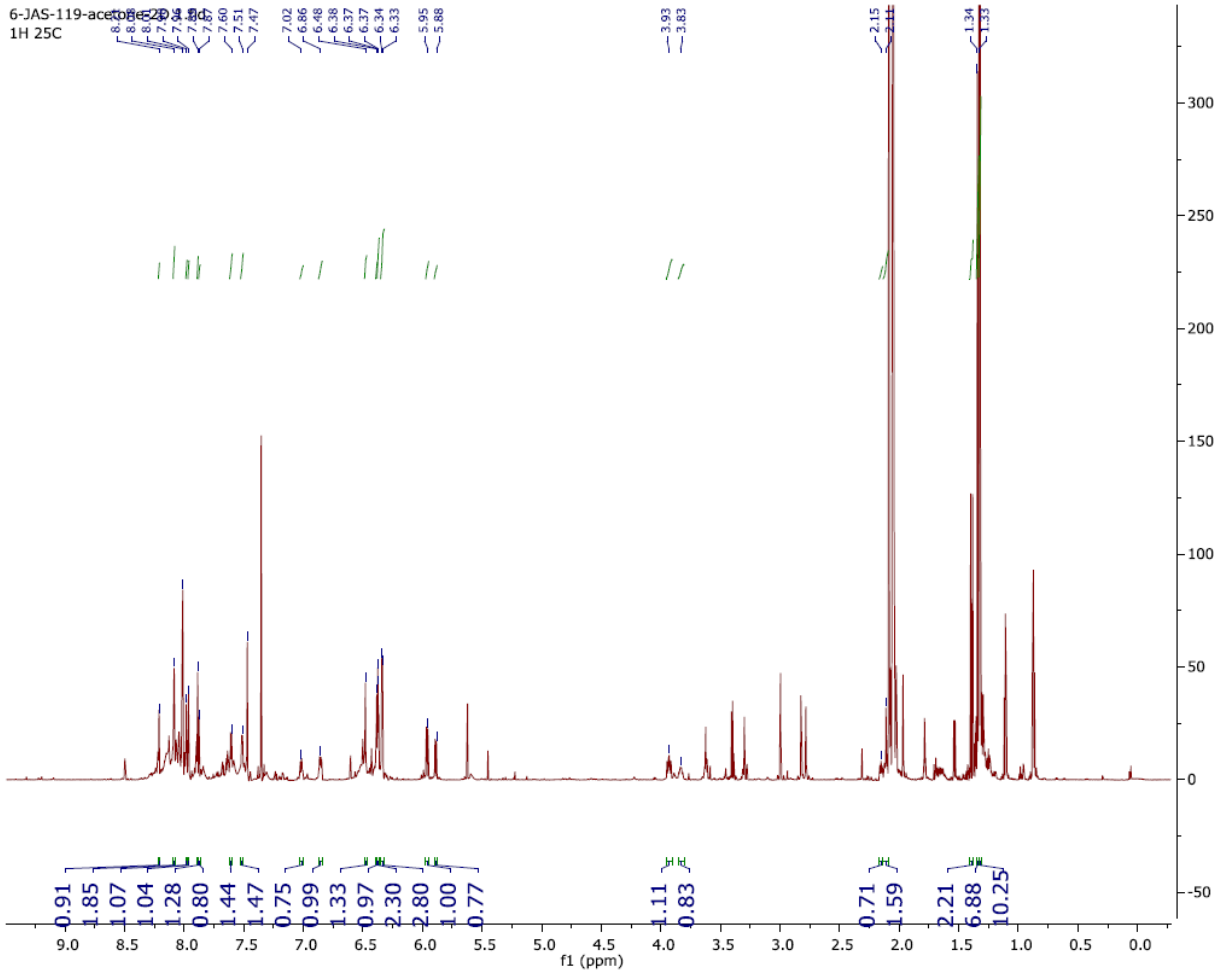

^{13}C {^{1}H} NMR Spectrum of 8A and 8B

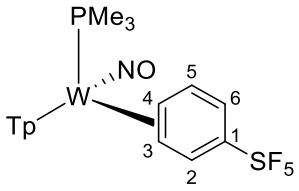

A

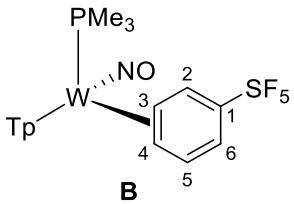

B

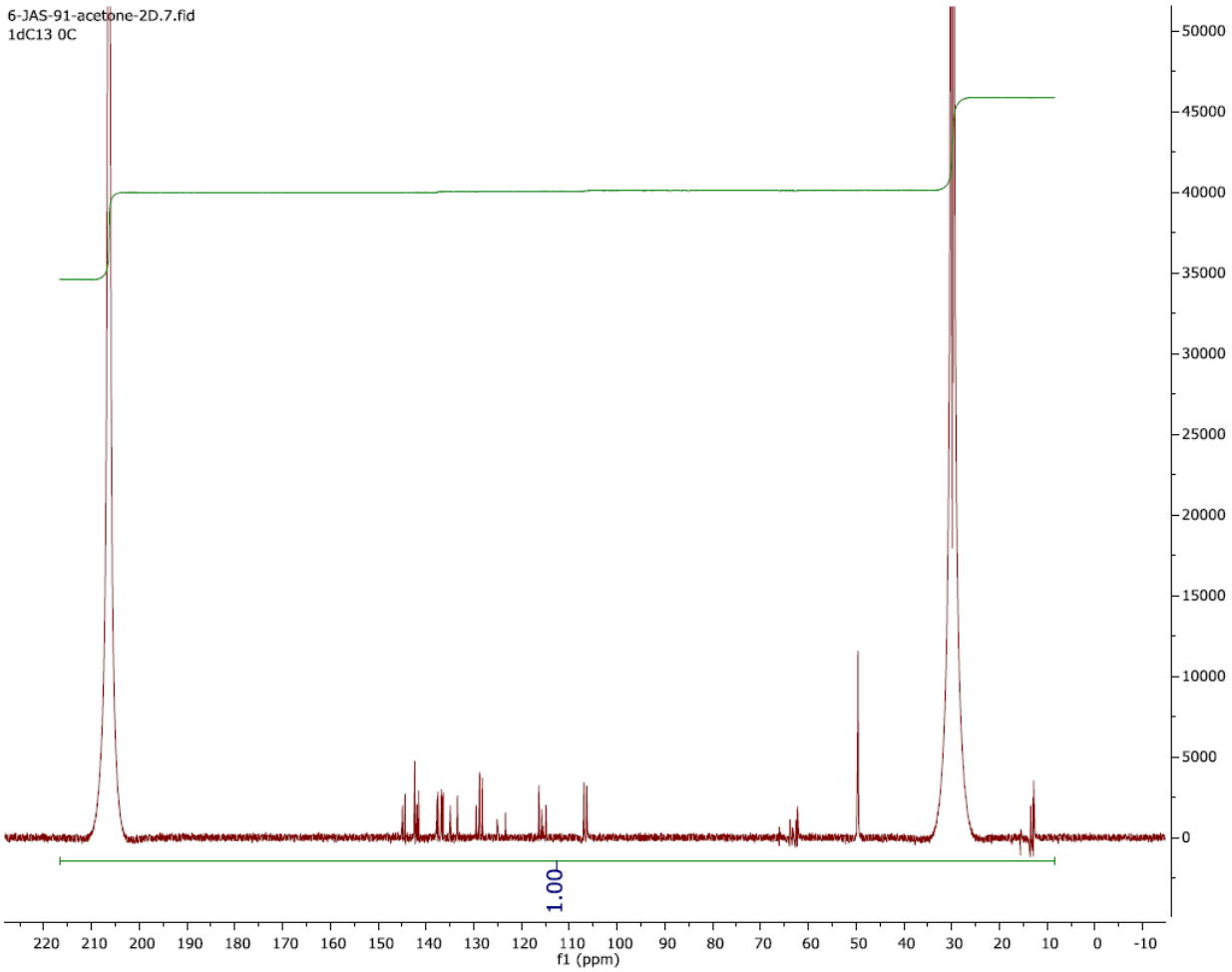

^{1}H NMR Spectrum of 9

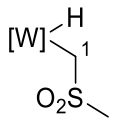

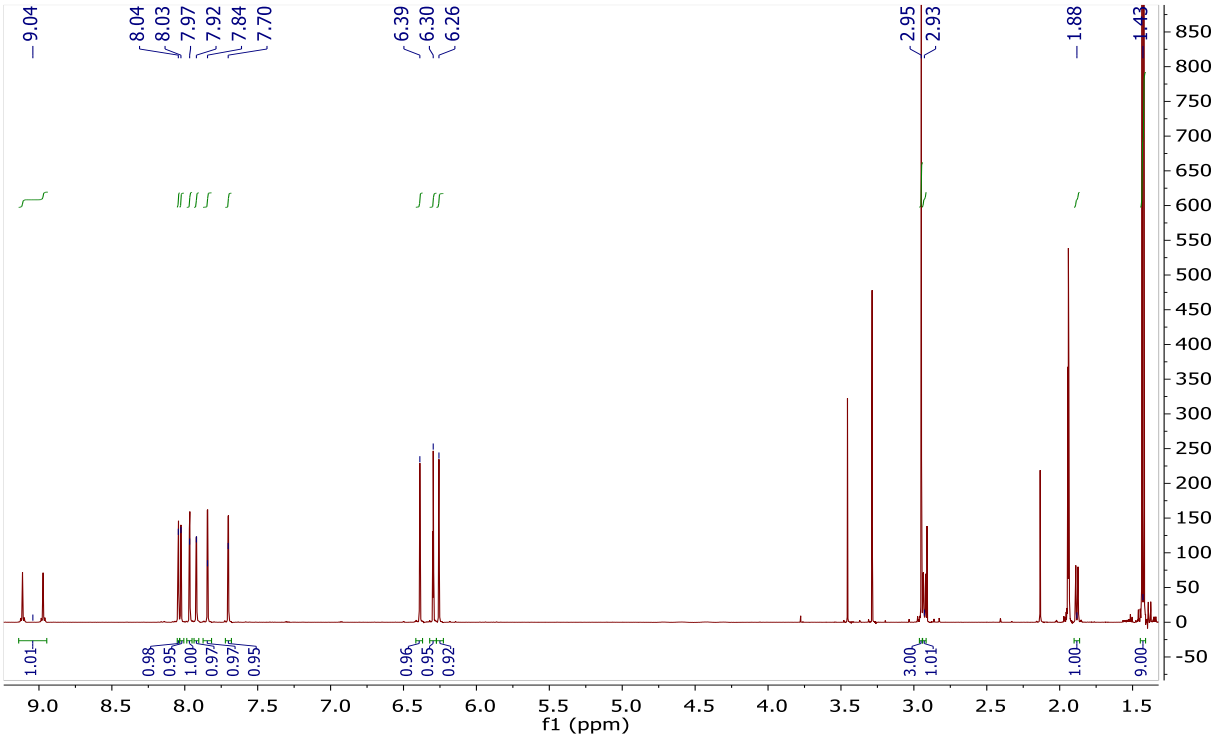

^{13}C {^{1}H} NMR Spectrum of 9

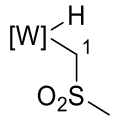

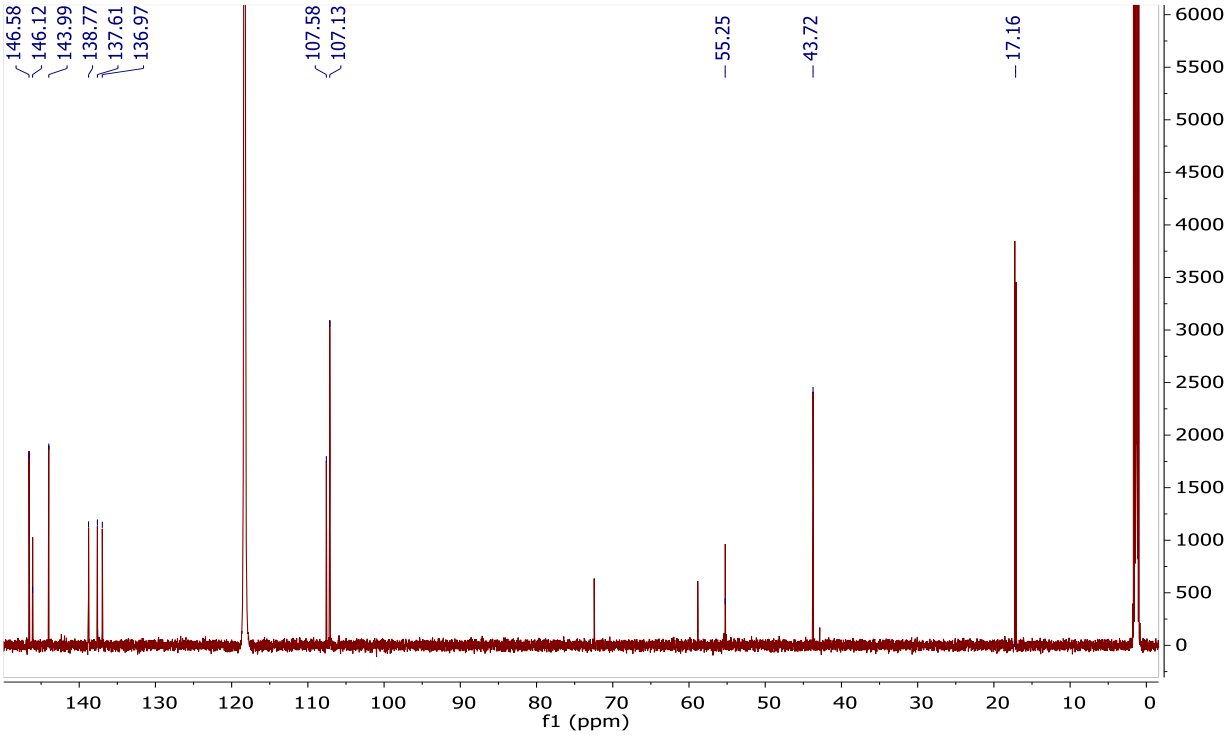

^{1}H NMR Spectrum of 10

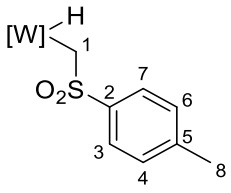

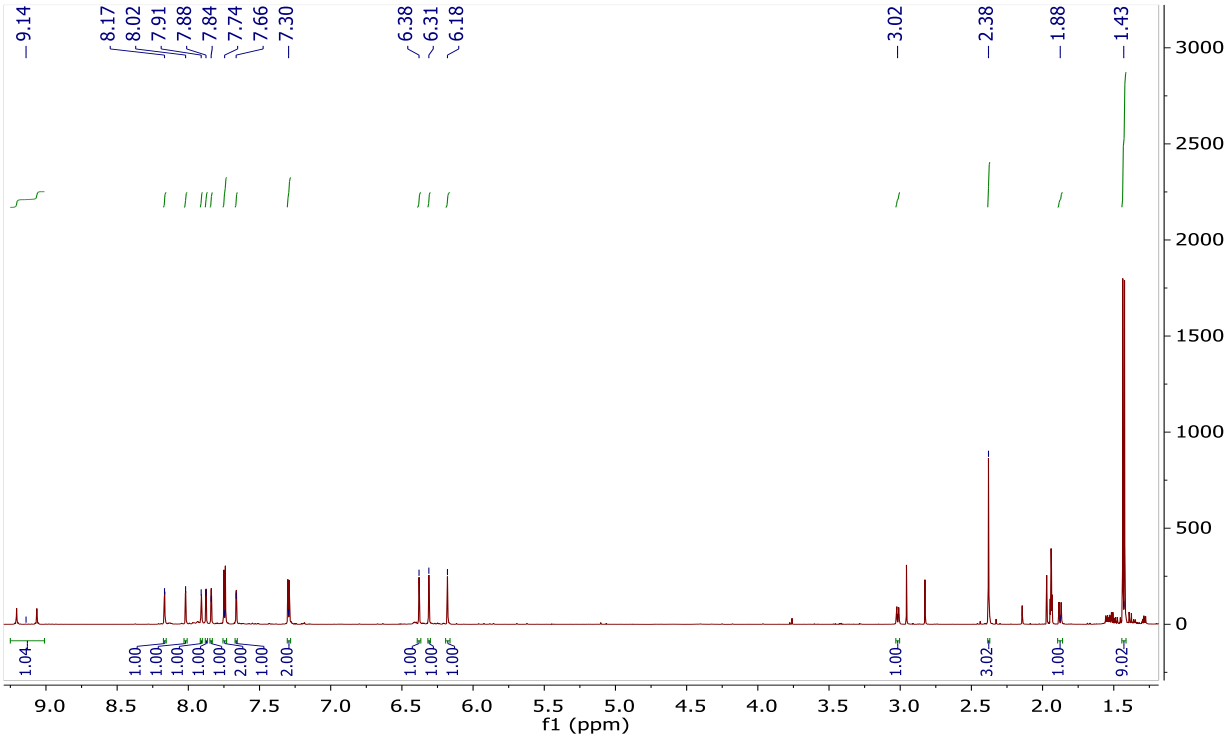

^{13}C {^{1}H} NMR Spectrum of 10

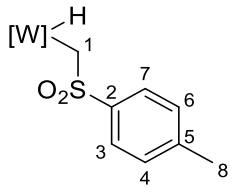

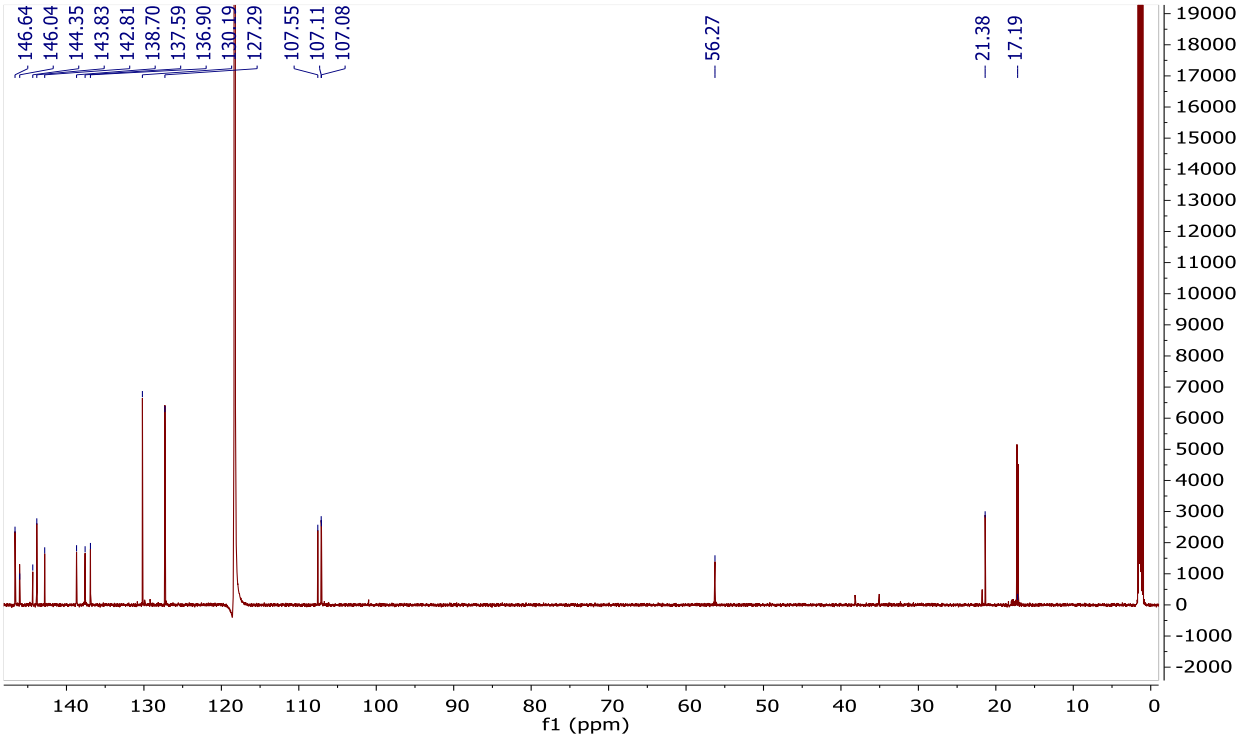

^{1}H NMR Spectrum of 11A and 11B

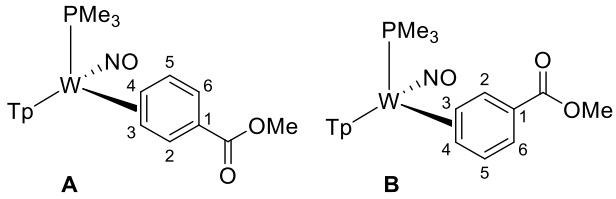

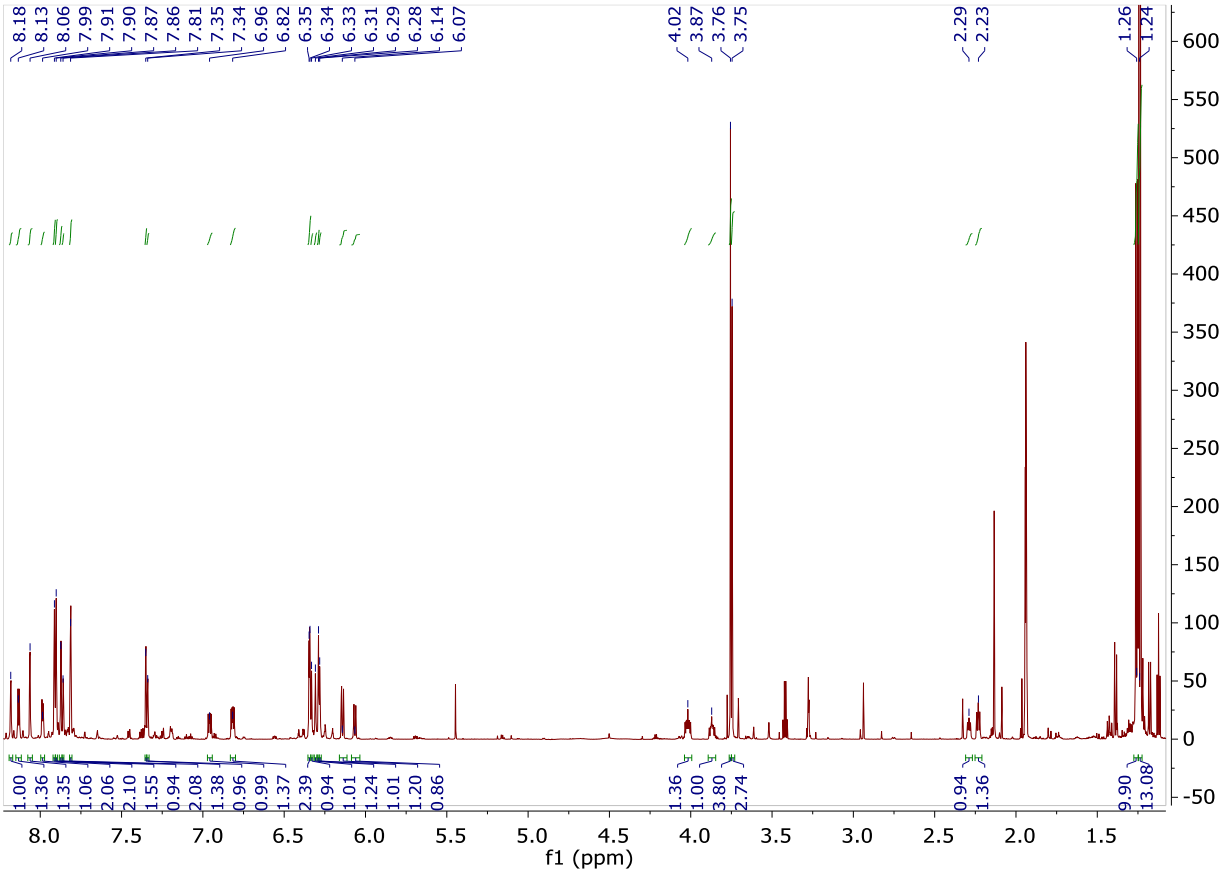

^{13}C {^{1}H} NMR Spectrum of 11A and 11B

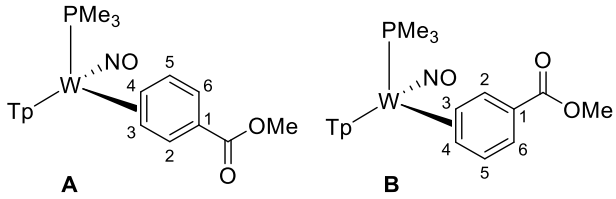

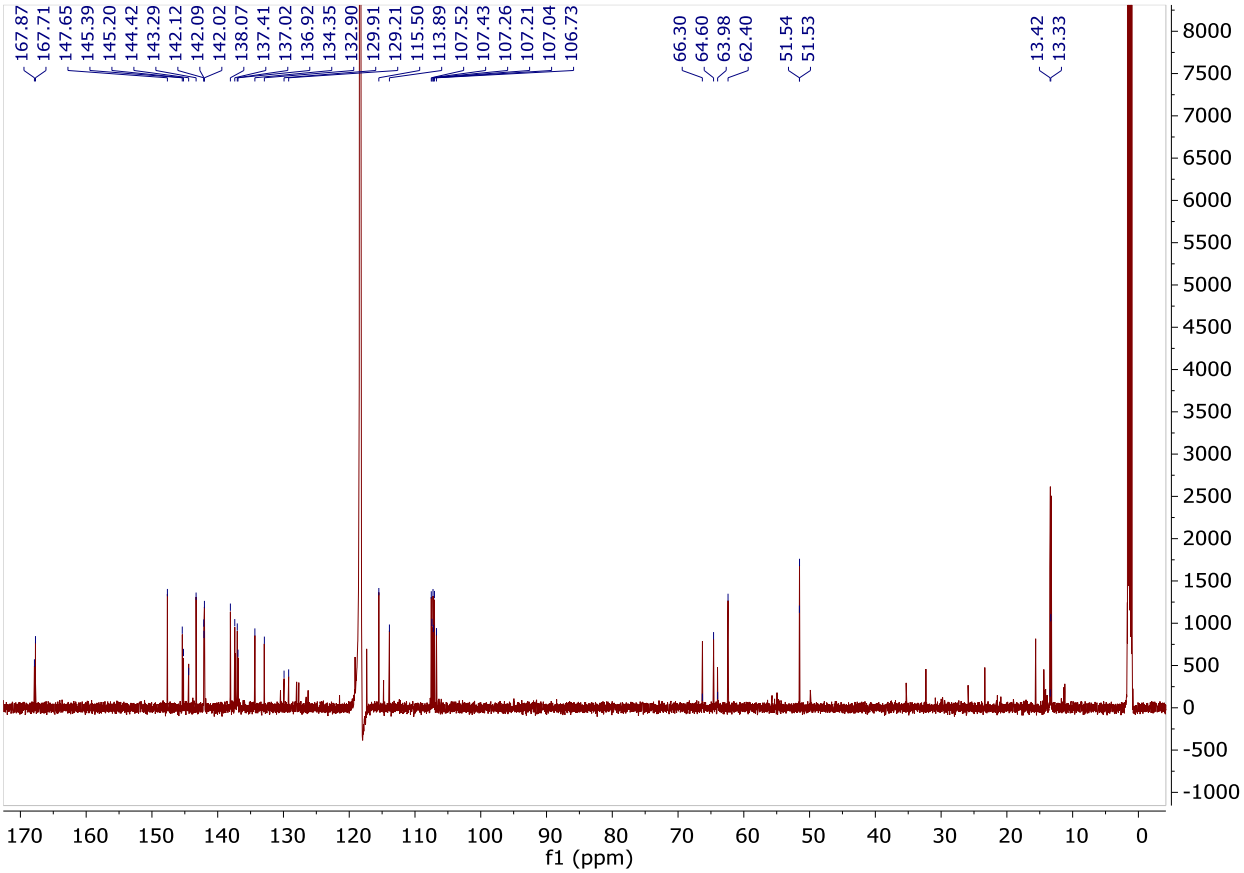

^{1}H NMR Spectrum of 12A and 12B

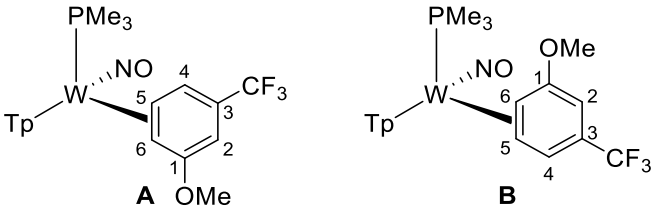

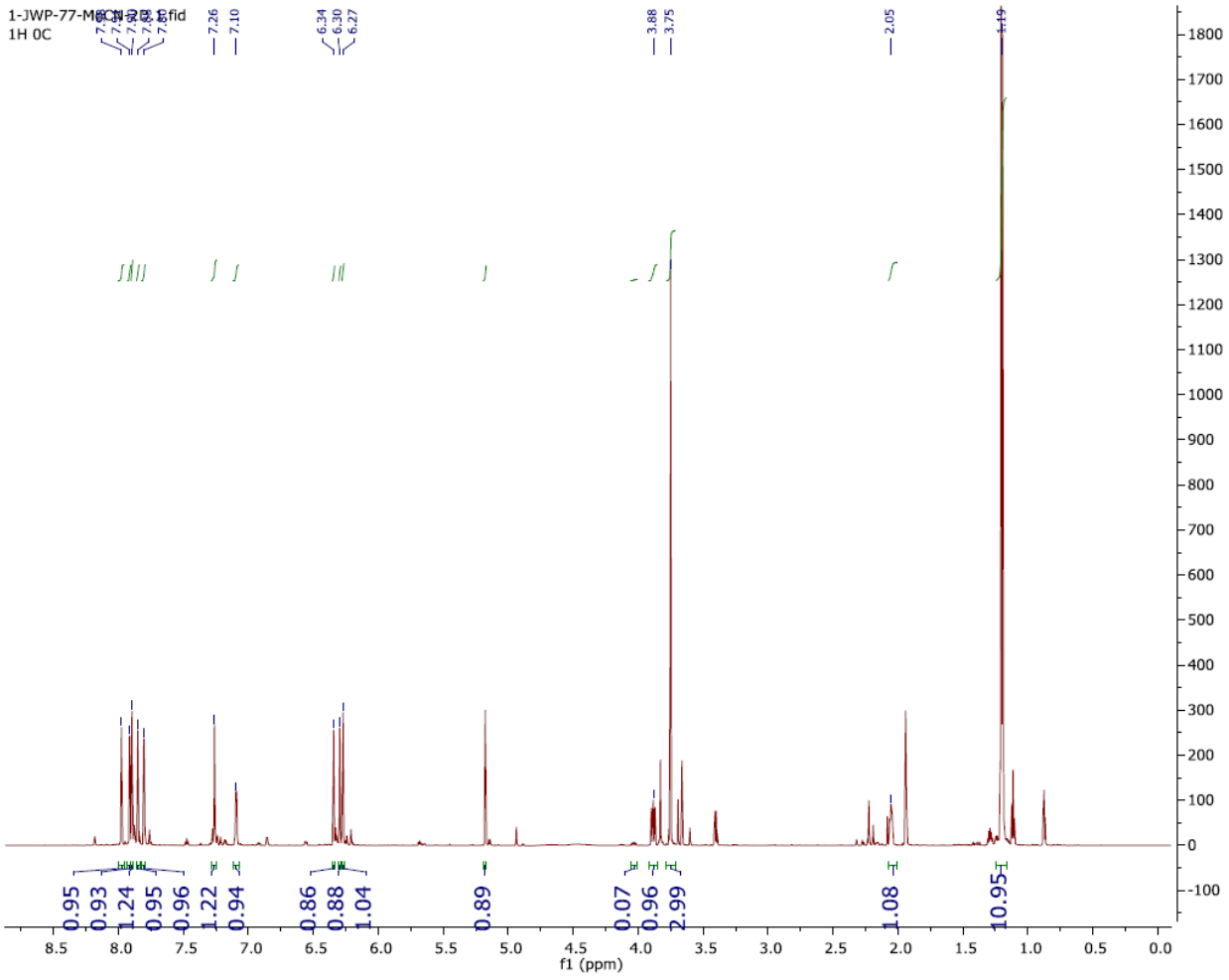

^{13}C {^{1}H} NMR Spectrum of 12A and 12B

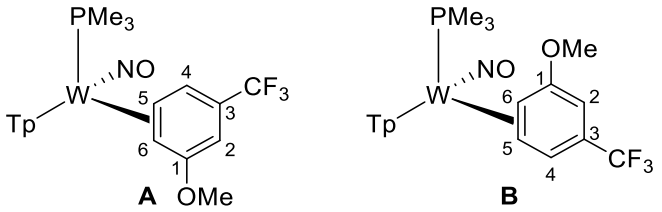

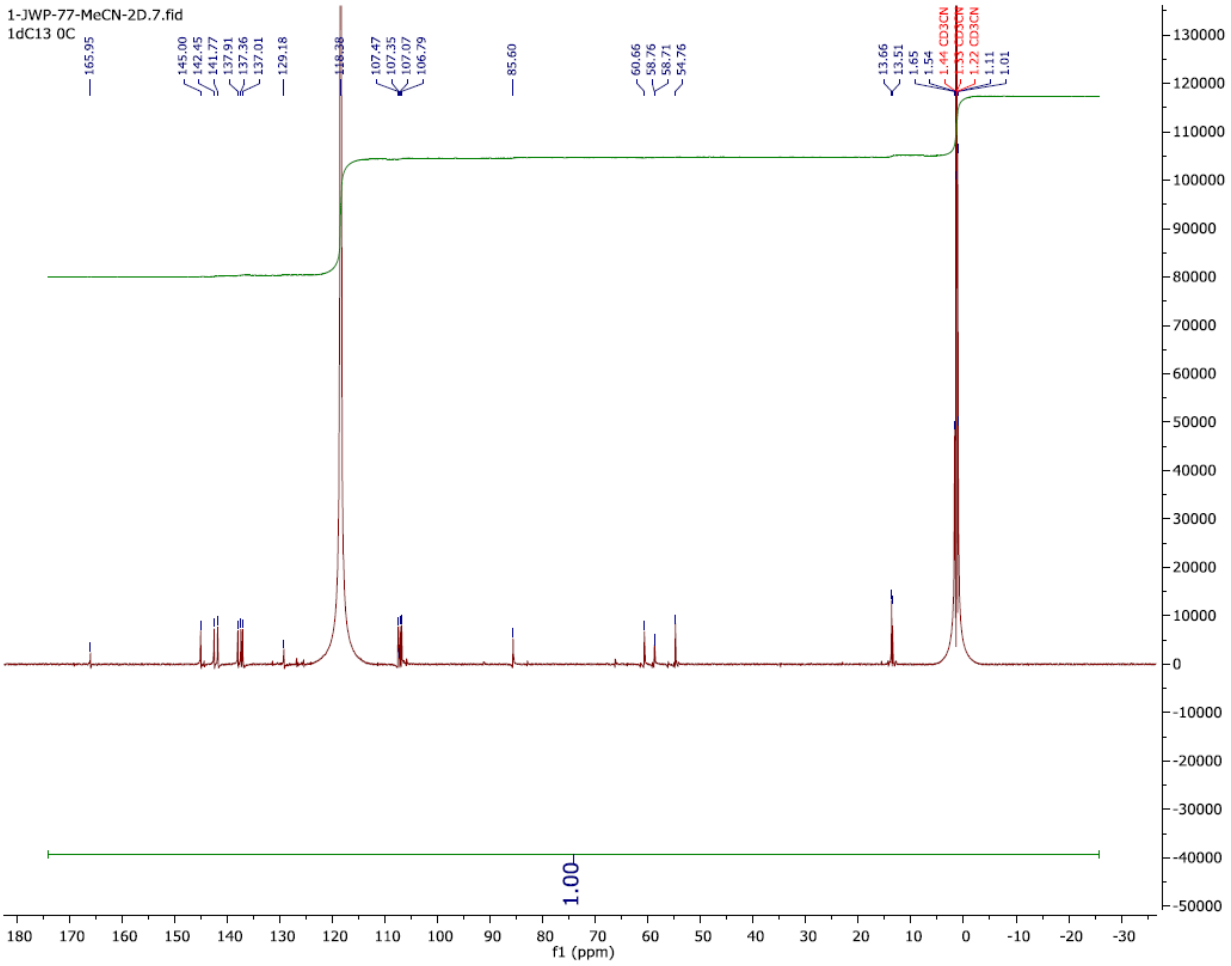

^{1}H NMR Spectrum of 13

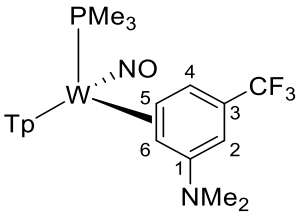

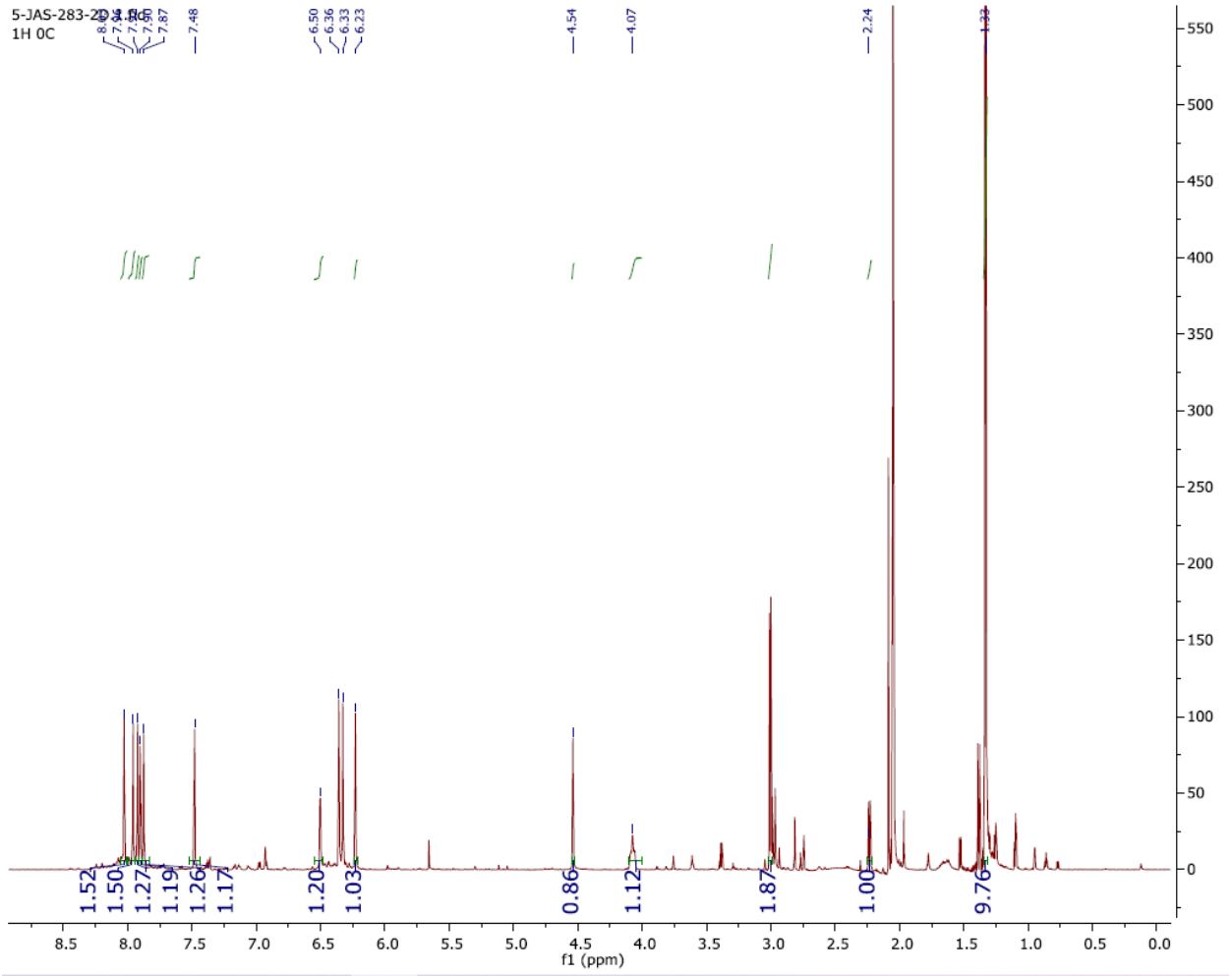

^{13}C {^{1}H} NMR Spectrum of 13

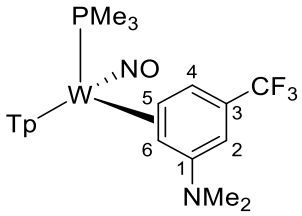

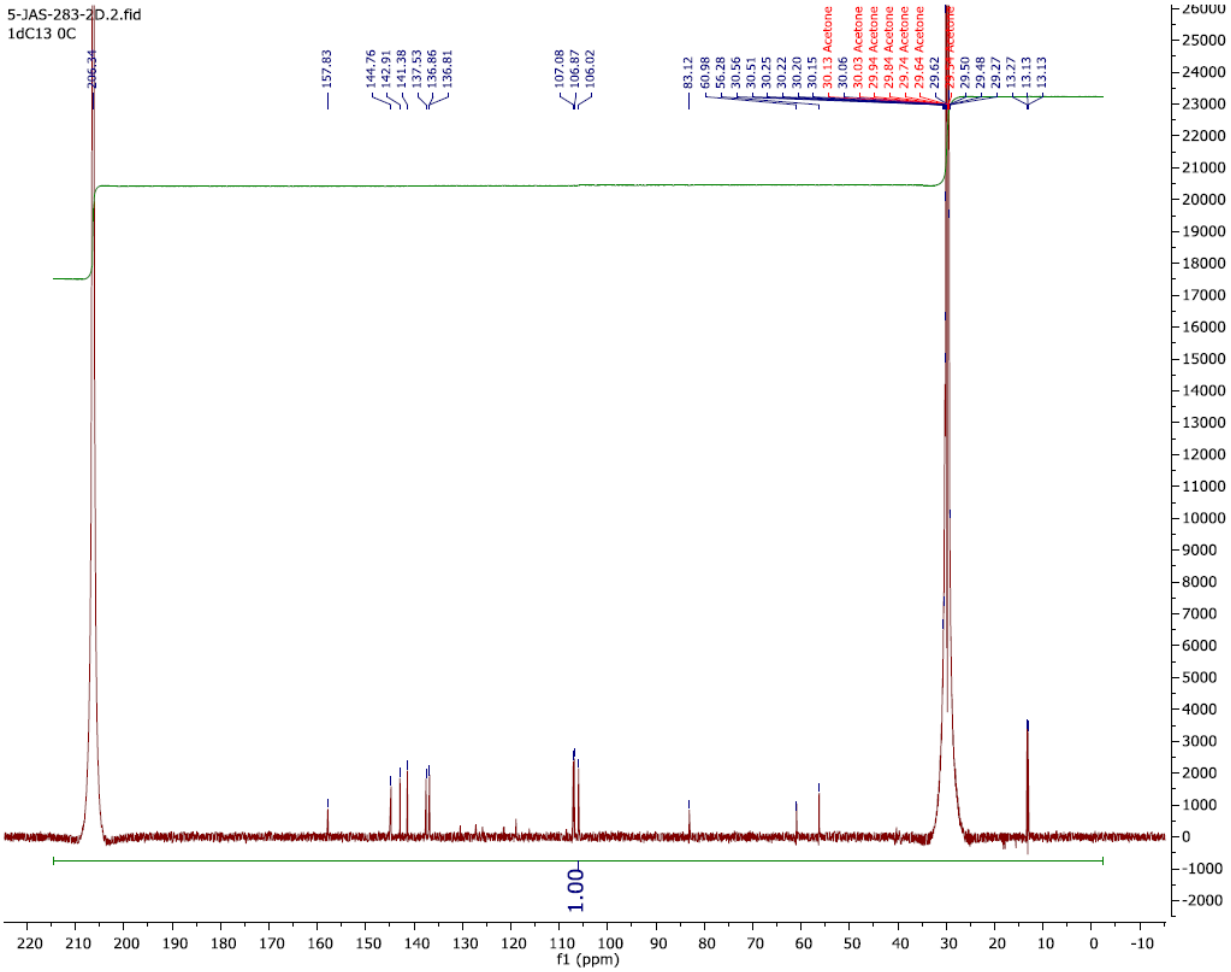

^{1}H NMR Spectrum of 14

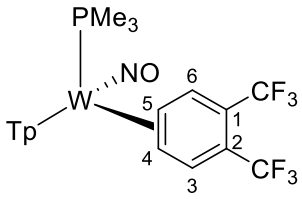

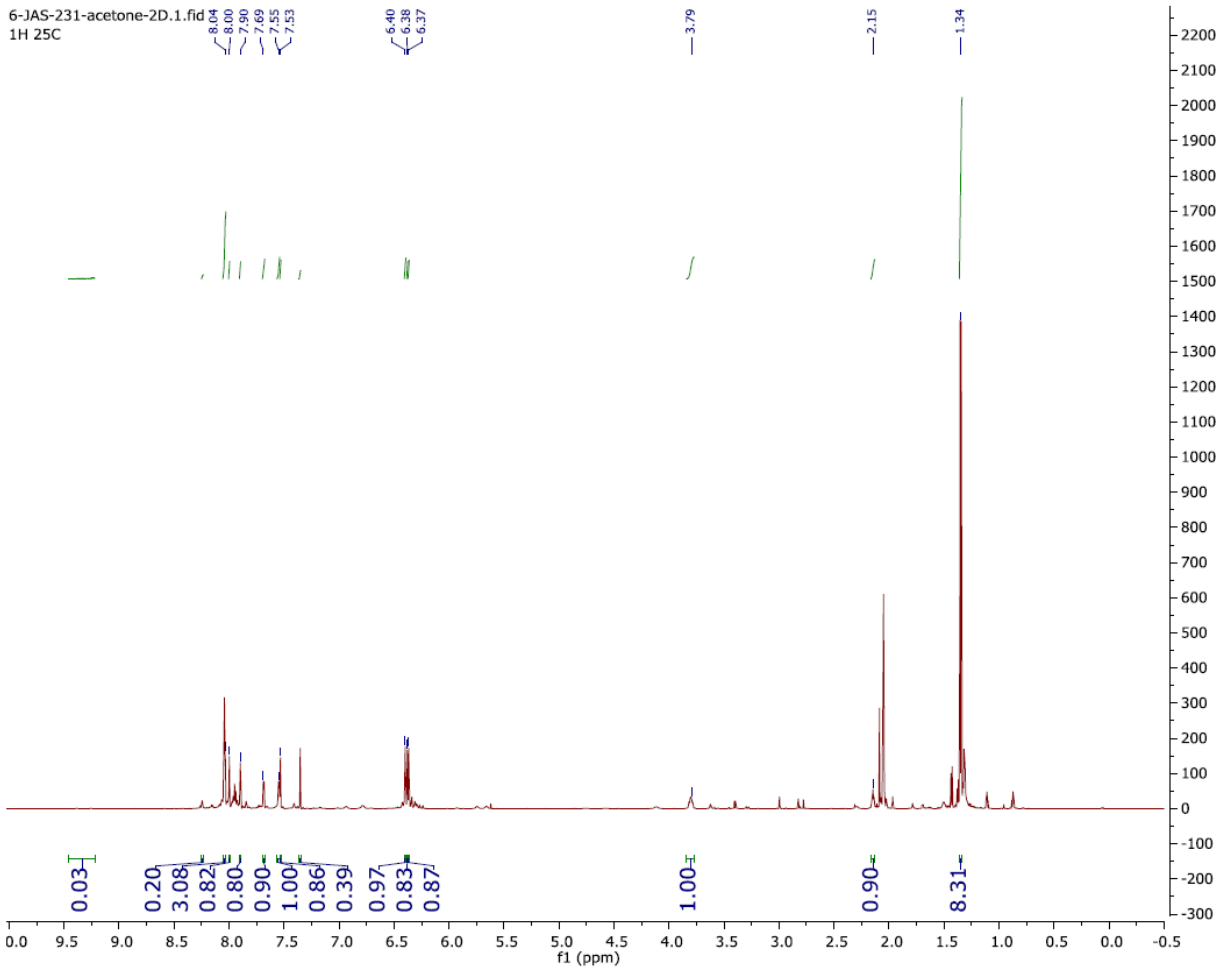

^{13}C {^{1}H} NMR Spectrum of 14

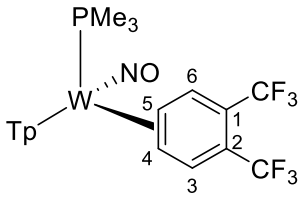

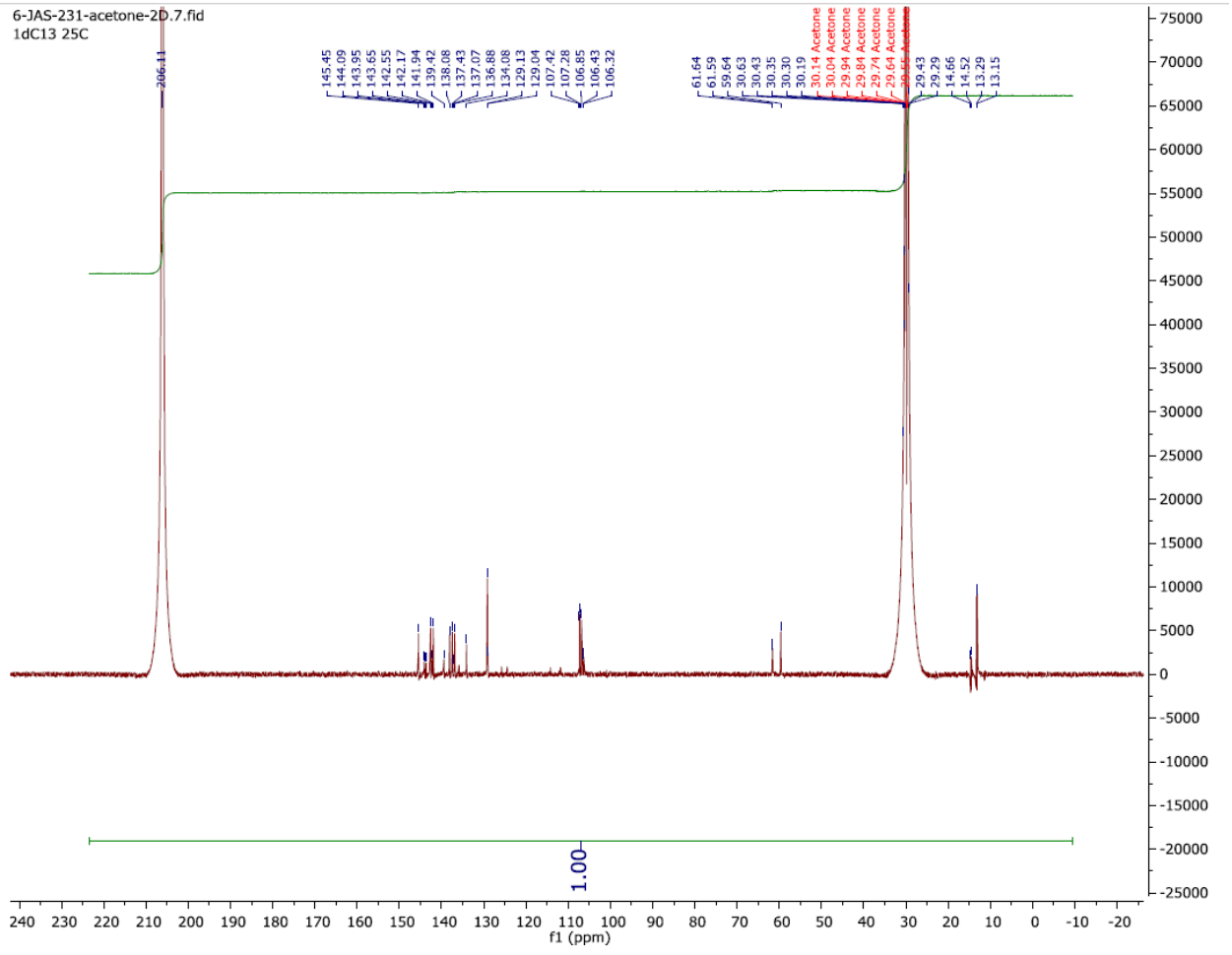

^{1}H NMR Spectrum of 15A and 15B

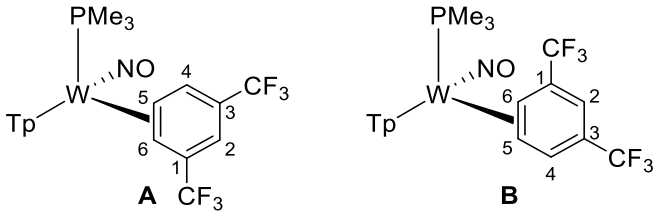

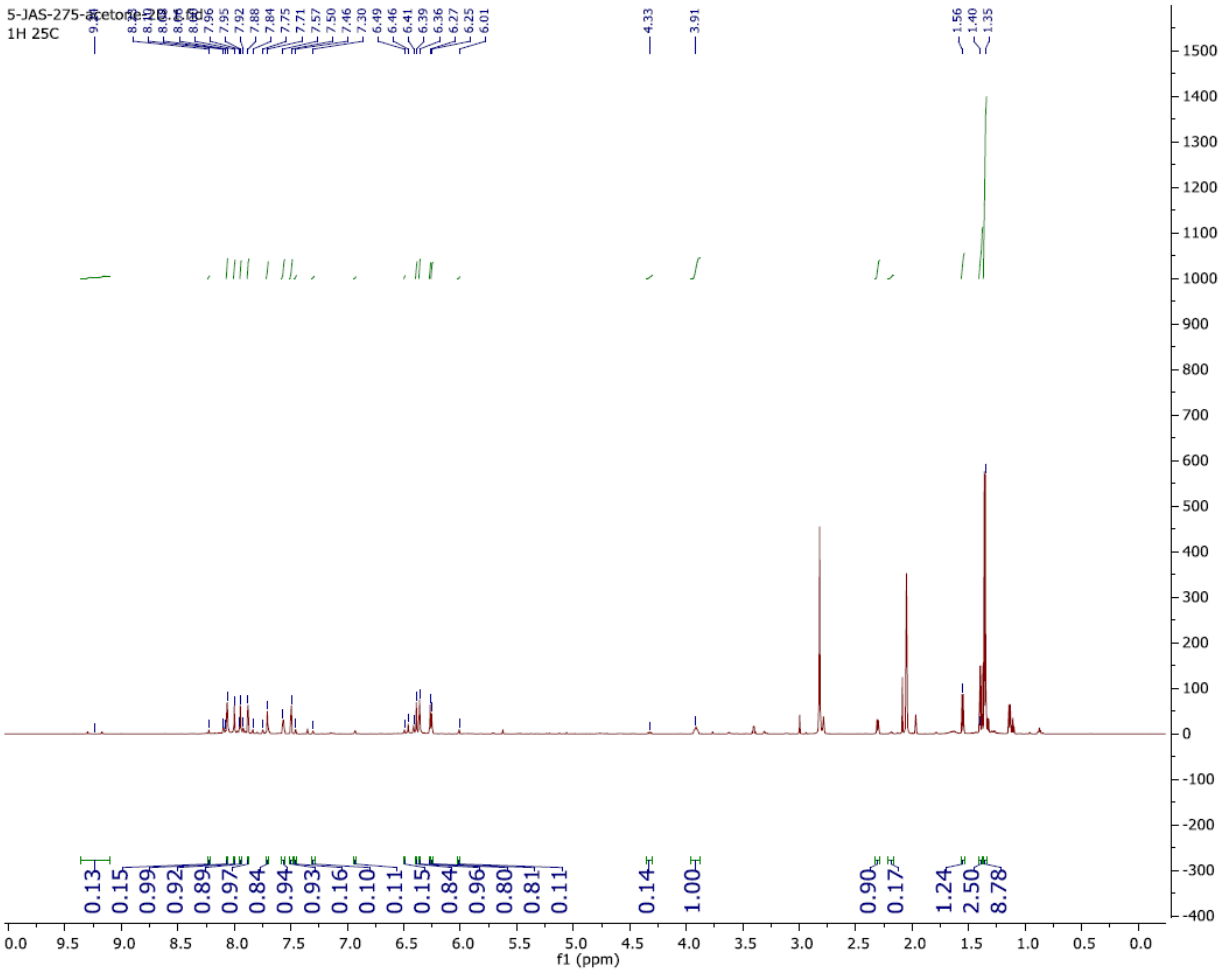

^{13}C {^{1}H} NMR Spectrum of 15A and 15B

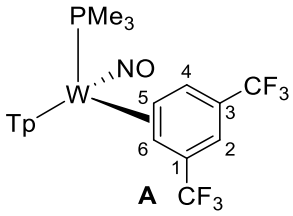

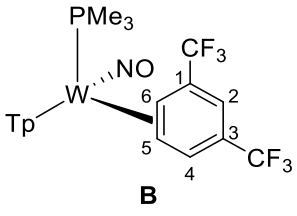

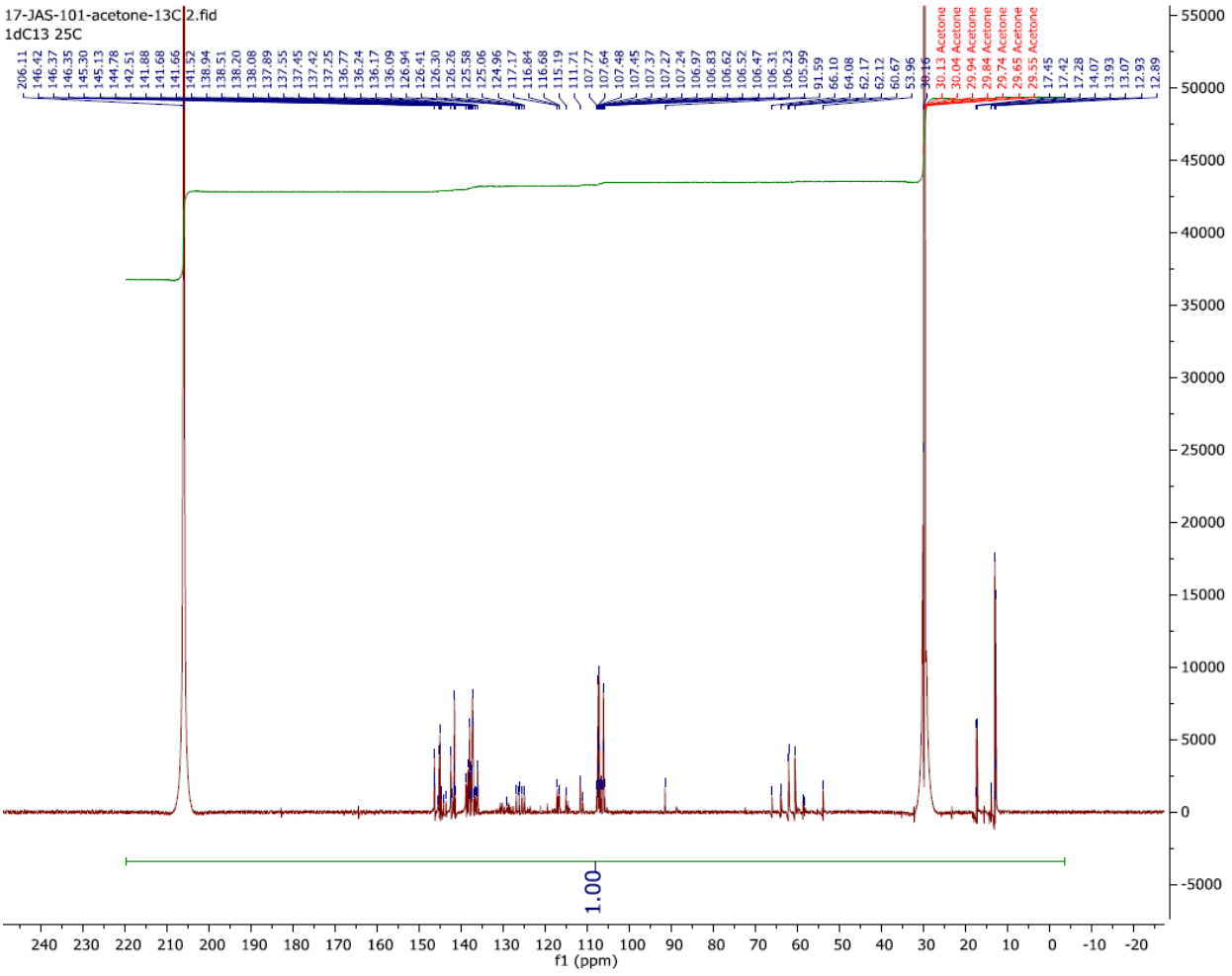

^{1}H NMR Spectrum of 16

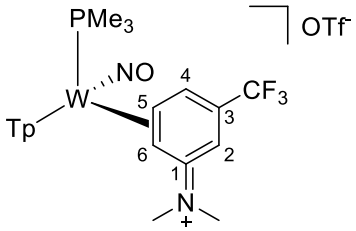

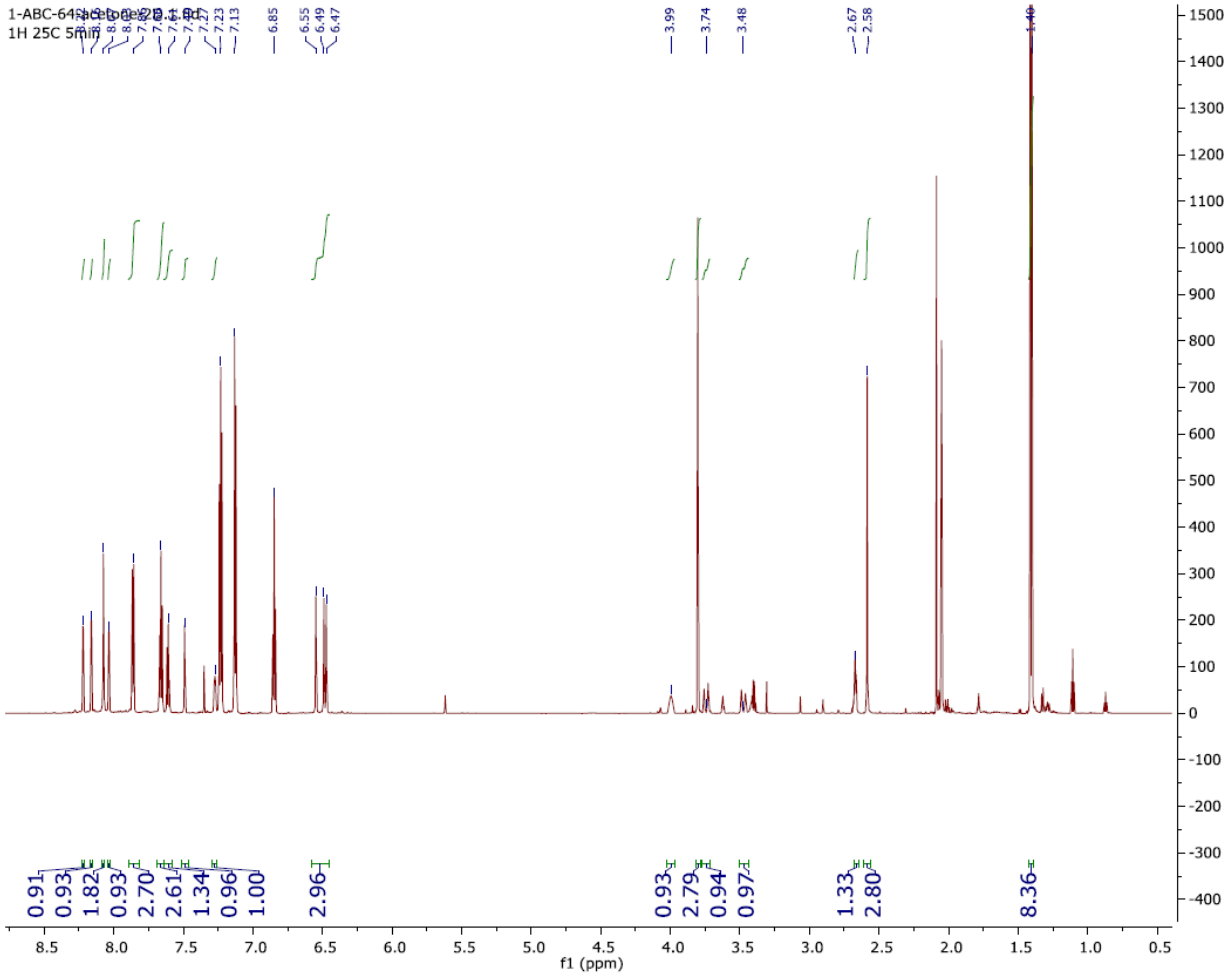

^{13}C {^{1}H} NMR Spectrum of 16

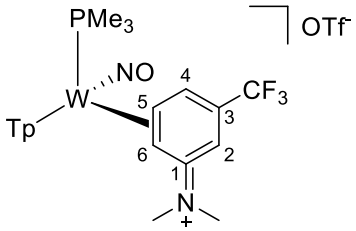

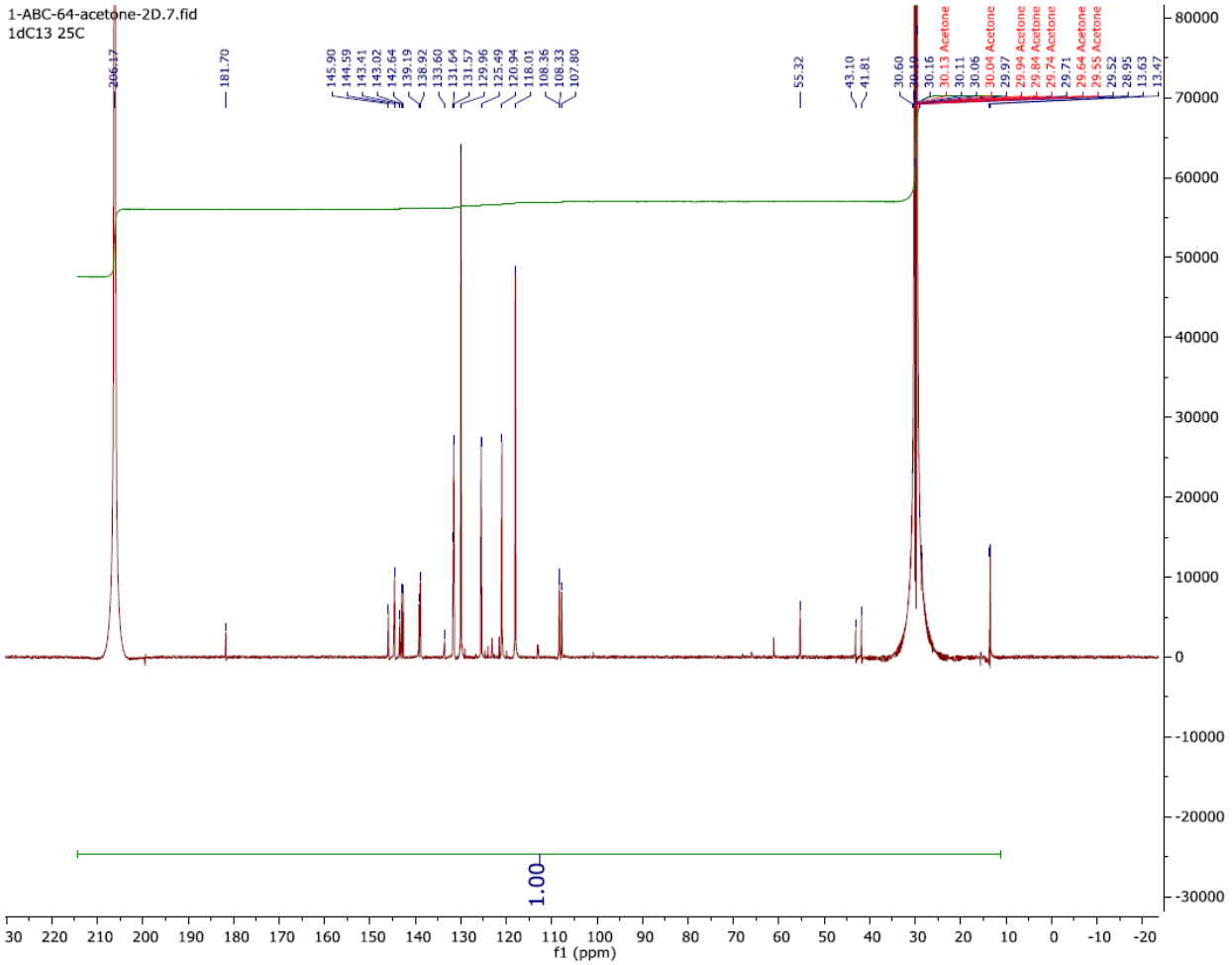

Supporting Crystallographic Data for Chapter 3

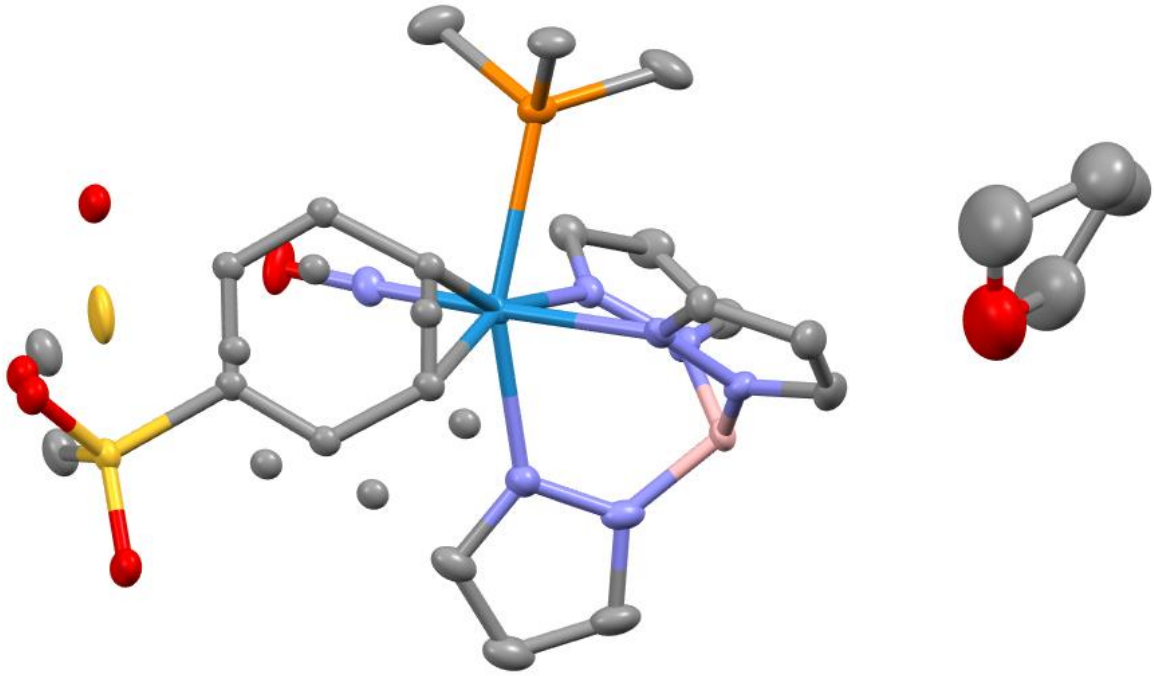

Crystal Structure Report for 6 in Chapter 3

A yellow plate-like specimen of $C_{23}H_{35}BN_7O_4PSW$, approximate dimensions 0.054 mm x 0.147 mm x 0.312 mm, was coated with Paratone oil and mounted on a MiTeGen MicroLoop. The X-ray intensity data were measured on a Bruker Kappa APEXII Duo system equipped with a fine-focus sealed tube (Mo K_α, λ = 0.71073 Å) and a graphite monochromator.

The total exposure time was 1.63 hours. The frames were integrated with the Bruker SAINT software package[1] using a narrow-frame algorithm. The integration of the data using a monoclinic unit cell yielded a total of 35588 reflections to a maximum θ angle of 28.30° (0.75 Å resolution), of which 7289 were independent (average redundancy 4.882, completeness = 99.8%, R_{int} = 6.18%, R_{sig} = 5.46%) and 5821 (79.86%) were greater than 2σ(F^2). The final cell constants of a = 12.8008(7) Å, b = 17.9773(9) Å, c = 13.4385(7) Å, β = 108.074(2)°, volume = 2939.9(3) $Å^3$, are based upon the refinement of the XYZ-centroids of 9744 reflections above 20 σ(I) with 4.458° < 2θ < 56.25°. Data were corrected for absorption effects using the Multi-Scan method (SADABS).[1] The ratio of minimum to maximum apparent transmission was 0.711. The calculated minimum and maximum transmission coefficients (based on crystal size) are 0.3610 and 0.8090.

The structure was solved and refined using the Bruker SHELXTL Software Package[2] within APEX3 [1] and OLEX2,[3] using the space group P $2_1/c$, with Z = 4 for the formula unit, $C_{23}H_{35}BN_7O_4PSW$. Non-hydrogen

[1] Bruker (2012). *Saint; SADABS; APEX3*. Bruker AXS Inc., Madison, Wisconsin, USA.
[2] Sheldrick, G. M. (2015). *Acta Cryst.* A**71**, 3-8.
[3] Dolomanov, O. V.; Bourhis, L. J.; Gildea, R. J.; Howard, J. A. K.; Puschmann, H. *J. Appl. Cryst.* (2009). **42**, 339-341.

atoms were refined anisotropically. The B-H atom was located in the diffraction map and refined isotropically. All other hydrogen atoms were placed in geometrically calculated positions with U_{iso} = 1.2U_{equiv} of the parent atom (U_{iso} = 1.5U_{equiv} for methyl). The relative occupancies of the disordered atoms was freely refined, and constraints were used on the anistropic displacement parameters of the disordered atoms. Restraints were needed on most of the disordered bonds. The final anisotropic full-matrix least-squares refinement on F^2 with 353 variables converged at R1 = 3.39%, for the observed data and wR2 = 7.26% for all data. The goodness-of-fit was 1.034. The largest peak in the final difference electron density synthesis was 2.128 $e^-/Å^3$ and the largest hole was -1.715 $e^-/Å^3$ with an RMS deviation of 0.141 $e^-/Å^3$. On the basis of the final model, the calculated density was 1.652 g/cm^3 and F(000), 1456 e^-.

Table 1. Sample and crystal data for Harman_SS4_176.

Identification code	Harman_SS4_176	
Chemical formula	$C_{23}H_{35}BN_7O_4PSW$	
Formula weight	731.27 g/mol	
Temperature	100(2) K	
Wavelength	0.71073 Å	
Crystal size	0.054 x 0.147 x 0.312 mm	
Crystal habit	yellow plate	
Crystal system	monoclinic	
Space group	P 2_1/c	
Unit cell dimensions	a = 12.8008(7) Å	α = 90°
	b = 17.9773(9) Å	β = 108.074(2)°
	c = 13.4385(7) Å	γ = 90°
Volume	2939.9(3) $Å^3$	
Z	4	
Density (calculated)	1.652 g/cm^3	
Absorption coefficient	4.096 mm^{-1}	
F(000)	1456	

Table 2. Data collection and structure refinement for Harman_SS4_176.

Diffractometer	Bruker Kappa APEXII Duo
Radiation source	fine-focus sealed tube (Mo K_α, λ = 0.71073 Å)
Theta range for data collection	1.96 to 28.30°
Index ranges	-17<=h<=17, -23<=k<=23, -17<=l<=17
Reflections collected	35588
Independent reflections	7289 [R(int) = 0.0618]
Coverage of independent reflections	99.8%
Absorption correction	Multi-Scan

Max. and min. transmission	0.8090 and 0.3610	
Structure solution technique	direct methods	
Structure solution program	SHELXT 2014/5 (Sheldrick, 2014)	
Refinement method	Full-matrix least-squares on F^2	
Refinement program	SHELXL-2018/3 (Sheldrick, 2018)	
Function minimized	$\Sigma\ w(F_o^2 - F_c^2)^2$	
Data / restraints / parameters	7289 / 5 / 353	
Goodness-of-fit on F^2	1.034	
Δ/σ_{max}	0.001	
Final R indices	5821 data; I>2σ(I)	R1 = 0.0339, wR2 = 0.0677
	all data	R1 = 0.0505, wR2 = 0.0726
Weighting scheme	$w=1/[\sigma^2(F_o^2)+(0.0231P)^2+4.9839P]$ where $P=(F_o^2+2F_c^2)/3$	
Largest diff. peak and hole	2.128 and -1.715 eÅ^{-3}	
R.M.S. deviation from mean	0.141 eÅ^{-3}	

Table 3. Atomic coordinates and equivalent isotropic atomic displacement parameters (Å²) for Harman_SS4_176.

U(eq) is defined as one third of the trace of the orthogonalized U_{ij} tensor.

	x/a	y/b	z/c	U(eq)
W1	0.81496(2)	0.37055(2)	0.28407(2)	0.01428(5)
P1	0.85827(9)	0.30762(6)	0.45875(8)	0.0193(2)
O1	0.9956(2)	0.28833(19)	0.2309(3)	0.0297(8)
O4	0.2992(5)	0.2570(4)	0.2407(5)	0.099(2)
N1	0.6826(3)	0.42967(19)	0.3307(3)	0.0174(7)
N2	0.5746(3)	0.4199(2)	0.2735(3)	0.0189(7)
N3	0.6960(3)	0.2788(2)	0.2376(2)	0.0173(7)
N4	0.5851(3)	0.2913(2)	0.2026(3)	0.0198(8)
N5	0.7124(3)	0.4052(2)	0.1257(3)	0.0198(8)
N6	0.6003(3)	0.4007(2)	0.0974(3)	0.0217(8)
N7	0.9193(3)	0.3216(2)	0.2498(3)	0.0198(8)
C1	0.6838(3)	0.4764(2)	0.4087(3)	0.0199(9)
C2	0.5774(4)	0.4978(3)	0.4018(3)	0.0251(10)
C3	0.5109(4)	0.4611(3)	0.3157(4)	0.0259(10)
C4	0.7101(4)	0.2052(3)	0.2367(3)	0.0216(9)
C5	0.6086(4)	0.1695(3)	0.2002(3)	0.0258(10)

C6	0.5324(4)	0.2259(3)	0.1801(3)	0.0272(10)
C7	0.7389(4)	0.4260(2)	0.0408(3)	0.0250(10)
C8	0.6439(4)	0.4352(3)	0.9570(3)	0.0292(11)
C9	0.5582(4)	0.4192(3)	0.9949(3)	0.0289(11)
C17	0.9086(4)	0.3608(2)	0.5806(3)	0.0256(10)
C18	0.9610(4)	0.2346(3)	0.4763(4)	0.0342(12)
C19	0.7409(4)	0.2625(3)	0.4824(4)	0.0340(12)
C20	0.3569(7)	0.2671(6)	0.3566(8)	0.102(3)
C21	0.2733(6)	0.2401(4)	0.4041(6)	0.069(2)
C22	0.2245(7)	0.1725(4)	0.3383(6)	0.074(2)
C23	0.2322(7)	0.1902(5)	0.2231(7)	0.089(3)
B1	0.5399(4)	0.3712(3)	0.1753(3)	0.0179(9)
S1	0.14821(9)	0.49426(7)	0.17346(8)	0.0166(3)
O2	0.2564(4)	0.5092(3)	0.2432(5)	0.0241(6)
O3	0.0972(3)	0.55230(19)	0.1005(3)	0.0241(6)
C10	0.9380(4)	0.4488(3)	0.3883(4)	0.0146(4)
C11	0.8892(4)	0.4830(3)	0.2856(3)	0.0146(4)
C12	0.9599(4)	0.4975(3)	0.2222(3)	0.0146(4)
C13	0.0640(4)	0.4731(3)	0.2505(3)	0.0146(4)
C14	0.1134(4)	0.4346(2)	0.3492(3)	0.0146(4)
C15	0.0535(4)	0.4256(3)	0.4154(4)	0.0146(4)
C16	0.1519(4)	0.4134(3)	0.1009(4)	0.0267(12)
S1A	0.2085(9)	0.4469(7)	0.2893(10)	0.032(3)
O2A	0.269(4)	0.493(2)	0.251(4)	0.0241(6)
O3A	0.260(2)	0.4139(16)	0.384(2)	0.0241(6)
C10A	0.851(3)	0.514(2)	0.275(2)	0.0146(4)
C11A	0.923(3)	0.465(2)	0.351(3)	0.0146(4)
C12A	0.041(3)	0.448(2)	0.370(3)	0.0146(4)
C13A	0.076(3)	0.464(2)	0.282(3)	0.0146(4)
C14A	0.003(2)	0.503(2)	0.193(3)	0.0146(4)
C15A	0.897(3)	0.518(2)	0.187(3)	0.0146(4)
C16A	0.208(4)	0.384(2)	0.185(3)	0.0267(12)

Table 4. Bond lengths (Å) for Harman_SS4_176.

W1-N7	1.775(3)	W1-C11A	2.20(4)
W1-N3	2.200(3)	W1-N5	2.216(3)
W1-C11	2.232(5)	W1-C10	2.248(5)
W1-N1	2.248(3)	W1-P1	2.5079(11)
W1-C10A	2.63(4)	P1-C19	1.820(5)

P1-C18	1.821(5)	P1-C17	1.833(4)
O1-N7	1.238(4)	O4-C23	1.451(9)
O4-C20	1.514(11)	N1-C1	1.339(5)
N1-N2	1.368(5)	N2-C3	1.350(5)
N2-B1	1.530(6)	N3-C4	1.336(6)
N3-N4	1.368(4)	N4-C6	1.342(6)
N4-B1	1.549(6)	N5-C7	1.339(5)
N5-N6	1.368(5)	N6-C9	1.356(5)
N6-B1	1.574(6)	C1-C2	1.391(6)
C1-H1	0.95	C2-C3	1.373(6)
C2-H2	0.95	C3-H3	0.95
C4-C5	1.394(6)	C4-H4	0.95
C5-C6	1.374(7)	C5-H5	0.95
C6-H6	0.95	C7-C8	1.387(6)
C7-H7	0.95	C8-C9	1.376(7)
C8-H8	0.95	C9-H9	0.95
C17-H17A	0.98	C17-H17B	0.98
C17-H17C	0.98	C18-H18A	0.98
C18-H18B	0.98	C18-H18C	0.98
C19-H19A	0.98	C19-H19B	0.98
C19-H19C	0.98	C20-C21	1.487(11)
C20-H20A	0.99	C20-H20B	0.99
C21-C22	1.518(10)	C21-H21A	0.99
C21-H21B	0.99	C22-C23	1.614(11)
C22-H22A	0.99	C22-H22B	0.99
C23-H23A	0.99	C23-H23B	0.99
B1-H1A	1.10(4)	S1-O2	1.436(6)
S1-O3	1.442(3)	S1-C13	1.752(5)
S1-C16	1.759(5)	C10-C11	1.463(6)
C10-C15	1.469(6)	C10-H10	0.95
C11-C12	1.445(6)	C11-H11	0.95
C12-C13	1.341(7)	C12-H12	0.95
C13-C14	1.455(6)	C14-C15	1.352(6)
C14-H14	0.95	C15-H15	0.95
C16-H16A	0.98	C16-H16B	0.98
C16-H16C	0.98	S1A-O2A	1.35(3)
S1A-O3A	1.37(3)	S1A-C13A	1.70(4)
S1A-C16A	1.80(4)	C10A-C11A	1.45(2)
C10A-C15A	1.48(2)	C10A-H10A	0.95

C11A-C12A	1.48(5)	C11A-H11A	0.95
C12A-C13A	1.41(5)	C12A-H12A	0.95
C13A-C14A	1.45(2)	C14A-C15A	1.36(2)
C14A-H14A	0.95	C15A-H15A	0.95
C16A-H16D	0.98	C16A-H16E	0.98
C16A-H16F	0.98		

Table 5. Bond angles (°) for Harman_SS4_176.

N7-W1-C11A	93.5(10)	N7-W1-N3	93.70(14)
C11A-W1-N3	170.8(11)	N7-W1-N5	99.20(14)
C11A-W1-N5	106.8(9)	N3-W1-N5	77.69(12)
N7-W1-C11	95.71(17)	N3-W1-C11	159.61(15)
N5-W1-C11	82.96(15)	N7-W1-C10	91.94(16)
N3-W1-C10	159.32(14)	N5-W1-C10	120.96(15)
C11-W1-C10	38.12(15)	N7-W1-N1	178.22(14)
C11A-W1-N1	87.4(10)	N3-W1-N1	85.30(13)
N5-W1-N1	82.04(12)	C11-W1-N1	85.70(15)
C10-W1-N1	88.50(15)	N7-W1-P1	93.04(12)
C11A-W1-P1	91.9(10)	N3-W1-P1	81.95(9)
N5-W1-P1	156.80(9)	C11-W1-P1	115.49(11)
C10-W1-P1	77.89(12)	N1-W1-P1	85.36(9)
N7-W1-C10A	108.5(7)	C11A-W1-C10A	33.4(7)
N3-W1-C10A	147.1(8)	N5-W1-C10A	75.0(7)
N1-W1-C10A	73.1(7)	P1-W1-C10A	119.6(6)
C19-P1-C18	105.0(3)	C19-P1-C17	99.0(2)
C18-P1-C17	102.8(2)	C19-P1-W1	114.18(16)
C18-P1-W1	112.79(17)	C17-P1-W1	121.04(15)
C23-O4-C20	110.0(6)	C1-N1-N2	106.6(3)
C1-N1-W1	133.4(3)	N2-N1-W1	120.0(3)
C3-N2-N1	109.2(3)	C3-N2-B1	128.7(4)
N1-N2-B1	122.1(3)	C4-N3-N4	106.8(3)
C4-N3-W1	131.4(3)	N4-N3-W1	121.8(3)
C6-N4-N3	109.2(4)	C6-N4-B1	129.3(4)
N3-N4-B1	120.4(3)	C7-N5-N6	107.5(3)
C7-N5-W1	131.7(3)	N6-N5-W1	120.5(2)
C9-N6-N5	108.7(4)	C9-N6-B1	129.5(4)
N5-N6-B1	121.6(3)	O1-N7-W1	176.8(3)
N1-C1-C2	110.3(4)	N1-C1-H1	124.8
C2-C1-H1	124.8	C3-C2-C1	105.2(4)

C3-C2-H2	127.4	C1-C2-H2	127.4
N2-C3-C2	108.7(4)	N2-C3-H3	125.6
C2-C3-H3	125.6	N3-C4-C5	110.2(4)
N3-C4-H4	124.9	C5-C4-H4	124.9
C6-C5-C4	104.9(4)	C6-C5-H5	127.6
C4-C5-H5	127.6	N4-C6-C5	109.0(4)
N4-C6-H6	125.5	C5-C6-H6	125.5
N5-C7-C8	109.6(4)	N5-C7-H7	125.2
C8-C7-H7	125.2	C9-C8-C7	105.9(4)
C9-C8-H8	127.1	C7-C8-H8	127.1
N6-C9-C8	108.4(4)	N6-C9-H9	125.8
C8-C9-H9	125.8	P1-C17-H17A	109.5
P1-C17-H17B	109.5	H17A-C17-H17B	109.5
P1-C17-H17C	109.5	H17A-C17-H17C	109.5
H17B-C17-H17C	109.5	P1-C18-H18A	109.5
P1-C18-H18B	109.5	H18A-C18-H18B	109.5
P1-C18-H18C	109.5	H18A-C18-H18C	109.5
H18B-C18-H18C	109.5	P1-C19-H19A	109.5
P1-C19-H19B	109.5	H19A-C19-H19B	109.5
P1-C19-H19C	109.5	H19A-C19-H19C	109.5
H19B-C19-H19C	109.5	C21-C20-O4	102.5(6)
C21-C20-H20A	111.3	O4-C20-H20A	111.3
C21-C20-H20B	111.3	O4-C20-H20B	111.3
H20A-C20-H20B	109.2	C20-C21-C22	103.5(7)
C20-C21-H21A	111.1	C22-C21-H21A	111.1
C20-C21-H21B	111.1	C22-C21-H21B	111.1
H21A-C21-H21B	109.0	C21-C22-C23	105.3(6)
C21-C22-H22A	110.7	C23-C22-H22A	110.7
C21-C22-H22B	110.7	C23-C22-H22B	110.7
H22A-C22-H22B	108.8	O4-C23-C22	102.5(7)
O4-C23-H23A	111.3	C22-C23-H23A	111.3
O4-C23-H23B	111.3	C22-C23-H23B	111.3
H23A-C23-H23B	109.2	N2-B1-N4	109.8(3)
N2-B1-N6	108.1(4)	N4-B1-N6	104.2(3)
N2-B1-H1A	114.(2)	N4-B1-H1A	112.(2)
N6-B1-H1A	108.(2)	O2-S1-O3	116.7(2)
O2-S1-C13	107.5(3)	O3-S1-C13	109.1(2)
O2-S1-C16	109.2(3)	O3-S1-C16	107.7(2)
C13-S1-C16	106.0(2)	C11-C10-C15	117.1(4)

C11-C10-W1	70.4(2)	C15-C10-W1	115.7(3)
C11-C10-H10	121.5	C15-C10-H10	121.5
W1-C10-H10	84.6	C12-C11-C10	118.0(4)
C12-C11-W1	120.0(3)	C10-C11-W1	71.5(3)
C12-C11-H11	121.0	C10-C11-H11	121.0
W1-C11-H11	79.8	C13-C12-C11	121.5(4)
C13-C12-H12	119.2	C11-C12-H12	119.2
C12-C13-C14	121.8(4)	C12-C13-S1	120.1(3)
C14-C13-S1	118.0(4)	C15-C14-C13	118.8(4)
C15-C14-H14	120.6	C13-C14-H14	120.6
C14-C15-C10	122.4(4)	C14-C15-H15	118.8
C10-C15-H15	118.8	S1-C16-H16A	109.5
S1-C16-H16B	109.5	H16A-C16-H16B	109.5
S1-C16-H16C	109.5	H16A-C16-H16C	109.5
H16B-C16-H16C	109.5	O2A-S1A-O3A	117.(3)
O2A-S1A-C13A	123.(2)	O3A-S1A-C13A	108.6(17)
O2A-S1A-C16A	87.(3)	O3A-S1A-C16A	109.(2)
C13A-S1A-C16A	108.(2)	C11A-C10A-C15A	106.(3)
C11A-C10A-W1	57.(2)	C15A-C10A-W1	102.(2)
C11A-C10A-H10A	127.0	C15A-C10A-H10A	127.0
W1-C10A-H10A	106.5	C10A-C11A-C12A	129.(4)
C10A-C11A-W1	90.(2)	C12A-C11A-W1	113.(3)
C10A-C11A-H11A	115.5	C12A-C11A-H11A	115.5
W1-C11A-H11A	62.9	C13A-C12A-C11A	113.(3)
C13A-C12A-H12A	123.6	C11A-C12A-H12A	123.6
C12A-C13A-C14A	120.(4)	C12A-C13A-S1A	119.(3)
C14A-C13A-S1A	121.(3)	C15A-C14A-C13A	121.(3)
C15A-C14A-H14A	119.5	C13A-C14A-H14A	119.5
C14A-C15A-C10A	125.(3)	C14A-C15A-H15A	117.3
C10A-C15A-H15A	117.3	S1A-C16A-H16D	109.5
S1A-C16A-H16E	109.5	H16D-C16A-H16E	109.5
S1A-C16A-H16F	109.5	H16D-C16A-H16F	109.5
H16E-C16A-H16F	109.5		

Table 6. Torsion angles (°) for Harman_SS4_176.

C1-N1-N2-C3	0.8(5)	W1-N1-N2-C3	-179.5(3)
C1-N1-N2-B1	178.4(4)	W1-N1-N2-B1	-1.9(5)

C4-N3-N4-C6	-0.3(4)	W1-N3-N4-C6	-179.9(3)
C4-N3-N4-B1	-169.2(3)	W1-N3-N4-B1	11.2(5)
C7-N5-N6-C9	-0.4(5)	W1-N5-N6-C9	-175.0(3)
C7-N5-N6-B1	174.8(4)	W1-N5-N6-B1	0.2(5)
N2-N1-C1-C2	-0.7(5)	W1-N1-C1-C2	179.6(3)
N1-C1-C2-C3	0.4(5)	N1-N2-C3-C2	-0.5(5)
B1-N2-C3-C2	-178.0(4)	C1-C2-C3-N2	0.1(5)
N4-N3-C4-C5	0.5(4)	W1-N3-C4-C5	-179.9(3)
N3-C4-C5-C6	-0.6(5)	N3-N4-C6-C5	-0.1(5)
B1-N4-C6-C5	167.6(4)	C4-C5-C6-N4	0.4(5)
N6-N5-C7-C8	0.2(5)	W1-N5-C7-C8	174.0(3)
N5-C7-C8-C9	0.0(5)	N5-N6-C9-C8	0.4(5)
B1-N6-C9-C8	-174.2(4)	C7-C8-C9-N6	-0.3(5)
C23-O4-C20-C21	-36.1(9)	O4-C20-C21-C22	40.1(9)
C20-C21-C22-C23	-31.0(9)	C20-O4-C23-C22	16.0(9)
C21-C22-C23-O4	9.3(8)	C3-N2-B1-N4	-125.6(4)
N1-N2-B1-N4	57.2(5)	C3-N2-B1-N6	121.3(4)
N1-N2-B1-N6	-55.8(5)	C6-N4-B1-N2	130.4(4)
N3-N4-B1-N2	-63.2(4)	C6-N4-B1-N6	-114.1(5)
N3-N4-B1-N6	52.4(4)	C9-N6-B1-N2	-128.5(4)
N5-N6-B1-N2	57.5(5)	C9-N6-B1-N4	114.8(5)
N5-N6-B1-N4	-59.2(5)	C15-C10-C11-C12	-5.2(6)
W1-C10-C11-C12	-114.8(4)	C15-C10-C11-W1	109.6(4)
C10-C11-C12-C13	7.3(7)	W1-C11-C12-C13	-76.6(5)
C11-C12-C13-C14	-3.5(7)	C11-C12-C13-S1	-178.0(4)
O2-S1-C13-C12	141.5(4)	O3-S1-C13-C12	14.0(5)
C16-S1-C13-C12	-101.8(5)	O2-S1-C13-C14	-33.2(5)
O3-S1-C13-C14	-160.7(4)	C16-S1-C13-C14	83.5(4)

C12-C13-C14-C15	-2.3(7)	S1-C13-C14-C15	172.3(4)
C13-C14-C15-C10	4.2(7)	C11-C10-C15-C14	-0.4(7)
W1-C10-C15-C14	79.6(5)	C15A-C10A-C11A-C12A	26.(5)
W1-C10A-C11A-C12A	120.(5)	C15A-C10A-C11A-W1	-94.(3)
C10A-C11A-C12A-C13A	-21.(6)	W1-C11A-C12A-C13A	89.(4)
C11A-C12A-C13A-C14A	9.(6)	C11A-C12A-C13A-S1A	-179.(3)
O2A-S1A-C13A-C12A	-139.(4)	O3A-S1A-C13A-C12A	4.(4)
C16A-S1A-C13A-C12A	122.(4)	O2A-S1A-C13A-C14A	34.(5)
O3A-S1A-C13A-C14A	176.(3)	C16A-S1A-C13A-C14A	-65.(4)
C12A-C13A-C14A-C15A	-7.(6)	S1A-C13A-C14A-C15A	-179.(3)
C13A-C14A-C15A-C10A	15.(6)	C11A-C10A-C15A-C14A	-22.(5)
W1-C10A-C15A-C14A	-81.(4)		

Table 7. Anisotropic atomic displacement parameters (Å^2) for Harman_SS4_176.

The anisotropic atomic displacement factor exponent takes the form: $-2\pi^2[h^2 a^{*2} U_{11} + ... + 2 h k a^* b^* U_{12}]$

	U_{11}	U_{22}	U_{33}	U_{23}	U_{13}	U_{12}
W1	0.01624(8)	0.01273(10)	0.01580(7)	-0.00176(7)	0.00778(5)	-0.00122(7)
P1	0.0240(6)	0.0144(6)	0.0175(5)	-0.0002(4)	0.0039(4)	0.0014(4)
O1	0.0201(16)	0.034(2)	0.0376(17)	-0.0174(15)	0.0126(14)	0.0030(14)
O4	0.072(4)	0.108(5)	0.128(5)	0.032(4)	0.044(4)	-0.003(3)
N1	0.0200(17)	0.014(2)	0.0203(17)	0.0046(14)	0.0096(14)	0.0033(14)
N2	0.0154(17)	0.020(2)	0.0197(17)	0.0042(14)	0.0027(14)	0.0031(14)
N3	0.0162(17)	0.019(2)	0.0168(17)	-0.0002(13)	0.0054(14)	-0.0024(14)
N4	0.0130(16)	0.022(2)	0.0227(17)	0.0017(15)	0.0032(14)	-0.0017(15)
N5	0.0207(18)	0.019(2)	0.0204(17)	0.0031(14)	0.0068(14)	0.0008(15)
N6	0.029(2)	0.017(2)	0.0158(16)	0.0007(14)	0.0022(14)	0.0049(16)

	U_{11}	U_{22}	U_{33}	U_{23}	U_{13}	U_{12}
N7	0.0203(18)	0.019(2)	0.0207(17)	-0.0058(14)	0.0076(14)	-0.0038(15)
C1	0.020(2)	0.019(2)	0.022(2)	-0.0019(17)	0.0089(17)	0.0008(17)
C2	0.026(2)	0.025(3)	0.028(2)	0.0014(19)	0.0130(19)	0.0083(19)
C3	0.021(2)	0.024(3)	0.035(2)	0.008(2)	0.0119(19)	0.0093(19)
C4	0.027(2)	0.018(3)	0.021(2)	-0.0027(16)	0.0097(17)	-0.0011(18)
C5	0.030(2)	0.017(3)	0.026(2)	-0.0031(18)	0.0031(19)	-0.007(2)
C6	0.023(2)	0.023(3)	0.030(2)	0.0008(19)	0.0007(19)	-0.010(2)
C7	0.040(3)	0.017(3)	0.021(2)	0.0007(17)	0.0142(19)	0.000(2)
C8	0.048(3)	0.022(3)	0.019(2)	0.0009(18)	0.011(2)	0.004(2)
C9	0.037(3)	0.023(3)	0.021(2)	0.0039(18)	0.0001(19)	0.008(2)
C17	0.035(2)	0.022(3)	0.0162(19)	0.0008(17)	0.0034(17)	0.003(2)
C18	0.045(3)	0.022(3)	0.029(2)	-0.001(2)	0.002(2)	0.011(2)
C19	0.050(3)	0.030(3)	0.023(2)	0.002(2)	0.014(2)	-0.011(2)
C20	0.071(6)	0.112(8)	0.116(8)	0.005(6)	0.018(6)	-0.027(5)
C21	0.060(5)	0.073(6)	0.068(5)	-0.007(4)	0.012(4)	-0.005(4)
C22	0.090(6)	0.054(5)	0.083(5)	0.015(4)	0.034(5)	-0.004(4)
C23	0.058(5)	0.080(6)	0.118(7)	0.016(5)	0.013(5)	-0.027(4)
B1	0.016(2)	0.022(3)	0.018(2)	0.0020(19)	0.0095(17)	0.002(2)
S1	0.0147(5)	0.0171(7)	0.0199(5)	0.0008(4)	0.0079(4)	-0.0020(4)
O2	0.0168(12)	0.0253(18)	0.0315(13)	0.0061(12)	0.0092(11)	-0.0005(11)
O3	0.0168(12)	0.0253(18)	0.0315(13)	0.0061(12)	0.0092(11)	-0.0005(11)
C10	0.0170(9)	0.0107(11)	0.0164(9)	0.0003(7)	0.0056(8)	-0.0012(7)
C11	0.0170(9)	0.0107(11)	0.0164(9)	0.0003(7)	0.0056(8)	-0.0012(7)
C12	0.0170(9)	0.0107(11)	0.0164(9)	0.0003(7)	0.0056(8)	-0.0012(7)
C13	0.0170(9)	0.0107(11)	0.0164(9)	0.0003(7)	0.0056(8)	-0.0012(7)
C14	0.0170(9)	0.0107(11)	0.0164(9)	0.0003(7)	0.0056(8)	-0.0012(7)
C15	0.0170(9)	0.0107(11)	0.0164(9)	0.0003(7)	0.0056(8)	-0.0012(7)
C16	0.029(3)	0.024(3)	0.033(3)	-0.005(2)	0.017(2)	-0.005(2)
S1A	0.021(5)	0.034(8)	0.050(7)	-0.009(6)	0.023(5)	-0.010(5)
O2A	0.0168(12)	0.0253(18)	0.0315(13)	0.0061(12)	0.0092(11)	-0.0005(11)
O3A	0.0168(12)	0.0253(18)	0.0315(13)	0.0061(12)	0.0092(11)	-0.0005(11)

	U_{11}	U_{22}	U_{33}	U_{23}	U_{13}	U_{12}
C10A	0.0170(9)	0.0107(11)	0.0164(9)	0.0003(7)	0.0056(8)	-0.0012(7)
C11A	0.0170(9)	0.0107(11)	0.0164(9)	0.0003(7)	0.0056(8)	-0.0012(7)
C12A	0.0170(9)	0.0107(11)	0.0164(9)	0.0003(7)	0.0056(8)	-0.0012(7)
C13A	0.0170(9)	0.0107(11)	0.0164(9)	0.0003(7)	0.0056(8)	-0.0012(7)
C14A	0.0170(9)	0.0107(11)	0.0164(9)	0.0003(7)	0.0056(8)	-0.0012(7)
C15A	0.0170(9)	0.0107(11)	0.0164(9)	0.0003(7)	0.0056(8)	-0.0012(7)
C16A	0.029(3)	0.024(3)	0.033(3)	-0.005(2)	0.017(2)	-0.005(2)

Table 8. Hydrogen atomic coordinates and isotropic atomic displacement parameters (Å^2) for Harman_SS4_176.

	x/a	y/b	z/c	U(eq)
H1	0.7483	0.4926	0.4613	0.024
H2	0.5554	0.5306	0.4470	0.03
H3	0.4331	0.4643	0.2901	0.031
H4	0.7793	0.1807	0.2578	0.026
H5	0.5951	0.1176	0.1912	0.031
H6	0.4550	0.2196	0.1545	0.033
H7	0.8115	0.4332	0.0383	0.03
H8	0.6391	0.4497	-0.1123	0.035
H9	0.4823	0.4208	-0.0442	0.035
H17A	0.9750	0.3882	0.5812	0.038
H17B	0.9259	0.3267	0.6404	0.038
H17C	0.8519	0.3960	0.5854	0.038
H18A	0.9331	0.1958	0.4234	0.051
H18B	0.9765	0.2129	0.5463	0.051
H18C	1.0286	0.2556	0.4685	0.051
H19A	0.6851	0.3000	0.4821	0.051
H19B	0.7647	0.2376	0.5506	0.051
H19C	0.7096	0.2258	0.4273	0.051
H20A	0.4249	0.2370	0.3802	0.123
H20B	0.3753	0.3200	0.3740	0.123
H21A	0.2165	0.2784	0.3996	0.083
H21B	0.3078	0.2262	0.4784	0.083
H22A	0.1471	0.1651	0.3359	0.089
H22B	0.2668	0.1271	0.3675	0.089
H23A	0.2679	0.1490	0.1972	0.106
H23B	0.1586	0.1994	0.1726	0.106

H1A	0.451(4)	0.371(2)	0.134(3)	0.019(11)
H10	0.8968	0.4418	0.4354	0.017
H11	0.8134	0.4955	0.2613	0.017
H12	0.9319	0.5248	0.1591	0.017
H14	1.1864	0.4161	0.3668	0.017
H15	1.0874	0.4035	0.4818	0.017
H16A	1.2034	0.4207	0.0609	0.04
H16B	1.0783	0.4034	0.0526	0.04
H16C	1.1760	0.3712	0.1486	0.04
H10A	0.7877	0.5385	0.2807	0.017
H11A	0.8902	0.4394	0.3961	0.017
H12A	1.0887	0.4290	0.4334	0.017
H14A	1.0296	0.5181	0.1372	0.017
H15A	0.8487	0.5327	0.1205	0.017
H16D	1.1771	0.4089	0.1175	0.04
H16E	1.1625	0.3403	0.1878	0.04
H16F	1.2830	0.3677	0.1929	0.04

NOESY of WTp(NO)(PMe$_3$)(η^2-benzonitrile) Isomers (2A-2E) at 25 °C

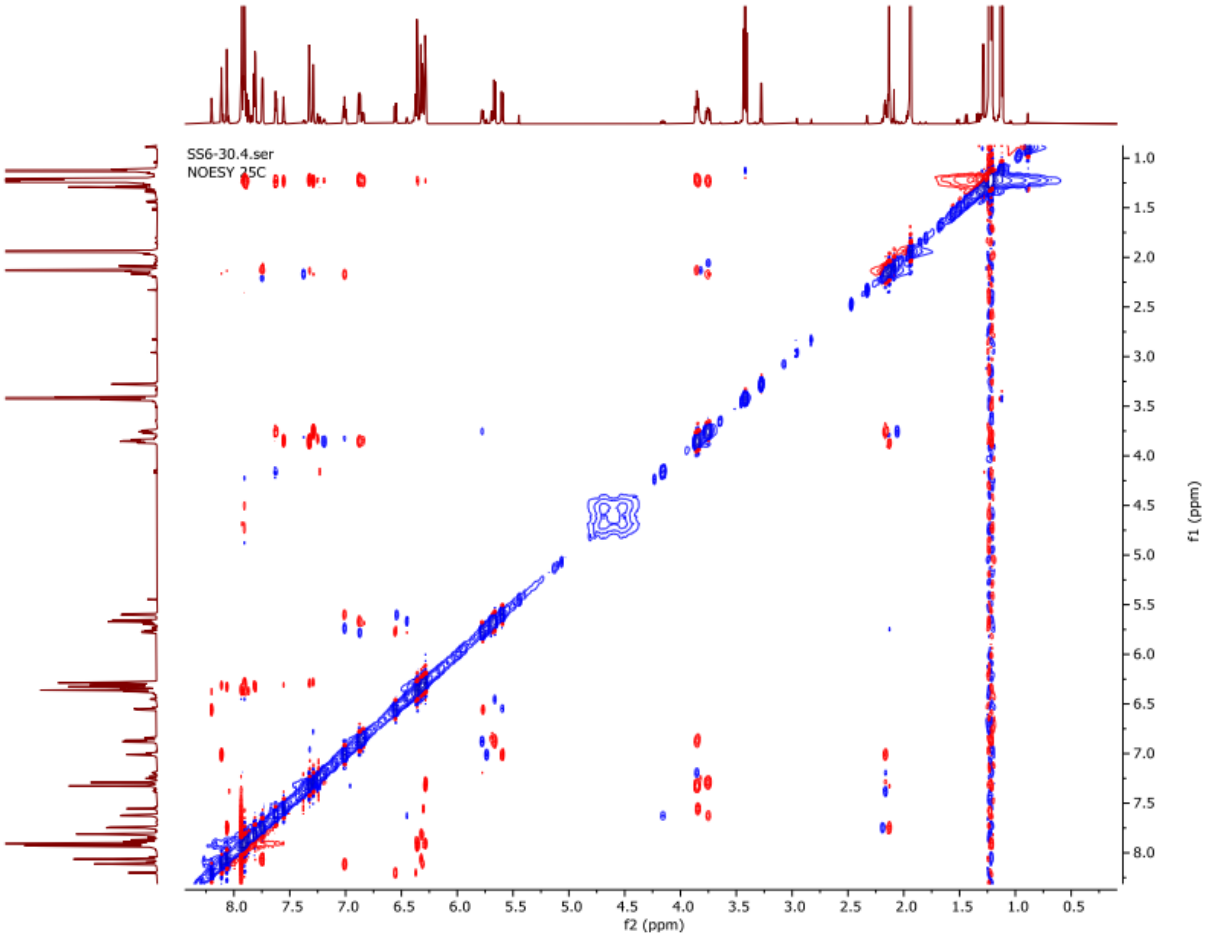

Details on DFT Calculations

All complexes were optimized in Gaussian 16 at the M06 level of theory, utilizing a hybrid basis set. This hybrid basis set used 6-31G(d,p) for all nonmetallic atoms, and LANL2DZ and its associated pseudopotentials for W and Mo. Initial starting geometries and optimized geometries are included as separate files.

Supporting Information for Chapter 4

^{1}H NMR Spectrum of 8

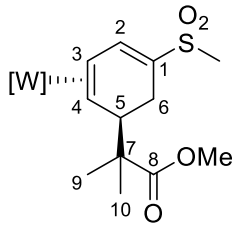

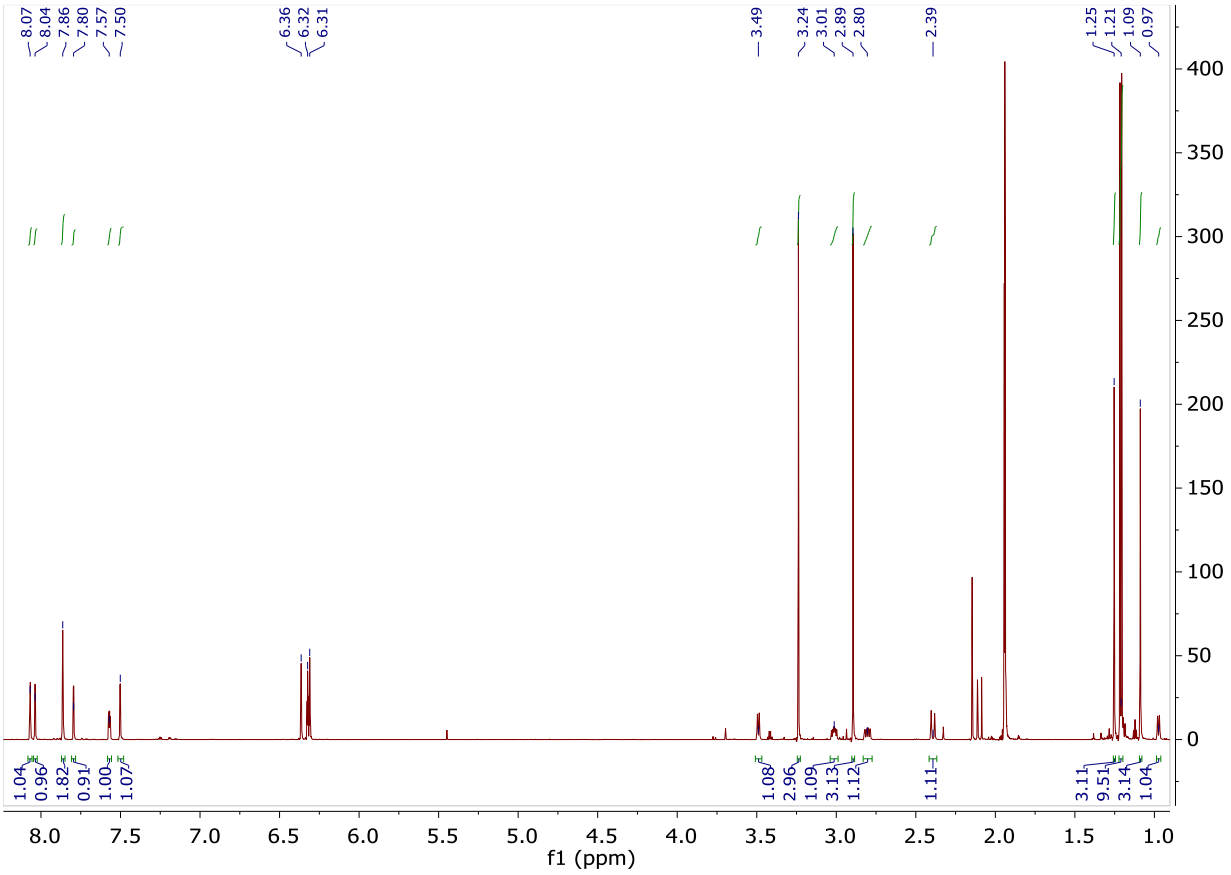

^{13}C {^{1}H} NMR Spectrum of 8

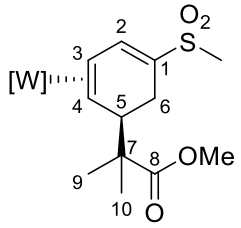

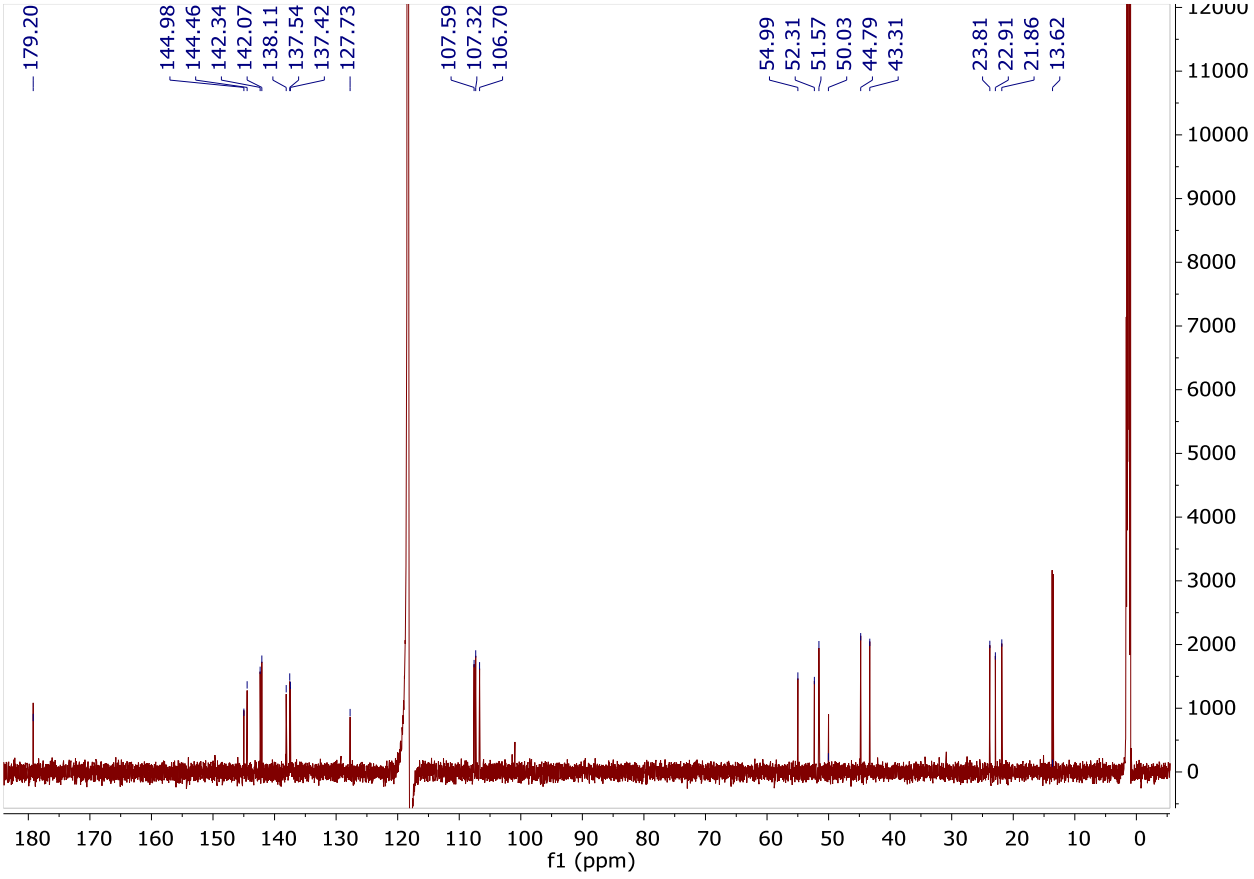

^{1}H NMR Spectrum of 9

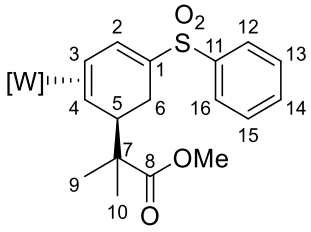

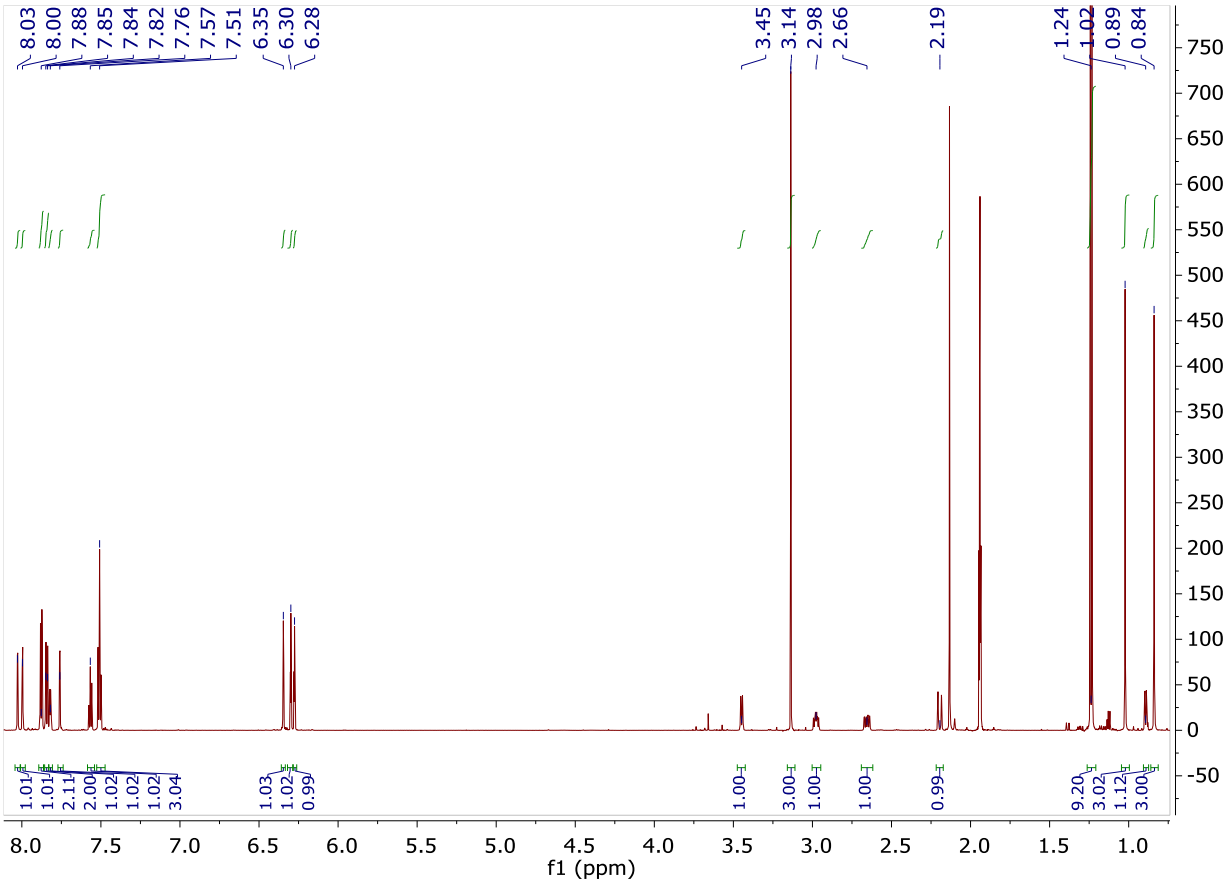

^{13}C {^{1}H} NMR Spectrum of 9

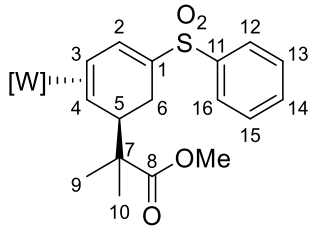

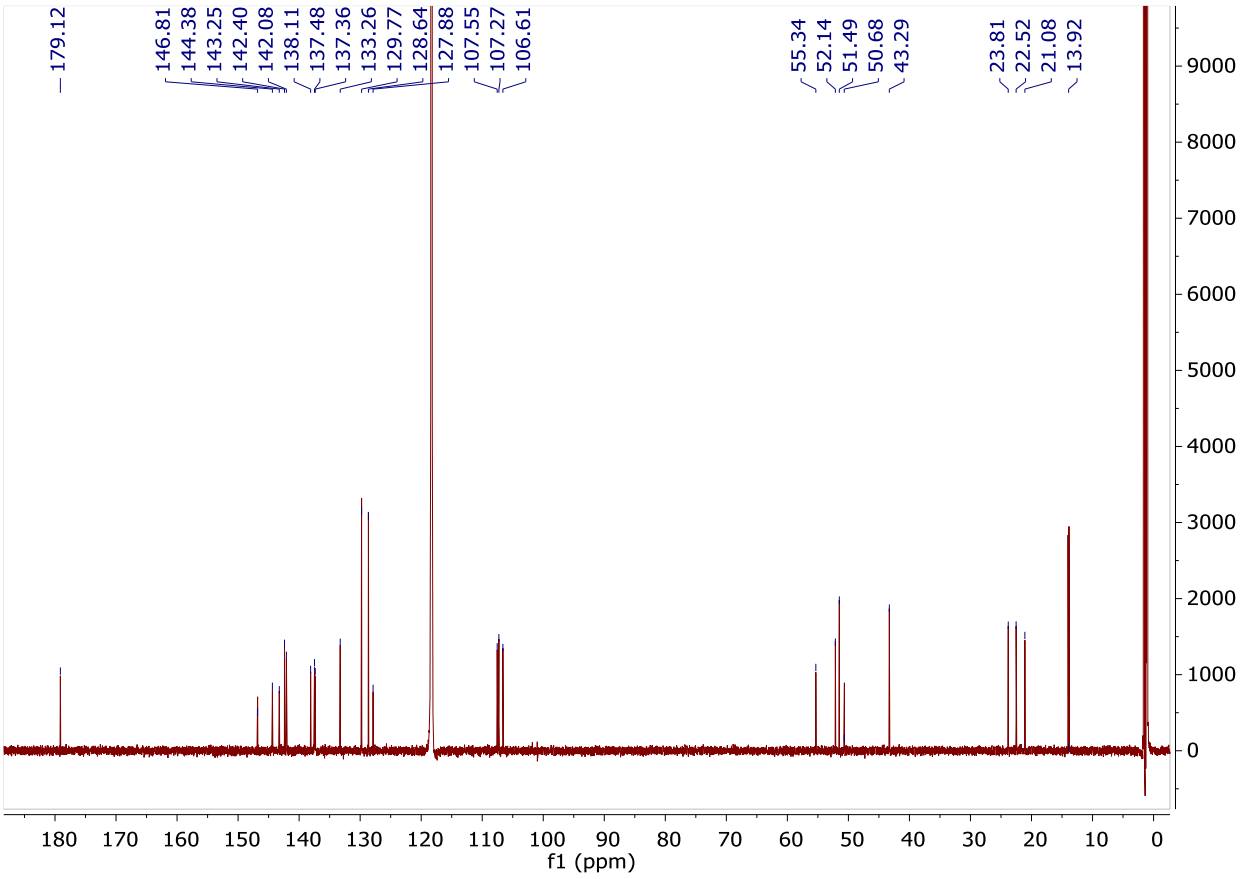

^{1}H NMR Spectrum of 10

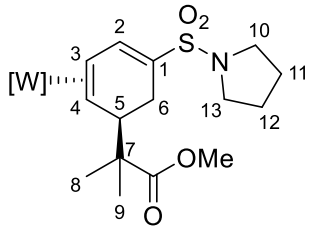

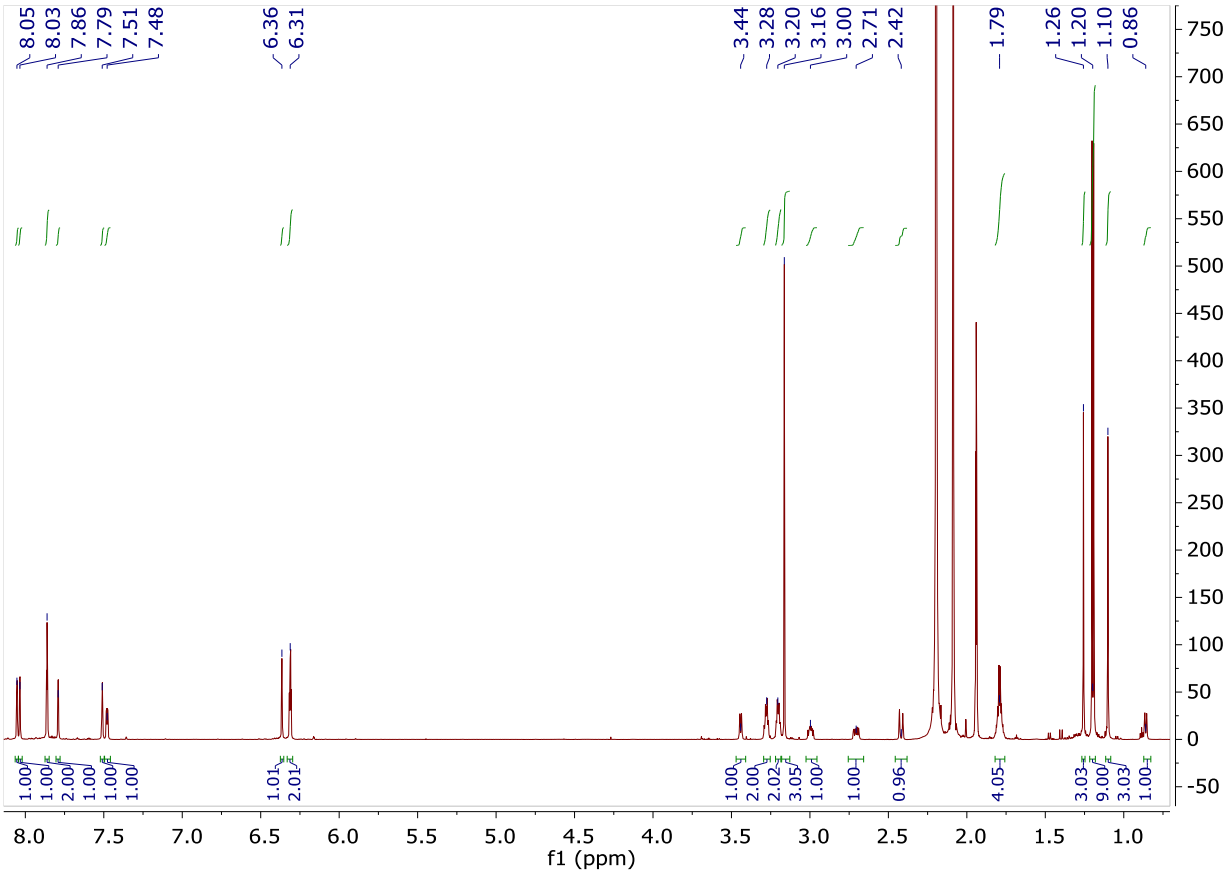

^{13}C {^{1}H} NMR Spectrum of 10

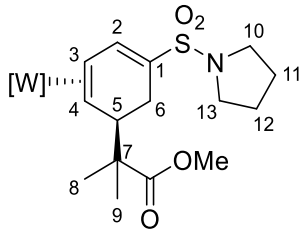

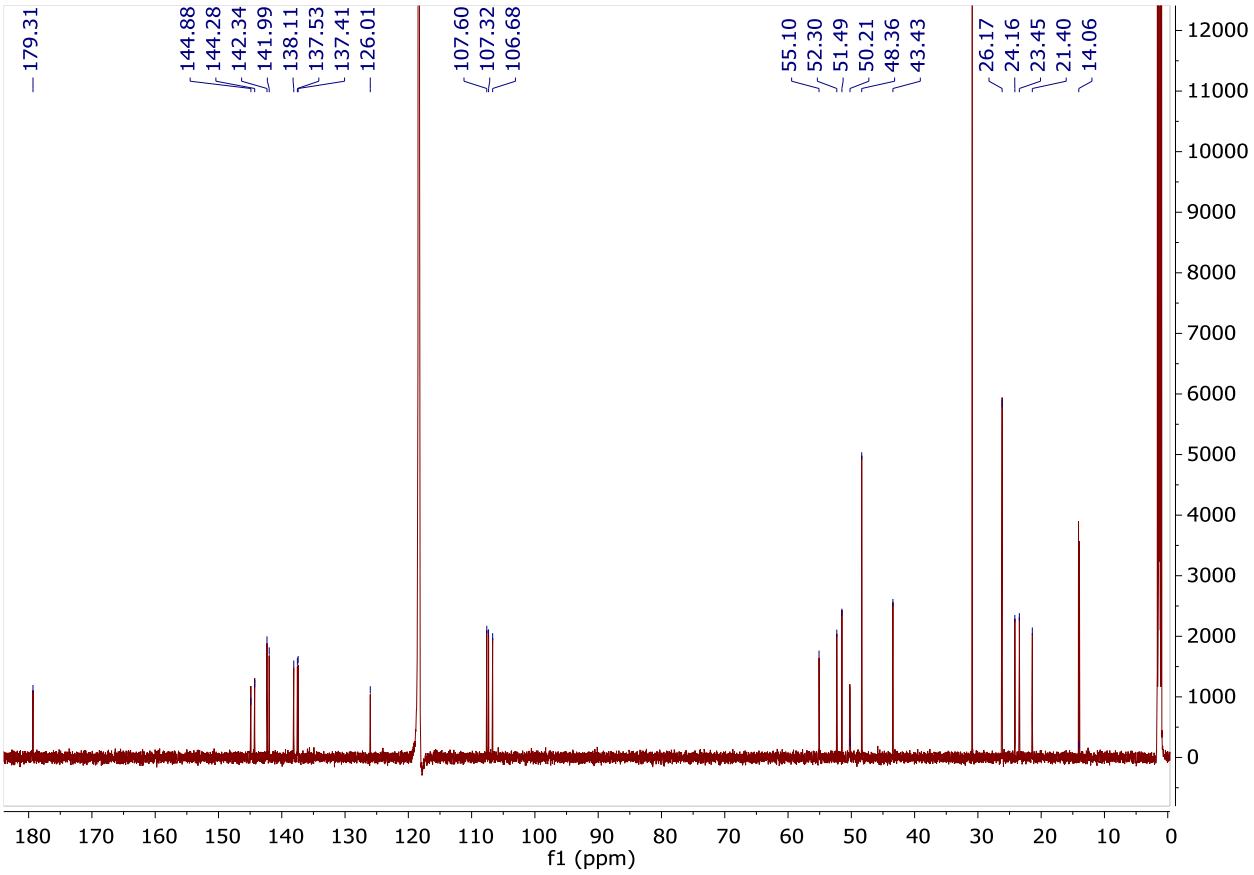

^{1}H NMR Spectrum of 11

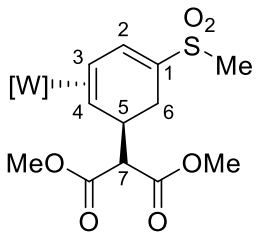

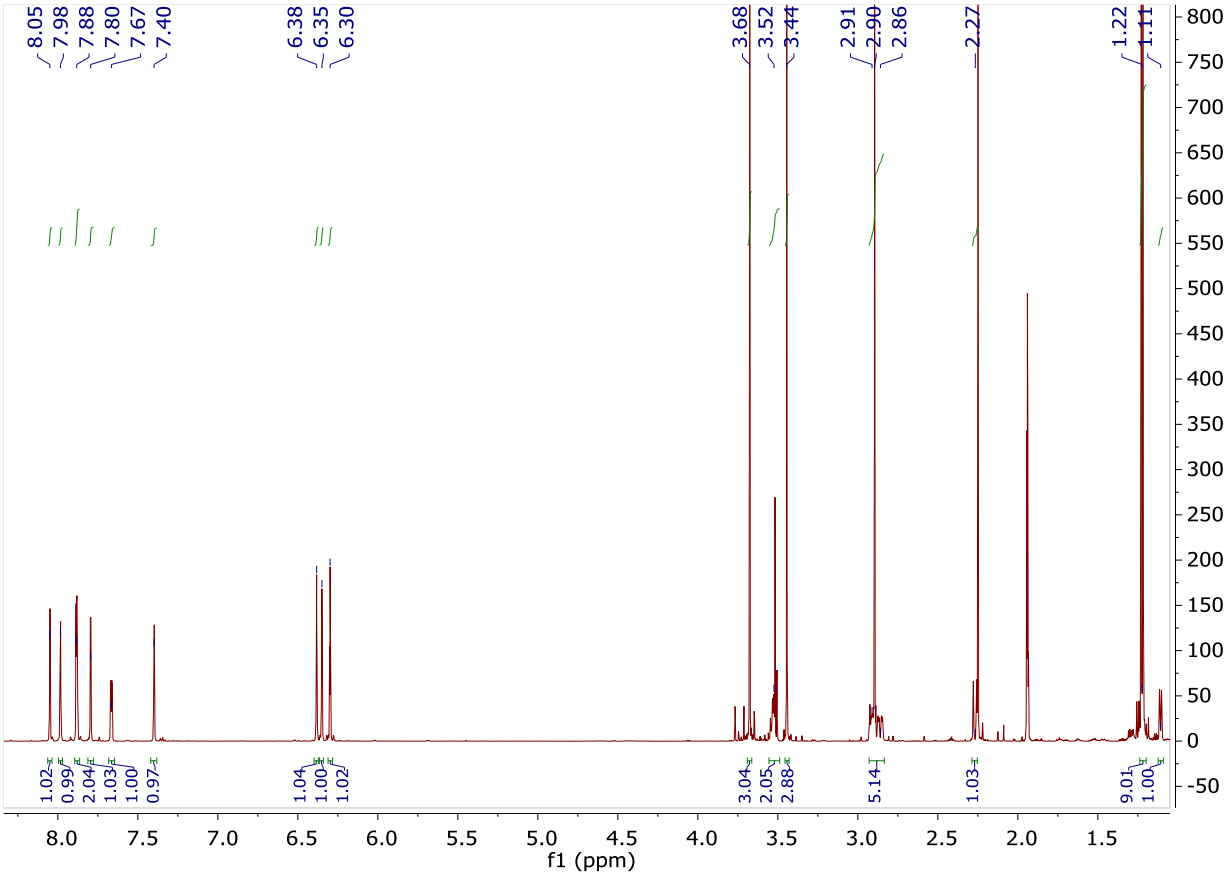

^{13}C {^{1}H} NMR Spectrum of 11

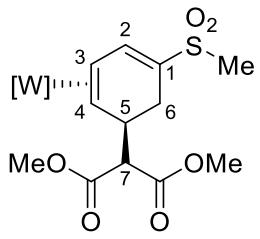

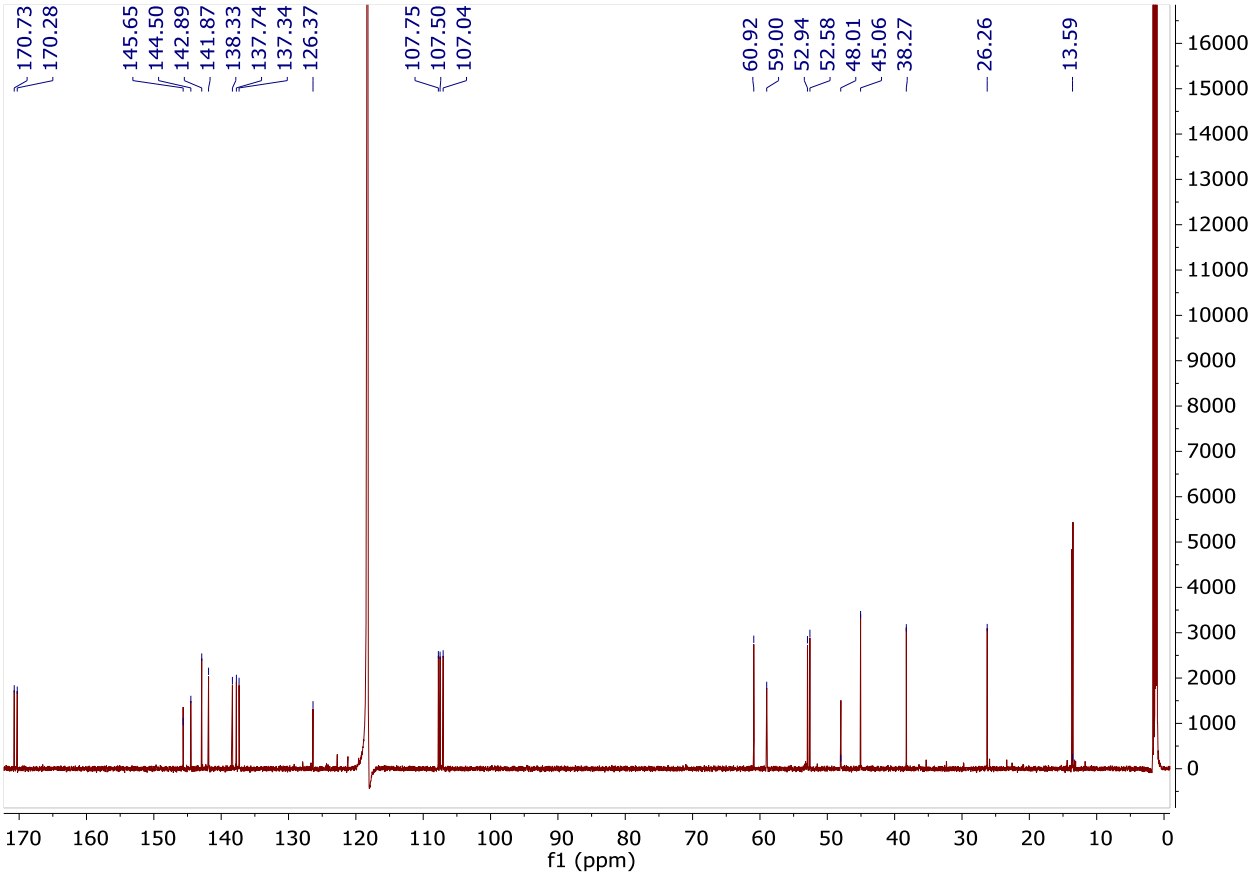

^{1}H NMR Spectrum of 12

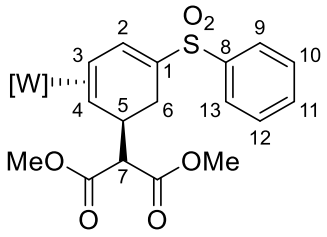

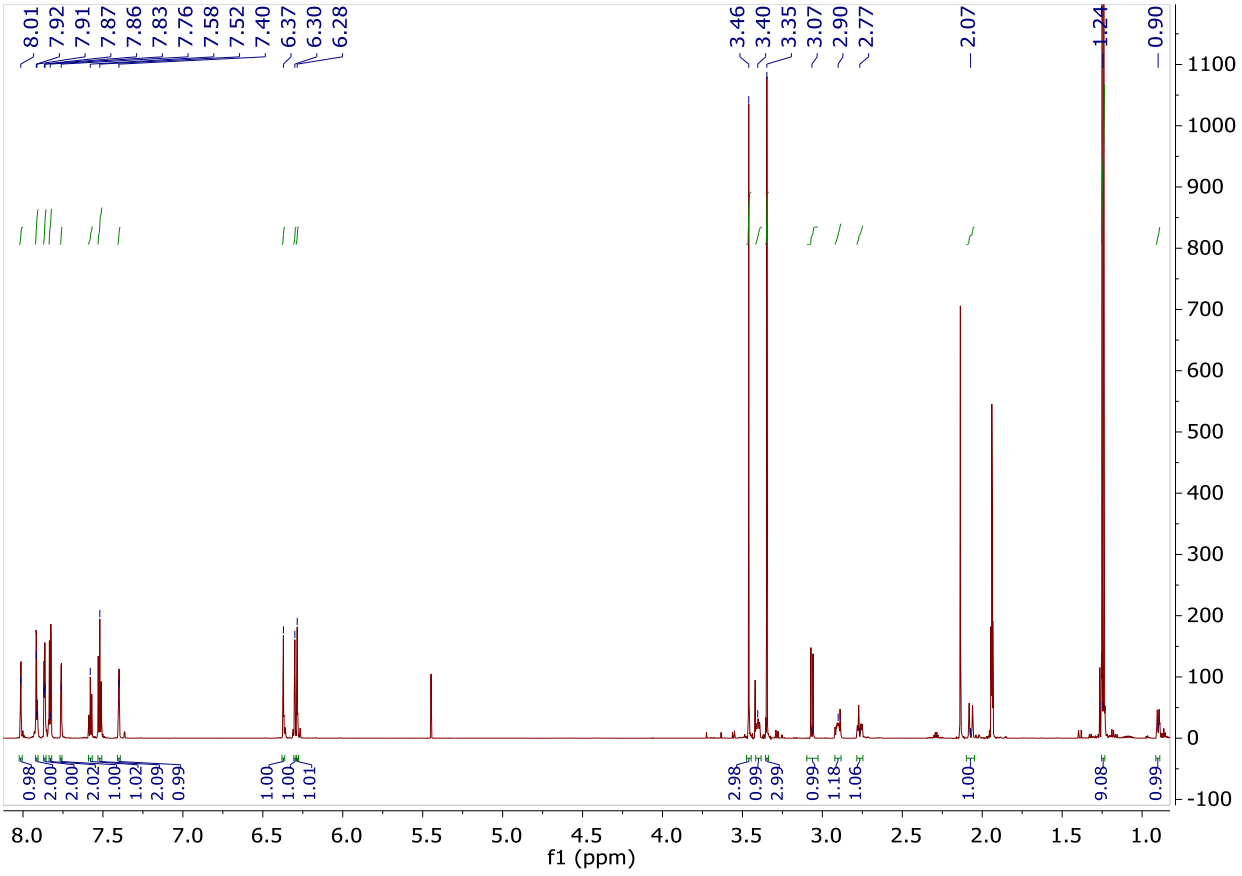

^{13}C {^{1}H} NMR Spectrum of 12

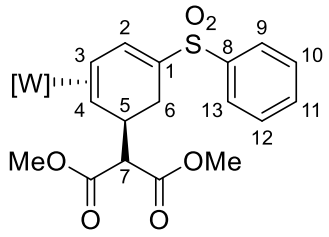

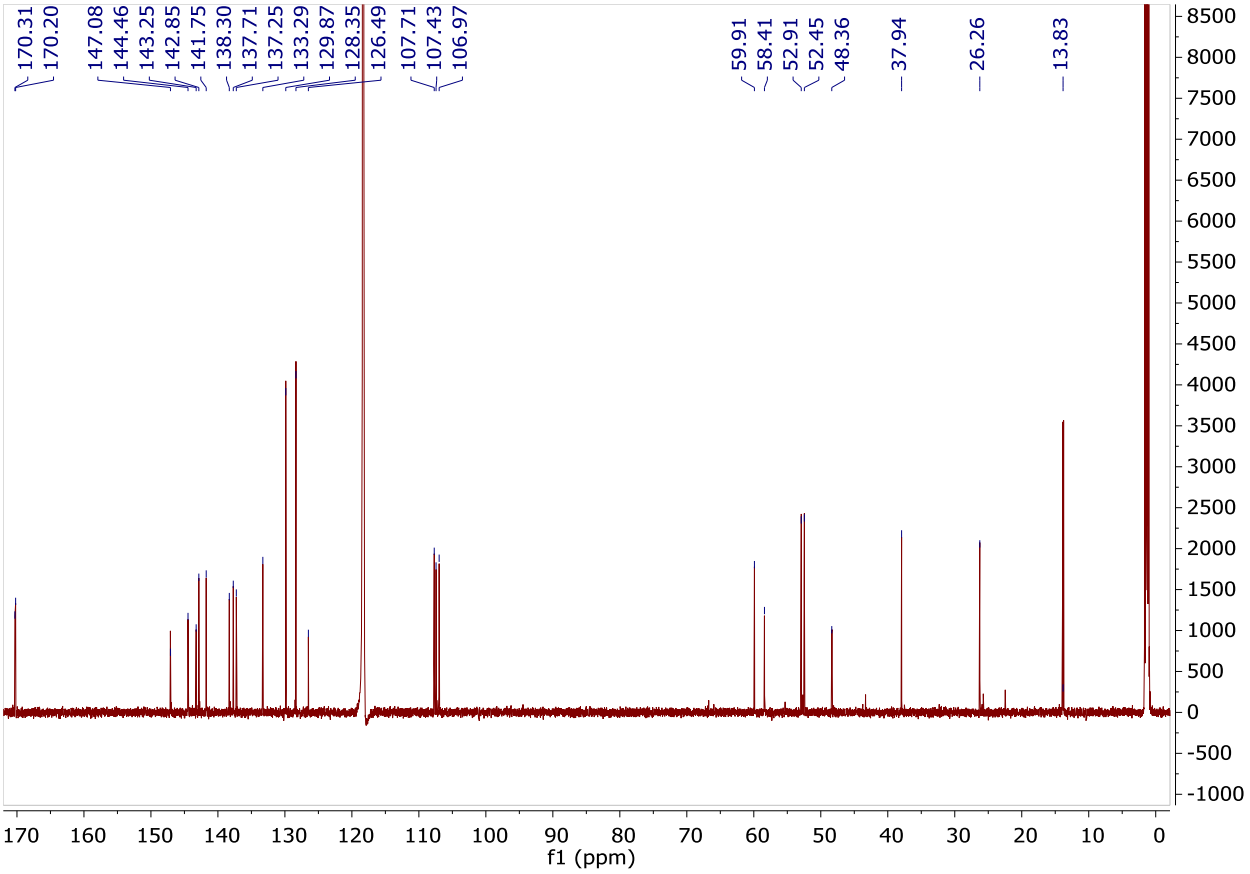

^{1}H NMR Spectrum of 13

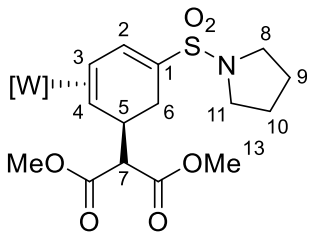

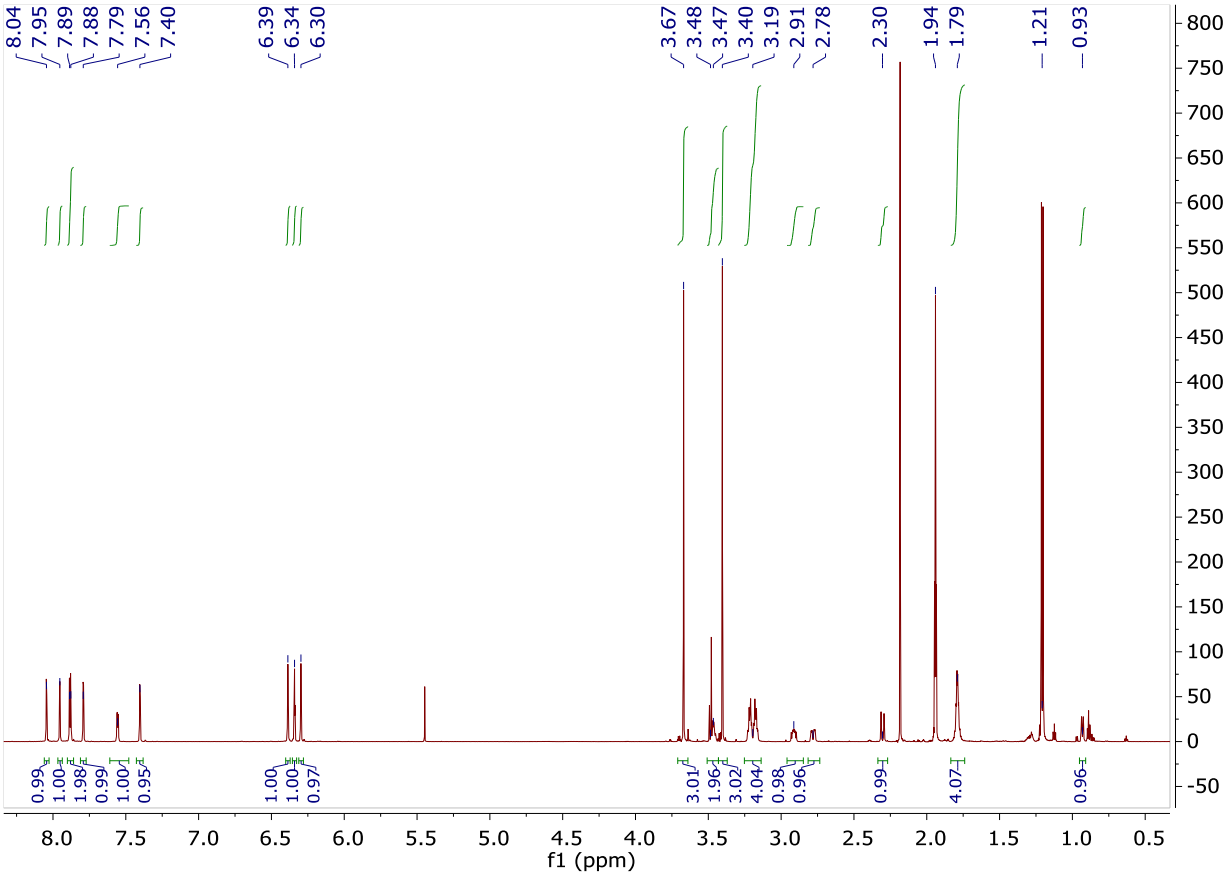

^{13}C {^{1}H} NMR Spectrum of 13

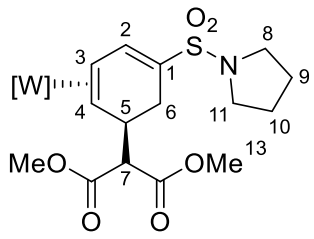

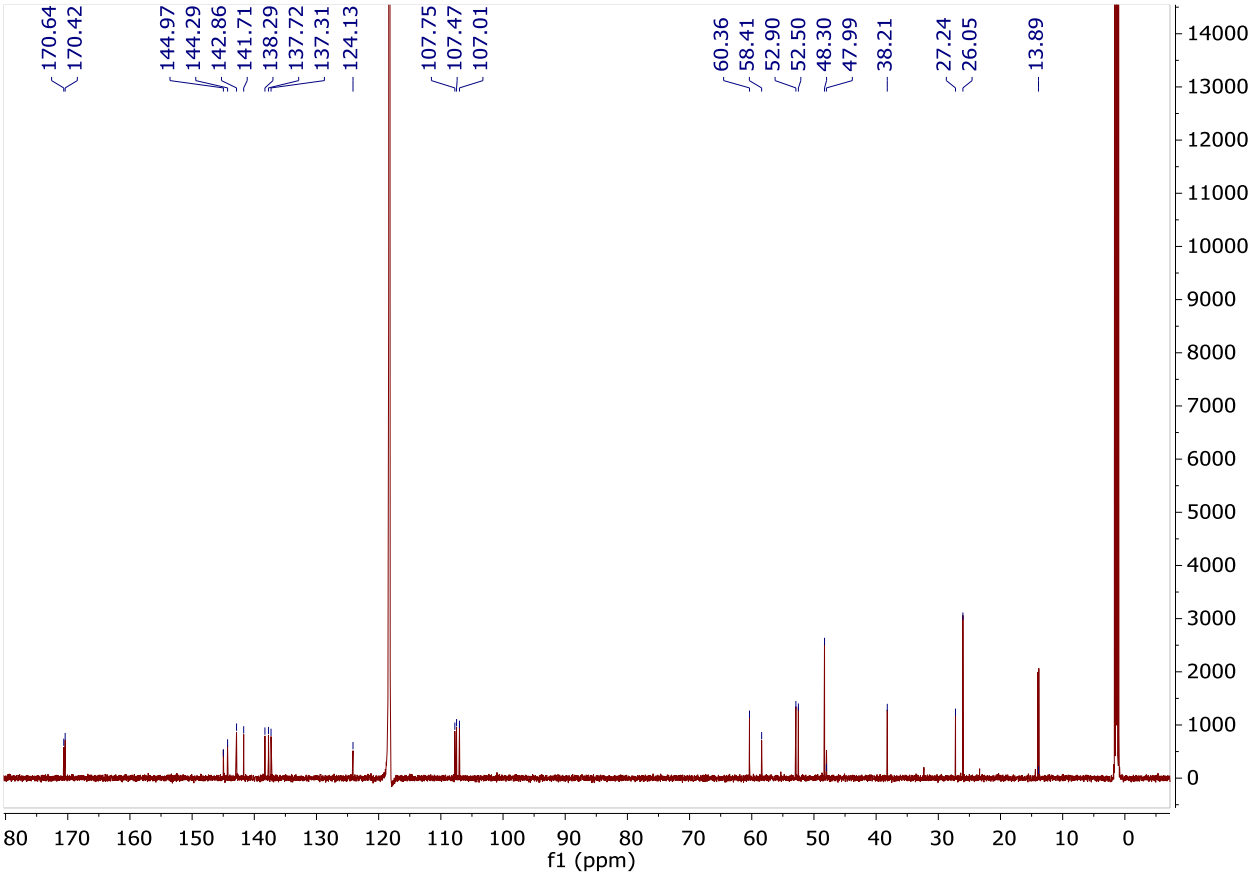

^{1}H NMR Spectrum of 14

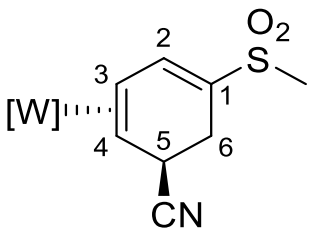

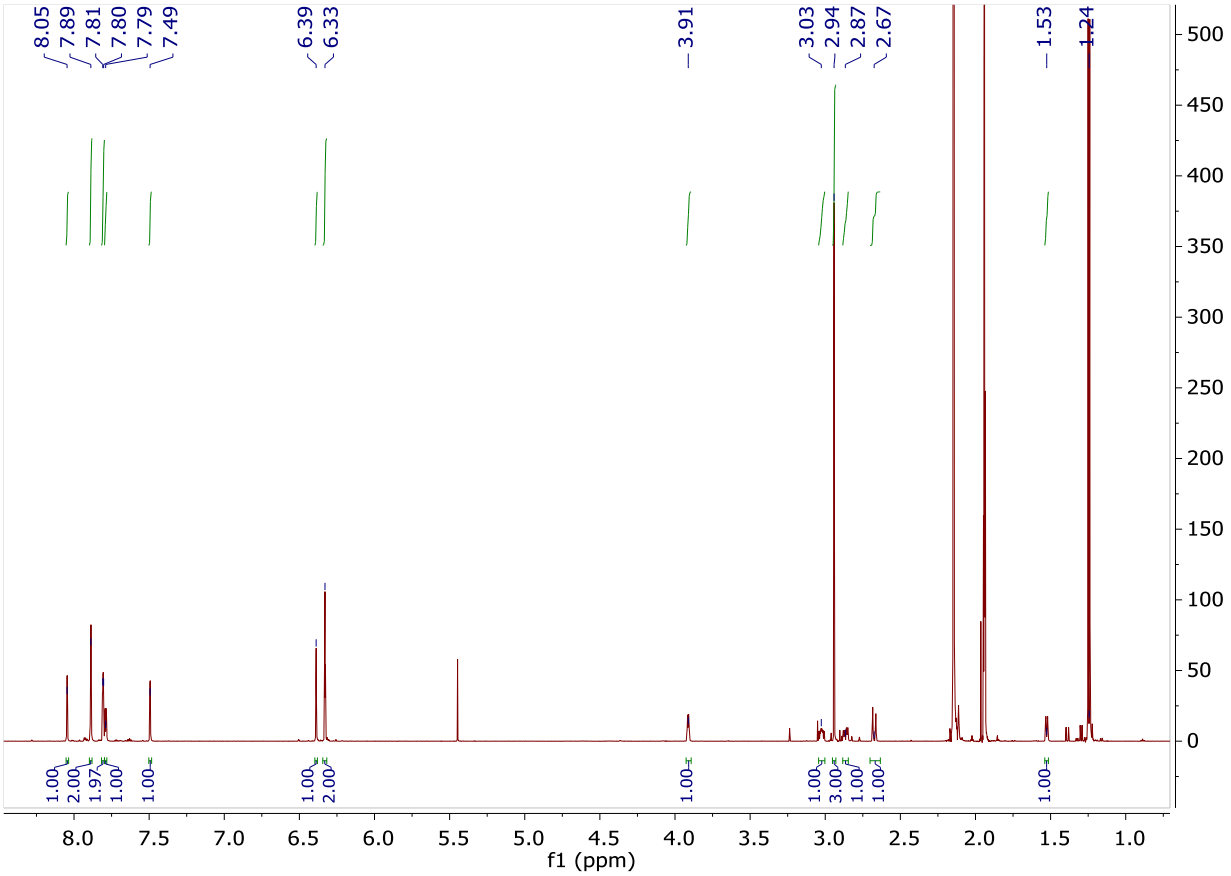

^{13}C {^{1}H} NMR Spectrum of 14

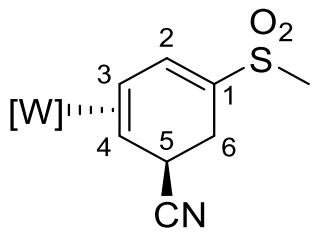

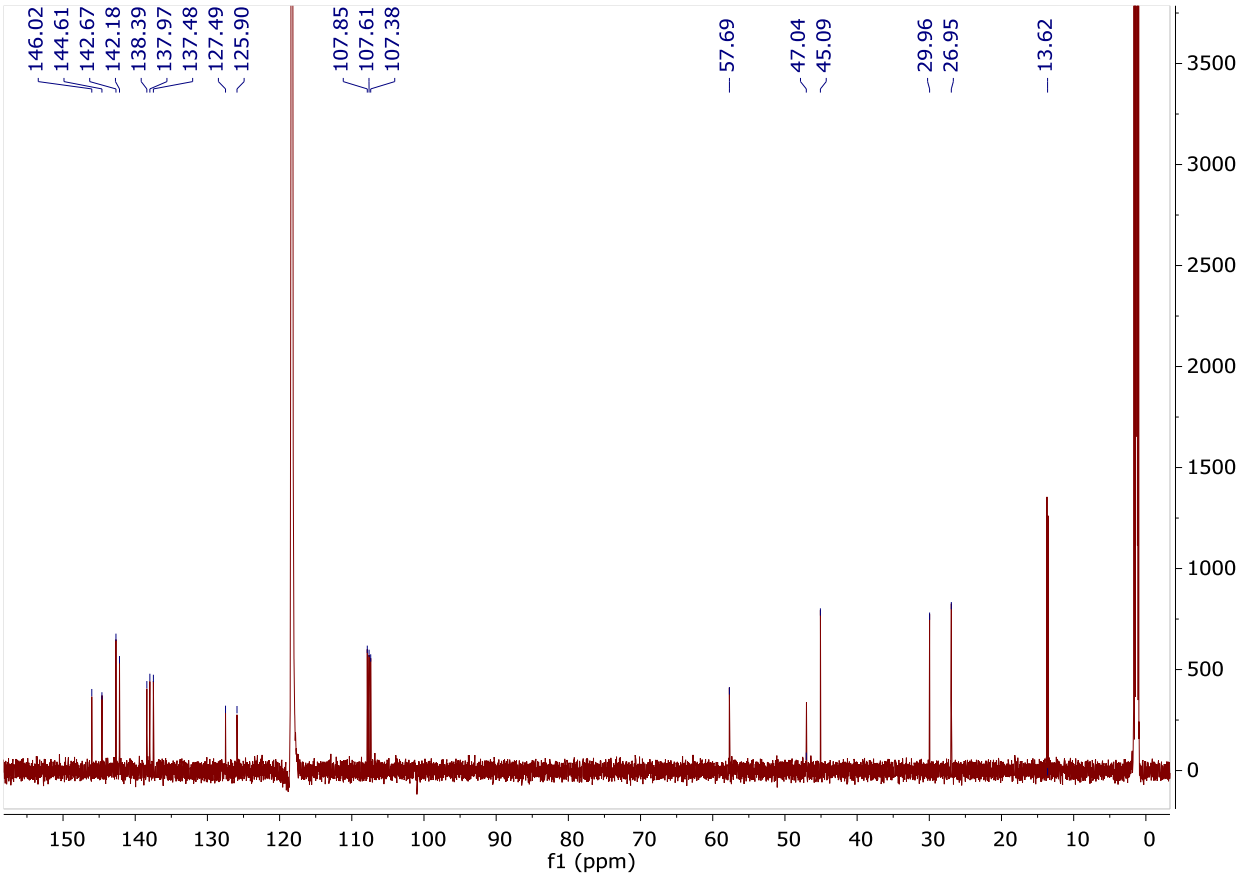

^{1}H NMR Spectrum of 15

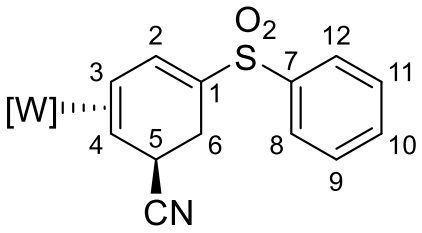

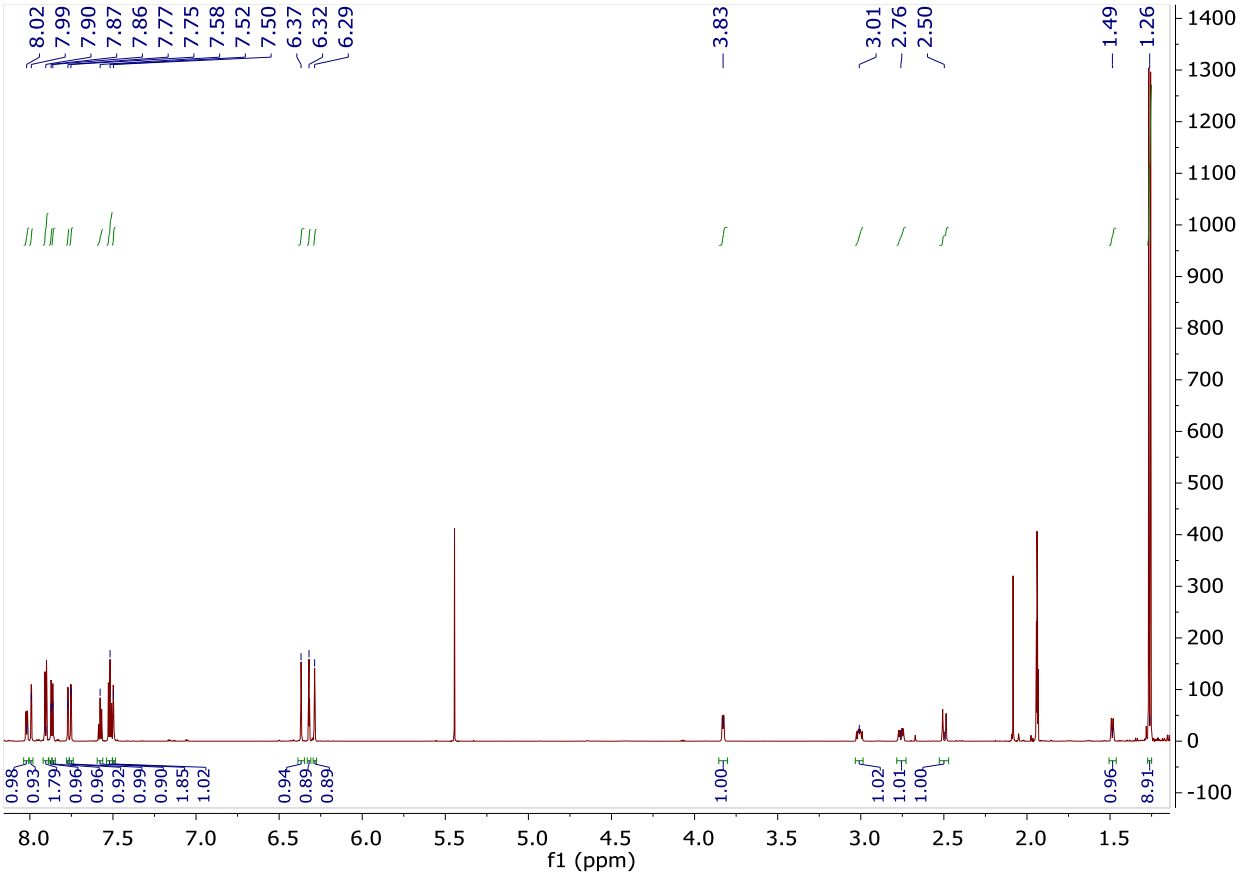

^{13}C {^{1}H} NMR Spectrum of 15

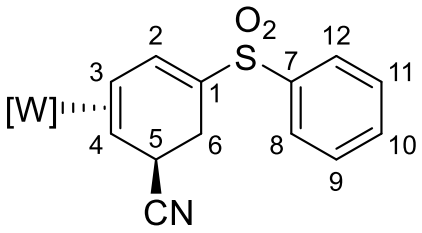

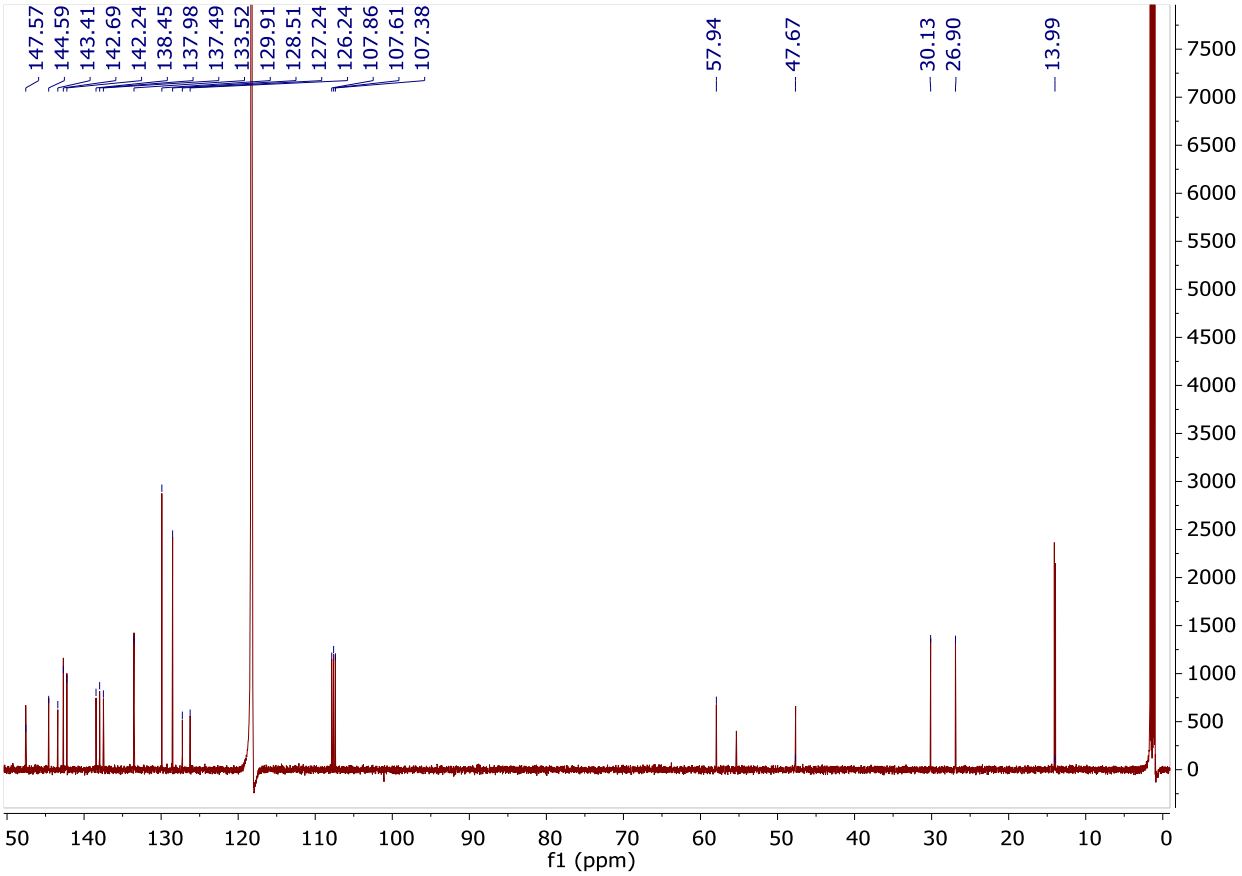

^{1}H NMR Spectrum of 16

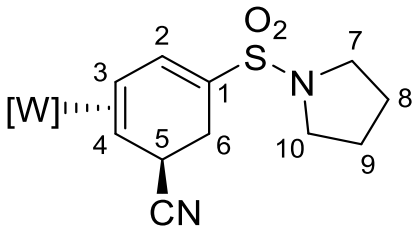

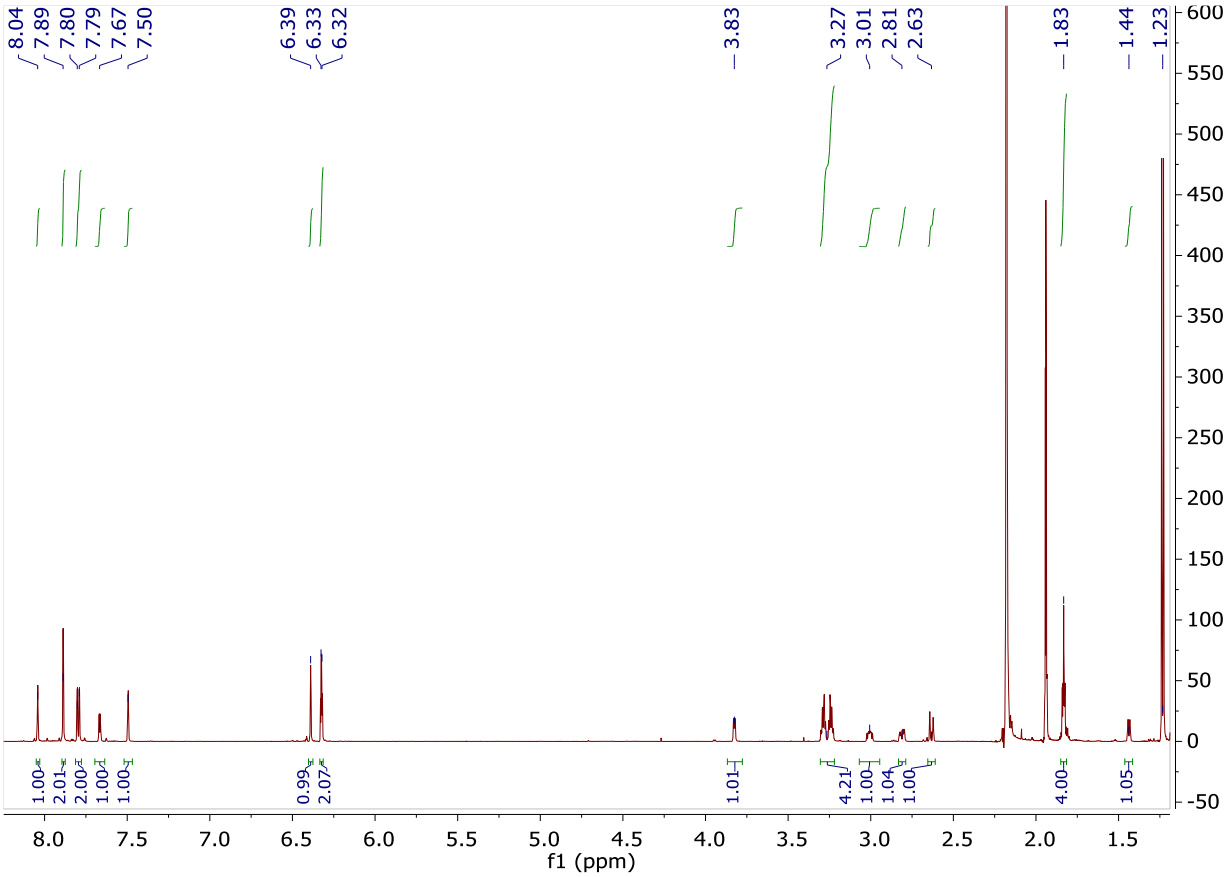

^{13}C {^{1}H} NMR Spectrum of 16

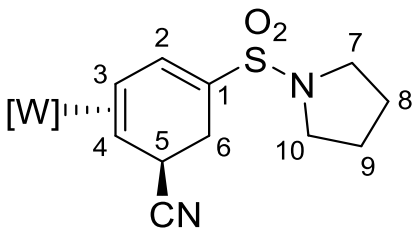

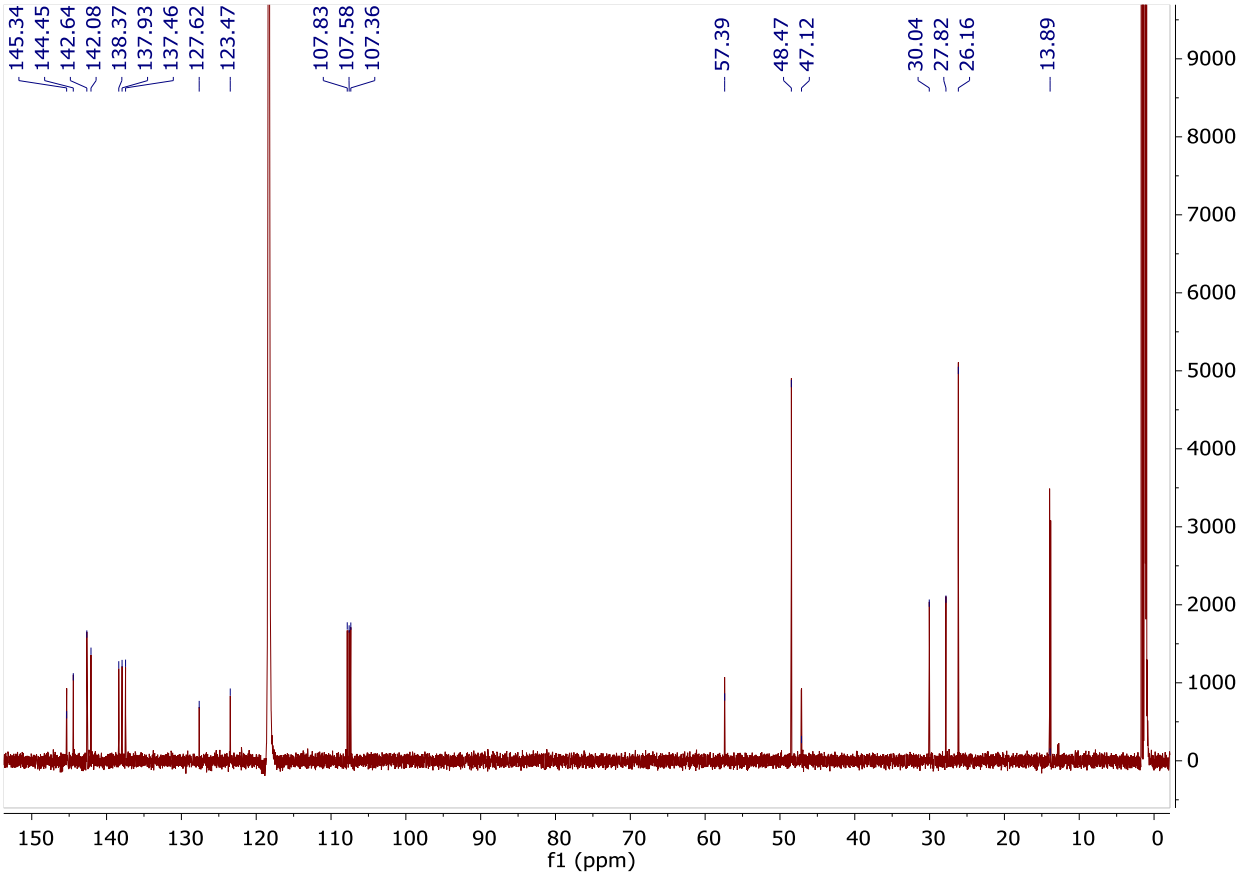

^{1}H NMR Spectrum of 17

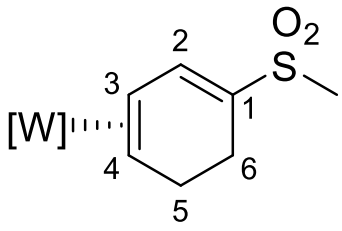

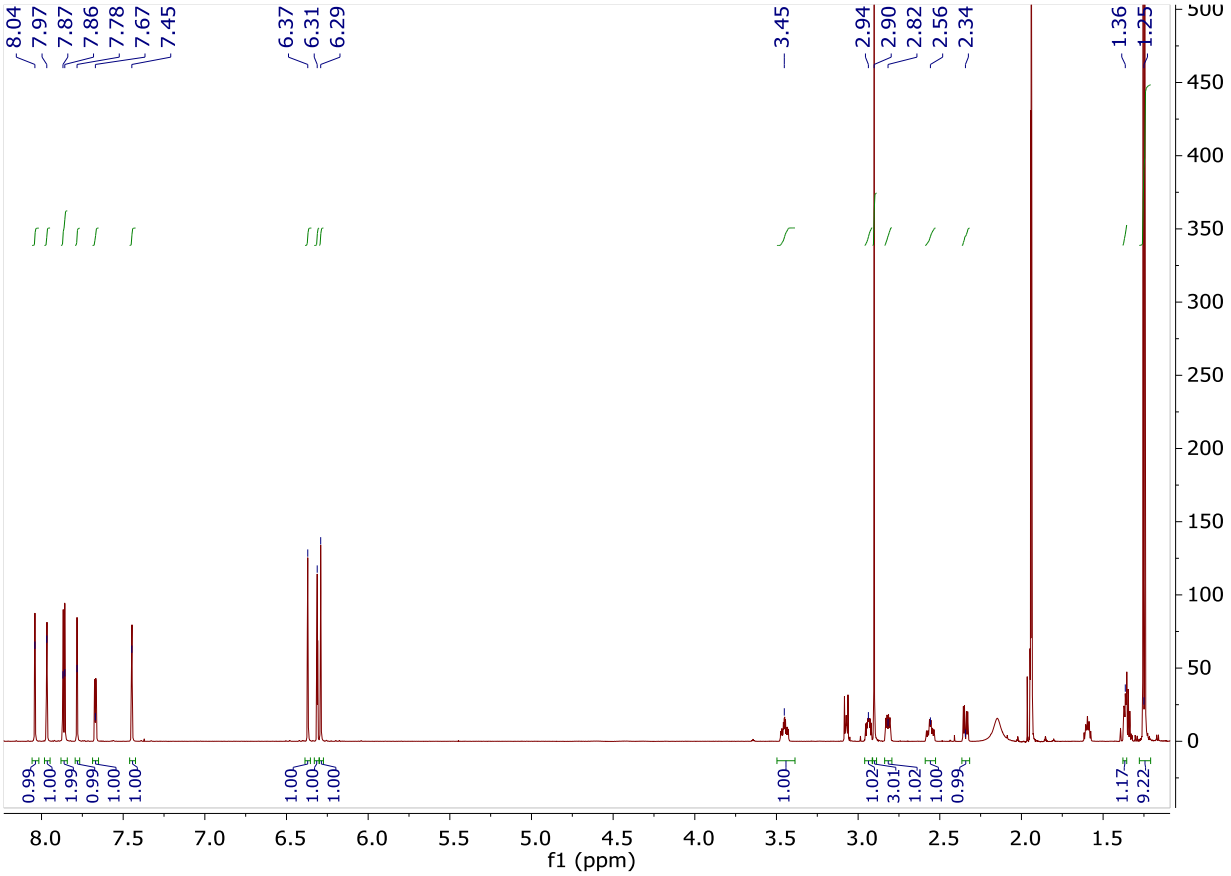

^{13}C {^{1}H} NMR Spectrum of 17

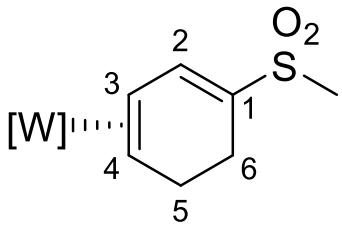

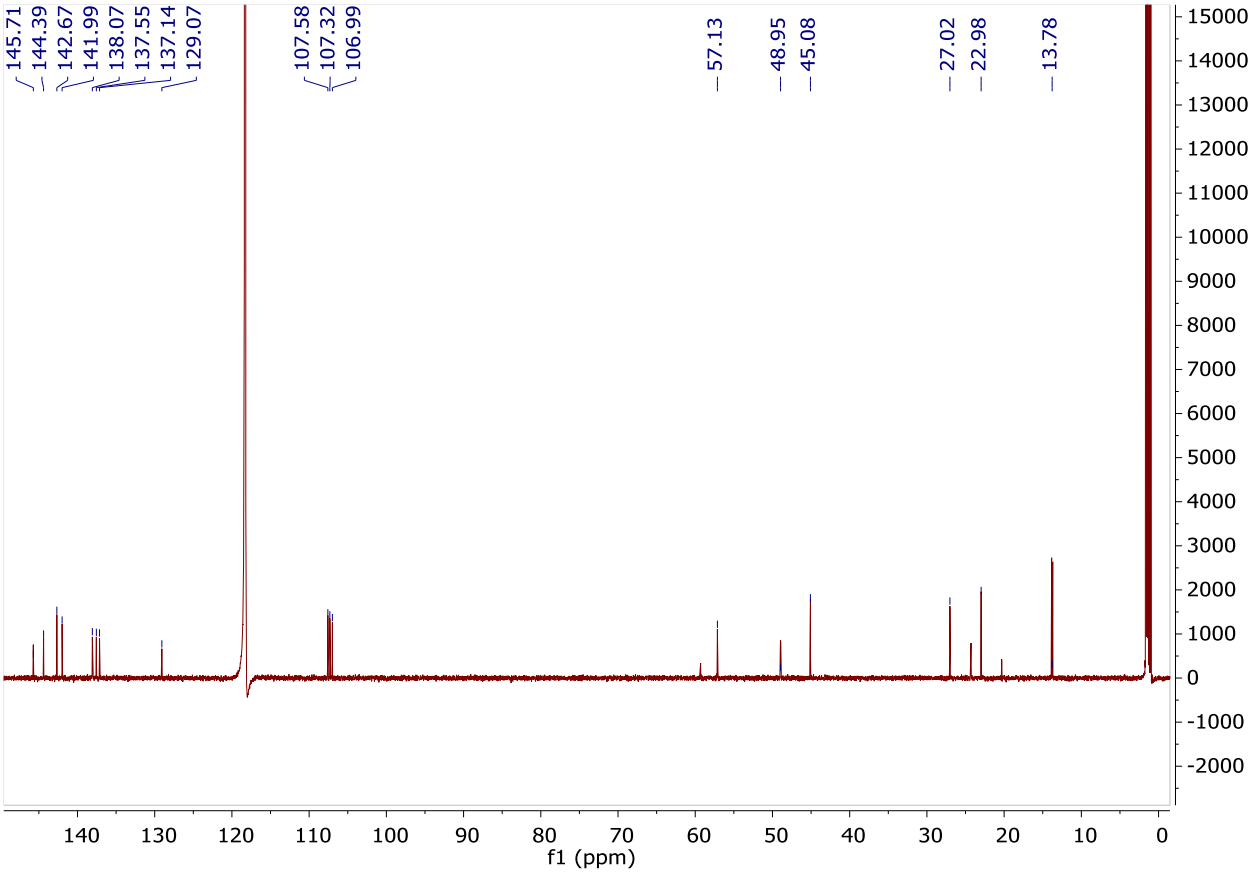

^{1}H NMR Spectrum of 18

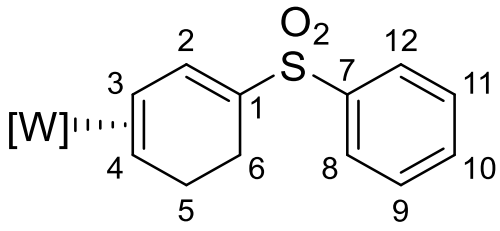

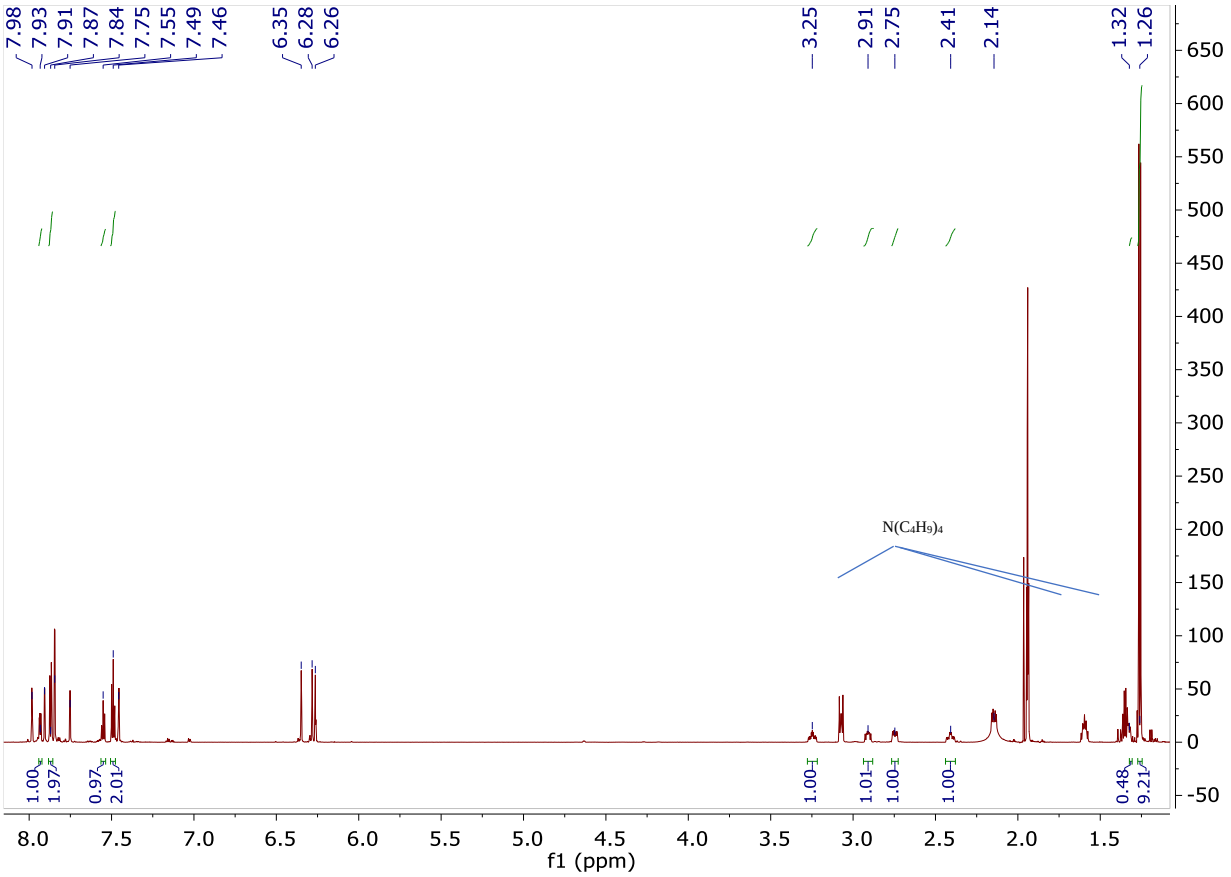

^{13}C {^{1}H} NMR Spectrum of 18

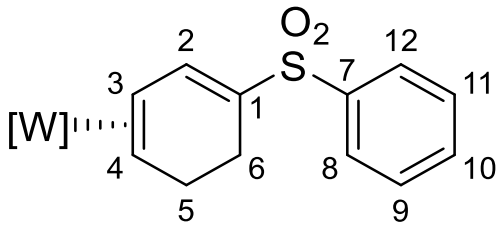

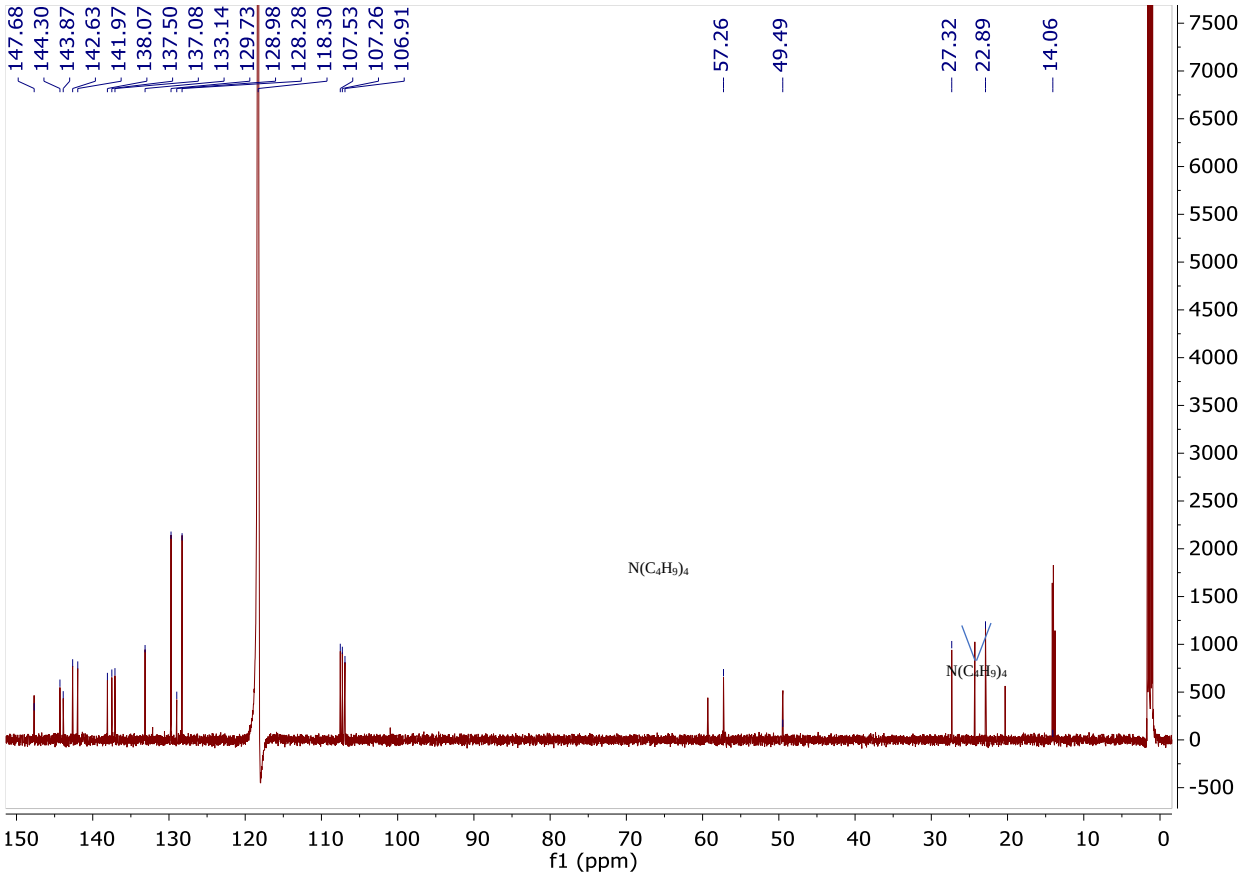

^{1}H NMR Spectrum of 22

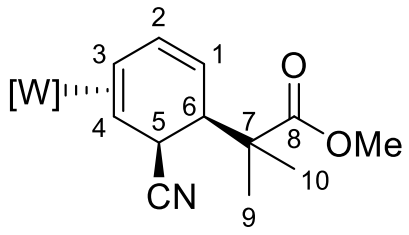

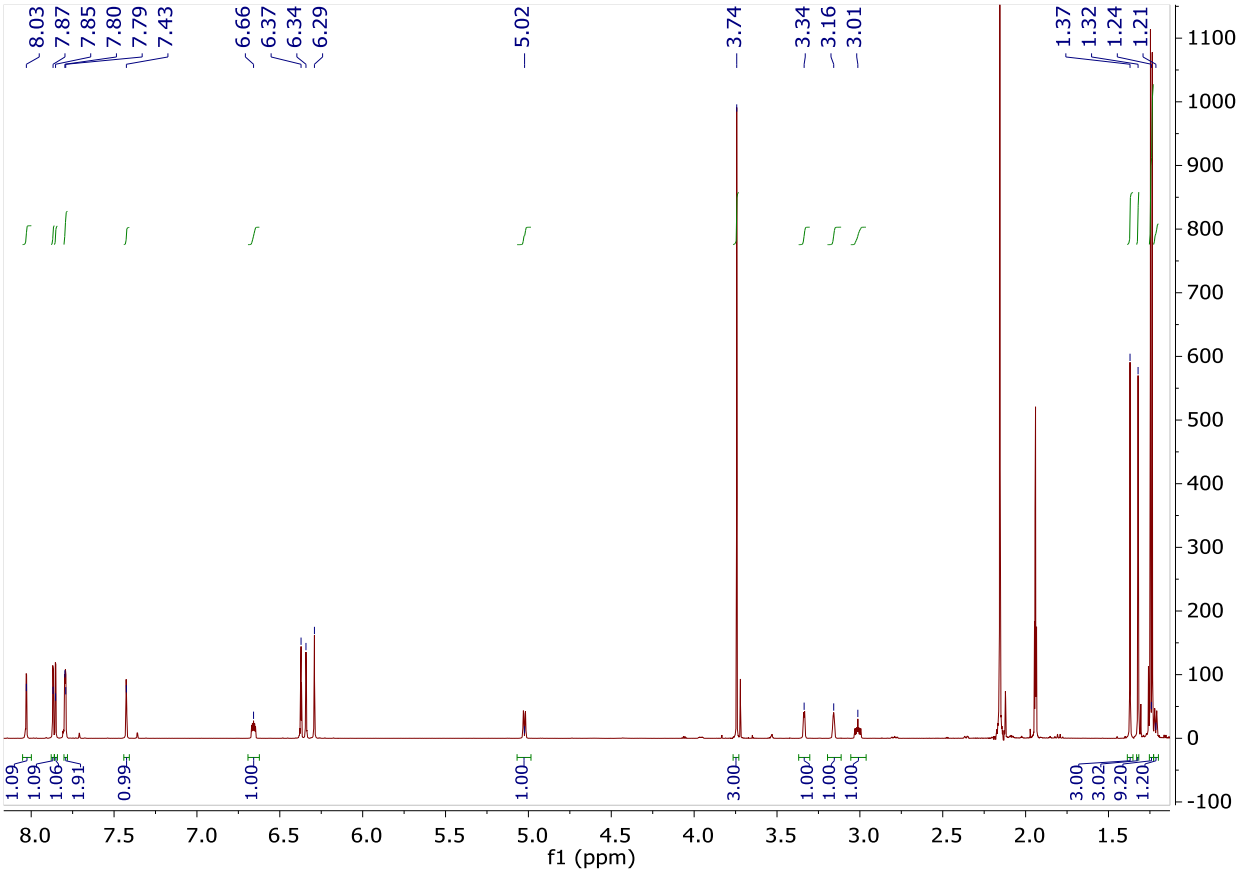

^{13}C {^{1}H} NMR Spectrum of 22

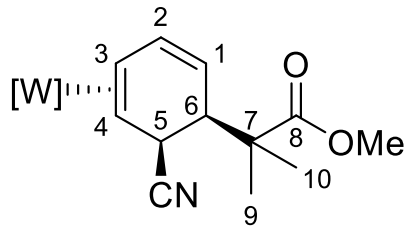

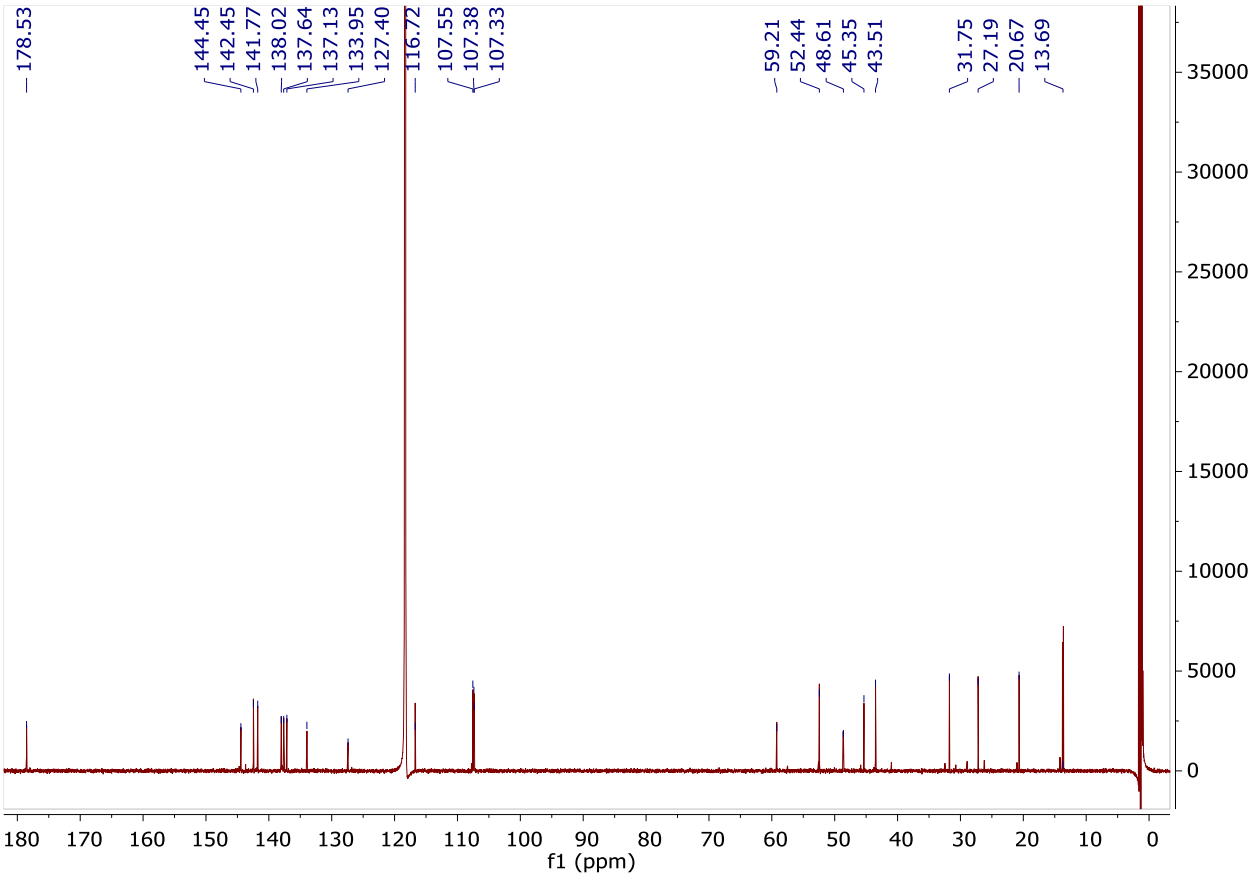

^{1}H NMR Spectrum of 23

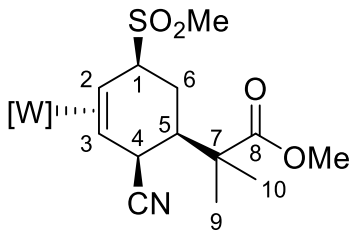

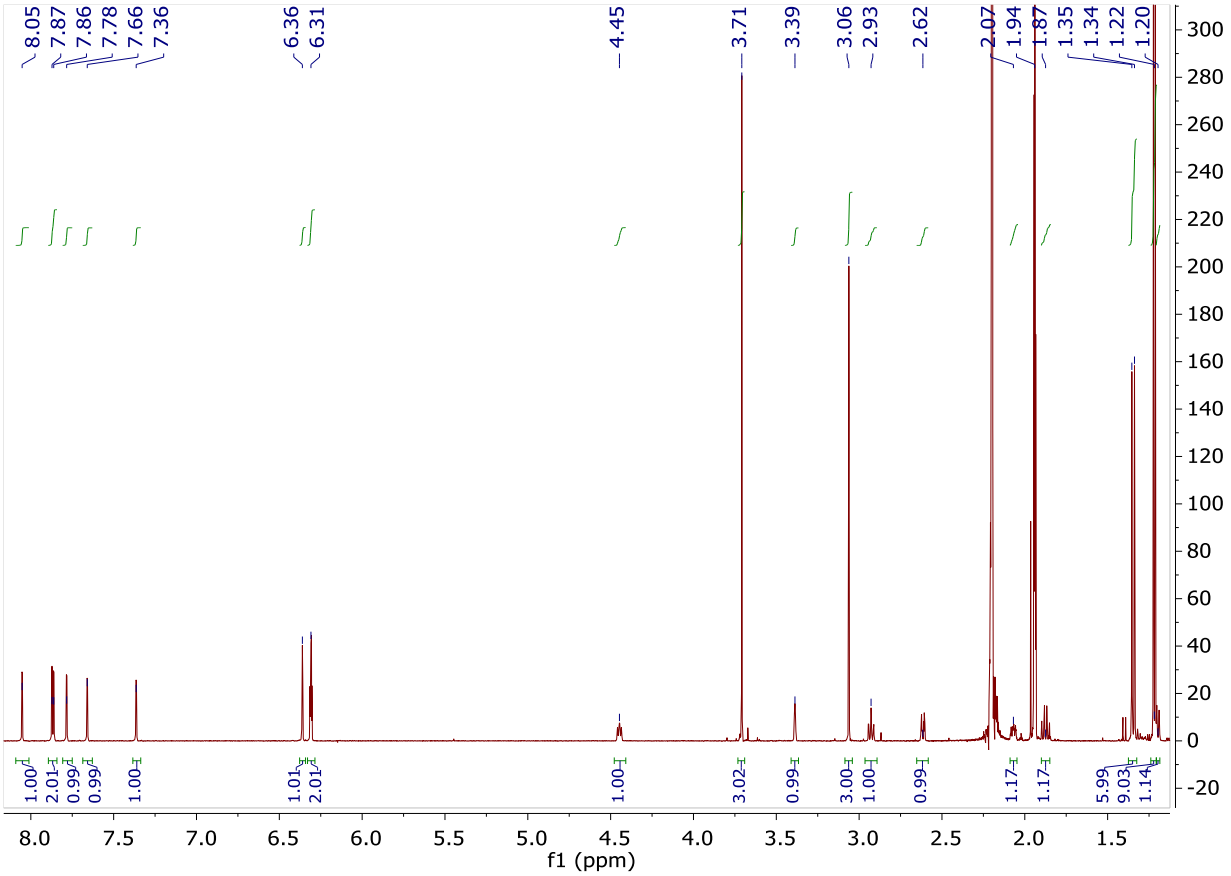

^{13}C {^{1}H} NMR Spectrum of 23

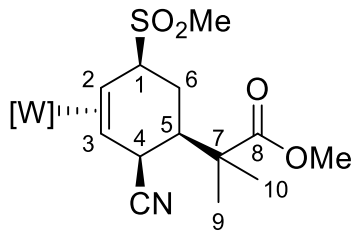

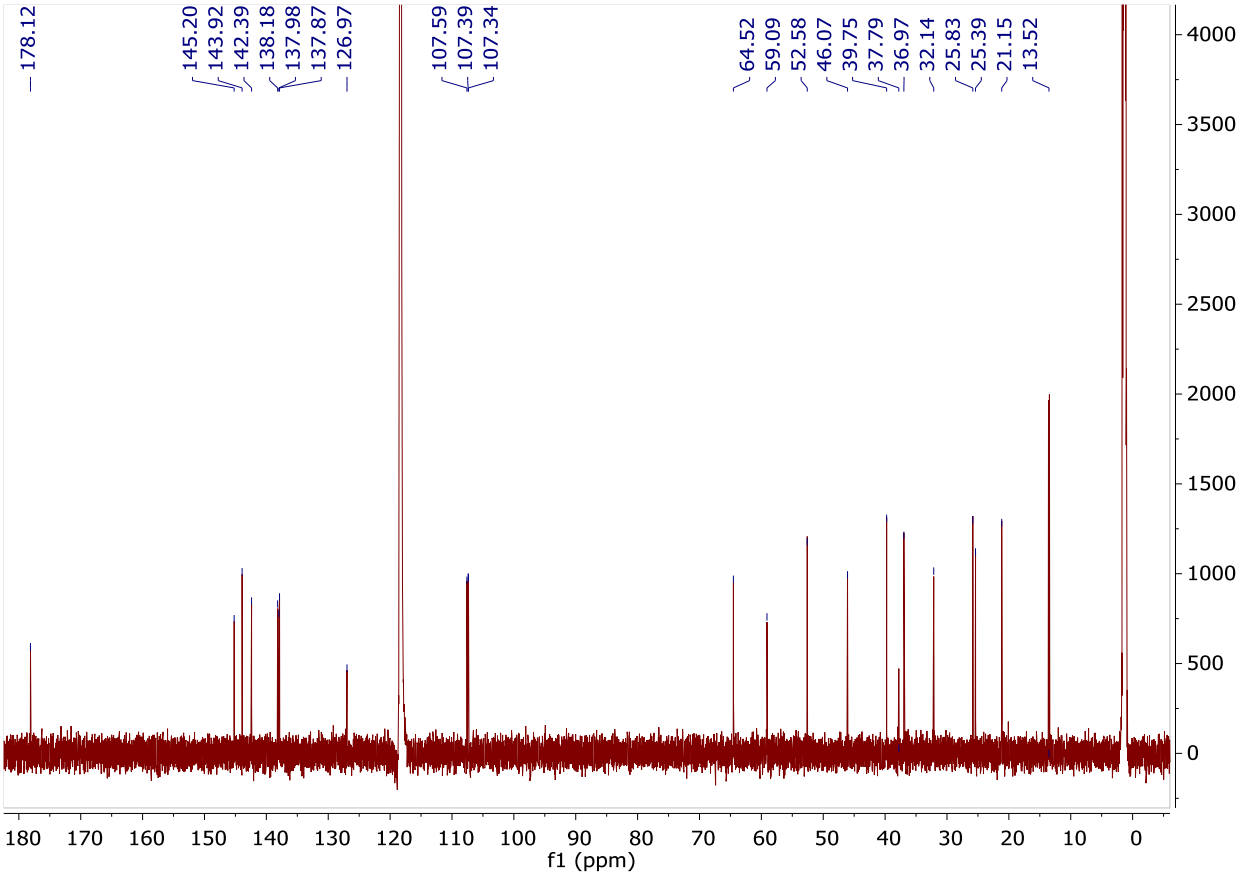

^{1}H NMR Spectrum of 24

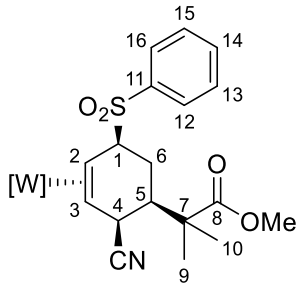

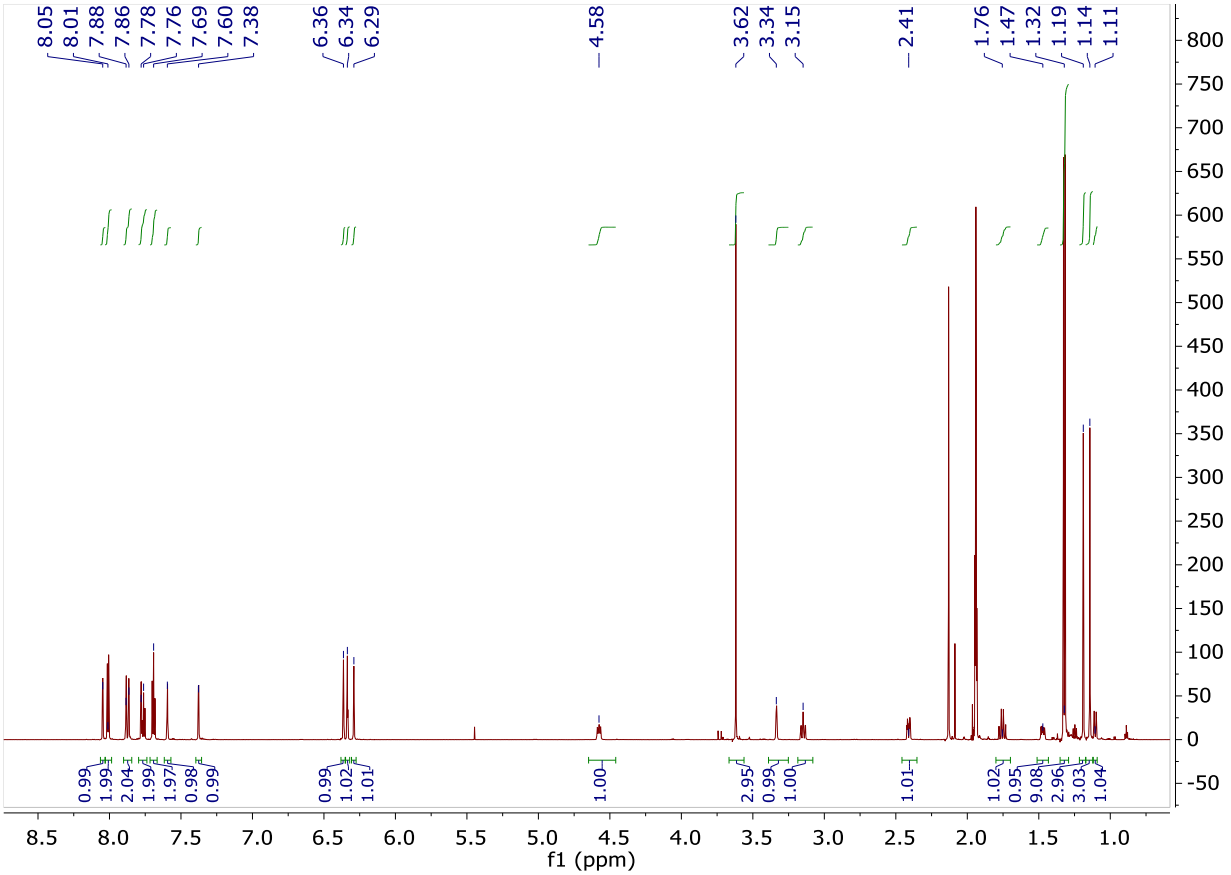

^{13}C {^{1}H} NMR Spectrum of 24

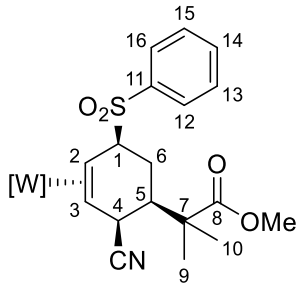

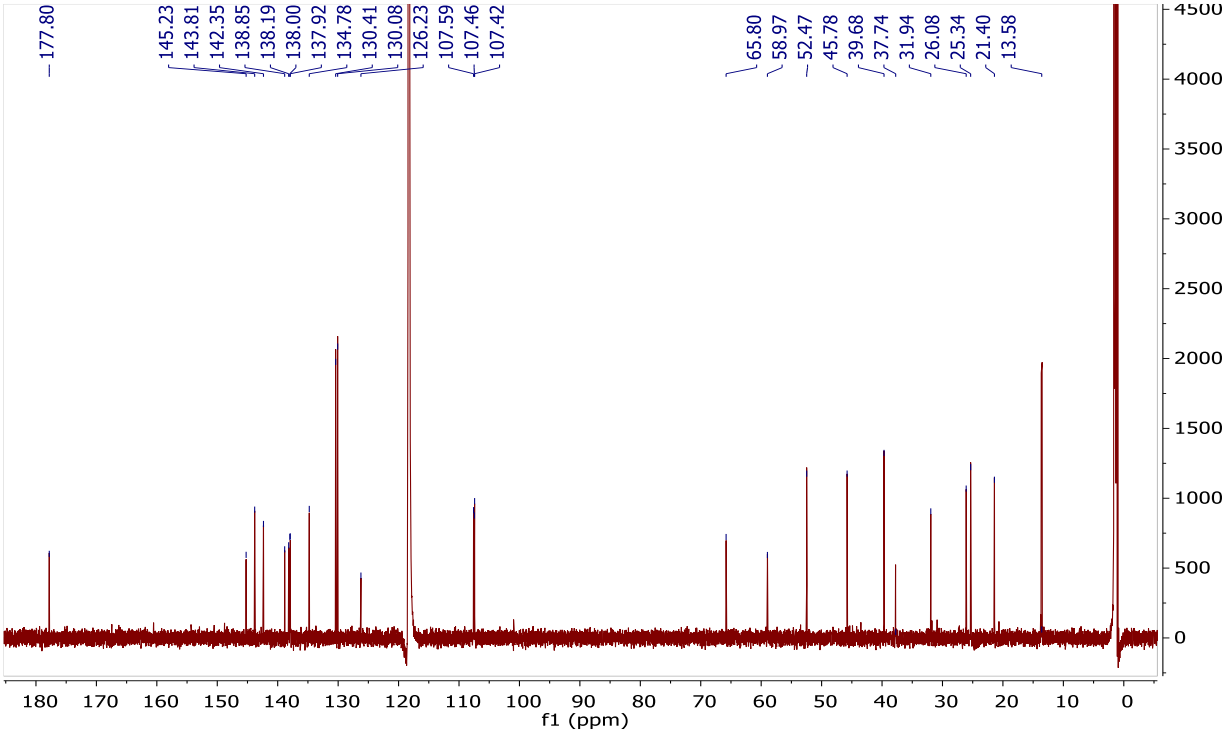

^{1}H NMR Spectrum of 25

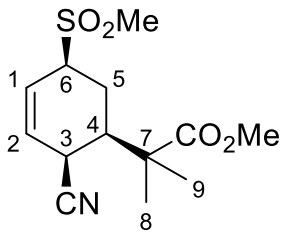

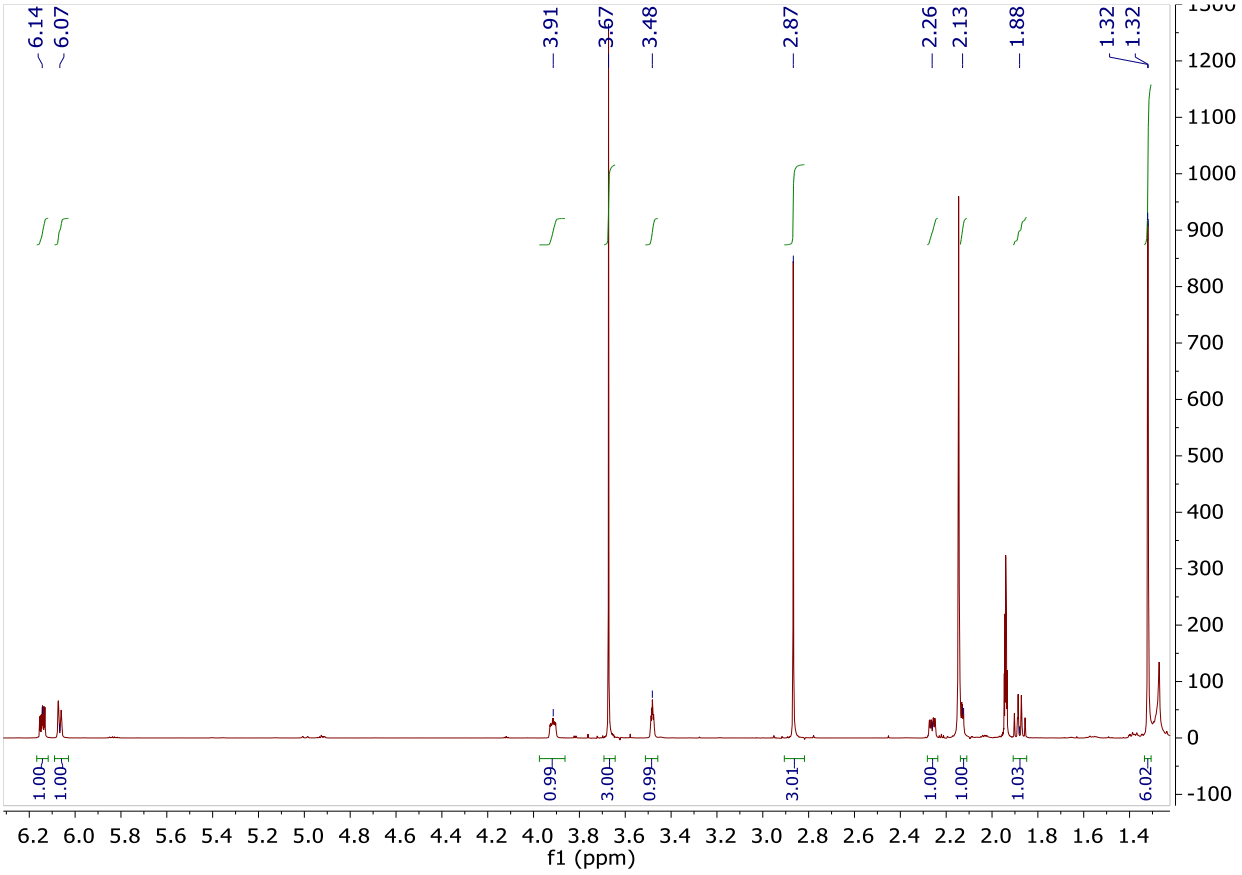

^{13}C {^{1}H} NMR Spectrum of 25

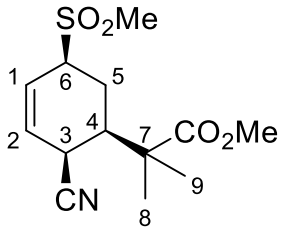

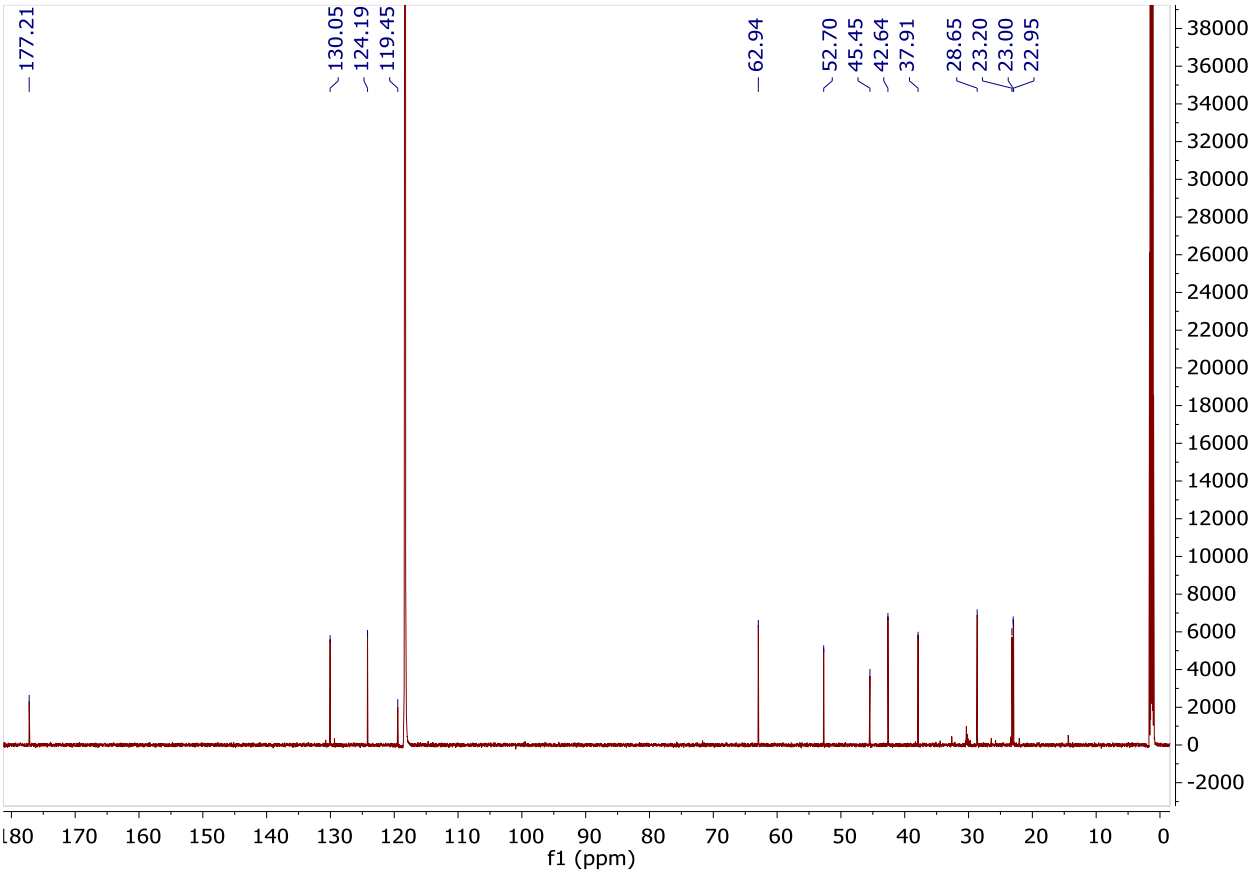

^{1}H NMR Spectrum of 26

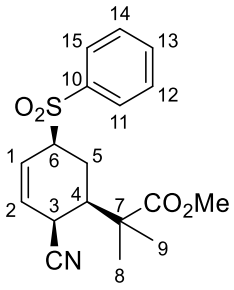

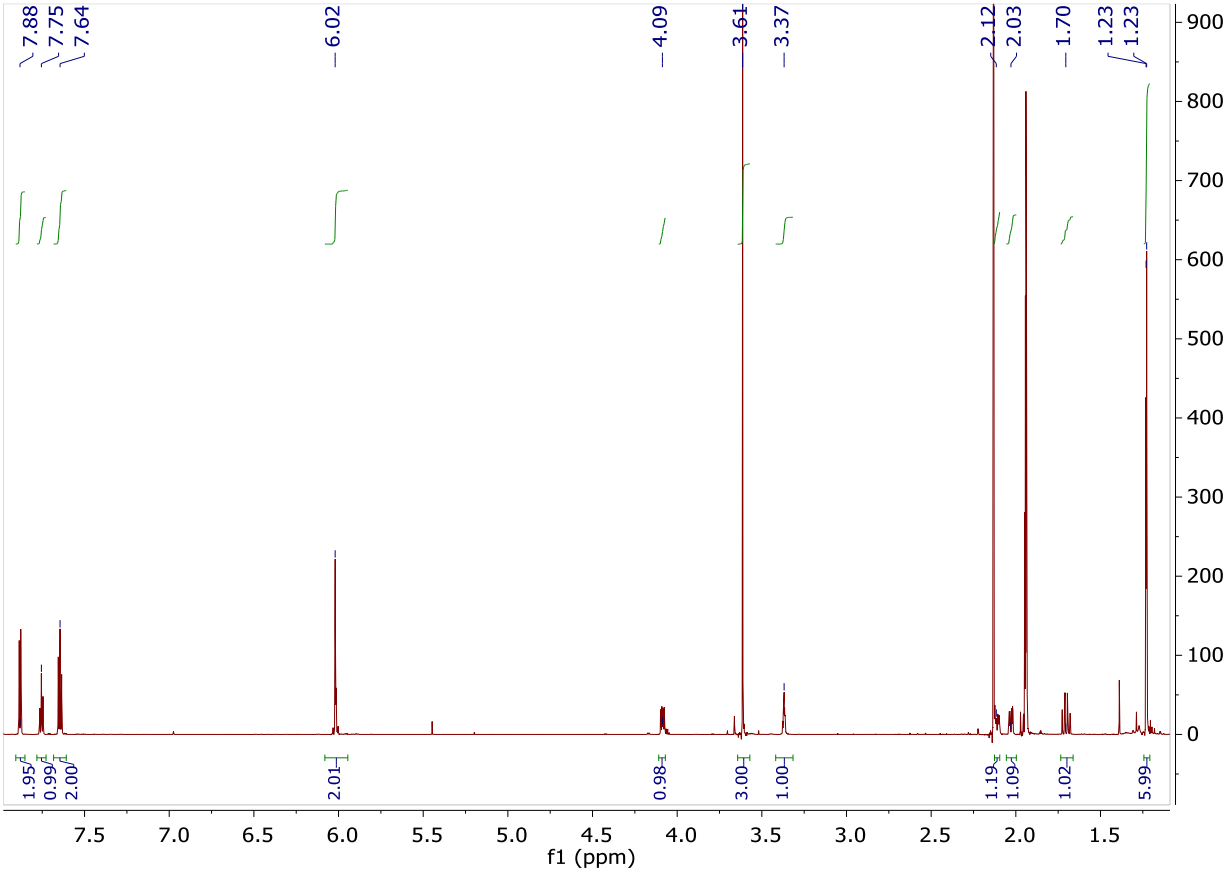

^{13}C {^{1}H} NMR Spectrum of 26

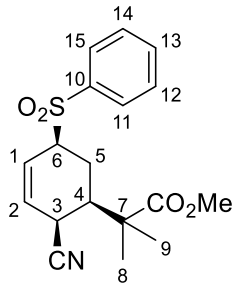

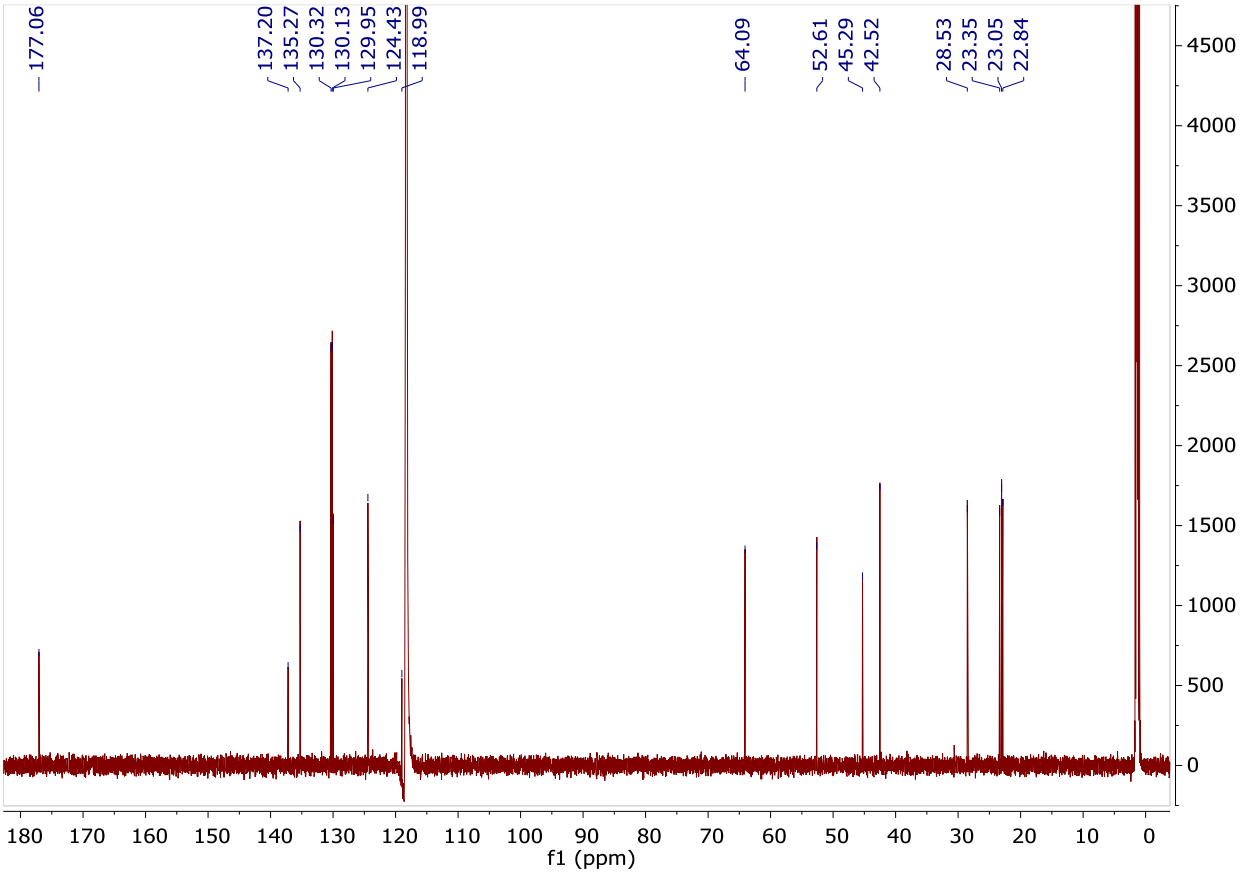

Supporting Crystallographic Data for Chapter 4

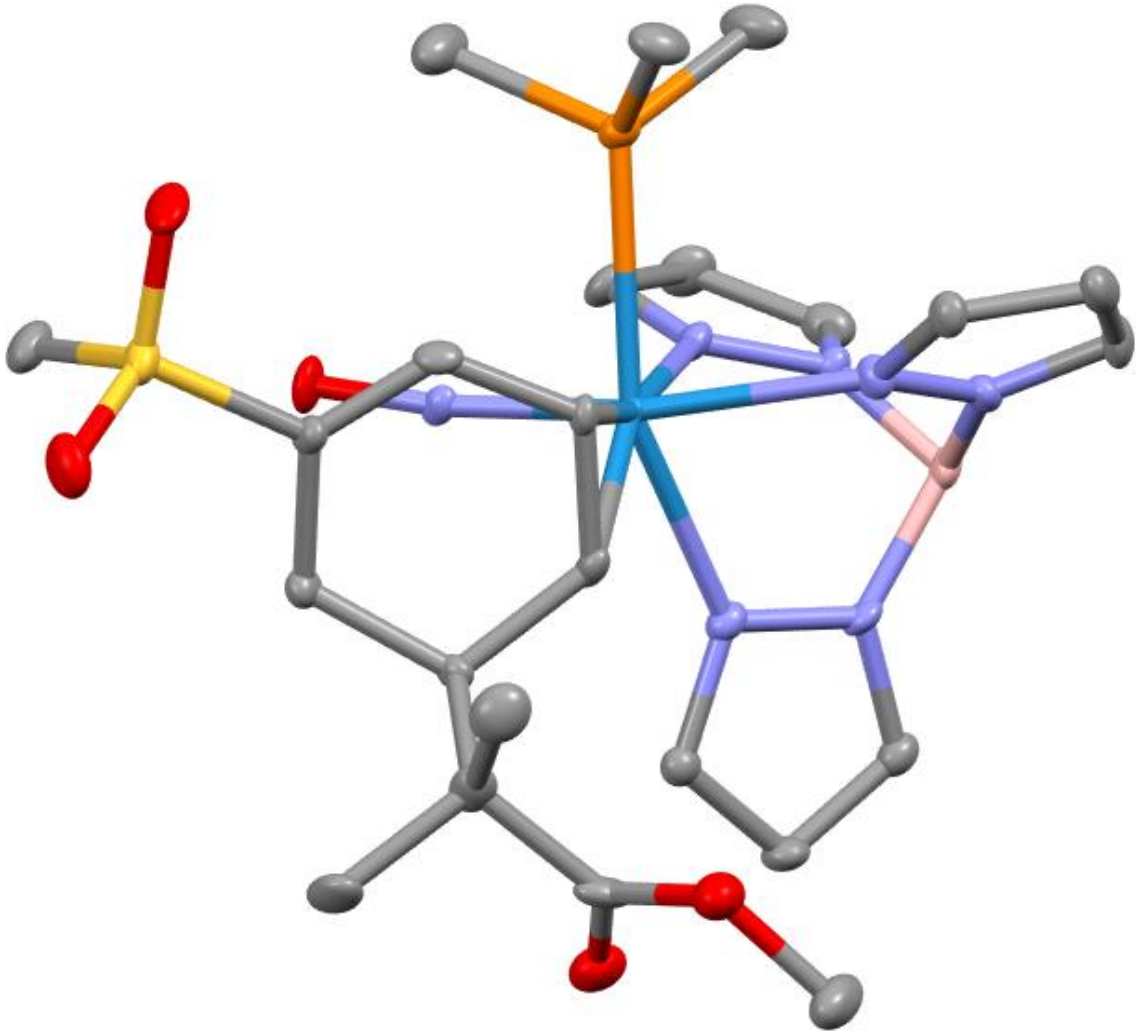

Crystal Structure Report for 8 in Chapter 4

A yellow plate-like specimen of $C_{24}H_{37}BN_7O_5PSW$, approximate dimensions 0.044 mm x 0.063 mm x 0.097 mm, was coated with Paratone oil and mounted on a MiTeGen MicroLoop. The X-ray intensity data were measured on a Bruker Kappa APEXII Duo system equipped with a fine-focus sealed tube (Mo K_α, λ = 0.71073 Å) and a graphite monochromator.

The total exposure time was 2.22 hours. The frames were integrated with the Bruker SAINT software package4 using a narrow-frame algorithm. The integration of the data using a monoclinic unit cell yielded a total of 32779 reflections to a maximum θ angle of 27.53° (0.77 Å resolution), of which 6782 were independent (average redundancy 4.833, completeness = 99.9%, R_{int} = 9.55%, R_{sig} = 8.21%) and 4736 (69.83%) were greater than

---

4 Bruker (2012). ***Saint; SADABS; APEX3***. Bruker AXS Inc., Madison, Wisconsin, USA.

2σ(F^2). The final cell constants of a = 11.5230(11) Å, b = 12.6655(12) Å, c = 20.3788(19) Å, β = 97.831(3)°, volume = 2946.4(5) $Å^3$, are based upon the refinement of the XYZ-centroids of 3256 reflections above 20 σ(I) with 4.803° < 2θ < 43.49°. Data were corrected for absorption effects using the Multi-Scan method (SADABS).[1] The ratio of minimum to maximum apparent transmission was 0.864. The calculated minimum and maximum transmission coefficients (based on crystal size) are 0.6920 and 0.8400.

The structure was solved and refined using the Bruker SHELXTL Software Package5 within APEX3 [1] and OLEX2,6 using the space group $P\,2_1/n$, with Z = 4 for the formula unit, $C_{24}H_{37}BN_7O_5PSW$. Non-hydrogen atoms were refined anisotropically. The B-H hydrogen atom, as well as H10 and H11, were located in the diffraction map and refined isotropically. All other hydrogen atoms were placed in geometrically calculated positions with U_{iso} = 1.2U_{equiv} of the parent atom (U_{iso} = 1.5U_{equiv} for methyl). The final anisotropic full-matrix least-squares refinement on F^2 with 379 variables converged at R1 = 3.74%, for the observed data and wR2 = 7.20% for all data. The goodness-of-fit was 1.000. The largest peak in the final difference electron density synthesis was 1.101 $e^-/Å^3$ and the largest hole was -0.914 $e^-/Å^3$ with an RMS deviation of 0.181 $e^-/Å^3$. On the basis of the final model, the calculated density was 1.716 g/cm^3 and F(000), 1520 e^-.

Table 1. Sample and crystal data for Harman_SS5_128_MTDA.

Identification code	Harman_SS5_128_MTDA	
Chemical formula	$C_{24}H_{37}BN_7O_5PSW$	
Formula weight	761.29 g/mol	
Temperature	100(2) K	
Wavelength	0.71073 Å	
Crystal size	0.044 x 0.063 x 0.097 mm	
Crystal habit	yellow plate	
Crystal system	monoclinic	
Space group	P 2_1/n	
Unit cell dimensions	a = 11.5230(11) Å	α = 90°
	b = 12.6655(12) Å	β = 97.831(3)°
	c = 20.3788(19) Å	γ = 90°
Volume	2946.4(5) $Å^3$	
Z	4	
Density (calculated)	1.716 g/cm^3	
Absorption coefficient	4.093 mm^{-1}	
F(000)	1520	

5 Sheldrick, G. M. (2015). ***Acta Cryst.*** A**71**, 3-8.

6 Dolomanov, O. V.; Bourhis, L. J.; Gildea, R. J.; Howard, J. A. K.; Puschmann, H. J. Appl. Cryst. (2009). 42, 339-341.

Table 2. Data collection and structure refinement for Harman_SS5_128_MTDA.

Diffractometer	Bruker Kappa APEXII Duo	
Radiation source	fine-focus sealed tube (Mo K_α, λ = 0.71073 Å)	
Theta range for data collection	1.90 to 27.53°	
Index ranges	-13<=h<=14, -16<=k<=16, -25<=l<=26	
Reflections collected	32779	
Independent reflections	6782 [R(int) = 0.0955]	
Coverage of independent reflections	99.9%	
Absorption correction	Multi-Scan	
Max. and min. transmission	0.8400 and 0.6920	
Structure solution technique	direct methods	
Structure solution program	SHELXT 2014/5 (Sheldrick, 2014)	
Refinement method	Full-matrix least-squares on F^2	
Refinement program	SHELXL-2018/3 (Sheldrick, 2018)	
Function minimized	$\Sigma\ w(F_o^2 - F_c^2)^2$	
Data / restraints / parameters	6782 / 0 / 379	
Goodness-of-fit on F^2	1.000	
Δ/σ_{max}	0.002	
Final R indices	4736 data; I>2σ(I)	R1 = 0.0374, wR2 = 0.0622
	all data	R1 = 0.0747, wR2 = 0.0720
Weighting scheme	$w=1/[\sigma^2(F_o^2)+(0.0217P)^2+0.3204P]$ where $P=(F_o^2+2F_c^2)/3$	
Largest diff. peak and hole	1.101 and -0.914 eÅ^{-3}	
R.M.S. deviation from mean	0.181 eÅ^{-3}	

Table 3. Atomic coordinates and equivalent isotropic atomic displacement parameters (Å²) for Harman_SS5_128_MTDA.

U(eq) is defined as one third of the trace of the orthogonalized U_{ij} tensor.

	x/a	y/b	z/c	U(eq)
W1	0.43213(2)	0.28555(2)	0.64649(2	0.01041(6)
S1	0.76386(12)	0.12337(11)	0.51810(7)	0.0184(3)
P1	0.33366(12)	0.28811(12)	0.52875(6)	0.0143(3)
O1	0.6302(3)	0.3985(3)	0.59531(17)	0.0185(9)
O2	0.6919(3)	0.0979(3)	0.45645(17)	0.0258(10)

O3	0.8609(3)	0.0545(3)	0.53973(19)	0.0252(10)
O4	0.6835(3)	0.1159(3)	0.84810(18)	0.0242(9)
O5	0.5901(3)	0.9649(3)	0.81816(18)	0.0251(10)
N1	0.2593(4)	0.2185(3)	0.66543(19)	0.0140(9)
N2	0.1856(4)	0.2761(3)	0.69909(19)	0.0148(9)
N3	0.3460(4)	0.4407(3)	0.6503(2)	0.0139(10)
N4	0.2590(4)	0.4622(3)	0.6877(2)	0.0136(10)
N5	0.4427(4)	0.3202(3)	0.7553(2)	0.0134(10)
N6	0.3447(4)	0.3512(3)	0.78118(19)	0.0144(10)
N7	0.5537(4)	0.3501(3)	0.61999(19)	0.0121(9)
C1	0.1950(4)	0.1351(4)	0.6405(2)	0.0149(11)
C2	0.0820(5)	0.1392(4)	0.6570(3)	0.0210(13)
C3	0.0795(5)	0.2291(4)	0.6942(3)	0.0182(12)
C4	0.3735(5)	0.5340(4)	0.6248(2)	0.0181(12)
C5	0.3055(5)	0.6146(4)	0.6440(3)	0.0217(13)
C6	0.2351(5)	0.5661(4)	0.6844(3)	0.0201(13)
C7	0.5289(5)	0.3166(4)	0.8067(2)	0.0142(12)
C8	0.4874(5)	0.3457(4)	0.8652(2)	0.0178(12)
C9	0.3713(5)	0.3666(4)	0.8465(2)	0.0156(12)
C10	0.5326(5)	0.1459(4)	0.6851(2)	0.0131(11)
C11	0.4831(5)	0.1217(4)	0.6174(2)	0.0118(11)
C12	0.5616(5)	0.1145(4)	0.5672(2)	0.0142(12)
C13	0.6758(4)	0.1356(4)	0.5800(2)	0.0137(11)
C14	0.7343(5)	0.1722(4)	0.6474(2)	0.0147(12)
C15	0.6653(4)	0.1462(4)	0.7049(2)	0.0120(11)
C16	0.8217(5)	0.2515(4)	0.5111(3)	0.0236(14)
C17	0.7083(5)	0.0415(4)	0.7416(3)	0.0194(13)
C18	0.6719(5)	0.9427(4)	0.7014(3)	0.0269(14)
C19	0.8422(5)	0.0426(5)	0.7615(3)	0.0264(15)
C20	0.6580(5)	0.0463(4)	0.8081(3)	0.0192(13)
C21	0.5494(6)	0.9678(5)	0.8827(3)	0.0311(16)
C22	0.4185(5)	0.3530(5)	0.4728(3)	0.0302(15)
C23	0.2864(5)	0.1691(4)	0.4830(3)	0.0229(13)
C24	0.1950(5)	0.3592(5)	0.5189(3)	0.0279(14)
B1	0.2290(6)	0.3774(5)	0.7373(3)	0.0153(13)

Table 4. Bond lengths (Å) for Harman_SS5_128_MTDA.

W1-N7	1.769(4)	W1-C10	2.200(5)

W1-N3	2.207(4)	W1-N1	2.247(4)
W1-N5	2.248(4)	W1-C11	2.258(5)
W1-P1	2.5109(13)	S1-O3	1.440(4)
S1-O2	1.445(4)	S1-C13	1.729(5)
S1-C16	1.768(5)	P1-C22	1.798(6)
P1-C23	1.816(5)	P1-C24	1.821(6)
O1-N7	1.236(5)	O4-C20	1.210(6)
O5-C20	1.327(6)	O5-C21	1.456(6)
N1-C1	1.348(6)	N1-N2	1.372(5)
N2-C3	1.351(6)	N2-B1	1.548(7)
N3-C4	1.346(6)	N3-N4	1.367(6)
N4-C6	1.344(6)	N4-B1	1.545(7)
N5-C7	1.342(6)	N5-N6	1.367(6)
N6-C9	1.338(6)	N6-B1	1.537(7)
C1-C2	1.390(7)	C1-H1	0.95
C2-C3	1.370(7)	C2-H2	0.95
C3-H3	0.95	C4-C5	1.376(7)
C4-H4	0.95	C5-C6	1.376(8)
C5-H5	0.95	C6-H6	0.95
C7-C8	1.393(7)	C7-H7	0.95
C8-C9	1.366(7)	C8-H8	0.95
C9-H9	0.95	C10-C11	1.452(7)
C10-C15	1.528(7)	C10-H10	0.98(5)
C11-C12	1.457(7)	C11-H11	1.01(5)
C12-C13	1.333(7)	C12-H12	0.95
C13-C14	1.519(7)	C14-C15	1.540(7)
C14-H14A	0.99	C14-H14B	0.99
C15-C17	1.569(7)	C15-H15	1.0
C16-H16A	0.98	C16-H16B	0.98
C16-H16C	0.98	C17-C18	1.524(7)
C17-C19	1.541(8)	C17-C20	1.545(8)
C18-H18A	0.98	C18-H18B	0.98
C18-H18C	0.98	C19-H19A	0.98
C19-H19B	0.98	C19-H19C	0.98
C21-H21A	0.98	C21-H21B	0.98
C21-H21C	0.98	C22-H22A	0.98
C22-H22B	0.98	C22-H22C	0.98
C23-H23A	0.98	C23-H23B	0.98
C23-H23C	0.98	C24-H24A	0.98

C24-H24B	0.98	C24-H24C	0.98
B1-H1A	1.10(5)		

Table 5. Bond angles (°) for Harman_SS5_128_MTDA.

N7-W1-C10	94.63(19)	N7-W1-N3	88.74(17)
C10-W1-N3	156.99(17)	N7-W1-N1	170.00(16)
C10-W1-N1	94.02(18)	N3-W1-N1	85.25(16)
N7-W1-N5	105.79(17)	C10-W1-N5	81.34(17)
N3-W1-N5	75.85(14)	N1-W1-N5	80.48(15)
N7-W1-C11	95.70(18)	C10-W1-C11	37.99(18)
N3-W1-C11	164.06(17)	N1-W1-C11	88.05(17)
N5-W1-C11	117.26(16)	N7-W1-P1	88.61(13)
C10-W1-P1	119.94(14)	N3-W1-P1	82.84(11)
N1-W1-P1	82.72(10)	N5-W1-P1	153.78(12)
C11-W1-P1	81.97(13)	O3-S1-O2	117.5(2)
O3-S1-C13	109.9(2)	O2-S1-C13	109.2(2)
O3-S1-C16	107.2(3)	O2-S1-C16	108.3(3)
C13-S1-C16	104.0(3)	C22-P1-C23	101.9(3)
C22-P1-C24	104.4(3)	C23-P1-C24	99.0(3)
C22-P1-W1	113.43(19)	C23-P1-W1	122.97(18)
C24-P1-W1	112.78(18)	C20-O5-C21	112.9(4)
C1-N1-N2	105.0(4)	C1-N1-W1	133.3(3)
N2-N1-W1	120.6(3)	C3-N2-N1	110.1(4)
C3-N2-B1	129.0(5)	N1-N2-B1	120.8(4)
C4-N3-N4	105.6(4)	C4-N3-W1	129.6(4)
N4-N3-W1	124.3(3)	C6-N4-N3	109.1(4)
C6-N4-B1	130.6(5)	N3-N4-B1	118.2(4)
C7-N5-N6	105.8(4)	C7-N5-W1	134.3(4)
N6-N5-W1	120.0(3)	C9-N6-N5	109.6(4)
C9-N6-B1	127.6(5)	N5-N6-B1	122.3(4)
O1-N7-W1	172.9(4)	N1-C1-C2	111.3(5)
N1-C1-H1	124.3	C2-C1-H1	124.3
C3-C2-C1	104.8(5)	C3-C2-H2	127.6
C1-C2-H2	127.6	N2-C3-C2	108.6(5)
N2-C3-H3	125.7	C2-C3-H3	125.7
N3-C4-C5	111.6(5)	N3-C4-H4	124.2
C5-C4-H4	124.2	C4-C5-C6	104.1(5)
C4-C5-H5	128.0	C6-C5-H5	128.0
N4-C6-C5	109.5(5)	N4-C6-H6	125.2

C5-C6-H6	125.2	N5-C7-C8	110.8(5)
N5-C7-H7	124.6	C8-C7-H7	124.6
C9-C8-C7	104.5(5)	C9-C8-H8	127.8
C7-C8-H8	127.8	N6-C9-C8	109.4(5)
N6-C9-H9	125.3	C8-C9-H9	125.3
C11-C10-C15	120.1(4)	C11-C10-W1	73.2(3)
C15-C10-W1	123.5(4)	C11-C10-H10	111.(3)
C15-C10-H10	113.(3)	W1-C10-H10	110.(3)
C10-C11-C12	118.6(5)	C10-C11-W1	68.8(3)
C12-C11-W1	116.8(3)	C10-C11-H11	122.(3)
C12-C11-H11	113.(3)	W1-C11-H11	110.(3)
C13-C12-C11	122.8(5)	C13-C12-H12	118.6
C11-C12-H12	118.6	C12-C13-C14	122.8(5)
C12-C13-S1	120.1(4)	C14-C13-S1	117.0(4)
C13-C14-C15	114.3(4)	C13-C14-H14A	108.7
C15-C14-H14A	108.7	C13-C14-H14B	108.7
C15-C14-H14B	108.7	H14A-C14-H14B	107.6
C10-C15-C14	113.7(4)	C10-C15-C17	111.3(4)
C14-C15-C17	112.4(4)	C10-C15-H15	106.3
C14-C15-H15	106.3	C17-C15-H15	106.3
S1-C16-H16A	109.5	S1-C16-H16B	109.5
H16A-C16-H16B	109.5	S1-C16-H16C	109.5
H16A-C16-H16C	109.5	H16B-C16-H16C	109.5
C18-C17-C19	110.0(5)	C18-C17-C20	113.3(5)
C19-C17-C20	104.5(4)	C18-C17-C15	113.1(4)
C19-C17-C15	111.0(4)	C20-C17-C15	104.6(4)
C17-C18-H18A	109.5	C17-C18-H18B	109.5
H18A-C18-H18B	109.5	C17-C18-H18C	109.5
H18A-C18-H18C	109.5	H18B-C18-H18C	109.5
C17-C19-H19A	109.5	C17-C19-H19B	109.5
H19A-C19-H19B	109.5	C17-C19-H19C	109.5
H19A-C19-H19C	109.5	H19B-C19-H19C	109.5
O4-C20-O5	123.8(5)	O4-C20-C17	122.3(5)
O5-C20-C17	113.9(4)	O5-C21-H21A	109.5
O5-C21-H21B	109.5	H21A-C21-H21B	109.5
O5-C21-H21C	109.5	H21A-C21-H21C	109.5
H21B-C21-H21C	109.5	P1-C22-H22A	109.5
P1-C22-H22B	109.5	H22A-C22-H22B	109.5
P1-C22-H22C	109.5	H22A-C22-H22C	109.5

H22B-C22-H22C	109.5	P1-C23-H23A	109.5
P1-C23-H23B	109.5	H23A-C23-H23B	109.5
P1-C23-H23C	109.5	H23A-C23-H23C	109.5
H23B-C23-H23C	109.5	P1-C24-H24A	109.5
P1-C24-H24B	109.5	H24A-C24-H24B	109.5
P1-C24-H24C	109.5	H24A-C24-H24C	109.5
H24B-C24-H24C	109.5	N6-B1-N4	106.1(4)
N6-B1-N2	108.0(4)	N4-B1-N2	109.4(4)
N6-B1-H1A	112.(3)	N4-B1-H1A	112.(3)
N2-B1-H1A	109.(3)		

Table 6. Torsion angles (°) for Harman_SS5_128_MTDA.

C1-N1-N2-C3	-0.4(5)	W1-N1-N2-C3	168.9(3)
C1-N1-N2-B1	177.8(4)	W1-N1-N2-B1	-12.9(6)
C4-N3-N4-C6	0.2(6)	W1-N3-N4-C6	173.4(3)
C4-N3-N4-B1	-165.1(4)	W1-N3-N4-B1	8.0(6)
C7-N5-N6-C9	0.4(5)	W1-N5-N6-C9	179.5(3)
C7-N5-N6-B1	172.9(4)	W1-N5-N6-B1	-8.0(6)
N2-N1-C1-C2	0.6(6)	W1-N1-C1-C2	-166.7(4)
N1-C1-C2-C3	-0.6(6)	N1-N2-C3-C2	0.0(6)
B1-N2-C3-C2	-178.0(5)	C1-C2-C3-N2	0.3(6)
N4-N3-C4-C5	-0.9(6)	W1-N3-C4-C5	-173.6(4)
N3-C4-C5-C6	1.2(6)	N3-N4-C6-C5	0.6(6)
B1-N4-C6-C5	163.5(5)	C4-C5-C6-N4	-1.1(6)
N6-N5-C7-C8	-0.4(5)	W1-N5-C7-C8	-179.4(3)
N5-C7-C8-C9	0.3(6)	N5-N6-C9-C8	-0.2(6)
B1-N6-C9-C8	-172.2(5)	C7-C8-C9-N6	0.0(6)
C15-C10-C11-C12	-9.6(7)	W1-C10-C11-C12	109.8(4)
C15-C10-C11-W1	-119.4(5)	C10-C11-C12-C13	-4.3(8)
W1-C11-C12-C13	75.0(6)	C11-C12-C13-C14	-1.8(8)
C11-C12-C13-S1	179.0(4)	O3-S1-C13-C12	-125.5(4)
O2-S1-C13-C12	4.7(5)	C16-S1-C13-C12	120.1(5)
O3-S1-C13-C14	55.3(5)	O2-S1-C13-C14	-174.5(4)
C16-S1-C13-C14	-59.1(4)	C12-C13-C14-C15	20.5(7)
S1-C13-C14-C15	-160.3(4)	C11-C10-C15-C14	27.5(7)
W1-C10-C15-C14	-61.5(5)	C11-C10-C15-C17	-100.7(5)
W1-C10-C15-C17	170.3(3)	C13-C14-C15-C10	-31.6(6)
C13-C14-C15-C17	96.0(5)	C10-C15-C17-C18	55.9(6)
C14-C15-C17-C18	-72.9(6)	C10-C15-C17-C19	-179.9(4)

C14-C15-C17-C19	51.2(6)	C10-C15-C17-C20	-67.8(5)
C14-C15-C17-C20	163.4(4)	C21-O5-C20-O4	-0.1(8)
C21-O5-C20-C17	176.5(4)	C18-C17-C20-O4	175.5(5)
C19-C17-C20-O4	55.7(7)	C15-C17-C20-O4	-61.0(7)
C18-C17-C20-O5	-1.2(7)	C19-C17-C20-O5	-120.9(5)
C15-C17-C20-O5	122.4(5)	C9-N6-B1-N4	116.4(5)
N5-N6-B1-N4	-54.6(6)	C9-N6-B1-N2	-126.3(5)
N5-N6-B1-N2	62.6(6)	C6-N4-B1-N6	-107.3(6)
N3-N4-B1-N6	54.4(6)	C6-N4-B1-N2	136.5(5)
N3-N4-B1-N2	-61.9(6)	C3-N2-B1-N6	128.3(5)
N1-N2-B1-N6	-49.6(6)	C3-N2-B1-N4	-116.7(6)
N1-N2-B1-N4	65.4(6)		

Table 7. Anisotropic atomic displacement parameters ($Å^2$) for Harman_SS5_128_MTDA.

The anisotropic atomic displacement factor exponent takes the form: $-2\pi^2[h^2 a^{*2} U_{11} + ... + 2 h k a^* b^* U_{12}]$

	U_{11}	U_{22}	U_{33}	U_{23}	U_{13}	U_{12}
W1	0.01142(10)	0.01137(9)	0.00880(10)	0.00042(11)	0.00269(7)	-0.00015(11)
S1	0.0172(8)	0.0227(8)	0.0168(7)	-0.0041(6)	0.0075(6)	-0.0051(6)
P1	0.0166(7)	0.0147(6)	0.0116(6)	0.0016(7)	0.0016(5)	-0.0001(7)
O1	0.018(2)	0.016(2)	0.024(2)	0.0029(17)	0.0119(18)	-0.0047(17)
O2	0.024(2)	0.041(3)	0.014(2)	-0.0096(18)	0.0079(18)	-0.009(2)
O3	0.018(2)	0.024(2)	0.035(2)	-0.0052(18)	0.0097(19)	0.0028(18)
O4	0.031(3)	0.024(2)	0.018(2)	0.0042(18)	0.0032(18)	-0.0001(19)
O5	0.025(2)	0.031(2)	0.019(2)	0.0016(18)	0.0017(18)	-0.0032(19)
N1	0.013(2)	0.013(2)	0.017(2)	-0.002(2)	0.0033(18)	0.002(2)
N2	0.011(2)	0.020(2)	0.014(2)	0.003(2)	0.0008(18)	0.001(2)
N3	0.016(3)	0.017(2)	0.010(2)	0.0002(19)	0.0050(19)	-0.0016(19)
N4	0.015(3)	0.013(2)	0.014(2)	0.0021(19)	0.0056(19)	0.0015(19)
N5	0.018(3)	0.012(2)	0.011(2)	-0.0008(17)	0.0038(19)	-0.0008(18)
N6	0.018(3)	0.018(2)	0.008(2)	0.0001(19)	0.0050(19)	0.001(2)
N7	0.013(2)	0.011(2)	0.013(2)	0.0024(18)	0.0049(19)	0.0042(19)
C1	0.014(3)	0.014(3)	0.018(3)	0.000(2)	0.005(2)	0.003(2)
C2	0.014(3)	0.025(3)	0.023(3)	0.007(3)	0.002(2)	-0.003(3)
C3	0.012(3)	0.020(3)	0.024(3)	0.002(2)	0.008(2)	0.000(2)
C4	0.025(3)	0.017(3)	0.013(3)	0.005(2)	0.006(2)	-0.001(2)
C5	0.031(4)	0.013(3)	0.022(3)	0.004(2)	0.004(3)	0.003(3)
C6	0.021(3)	0.018(3)	0.020(3)	-0.004(2)	-0.001(3)	0.004(2)

C7	0.015(3)	0.013(3)	0.014(3)	0.001(2)	0.002(2)	-0.001(2)
C8	0.020(3)	0.022(3)	0.010(3)	0.000(2)	0.000(2)	0.001(2)
C9	0.020(3)	0.015(3)	0.013(3)	0.000(2)	0.005(2)	-0.002(2)
C10	0.015(3)	0.013(3)	0.012(3)	0.004(2)	0.006(2)	0.004(2)
C11	0.010(3)	0.012(3)	0.014(3)	0.001(2)	0.005(2)	0.000(2)
C12	0.020(3)	0.012(3)	0.010(3)	-0.003(2)	-0.002(2)	0.001(2)
C13	0.012(3)	0.018(3)	0.012(3)	0.001(2)	0.004(2)	0.003(2)
C14	0.013(3)	0.017(3)	0.014(3)	0.000(2)	0.002(2)	-0.004(2)
C15	0.010(3)	0.014(3)	0.012(3)	0.000(2)	0.001(2)	0.003(2)
C16	0.028(4)	0.028(3)	0.016(3)	-0.001(2)	0.009(3)	-0.008(3)
C17	0.020(3)	0.018(3)	0.021(3)	0.007(2)	0.004(3)	0.006(3)
C18	0.036(4)	0.016(3)	0.029(3)	0.002(3)	0.007(3)	0.003(3)
C19	0.022(4)	0.038(4)	0.018(3)	0.010(3)	0.000(3)	0.013(3)
C20	0.025(3)	0.015(3)	0.014(3)	0.001(2)	-0.009(2)	-0.003(2)
C21	0.034(4)	0.040(4)	0.020(3)	0.001(3)	0.006(3)	-0.015(3)
C22	0.034(4)	0.037(4)	0.019(3)	0.002(3)	0.002(3)	-0.015(3)
C23	0.025(3)	0.020(3)	0.021(3)	-0.001(2)	-0.007(3)	-0.003(3)
C24	0.028(4)	0.035(4)	0.020(3)	-0.004(3)	-0.003(3)	0.014(3)
B1	0.014(3)	0.020(3)	0.014(3)	0.000(3)	0.007(3)	-0.001(3)

Table 8. Hydrogen atomic coordinates and isotropic atomic displacement parameters ($Å^2$) for Harman_SS5_128_MTDA.

	x/a	y/b	z/c	U(eq)
H1	0.2234	0.0806	0.6149	0.018
H2	0.0201	0.0904	0.6451	0.025
H3	0.0140	0.2542	0.7133	0.022
H4	0.4326	0.5430	0.5970	0.022
H5	0.3068	0.6870	0.6321	0.026
H6	0.1783	0.6007	0.7064	0.024
H7	0.6075	0.2969	0.8036	0.017
H8	0.5302	0.3500	0.9083	0.021
H9	0.3178	0.3886	0.8753	0.019
H10	0.491(5)	0.108(4)	0.717(3)	0.029(17)
H11	0.411(4)	0.076(4)	0.607(2)	0.014
H12	0.5301	0.0938	0.5236	0.017
H14A	0.7459	0.2496	0.6459	0.018
H14B	0.8127	0.1391	0.6564	0.018
H15	0.6825	0.2044	0.7380	0.014

H16A	0.8626	0.2548	0.4720	0.035
H16B	0.8769	0.2675	0.5508	0.035
H16C	0.7578	0.3031	0.5066	0.035
H18A	0.5863	-0.0599	0.6915	0.04
H18B	0.7001	-0.1200	0.7268	0.04
H18C	0.7058	-0.0556	0.6598	0.04
H19A	0.8809	0.0333	0.7219	0.04
H19B	0.8649	-0.0150	0.7927	0.04
H19C	0.8660	0.1103	0.7825	0.04
H21A	0.4952	-0.0909	0.8862	0.047
H21B	0.5092	0.0348	0.8878	0.047
H21C	0.6166	-0.0386	0.9176	0.047
H22A	0.4418	0.4232	0.4901	0.045
H22B	0.3713	0.3600	0.4293	0.045
H22C	0.4886	0.3111	0.4687	0.045
H23A	0.3542	0.1234	0.4802	0.034
H23B	0.2501	0.1881	0.4383	0.034
H23C	0.2293	0.1315	0.5059	0.034
H24A	0.1413	0.3255	0.5459	0.042
H24B	0.1604	0.3580	0.4722	0.042
H24C	0.2086	0.4326	0.5333	0.042
H1A	0.161(5)	0.404(4)	0.767(2)	0.025(15)

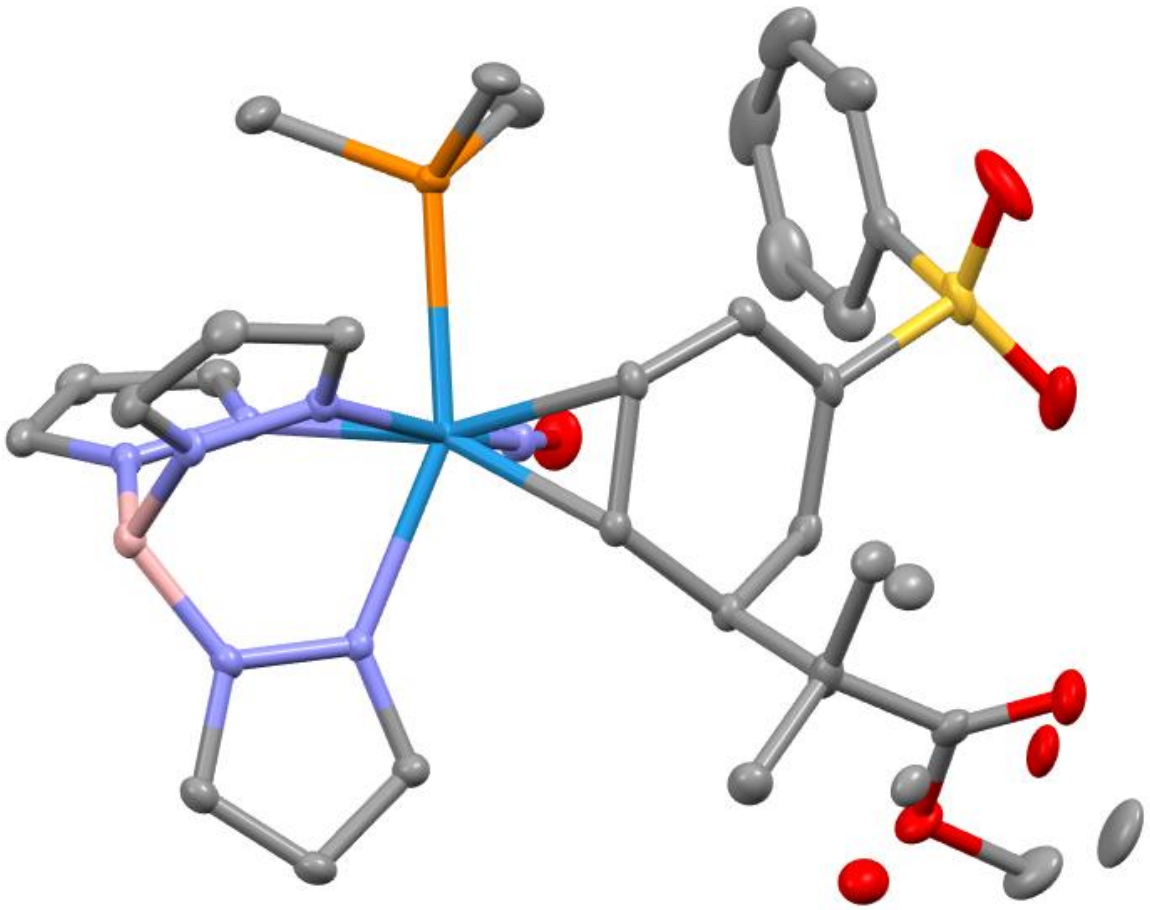

Crystal Structure Report for 9 in Chapter 4

A **yellow block-like** specimen of **$C_{29}H_{39}BN_7O_5PSW$**, approximate dimensions **0.130** mm x **0.260** mm x **0.339** mm, was coated with Paratone oil and mounted on a MiTeGen MicroLoop. The X-ray intensity data were measured on a Bruker Kappa APEXII Duo system equipped with a fine-focus sealed tube (Mo K_α, λ = 0.71073 Å) and a graphite monochromator.

The total exposure time was 1.54 hours. The frames were integrated with the Bruker SAINT software package[7] using a narrow-frame algorithm. The integration of the data using a **monoclinic** unit cell yielded a total of **92725** reflections to a maximum θ angle of **31.54**° (**0.68** Å resolution), of which **10767** were independent (average redundancy **8.612**, completeness = **99.9**%, R_{int} = **3.88**%, R_{sig} = **2.18**%) and **9831** (**91.31**%) were greater than 2σ(F^2). The final cell constants of a = **12.6795(14)** Å, b = **21.036(2)** Å, c = **12.8270(14)** Å, β = **109.402(2)**°, volume = **3227.0(6)** $Å^3$, are based upon the refinement of the XYZ-centroids of **9795** reflections above 20 σ(I) with **5.132**° < 2θ < **62.90**°. Data were corrected for absorption effects using the Multi-Scan method (SADABS).[1] The ratio of minimum to maximum apparent transmission was **0.718**. The calculated minimum and maximum transmission coefficients (based on crystal size) are **0.3630** and **0.6420**.

7 Bruker (2012). Saint; SADABS; APEX3. Bruker AXS Inc., Madison, Wisconsin, USA.

The structure was solved and refined using the Bruker SHELXTL Software Package[8] within APEX3 [1] and OLEX2,[9] using the space group **P 2_1/n**, with Z = **4** for the formula unit, **$C_{29}H_{39}BN_7O_5PSW$**. Non-hydrogen atoms were refined anisotropically. The B-H hydrogen atom was located in the electron density map and refined isotropcially. All other hydrogen atoms were placed in geometrically calculated positions with U_{iso} = 1.2U_{equiv} of the parent atom (U_{iso} = 1.5U_{equiv} for methyl). The relative occupancy of the two positions of the disordered ester fragment was freely refined and no constraints or restraints were needed. The final anisotropic full-matrix least-squares refinement on F^2 with **464** variables converged at R1 = **2.47**%, for the observed data and wR2 = **4.51**% for all data. The goodness-of-fit was **1.216**. The largest peak in the final difference electron density synthesis was **0.830** $e^-/Å^3$ and the largest hole was **-1.204** $e^-/Å^3$ with an RMS deviation of **0.095** $e^-/Å^3$. On the basis of the final model, the calculated density was **1.695** g/cm^3 and F(000), **1648** e^-.

Table 1. Sample and crystal data for Harman_SS7_34_2.

Identification code	Harman_SS7_34_2	
Chemical formula	$C_{29}H_{39}BN_7O_5PSW$	
Formula weight	823.36 g/mol	
Temperature	100(2) K	
Wavelength	0.71073 Å	
Crystal size	0.130 x 0.260 x 0.339 mm	
Crystal habit	yellow block	
Crystal system	monoclinic	
Space group	P 2_1/n	
Unit cell dimensions	a = 12.6795(14) Å	α = 90°
	b = 21.036(2) Å	β = 109.402(2)°
	c = 12.8270(14) Å	γ = 90°
Volume	3227.0(6) $Å^3$	
Z	4	
Density (calculated)	1.695 g/cm^3	
Absorption coefficient	3.744 mm^{-1}	
F(000)	1648	

Table 2. Data collection and structure refinement for Harman_SS7_34_2.

Diffractometer	Bruker Kappa APEXII Duo
Radiation source	fine-focus sealed tube (Mo K_α, λ = 0.71073 Å)
Theta range for data collection	1.94 to 31.54°
Index ranges	-18<=h<=18, -30<=k<=30, -18<=l<=18
Reflections collected	92725
Independent reflections	10767 [R(int) = 0.0388]

8 Sheldrick, G. M. (2015). Acta Cryst. A**71**, 3-8.
9 Dolomanov, O. V.; Bourhis, L. J.; Gildea, R. J.; Howard, J. A. K.; Puschmann, H. J. Appl. Cryst. (2009). 42, 339-341.

Coverage of independent reflections	99.9%	
Absorption correction	Multi-Scan	
Max. and min. transmission	0.6420 and 0.3630	
Structure solution technique	direct methods	
Structure solution program	SHELXT 2018/2 (Sheldrick, 2018)	
Refinement method	Full-matrix least-squares on F^2	
Refinement program	SHELXL-2018/3 (Sheldrick, 2018)	
Function minimized	$\Sigma w(F_o^2 - F_c^2)^2$	
Data / restraints / parameters	10767 / 0 / 464	
Goodness-of-fit on F^2	1.216	
Δ/σ_{max}	0.002	
Final R indices	9831 data; I>2σ(I)	R1 = 0.0247, wR2 = 0.0441
	all data	R1 = 0.0293, wR2 = 0.0451
Weighting scheme	$w=1/[\sigma^2(F_o^2)+4.6293P]$ where $P=(F_o^2+2F_c^2)/3$	
Largest diff. peak and hole	0.830 and -1.204 eÅ^{-3}	
R.M.S. deviation from mean	0.095 eÅ^{-3}	

Table 3. Atomic coordinates and equivalent isotropic atomic displacement parameters (Å^2) for Harman_SS7_34_2.

U(eq) is defined as one third of the trace of the orthogonalized U_{ij} tensor.

	x/a	y/b	z/c	U(eq)
W1	0.41518(2)	0.35609(2)	0.68423(2)	0.00986(2)
S1	0.35038(5)	0.39169(3)	0.07284(4)	0.02054(11)
P1	0.60522(5)	0.33241(3)	0.81990(4)	0.01456(10)
O1	0.31295(16)	0.25745(8)	0.79032(15)	0.0263(4)
O2	0.44194(19)	0.42614(9)	0.14925(14)	0.0363(5)
O3	0.23960(18)	0.39850(9)	0.08103(15)	0.0330(4)
N1	0.51709(15)	0.41333(8)	0.60109(14)	0.0129(3)
N2	0.52126(15)	0.39363(8)	0.50060(14)	0.0132(3)
N3	0.45112(15)	0.27358(8)	0.59424(14)	0.0128(3)
N4	0.46924(15)	0.27816(8)	0.49579(14)	0.0132(3)
N5	0.28855(14)	0.36537(8)	0.51454(13)	0.0118(3)
N6	0.32125(15)	0.35974(8)	0.42341(13)	0.0133(3)
N7	0.35074(16)	0.30062(8)	0.74839(15)	0.0150(3)

C00F	0.6977(2)	0.29244(12)	0.7580(2)	0.0245(5)
C00X	0.6030(2)	0.28097(13)	0.9328(2)	0.0284(5)
C1	0.59106(18)	0.46129(10)	0.63312(18)	0.0158(4)
C2	0.64346(19)	0.47233(10)	0.55516(19)	0.0186(4)
C3	0.59604(18)	0.42864(10)	0.47248(18)	0.0175(4)
C4	0.46102(18)	0.21188(10)	0.62276(18)	0.0163(4)
C5	0.48768(19)	0.17623(10)	0.54296(19)	0.0190(4)
C6	0.49116(18)	0.21990(10)	0.46374(18)	0.0170(4)
C7	0.17959(18)	0.38033(10)	0.47625(17)	0.0152(4)
C8	0.14152(19)	0.38496(10)	0.36128(17)	0.0172(4)
C9	0.23400(19)	0.37169(10)	0.33101(17)	0.0157(4)
C10	0.43397(18)	0.43802(9)	0.80305(16)	0.0136(4)
C11	0.32761(17)	0.44081(9)	0.71339(16)	0.0130(4)
C12	0.21904(18)	0.44021(10)	0.74129(17)	0.0143(4)
C13	0.23013(19)	0.40094(10)	0.84675(18)	0.0166(4)
C013	0.69702(19)	0.39695(12)	0.89093(19)	0.0228(5)
C14	0.34102(19)	0.40925(10)	0.93647(17)	0.0161(4)
C15	0.43457(19)	0.42517(10)	0.91516(17)	0.0158(4)
C16	0.3872(2)	0.30988(11)	0.09109(18)	0.0183(4)
C17	0.3061(2)	0.26440(12)	0.0419(2)	0.0272(5)
C18	0.3365(3)	0.20040(13)	0.0532(3)	0.0407(8)
C19	0.4449(3)	0.18282(15)	0.1134(3)	0.0470(9)
C20	0.5235(3)	0.22781(17)	0.1617(3)	0.0431(8)
C21	0.4958(2)	0.29206(14)	0.1509(2)	0.0296(6)
C22	0.1740(2)	0.50991(11)	0.74476(19)	0.0195(4)
C23	0.1338(2)	0.53885(11)	0.62792(19)	0.0215(4)
B1	0.4422(2)	0.34170(11)	0.43267(19)	0.0138(4)
O4	0.0837(3)	0.54064(16)	0.8770(2)	0.0276(8)
O5	0.0023(3)	0.47072(16)	0.7411(3)	0.0220(7)
C24	0.2713(4)	0.5567(2)	0.8175(4)	0.0192(8)
C25	0.0858(3)	0.51063(18)	0.7970(3)	0.0174(7)
C26	0.9148(3)	0.4622(2)	0.7902(4)	0.0309(10)
O4A	0.9721(5)	0.4641(3)	0.6762(6)	0.0265(14)
O5A	0.0348(5)	0.5121(3)	0.8425(5)	0.0236(14)
C24A	0.2331(8)	0.5473(4)	0.8304(8)	0.0229(18)
C25A	0.0451(8)	0.4915(4)	0.7470(7)	0.0158(14)
C26A	0.9303(7)	0.4921(4)	0.8561(8)	0.033(2)

Table 4. Bond lengths (Å) for Harman_SS7_34_2.

W1-N7	1.7757(18)	W1-C11	2.197(2)
W1-N3	2.2140(17)	W1-N5	2.2431(17)
W1-C10	2.2602(19)	W1-N1	2.2743(17)
W1-P1	2.5094(6)	S1-O2	1.441(2)
S1-O3	1.450(2)	S1-C14	1.753(2)
S1-C16	1.778(2)	P1-C00X	1.816(2)
P1-C013	1.823(2)	P1-C00F	1.825(2)
O1-N7	1.231(2)	N1-C1	1.345(3)
N1-N2	1.372(2)	N2-C3	1.341(3)
N2-B1	1.542(3)	N3-C4	1.343(3)
N3-N4	1.360(2)	N4-C6	1.350(3)
N4-B1	1.541(3)	N5-C7	1.341(3)
N5-N6	1.369(2)	N6-C9	1.349(3)
N6-B1	1.545(3)	C00F-H00A	0.98
C00F-H00B	0.98	C00F-H00C	0.98
C00X-H00D	0.98	C00X-H00E	0.98
C00X-H00F	0.98	C1-C2	1.392(3)
C1-H1	0.95	C2-C3	1.381(3)
C2-H2	0.95	C3-H3	0.95
C4-C5	1.398(3)	C4-H4	0.95
C5-C6	1.381(3)	C5-H5	0.95
C6-H6	0.95	C7-C8	1.394(3)
C7-H7	0.95	C8-C9	1.381(3)
C8-H8	0.95	C9-H9	0.95
C10-C11	1.454(3)	C10-C15	1.461(3)
C10-H10	1.0	C11-C12	1.533(3)
C11-H11	1.0	C12-C13	1.551(3)
C12-C22	1.580(3)	C12-H12	1.0
C13-C14	1.502(3)	C13-H13A	0.99
C13-H13B	0.99	C013-H01A	0.98
C013-H01B	0.98	C013-H01C	0.98
C14-C15	1.345(3)	C15-H15	0.95
C16-C21	1.387(3)	C16-C17	1.393(3)
C17-C18	1.395(4)	C17-H17	0.95
C18-C19	1.385(5)	C18-H18	0.95
C19-C20	1.365(5)	C19-H19	0.95
C20-C21	1.392(4)	C20-H20	0.95
C21-H21	0.95	C22-C24A	1.357(9)
C22-C25	1.482(4)	C22-C23	1.539(3)

C22-C24	1.611(5)	C22-C25A	1.689(10)
C23-H23A	0.98	C23-H23B	0.98
C23-H23C	0.98	B1-H1A	1.06(3)
O4-C25	1.213(5)	O5-C25	1.355(5)
O5-C26	1.457(5)	C24-H24A	0.98
C24-H24B	0.98	C24-H24C	0.98
C26-H26A	0.98	C26-H26B	0.98
C26-H26C	0.98	O4A-C25A	1.207(10)
O5A-C25A	1.346(9)	O5A-C26A	1.455(10)
C24A-H24D	0.98	C24A-H24E	0.98
C24A-H24F	0.98	C26A-H26D	0.98
C26A-H26E	0.98	C26A-H26F	0.98

Table 5. Bond angles (°) for Harman_SS7_34_2.

N7-W1-C11	96.76(8)	N7-W1-N3	86.14(7)
C11-W1-N3	158.13(7)	N7-W1-N5	102.45(7)
C11-W1-N5	81.68(7)	N3-W1-N5	76.54(6)
N7-W1-C10	98.63(8)	C11-W1-C10	38.05(7)
N3-W1-C10	162.84(7)	N5-W1-C10	117.98(7)
N7-W1-N1	170.33(7)	C11-W1-N1	92.78(7)
N3-W1-N1	85.59(6)	N5-W1-N1	80.44(6)
C10-W1-N1	87.91(7)	N7-W1-P1	91.83(6)
C11-W1-P1	117.79(6)	N3-W1-P1	83.65(5)
N5-W1-P1	154.57(4)	C10-W1-P1	79.74(6)
N1-W1-P1	82.30(5)	O2-S1-O3	118.80(13)
O2-S1-C14	110.18(11)	O3-S1-C14	107.78(11)
O2-S1-C16	106.27(12)	O3-S1-C16	107.71(11)
C14-S1-C16	105.26(10)	C00X-P1-C013	102.80(12)
C00X-P1-C00F	104.78(12)	C013-P1-C00F	99.48(12)
C00X-P1-W1	113.95(9)	C013-P1-W1	120.35(8)
C00F-P1-W1	113.41(8)	C1-N1-N2	105.84(17)
C1-N1-W1	134.49(14)	N2-N1-W1	119.08(12)
C3-N2-N1	109.77(17)	C3-N2-B1	128.48(18)
N1-N2-B1	121.62(16)	C4-N3-N4	106.97(17)
C4-N3-W1	129.23(14)	N4-N3-W1	123.79(13)
C6-N4-N3	109.50(17)	C6-N4-B1	131.26(18)
N3-N4-B1	118.19(16)	C7-N5-N6	105.96(16)
C7-N5-W1	133.95(14)	N6-N5-W1	119.92(12)
C9-N6-N5	109.96(17)	C9-N6-B1	128.05(17)

N5-N6-B1	121.99(16)	O1-N7-W1	173.33(16)
P1-C00F-H00A	109.5	P1-C00F-H00B	109.5
H00A-C00F-H00B	109.5	P1-C00F-H00C	109.5
H00A-C00F-H00C	109.5	H00B-C00F-H00C	109.5
P1-C00X-H00D	109.5	P1-C00X-H00E	109.5
H00D-C00X-H00E	109.5	P1-C00X-H00F	109.5
H00D-C00X-H00F	109.5	H00E-C00X-H00F	109.5
N1-C1-C2	110.88(19)	N1-C1-H1	124.6
C2-C1-H1	124.6	C3-C2-C1	104.52(19)
C3-C2-H2	127.7	C1-C2-H2	127.7
N2-C3-C2	108.98(19)	N2-C3-H3	125.5
C2-C3-H3	125.5	N3-C4-C5	110.03(19)
N3-C4-H4	125.0	C5-C4-H4	125.0
C6-C5-C4	104.86(18)	C6-C5-H5	127.6
C4-C5-H5	127.6	N4-C6-C5	108.62(19)
N4-C6-H6	125.7	C5-C6-H6	125.7
N5-C7-C8	110.87(19)	N5-C7-H7	124.6
C8-C7-H7	124.6	C9-C8-C7	104.79(19)
C9-C8-H8	127.6	C7-C8-H8	127.6
N6-C9-C8	108.41(18)	N6-C9-H9	125.8
C8-C9-H9	125.8	C11-C10-C15	119.10(19)
C11-C10-W1	68.60(11)	C15-C10-W1	119.19(14)
C11-C10-H10	114.2	C15-C10-H10	114.2
W1-C10-H10	114.2	C10-C11-C12	118.93(17)
C10-C11-W1	73.34(11)	C12-C11-W1	125.23(14)
C10-C11-H11	111.4	C12-C11-H11	111.4
W1-C11-H11	111.4	C11-C12-C13	112.31(17)
C11-C12-C22	111.11(17)	C13-C12-C22	113.50(17)
C11-C12-H12	106.5	C13-C12-H12	106.5
C22-C12-H12	106.5	C14-C13-C12	113.38(18)
C14-C13-H13A	108.9	C12-C13-H13A	108.9
C14-C13-H13B	108.9	C12-C13-H13B	108.9
H13A-C13-H13B	107.7	P1-C013-H01A	109.5
P1-C013-H01B	109.5	H01A-C013-H01B	109.5
P1-C013-H01C	109.5	H01A-C013-H01C	109.5
H01B-C013-H01C	109.5	C15-C14-C13	122.50(19)
C15-C14-S1	118.90(17)	C13-C14-S1	118.42(16)
C14-C15-C10	122.0(2)	C14-C15-H15	119.0
C10-C15-H15	119.0	C21-C16-C17	120.9(2)

C21-C16-S1	120.2(2)	C17-C16-S1	118.90(19)
C16-C17-C18	118.6(3)	C16-C17-H17	120.7
C18-C17-H17	120.7	C19-C18-C17	120.3(3)
C19-C18-H18	119.8	C17-C18-H18	119.8
C20-C19-C18	120.5(3)	C20-C19-H19	119.7
C18-C19-H19	119.7	C19-C20-C21	120.4(3)
C19-C20-H20	119.8	C21-C20-H20	119.8
C16-C21-C20	119.3(3)	C16-C21-H21	120.4
C20-C21-H21	120.4	C24A-C22-C23	118.3(5)
C25-C22-C23	112.4(2)	C24A-C22-C12	116.9(5)
C25-C22-C12	110.9(2)	C23-C22-C12	110.21(18)
C25-C22-C24	106.2(3)	C23-C22-C24	105.4(2)
C12-C22-C24	111.6(2)	C24A-C22-C25A	113.4(5)
C23-C22-C25A	95.6(3)	C12-C22-C25A	98.6(3)
C22-C23-H23A	109.5	C22-C23-H23B	109.5
H23A-C23-H23B	109.5	C22-C23-H23C	109.5
H23A-C23-H23C	109.5	H23B-C23-H23C	109.5
N4-B1-N2	109.16(17)	N4-B1-N6	107.18(17)
N2-B1-N6	108.17(16)	N4-B1-H1A	110.8(14)
N2-B1-H1A	110.9(14)	N6-B1-H1A	110.5(14)
C25-O5-C26	115.0(4)	C22-C24-H24A	109.5
C22-C24-H24B	109.5	H24A-C24-H24B	109.5
C22-C24-H24C	109.5	H24A-C24-H24C	109.5
H24B-C24-H24C	109.5	O4-C25-O5	122.4(3)
O4-C25-C22	128.3(4)	O5-C25-C22	109.3(3)
O5-C26-H26A	109.5	O5-C26-H26B	109.5
H26A-C26-H26B	109.5	O5-C26-H26C	109.5
H26A-C26-H26C	109.5	H26B-C26-H26C	109.5
C25A-O5A-C26A	112.6(8)	C22-C24A-H24D	109.5
C22-C24A-H24E	109.5	H24D-C24A-H24E	109.5
C22-C24A-H24F	109.5	H24D-C24A-H24F	109.5
H24E-C24A-H24F	109.5	O4A-C25A-O5A	123.8(8)
O4A-C25A-C22	127.0(6)	O5A-C25A-C22	109.2(7)
O5A-C26A-H26D	109.5	O5A-C26A-H26E	109.5
H26D-C26A-H26E	109.5	O5A-C26A-H26F	109.5
H26D-C26A-H26F	109.5	H26E-C26A-H26F	109.5

Table 6. Torsion angles (°) for Harman_SS7_34_2.

C1-N1-N2-C3	0.1(2)	W1-N1-N2-C3	-172.29(14)
C1-N1-N2-B1	-175.97(18)	W1-N1-N2-B1	11.6(2)
C4-N3-N4-C6	-0.5(2)	W1-N3-N4-C6	178.68(14)
C4-N3-N4-B1	169.06(18)	W1-N3-N4-B1	-11.7(2)
C7-N5-N6-C9	0.6(2)	W1-N5-N6-C9	-175.34(13)
C7-N5-N6-B1	-179.05(18)	W1-N5-N6-B1	5.0(2)
N2-N1-C1-C2	-0.5(2)	W1-N1-C1-C2	170.18(15)
N1-C1-C2-C3	0.7(3)	N1-N2-C3-C2	0.3(2)
B1-N2-C3-C2	176.1(2)	C1-C2-C3-N2	-0.6(2)
N4-N3-C4-C5	1.0(2)	W1-N3-C4-C5	-178.12(15)
N3-C4-C5-C6	-1.1(3)	N3-N4-C6-C5	-0.2(2)
B1-N4-C6-C5	-167.9(2)	C4-C5-C6-N4	0.8(2)
N6-N5-C7-C8	-0.5(2)	W1-N5-C7-C8	174.64(14)
N5-C7-C8-C9	0.2(2)	N5-N6-C9-C8	-0.5(2)
B1-N6-C9-C8	179.12(19)	C7-C8-C9-N6	0.2(2)
C15-C10-C11-C12	9.1(3)	W1-C10-C11-C12	121.51(17)
C15-C10-C11-W1	-112.42(17)	C10-C11-C12-C13	-32.0(2)
W1-C11-C12-C13	57.4(2)	C10-C11-C12-C22	96.3(2)
W1-C11-C12-C22	-174.26(14)	C11-C12-C13-C14	39.3(2)
C22-C12-C13-C14	-87.8(2)	C12-C13-C14-C15	-26.5(3)
C12-C13-C14-S1	158.33(15)	O2-S1-C14-C15	28.9(2)
O3-S1-C14-C15	160.01(18)	C16-S1-C14-C15	-85.25(19)
O2-S1-C14-C13	-155.75(17)	O3-S1-C14-C13	-24.7(2)
C16-S1-C14-C13	90.06(18)	C13-C14-C15-C10	2.5(3)
S1-C14-C15-C10	177.59(15)	C11-C10-C15-C14	7.1(3)
W1-C10-C15-C14	-73.2(2)	O2-S1-C16-C21	-12.9(2)
O3-S1-C16-C21	-141.19(19)	C14-S1-C16-C21	104.0(2)
O2-S1-C16-C17	168.91(19)	O3-S1-C16-C17	40.6(2)
C14-S1-C16-C17	-74.2(2)	C21-C16-C17-C18	-0.4(4)
S1-C16-C17-C18	177.8(2)	C16-C17-C18-C19	0.7(4)
C17-C18-C19-C20	-0.5(4)	C18-C19-C20-C21	-0.1(4)
C17-C16-C21-C20	-0.2(4)	S1-C16-C21-C20	-178.3(2)

C19-C20-C21-C16	0.5(4)	C11-C12-C22-C24A	-70.6(5)
C13-C12-C22-C24A	57.1(6)	C11-C12-C22-C25	-166.6(2)
C13-C12-C22-C25	-38.8(3)	C11-C12-C22-C23	68.4(2)
C13-C12-C22-C23	-163.92(19)	C11-C12-C22-C24	-48.3(3)
C13-C12-C22-C24	79.4(3)	C11-C12-C22-C25A	167.7(3)
C13-C12-C22-C25A	-64.6(3)	C6-N4-B1-N2	-128.0(2)
N3-N4-B1-N2	65.1(2)	C6-N4-B1-N6	115.0(2)
N3-N4-B1-N6	-51.9(2)	C3-N2-B1-N4	119.1(2)
N1-N2-B1-N4	-65.6(2)	C3-N2-B1-N6	-124.6(2)
N1-N2-B1-N6	50.7(2)	C9-N6-B1-N4	-123.5(2)
N5-N6-B1-N4	56.1(2)	C9-N6-B1-N2	118.9(2)
N5-N6-B1-N2	-61.5(2)	C26-O5-C25-O4	-5.3(5)
C26-O5-C25-C22	174.4(3)	C23-C22-C25-O4	-113.5(4)
C12-C22-C25-O4	122.7(4)	C24-C22-C25-O4	1.2(5)
C23-C22-C25-O5	66.9(3)	C12-C22-C25-O5	-57.0(3)
C24-C22-C25-O5	-178.4(3)	C26A-O5A-C25A-O4A	5.7(10)
C26A-O5A-C25A-C22	-173.8(5)	C24A-C22-C25A-O4A	172.9(8)
C23-C22-C25A-O4A	48.7(7)	C12-C22-C25A-O4A	-62.8(7)
C24A-C22-C25A-O5A	-7.6(7)	C23-C22-C25A-O5A	-131.8(5)
C12-C22-C25A-O5A	116.7(5)		

Table 7. Anisotropic atomic displacement parameters (Å^2) for Harman_SS7_34_2.

The anisotropic atomic displacement factor exponent takes the form:
$-2\pi^2[h^2 a^{*2} U_{11} + ... + 2 h k a^* b^* U_{12}]$

	U_{11}	U_{22}	U_{33}	U_{23}	U_{13}	U_{12}
W1	0.01053(3)	0.01043(3)	0.00854(3)	0.00106(3)	0.00305(2)	0.00058(3)
S1	0.0330(3)	0.0190(2)	0.0130(2)	-0.00002(19)	0.0122(2)	-0.0007(2)
P1	0.0125(3)	0.0183(2)	0.0118(2)	0.00125(19)	0.0025(2)	0.00303(19)
O1	0.0351(10)	0.0194(8)	0.0318(9)	0.0089(7)	0.0210(8)	-0.0012(7)

O2	0.0629(14)	0.0294(9)	0.0157(8)	-0.0056(7)	0.0116(9)	-0.0194(9)
O3	0.0430(12)	0.0396(11)	0.0269(9)	0.0087(8)	0.0255(9)	0.0161(9)
N1	0.0134(8)	0.0127(7)	0.0127(7)	0.0012(6)	0.0046(6)	0.0002(6)
N2	0.0142(8)	0.0143(8)	0.0132(8)	0.0014(6)	0.0075(6)	-0.0003(6)
N3	0.0144(8)	0.0133(7)	0.0109(7)	0.0007(6)	0.0044(6)	0.0017(6)
N4	0.0131(8)	0.0153(8)	0.0113(7)	-0.0016(6)	0.0042(6)	0.0009(6)
N5	0.0122(8)	0.0135(8)	0.0105(7)	-0.0004(6)	0.0048(6)	0.0003(6)
N6	0.0151(8)	0.0149(7)	0.0098(7)	0.0005(6)	0.0040(6)	0.0007(7)
N7	0.0177(9)	0.0131(8)	0.0151(8)	0.0016(6)	0.0066(7)	0.0009(6)
C00F	0.0149(11)	0.0310(12)	0.0250(11)	-0.0050(9)	0.0031(9)	0.0058(9)
C00X	0.0318(14)	0.0313(13)	0.0196(11)	0.0123(10)	0.0051(10)	0.0076(11)
C1	0.0144(10)	0.0139(9)	0.0180(10)	0.0010(7)	0.0038(8)	-0.0007(7)
C2	0.0167(10)	0.0165(9)	0.0243(11)	0.0028(8)	0.0090(9)	-0.0028(8)
C3	0.0172(10)	0.0176(9)	0.0214(10)	0.0041(8)	0.0115(8)	0.0003(8)
C4	0.0162(10)	0.0133(9)	0.0180(10)	0.0022(7)	0.0039(8)	0.0004(7)
C5	0.0173(11)	0.0128(9)	0.0250(11)	-0.0021(8)	0.0046(9)	0.0012(8)
C6	0.0140(10)	0.0171(9)	0.0191(10)	-0.0064(8)	0.0045(8)	0.0008(8)
C7	0.0130(10)	0.0177(9)	0.0142(9)	-0.0001(7)	0.0036(7)	0.0013(7)
C8	0.0159(10)	0.0188(10)	0.0136(9)	0.0015(7)	0.0005(8)	0.0023(8)
C9	0.0181(10)	0.0159(9)	0.0116(8)	0.0006(7)	0.0028(8)	0.0008(7)
C10	0.0176(10)	0.0128(8)	0.0114(8)	-0.0015(7)	0.0062(7)	-0.0005(7)
C11	0.0156(10)	0.0119(8)	0.0125(8)	0.0001(7)	0.0060(7)	0.0011(7)
C12	0.0150(10)	0.0156(9)	0.0138(9)	0.0008(7)	0.0067(7)	0.0022(7)
C13	0.0196(11)	0.0161(9)	0.0186(10)	0.0026(8)	0.0123(8)	0.0021(8)
C013	0.0145(10)	0.0295(12)	0.0188(10)	-0.0038(9)	-0.0021(8)	0.0011(9)
C14	0.0236(11)	0.0151(9)	0.0117(9)	0.0007(7)	0.0088(8)	0.0028(8)
C15	0.0196(10)	0.0138(9)	0.0129(9)	-0.0009(7)	0.0039(8)	0.0013(8)
C16	0.0215(11)	0.0217(10)	0.0145(9)	0.0033(8)	0.0098(8)	-0.0002(8)
C17	0.0295(14)	0.0286(12)	0.0261(12)	0.0026(10)	0.0129(10)	-0.0067(10)
C18	0.066(2)	0.0242(13)	0.0442(17)	-0.0018(12)	0.0347(17)	-0.0130(14)
C19	0.077(3)	0.0316(15)	0.053(2)	0.0209(14)	0.050(2)	0.0205(16)
C20	0.0433(18)	0.057(2)	0.0384(16)	0.0269(15)	0.0261(14)	0.0272(16)
C21	0.0261(13)	0.0447(15)	0.0197(11)	0.0109(11)	0.0100(10)	0.0044(11)
C22	0.0244(12)	0.0189(10)	0.0187(10)	0.0042(8)	0.0119(9)	0.0087(9)
C23	0.0222(12)	0.0221(11)	0.0196(10)	0.0040(8)	0.0063(9)	0.0052(9)
B1	0.0151(11)	0.0151(10)	0.0121(9)	0.0001(7)	0.0058(8)	0.0009(8)
O4	0.0272(17)	0.0344(17)	0.0266(15)	-0.0079(12)	0.0162(13)	0.0024(13)
O5	0.0135(15)	0.0238(15)	0.0304(19)	-0.0008(13)	0.0095(14)	-0.0026(12)
C24	0.018(2)	0.0136(18)	0.024(2)	-0.0050(14)	0.0043(16)	0.0003(16)

C25	0.0146(16)	0.0173(15)	0.0207(18)	0.0034(14)	0.0064(15)	0.0057(14)
C26	0.0192(19)	0.034(2)	0.044(3)	0.0105(19)	0.0173(18)	0.0009(16)
O4A	0.022(3)	0.026(3)	0.028(3)	-0.006(2)	0.004(3)	0.000(2)
O5A	0.025(3)	0.029(3)	0.023(3)	0.000(2)	0.017(2)	0.006(2)
C24A	0.022(5)	0.018(4)	0.027(4)	-0.004(3)	0.005(4)	-0.003(3)
C25A	0.016(4)	0.010(3)	0.023(4)	-0.001(3)	0.008(4)	0.001(3)
C26A	0.035(5)	0.033(4)	0.046(5)	0.009(4)	0.034(4)	0.006(3)

Table 8. Hydrogen atomic coordinates and isotropic atomic displacement parameters (Å^2) for Harman_SS7_34_2.

	x/a	y/b	z/c	U(eq)
H00A	0.6642	0.2520	0.7256	0.037
H00B	0.7701	0.2844	0.8149	0.037
H00C	0.7084	0.3195	0.7001	0.037
H00D	0.5666	0.3031	0.9789	0.043
H00E	0.6798	0.2700	0.9777	0.043
H00F	0.5615	0.2421	0.9028	0.043
H1	0.6056	0.4845	0.7000	0.019
H2	0.6993	0.5030	0.5581	0.022
H3	0.6136	0.4241	0.4064	0.021
H4	0.4513	0.1949	0.6876	0.02
H5	0.5006	0.1317	0.5432	0.023
H6	0.5064	0.2105	0.3977	0.02
H7	0.1344	0.3869	0.5214	0.018
H8	0.0681	0.3950	0.3142	0.021
H9	0.2359	0.3711	0.2576	0.019
H10	0.4891	0.4710	0.7986	0.016
H11	0.3271	0.4755	0.6600	0.016
H12	0.1619	0.4180	0.6787	0.017
H13A	0.1699	0.4137	0.8756	0.02
H13B	0.2195	0.3554	0.8267	0.02
H01A	0.7215	0.4210	0.8376	0.034
H01B	0.7624	0.3793	0.9483	0.034
H01C	0.6565	0.4253	0.9251	0.034
H15	0.5031	0.4282	0.9748	0.019
H17	0.2316	0.2767	1.0014	0.033
H18	0.2825	0.1687	1.0195	0.049
H19	0.4647	0.1391	1.1212	0.056

H20	0.5976	0.2152	1.2030	0.052
H21	0.5507	0.3234	1.1840	0.036
H23A	0.1972	0.5428	0.6008	0.032
H23B	0.1018	0.5810	0.6304	0.032
H23C	0.0768	0.5112	0.5782	0.032
H1A	0.450(2)	0.3374(12)	0.353(2)	0.017(7)
H24A	0.3021	0.5401	0.8930	0.029
H24B	0.2402	0.5991	0.8192	0.029
H24C	0.3307	0.5591	0.7846	0.029
H26A	-0.0518	0.4479	0.8668	0.046
H26B	-0.1388	0.4303	0.7480	0.046
H26C	-0.1240	0.5027	0.7886	0.046
H24D	0.2362	0.5272	0.9003	0.034
H24E	0.1966	0.5889	0.8243	0.034
H24F	0.3092	0.5529	0.8285	0.034
H26D	-0.1327	0.5102	0.7967	0.05
H26E	-0.0721	0.5069	0.9277	0.05
H26F	-0.0747	0.4456	0.8532	0.05

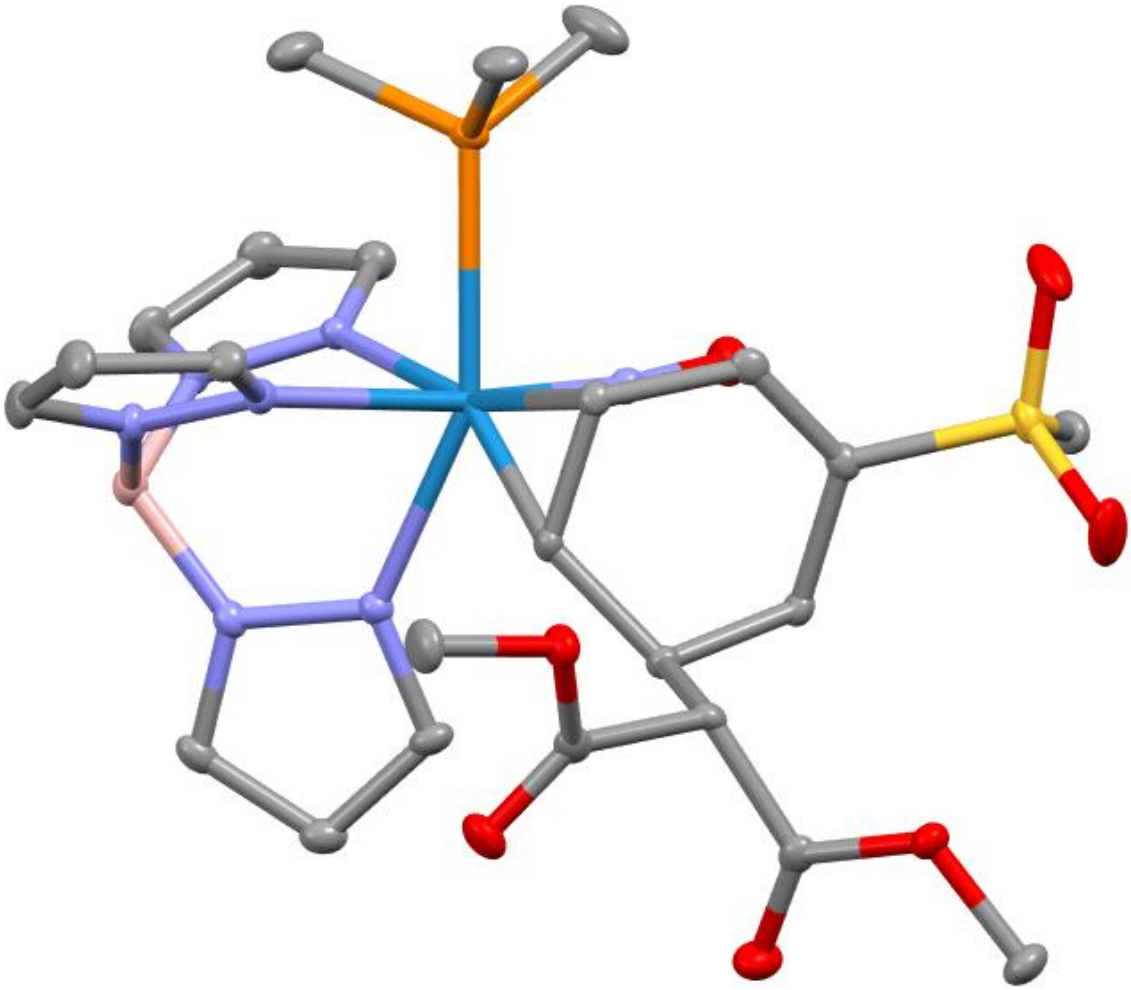

Crystal Structure Report for 11 in Chapter 4

A **yellow block-like** specimen of **$C_{24}H_{35}BN_7O_7PSW$**, approximate dimensions **0.062** mm x **0.110** mm x **0.170** mm, was coated with Paratone oil and mounted on a MiTeGen MicroLoop. The X-ray intensity data were measured on a Bruker Kappa APEXII Duo system equipped with a fine-focus sealed tube (Mo K_α, λ = 0.71073 Å) and a graphite monochromator.

The total exposure time was 1.95 hours. The frames were integrated with the Bruker SAINT software package[10] using a narrow-frame algorithm. The integration of the data using a **monoclinic** unit cell yielded a total of **47255** reflections to a maximum θ angle of **29.61**° (**0.72** Å resolution), of which **8246** were independent (average redundancy **5.731**, completeness = **99.8**%, R_{int} = **4.72**%, R_{sig} = **3.47**%) and **6872** (**83.34**%) were greater than 2σ(F^2). The final cell constants of a = **12.6337(8)** Å, b = **14.1105(9)** Å, c = **17.1373(13)** Å, β = **106.327(2)**°, volume = **2931.8(3)** $Å^3$, are based upon the refinement of the XYZ-centroids of **9902** reflections above 20 σ(I) with **4.429**° < 2θ < **58.93**°. Data were corrected for absorption effects using the Multi-Scan method (SADABS).[1] The ratio of minimum to maximum apparent transmission was **0.833**. The calculated minimum and maximum transmission coefficients (based on crystal size) are **0.5410** and **0.7840**.

10 Bruker (2012). Saint; SADABS; APEX3. Bruker AXS Inc., Madison, Wisconsin, USA.

The structure was solved and refined using the Bruker SHELXTL Software Package[11] within APEX3 [1] and OLEX2,[12] using the space group **P 2_1/c**, with Z = **4** for the formula unit, **$C_{24}H_{35}BN_7O_7PSW$**. Non-hydrogen atoms were refined anisotropically. The B-H hydrogen atom, as well as H10 and H11 were located in the electron density map and refined isotropically. All other hydrogen atoms were placed in geometrically calculated positions with U_{iso} = 1.2U_{equiv} of the parent atom (U_{iso} = 1.5U_{equiv} for methyl). The final anisotropic full-matrix least-squares refinement on F^2 with **396** variables converged at R1 = **2.25**%, for the observed data and wR2 = **4.49**% for all data. The goodness-of-fit was **1.008**. The largest peak in the final difference electron density synthesis was **0.620** $e^-/Å^3$ and the largest hole was **-0.709** $e^-/Å^3$ with an RMS deviation of **0.114** $e^-/Å^3$. On the basis of the final model, the calculated density was **1.793** g/cm^3 and F(000), **1576** e^-.

Table 1. Sample and crystal data for Harman_SS7_200_5_X1.

Identification code	Harman_SS7_200_5_X1	
Chemical formula	$C_{24}H_{35}BN_7O_7PSW$	
Formula weight	791.28 g/mol	
Temperature	100(2) K	
Wavelength	0.71073 Å	
Crystal size	0.062 x 0.110 x 0.170 mm	
Crystal habit	yellow block	
Crystal system	monoclinic	
Space group	P 2_1/c	
Unit cell dimensions	a = 12.6337(8) Å	α = 90°
	b = 14.1105(9) Å	β = 106.327(2)°
	c = 17.1373(13) Å	γ = 90°
Volume	2931.8(3) $Å^3$	
Z	4	
Density (calculated)	1.793 g/cm^3	
Absorption coefficient	4.122 mm^{-1}	
F(000)	1576	

Table 2. Data collection and structure refinement for Harman_SS7_200_5_X1.

Diffractometer	Bruker Kappa APEXII Duo
Radiation source	fine-focus sealed tube (Mo K_α, λ = 0.71073 Å)
Theta range for data collection	1.68 to 29.61°
Index ranges	-17<=h<=17, -19<=k<=19, -23<=l<=23
Reflections collected	47255

11 Sheldrick, G. M. (2015). Acta Cryst. A**71**, 3-8.
12 Dolomanov, O. V.; Bourhis, L. J.; Gildea, R. J.; Howard, J. A. K.; Puschmann, H. J. Appl. Cryst. (2009). 42, 339-341.

Independent reflections	8246 [R(int) = 0.0472]	
Coverage of independent reflections	99.8%	
Absorption correction	Multi-Scan	
Max. and min. transmission	0.7840 and 0.5410	
Structure solution technique	direct methods	
Structure solution program	SHELXT 2018/2 (Sheldrick, 2018)	
Refinement method	Full-matrix least-squares on F^2	
Refinement program	SHELXL-2018/3 (Sheldrick, 2018)	
Function minimized	$\Sigma\ w(F_o^2 - F_c^2)^2$	
Data / restraints / parameters	8246 / 0 / 396	
Goodness-of-fit on F^2	1.008	
Δ/σ_{max}	0.002	
Final R indices	6872 data; I>2σ(I)	R1 = 0.0225, wR2 = 0.0418
	all data	R1 = 0.0342, wR2 = 0.0449
Weighting scheme	$w=1/[\sigma^2(F_o^2)+(0.0141P)^2+2.6132P]$ where $P=(F_o^2+2F_c^2)/3$	
Largest diff. peak and hole	0.620 and -0.709 eÅ^{-3}	
R.M.S. deviation from mean	0.114 eÅ^{-3}	

Table 3. Atomic coordinates and equivalent isotropic atomic displacement parameters (Å^2) for Harman_SS7_200_5_X1.

U(eq) is defined as one third of the trace of the orthogonalized U_{ij} tensor.

	x/a	y/b	z/c	U(eq)
W1	0.31924(2)	0.68772(2)	0.38272(2)	0.00821(3)
S1	0.17246(5)	0.37840(5)	0.49429(4)	0.01473(13)
P1	0.22565(5)	0.78789(5)	0.46456(4)	0.01243(13)
O1	0.42297(15)	0.57428(13)	0.53270(11)	0.0193(4)
O2	0.10420(15)	0.42109(15)	0.53972(12)	0.0255(5)
O3	0.13567(18)	0.28997(14)	0.45286(13)	0.0303(5)
O4	0.99706(14)	0.52321(12)	0.15764(11)	0.0156(4)
O5	0.14204(15)	0.49753(14)	0.10838(11)	0.0193(4)
O6	0.11467(14)	0.26012(12)	0.24205(11)	0.0140(4)
O7	0.24808(15)	0.31147(13)	0.18879(12)	0.0208(4)
N1	0.24878(16)	0.79531(14)	0.28441(12)	0.0116(4)
N2	0.31807(17)	0.85604(15)	0.25974(13)	0.0132(4)

N3	0.45180(16)	0.79264(14)	0.42859(12)	0.0108(4)
N4	0.48960(16)	0.85216(14)	0.37924(13)	0.0124(4)
N5	0.43268(16)	0.66223(14)	0.30621(12)	0.0114(4)
N6	0.46809(16)	0.73619(15)	0.26848(12)	0.0116(4)
N7	0.38039(16)	0.61539(14)	0.46864(12)	0.0117(4)
C1	0.1457(2)	0.82142(18)	0.24330(15)	0.0151(5)
C2	0.1475(2)	0.89839(19)	0.19331(16)	0.0182(5)
C3	0.2576(2)	0.91800(18)	0.20519(16)	0.0171(5)
C4	0.5179(2)	0.80506(18)	0.50397(16)	0.0156(5)
C5	0.5983(2)	0.87203(19)	0.50423(17)	0.0195(6)
C6	0.5788(2)	0.89934(18)	0.42409(17)	0.0175(5)
C7	0.47501(19)	0.58386(18)	0.28285(15)	0.0135(5)
C8	0.5363(2)	0.60585(19)	0.22938(16)	0.0159(5)
C9	0.53059(19)	0.70374(18)	0.22280(15)	0.0142(5)
C10	0.15512(19)	0.61295(17)	0.35301(15)	0.0105(5)
C11	0.21961(19)	0.58354(17)	0.29875(14)	0.0099(5)
C12	0.24225(19)	0.47832(17)	0.29254(14)	0.0107(5)
C13	0.27421(19)	0.43068(17)	0.37647(14)	0.0110(5)
C14	0.19510(19)	0.46014(17)	0.42391(14)	0.0113(5)
C15	0.14198(19)	0.54367(17)	0.41340(14)	0.0118(5)
C16	0.3050(2)	0.35978(19)	0.56106(16)	0.0172(5)
C17	0.13889(19)	0.42653(17)	0.23677(14)	0.0106(5)
C18	0.0954(2)	0.48432(17)	0.15956(15)	0.0125(5)
C19	0.9555(2)	0.5926(2)	0.09407(17)	0.0210(6)
C20	0.17431(19)	0.32786(17)	0.21815(15)	0.0126(5)
C21	0.1471(2)	0.16306(18)	0.23108(18)	0.0189(6)
C22	0.0760(2)	0.78974(19)	0.44112(17)	0.0189(6)
C23	0.2667(2)	0.7651(3)	0.57273(17)	0.0296(7)
C24	0.2544(2)	0.91370(19)	0.45756(19)	0.0240(6)
B1	0.4443(2)	0.8402(2)	0.28664(18)	0.0138(6)

Table 4. Bond lengths (Å) for Harman_SS7_200_5_X1.

W1-N7	1.780(2)	W1-C11	2.190(2)
W1-N3	2.208(2)	W1-N5	2.227(2)
W1-C10	2.253(2)	W1-N1	2.257(2)
W1-P1	2.5090(7)	S1-O2	1.446(2)
S1-O3	1.446(2)	S1-C14	1.750(2)
S1-C16	1.762(3)	P1-C23	1.808(3)

P1-C22	1.819(3)	P1-C24	1.823(3)
O1-N7	1.224(3)	O4-C18	1.350(3)
O4-C19	1.449(3)	O5-C18	1.201(3)
O6-C20	1.350(3)	O6-C21	1.457(3)
O7-C20	1.199(3)	N1-C1	1.346(3)
N1-N2	1.374(3)	N2-C3	1.349(3)
N2-B1	1.547(3)	N3-C4	1.338(3)
N3-N4	1.370(3)	N4-C6	1.348(3)
N4-B1	1.537(4)	N5-C7	1.338(3)
N5-N6	1.368(3)	N6-C9	1.339(3)
N6-B1	1.546(4)	C1-C2	1.387(4)
C1-H1	0.95	C2-C3	1.377(4)
C2-H2	0.95	C3-H3	0.95
C4-C5	1.387(4)	C4-H4	0.95
C5-C6	1.380(4)	C5-H5	0.95
C6-H6	0.95	C7-C8	1.391(4)
C7-H7	0.95	C8-C9	1.386(4)
C8-H8	0.95	C9-H9	0.95
C10-C11	1.458(3)	C10-C15	1.467(3)
C10-H10	0.95(3)	C11-C12	1.521(3)
C11-H11	0.95(3)	C12-C13	1.535(3)
C12-C17	1.566(3)	C12-H12	1.0
C13-C14	1.513(3)	C13-H13A	0.99
C13-H13B	0.99	C14-C15	1.343(3)
C15-H15	0.95	C16-H16A	0.98
C16-H16B	0.98	C16-H16C	0.98
C17-C18	1.520(3)	C17-C20	1.523(3)
C17-H17	1.0	C19-H19A	0.98
C19-H19B	0.98	C19-H19C	0.98
C21-H21A	0.98	C21-H21B	0.98
C21-H21C	0.98	C22-H22A	0.98
C22-H22B	0.98	C22-H22C	0.98
C23-H23A	0.98	C23-H23B	0.98
C23-H23C	0.98	C24-H24A	0.98
C24-H24B	0.98	C24-H24C	0.98
B1-H1A	1.11(3)		

Table 5. Bond angles (°) for Harman_SS7_200_5_X1.

N7-W1-C11	101.20(9)	N7-W1-N3	88.89(8)

C11-W1-N3	157.26(8)	N7-W1-N5	101.13(8)
C11-W1-N5	81.42(8)	N3-W1-N5	76.62(7)
N7-W1-C10	94.38(9)	C11-W1-C10	38.28(8)
N3-W1-C10	162.19(8)	N5-W1-C10	119.67(8)
N7-W1-N1	172.71(8)	C11-W1-N1	85.86(8)
N3-W1-N1	85.14(7)	N5-W1-N1	81.56(7)
C10-W1-N1	90.09(8)	N7-W1-P1	91.36(7)
C11-W1-P1	118.12(6)	N3-W1-P1	81.53(5)
N5-W1-P1	154.49(5)	C10-W1-P1	80.90(6)
N1-W1-P1	83.65(5)	O2-S1-O3	117.77(13)
O2-S1-C14	109.54(12)	O3-S1-C14	108.82(12)
O2-S1-C16	108.31(12)	O3-S1-C16	107.80(13)
C14-S1-C16	103.67(12)	C23-P1-C22	102.11(13)
C23-P1-C24	103.61(15)	C22-P1-C24	100.67(13)
C23-P1-W1	115.39(10)	C22-P1-W1	120.56(9)
C24-P1-W1	112.21(9)	C18-O4-C19	115.4(2)
C20-O6-C21	115.16(19)	C1-N1-N2	105.9(2)
C1-N1-W1	134.06(17)	N2-N1-W1	119.84(15)
C3-N2-N1	109.4(2)	C3-N2-B1	129.5(2)
N1-N2-B1	120.7(2)	C4-N3-N4	106.54(19)
C4-N3-W1	129.53(17)	N4-N3-W1	123.54(15)
C6-N4-N3	109.4(2)	C6-N4-B1	130.7(2)
N3-N4-B1	118.47(19)	C7-N5-N6	106.1(2)
C7-N5-W1	133.42(17)	N6-N5-W1	120.35(15)
C9-N6-N5	109.9(2)	C9-N6-B1	128.4(2)
N5-N6-B1	121.4(2)	O1-N7-W1	173.08(18)
N1-C1-C2	110.9(2)	N1-C1-H1	124.6
C2-C1-H1	124.6	C3-C2-C1	104.9(2)
C3-C2-H2	127.6	C1-C2-H2	127.6
N2-C3-C2	108.9(2)	N2-C3-H3	125.6
C2-C3-H3	125.6	N3-C4-C5	110.5(2)
N3-C4-H4	124.8	C5-C4-H4	124.8
C6-C5-C4	105.1(2)	C6-C5-H5	127.4
C4-C5-H5	127.4	N4-C6-C5	108.5(2)
N4-C6-H6	125.8	C5-C6-H6	125.8
N5-C7-C8	110.9(2)	N5-C7-H7	124.6
C8-C7-H7	124.6	C9-C8-C7	104.5(2)
C9-C8-H8	127.8	C7-C8-H8	127.8
N6-C9-C8	108.6(2)	N6-C9-H9	125.7

C8-C9-H9	125.7	C11-C10-C15	117.0(2)
C11-C10-W1	68.51(13)	C15-C10-W1	115.60(16)
C11-C10-H10	119.3(18)	C15-C10-H10	115.4(17)
W1-C10-H10	112.4(17)	C10-C11-C12	118.2(2)
C10-C11-W1	73.20(13)	C12-C11-W1	128.05(16)
C10-C11-H11	114.0(16)	C12-C11-H11	112.7(16)
W1-C11-H11	105.1(16)	C11-C12-C13	111.52(19)
C11-C12-C17	110.94(19)	C13-C12-C17	108.78(19)
C11-C12-H12	108.5	C13-C12-H12	108.5
C17-C12-H12	108.5	C14-C13-C12	110.10(19)
C14-C13-H13A	109.6	C12-C13-H13A	109.6
C14-C13-H13B	109.6	C12-C13-H13B	109.6
H13A-C13-H13B	108.2	C15-C14-C13	123.3(2)
C15-C14-S1	119.90(19)	C13-C14-S1	116.74(17)
C14-C15-C10	121.9(2)	C14-C15-H15	119.1
C10-C15-H15	119.1	S1-C16-H16A	109.5
S1-C16-H16B	109.5	H16A-C16-H16B	109.5
S1-C16-H16C	109.5	H16A-C16-H16C	109.5
H16B-C16-H16C	109.5	C18-C17-C20	111.33(19)
C18-C17-C12	108.45(19)	C20-C17-C12	108.11(18)
C18-C17-H17	109.6	C20-C17-H17	109.6
C12-C17-H17	109.6	O5-C18-O4	123.8(2)
O5-C18-C17	126.0(2)	O4-C18-C17	110.2(2)
O4-C19-H19A	109.5	O4-C19-H19B	109.5
H19A-C19-H19B	109.5	O4-C19-H19C	109.5
H19A-C19-H19C	109.5	H19B-C19-H19C	109.5
O7-C20-O6	123.8(2)	O7-C20-C17	124.9(2)
O6-C20-C17	111.2(2)	O6-C21-H21A	109.5
O6-C21-H21B	109.5	H21A-C21-H21B	109.5
O6-C21-H21C	109.5	H21A-C21-H21C	109.5
H21B-C21-H21C	109.5	P1-C22-H22A	109.5
P1-C22-H22B	109.5	H22A-C22-H22B	109.5
P1-C22-H22C	109.5	H22A-C22-H22C	109.5
H22B-C22-H22C	109.5	P1-C23-H23A	109.5
P1-C23-H23B	109.5	H23A-C23-H23B	109.5
P1-C23-H23C	109.5	H23A-C23-H23C	109.5
H23B-C23-H23C	109.5	P1-C24-H24A	109.5
P1-C24-H24B	109.5	H24A-C24-H24B	109.5
P1-C24-H24C	109.5	H24A-C24-H24C	109.5

H24B-C24-H24C	109.5	N4-B1-N6	106.0(2)
N4-B1-N2	110.2(2)	N6-B1-N2	108.6(2)
N4-B1-H1A	112.1(14)	N6-B1-H1A	107.7(14)
N2-B1-H1A	112.0(14)		

Table 6. Torsion angles (°) for Harman_SS7_200_5_X1.

C1-N1-N2-C3	0.4(3)	W1-N1-N2-C3	-175.57(16)
C1-N1-N2-B1	-172.7(2)	W1-N1-N2-B1	11.3(3)
C4-N3-N4-C6	0.8(3)	W1-N3-N4-C6	-172.72(16)
C4-N3-N4-B1	168.4(2)	W1-N3-N4-B1	-5.2(3)
C7-N5-N6-C9	0.2(3)	W1-N5-N6-C9	-176.86(15)
C7-N5-N6-B1	-174.5(2)	W1-N5-N6-B1	8.5(3)
N2-N1-C1-C2	-0.6(3)	W1-N1-C1-C2	174.57(18)
N1-C1-C2-C3	0.5(3)	N1-N2-C3-C2	-0.1(3)
B1-N2-C3-C2	172.2(2)	C1-C2-C3-N2	-0.3(3)
N4-N3-C4-C5	0.0(3)	W1-N3-C4-C5	173.01(17)
N3-C4-C5-C6	-0.8(3)	N3-N4-C6-C5	-1.3(3)
B1-N4-C6-C5	-166.9(2)	C4-C5-C6-N4	1.3(3)
N6-N5-C7-C8	-0.8(3)	W1-N5-C7-C8	175.61(17)
N5-C7-C8-C9	1.2(3)	N5-N6-C9-C8	0.6(3)
B1-N6-C9-C8	174.8(2)	C7-C8-C9-N6	-1.1(3)
C15-C10-C11-C12	16.0(3)	W1-C10-C11-C12	124.7(2)
C15-C10-C11-W1	-108.7(2)	C10-C11-C12-C13	-43.1(3)
W1-C11-C12-C13	47.1(3)	C10-C11-C12-C17	78.3(3)
W1-C11-C12-C17	168.51(16)	C11-C12-C13-C14	46.9(3)
C17-C12-C13-C14	-75.8(2)	C12-C13-C14-C15	-28.6(3)
C12-C13-C14-S1	150.37(17)	O2-S1-C14-C15	-6.7(2)
O3-S1-C14-C15	123.3(2)	C16-S1-C14-C15	-122.1(2)
O2-S1-C14-C13	174.27(17)	O3-S1-C14-C13	-55.7(2)
C16-S1-C14-C13	58.8(2)	C13-C14-C15-C10	1.3(4)
S1-C14-C15-C10	-177.69(18)	C11-C10-C15-C14	6.1(3)
W1-C10-C15-C14	-71.7(3)	C11-C12-C17-C18	46.9(3)
C13-C12-C17-C18	169.96(19)	C11-C12-C17-C20	167.76(19)
C13-C12-C17-C20	-69.2(2)	C19-O4-C18-O5	-7.2(3)
C19-O4-C18-C17	170.1(2)	C20-C17-C18-O5	-52.6(3)
C12-C17-C18-O5	66.3(3)	C20-C17-C18-O4	130.1(2)
C12-C17-C18-O4	-111.1(2)	C21-O6-C20-O7	1.0(3)
C21-O6-C20-C17	-176.5(2)	C18-C17-C20-O7	63.9(3)
C12-C17-C20-O7	-55.2(3)	C18-C17-C20-O6	-118.7(2)

C12-C17-C20-O6	122.3(2)	C6-N4-B1-N6	108.0(3)
N3-N4-B1-N6	-56.4(3)	C6-N4-B1-N2	-134.6(3)
N3-N4-B1-N2	60.9(3)	C9-N6-B1-N4	-118.6(3)
N5-N6-B1-N4	55.0(3)	C9-N6-B1-N2	123.0(3)
N5-N6-B1-N2	-63.4(3)	C3-N2-B1-N4	123.4(3)
N1-N2-B1-N4	-65.0(3)	C3-N2-B1-N6	-121.0(3)
N1-N2-B1-N6	50.6(3)		

Table 7. Anisotropic atomic displacement parameters (Å^2) for Harman_SS7_200_5_X1.

The anisotropic atomic displacement factor exponent takes the form: $-2\pi^2[h^2 a^{*2} U_{11} + ... + 2 h k a^* b^* U_{12}]$

	U_{11}	U_{22}	U_{33}	U_{23}	U_{13}	U_{12}
W1	0.00832(4)	0.00777(5)	0.00845(4)	-0.00084(4)	0.00223(3)	-0.00053(4)
S1	0.0146(3)	0.0160(3)	0.0130(3)	0.0039(2)	0.0028(2)	-0.0025(2)
P1	0.0118(3)	0.0150(3)	0.0106(3)	-0.0014(2)	0.0033(2)	0.0010(2)
O1	0.0211(9)	0.0205(10)	0.0132(9)	0.0044(8)	-0.0003(7)	0.0035(8)
O2	0.0208(10)	0.0349(12)	0.0256(11)	0.0150(9)	0.0142(8)	0.0098(9)
O3	0.0448(13)	0.0186(11)	0.0226(11)	0.0013(9)	0.0014(9)	-0.0174(9)
O4	0.0157(9)	0.0162(9)	0.0148(9)	0.0041(7)	0.0041(7)	0.0020(7)
O5	0.0220(9)	0.0251(10)	0.0122(9)	0.0011(8)	0.0070(7)	-0.0033(8)
O6	0.0157(8)	0.0107(9)	0.0158(9)	-0.0019(7)	0.0049(7)	-0.0010(7)
O7	0.0198(9)	0.0187(10)	0.0279(10)	-0.0047(9)	0.0132(8)	-0.0014(8)
N1	0.0130(10)	0.0099(10)	0.0124(10)	0.0007(8)	0.0044(8)	-0.0003(8)
N2	0.0155(10)	0.0101(10)	0.0140(10)	0.0013(9)	0.0041(8)	-0.0020(8)
N3	0.0121(9)	0.0102(10)	0.0105(10)	-0.0014(8)	0.0038(8)	-0.0020(8)
N4	0.0140(10)	0.0083(10)	0.0145(10)	0.0000(8)	0.0033(8)	-0.0029(8)
N5	0.0112(9)	0.0120(10)	0.0112(10)	-0.0012(8)	0.0036(8)	-0.0014(8)
N6	0.0096(9)	0.0131(11)	0.0117(10)	0.0002(8)	0.0026(8)	-0.0023(8)
N7	0.0109(9)	0.0113(10)	0.0123(10)	-0.0014(8)	0.0019(8)	-0.0016(8)
C1	0.0117(11)	0.0163(13)	0.0161(12)	0.0004(11)	0.0022(9)	0.0030(10)
C2	0.0177(13)	0.0167(13)	0.0182(13)	0.0057(11)	0.0017(10)	0.0051(11)
C3	0.0209(13)	0.0128(13)	0.0173(13)	0.0051(10)	0.0046(10)	0.0004(10)
C4	0.0163(12)	0.0158(13)	0.0145(12)	-0.0013(11)	0.0039(9)	-0.0010(11)
C5	0.0192(13)	0.0184(14)	0.0190(14)	-0.0043(11)	0.0020(10)	-0.0058(11)
C6	0.0162(12)	0.0134(13)	0.0207(14)	-0.0036(11)	0.0017(10)	-0.0073(10)

C7	0.0120(11)	0.0114(12)	0.0163(12)	-0.0048(10)	0.0025(9)	0.0006(10)
C8	0.0136(12)	0.0177(13)	0.0169(13)	-0.0056(11)	0.0052(10)	-0.0015(10)
C9	0.0116(11)	0.0213(14)	0.0102(11)	-0.0022(10)	0.0038(9)	-0.0038(10)
C10	0.0076(10)	0.0105(12)	0.0125(11)	-0.0003(9)	0.0014(9)	-0.0007(9)
C11	0.0114(11)	0.0094(12)	0.0081(11)	0.0003(9)	0.0017(9)	-0.0015(9)
C12	0.0110(11)	0.0103(12)	0.0104(11)	-0.0013(9)	0.0024(9)	-0.0009(9)
C13	0.0108(11)	0.0092(11)	0.0122(11)	0.0008(9)	0.0020(9)	0.0002(9)
C14	0.0087(11)	0.0135(12)	0.0107(11)	0.0001(9)	0.0013(9)	-0.0022(9)
C15	0.0087(11)	0.0148(12)	0.0107(11)	-0.0028(10)	0.0009(9)	-0.0036(9)
C16	0.0192(13)	0.0182(14)	0.0135(12)	0.0038(11)	0.0035(10)	0.0045(11)
C17	0.0109(11)	0.0126(12)	0.0093(11)	-0.0016(9)	0.0046(9)	-0.0011(9)
C18	0.0134(11)	0.0124(12)	0.0103(11)	-0.0033(10)	0.0010(9)	-0.0042(10)
C19	0.0232(14)	0.0210(14)	0.0170(13)	0.0085(11)	0.0026(11)	0.0035(12)
C20	0.0136(11)	0.0114(12)	0.0108(11)	-0.0019(9)	0.0002(9)	-0.0026(9)
C21	0.0210(13)	0.0106(13)	0.0260(15)	-0.0028(11)	0.0081(11)	0.0006(10)
C22	0.0147(12)	0.0220(15)	0.0202(13)	-0.0062(11)	0.0052(10)	0.0029(10)
C23	0.0257(15)	0.051(2)	0.0131(13)	0.0028(14)	0.0065(11)	0.0112(15)
C24	0.0235(14)	0.0180(14)	0.0335(17)	-0.0095(13)	0.0129(12)	-0.0018(12)
B1	0.0151(13)	0.0119(14)	0.0143(13)	-0.0005(11)	0.0040(11)	-0.0032(11)

Table 8. Hydrogen atomic coordinates and isotropic atomic displacement parameters (Å^2) for Harman_SS7_200_5_X1.

	x/a	y/b	z/c	U(eq)
H1	0.0805	0.7912	0.2479	0.018
H2	0.0861	0.9305	0.1585	0.022
H3	0.2864	0.9672	0.1792	0.021
H4	0.5107	0.7726	0.5508	0.019
H5	0.6547	0.8943	0.5497	0.023
H6	0.6210	0.9439	0.4040	0.021
H7	0.4646	0.5216	0.3004	0.016
H8	0.5738	0.5633	0.2033	0.019
H9	0.5652	0.7415	0.1912	0.017
H10	0.095(2)	0.655(2)	0.3334(18)	0.019(8)
H11	0.199(2)	0.6140(19)	0.2476(17)	0.012
H12	0.3049	0.4710	0.2680	0.013
H13A	0.2723	0.3610	0.3698	0.013
H13B	0.3502	0.4492	0.4067	0.013
H15	0.0945	0.5583	0.4460	0.014
H16A	0.3352	0.4202	0.5857	0.026
H16B	0.3534	0.3334	0.5308	0.026
H16C	0.3001	0.3154	0.6039	0.026
H17	0.0806	0.4212	0.2658	0.013
H19A	-0.0553	0.5625	0.0409	0.032
H19B	0.0087	0.6445	0.1001	0.032
H19C	-0.1150	0.6177	0.0983	0.032
H21A	0.1323	0.1496	0.1729	0.028
H21B	0.1049	0.1192	0.2551	0.028
H21C	0.2260	0.1551	0.2579	0.028
H22A	0.0440	0.8009	0.3828	0.028
H22B	0.0535	0.8406	0.4720	0.028
H22C	0.0500	0.7287	0.4560	0.028
H23A	0.2465	0.7002	0.5828	0.044
H23B	0.2292	0.8098	0.5998	0.044
H23C	0.3467	0.7731	0.5942	0.044
H24A	0.3343	0.9241	0.4751	0.036
H24B	0.2197	0.9497	0.4927	0.036
H24C	0.2246	0.9349	0.4012	0.036
H1A	0.488(2)	0.8868(19)	0.2529(17)	0.013(7)

x/a	y/b	z/c	U(eq)

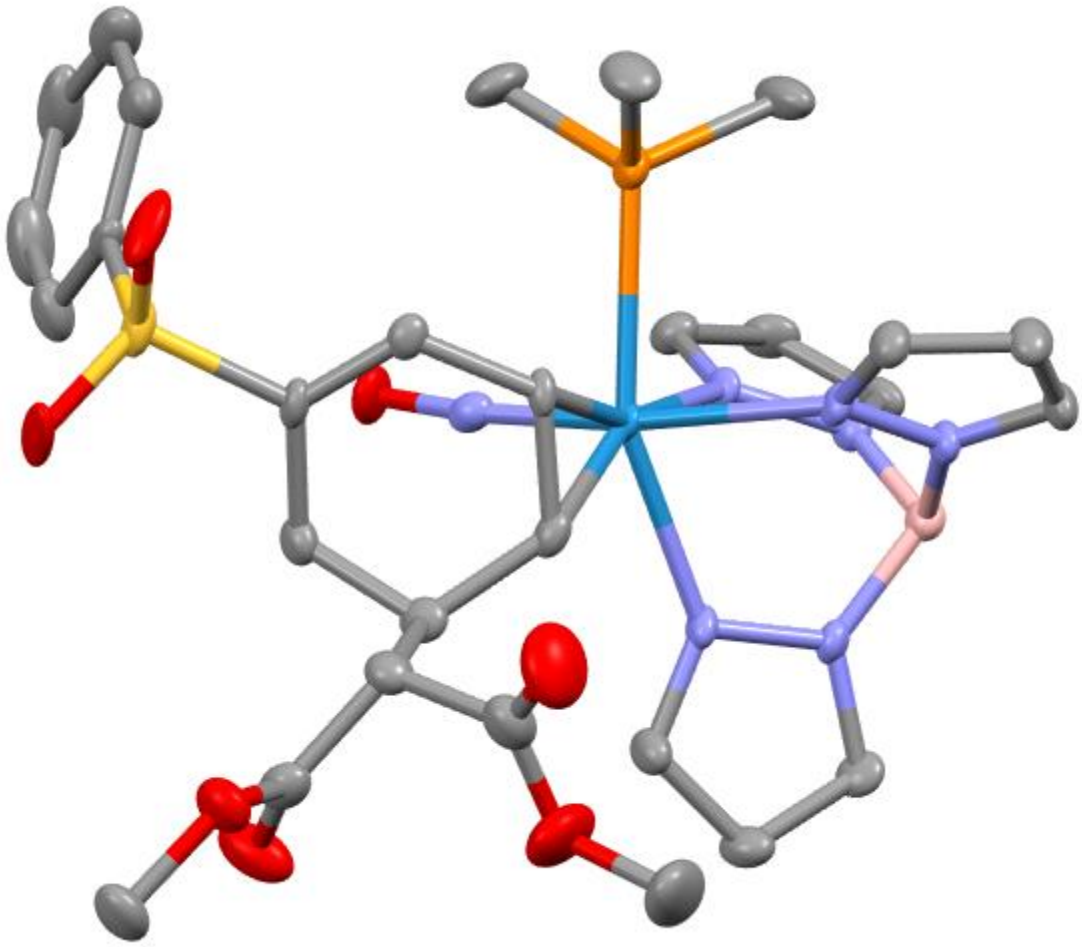

Crystal Structure Report for 12

A **yellow blocks-like** specimen of **$C_{29}H_{37}BN_7O_7PSW$**, approximate dimensions **0.075** mm x **0.081** mm x **0.244** mm, was coated with Paratone oil and mounted on a MiTeGen MicroLoop. The X-ray intensity data were measured on a Bruker Kappa APEXII Duo system equipped with a fine-focus sealed tube (Mo K_α, λ = 0.71073 Å) and a graphite monochromator.

The total exposure time was 3.08 hours. The frames were integrated with the Bruker SAINT software package[13] using a narrow-frame algorithm. The integration of the data using a **monoclinic** unit cell yielded a total of **53711** reflections to a maximum θ angle of **28.34**° (**0.75** Å resolution), of which **8375** were independent (average redundancy **6.413**, completeness = **99.8**%, R_{int} = **7.89**%, R_{sig} = **5.82**%) and **6486** (**77.44**%) were greater than 2σ(F^2). The final cell constants of a = **12.5334(8)** Å, b = **22.9625(17)** Å, c = **12.6358(9)** Å, β = **112.263(2)**°, volume = **3365.5(4)** Å^3, are based upon the refinement of the XYZ-centroids of **8009** reflections above 20 σ(I) with **4.972**° < 2θ < **49.28**°. Data were corrected for absorption effects using the Multi-Scan method (SADABS).[1] The ratio of minimum to maximum apparent transmission was **0.805**. The calculated minimum and maximum transmission coefficients (based on

13 Bruker (2012). Saint; SADABS; APEX3. Bruker AXS Inc., Madison, Wisconsin, USA.

crystal size) are **0.4740** and **0.7740**.

The structure was solved and refined using the Bruker SHELXTL Software Package[14] within APEX3 [1] and OLEX2,[15] using the space group **P 2_1/n**, with Z = **4** for the formula unit, **$C_{29}H_{37}BN_7O_7PSW$**. Non-hydrogen atoms were refined anisotropically. The B-H hydrogen atom, as well as H10 and H11 were located in the electron density map and refined isotropically. All other hydrogen atoms were placed in geometrically calculated positions with U_{iso} = 1.2U_{equiv} of the parent atom (U_{iso} = 1.5U_{equiv} for methyl). The final anisotropic full-matrix least-squares refinement on F^2 with **440** variables converged at R1 = **4.31**%, for the observed data and wR2 = **7.60**% for all data. The goodness-of-fit was **1.072**. The largest peak in the final difference electron density synthesis was **1.008** $e^-/Å^3$ and the largest hole was **-1.311** $e^-/Å^3$ with an RMS deviation of **0.153** $e^-/Å^3$. On the basis of the final model, the calculated density was **1.684** g/cm^3 and F(000), **1704** e^-.

Table 1. Sample and crystal data for Harman_SS7_200_8_X1.

Identification code	Harman_SS7_200_8_X1	
Chemical formula	$C_{29}H_{37}BN_7O_7PSW$	
Formula weight	853.34 g/mol	
Temperature	100(2) K	
Wavelength	0.71073 Å	
Crystal size	0.075 x 0.081 x 0.244 mm	
Crystal habit	yellow blocks	
Crystal system	monoclinic	
Space group	P 2_1/n	
Unit cell dimensions	a = 12.5334(8) Å	α = 90°
	b = 22.9625(17) Å	β = 112.263(2)°
	c = 12.6358(9) Å	γ = 90°
Volume	3365.5(4) $Å^3$	
Z	4	
Density (calculated)	1.684 g/cm^3	
Absorption coefficient	3.598 mm^{-1}	
F(000)	1704	

Table 2. Data collection and structure refinement for Harman_SS7_200_8_X1.

Diffractometer	Bruker Kappa APEXII Duo
Radiation source	fine-focus sealed tube (Mo K_α, λ = 0.71073 Å)
Theta range for data collection	1.77 to 28.34°
Index ranges	-16<=h<=16, -30<=k<=30, -16<=l<=16
Reflections collected	53711

14 Sheldrick, G. M. (2015). Acta Cryst. A**71**, 3-8.
15 Dolomanov, O. V.; Bourhis, L. J.; Gildea, R. J.; Howard, J. A. K.; Puschmann, H. J. Appl. Cryst. (2009). 42, 339-341.

Independent reflections	8375 [R(int) = 0.0789]	
Coverage of independent reflections	99.8%	
Absorption correction	Multi-Scan	
Max. and min. transmission	0.7740 and 0.4740	
Structure solution technique	direct methods	
Structure solution program	SHELXT 2018/2 (Sheldrick, 2018)	
Refinement method	Full-matrix least-squares on F^2	
Refinement program	SHELXL-2018/3 (Sheldrick, 2018)	
Function minimized	$\Sigma\, w(F_o^2 - F_c^2)^2$	
Data / restraints / parameters	8375 / 0 / 440	
Goodness-of-fit on F^2	1.072	
Δ/σ_{max}	0.002	
Final R indices	6486 data; I>2σ(I)	R1 = 0.0431, wR2 = 0.0702
	all data	R1 = 0.0681, wR2 = 0.0760
Weighting scheme	$w=1/[\sigma^2(F_o^2)+(0.0100P)^2+15.7645P]$ where $P=(F_o^2+2F_c^2)/3$	
Largest diff. peak and hole	1.008 and -1.311 eÅ^{-3}	
R.M.S. deviation from mean	0.153 eÅ^{-3}	

Table 3. Atomic coordinates and equivalent isotropic atomic displacement parameters (Å^2) for Harman_SS7_200_8_X1.

U(eq) is defined as one third of the trace of the orthogonalized U_{ij} tensor.

	x/a	y/b	z/c	U(eq)
W1	0.44433(2)	0.63752(2)	0.22078(2)	0.01447(5)
S1	0.37858(12)	0.61056(6)	0.61261(10)	0.0216(3)
P1	0.64745(12)	0.65170(6)	0.36032(10)	0.0200(3)
O1	0.3778(3)	0.73421(15)	0.3419(3)	0.0265(9)
O2	0.4652(4)	0.57333(17)	0.6898(3)	0.0374(10)
O3	0.2635(3)	0.60975(17)	0.6146(3)	0.0323(10)
O4	0.0004(3)	0.55914(19)	0.2532(4)	0.0416(11)
O5	0.0391(3)	0.47737(17)	0.3541(3)	0.0299(9)
O6	0.2555(4)	0.4231(2)	0.2560(4)	0.0537(13)
O7	0.1153(4)	0.4727(2)	0.1187(4)	0.0501(12)
N1	0.3024(3)	0.63719(19)	0.0474(3)	0.0169(8)
N2	0.3293(3)	0.63925(18)	0.9517(3)	0.0165(8)

N3	0.4904(3)	0.71006(18)	0.1313(3)	0.0157(9)
N4	0.4966(3)	0.70436(18)	0.0259(3)	0.0184(9)
N5	0.5282(3)	0.57984(18)	0.1287(3)	0.0168(9)
N6	0.5273(3)	0.59689(18)	0.0248(3)	0.0186(9)
N7	0.3989(4)	0.69204(18)	0.2928(3)	0.0186(9)
C1	0.1886(4)	0.6311(2)	0.0097(4)	0.0227(11)
C2	0.1409(4)	0.6291(2)	0.8908(4)	0.0252(12)
C3	0.2321(4)	0.6343(2)	0.8575(4)	0.0208(10)
C4	0.5129(4)	0.7655(2)	0.1609(4)	0.0221(11)
C5	0.5349(4)	0.7965(2)	0.0771(4)	0.0263(12)
C6	0.5234(4)	0.7561(2)	0.9930(4)	0.0226(11)
C7	0.5980(4)	0.5330(2)	0.1596(4)	0.0213(11)
C8	0.6431(4)	0.5205(2)	0.0771(4)	0.0241(12)
C9	0.5953(4)	0.5614(2)	0.9933(4)	0.0243(12)
C10	0.4525(4)	0.5629(2)	0.3397(4)	0.0150(10)
C11	0.3421(4)	0.5655(2)	0.2466(4)	0.0176(10)
C12	0.2342(4)	0.5726(2)	0.2743(4)	0.0207(11)
C13	0.2553(4)	0.6128(2)	0.3779(4)	0.0209(11)
C14	0.3662(4)	0.5969(2)	0.4732(4)	0.0179(10)
C15	0.4558(4)	0.5748(2)	0.4536(4)	0.0171(10)
C16	0.4312(4)	0.6827(2)	0.6412(4)	0.0170(10)
C17	0.3524(5)	0.7281(2)	0.6053(5)	0.0299(13)
C18	0.3928(7)	0.7856(3)	0.6244(6)	0.0442(17)
C19	0.5083(7)	0.7954(3)	0.6796(6)	0.0457(18)
C20	0.5870(6)	0.7502(3)	0.7144(5)	0.0422(17)
C21	0.5477(5)	0.6931(3)	0.6940(5)	0.0314(13)
C22	0.1893(4)	0.5140(2)	0.3023(4)	0.0221(11)
C23	0.0670(5)	0.5207(2)	0.2983(4)	0.0249(12)
C24	0.9228(5)	0.4807(3)	0.3543(5)	0.0344(14)
C25	0.1919(5)	0.4643(3)	0.2251(5)	0.0314(13)
C26	0.1089(6)	0.4261(3)	0.0387(6)	0.059(2)
C27	0.6661(5)	0.7102(3)	0.4611(5)	0.0346(14)
C28	0.7462(5)	0.6703(3)	0.2899(5)	0.0371(15)
C29	0.7271(5)	0.5927(3)	0.4525(5)	0.0331(14)
B1	0.4535(5)	0.6478(2)	0.9593(4)	0.0190(12)

Table 4. Bond lengths (Å) for Harman_SS7_200_8_X1.

W1-N7	1.764(4)	W1-C11	2.191(5)

W1-N3	2.210(4)	W1-N1	2.238(4)
W1-C10	2.256(4)	W1-N5	2.267(4)
W1-P1	2.5089(13)	S1-O2	1.435(4)
S1-O3	1.452(4)	S1-C14	1.737(5)
S1-C16	1.768(5)	P1-C27	1.804(6)
P1-C29	1.818(5)	P1-C28	1.828(5)
O1-N7	1.232(5)	O4-C23	1.200(6)
O5-C23	1.339(6)	O5-C24	1.461(6)
O6-C25	1.203(7)	O7-C25	1.337(7)
O7-C26	1.453(7)	N1-C1	1.329(6)
N1-N2	1.374(5)	N2-C3	1.346(6)
N2-B1	1.536(7)	N3-C4	1.328(6)
N3-N4	1.369(5)	N4-C6	1.343(6)
N4-B1	1.531(7)	N5-C7	1.348(6)
N5-N6	1.366(5)	N6-C9	1.345(6)
N6-B1	1.525(7)	C1-C2	1.392(6)
C1-H1	0.95	C2-C3	1.365(7)
C2-H2	0.95	C3-H3	0.95
C4-C5	1.388(7)	C4-H4	0.95
C5-C6	1.377(7)	C5-H5	0.95
C6-H6	0.95	C7-C8	1.390(7)
C7-H7	0.95	C8-C9	1.372(7)
C8-H8	0.95	C9-H9	0.95
C10-C11	1.438(7)	C10-C15	1.451(6)
C10-H10	0.88(5)	C11-C12	1.528(7)
C11-H11	0.81(5)	C12-C13	1.541(7)
C12-C22	1.551(7)	C12-H12	1.0
C13-C14	1.500(7)	C13-H13A	0.99
C13-H13B	0.99	C14-C15	1.338(7)
C15-H15	0.95	C16-C21	1.377(7)
C16-C17	1.389(7)	C17-C18	1.402(8)
C17-H17	0.95	C18-C19	1.367(10)
C18-H18	0.95	C19-C20	1.384(10)
C19-H19	0.95	C20-C21	1.392(8)
C20-H20	0.95	C21-H21	0.95
C22-C25	1.509(8)	C22-C23	1.523(7)
C22-H22	1.0	C24-H24A	0.98
C24-H24B	0.98	C24-H24C	0.98
C26-H26A	0.98	C26-H26B	0.98

C26-H26C	0.98	C27-H27A	0.98
C27-H27B	0.98	C27-H27C	0.98
C28-H28A	0.98	C28-H28B	0.98
C28-H28C	0.98	C29-H29A	0.98
C29-H29B	0.98	C29-H29C	0.98
B1-H1A	1.11(5)		

Table 5. Bond angles (°) for Harman_SS7_200_8_X1.

N7-W1-C11	97.90(18)	N7-W1-N3	85.82(16)
C11-W1-N3	157.87(16)	N7-W1-N1	102.42(17)
C11-W1-N1	81.40(16)	N3-W1-N1	76.50(14)
N7-W1-C10	97.92(17)	C11-W1-C10	37.70(17)
N3-W1-C10	163.53(16)	N1-W1-C10	117.90(17)
N7-W1-N5	169.20(17)	C11-W1-N5	92.68(17)
N3-W1-N5	85.17(15)	N1-W1-N5	81.21(14)
C10-W1-N5	89.14(16)	N7-W1-P1	89.15(13)
C11-W1-P1	119.23(13)	N3-W1-P1	82.50(11)
N1-W1-P1	155.06(10)	C10-W1-P1	81.53(13)
N5-W1-P1	83.80(10)	O2-S1-O3	118.8(2)
O2-S1-C14	109.6(2)	O3-S1-C14	107.9(2)
O2-S1-C16	106.9(2)	O3-S1-C16	107.7(2)
C14-S1-C16	105.0(2)	C27-P1-C29	102.1(3)
C27-P1-C28	103.8(3)	C29-P1-C28	100.2(3)
C27-P1-W1	114.7(2)	C29-P1-W1	121.2(2)
C28-P1-W1	112.47(18)	C23-O5-C24	114.9(4)
C25-O7-C26	115.1(5)	C1-N1-N2	106.0(3)
C1-N1-W1	134.3(3)	N2-N1-W1	119.5(3)
C3-N2-N1	109.5(4)	C3-N2-B1	128.4(4)
N1-N2-B1	122.0(4)	C4-N3-N4	106.4(4)
C4-N3-W1	130.4(3)	N4-N3-W1	123.2(3)
C6-N4-N3	109.3(4)	C6-N4-B1	131.2(4)
N3-N4-B1	118.5(4)	C7-N5-N6	106.0(4)
C7-N5-W1	134.0(3)	N6-N5-W1	119.3(3)
C9-N6-N5	109.6(4)	C9-N6-B1	128.7(4)
N5-N6-B1	121.6(4)	O1-N7-W1	172.2(4)
N1-C1-C2	110.8(4)	N1-C1-H1	124.6
C2-C1-H1	124.6	C3-C2-C1	105.2(4)
C3-C2-H2	127.4	C1-C2-H2	127.4
N2-C3-C2	108.5(4)	N2-C3-H3	125.7

C2-C3-H3	125.7	N3-C4-C5	111.0(5)
N3-C4-H4	124.5	C5-C4-H4	124.5
C6-C5-C4	104.6(5)	C6-C5-H5	127.7
C4-C5-H5	127.7	N4-C6-C5	108.8(4)
N4-C6-H6	125.6	C5-C6-H6	125.6
N5-C7-C8	110.6(4)	N5-C7-H7	124.7
C8-C7-H7	124.7	C9-C8-C7	104.8(5)
C9-C8-H8	127.6	C7-C8-H8	127.6
N6-C9-C8	109.1(4)	N6-C9-H9	125.5
C8-C9-H9	125.5	C11-C10-C15	117.4(4)
C11-C10-W1	68.7(3)	C15-C10-W1	119.7(3)
C11-C10-H10	119.(3)	C15-C10-H10	115.(3)
W1-C10-H10	110.(3)	C10-C11-C12	118.6(4)
C10-C11-W1	73.6(3)	C12-C11-W1	124.9(3)
C10-C11-H11	112.(4)	C12-C11-H11	115.(4)
W1-C11-H11	105.(4)	C11-C12-C13	112.1(4)
C11-C12-C22	112.9(4)	C13-C12-C22	106.6(4)
C11-C12-H12	108.4	C13-C12-H12	108.4
C22-C12-H12	108.4	C14-C13-C12	110.2(4)
C14-C13-H13A	109.6	C12-C13-H13A	109.6
C14-C13-H13B	109.6	C12-C13-H13B	109.6
H13A-C13-H13B	108.1	C15-C14-C13	122.1(4)
C15-C14-S1	119.8(4)	C13-C14-S1	118.0(4)
C14-C15-C10	123.0(4)	C14-C15-H15	118.5
C10-C15-H15	118.5	C21-C16-C17	121.4(5)
C21-C16-S1	120.4(4)	C17-C16-S1	118.2(4)
C16-C17-C18	119.0(6)	C16-C17-H17	120.5
C18-C17-H17	120.5	C19-C18-C17	119.2(6)
C19-C18-H18	120.4	C17-C18-H18	120.4
C18-C19-C20	121.9(6)	C18-C19-H19	119.1
C20-C19-H19	119.1	C19-C20-C21	119.3(6)
C19-C20-H20	120.4	C21-C20-H20	120.4
C16-C21-C20	119.3(6)	C16-C21-H21	120.3
C20-C21-H21	120.3	C25-C22-C23	108.8(4)
C25-C22-C12	114.2(4)	C23-C22-C12	110.7(4)
C25-C22-H22	107.6	C23-C22-H22	107.6
C12-C22-H22	107.6	O4-C23-O5	121.6(5)
O4-C23-C22	126.9(5)	O5-C23-C22	111.5(4)
O5-C24-H24A	109.5	O5-C24-H24B	109.5

H24A-C24-H24B	109.5	O5-C24-H24C	109.5
H24A-C24-H24C	109.5	H24B-C24-H24C	109.5
O6-C25-O7	125.1(6)	O6-C25-C22	123.9(6)
O7-C25-C22	111.0(5)	O7-C26-H26A	109.5
O7-C26-H26B	109.5	H26A-C26-H26B	109.5
O7-C26-H26C	109.5	H26A-C26-H26C	109.5
H26B-C26-H26C	109.5	P1-C27-H27A	109.5
P1-C27-H27B	109.5	H27A-C27-H27B	109.5
P1-C27-H27C	109.5	H27A-C27-H27C	109.5
H27B-C27-H27C	109.5	P1-C28-H28A	109.5
P1-C28-H28B	109.5	H28A-C28-H28B	109.5
P1-C28-H28C	109.5	H28A-C28-H28C	109.5
H28B-C28-H28C	109.5	P1-C29-H29A	109.5
P1-C29-H29B	109.5	H29A-C29-H29B	109.5
P1-C29-H29C	109.5	H29A-C29-H29C	109.5
H29B-C29-H29C	109.5	N6-B1-N4	109.7(4)
N6-B1-N2	109.2(4)	N4-B1-N2	106.3(4)
N6-B1-H1A	108.(3)	N4-B1-H1A	110.(3)
N2-B1-H1A	114.(3)		

Table 6. Torsion angles (°) for Harman_SS7_200_8_X1.

C1-N1-N2-C3	-0.1(6)	W1-N1-N2-C3	175.5(3)
C1-N1-N2-B1	178.3(4)	W1-N1-N2-B1	-6.1(6)
C4-N3-N4-C6	0.4(5)	W1-N3-N4-C6	178.4(3)
C4-N3-N4-B1	-169.2(4)	W1-N3-N4-B1	8.8(6)
C7-N5-N6-C9	-0.3(5)	W1-N5-N6-C9	171.0(3)
C7-N5-N6-B1	177.7(4)	W1-N5-N6-B1	-11.1(6)
N2-N1-C1-C2	0.1(6)	W1-N1-C1-C2	-174.6(4)
N1-C1-C2-C3	0.0(6)	N1-N2-C3-C2	0.1(6)
B1-N2-C3-C2	-178.2(5)	C1-C2-C3-N2	-0.1(6)
N4-N3-C4-C5	-0.5(6)	W1-N3-C4-C5	-178.3(3)
N3-C4-C5-C6	0.4(6)	N3-N4-C6-C5	-0.2(6)
B1-N4-C6-C5	167.6(5)	C4-C5-C6-N4	-0.1(6)
N6-N5-C7-C8	0.9(6)	W1-N5-C7-C8	-168.5(4)
N5-C7-C8-C9	-1.2(6)	N5-N6-C9-C8	-0.5(6)
B1-N6-C9-C8	-178.2(5)	C7-C8-C9-N6	1.0(6)
C15-C10-C11-C12	-7.9(7)	W1-C10-C11-C12	-121.2(4)
C15-C10-C11-W1	113.3(4)	C10-C11-C12-C13	36.7(6)
W1-C11-C12-C13	-52.6(5)	C10-C11-C12-C22	-83.6(5)

W1-C11-C12-C22	-173.0(3)	C11-C12-C13-C14	-46.0(5)
C22-C12-C13-C14	78.0(5)	C12-C13-C14-C15	30.9(6)
C12-C13-C14-S1	-151.6(3)	O2-S1-C14-C15	-25.3(5)
O3-S1-C14-C15	-156.0(4)	C16-S1-C14-C15	89.3(4)
O2-S1-C14-C13	157.1(4)	O3-S1-C14-C13	26.4(4)
C16-S1-C14-C13	-88.3(4)	C13-C14-C15-C10	-1.7(7)
S1-C14-C15-C10	-179.3(4)	C11-C10-C15-C14	-11.1(7)
W1-C10-C15-C14	68.8(6)	O2-S1-C16-C21	22.1(5)
O3-S1-C16-C21	150.9(4)	C14-S1-C16-C21	-94.3(4)
O2-S1-C16-C17	-160.2(4)	O3-S1-C16-C17	-31.4(4)
C14-S1-C16-C17	83.4(4)	C21-C16-C17-C18	-0.6(8)
S1-C16-C17-C18	-178.2(4)	C16-C17-C18-C19	-1.2(8)
C17-C18-C19-C20	1.9(9)	C18-C19-C20-C21	-0.9(9)
C17-C16-C21-C20	1.6(8)	S1-C16-C21-C20	179.2(4)
C19-C20-C21-C16	-0.9(8)	C11-C12-C22-C25	-42.0(6)
C13-C12-C22-C25	-165.5(4)	C11-C12-C22-C23	-165.2(4)
C13-C12-C22-C23	71.3(5)	C24-O5-C23-O4	0.4(7)
C24-O5-C23-C22	179.9(4)	C25-C22-C23-O4	-108.2(6)
C12-C22-C23-O4	18.1(7)	C25-C22-C23-O5	72.4(5)
C12-C22-C23-O5	-161.4(4)	C26-O7-C25-O6	2.4(9)
C26-O7-C25-C22	-178.2(5)	C23-C22-C25-O6	-124.5(6)
C12-C22-C25-O6	111.3(6)	C23-C22-C25-O7	56.0(6)
C12-C22-C25-O7	-68.1(6)	C9-N6-B1-N4	-117.2(5)
N5-N6-B1-N4	65.3(6)	C9-N6-B1-N2	126.7(5)
N5-N6-B1-N2	-50.8(6)	C6-N4-B1-N6	129.7(5)
N3-N4-B1-N6	-63.4(5)	C6-N4-B1-N2	-112.4(5)
N3-N4-B1-N2	54.5(5)	C3-N2-B1-N6	-120.0(5)
N1-N2-B1-N6	61.8(6)	C3-N2-B1-N4	121.7(5)
N1-N2-B1-N4	-56.4(6)		

Table 7. Anisotropic atomic displacement parameters (Å^2) for Harman_SS7_200_8_X1.

The anisotropic atomic displacement factor exponent takes the form: $-2\pi^2[h^2 a^{*2} U_{11} + ... + 2 h k a^* b^* U_{12}]$

	U_{11}	U_{22}	U_{33}	U_{23}	U_{13}	U_{12}
W1	0.01856(10)	0.01692(9)	0.00925(8)	0.00221(8)	0.00676(6)	0.00036(10)
S1	0.0392(8)	0.0149(6)	0.0172(6)	0.0003(5)	0.0180(6)	-0.0032(6)
P1	0.0227(7)	0.0257(7)	0.0126(6)	0.0023(5)	0.0080(5)	0.0011(5)
O1	0.038(2)	0.0194(19)	0.027(2)	-0.0105(15)	0.0183(17)	-0.0019(17)

O2	0.072(3)	0.027(2)	0.0161(19)	0.0062(15)	0.0192(19)	0.017(2)
O3	0.044(2)	0.036(2)	0.032(2)	-0.0146(17)	0.0323(19)	-0.023(2)
O4	0.027(2)	0.038(3)	0.060(3)	0.024(2)	0.017(2)	0.004(2)
O5	0.027(2)	0.030(2)	0.036(2)	0.0073(17)	0.0167(18)	-0.0028(18)
O6	0.068(3)	0.034(3)	0.068(3)	0.005(2)	0.036(3)	0.018(3)
O7	0.057(3)	0.046(3)	0.037(3)	-0.021(2)	0.006(2)	-0.003(2)
N1	0.021(2)	0.020(2)	0.0113(17)	0.0033(17)	0.0084(15)	0.004(2)
N2	0.023(2)	0.0159(19)	0.0125(17)	-0.0013(16)	0.0089(15)	-0.0005(19)
N3	0.020(2)	0.018(2)	0.0111(18)	0.0042(15)	0.0080(16)	-0.0012(18)
N4	0.021(2)	0.021(2)	0.0147(19)	0.0049(16)	0.0081(17)	0.0010(18)
N5	0.022(2)	0.020(2)	0.0102(18)	0.0015(15)	0.0077(16)	0.0010(18)
N6	0.020(2)	0.026(2)	0.0128(19)	0.0023(16)	0.0094(17)	0.0014(19)
N7	0.021(2)	0.019(2)	0.015(2)	0.0020(16)	0.0052(17)	-0.0048(18)
C1	0.021(3)	0.031(3)	0.018(2)	0.007(2)	0.010(2)	0.002(2)
C2	0.021(3)	0.031(3)	0.020(2)	0.008(2)	0.003(2)	-0.004(2)
C3	0.026(3)	0.020(2)	0.015(2)	0.008(2)	0.0055(19)	0.000(2)
C4	0.024(3)	0.023(3)	0.017(2)	0.0004(19)	0.005(2)	-0.005(2)
C5	0.024(3)	0.024(3)	0.028(3)	0.005(2)	0.006(2)	-0.011(2)
C6	0.017(3)	0.033(3)	0.021(2)	0.011(2)	0.009(2)	-0.003(2)
C7	0.025(3)	0.023(3)	0.016(2)	0.0037(19)	0.008(2)	0.004(2)
C8	0.023(3)	0.029(3)	0.020(3)	0.006(2)	0.008(2)	0.009(2)
C9	0.021(3)	0.038(3)	0.018(2)	0.002(2)	0.012(2)	0.004(2)
C10	0.023(3)	0.012(2)	0.015(2)	0.0042(17)	0.013(2)	0.004(2)
C11	0.028(3)	0.014(2)	0.013(2)	0.0009(18)	0.009(2)	-0.001(2)
C12	0.024(3)	0.019(3)	0.018(2)	0.0066(19)	0.007(2)	-0.001(2)
C13	0.023(3)	0.024(3)	0.020(2)	0.004(2)	0.013(2)	0.001(2)
C14	0.028(3)	0.015(2)	0.015(2)	-0.0016(18)	0.014(2)	-0.002(2)
C15	0.025(3)	0.011(2)	0.017(2)	0.0008(17)	0.009(2)	-0.002(2)
C16	0.021(3)	0.018(2)	0.014(2)	-0.0043(18)	0.0097(19)	-0.010(2)
C17	0.036(3)	0.025(3)	0.040(3)	0.000(2)	0.027(3)	-0.001(3)
C18	0.072(5)	0.025(3)	0.057(4)	0.002(3)	0.048(4)	0.006(3)
C19	0.077(5)	0.031(4)	0.051(4)	-0.017(3)	0.049(4)	-0.025(4)
C20	0.041(4)	0.055(4)	0.039(3)	-0.018(3)	0.024(3)	-0.027(4)
C21	0.029(3)	0.044(4)	0.025(3)	-0.005(2)	0.015(2)	-0.006(3)
C22	0.020(3)	0.023(3)	0.022(3)	0.005(2)	0.006(2)	0.003(2)
C23	0.028(3)	0.024(3)	0.022(3)	0.000(2)	0.008(2)	-0.009(2)

C24	0.027(3)	0.036(3)	0.047(4)	-0.002(3)	0.022(3)	-0.008(3)
C25	0.028(3)	0.031(3)	0.039(3)	0.000(3)	0.017(3)	-0.003(3)
C26	0.055(5)	0.072(6)	0.051(4)	-0.037(4)	0.021(4)	-0.012(4)
C27	0.033(3)	0.039(3)	0.021(3)	-0.008(2)	-0.002(2)	-0.006(3)
C28	0.020(3)	0.063(4)	0.025(3)	0.012(3)	0.006(2)	-0.007(3)
C29	0.025(3)	0.041(4)	0.030(3)	0.015(3)	0.006(2)	0.008(3)
B1	0.021(3)	0.021(3)	0.015(2)	0.003(2)	0.007(2)	0.001(2)

Table 8. Hydrogen atomic coordinates and isotropic atomic displacement parameters (Å^2) for Harman_SS7_200_8_X1.

	x/a	y/b	z/c	U(eq)
H1	0.1457	0.6284	0.0574	0.027
H2	0.0618	0.6249	-0.1570	0.03
H3	0.2278	0.6344	-0.2192	0.025
H4	0.5139	0.7819	0.2304	0.027
H5	0.5536	0.8366	0.0776	0.032
H6	0.5330	0.7636	-0.0769	0.027
H7	0.6142	0.5115	0.2281	0.026
H8	0.6953	0.4902	0.0784	0.029
H9	0.6082	0.5642	-0.0760	0.029
H10	0.503(4)	0.537(2)	0.337(4)	0.018
H11	0.337(4)	0.542(2)	0.197(4)	0.013(13)
H12	0.1721	0.5902	0.2063	0.025
H13A	0.2586	0.6538	0.3552	0.025
H13B	0.1906	0.6090	0.4044	0.025
H15	0.5248	0.5665	0.5173	0.021
H17	0.2723	0.7203	0.5684	0.036
H18	0.3406	0.8173	0.5992	0.053
H19	0.5353	0.8344	0.6945	0.055
H20	0.6670	0.7582	0.7517	0.051
H21	0.6007	0.6615	0.7163	0.038
H22	0.2399	0.5031	0.3823	0.027
H24A	-0.1337	0.4787	0.2755	0.052
H24B	-0.0864	0.5176	0.3890	0.052
H24C	-0.0895	0.4481	0.3984	0.052
H26A	0.0345	0.4279	-0.0259	0.089
H26B	0.1164	0.3884	0.0773	0.089
H26C	0.1714	0.4305	0.0107	0.089

H27A	0.6391	0.7467	0.4196	0.052
H27B	0.7479	0.7137	0.5102	0.052
H27C	0.6214	0.7018	0.5084	0.052
H28A	0.7427	0.6402	0.2338	0.056
H28B	0.8250	0.6729	0.3472	0.056
H28C	0.7239	0.7079	0.2509	0.056
H29A	0.6968	0.5860	0.5125	0.05
H29B	0.8089	0.6032	0.4876	0.05
H29C	0.7186	0.5572	0.4070	0.05
H1A	0.462(4)	0.650(2)	-0.125(4)	0.024(14)

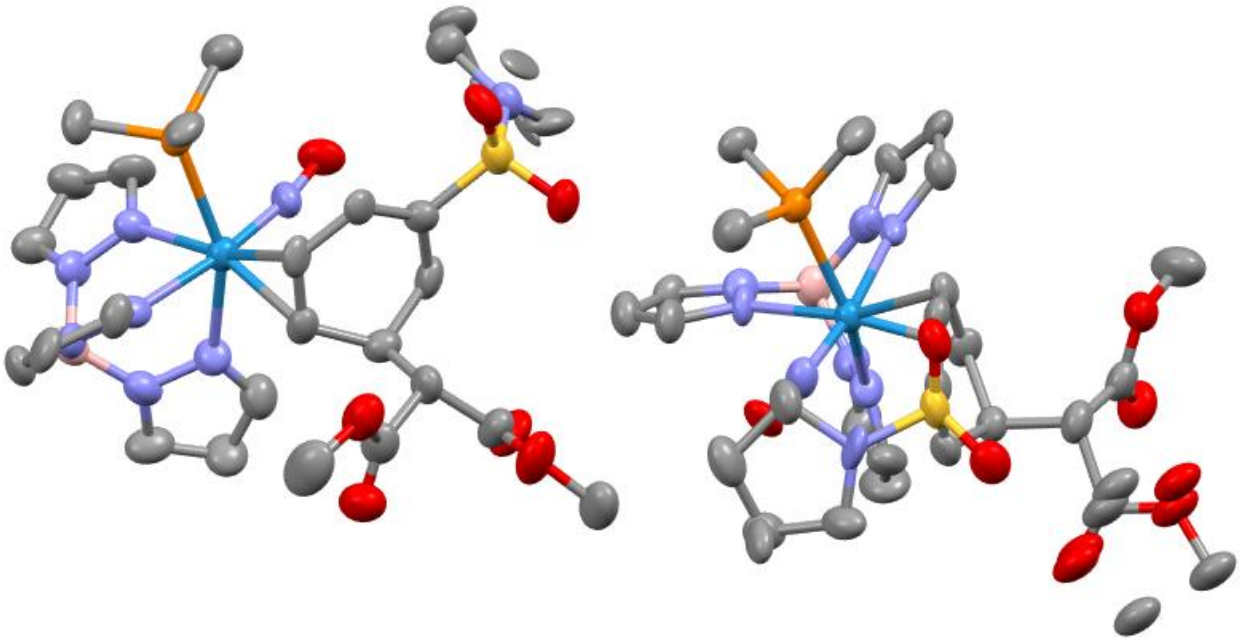

Crystal Structure Report for 13 in Chapter 4

A colorless plate-like specimen of $C_{27}H_{40}BN_8O_7PSW$, approximate dimensions 0.029 mm x 0.052 mm x 0.062 mm, was coated with Paratone oil and mounted on a MiTeGen MicroLoop. The X-ray intensity data were measured on a Bruker D8 Venture Photon III Kappa four-circle diffractometer system equipped with an Incoatec IμS 3.0 micro-focus sealed X-ray tube (Cu Kα, λ = 1.54178 Å) and a HELIOS MX double bounce multilayer mirror monochromator.

The total exposure time was 17.76 hours. The frames were integrated with the Bruker SAINT software package[16] using a narrow-frame algorithm. The integration of the data using a triclinic unit cell yielded a total of 46447 reflections to a maximum θ angle of 68.49° (0.83 Å resolution), of which 12982 were independent (average redundancy 3.578, completeness = 99.2%, R_{int} = 12.44%, R_{sig} = 9.51%) and 9144 (70.44%) were greater than $2\sigma(F^2)$. The final cell constants of a = 12.7593(4) Å, b = 15.3175(5) Å, c = 19.5201(6) Å, α = 104.356(2)°, β = 90.005(2)°, γ = 105.656(2)°, volume = 3549.6(2) $Å^3$, are based upon the refinement of the XYZ-centroids of 9881 reflections above 20 σ(I) with 6.201° < 2θ < 136.9°. Data were corrected for absorption effects using the Multi-Scan method (SADABS).[1] The ratio of minimum to maximum apparent transmission was 0.522. The calculated minimum and maximum transmission coefficients (based on crystal size) are 0.6550 and 0.8130.

The structure was solved and refined as a two-component twin using the Bruker SHELXTL Software Package[17] within APEX3[1] and OLEX2,[18] using the space group P -1, with Z = 4 for the formula unit, $C_{27}H_{40}BN_8O_7PSW$. The TWINROTMAT feature of Platon[19] was used to identify the twin law, and the BASF

[16] Bruker (2012). *Saint; SADABS; APEX3*. Bruker AXS Inc., Madison, Wisconsin, USA.
[17] Sheldrick, G. M. (2015). *Acta Cryst.* A**71**, 3-8.
[18] Dolomanov, O. V.; Bourhis, L. J.; Gildea, R. J.; Howard, J. A. K.; Puschmann, H. *J. Appl. Cryst.* (2009). **42**, 339-341.
[19] Spek, A. L. *Acta Cryst.* (2009) **D65**, 148-155.

refined to 0.02639. Non-hydrogen atoms were refined anisotropically. Hydrogen atoms were placed in geometrically calculated positions with U_{iso} = 1.2U_{equiv} of the parent atom (1.5U_{equiv} for methyl). The relative occupancy of the disordered sites was freely refined, with constraints and restraints on most of the disordered atoms and bonds. The final anisotropic full-matrix least-squares refinement on F^2 with 865 variables converged at R1 = 11.39%, for the observed data and wR2 = 28.43% for all data. The goodness-of-fit was 1.612. The largest peak in the final difference electron density synthesis was 11.006 $e^-/Å^3$ and the largest hole was -1.524 $e^-/Å^3$ with an RMS deviation of 0.362 $e^-/Å^3$. On the basis of the final model, the calculated density was 1.584 g/cm^3 and F(000), 1696 e^-.

Table 1. Sample and crystal data for Harman_SS7_198_6_X2.

Identification code	Harman_SS7_198_6_X2	
Chemical formula	$C_{27}H_{40}BN_8O_7PSW$	
Formula weight	846.36 g/mol	
Temperature	100(2) K	
Wavelength	1.54178 Å	
Crystal size	0.029 x 0.052 x 0.062 mm	
Crystal habit	colorless plate	
Crystal system	triclinic	
Space group	P -1	
Unit cell dimensions	a = 12.7593(4) Å	α = 104.356(2)°
	b = 15.3175(5) Å	β = 90.005(2)°
	c = 19.5201(6) Å	γ = 105.656(2)°
Volume	3549.6(2) $Å^3$	
Z	4	
Density (calculated)	1.584 g/cm^3	
Absorption coefficient	7.455 mm^{-1}	
F(000)	1696	

Table 2. Data collection and structure refinement for Harman_SS7_198_6_X2.

Diffractometer	Bruker D8 Venture Photon III Kappa four-circle diffractometer
Radiation source	Incoatec IμS 3.0 micro-focus sealed X-ray tube (Cu Kα, λ = 1.54178 Å)
Theta range for data collection	2.34 to 68.49°
Index ranges	-15<=h<=15, -18<=k<=18, -23<=l<=23
Reflections collected	46447
Independent reflections	12982 [R(int) = 0.1244]
Coverage of independent reflections	99.2%
Absorption correction	Multi-Scan

Max. and min. transmission	0.8130 and 0.6550
Structure solution technique	direct methods
Structure solution program	SHELXT 2018/2 (Sheldrick, 2018)
Refinement method	Full-matrix least-squares on F^2
Refinement program	SHELXL-2018/3 (Sheldrick, 2018)
Function minimized	$\Sigma\, w(F_o^2 - F_c^2)^2$
Data / restraints / parameters	12982 / 55 / 865
Goodness-of-fit on F^2	1.612
Final R indices	9144 data; I>2σ(I) R1 = 0.1139, wR2 = 0.2632
	all data R1 = 0.1455, wR2 = 0.2843
Weighting scheme	$w=1/[\sigma^2(F_o^2)+(0.1000P)^2]$ where $P=(F_o^2+2F_c^2)/3$
Largest diff. peak and hole	11.006 and -1.524 eÅ^{-3}
R.M.S. deviation from mean	0.362 eÅ^{-3}

Table 3. Atomic coordinates and equivalent isotropic atomic displacement parameters (Å^2) for Harman_SS7_198_6_X2.

U(eq) is defined as one third of the trace of the orthogonalized U_{ij} tensor.

	x/a	y/b	z/c	U(eq)
S1	0.2534(3)	0.0746(3)	0.0632(2)	0.0447(9)
P1	0.4851(4)	0.0876(3)	0.8131(2)	0.0415(8)
O1	0.3073(11)	0.2400(10)	0.9089(8)	0.059(3)
O2	0.2422(10)	0.9782(10)	0.0333(7)	0.054(3)
O3	0.2524(11)	0.1086(11)	0.1385(6)	0.059(3)
O4	0.7638(13)	0.3450(13)	0.1643(9)	0.074(4)
O5	0.7170(13)	0.1900(13)	0.1294(8)	0.070(4)
O6	0.5081(15)	0.3819(14)	0.2187(8)	0.080(5)
O7	0.5779(15)	0.2936(15)	0.2685(8)	0.080(5)
N1	0.6263(12)	0.3964(10)	0.9438(8)	0.044(3)
N2	0.7101(12)	0.4393(11)	0.9077(8)	0.050(3)
N3	0.5412(12)	0.2994(10)	0.8083(7)	0.041(3)
N4	0.6289(13)	0.3517(11)	0.7866(7)	0.047(3)
N5	0.7124(12)	0.2398(9)	0.8781(7)	0.042(3)
N6	0.7734(12)	0.3018(10)	0.8438(6)	0.043(3)

N7	0.4032(12)	0.2434(11)	0.9125(7)	0.047(3)
N8	0.1491(11)	0.0938(11)	0.0286(8)	0.047(3)
C1	0.6134(17)	0.4622(15)	0.9952(10)	0.056(4)
C2	0.6852(19)	0.5464(14)	0.9991(11)	0.059(5)
C3	0.7428(19)	0.5300(13)	0.9384(11)	0.059(5)
C4	0.4549(17)	0.3001(15)	0.7698(10)	0.058(5)
C5	0.4884(18)	0.3548(16)	0.7235(12)	0.063(5)
C6	0.6020(18)	0.3887(14)	0.7351(10)	0.056(5)
C7	0.7685(16)	0.1788(14)	0.8784(9)	0.050(4)
C8	0.8682(17)	0.2022(14)	0.8466(8)	0.052(4)
C9	0.8669(15)	0.2830(15)	0.8263(10)	0.052(4)
C10	0.5419(14)	0.1456(12)	0.9750(7)	0.041(3)
C11	0.5891(13)	0.2455(13)	0.0120(8)	0.044(4)
C12	0.5336(15)	0.2823(12)	0.0790(9)	0.045(4)
C13	0.4073(15)	0.2455(13)	0.0718(8)	0.045(4)
C14	0.3753(13)	0.1432(12)	0.0391(8)	0.041(3)
C15	0.4375(13)	0.0986(12)	0.9943(7)	0.038(3)
C16	0.100(4)	0.175(3)	0.0616(16)	0.065(11)
C17	0.090(2)	0.2103(18)	0.9936(12)	0.050(7)
C18	0.0553(17)	0.1181(16)	0.9317(10)	0.063(5)
C19	0.1264(16)	0.0630(14)	0.9497(10)	0.053(4)
C20	0.5727(14)	0.2580(15)	0.1428(9)	0.049(4)
C21	0.6965(16)	0.2725(15)	0.1471(9)	0.051(4)
C22	0.837(2)	0.201(2)	0.1234(15)	0.093(10)
C23	0.5469(17)	0.3224(18)	0.2140(10)	0.063(6)
C24	0.5674(19)	0.352(2)	0.3395(12)	0.079(8)
C25	0.3375(16)	0.0442(15)	0.7935(10)	0.056(4)
C26	0.5246(17)	0.9870(12)	0.8288(8)	0.049(4)
C27	0.5409(18)	0.0927(14)	0.7281(9)	0.055(4)
B1	0.7349(16)	0.3846(15)	0.8332(11)	0.048(4)
W1	0.54299(6)	0.24304(5)	0.90347(4)	0.0382(2)
S2	0.2935(3)	0.0726(3)	0.5627(2)	0.0439(9)
P2	0.0730(3)	0.0947(3)	0.31494(19)	0.0392(8)
O8	0.3501(9)	0.2498(11)	0.4157(7)	0.056(3)
O9	0.2408(10)	0.9777(10)	0.5300(7)	0.051(3)
O10	0.3157(11)	0.1038(11)	0.6365(7)	0.061(3)
O11	0.9615(13)	0.3440(12)	0.6667(8)	0.066(4)
O12	0.9021(11)	0.1858(11)	0.6296(7)	0.059(3)
O13	0.221(3)	0.386(3)	0.7215(16)	0.070(4)

O14	0.119(3)	0.301(3)	0.7731(15)	0.070(4)
N9	0.9447(11)	0.2438(9)	0.3806(6)	0.038(3)
N10	0.9212(12)	0.3070(11)	0.3465(7)	0.043(3)
N11	0.1544(12)	0.3049(10)	0.3130(6)	0.039(3)
N12	0.0987(13)	0.3579(10)	0.2908(7)	0.045(3)
N13	0.1297(12)	0.3989(9)	0.4473(7)	0.041(3)
N14	0.0745(13)	0.4427(10)	0.4109(7)	0.046(3)
N15	0.2540(13)	0.2497(12)	0.4158(7)	0.050(4)
N16	0.4127(13)	0.0928(13)	0.5280(7)	0.054(4)
C28	0.8436(14)	0.1844(14)	0.3824(9)	0.047(4)
C29	0.7637(15)	0.2074(14)	0.3473(8)	0.049(4)
C30	0.8170(13)	0.2847(13)	0.3261(9)	0.046(4)
C31	0.2408(18)	0.3041(15)	0.2702(9)	0.055(4)
C32	0.2365(17)	0.3553(14)	0.2249(10)	0.055(4)
C33	0.1486(15)	0.3884(11)	0.2372(8)	0.041(3)
C34	0.1878(17)	0.4661(16)	0.5018(10)	0.061(5)
C35	0.175(2)	0.5554(15)	0.5026(14)	0.075(7)
C36	0.108(2)	0.5416(15)	0.4461(10)	0.064(5)
C37	0.0527(12)	0.1493(11)	0.4756(8)	0.036(3)
C38	0.0707(14)	0.2465(13)	0.5148(8)	0.043(4)
C39	0.1493(13)	0.2830(12)	0.5830(8)	0.041(3)
C40	0.2491(12)	0.2458(12)	0.5719(8)	0.040(3)
C41	0.2159(12)	0.1420(11)	0.5390(7)	0.036(3)
C42	0.1273(13)	0.0994(12)	0.4949(7)	0.039(3)
C43	0.4925(15)	0.1760(14)	0.5595(11)	0.058(5)
C44	0.547(3)	0.221(2)	0.5001(11)	0.056(8)
C45	0.5202(18)	0.1277(16)	0.4380(12)	0.066(6)
C46	0.4139(16)	0.0623(15)	0.4501(10)	0.056(4)
C47	0.0903(17)	0.2561(15)	0.6480(9)	0.052(4)
C48	0.9796(17)	0.2694(14)	0.6501(8)	0.050(4)
C49	0.794(2)	0.194(2)	0.6242(17)	0.093(9)
C50	0.165(5)	0.325(4)	0.719(3)	0.070(4)
C51	0.164(4)	0.345(3)	0.8387(18)	0.070(4)
C52	0.9710(19)	0.9924(13)	0.3269(9)	0.057(5)
C53	0.0211(16)	0.1013(14)	0.2287(9)	0.051(4)
C54	0.1913(18)	0.0507(16)	0.2931(10)	0.059(5)
B2	0.0144(18)	0.3923(16)	0.3380(11)	0.050(4)
W2	0.11575(6)	0.24900(5)	0.40730(3)	0.0359(2)
O13A	0.104(4)	0.254(3)	0.7648(18)	0.070(4)

C50A	0.139(6)	0.297(5)	0.716(3)	0.070(4)
O14A	0.249(4)	0.373(4)	0.728(2)	0.070(4)
C51A	0.256(5)	0.419(4)	0.803(2)	0.070(4)
C44A	0.590(3)	0.180(4)	0.5098(13)	0.055(15)
C17A	0.026(4)	0.185(3)	0.9989(14)	0.050(10)
C16A	0.123(3)	0.188(2)	0.050(3)	0.039(10)

Table 4. Bond lengths (Å) for Harman_SS7_198_6_X2.

S1-O2	1.414(15)	S1-O3	1.433(13)
S1-N8	1.620(13)	S1-C14	1.763(18)
P1-C27	1.817(17)	P1-C25	1.83(2)
P1-C26	1.837(17)	P1-W1	2.509(4)
O1-N7	1.21(2)	O4-C21	1.18(3)
O5-C21	1.32(2)	O5-C22	1.50(3)
O6-C23	1.13(3)	O7-C23	1.35(3)
O7-C24	1.48(3)	N1-C1	1.28(2)
N1-N2	1.39(2)	N1-W1	2.236(14)
N2-C3	1.32(2)	N2-B1	1.57(3)
N3-N4	1.33(2)	N3-C4	1.34(2)
N3-W1	2.236(13)	N4-C6	1.36(2)
N4-B1	1.52(2)	N5-C7	1.32(2)
N5-N6	1.37(2)	N5-W1	2.228(15)
N6-C9	1.33(2)	N6-B1	1.54(2)
N7-W1	1.794(14)	N8-C19	1.50(2)
N8-C16A	1.53(3)	N8-C16	1.53(3)
C1-C2	1.35(3)	C1-H1	0.95
C2-C3	1.40(3)	C2-H2A	0.95
C3-H3	0.95	C4-C5	1.37(3)
C4-H4	0.95	C5-C6	1.40(3)
C5-H5	0.95	C6-H6	0.95
C7-C8	1.41(3)	C7-H7	0.95
C8-C9	1.39(3)	C8-H8	0.95
C9-H9	0.95	C10-C15	1.43(2)
C10-C11	1.48(3)	C10-W1	2.280(13)
C10-H10	1.0	C11-C12	1.54(2)
C11-W1	2.187(14)	C11-H11	1.0
C12-C20	1.51(2)	C12-C13	1.55(2)
C12-H12	1.0	C13-C14	1.48(2)

C13-H13A	0.99	C13-H13B	0.99
C14-C15	1.36(2)	C15-H15	0.95
C16-C17	1.57(3)	C16-H16A	0.99
C16-H16B	0.99	C17-C18	1.57(3)
C17-H17A	0.99	C17-H17B	0.99
C18-C19	1.49(2)	C18-C17A	1.56(3)
C18-H18A	0.99	C18-H18B	0.99
C18-H18C	0.99	C18-H18D	0.99
C19-H19A	0.99	C19-H19B	0.99
C20-C21	1.53(2)	C20-C23	1.58(2)
C20-H20	1.0	C22-H22A	0.98
C22-H22B	0.98	C22-H22C	0.98
C24-H24A	0.98	C24-H24B	0.98
C24-H24C	0.98	C25-H25A	0.98
C25-H25B	0.98	C25-H25C	0.98
C26-H26A	0.98	C26-H26B	0.98
C26-H26C	0.98	C27-H27A	0.98
C27-H27B	0.98	C27-H27C	0.98
B1-H1A	1.0	S2-O10	1.404(15)
S2-O9	1.408(15)	S2-N16	1.648(15)
S2-C41	1.772(14)	P2-C52	1.81(2)
P2-C54	1.82(2)	P2-C53	1.843(15)
P2-W2	2.514(4)	O8-N15	1.23(2)
O11-C48	1.19(2)	O12-C48	1.36(3)
O12-C49	1.42(3)	O13-C50	1.00(7)
O14-C50	1.29(7)	O14-C51	1.33(4)
N9-C28	1.37(2)	N9-N10	1.395(19)
N9-W2	2.220(14)	N10-C30	1.32(2)
N10-B2	1.55(3)	N11-N12	1.357(18)
N11-C31	1.38(2)	N11-W2	2.218(12)
N12-C33	1.34(2)	N12-B2	1.53(3)
N13-C34	1.34(2)	N13-N14	1.394(19)
N13-W2	2.191(13)	N14-C36	1.44(2)
N14-B2	1.53(2)	N15-W2	1.769(14)
N16-C43	1.40(3)	N16-C46	1.48(2)
C28-C29	1.39(2)	C28-H28	0.95
C29-C30	1.36(3)	C29-H29	0.95
C30-H30	0.95	C31-C32	1.33(3)
C31-H31	0.95	C32-C33	1.35(3)

C32-H32	0.95	C33-H33	0.95
C34-C35	1.42(3)	C34-H34	0.95
C35-C36	1.33(3)	C35-H35	0.95
C36-H36	0.95	C37-C38	1.45(2)
C37-C42	1.47(2)	C37-W2	2.259(14)
C37-H37	1.0	C38-C39	1.55(2)
C38-W2	2.183(16)	C38-H38	1.0
C39-C40	1.52(2)	C39-C47	1.56(2)
C39-H39	1.0	C40-C41	1.50(2)
C40-H40A	0.99	C40-H40B	0.99
C41-C42	1.33(2)	C42-H42	0.95
C43-C44	1.56(3)	C43-C44A	1.58(3)
C43-H43A	0.99	C43-H43B	0.99
C43-H43C	0.99	C43-H43D	0.99
C44-C45	1.58(3)	C44-H44A	0.99
C44-H44B	0.99	C45-C46	1.51(3)
C45-C44A	1.57(3)	C45-H45A	0.99
C45-H45B	0.99	C45-H45C	0.99
C45-H45D	0.99	C46-H46A	0.99
C46-H46B	0.99	C47-C50A	1.38(6)
C47-C48	1.48(3)	C47-C50	1.63(5)
C47-H47	1.0	C47-H47A	1.0
C49-H49A	0.98	C49-H49B	0.98
C49-H49C	0.98	C51-H51A	0.98
C51-H51B	0.98	C51-H51C	0.98
C52-H52A	0.98	C52-H52B	0.98
C52-H52C	0.98	C53-H53A	0.98
C53-H53B	0.98	C53-H53C	0.98
C54-H54A	0.98	C54-H54B	0.98
C54-H54C	0.98	B2-H2	1.0
O13A-C50A	1.30(9)	C50A-O14A	1.53(9)
O14A-C51A	1.45(6)	C51A-H51D	0.98
C51A-H51E	0.98	C51A-H51F	0.98
C44A-H44C	0.99	C44A-H44D	0.99
C17A-C16A	1.57(3)	C17A-H17C	0.99
C17A-H17D	0.99	C16A-H16C	0.99
C16A-H16D	0.99		

Table 5. Bond angles (°) for Harman_SS7_198_6_X2.

O2-S1-O3	119.5(9)	O2-S1-N8	104.5(8)
O3-S1-N8	106.4(8)	O2-S1-C14	110.2(8)
O3-S1-C14	106.1(8)	N8-S1-C14	110.0(8)
C27-P1-C25	105.0(10)	C27-P1-C26	100.8(9)
C25-P1-C26	104.3(10)	C27-P1-W1	112.5(7)
C25-P1-W1	113.0(6)	C26-P1-W1	119.7(5)
C21-O5-C22	111.(2)	C23-O7-C24	114.5(19)
C1-N1-N2	105.3(16)	C1-N1-W1	134.8(14)
N2-N1-W1	119.9(11)	C3-N2-N1	109.4(17)
C3-N2-B1	129.1(17)	N1-N2-B1	120.0(14)
N4-N3-C4	107.0(15)	N4-N3-W1	124.0(10)
C4-N3-W1	128.3(14)	N3-N4-C6	111.5(16)
N3-N4-B1	118.4(13)	C6-N4-B1	127.5(16)
C7-N5-N6	105.3(15)	C7-N5-W1	133.6(13)
N6-N5-W1	120.1(10)	C9-N6-N5	111.6(14)
C9-N6-B1	127.4(15)	N5-N6-B1	120.9(14)
O1-N7-W1	171.3(13)	C19-N8-C16A	104.(2)
C19-N8-C16	111.2(16)	C19-N8-S1	119.0(11)
C16A-N8-S1	122.9(18)	C16-N8-S1	124.6(16)
N1-C1-C2	114.(2)	N1-C1-H1	123.1
C2-C1-H1	123.1	C1-C2-C3	103.7(18)
C1-C2-H2A	128.1	C3-C2-H2A	128.1
N2-C3-C2	108.(2)	N2-C3-H3	126.2
C2-C3-H3	126.2	N3-C4-C5	109.9(19)
N3-C4-H4	125.1	C5-C4-H4	125.1
C4-C5-C6	106.1(17)	C4-C5-H5	126.9
C6-C5-H5	126.9	N4-C6-C5	105.5(19)
N4-C6-H6	127.3	C5-C6-H6	127.3
N5-C7-C8	111.4(17)	N5-C7-H7	124.3
C8-C7-H7	124.3	C9-C8-C7	103.8(15)
C9-C8-H8	128.1	C7-C8-H8	128.1
N6-C9-C8	107.9(16)	N6-C9-H9	126.1
C8-C9-H9	126.1	C15-C10-C11	117.6(14)
C15-C10-W1	116.7(10)	C11-C10-W1	67.3(8)
C15-C10-H10	115.6	C11-C10-H10	115.6
W1-C10-H10	115.6	C10-C11-C12	115.6(15)
C10-C11-W1	74.1(8)	C12-C11-W1	126.0(10)
C10-C11-H11	111.9	C12-C11-H11	111.9
W1-C11-H11	111.9	C20-C12-C11	111.9(13)

C20-C12-C13	107.3(15)	C11-C12-C13	114.2(13)
C20-C12-H12	107.7	C11-C12-H12	107.7
C13-C12-H12	107.7	C14-C13-C12	108.9(13)
C14-C13-H13A	109.9	C12-C13-H13A	109.9
C14-C13-H13B	109.9	C12-C13-H13B	109.9
H13A-C13-H13B	108.3	C15-C14-C13	123.6(16)
C15-C14-S1	118.3(13)	C13-C14-S1	118.0(12)
C14-C15-C10	123.6(16)	C14-C15-H15	118.2
C10-C15-H15	118.2	N8-C16-C17	98.5(19)
N8-C16-H16A	112.1	C17-C16-H16A	112.1
N8-C16-H16B	112.1	C17-C16-H16B	112.1
H16A-C16-H16B	109.7	C18-C17-C16	104.(2)
C18-C17-H17A	110.9	C16-C17-H17A	110.9
C18-C17-H17B	110.9	C16-C17-H17B	110.9
H17A-C17-H17B	108.9	C19-C18-C17A	112.4(19)
C19-C18-C17	101.8(15)	C19-C18-H18A	111.4
C17-C18-H18A	111.4	C19-C18-H18B	111.4
C17-C18-H18B	111.4	H18A-C18-H18B	109.3
C19-C18-H18C	109.1	C17A-C18-H18C	109.1
C19-C18-H18D	109.1	C17A-C18-H18D	109.1
H18C-C18-H18D	107.9	C18-C19-N8	106.6(15)
C18-C19-H19A	110.4	N8-C19-H19A	110.4
C18-C19-H19B	110.4	N8-C19-H19B	110.4
H19A-C19-H19B	108.6	C12-C20-C21	112.3(15)
C12-C20-C23	111.1(15)	C21-C20-C23	106.3(15)
C12-C20-H20	109.0	C21-C20-H20	109.0
C23-C20-H20	109.0	O4-C21-O5	124.5(18)
O4-C21-C20	126.1(18)	O5-C21-C20	109.4(18)
O5-C22-H22A	109.5	O5-C22-H22B	109.5
H22A-C22-H22B	109.5	O5-C22-H22C	109.5
H22A-C22-H22C	109.5	H22B-C22-H22C	109.5
O6-C23-O7	125.6(19)	O6-C23-C20	126.4(19)
O7-C23-C20	108.1(18)	O7-C24-H24A	109.5
O7-C24-H24B	109.5	H24A-C24-H24B	109.5
O7-C24-H24C	109.5	H24A-C24-H24C	109.5
H24B-C24-H24C	109.5	P1-C25-H25A	109.5
P1-C25-H25B	109.5	H25A-C25-H25B	109.5
P1-C25-H25C	109.5	H25A-C25-H25C	109.5
H25B-C25-H25C	109.5	P1-C26-H26A	109.5

P1-C26-H26B	109.5	H26A-C26-H26B	109.5
P1-C26-H26C	109.5	H26A-C26-H26C	109.5
H26B-C26-H26C	109.5	P1-C27-H27A	109.5
P1-C27-H27B	109.5	H27A-C27-H27B	109.5
P1-C27-H27C	109.5	H27A-C27-H27C	109.5
H27B-C27-H27C	109.5	N4-B1-N6	111.8(16)
N4-B1-N2	106.7(15)	N6-B1-N2	107.5(13)
N4-B1-H1A	110.2	N6-B1-H1A	110.2
N2-B1-H1A	110.2	N7-W1-C11	99.7(6)
N7-W1-N5	173.0(6)	C11-W1-N5	87.2(5)
N7-W1-N1	100.3(6)	C11-W1-N1	81.1(6)
N5-W1-N1	81.5(5)	N7-W1-N3	88.6(6)
C11-W1-N3	156.6(6)	N5-W1-N3	85.3(5)
N1-W1-N3	75.9(5)	N7-W1-C10	95.5(7)
C11-W1-C10	38.6(6)	N5-W1-C10	89.4(5)
N1-W1-C10	119.5(6)	N3-W1-C10	162.9(6)
N7-W1-P1	90.6(5)	C11-W1-P1	118.4(5)
N5-W1-P1	85.3(4)	N1-W1-P1	155.9(4)
N3-W1-P1	83.1(4)	C10-W1-P1	80.3(4)
O10-S2-O9	120.8(9)	O10-S2-N16	106.3(8)
O9-S2-N16	104.6(8)	O10-S2-C41	106.7(8)
O9-S2-C41	108.2(7)	N16-S2-C41	110.1(8)
C52-P2-C54	102.8(11)	C52-P2-C53	100.2(9)
C54-P2-C53	103.4(9)	C52-P2-W2	121.3(6)
C54-P2-W2	113.8(7)	C53-P2-W2	113.0(6)
C48-O12-C49	113.9(19)	C50-O14-C51	121.(4)
C28-N9-N10	102.5(13)	C28-N9-W2	136.1(11)
N10-N9-W2	121.1(10)	C30-N10-N9	112.1(15)
C30-N10-B2	128.3(14)	N9-N10-B2	119.6(13)
N12-N11-C31	105.7(13)	N12-N11-W2	123.5(10)
C31-N11-W2	130.5(11)	C33-N12-N11	109.0(14)
C33-N12-B2	130.3(14)	N11-N12-B2	118.7(13)
C34-N13-N14	106.2(14)	C34-N13-W2	133.4(13)
N14-N13-W2	120.2(10)	N13-N14-C36	107.2(14)
N13-N14-B2	121.9(13)	C36-N14-B2	129.4(15)
O8-N15-W2	174.6(13)	C43-N16-C46	114.1(17)
C43-N16-S2	118.1(12)	C46-N16-S2	117.9(13)
N9-C28-C29	111.1(16)	N9-C28-H28	124.5
C29-C28-H28	124.5	C30-C29-C28	105.5(16)

C30-C29-H29	127.3	C28-C29-H29	127.3
N10-C30-C29	108.7(15)	N10-C30-H30	125.6
C29-C30-H30	125.6	C32-C31-N11	108.9(17)
C32-C31-H31	125.5	N11-C31-H31	125.5
C31-C32-C33	108.2(17)	C31-C32-H32	125.9
C33-C32-H32	125.9	N12-C33-C32	108.3(14)
N12-C33-H33	125.8	C32-C33-H33	125.8
N13-C34-C35	112.0(18)	N13-C34-H34	124.0
C35-C34-H34	124.0	C36-C35-C34	105.9(18)
C36-C35-H35	127.1	C34-C35-H35	127.1
C35-C36-N14	108.6(18)	C35-C36-H36	125.7
N14-C36-H36	125.7	C38-C37-C42	116.7(13)
C38-C37-W2	68.1(8)	C42-C37-W2	117.3(10)
C38-C37-H37	115.5	C42-C37-H37	115.5
W2-C37-H37	115.5	C37-C38-C39	117.6(12)
C37-C38-W2	73.8(8)	C39-C38-W2	126.4(12)
C37-C38-H38	111.3	C39-C38-H38	111.3
W2-C38-H38	111.3	C40-C39-C38	111.1(13)
C40-C39-C47	110.0(13)	C38-C39-C47	111.4(15)
C40-C39-H39	108.1	C38-C39-H39	108.1
C47-C39-H39	108.1	C41-C40-C39	110.8(13)
C41-C40-H40A	109.5	C39-C40-H40A	109.5
C41-C40-H40B	109.5	C39-C40-H40B	109.5
H40A-C40-H40B	108.1	C42-C41-C40	122.3(13)
C42-C41-S2	118.6(13)	C40-C41-S2	119.0(11)
C41-C42-C37	123.1(15)	C41-C42-H42	118.4
C37-C42-H42	118.4	N16-C43-C44	108.8(16)
N16-C43-C44A	106.(2)	N16-C43-H43A	109.9
C44-C43-H43A	109.9	N16-C43-H43B	109.9
C44-C43-H43B	109.9	H43A-C43-H43B	108.3
N16-C43-H43C	110.6	C44A-C43-H43C	110.6
N16-C43-H43D	110.6	C44A-C43-H43D	110.6
H43C-C43-H43D	108.7	C43-C44-C45	97.4(18)
C43-C44-H44A	112.3	C45-C44-H44A	112.3
C43-C44-H44B	112.3	C45-C44-H44B	112.3
H44A-C44-H44B	109.9	C46-C45-C44A	111.(2)
C46-C45-C44	108.9(17)	C46-C45-H45A	109.9
C44-C45-H45A	109.9	C46-C45-H45B	109.9
C44-C45-H45B	109.9	H45A-C45-H45B	108.3

C46-C45-H45C	109.5	C44A-C45-H45C	109.5
C46-C45-H45D	109.5	C44A-C45-H45D	109.5
H45C-C45-H45D	108.0	N16-C46-C45	101.1(17)
N16-C46-H46A	111.6	C45-C46-H46A	111.6
N16-C46-H46B	111.6	C45-C46-H46B	111.6
H46A-C46-H46B	109.4	C50A-C47-C48	106.(3)
C50A-C47-C39	120.(4)	C48-C47-C39	111.8(14)
C48-C47-C50	110.(2)	C39-C47-C50	107.(3)
C48-C47-H47	109.6	C39-C47-H47	109.6
C50-C47-H47	109.6	C50A-C47-H47A	105.8
C48-C47-H47A	105.8	C39-C47-H47A	105.8
O11-C48-O12	124.8(19)	O11-C48-C47	124.(2)
O12-C48-C47	111.0(16)	O12-C49-H49A	109.5
O12-C49-H49B	109.5	H49A-C49-H49B	109.5
O12-C49-H49C	109.5	H49A-C49-H49C	109.5
H49B-C49-H49C	109.5	O13-C50-O14	124.(5)
O13-C50-C47	126.(6)	O14-C50-C47	107.(4)
O14-C51-H51A	109.5	O14-C51-H51B	109.5
H51A-C51-H51B	109.5	O14-C51-H51C	109.5
H51A-C51-H51C	109.5	H51B-C51-H51C	109.5
P2-C52-H52A	109.5	P2-C52-H52B	109.5
H52A-C52-H52B	109.5	P2-C52-H52C	109.5
H52A-C52-H52C	109.5	H52B-C52-H52C	109.5
P2-C53-H53A	109.5	P2-C53-H53B	109.5
H53A-C53-H53B	109.5	P2-C53-H53C	109.5
H53A-C53-H53C	109.5	H53B-C53-H53C	109.5
P2-C54-H54A	109.5	P2-C54-H54B	109.5
H54A-C54-H54B	109.5	P2-C54-H54C	109.5
H54A-C54-H54C	109.5	H54B-C54-H54C	109.5
N14-B2-N12	106.0(15)	N14-B2-N10	108.0(14)
N12-B2-N10	109.9(15)	N14-B2-H2	110.9
N12-B2-H2	110.9	N10-B2-H2	110.9
N15-W2-C38	99.7(6)	N15-W2-N13	100.7(7)
C38-W2-N13	82.6(6)	N15-W2-N11	88.0(6)
C38-W2-N11	158.5(6)	N13-W2-N11	76.3(5)
N15-W2-N9	172.1(5)	C38-W2-N9	88.0(5)
N13-W2-N9	81.9(5)	N11-W2-N9	85.3(5)
N15-W2-C37	96.1(6)	C38-W2-C37	38.1(6)
N13-W2-C37	120.3(5)	N11-W2-C37	161.4(6)

N9-W2-C37	88.9(5)	N15-W2-P2	90.7(5)
C38-W2-P2	117.6(5)	N13-W2-P2	155.0(4)
N11-W2-P2	82.0(4)	N9-W2-P2	84.1(3)
C37-W2-P2	79.8(4)	O13A-C50A-C47	118.(5)
O13A-C50A-O14A	120.(4)	C47-C50A-O14A	120.(6)
C51A-O14A-C50A	104.(5)	O14A-C51A-H51D	109.5
O14A-C51A-H51E	109.5	H51D-C51A-H51E	109.5
O14A-C51A-H51F	109.5	H51D-C51A-H51F	109.5
H51E-C51A-H51F	109.5	C45-C44A-C43	97.(2)
C45-C44A-H44C	112.3	C43-C44A-H44C	112.3
C45-C44A-H44D	112.3	C43-C44A-H44D	112.3
H44C-C44A-H44D	109.9	C18-C17A-C16A	97.(3)
C18-C17A-H17C	112.3	C16A-C17A-H17C	112.3
C18-C17A-H17D	112.3	C16A-C17A-H17D	112.3
H17C-C17A-H17D	109.9	N8-C16A-C17A	108.(3)
N8-C16A-H16C	110.0	C17A-C16A-H16C	110.0
N8-C16A-H16D	110.0	C17A-C16A-H16D	110.0
H16C-C16A-H16D	108.4		

Table 6. Torsion angles (°) for Harman_SS7_198_6_X2.

C1-N1-N2-C3	-1.2(18)	W1-N1-N2-C3	176.5(11)
C1-N1-N2-B1	-168.7(15)	W1-N1-N2-B1	9.0(18)
C4-N3-N4-C6	1.(2)	W1-N3-N4-C6	-170.0(12)
C4-N3-N4-B1	164.1(17)	W1-N3-N4-B1	-7.(2)
C7-N5-N6-C9	-3.1(19)	W1-N5-N6-C9	-173.1(12)
C7-N5-N6-B1	-179.6(15)	W1-N5-N6-B1	10.4(19)
O2-S1-N8-C19	-51.0(16)	O3-S1-N8-C19	-178.3(15)
C14-S1-N8-C19	67.2(16)	O2-S1-N8-C16A	175.(2)
O3-S1-N8-C16A	48.(3)	C14-S1-N8-C16A	-66.(2)
O2-S1-N8-C16	157.(3)	O3-S1-N8-C16	30.(3)
C14-S1-N8-C16	-85.(3)	N2-N1-C1-C2	-3.(2)
W1-N1-C1-C2	180.0(13)	N1-C1-C2-C3	5.(2)
N1-N2-C3-C2	4.(2)	B1-N2-C3-C2	170.5(16)
C1-C2-C3-N2	-6.(2)	N4-N3-C4-C5	-1.(2)
W1-N3-C4-C5	169.9(14)	N3-C4-C5-C6	0.(3)

N3-N4-C6-C5	-1.(2)	B1-N4-C6-C5	-162.1(19)
C4-C5-C6-N4	1.(2)	N6-N5-C7-C8	2.2(19)
W1-N5-C7-C8	170.2(12)	N5-C7-C8-C9	-1.(2)
N5-N6-C9-C8	3.(2)	B1-N6-C9-C8	179.0(16)
C7-C8-C9-N6	-1.(2)	C15-C10-C11-C12	13.5(18)
W1-C10-C11-C12	122.8(12)	C15-C10-C11-W1	-109.4(12)
C10-C11-C12-C20	81.4(18)	W1-C11-C12-C20	169.9(13)
C10-C11-C12-C13	-40.7(19)	W1-C11-C12-C13	48.(2)
C20-C12-C13-C14	-78.7(16)	C11-C12-C13-C14	45.9(18)
C12-C13-C14-C15	-27.9(19)	C12-C13-C14-S1	148.7(11)
O2-S1-C14-C15	3.3(14)	O3-S1-C14-C15	134.0(12)
N8-S1-C14-C15	-111.4(12)	O2-S1-C14-C13	-173.5(11)
O3-S1-C14-C13	-42.8(13)	N8-S1-C14-C13	71.8(13)
C13-C14-C15-C10	1.(2)	S1-C14-C15-C10	-175.2(10)
C11-C10-C15-C14	7.(2)	W1-C10-C15-C14	-70.1(16)
C19-N8-C16-C17	-21.(4)	S1-N8-C16-C17	133.(2)
N8-C16-C17-C18	38.(3)	C16-C17-C18-C19	-42.(3)
C17A-C18-C19-N8	-2.(3)	C17-C18-C19-N8	28.(2)
C16A-N8-C19-C18	-19.(2)	C16-N8-C19-C18	-4.(3)
S1-N8-C19-C18	-160.0(15)	C11-C12-C20-C21	42.(2)
C13-C12-C20-C21	168.3(15)	C11-C12-C20-C23	161.3(16)
C13-C12-C20-C23	-72.8(19)	C22-O5-C21-O4	-8.(3)
C22-O5-C21-C20	172.5(16)	C12-C20-C21-O4	75.(2)
C23-C20-C21-O4	-47.(3)	C12-C20-C21-O5	-105.8(18)
C23-C20-C21-O5	132.5(17)	C24-O7-C23-O6	-6.(4)
C24-O7-C23-C20	175.2(19)	C12-C20-C23-O6	-3.(3)
C21-C20-C23-O6	120.(3)	C12-C20-C23-O7	176.4(18)
C21-C20-C23-O7	-61.(2)	N3-N4-B1-N6	61.(2)
C6-N4-B1-N6	-139.2(19)	N3-N4-B1-N2	-56.(2)
C6-N4-B1-N2	103.(2)	C9-N6-B1-N4	120.3(19)
N5-N6-B1-N4	-64.(2)	C9-N6-B1-N2	-122.8(18)
N5-N6-B1-N2	53.(2)	C3-N2-B1-N4	-109.(2)

N1-N2-B1-N4	55.4(18)	C3-N2-B1-N6	130.5(18)
N1-N2-B1-N6	-64.7(19)	C28-N9-N10-C30	-3.3(17)
W2-N9-N10-C30	170.9(11)	C28-N9-N10-B2	175.6(14)
W2-N9-N10-B2	-10.2(18)	C31-N11-N12-C33	-0.2(19)
W2-N11-N12-C33	173.7(11)	C31-N11-N12-B2	-165.6(17)
W2-N11-N12-B2	8.(2)	C34-N13-N14-C36	2.(2)
W2-N13-N14-C36	-174.6(12)	C34-N13-N14-B2	169.4(17)
W2-N13-N14-B2	-8.(2)	O10-S2-N16-C43	-39.2(17)
O9-S2-N16-C43	-168.0(14)	C41-S2-N16-C43	76.0(16)
O10-S2-N16-C46	177.1(15)	O9-S2-N16-C46	48.3(16)
C41-S2-N16-C46	-67.7(17)	N10-N9-C28-C29	3.3(17)
W2-N9-C28-C29	-169.5(11)	N9-C28-C29-C30	-2.3(19)
N9-N10-C30-C29	2.0(19)	B2-N10-C30-C29	-176.8(15)
C28-C29-C30-N10	0.1(19)	N12-N11-C31-C32	0.(2)
W2-N11-C31-C32	-172.9(14)	N11-C31-C32-C33	-1.(2)
N11-N12-C33-C32	0.(2)	B2-N12-C33-C32	163.1(19)
C31-C32-C33-N12	0.(2)	N14-N13-C34-C35	-1.(2)
W2-N13-C34-C35	175.5(16)	N13-C34-C35-C36	-1.(3)
C34-C35-C36-N14	2.(3)	N13-N14-C36-C35	-3.(3)
B2-N14-C36-C35	-169.(2)	C42-C37-C38-C39	-12.(2)
W2-C37-C38-C39	-123.0(15)	C42-C37-C38-W2	110.6(12)
C37-C38-C39-C40	41.(2)	W2-C38-C39-C40	-48.6(19)
C37-C38-C39-C47	-82.1(18)	W2-C38-C39-C47	-171.7(11)
C38-C39-C40-C41	-48.1(18)	C47-C39-C40-C41	75.8(17)
C39-C40-C41-C42	30.9(19)	C39-C40-C41-S2	-146.0(11)
O10-S2-C41-C42	-133.6(13)	O9-S2-C41-C42	-2.2(14)
N16-S2-C41-C42	111.5(13)	O10-S2-C41-C40	43.4(14)
O9-S2-C41-C40	174.8(11)	N16-S2-C41-C40	-71.5(13)
C40-C41-C42-C37	-1.(2)	S2-C41-C42-C37	175.6(11)
C38-C37-C42-C41	-9.(2)	W2-C37-C42-C41	69.1(17)

C46-N16-C43-C44	9.(2)	S2-N16-C43-C44	-135.5(16)
C46-N16-C43-C44A	-29.(3)	S2-N16-C43-C44A	-174.(2)
N16-C43-C44-C45	-24.(2)	C43-C44-C45-C46	31.(2)
C43-N16-C46-C45	11.(2)	S2-N16-C46-C45	155.8(14)
C44A-C45-C46-N16	12.(3)	C44-C45-C46-N16	-27.(2)
C40-C39-C47-C50A	69.(4)	C38-C39-C47-C50A	-168.(4)
C40-C39-C47-C48	-165.8(16)	C38-C39-C47-C48	-42.(2)
C40-C39-C47-C50	74.(3)	C38-C39-C47-C50	-162.(3)
C49-O12-C48-O11	4.(3)	C49-O12-C48-C47	-174.7(19)
C50A-C47-C48-O11	59.(4)	C39-C47-C48-O11	-74.(2)
C50-C47-C48-O11	44.(3)	C50A-C47-C48-O12	-122.(4)
C39-C47-C48-O12	104.9(18)	C50-C47-C48-O12	-137.(3)
C51-O14-C50-O13	-18.(9)	C51-O14-C50-C47	179.(4)
C48-C47-C50-O13	-102.(6)	C39-C47-C50-O13	20.(7)
C48-C47-C50-O14	61.(4)	C39-C47-C50-O14	-178.(3)
N13-N14-B2-N12	-55.(2)	C36-N14-B2-N12	109.(2)
N13-N14-B2-N10	63.(2)	C36-N14-B2-N10	-133.(2)
C33-N12-B2-N14	-108.1(19)	N11-N12-B2-N14	54.(2)
C33-N12-B2-N10	135.4(18)	N11-N12-B2-N10	-63.(2)
C30-N10-B2-N14	127.6(17)	N9-N10-B2-N14	-51.1(19)
C30-N10-B2-N12	-117.2(18)	N9-N10-B2-N12	64.1(18)
C48-C47-C50A-O13A	71.(6)	C39-C47-C50A-O13A	-160.(4)
C48-C47-C50A-O14A	-124.(5)	C39-C47-C50A-O14A	4.(7)
O13A-C50A-O14A-C51A	-35.(7)	C47-C50A-O14A-C51A	161.(5)
C46-C45-C44A-C43	-27.(4)	N16-C43-C44A-C45	32.(4)
C19-C18-C17A-C16A	21.(3)	C19-N8-C16A-C17A	33.(3)
S1-N8-C16A-C17A	173.(2)	C18-C17A-C16A-N8	-32.(4)

Table 7. Anisotropic atomic displacement parameters (Å^2) for Harman_SS7_198_6_X2.

The anisotropic atomic displacement factor exponent takes the form: $-2\pi^2[h^2 a^{*2} U_{11} + ... + 2 h k a^* b^* U_{12}]$

	U_{11}	U_{22}	U_{33}	U_{23}	U_{13}	U_{12}
S1	0.0374(18)	0.063(3)	0.0408(18)	0.0226(17)	0.0047(15)	0.0182(18)
P1	0.049(2)	0.046(2)	0.0339(17)	0.0145(15)	0.0046(15)	0.0177(18)
O1	0.042(7)	0.066(9)	0.068(8)	0.015(7)	-0.014(6)	0.018(6)
O2	0.035(6)	0.065(8)	0.071(8)	0.038(7)	0.009(5)	0.013(6)
O3	0.050(7)	0.093(11)	0.038(6)	0.019(6)	0.010(5)	0.028(7)
O4	0.055(8)	0.082(11)	0.072(9)	0.006(8)	-0.005(7)	0.010(8)
O5	0.065(9)	0.102(12)	0.052(7)	0.014(7)	0.002(6)	0.043(9)
O6	0.082(11)	0.101(13)	0.049(8)	-0.013(8)	0.009(7)	0.040(11)
O7	0.081(11)	0.132(16)	0.042(7)	0.029(8)	0.007(7)	0.048(11)
N1	0.048(7)	0.038(7)	0.050(7)	0.012(6)	0.005(6)	0.019(6)
N2	0.041(7)	0.055(9)	0.052(8)	0.022(7)	-0.004(6)	0.004(7)
N3	0.043(7)	0.041(7)	0.042(7)	0.020(6)	-0.005(5)	0.007(6)
N4	0.055(8)	0.050(8)	0.039(7)	0.027(6)	-0.001(6)	0.005(7)
N5	0.047(7)	0.035(7)	0.044(7)	0.015(5)	-0.005(6)	0.005(6)
N6	0.047(7)	0.052(8)	0.029(6)	0.018(5)	0.006(5)	0.007(6)
N7	0.037(7)	0.057(9)	0.043(7)	0.009(6)	0.012(6)	0.009(6)
N8	0.033(7)	0.064(9)	0.047(7)	0.019(7)	0.006(5)	0.016(6)
C1	0.061(11)	0.063(12)	0.055(10)	0.027(9)	0.012(8)	0.027(10)
C2	0.072(13)	0.038(9)	0.066(11)	0.015(8)	0.008(10)	0.014(9)
C3	0.074(13)	0.038(9)	0.062(11)	0.010(8)	-0.015(10)	0.014(9)
C4	0.053(11)	0.067(12)	0.054(10)	0.022(9)	-0.026(8)	0.010(9)
C5	0.052(11)	0.067(13)	0.067(12)	0.027(10)	-0.016(9)	0.002(10)
C6	0.067(12)	0.052(10)	0.049(9)	0.020(8)	-0.012(8)	0.011(9)
C7	0.060(11)	0.066(12)	0.038(8)	0.021(8)	0.011(7)	0.034(10)
C8	0.066(11)	0.066(11)	0.033(7)	0.008(7)	0.015(7)	0.040(10)
C9	0.040(9)	0.069(12)	0.049(9)	0.025(8)	0.013(7)	0.010(8)
C10	0.054(9)	0.052(9)	0.031(7)	0.027(6)	0.010(6)	0.026(8)
C11	0.038(8)	0.067(11)	0.032(7)	0.016(7)	0.001(6)	0.021(8)
C12	0.048(9)	0.045(9)	0.041(8)	0.006(7)	-0.005(7)	0.014(8)
C13	0.054(10)	0.063(11)	0.030(7)	0.016(7)	0.013(6)	0.032(9)
C14	0.034(7)	0.049(9)	0.040(7)	0.010(6)	-0.003(6)	0.013(7)
C15	0.044(8)	0.048(9)	0.028(6)	0.021(6)	-0.001(6)	0.014(7)
C16	0.07(2)	0.045(15)	0.058(17)	-0.002(13)	-0.026(16)	-0.003(15)
C17	0.031(14)	0.052(15)	0.077(16)	0.044(12)	0.018(11)	0.003(11)

C18	0.050(10)	0.086(15)	0.048(9)	0.005(9)	-0.023(8)	0.022(10)
C19	0.052(10)	0.061(11)	0.047(9)	0.012(8)	-0.001(7)	0.021(9)
C20	0.034(8)	0.072(12)	0.044(8)	0.013(8)	0.009(6)	0.020(8)
C21	0.046(10)	0.074(13)	0.047(9)	0.024(8)	-0.002(7)	0.030(10)
C22	0.078(17)	0.14(3)	0.077(15)	0.010(16)	0.004(13)	0.074(19)
C23	0.050(10)	0.095(16)	0.038(9)	0.001(9)	0.003(7)	0.023(11)
C24	0.049(11)	0.13(2)	0.059(12)	0.015(13)	0.010(9)	0.039(14)
C25	0.052(10)	0.064(12)	0.048(9)	0.004(8)	-0.005(8)	0.020(9)
C26	0.073(12)	0.034(8)	0.035(7)	0.002(6)	-0.001(7)	0.012(8)
C27	0.072(12)	0.057(11)	0.041(8)	0.024(8)	0.017(8)	0.015(10)
B1	0.042(10)	0.048(11)	0.059(11)	0.030(9)	0.004(8)	0.010(8)
W1	0.0395(4)	0.0442(4)	0.0354(4)	0.0142(3)	0.0011(3)	0.0154(3)
S2	0.0355(18)	0.064(3)	0.0444(19)	0.0281(18)	0.0119(15)	0.0202(18)
P2	0.044(2)	0.044(2)	0.0320(16)	0.0132(15)	0.0035(15)	0.0134(17)
O8	0.022(5)	0.082(9)	0.065(8)	0.031(7)	-0.001(5)	0.004(6)
O9	0.042(6)	0.069(8)	0.055(7)	0.033(6)	0.014(5)	0.020(6)
O10	0.047(7)	0.085(10)	0.060(8)	0.032(7)	0.000(6)	0.023(7)
O11	0.067(9)	0.080(10)	0.058(8)	0.013(7)	0.014(7)	0.037(8)
O12	0.051(7)	0.077(9)	0.045(6)	0.020(6)	0.008(5)	0.008(7)
O13	0.073(10)	0.088(12)	0.039(5)	-0.008(6)	-0.015(5)	0.030(8)
O14	0.073(10)	0.088(12)	0.039(5)	-0.008(6)	-0.015(5)	0.030(8)
N9	0.042(7)	0.033(6)	0.033(6)	0.005(5)	0.012(5)	0.002(5)
N10	0.042(7)	0.060(9)	0.035(6)	0.016(6)	0.001(5)	0.025(7)
N11	0.049(7)	0.046(7)	0.031(6)	0.021(5)	0.019(5)	0.021(6)
N12	0.057(8)	0.040(7)	0.045(7)	0.021(6)	0.006(6)	0.014(7)
N13	0.053(8)	0.032(6)	0.044(7)	0.018(5)	0.010(6)	0.016(6)
N14	0.056(8)	0.039(7)	0.046(7)	0.008(6)	0.008(6)	0.019(7)
N15	0.046(8)	0.073(10)	0.039(7)	0.019(7)	0.008(6)	0.028(8)
N16	0.051(8)	0.096(12)	0.026(6)	0.009(7)	0.017(5)	0.042(9)
C28	0.044(9)	0.060(11)	0.045(8)	0.022(8)	0.012(7)	0.019(8)
C29	0.045(9)	0.071(12)	0.023(6)	-0.002(7)	0.004(6)	0.013(8)
C30	0.033(8)	0.064(11)	0.049(8)	0.025(8)	0.011(6)	0.019(8)
C31	0.065(11)	0.066(12)	0.041(8)	0.026(8)	0.018(8)	0.018(10)
C32	0.060(11)	0.061(11)	0.049(9)	0.021(8)	0.023(8)	0.019(9)
C33	0.058(10)	0.039(8)	0.032(7)	0.017(6)	0.003(6)	0.015(7)
C34	0.053(10)	0.068(13)	0.046(9)	0.017(9)	-0.010(8)	-0.010(9)
C35	0.083(16)	0.042(11)	0.082(15)	-0.008(10)	0.000(12)	0.008(11)
C36	0.098(17)	0.052(11)	0.045(9)	0.016(8)	0.012(10)	0.024(11)
C37	0.034(7)	0.046(8)	0.036(7)	0.025(6)	0.007(6)	0.010(6)

C38	0.044(8)	0.062(10)	0.034(7)	0.019(7)	-0.003(6)	0.026(8)
C39	0.041(8)	0.047(9)	0.038(7)	0.013(6)	0.007(6)	0.015(7)
C40	0.024(6)	0.058(10)	0.041(7)	0.017(7)	0.004(6)	0.013(7)
C41	0.038(7)	0.045(8)	0.034(7)	0.022(6)	0.011(6)	0.016(7)
C42	0.043(8)	0.049(9)	0.028(6)	0.012(6)	0.011(6)	0.018(7)
C43	0.044(9)	0.049(10)	0.067(11)	-0.009(9)	-0.001(8)	0.013(8)
C44	0.057(17)	0.057(17)	0.056(15)	0.023(12)	-0.007(12)	0.011(13)
C45	0.057(11)	0.081(15)	0.079(14)	0.051(12)	0.020(10)	0.024(11)
C46	0.050(10)	0.068(12)	0.056(10)	0.019(9)	0.022(8)	0.025(9)
C47	0.062(11)	0.063(11)	0.036(8)	0.016(7)	0.013(7)	0.026(9)
C48	0.061(11)	0.065(12)	0.030(7)	0.013(7)	0.007(7)	0.025(10)
C49	0.054(13)	0.11(2)	0.097(19)	-0.006(16)	-0.010(13)	0.012(14)
C50	0.073(10)	0.088(12)	0.039(5)	-0.008(6)	-0.015(5)	0.030(8)
C51	0.073(10)	0.088(12)	0.039(5)	-0.008(6)	-0.015(5)	0.030(8)
C52	0.084(14)	0.043(10)	0.037(8)	0.008(7)	0.004(8)	0.007(9)
C53	0.058(10)	0.056(10)	0.037(8)	0.018(7)	-0.007(7)	0.011(9)
C54	0.062(11)	0.068(13)	0.052(10)	0.012(9)	0.006(8)	0.027(10)
B2	0.054(11)	0.059(12)	0.045(10)	0.025(9)	0.004(8)	0.021(10)
W2	0.0349(4)	0.0440(4)	0.0326(3)	0.0149(3)	0.0060(2)	0.0126(3)
O13A	0.073(10)	0.088(12)	0.039(5)	-0.008(6)	-0.015(5)	0.030(8)
C50A	0.073(10)	0.088(12)	0.039(5)	-0.008(6)	-0.015(5)	0.030(8)
O14A	0.073(10)	0.088(12)	0.039(5)	-0.008(6)	-0.015(5)	0.030(8)
C51A	0.073(10)	0.088(12)	0.039(5)	-0.008(6)	-0.015(5)	0.030(8)
C44A	0.06(3)	0.05(3)	0.05(2)	0.01(2)	0.03(2)	0.02(2)
C17A	0.044(19)	0.045(17)	0.053(17)	0.035(14)	-0.007(16)	-0.023(16)
C16A	0.016(14)	0.030(17)	0.060(18)	0.002(14)	0.024(14)	-0.002(13)

Table 8. Hydrogen atomic coordinates and isotropic atomic displacement parameters (Å^2) for Harman_SS7_198_6_X2.

	x/a	y/b	z/c	U(eq)
H1	0.5585	0.4526	0.0276	0.067
H2A	0.6944	0.6034	0.0347	0.07
H3	0.7958	0.5758	-0.0777	0.071
H4	0.3813	0.2676	-0.2261	0.07
H5	0.4435	0.3671	-0.3097	0.076
H6	0.6501	0.4292	-0.2883	0.067
H7	0.7448	0.1260	-0.1026	0.06
H8	0.9233	0.1704	-0.1595	0.062

H9	0.9229	0.3182	-0.1960	0.062
H10	0.5950	0.1073	-0.0353	0.049
H11	0.6701	0.2616	0.0211	0.053
H12	0.5536	0.3522	0.0891	0.054
H13A	0.3782	0.2588	0.1191	0.054
H13B	0.3769	0.2776	0.0418	0.054
H15	0.4101	0.0328	-0.0252	0.045
H16A	0.1499	0.2232	0.0997	0.077
H16B	0.0284	0.1520	0.0800	0.077
H17A	0.0340	0.2448	-0.0020	0.061
H17B	0.1606	0.2519	-0.0143	0.061
H18A	-0.0230	0.0850	-0.0684	0.075
H18B	0.0700	0.1315	-0.1150	0.075
H18C	-0.0130	0.0743	-0.0941	0.075
H18D	0.0929	0.1559	-0.1001	0.075
H19A	0.1953	0.0754	-0.0741	0.064
H19B	0.0889	-0.0050	-0.0656	0.064
H20	0.5351	0.1909	0.1406	0.059
H22A	0.8586	0.2184	0.0795	0.139
H22B	0.8521	0.1413	0.1229	0.139
H22C	0.8779	0.2499	0.1641	0.139
H24A	0.5817	0.4178	0.3376	0.119
H24B	0.6201	0.3476	0.3739	0.119
H24C	0.4933	0.3304	0.3538	0.119
H25A	0.3199	-0.0153	-0.2433	0.084
H25B	0.3114	0.0902	-0.2234	0.084
H25C	0.3021	0.0342	-0.1635	0.084
H26A	0.5037	-0.0211	-0.1244	0.074
H26B	0.6037	-0.0018	-0.1732	0.074
H26C	0.4874	-0.0699	-0.2077	0.074
H27A	0.5340	0.0289	-0.3007	0.083
H27B	0.6181	0.1284	-0.2643	0.083
H27C	0.5007	0.1235	-0.2965	0.083
H1A	0.7929	0.4268	-0.1875	0.057
H28	-0.1703	0.1342	0.4046	0.056
H29	-0.3120	0.1757	0.3399	0.059
H30	-0.2156	0.3173	0.3007	0.055
H31	0.2945	0.2722	0.2727	0.066
H32	0.2867	0.3666	0.1900	0.066

H33	0.1259	0.4268	0.2121	0.05
H34	0.2326	0.4554	0.5360	0.073
H35	0.2071	0.6132	0.5364	0.09
H36	0.0857	0.5890	0.4314	0.077
H37	-0.0254	0.1117	0.4647	0.044
H38	0.0000	0.2623	0.5241	0.052
H39	0.1749	0.3530	0.5936	0.049
H40A	0.2976	0.2780	0.5408	0.048
H40B	0.2902	0.2593	0.6181	0.048
H42	0.1113	0.0337	0.4750	0.046
H43A	0.5481	0.1627	0.5876	0.069
H43B	0.4589	0.2201	0.5917	0.069
H43C	0.5164	0.1759	0.6077	0.069
H43D	0.4639	0.2308	0.5629	0.069
H44A	0.6266	0.2495	0.5109	0.067
H44B	0.5125	0.2674	0.4905	0.067
H45A	0.5139	0.1427	0.3920	0.079
H45B	0.5796	0.0972	0.4369	0.079
H45C	0.5047	0.1744	0.4154	0.079
H45D	0.5618	0.0914	0.4055	0.079
H46A	0.3509	0.0711	0.4259	0.067
H46B	0.4144	-0.0042	0.4341	0.067
H47	0.0854	0.1893	0.6461	0.062
H47A	0.0795	0.1871	0.6400	0.062
H49A	-0.2189	0.2072	0.5790	0.14
H49B	-0.2145	0.2449	0.6634	0.14
H49C	-0.2579	0.1348	0.6267	0.14
H51A	0.1839	0.4129	0.8444	0.104
H51B	0.2288	0.3256	0.8467	0.104
H51C	0.1107	0.3285	0.8730	0.104
H52A	-0.1006	0.0048	0.3294	0.086
H52B	-0.0101	-0.0213	0.3710	0.086
H52C	-0.0315	-0.0615	0.2868	0.086
H53A	0.0053	0.0393	0.1950	0.076
H53B	0.0763	0.1466	0.2106	0.076
H53C	-0.0458	0.1213	0.2347	0.076
H54A	0.2148	0.0312	0.3333	0.089
H54B	0.2508	0.1004	0.2828	0.089
H54C	0.1718	-0.0031	0.2514	0.089

H2	-0.0153	0.4358	0.3182	0.06
H51D	0.2343	0.4774	0.8095	0.104
H51E	0.3306	0.4338	0.8232	0.104
H51F	0.2064	0.3777	0.8277	0.104
H44C	0.6318	0.2448	0.5108	0.066
H44D	0.6405	0.1452	0.5210	0.066
H17C	-0.0458	0.1573	0.0150	0.06
H17D	0.0297	0.2473	-0.0082	0.06
H16C	0.1879	0.2396	0.0467	0.046
H16D	0.1021	0.2006	0.0997	0.046

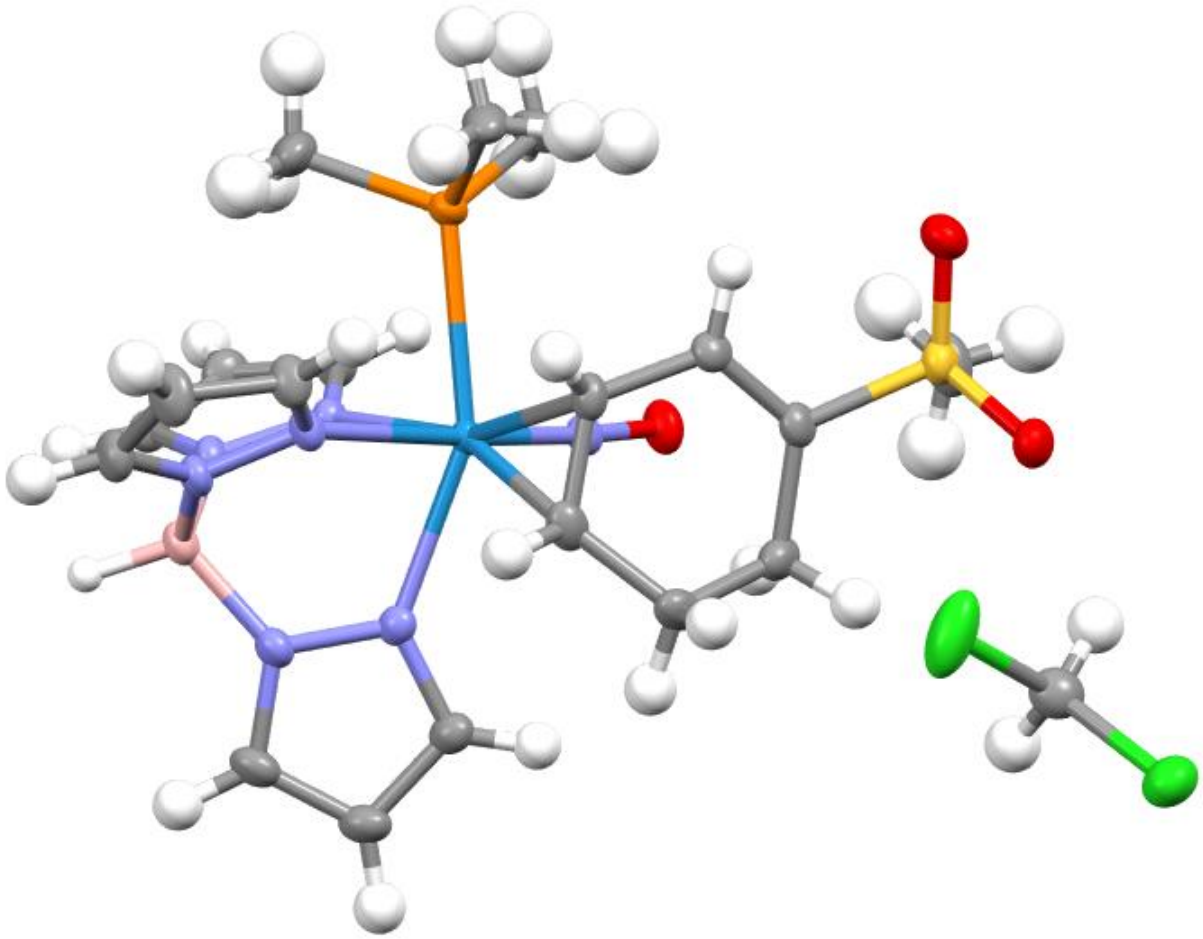

Crystal Structure Report for 17 in Chapter 4

A yellow plate-like specimen of $C_{20}H_{31}BCl_2N_7O_3PSW$, approximate dimensions 0.079 mm x 0.144 mm x 0.223 mm, was coated with Paratone oil and mounted on a MiTeGen MicroLoop. The X-ray intensity data were measured on a Bruker Kappa APEXII Duo system equipped with a fine-focus sealed tube (Mo K_α, λ = 0.71073 Å) and a graphite monochromator.

The total exposure time was 3.56 hours. The frames were integrated with the Bruker SAINT software package[20] using a narrow-frame algorithm. The integration of the data using a monoclinic unit cell yielded a total of 37280 reflections to a maximum θ angle of 28.33° (0.75 Å resolution), of which 6837 were independent (average redundancy 5.453, completeness = 99.8%, R_{int} = 3.83%, R_{sig} = 2.79%) and 6005 (87.83%) were greater than $2\sigma(F^2)$. The final cell constants of a = 8.4005(6) Å, b = 12.5289(9) Å, c = 26.2545(17) Å, β = 95.218(2)°, volume = 2751.8(3) $Å^3$, are based upon the refinement of the XYZ-centroids of 9938 reflections above 20 σ(I) with 4.503° < 2θ < 56.44°. Data were corrected for absorption effects using the Multi-Scan method (SADABS).[1] The ratio of minimum to maximum apparent transmission was 0.814. The calculated minimum and maximum transmission coefficients (based on

[20] Bruker (2012). *Saint; SADABS; APEX3*. Bruker AXS Inc., Madison, Wisconsin, USA.

crystal size) are 0.4007 and 0.4920.

The structure was solved and refined using the Bruker SHELXTL Software Package[21] within APEX3 [1] and OLEX2,[22] using the space group P $2_1/c$, with Z = 4 for the formula unit, $C_{20}H_{31}BCl_2N_7O_3PSW$. Non-hydrogen atoms were refined anisotropically. The B-H hydrogen atom, as well as H10 and H11, were located in the electron density map and refined isotropically. All other hydrogen atoms were placed in geometrically calculated positions with U_{iso} = 1.2U_{equiv} of the parent atom (U_{iso} = 1.5U_{equiv} for methyl). The final anisotropic full-matrix least-squares refinement on F^2 with 341 variables converged at R1 = 2.76%, for the observed data and wR2 = 5.84% for all data. The goodness-of-fit was 1.076. The largest peak in the final difference electron density synthesis was 2.123 $e^-/Å^3$ and the largest hole was -1.183 $e^-/Å^3$ with an RMS deviation of 0.113 $e^-/Å^3$. On the basis of the final model, the calculated density was 1.801 g/cm^3 and F(000), 1472 e^-.

Table 1. Sample and crystal data for Harman_SS7_198_3_X1.

Identification code	Harman_SS7_198_3_X1	
Chemical formula	$C_{20}H_{31}BCl_2N_7O_3PSW$	
Formula weight	746.11 g/mol	
Temperature	100(2) K	
Wavelength	0.71073 Å	
Crystal size	0.079 x 0.144 x 0.223 mm	
Crystal habit	yellow plate	
Crystal system	monoclinic	
Space group	P $2_1/c$	
Unit cell dimensions	a = 8.4005(6) Å	α = 90°
	b = 12.5289(9) Å	β = 95.218(2)°
	c = 26.2545(17) Å	γ = 90°
Volume	2751.8(3) $Å^3$	
Z	4	
Density (calculated)	1.801 g/cm^3	
Absorption coefficient	4.563 mm^{-1}	
F(000)	1472	

Table 2. Data collection and structure refinement for Harman_SS7_198_3_X1.

Diffractometer	Bruker Kappa APEXII Duo

[21] Sheldrick, G. M. (2015). *Acta Cryst.* A**71**, 3-8.
[22] Dolomanov, O. V.; Bourhis, L. J.; Gildea, R. J.; Howard, J. A. K.; Puschmann, H. *J. Appl. Cryst.* (2009). **42**, 339-341.

Radiation source	fine-focus sealed tube (Mo K_α, λ = 0.71073 Å)	
Theta range for data collection	1.56 to 28.33°	
Index ranges	-11<=h<=11, -16<=k<=16, -33<=l<=34	
Reflections collected	37280	
Independent reflections	6837 [R(int) = 0.0383]	
Coverage of independent reflections	99.8%	
Absorption correction	Multi-Scan	
Max. and min. transmission	0.4920 and 0.4007	
Structure solution technique	direct methods	
Structure solution program	SHELXT 2018/2 (Sheldrick, 2018)	
Refinement method	Full-matrix least-squares on F^2	
Refinement program	SHELXL-2018/3 (Sheldrick, 2018)	
Function minimized	$\Sigma\, w(F_o^2 - F_c^2)^2$	
Data / restraints / parameters	6837 / 0 / 341	
Goodness-of-fit on F^2	1.076	
Δ/σ_{max}	0.002	
Final R indices	6005 data; I>2σ(I)	R1 = 0.0276, wR2 = 0.0562
	all data	R1 = 0.0348, wR2 = 0.0584
Weighting scheme	$w=1/[\sigma^2(F_o^2)+(0.0182P)^2+6.9716P]$ where $P=(F_o^2+2F_c^2)/3$	
Largest diff. peak and hole	2.123 and -1.183 eÅ^{-3}	
R.M.S. deviation from mean	0.113 eÅ^{-3}	

Table 3. Atomic coordinates and equivalent isotropic atomic displacement parameters (Å^2) for Harman_SS7_198_3_X1.

U(eq) is defined as one third of the trace of the orthogonalized U_{ij} tensor.

	x/a	y/b	z/c	U(eq)
W1	0.34589(2)	0.69785(2)	0.39085(2)	0.01502(4)
Cl1	0.74593(18)	0.79483(10)	0.63040(5)	0.0577(4)
Cl2	0.82830(14)	0.97932(9)	0.69460(4)	0.0407(2)
S1	0.21809(11)	0.82372(7)	0.57469(3)	0.02406(19)
P1	0.12030(11)	0.56752(8)	0.39641(3)	0.02144(19)

O1	0.1446(3)	0.8797(2)	0.42275(10)	0.0282(6)
O2	0.1235(3)	0.7361(2)	0.59110(11)	0.0329(6)
O3	0.3196(3)	0.8789(2)	0.61359(10)	0.0304(6)
N1	0.4726(3)	0.5566(2)	0.36044(10)	0.0192(6)
N2	0.5127(3)	0.5551(2)	0.31113(11)	0.0208(6)
N3	0.2331(3)	0.7143(2)	0.31217(10)	0.0179(6)
N4	0.3049(3)	0.6807(2)	0.27036(10)	0.0198(6)
N5	0.5279(3)	0.7847(2)	0.35055(11)	0.0197(6)
N6	0.5686(3)	0.7503(2)	0.30401(11)	0.0218(6)
N7	0.2318(3)	0.8071(2)	0.41044(10)	0.0194(6)
C1	0.5167(5)	0.4612(3)	0.38015(14)	0.0264(8)
C2	0.5837(5)	0.3988(3)	0.34427(16)	0.0343(9)
C3	0.5797(5)	0.4613(3)	0.30131(15)	0.0285(8)
C4	0.0902(4)	0.7535(3)	0.29437(14)	0.0221(7)
C5	0.0699(5)	0.7455(3)	0.24144(14)	0.0262(8)
C6	0.2078(4)	0.6996(3)	0.22764(13)	0.0245(7)
C7	0.6105(4)	0.8754(3)	0.36046(14)	0.0243(7)
C8	0.7040(4)	0.8986(3)	0.32093(15)	0.0290(8)
C9	0.6748(4)	0.8185(3)	0.28634(15)	0.0273(8)
C10	0.4106(4)	0.6368(3)	0.46998(13)	0.0232(7)
C11	0.5378(4)	0.7010(3)	0.45355(13)	0.0252(7)
C12	0.5936(4)	0.7960(3)	0.48671(14)	0.0290(8)
C13	0.4557(5)	0.8568(3)	0.50854(14)	0.0274(8)
C14	0.3370(4)	0.7796(3)	0.52755(13)	0.0217(7)
C15	0.3164(4)	0.6795(3)	0.50983(13)	0.0214(7)
C16	0.0887(5)	0.9189(4)	0.54439(16)	0.0386(10)
C17	0.9315(5)	0.6286(4)	0.40946(18)	0.0373(10)
C18	0.1390(5)	0.4590(3)	0.44305(15)	0.0319(9)
C19	0.0698(5)	0.4928(3)	0.33746(16)	0.0354(9)
C20	0.7011(5)	0.9279(3)	0.64311(16)	0.0338(9)
B1	0.4847(5)	0.6540(3)	0.27679(15)	0.0227(8)

Table 4. Bond lengths (Å) for Harman_SS7_198_3_X1.

W1-N7	1.774(3)	W1-C11	2.197(3)
W1-N3	2.203(3)	W1-N5	2.222(3)
W1-C10	2.234(4)	W1-N1	2.249(3)

W1-P1	2.5158(9)	Cl1-C20	1.748(4)
Cl2-C20	1.767(4)	S1-O2	1.444(3)
S1-O3	1.446(3)	S1-C14	1.749(4)
S1-C16	1.754(4)	P1-C17	1.822(4)
P1-C19	1.825(4)	P1-C18	1.827(4)
O1-N7	1.230(4)	N1-C1	1.341(4)
N1-N2	1.367(4)	N2-C3	1.339(5)
N2-B1	1.537(5)	N3-C4	1.341(4)
N3-N4	1.366(4)	N4-C6	1.346(4)
N4-B1	1.541(5)	N5-C7	1.345(5)
N5-N6	1.368(4)	N6-C9	1.349(5)
N6-B1	1.540(5)	C1-C2	1.383(5)
C1-H1	0.95	C2-C3	1.371(6)
C2-H2	0.95	C3-H3	0.95
C4-C5	1.388(5)	C4-H4	0.95
C5-C6	1.371(5)	C5-H5	0.95
C6-H6	0.95	C7-C8	1.388(5)
C7-H7	0.95	C8-C9	1.360(6)
C8-H8	0.95	C9-H9	0.95
C10-C11	1.435(5)	C10-C15	1.469(5)
C10-H10	0.85(5)	C11-C12	1.524(5)
C11-H11	0.97(4)	C12-C13	1.540(5)
C12-H12A	0.99	C12-H12B	0.99
C13-C14	1.506(5)	C13-H13A	0.99
C13-H13B	0.99	C14-C15	1.343(5)
C15-H15	0.95	C16-H16A	0.98
C16-H16B	0.98	C16-H16C	0.98
C17-H17A	0.98	C17-H17B	0.98
C17-H17C	0.98	C18-H18A	0.98
C18-H18B	0.98	C18-H18C	0.98
C19-H19A	0.98	C19-H19B	0.98
C19-H19C	0.98	C20-H20A	0.99
C20-H20B	0.99	B1-H1A	1.11(3)

Table 5. Bond angles (°) for Harman_SS7_198_3_X1.

N7-W1-C11	98.50(14)	N7-W1-N3	90.12(11)
C11-W1-N3	157.62(12)	N7-W1-N5	100.01(12)

C11-W1-N5	81.84(12)	N3-W1-N5	76.33(10)
N7-W1-C10	94.99(13)	C11-W1-C10	37.77(14)
N3-W1-C10	162.11(13)	N5-W1-C10	119.38(12)
N7-W1-N1	174.82(12)	C11-W1-N1	86.64(12)
N3-W1-N1	85.28(10)	N5-W1-N1	81.24(10)
C10-W1-N1	88.71(12)	N7-W1-P1	93.11(10)
C11-W1-P1	118.26(11)	N3-W1-P1	81.55(8)
N5-W1-P1	154.19(8)	C10-W1-P1	81.07(10)
N1-W1-P1	83.87(8)	O2-S1-O3	117.28(17)
O2-S1-C14	109.63(17)	O3-S1-C14	108.24(17)
O2-S1-C16	108.5(2)	O3-S1-C16	107.2(2)
C14-S1-C16	105.30(18)	C17-P1-C19	103.7(2)
C17-P1-C18	102.1(2)	C19-P1-C18	100.72(19)
C17-P1-W1	114.29(15)	C19-P1-W1	113.68(14)
C18-P1-W1	120.16(14)	C1-N1-N2	105.7(3)
C1-N1-W1	133.4(2)	N2-N1-W1	120.8(2)
C3-N2-N1	109.8(3)	C3-N2-B1	129.7(3)
N1-N2-B1	120.5(3)	C4-N3-N4	106.2(3)
C4-N3-W1	131.0(2)	N4-N3-W1	122.7(2)
C6-N4-N3	109.7(3)	C6-N4-B1	130.0(3)
N3-N4-B1	118.6(3)	C7-N5-N6	105.8(3)
C7-N5-W1	133.4(2)	N6-N5-W1	120.6(2)
C9-N6-N5	109.5(3)	C9-N6-B1	128.8(3)
N5-N6-B1	121.4(3)	O1-N7-W1	176.1(3)
N1-C1-C2	110.9(3)	N1-C1-H1	124.6
C2-C1-H1	124.6	C3-C2-C1	104.8(3)
C3-C2-H2	127.6	C1-C2-H2	127.6
N2-C3-C2	108.8(3)	N2-C3-H3	125.6
C2-C3-H3	125.6	N3-C4-C5	110.3(3)
N3-C4-H4	124.8	C5-C4-H4	124.8
C6-C5-C4	105.4(3)	C6-C5-H5	127.3
C4-C5-H5	127.3	N4-C6-C5	108.4(3)
N4-C6-H6	125.8	C5-C6-H6	125.8
N5-C7-C8	110.4(3)	N5-C7-H7	124.8
C8-C7-H7	124.8	C9-C8-C7	105.4(3)
C9-C8-H8	127.3	C7-C8-H8	127.3
N6-C9-C8	108.8(3)	N6-C9-H9	125.6

C8-C9-H9	125.6	C11-C10-C15	118.3(3)
C11-C10-W1	69.7(2)	C15-C10-W1	115.8(2)
C11-C10-H10	119.(3)	C15-C10-H10	112.(3)
W1-C10-H10	115.(3)	C10-C11-C12	117.7(3)
C10-C11-W1	72.5(2)	C12-C11-W1	127.5(3)
C10-C11-H11	113.(3)	C12-C11-H11	113.(3)
W1-C11-H11	107.(3)	C11-C12-C13	113.4(3)
C11-C12-H12A	108.9	C13-C12-H12A	108.9
C11-C12-H12B	108.9	C13-C12-H12B	108.9
H12A-C12-H12B	107.7	C14-C13-C12	110.4(3)
C14-C13-H13A	109.6	C12-C13-H13A	109.6
C14-C13-H13B	109.6	C12-C13-H13B	109.6
H13A-C13-H13B	108.1	C15-C14-C13	123.6(3)
C15-C14-S1	118.4(3)	C13-C14-S1	118.0(3)
C14-C15-C10	121.8(3)	C14-C15-H15	119.1
C10-C15-H15	119.1	S1-C16-H16A	109.5
S1-C16-H16B	109.5	H16A-C16-H16B	109.5
S1-C16-H16C	109.5	H16A-C16-H16C	109.5
H16B-C16-H16C	109.5	P1-C17-H17A	109.5
P1-C17-H17B	109.5	H17A-C17-H17B	109.5
P1-C17-H17C	109.5	H17A-C17-H17C	109.5
H17B-C17-H17C	109.5	P1-C18-H18A	109.5
P1-C18-H18B	109.5	H18A-C18-H18B	109.5
P1-C18-H18C	109.5	H18A-C18-H18C	109.5
H18B-C18-H18C	109.5	P1-C19-H19A	109.5
P1-C19-H19B	109.5	H19A-C19-H19B	109.5
P1-C19-H19C	109.5	H19A-C19-H19C	109.5
H19B-C19-H19C	109.5	Cl1-C20-Cl2	111.6(2)
Cl1-C20-H20A	109.3	Cl2-C20-H20A	109.3
Cl1-C20-H20B	109.3	Cl2-C20-H20B	109.3
H20A-C20-H20B	108.0	N2-B1-N6	108.7(3)
N2-B1-N4	109.6(3)	N6-B1-N4	106.4(3)
N2-B1-H1A	110.3(19)	N6-B1-H1A	113.1(19)
N4-B1-H1A	108.8(19)		

Table 6. Torsion angles (°) for Harman_SS7_198_3_X1.

C1-N1-N2-C3	-0.1(4)	W1-N1-N2-C3	-177.1(2)

C1-N1-N2-B1	-177.9(3)	W1-N1-N2-B1	5.2(4)
C4-N3-N4-C6	0.3(4)	W1-N3-N4-C6	179.2(2)
C4-N3-N4-B1	167.0(3)	W1-N3-N4-B1	-14.2(4)
C7-N5-N6-C9	0.5(4)	W1-N5-N6-C9	177.0(2)
C7-N5-N6-B1	-173.6(3)	W1-N5-N6-B1	2.9(4)
N2-N1-C1-C2	-0.2(4)	W1-N1-C1-C2	176.2(3)
N1-C1-C2-C3	0.4(5)	N1-N2-C3-C2	0.4(4)
B1-N2-C3-C2	177.9(4)	C1-C2-C3-N2	-0.5(5)
N4-N3-C4-C5	-0.1(4)	W1-N3-C4-C5	-178.9(2)
N3-C4-C5-C6	-0.1(4)	N3-N4-C6-C5	-0.4(4)
B1-N4-C6-C5	-165.0(3)	C4-C5-C6-N4	0.3(4)
N6-N5-C7-C8	-0.4(4)	W1-N5-C7-C8	-176.3(3)
N5-C7-C8-C9	0.2(4)	N5-N6-C9-C8	-0.4(4)
B1-N6-C9-C8	173.2(3)	C7-C8-C9-N6	0.1(4)
C15-C10-C11-C12	14.6(5)	W1-C10-C11-C12	123.7(3)
C15-C10-C11-W1	-109.2(3)	C10-C11-C12-C13	-39.7(5)
W1-C11-C12-C13	48.9(4)	C11-C12-C13-C14	43.0(4)
C12-C13-C14-C15	-25.3(5)	C12-C13-C14-S1	155.5(3)
O2-S1-C14-C15	6.0(3)	O3-S1-C14-C15	135.1(3)
C16-S1-C14-C15	-110.5(3)	O2-S1-C14-C13	-174.7(3)
O3-S1-C14-C13	-45.7(3)	C16-S1-C14-C13	68.7(3)
C13-C14-C15-C10	0.3(5)	S1-C14-C15-C10	179.5(3)
C11-C10-C15-C14	6.1(5)	W1-C10-C15-C14	-73.7(4)
C3-N2-B1-N6	-122.4(4)	N1-N2-B1-N6	54.8(4)
C3-N2-B1-N4	121.7(4)	N1-N2-B1-N4	-61.1(4)
C9-N6-B1-N2	126.7(4)	N5-N6-B1-N2	-60.4(4)
C9-N6-B1-N4	-115.3(4)	N5-N6-B1-N4	57.5(4)
C6-N4-B1-N2	-129.9(4)	N3-N4-B1-N2	66.6(4)
C6-N4-B1-N6	112.7(4)	N3-N4-B1-N6	-50.7(4)

Table 7. Anisotropic atomic displacement parameters (Å^2) for Harman_SS7_198_3_X1.

The anisotropic atomic displacement factor exponent takes the form: $-2\pi^2[h^2 a^{*2} U_{11} + ... + 2 h k a^* b^* U_{12}]$

	U_{11}	U_{22}	U_{33}	U_{23}	U_{13}	U_{12}
W1	0.01482(6)	0.01780(7)	0.01235(6)	-0.00013(5)	0.00071(4)	0.00220(5)

	U_{11}	U_{22}	U_{33}	U_{23}	U_{13}	U_{12}
Cl1	0.0766(9)	0.0460(7)	0.0452(7)	-0.0168(6)	-0.0237(6)	0.0237(7)
Cl2	0.0425(6)	0.0364(6)	0.0426(6)	-0.0044(5)	0.0011(5)	-0.0078(5)
S1	0.0274(4)	0.0269(5)	0.0179(4)	-0.0018(3)	0.0021(3)	0.0008(4)
P1	0.0194(4)	0.0236(5)	0.0220(4)	-0.0010(4)	0.0055(3)	-0.0039(4)
O1	0.0326(15)	0.0271(14)	0.0256(13)	-0.0012(11)	0.0061(11)	0.0098(11)
O2	0.0327(15)	0.0378(16)	0.0295(14)	-0.0007(12)	0.0100(12)	-0.0053(12)
O3	0.0344(15)	0.0358(16)	0.0210(13)	-0.0045(11)	0.0021(11)	-0.0036(12)
N1	0.0198(14)	0.0219(15)	0.0161(13)	0.0016(11)	0.0026(11)	0.0044(11)
N2	0.0212(14)	0.0243(15)	0.0178(14)	-0.0027(12)	0.0059(11)	0.0015(12)
N3	0.0197(14)	0.0198(15)	0.0139(13)	0.0002(11)	0.0006(10)	0.0003(11)
N4	0.0240(14)	0.0219(15)	0.0136(13)	0.0010(11)	0.0025(11)	0.0006(12)
N5	0.0177(13)	0.0196(15)	0.0218(14)	-0.0020(11)	0.0008(11)	0.0021(11)
N6	0.0198(14)	0.0246(16)	0.0216(15)	-0.0004(12)	0.0055(12)	0.0009(12)
N7	0.0190(13)	0.0232(15)	0.0158(13)	0.0011(12)	0.0010(10)	0.0022(12)
C1	0.032(2)	0.0253(19)	0.0223(18)	0.0038(15)	0.0023(15)	0.0098(16)
C2	0.041(2)	0.030(2)	0.033(2)	0.0000(17)	0.0062(18)	0.0179(18)
C3	0.032(2)	0.027(2)	0.027(2)	-0.0045(16)	0.0068(16)	0.0070(16)
C4	0.0204(17)	0.0219(18)	0.0237(18)	-0.0024(14)	0.0008(14)	0.0028(14)
C5	0.0282(19)	0.028(2)	0.0206(18)	0.0047(15)	-0.0063(14)	0.0017(16)
C6	0.0311(19)	0.0276(18)	0.0139(15)	0.0032(15)	-0.0022(13)	-0.0058(16)
C7	0.0222(17)	0.0214(18)	0.0291(19)	-0.0021(15)	0.0010(14)	-0.0004(14)
C8	0.0218(18)	0.027(2)	0.038(2)	0.0027(17)	0.0048(16)	-0.0038(15)
C9	0.0201(17)	0.031(2)	0.032(2)	0.0062(16)	0.0077(15)	0.0003(15)
C10	0.0272(19)	0.0234(19)	0.0186(17)	-0.0020(14)	0.0010(14)	0.0050(15)

	U_{11}	U_{22}	U_{33}	U_{23}	U_{13}	U_{12}
C11	0.0203(16)	0.036(2)	0.0189(16)	0.0016(16)	-0.0020(13)	0.0064(16)
C12	0.0219(17)	0.043(2)	0.0218(18)	-0.0008(17)	-0.0015(14)	-0.0084(17)
C13	0.033(2)	0.029(2)	0.0198(18)	-0.0017(15)	-0.0011(15)	-0.0075(16)
C14	0.0245(17)	0.0270(19)	0.0131(15)	0.0016(13)	-0.0005(13)	0.0014(14)
C15	0.0242(17)	0.0231(18)	0.0165(16)	0.0045(13)	0.0000(13)	-0.0005(14)
C16	0.039(2)	0.045(3)	0.031(2)	-0.0004(19)	0.0044(18)	0.016(2)
C17	0.0210(19)	0.040(2)	0.053(3)	0.002(2)	0.0148(18)	-0.0004(17)
C18	0.043(2)	0.0235(19)	0.031(2)	-0.0005(16)	0.0111(18)	-0.0106(17)
C19	0.041(2)	0.034(2)	0.031(2)	-0.0078(18)	0.0029(18)	-0.0131(19)
C20	0.033(2)	0.035(2)	0.033(2)	0.0075(18)	0.0001(17)	0.0018(17)
B1	0.025(2)	0.025(2)	0.0188(19)	-0.0004(16)	0.0059(16)	0.0019(16)

Table 8. Hydrogen atomic coordinates and isotropic atomic displacement parameters (Å^2) for Harman_SS7_198_3_X1.

	x/a	y/b	z/c	U(eq)
H1	0.5037	0.4394	0.4142	0.032
H2	0.6238	0.3281	0.3485	0.041
H3	0.6181	0.4413	0.2697	0.034
H4	0.0138	0.7825	0.3150	0.026
H5	-0.0203	0.7672	0.2195	0.031
H6	0.2309	0.6838	0.1937	0.029
H7	0.6056	0.9176	0.3903	0.029
H8	0.7735	0.9578	0.3185	0.035
H9	0.7217	0.8118	0.2549	0.033
H10	0.423(5)	0.569(4)	0.4722(16)	0.034(12)
H11	0.625(5)	0.659(3)	0.4424(16)	0.034(12)
H12A	0.6528	0.8459	0.4661	0.035

H12B	0.6685	0.7705	0.5154	0.035
H13A	0.4989	0.9032	0.5370	0.033
H13B	0.4015	0.9028	0.4816	0.033
H15	0.2389	0.6352	0.5234	0.026
H16A	0.0150	0.8836	0.5186	0.058
H16B	0.1512	0.9726	0.5278	0.058
H16C	0.0276	0.9535	0.5698	0.058
H17A	-0.1531	0.5746	0.4066	0.056
H17B	-0.0953	0.6857	0.3846	0.056
H17C	-0.0586	0.6585	0.4441	0.056
H18A	0.1454	0.4887	0.4777	0.048
H18B	0.2361	0.4180	0.4387	0.048
H18C	0.0456	0.4121	0.4378	0.048
H19A	0.1637	0.4528	0.3286	0.053
H19B	0.0362	0.5425	0.3097	0.053
H19C	-0.0175	0.4431	0.3424	0.053
H20A	0.5887	0.9331	0.6514	0.041
H20B	0.7123	0.9714	0.6122	0.041
H1A	0.526(4)	0.638(3)	0.2385(13)	0.016(9)

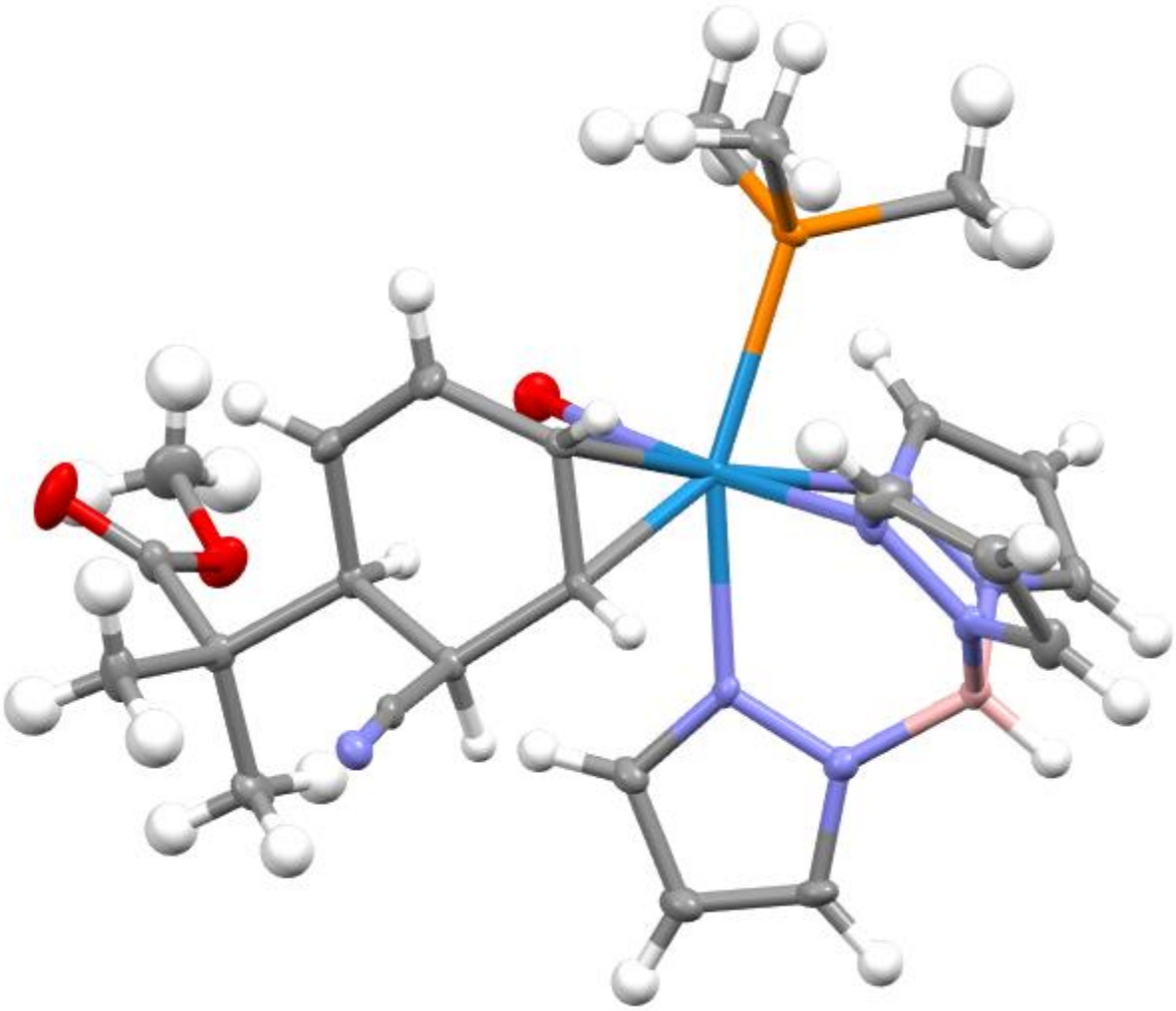

Crystal Structure Report for 22 in Chapter 4

A yellow block-like specimen of $C_{24}H_{34}BN_8O_3PW$, approximate dimensions 0.270 mm x 0.319 mm x 0.386 mm, was coated with Paratone oil and mounted on a MiTeGen MicroLoop. The X-ray intensity data were measured on a Bruker Kappa APEXII Duo system equipped with a fine-focus sealed tube (Mo K_α, λ = 0.71073 Å) and a graphite monochromator.

The total exposure time was 0.90 hours. The frames were integrated with the Bruker SAINT software package[23] using a narrow-frame algorithm. The integration of the data using a monoclinic unit cell yielded a total of 46743 reflections to a maximum θ angle of 31.52° (0.68 Å resolution), of which 9416 were independent (average redundancy 4.964, completeness = 99.9%, R_{int} = 2.35%, R_{sig} = 1.82%) and 8354 (88.72%) were greater than 2σ(F^2). The final cell constants of a = 11.9916(7) Å, b = 12.5032(7) Å, c = 19.5817(11) Å, β = 105.9270(10)°, volume = 2823.2(3) $Å^3$, are based upon the refinement of the XYZ-centroids of 9997 reflections above 20 σ(I) with 4.805° < 2θ < 63.00°. Data were corrected for absorption effects using the Multi-Scan method (SADABS).[1] The ratio of minimum to maximum apparent transmission was 0.866. The calculated minimum and maximum transmission coefficients (based on

[23] Bruker (2012). *Saint; SADABS; APEX3*. Bruker AXS Inc., Madison, Wisconsin, USA.

crystal size) are 0.2950 and 0.3980.

The structure was solved and refined using the Bruker SHELXTL Software Package[24] within APEX3 [1] and OLEX2,[25] using the space group P $2_1/c$, with Z = 4 for the formula unit, $C_{24}H_{34}BN_8O_3PW$. Non-hydrogen atoms were refined anisotropically. Hydrogen atoms were placed in geometrically calculated positions with U_{iso} = 1.2U_{equiv} of the parent atom (U_{iso} = 1.5U_{equiv} for methyl). Most of the molecule was disordered over two positions. The relative occupancies were freely refined, and no constraints or restraints were needed. The final anisotropic full-matrix least-squares refinement on F^2 with 644 variables converged at R1 = 1.56%, for the observed data and wR2 = 3.65% for all data. The goodness-of-fit was 1.062. The largest peak in the final difference electron density synthesis was 1.330 $e^-/Å^3$ and the largest hole was -1.484 $e^-/Å^3$ with an RMS deviation of 0.086 $e^-/Å^3$. On the basis of the final model, the calculated density was 1.666 g/cm^3 and F(000), 1408 e^-.

Table 1. Sample and crystal data for Harman_SS5_44.

Identification code	Harman_SS5_44	
Chemical formula	$C_{24}H_{34}BN_8O_3PW$	
Formula weight	708.22 g/mol	
Temperature	100(2) K	
Wavelength	0.71073 Å	
Crystal size	0.270 x 0.319 x 0.386 mm	
Crystal habit	yellow block	
Crystal system	monoclinic	
Space group	P $2_1/c$	
Unit cell dimensions	a = 11.9916(7) Å	α = 90°
	b = 12.5032(7) Å	β = 105.9270(10)°
	c = 19.5817(11) Å	γ = 90°
Volume	2823.2(3) $Å^3$	
Z	4	
Density (calculated)	1.666 g/cm^3	
Absorption coefficient	4.189 mm^{-1}	
F(000)	1408	

Table 2. Data collection and structure refinement for Harman_SS5_44.

Diffractometer	Bruker Kappa APEXII Duo
Radiation source	fine-focus sealed tube (Mo K_α, λ = 0.71073 Å)
Theta range for data collection	1.77 to 31.52°
Index ranges	-17<=h<=17, -18<=k<=18, -23<=l<=28
Reflections collected	46743

[24] Sheldrick, G. M. (2015). *Acta Cryst.* A**71**, 3-8.
[25] Dolomanov, O. V.; Bourhis, L. J.; Gildea, R. J.; Howard, J. A. K.; Puschmann, H. *J. Appl. Cryst.* (2009). **42**, 339-341.

Independent reflections	9416 [R(int) = 0.0235]	
Coverage of independent reflections	99.9%	
Absorption correction	Multi-Scan	
Max. and min. transmission	0.3980 and 0.2950	
Structure solution technique	direct methods	
Structure solution program	SHELXT 2014/5 (Sheldrick, 2014)	
Refinement method	Full-matrix least-squares on F^2	
Refinement program	SHELXL-2018/3 (Sheldrick, 2018)	
Function minimized	$\Sigma\ w(F_o^2 - F_c^2)^2$	
Data / restraints / parameters	9416 / 0 / 644	
Goodness-of-fit on F^2	1.062	
Δ/σ_{max}	0.003	
Final R indices	8354 data; I>2σ(I)	R1 = 0.0156, wR2 = 0.0344
	all data	R1 = 0.0209, wR2 = 0.0365
Weighting scheme	$w=1/[\sigma^2(F_o^2)+(0.0155P)^2+1.4980P]$ where $P=(F_o^2+2F_c^2)/3$	
Largest diff. peak and hole	1.330 and -1.484 eÅ^{-3}	
R.M.S. deviation from mean	0.086 eÅ^{-3}	

Table 3. Atomic coordinates and equivalent isotropic atomic displacement parameters (Å^2) for Harman_SS5_44.

U(eq) is defined as one third of the trace of the orthogonalized U_{ij} tensor.

	x/a	y/b	z/c	U(eq)
W1	0.20866(2)	0.44423(2)	0.81862(2)	0.00945(2)
O1	0.05505(10)	0.47871(10)	0.67110(6)	0.0212(2)
N1	0.30213(11)	0.42098(11)	0.93422(7)	0.0165(2)
N7	0.12150(10)	0.46492(10)	0.73025(7)	0.0133(2)
C1	0.38336(15)	0.35329(14)	0.96995(9)	0.0241(3)
C2	0.41808(15)	0.37871(15)	0.04182(9)	0.0239(3)
P1	0.10664(9)	0.27123(8)	0.82834(6)	0.01313(18)
O2	0.2901(2)	0.4904(3)	0.49581(14)	0.0334(7)
O3	0.1817(2)	0.5935(2)	0.54501(13)	0.0237(5)
N2	0.2978(3)	0.5078(3)	0.9833(2)	0.0148(7)
N3	0.0719(3)	0.5148(3)	0.86536(17)	0.0126(6)
N4	0.0991(2)	0.5787(2)	0.92398(13)	0.0135(5)

N5	0.2634(3)	0.6145(4)	0.8390(2)	0.0113(7)
N6	0.2694(2)	0.6658(2)	0.90132(14)	0.0149(5)
N8	0.6444(2)	0.4970(2)	0.77501(14)	0.0159(5)
C3	0.3630(6)	0.4815(5)	0.0483(4)	0.0198(11)
C4	0.9556(3)	0.5151(3)	0.84048(17)	0.0147(5)
C5	0.9074(3)	0.5781(3)	0.88401(17)	0.0175(6)
C6	0.0009(3)	0.6185(3)	0.93518(17)	0.0167(6)
C7	0.2913(3)	0.6864(2)	0.79596(19)	0.0154(6)
C8	0.3173(3)	0.7850(3)	0.83000(18)	0.0197(6)
C9	0.3024(3)	0.7689(3)	0.8965(2)	0.0187(6)
C10	0.3536(4)	0.3538(4)	0.7885(3)	0.0118(8)
C11	0.3830(7)	0.4651(4)	0.8045(4)	0.0105(10)
C12	0.4204(2)	0.5314(3)	0.74859(16)	0.0112(5)
C13	0.3471(2)	0.5049(3)	0.67225(15)	0.0119(5)
C14	0.3411(3)	0.3862(3)	0.66143(17)	0.0175(6)
C15	0.3388(3)	0.3177(3)	0.71400(18)	0.0182(6)
C16	0.5463(2)	0.5120(2)	0.76020(15)	0.0125(5)
C17	0.3792(4)	0.5687(4)	0.6105(3)	0.0136(8)
C18	0.3822(3)	0.6895(3)	0.62672(17)	0.0203(6)
C19	0.4933(3)	0.5342(3)	0.59741(18)	0.0240(7)
C20	0.2807(3)	0.5455(3)	0.54417(17)	0.0175(6)
C21	0.0833(3)	0.5694(3)	0.4856(2)	0.0316(8)
C22	0.1857(3)	0.1455(3)	0.84533(19)	0.0197(6)
C23	0.0278(4)	0.2620(3)	0.8960(2)	0.0276(8)
C24	0.9967(3)	0.2454(3)	0.7459(2)	0.0224(7)
B1	0.2263(3)	0.6099(3)	0.95890(19)	0.0143(6)
P1A	0.13785(10)	0.25333(8)	0.81444(6)	0.01443(19)
O2A	0.4785(2)	0.64067(19)	0.59594(14)	0.0218(5)
O3A	0.30836(18)	0.66521(17)	0.62030(12)	0.0161(4)
N2A	0.2710(3)	0.4747(3)	0.9828(2)	0.0117(6)
N3A	0.0556(3)	0.4732(3)	0.85442(17)	0.0124(6)
N4A	0.0625(2)	0.5191(2)	0.91854(14)	0.0128(5)
N5A	0.2337(3)	0.6139(4)	0.8506(2)	0.0111(7)
N6A	0.2195(2)	0.6445(2)	0.91515(14)	0.0130(5)
N8A	0.6242(3)	0.4023(3)	0.75391(17)	0.0276(7)
C3A	0.3444(6)	0.4516(5)	0.0472(4)	0.0146(10)
C4A	0.9424(3)	0.4596(3)	0.82193(18)	0.0154(6)
C5A	0.8755(3)	0.4970(3)	0.86488(17)	0.0189(6)
C6A	0.9542(3)	0.5344(3)	0.92566(17)	0.0184(6)

C7A	0.2584(3)	0.7022(3)	0.8194(2)	0.0159(6)
C8A	0.2610(3)	0.7912(3)	0.8627(2)	0.0181(6)
C9A	0.2351(3)	0.7515(2)	0.92253(18)	0.0178(6)
C10A	0.3289(4)	0.3268(4)	0.7931(3)	0.0113(8)
C11A	0.3773(7)	0.4334(4)	0.7990(4)	0.0100(12)
C12A	0.4129(2)	0.4774(3)	0.73472(17)	0.0122(5)
C13A	0.3246(2)	0.4476(3)	0.66362(15)	0.0105(5)
C14A	0.2970(3)	0.3305(3)	0.66289(17)	0.0149(5)
C15A	0.2979(3)	0.2770(3)	0.72240(17)	0.0144(5)
C16A	0.5314(3)	0.4344(3)	0.74245(17)	0.0174(6)
C17A	0.3537(3)	0.4867(2)	0.59406(16)	0.0142(5)
C18A	0.4501(3)	0.4223(3)	0.5759(2)	0.0230(7)
C19A	0.2420(3)	0.4805(3)	0.53174(18)	0.0227(7)
C20A	0.3894(5)	0.6050(3)	0.6042(3)	0.0133(8)
C21A	0.3393(3)	0.7763(2)	0.63423(19)	0.0198(6)
C22A	0.2371(3)	0.1396(3)	0.8314(2)	0.0223(7)
C23A	0.0588(4)	0.2249(3)	0.8800(2)	0.0296(8)
C24A	0.0384(3)	0.2201(3)	0.7294(2)	0.0275(8)
B1A	0.1795(3)	0.5643(3)	0.96268(18)	0.0138(6)

Table 4. Bond lengths (Å) for Harman_SS5_44.

W1-N7	1.7778(12)	W1-C11A	2.164(8)
W1-N3A	2.167(3)	W1-C11	2.197(8)
W1-N5A	2.209(5)	W1-C10A	2.209(6)
W1-N5	2.231(5)	W1-N1	2.2522(13)
W1-N3	2.265(3)	W1-C10	2.283(5)
W1-P1	2.5179(10)	W1-P1A	2.5272(10)
O1-N7	1.2248(16)	N1-N2A	1.300(4)
N1-C1	1.334(2)	N1-N2	1.459(4)
C1-C2	1.390(2)	C1-H1	0.95
C2-C3A	1.293(8)	C2-C3	1.467(8)
C2-H2A	0.95	C2-H2B	0.95
P1-C24	1.812(4)	P1-C22	1.819(3)
P1-C23	1.830(4)	O2-C20	1.201(4)
O3-C20	1.334(4)	O3-C21	1.444(4)
N2-C3	1.340(9)	N2-B1	1.540(5)
N3-C4	1.345(4)	N3-N4	1.363(4)
N4-C6	1.351(4)	N4-B1	1.540(4)
N5-C7	1.336(5)	N5-N6	1.363(5)

N6-C9	1.359(4)	N6-B1	1.532(5)
N8-C16	1.147(4)	C3-H3	0.95
C4-C5	1.398(5)	C4-H4	0.95
C5-C6	1.378(4)	C5-H5	0.95
C6-H6	0.95	C7-C8	1.396(4)
C7-H7	0.95	C8-C9	1.378(5)
C8-H8	0.95	C9-H9	0.95
C10-C11	1.448(7)	C10-C15	1.491(6)
C10-H10	1.0	C11-C12	1.536(9)
C11-H11	1.0	C12-C16	1.484(4)
C12-C13	1.548(4)	C12-H12	1.0
C13-C14	1.498(5)	C13-C17	1.581(6)
C13-H13	1.0	C14-C15	1.346(5)
C14-H14	0.95	C15-H15	0.95
C17-C19	1.523(6)	C17-C20	1.524(6)
C17-C18	1.541(6)	C18-H18A	0.98
C18-H18B	0.98	C18-H18C	0.98
C19-H19A	0.98	C19-H19B	0.98
C19-H19C	0.98	C21-H21A	0.98
C21-H21B	0.98	C21-H21C	0.98
C22-H22A	0.98	C22-H22B	0.98
C22-H22C	0.98	C23-H23A	0.98
C23-H23B	0.98	C23-H23C	0.98
C24-H24A	0.98	C24-H24B	0.98
C24-H24C	0.98	B1-H1A	1.0
P1A-C24A	1.811(4)	P1A-C22A	1.825(4)
P1A-C23A	1.828(4)	O2A-C20A	1.209(5)
O3A-C20A	1.334(6)	O3A-C21A	1.444(4)
N2A-C3A	1.356(9)	N2A-B1A	1.542(5)
N3A-C4A	1.343(4)	N3A-N4A	1.362(4)
N4A-C6A	1.357(4)	N4A-B1A	1.540(4)
N5A-C7A	1.334(5)	N5A-N6A	1.375(5)
N6A-C9A	1.352(4)	N6A-B1A	1.532(5)
N8A-C16A	1.146(4)	C3A-H3A	0.95
C4A-C5A	1.393(5)	C4A-H4A	0.95
C5A-C6A	1.382(5)	C5A-H5A	0.95
C6A-H6A	0.95	C7A-C8A	1.393(5)
C7A-H7A	0.95	C8A-C9A	1.384(5)
C8A-H8A	0.95	C9A-H9A	0.95

C10A-C11A	1.445(7)	C10A-C15A	1.470(6)
C10A-H10A	1.0	C11A-C12A	1.537(9)
C11A-H11A	1.0	C12A-C16A	1.488(4)
C12A-C13A	1.546(4)	C12A-H12A	1.0
C13A-C14A	1.500(5)	C13A-C17A	1.574(4)
C13A-H13A	1.0	C14A-C15A	1.341(4)
C14A-H14A	0.95	C15A-H15A	0.95
C17A-C18A	1.529(4)	C17A-C20A	1.538(5)
C17A-C19A	1.546(4)	C18A-H18D	0.98
C18A-H18E	0.98	C18A-H18F	0.98
C19A-H19D	0.98	C19A-H19E	0.98
C19A-H19F	0.98	C21A-H21D	0.98
C21A-H21E	0.98	C21A-H21F	0.98
C22A-H22D	0.98	C22A-H22E	0.98
C22A-H22F	0.98	C23A-H23D	0.98
C23A-H23E	0.98	C23A-H23F	0.98
C24A-H24D	0.98	C24A-H24E	0.98
C24A-H24F	0.98	B1A-H1B	1.0

Table 5. Bond angles (°) for Harman_SS5_44.

N7-W1-C11A	99.5(2)	N7-W1-N3A	88.09(10)
C11A-W1-N3A	169.60(19)	N7-W1-C11	100.7(2)
N7-W1-N5A	97.71(12)	C11A-W1-N5A	92.86(15)
N3A-W1-N5A	78.98(13)	N7-W1-C10A	97.04(15)
C11A-W1-C10A	38.57(16)	N3A-W1-C10A	147.96(14)
N5A-W1-C10A	130.99(15)	N7-W1-N5	95.79(12)
C11-W1-N5	70.49(16)	N7-W1-N1	173.99(5)
C11A-W1-N1	86.5(2)	N3A-W1-N1	85.90(9)
C11-W1-N1	85.0(2)	N5A-W1-N1	81.22(12)
C10A-W1-N1	88.04(14)	N5-W1-N1	84.41(12)
N7-W1-N3	92.25(9)	C11-W1-N3	145.46(16)
N5-W1-N3	76.48(12)	N1-W1-N3	81.94(9)
N7-W1-C10	96.12(14)	C11-W1-C10	37.65(16)
N5-W1-C10	108.13(14)	N1-W1-C10	89.51(14)
N3-W1-C10	169.92(15)	N7-W1-P1	91.75(5)
C11-W1-P1	127.59(15)	N5-W1-P1	158.64(9)
N1-W1-P1	86.06(4)	N3-W1-P1	83.30(9)
C10-W1-P1	90.83(11)	N7-W1-P1A	90.19(5)
C11A-W1-P1A	104.89(13)	N3A-W1-P1A	82.05(10)

N5A-W1-P1A	159.15(9)	C10A-W1-P1A	66.39(12)
N1-W1-P1A	88.90(4)	N2A-N1-C1	105.0(2)
C1-N1-N2	106.2(2)	N2A-N1-W1	120.35(18)
C1-N1-W1	134.36(12)	N2-N1-W1	117.88(18)
O1-N7-W1	175.69(12)	N1-C1-C2	111.01(16)
N1-C1-H1	124.5	C2-C1-H1	124.5
C3A-C2-C1	102.8(4)	C1-C2-C3	105.8(3)
C1-C2-H2A	127.1	C3-C2-H2A	127.1
C3A-C2-H2B	128.6	C1-C2-H2B	128.6
C24-P1-C22	102.93(17)	C24-P1-C23	103.9(2)
C22-P1-C23	99.21(19)	C24-P1-W1	109.62(12)
C22-P1-W1	121.12(13)	C23-P1-W1	117.86(14)
C20-O3-C21	115.4(3)	C3-N2-N1	109.1(4)
C3-N2-B1	128.9(4)	N1-N2-B1	122.0(3)
C4-N3-N4	106.7(3)	C4-N3-W1	130.4(3)
N4-N3-W1	122.4(2)	C6-N4-N3	109.6(3)
C6-N4-B1	129.5(3)	N3-N4-B1	120.1(2)
C7-N5-N6	106.7(4)	C7-N5-W1	129.9(3)
N6-N5-W1	123.3(3)	C9-N6-N5	109.2(3)
C9-N6-B1	130.3(3)	N5-N6-B1	120.0(3)
N2-C3-C2	106.9(5)	N2-C3-H3	126.5
C2-C3-H3	126.5	N3-C4-C5	110.0(3)
N3-C4-H4	125.0	C5-C4-H4	125.0
C6-C5-C4	105.0(3)	C6-C5-H5	127.5
C4-C5-H5	127.5	N4-C6-C5	108.6(3)
N4-C6-H6	125.7	C5-C6-H6	125.7
N5-C7-C8	110.8(4)	N5-C7-H7	124.6
C8-C7-H7	124.6	C9-C8-C7	104.6(3)
C9-C8-H8	127.7	C7-C8-H8	127.7
N6-C9-C8	108.7(3)	N6-C9-H9	125.7
C8-C9-H9	125.7	C11-C10-C15	117.4(4)
C11-C10-W1	68.0(4)	C15-C10-W1	120.5(3)
C11-C10-H10	114.4	C15-C10-H10	114.4
W1-C10-H10	114.4	C10-C11-C12	117.7(5)
C10-C11-W1	74.4(3)	C12-C11-W1	128.9(5)
C10-C11-H11	110.3	C12-C11-H11	110.3
W1-C11-H11	110.3	C16-C12-C11	106.6(4)
C16-C12-C13	113.4(2)	C11-C12-C13	111.9(4)
C16-C12-H12	108.2	C11-C12-H12	108.2

C13-C12-H12	108.2	C14-C13-C12	109.9(3)
C14-C13-C17	113.8(3)	C12-C13-C17	115.9(3)
C14-C13-H13	105.4	C12-C13-H13	105.4
C17-C13-H13	105.4	C15-C14-C13	122.2(3)
C15-C14-H14	118.9	C13-C14-H14	118.9
C14-C15-C10	122.2(3)	C14-C15-H15	118.9
C10-C15-H15	118.9	N8-C16-C12	174.4(3)
C19-C17-C20	108.9(4)	C19-C17-C18	109.9(3)
C20-C17-C18	109.3(3)	C19-C17-C13	113.9(3)
C20-C17-C13	105.2(3)	C18-C17-C13	109.5(4)
C17-C18-H18A	109.5	C17-C18-H18B	109.5
H18A-C18-H18B	109.5	C17-C18-H18C	109.5
H18A-C18-H18C	109.5	H18B-C18-H18C	109.5
C17-C19-H19A	109.5	C17-C19-H19B	109.5
H19A-C19-H19B	109.5	C17-C19-H19C	109.5
H19A-C19-H19C	109.5	H19B-C19-H19C	109.5
O2-C20-O3	123.0(3)	O2-C20-C17	124.2(3)
O3-C20-C17	112.8(3)	O3-C21-H21A	109.5
O3-C21-H21B	109.5	H21A-C21-H21B	109.5
O3-C21-H21C	109.5	H21A-C21-H21C	109.5
H21B-C21-H21C	109.5	P1-C22-H22A	109.5
P1-C22-H22B	109.5	H22A-C22-H22B	109.5
P1-C22-H22C	109.5	H22A-C22-H22C	109.5
H22B-C22-H22C	109.5	P1-C23-H23A	109.5
P1-C23-H23B	109.5	H23A-C23-H23B	109.5
P1-C23-H23C	109.5	H23A-C23-H23C	109.5
H23B-C23-H23C	109.5	P1-C24-H24A	109.5
P1-C24-H24B	109.5	H24A-C24-H24B	109.5
P1-C24-H24C	109.5	H24A-C24-H24C	109.5
H24B-C24-H24C	109.5	N6-B1-N2	109.5(3)
N6-B1-N4	106.4(3)	N2-B1-N4	109.1(3)
N6-B1-H1A	110.6	N2-B1-H1A	110.6
N4-B1-H1A	110.6	C24A-P1A-C22A	102.72(18)
C24A-P1A-C23A	105.3(2)	C22A-P1A-C23A	99.1(2)
C24A-P1A-W1	112.17(14)	C22A-P1A-W1	122.25(13)
C23A-P1A-W1	113.28(15)	C20A-O3A-C21A	114.9(3)
N1-N2A-C3A	109.1(4)	N1-N2A-B1A	121.0(3)
C3A-N2A-B1A	128.9(4)	C4A-N3A-N4A	106.7(3)
C4A-N3A-W1	131.4(3)	N4A-N3A-W1	121.8(2)

C6A-N4A-N3A	109.7(3)	C6A-N4A-B1A	129.8(3)
N3A-N4A-B1A	119.2(3)	C7A-N5A-N6A	106.8(4)
C7A-N5A-W1	134.0(3)	N6A-N5A-W1	119.1(3)
C9A-N6A-N5A	109.0(3)	C9A-N6A-B1A	129.7(3)
N5A-N6A-B1A	121.0(3)	C2-C3A-N2A	111.0(6)
C2-C3A-H3A	124.5	N2A-C3A-H3A	124.5
N3A-C4A-C5A	110.3(3)	N3A-C4A-H4A	124.9
C5A-C4A-H4A	124.9	C6A-C5A-C4A	105.3(3)
C6A-C5A-H5A	127.4	C4A-C5A-H5A	127.4
N4A-C6A-C5A	108.1(3)	N4A-C6A-H6A	126.0
C5A-C6A-H6A	126.0	N5A-C7A-C8A	110.7(4)
N5A-C7A-H7A	124.7	C8A-C7A-H7A	124.7
C9A-C8A-C7A	104.8(3)	C9A-C8A-H8A	127.6
C7A-C8A-H8A	127.6	N6A-C9A-C8A	108.7(3)
N6A-C9A-H9A	125.7	C8A-C9A-H9A	125.7
C11A-C10A-C15A	117.3(4)	C11A-C10A-W1	69.0(3)
C15A-C10A-W1	118.9(3)	C11A-C10A-H10A	114.7
C15A-C10A-H10A	114.7	W1-C10A-H10A	114.7
C10A-C11A-C12A	117.4(5)	C10A-C11A-W1	72.4(3)
C12A-C11A-W1	127.3(4)	C10A-C11A-H11A	111.3
C12A-C11A-H11A	111.3	W1-C11A-H11A	111.3
C16A-C12A-C11A	105.0(4)	C16A-C12A-C13A	113.8(3)
C11A-C12A-C13A	112.1(3)	C16A-C12A-H12A	108.6
C11A-C12A-H12A	108.6	C13A-C12A-H12A	108.6
C14A-C13A-C12A	109.8(3)	C14A-C13A-C17A	113.3(3)
C12A-C13A-C17A	116.4(2)	C14A-C13A-H13A	105.4
C12A-C13A-H13A	105.4	C17A-C13A-H13A	105.4
C15A-C14A-C13A	122.0(3)	C15A-C14A-H14A	119.0
C13A-C14A-H14A	119.0	C14A-C15A-C10A	123.1(3)
C14A-C15A-H15A	118.5	C10A-C15A-H15A	118.5
N8A-C16A-C12A	174.7(4)	C18A-C17A-C20A	109.6(3)
C18A-C17A-C19A	109.7(3)	C20A-C17A-C19A	107.5(3)
C18A-C17A-C13A	113.5(3)	C20A-C17A-C13A	107.9(3)
C19A-C17A-C13A	108.5(2)	C17A-C18A-H18D	109.5
C17A-C18A-H18E	109.5	H18D-C18A-H18E	109.5
C17A-C18A-H18F	109.5	H18D-C18A-H18F	109.5
H18E-C18A-H18F	109.5	C17A-C19A-H19D	109.5
C17A-C19A-H19E	109.5	H19D-C19A-H19E	109.5
C17A-C19A-H19F	109.5	H19D-C19A-H19F	109.5

H19E-C19A-H19F	109.5	O2A-C20A-O3A	123.5(4)
O2A-C20A-C17A	124.2(4)	O3A-C20A-C17A	112.2(4)
O3A-C21A-H21D	109.5	O3A-C21A-H21E	109.5
H21D-C21A-H21E	109.5	O3A-C21A-H21F	109.5
H21D-C21A-H21F	109.5	H21E-C21A-H21F	109.5
P1A-C22A-H22D	109.5	P1A-C22A-H22E	109.5
H22D-C22A-H22E	109.5	P1A-C22A-H22F	109.5
H22D-C22A-H22F	109.5	H22E-C22A-H22F	109.5
P1A-C23A-H23D	109.5	P1A-C23A-H23E	109.5
H23D-C23A-H23E	109.5	P1A-C23A-H23F	109.5
H23D-C23A-H23F	109.5	H23E-C23A-H23F	109.5
P1A-C24A-H24D	109.5	P1A-C24A-H24E	109.5
H24D-C24A-H24E	109.5	P1A-C24A-H24F	109.5
H24D-C24A-H24F	109.5	H24E-C24A-H24F	109.5
N6A-B1A-N4A	106.8(2)	N6A-B1A-N2A	108.1(3)
N4A-B1A-N2A	110.6(3)	N6A-B1A-H1B	110.4
N4A-B1A-H1B	110.4	N2A-B1A-H1B	110.4

Table 6. Torsion angles (°) for Harman_SS5_44.

N2A-N1-C1-C2	-11.0(2)	N2-N1-C1-C2	10.6(2)
W1-N1-C1-C2	175.49(12)	N1-C1-C2-C3A	8.5(3)
N1-C1-C2-C3	-8.4(3)	C1-N1-N2-C3	-8.9(4)
W1-N1-N2-C3	-176.7(3)	C1-N1-N2-B1	171.5(3)
W1-N1-N2-B1	3.6(4)	C4-N3-N4-C6	-0.2(4)
W1-N3-N4-C6	173.3(2)	C4-N3-N4-B1	-170.6(3)
W1-N3-N4-B1	2.9(4)	C7-N5-N6-C9	-0.8(4)
W1-N5-N6-C9	-178.4(3)	C7-N5-N6-B1	171.6(3)
W1-N5-N6-B1	-6.1(4)	N1-N2-C3-C2	3.8(5)
B1-N2-C3-C2	-176.6(3)	C1-C2-C3-N2	2.4(5)
N4-N3-C4-C5	-1.0(4)	W1-N3-C4-C5	-173.8(2)
N3-C4-C5-C6	1.8(4)	N3-N4-C6-C5	1.4(4)
B1-N4-C6-C5	170.5(3)	C4-C5-C6-N4	-1.9(4)
N6-N5-C7-C8	0.8(4)	W1-N5-C7-C8	178.3(3)
N5-C7-C8-C9	-0.5(4)	N5-N6-C9-C8	0.5(4)
B1-N6-C9-C8	-170.9(3)	C7-C8-C9-N6	0.0(4)
C15-C10-C11-C12	-12.0(7)	W1-C10-C11-C12	-126.1(6)
C15-C10-C11-W1	114.1(4)	C10-C11-C12-C16	-84.5(6)

W1-C11-C12-C16	-176.4(3)	C10-C11-C12-C13	40.1(7)
W1-C11-C12-C13	-51.8(5)	C16-C12-C13-C14	71.9(3)
C11-C12-C13-C14	-48.9(4)	C16-C12-C13-C17	-59.0(4)
C11-C12-C13-C17	-179.7(4)	C12-C13-C14-C15	34.1(4)
C17-C13-C14-C15	166.0(3)	C13-C14-C15-C10	-6.1(5)
C11-C10-C15-C14	-6.3(6)	W1-C10-C15-C14	73.1(4)
C14-C13-C17-C19	-56.9(4)	C12-C13-C17-C19	72.1(4)
C14-C13-C17-C20	62.3(4)	C12-C13-C17-C20	-168.7(3)
C14-C13-C17-C18	179.7(3)	C12-C13-C17-C18	-51.4(4)
C21-O3-C20-O2	3.9(5)	C21-O3-C20-C17	-176.3(3)
C19-C17-C20-O2	13.3(5)	C18-C17-C20-O2	133.4(4)
C13-C17-C20-O2	-109.1(4)	C19-C17-C20-O3	-166.4(3)
C18-C17-C20-O3	-46.3(4)	C13-C17-C20-O3	71.1(4)
C9-N6-B1-N2	-128.1(4)	N5-N6-B1-N2	61.3(4)
C9-N6-B1-N4	114.1(4)	N5-N6-B1-N4	-56.4(4)
C3-N2-B1-N6	120.7(5)	N1-N2-B1-N6	-59.7(4)
C3-N2-B1-N4	-123.2(5)	N1-N2-B1-N4	56.3(4)
C6-N4-B1-N6	-110.4(3)	N3-N4-B1-N6	57.8(4)
C6-N4-B1-N2	131.5(3)	N3-N4-B1-N2	-60.3(4)
C1-N1-N2A-C3A	9.0(3)	W1-N1-N2A-C3A	-176.3(2)
C1-N1-N2A-B1A	178.4(3)	W1-N1-N2A-B1A	-7.0(4)
C4A-N3A-N4A-C6A	-0.4(4)	W1-N3A-N4A-C6A	176.0(2)
C4A-N3A-N4A-B1A	-168.5(3)	W1-N3A-N4A-B1A	7.8(4)
C7A-N5A-N6A-C9A	0.3(4)	W1-N5A-N6A-C9A	-178.0(2)
C7A-N5A-N6A-B1A	174.5(3)	W1-N5A-N6A-B1A	-3.8(4)
C1-C2-C3A-N2A	-2.7(4)	N1-N2A-C3A-C2	-4.0(5)
B1A-N2A-C3A-C2	-172.3(3)	N4A-N3A-C4A-C5A	0.2(4)
W1-N3A-C4A-C5A	-175.6(3)	N3A-C4A-C5A-C6A	0.0(4)
N3A-N4A-C6A-C5A	0.4(4)	B1A-N4A-C6A-C5A	166.9(3)
C4A-C5A-C6A-N4A	-0.3(4)	N6A-N5A-C7A-C8A	0.1(4)
W1-N5A-C7A-C8A	178.0(3)	N5A-C7A-C8A-C9A	-0.5(4)
N5A-N6A-C9A-C8A	-0.6(4)	B1A-N6A-C9A-C8A	-174.1(3)
C7A-C8A-C9A-N6A	0.7(4)	C15A-C10A-C11A-C12A	-10.9(7)

W1-C10A-C11A-C12A	-123.5(6)	C15A-C10A-C11A-W1	112.6(4)
C10A-C11A-C12A-C16A	-83.7(6)	W1-C11A-C12A-C16A	-171.9(3)
C10A-C11A-C12A-C13A	40.2(6)	W1-C11A-C12A-C13A	-47.9(5)
C16A-C12A-C13A-C14A	70.6(3)	C11A-C12A-C13A-C14A	-48.3(4)
C16A-C12A-C13A-C17A	-59.9(4)	C11A-C12A-C13A-C17A	-178.8(3)
C12A-C13A-C14A-C15A	31.3(4)	C17A-C13A-C14A-C15A	163.4(3)
C13A-C14A-C15A-C10A	-1.8(5)	C11A-C10A-C15A-C14A	-9.7(6)
W1-C10A-C15A-C14A	70.2(4)	C14A-C13A-C17A-C18A	-54.0(3)
C12A-C13A-C17A-C18A	74.8(4)	C14A-C13A-C17A-C20A	-175.6(3)
C12A-C13A-C17A-C20A	-46.8(4)	C14A-C13A-C17A-C19A	68.2(3)
C12A-C13A-C17A-C19A	-163.0(3)	C21A-O3A-C20A-O2A	-5.9(7)
C21A-O3A-C20A-C17A	176.9(3)	C18A-C17A-C20A-O2A	2.9(6)
C19A-C17A-C20A-O2A	-116.2(5)	C13A-C17A-C20A-O2A	126.9(5)
C18A-C17A-C20A-O3A	-179.9(3)	C19A-C17A-C20A-O3A	61.0(5)
C13A-C17A-C20A-O3A	-55.9(4)	C9A-N6A-B1A-N4A	115.5(3)
N5A-N6A-B1A-N4A	-57.3(4)	C9A-N6A-B1A-N2A	-125.5(3)
N5A-N6A-B1A-N2A	61.7(4)	C6A-N4A-B1A-N6A	-110.1(3)
N3A-N4A-B1A-N6A	55.3(4)	C6A-N4A-B1A-N2A	132.5(3)
N3A-N4A-B1A-N2A	-62.1(4)	N1-N2A-B1A-N6A	-55.0(4)
C3A-N2A-B1A-N6A	112.1(4)	N1-N2A-B1A-N4A	61.6(4)
C3A-N2A-B1A-N4A	-131.4(4)		

Table 7. Anisotropic atomic displacement parameters (Å^2) for Harman_SS5_44.

The anisotropic atomic displacement factor exponent takes the form: $-2\pi^2[h^2 a^{*2} U_{11} + ... + 2 h k a^* b^* U_{12}]$

	U_{11}	U_{22}	U_{33}	U_{23}	U_{13}	U_{12}
W1	0.00768(2)	0.01007(3)	0.01014(3)	0.00082(2)	0.00168(2)	-0.00090(2)
O1	0.0166(5)	0.0282(6)	0.0141(5)	0.0035(5)	-0.0035(4)	0.0019(4)
N1	0.0125(5)	0.0242(7)	0.0133(6)	0.0043(5)	0.0044(5)	0.0028(5)
N7	0.0115(5)	0.0136(5)	0.0136(6)	0.0007(4)	0.0016(4)	-0.0001(4)
C1	0.0231(8)	0.0190(8)	0.0232(8)	0.0017(6)	-0.0056(6)	0.0028(6)
C2	0.0198(7)	0.0278(9)	0.0200(8)	0.0075(7)	-0.0017(6)	-0.0002(6)
P1	0.0120(4)	0.0117(4)	0.0165(5)	0.0003(3)	0.0051(3)	-0.0015(3)
O2	0.0270(13)	0.0550(19)	0.0168(13)	-0.0117(12)	0.0034(10)	0.0041(13)
O3	0.0147(10)	0.0332(13)	0.0191(12)	-0.0044(10)	-0.0024(9)	0.0015(9)
N2	0.0113(15)	0.0203(19)	0.0131(13)	-0.0036(14)	0.0038(11)	-0.0035(12)
N3	0.0093(12)	0.0137(15)	0.0137(14)	-0.0018(12)	0.0014(10)	-0.0008(11)
N4	0.0129(11)	0.0175(13)	0.0114(12)	-0.0037(9)	0.0052(9)	-0.0010(10)
N5	0.0092(17)	0.0143(13)	0.0113(16)	-0.0037(11)	0.0043(11)	-0.0003(13)
N6	0.0152(12)	0.0152(12)	0.0147(12)	-0.0026(10)	0.0047(10)	-0.0012(10)
N8	0.0162(11)	0.0167(12)	0.0155(12)	0.0013(10)	0.0054(9)	-0.0004(9)
C3	0.013(2)	0.031(4)	0.0143(18)	0.000(3)	0.0014(15)	0.002(2)
C4	0.0115(12)	0.0174(15)	0.0148(14)	0.0016(12)	0.0030(10)	0.0000(11)
C5	0.0103(12)	0.0225(15)	0.0213(16)	0.0043(12)	0.0068(11)	0.0037(10)
C6	0.0154(13)	0.0211(14)	0.0164(14)	0.0031(11)	0.0091(11)	0.0033(11)
C7	0.0158(14)	0.0128(14)	0.0192(15)	0.0020(11)	0.0075(12)	0.0009(11)
C8	0.0202(14)	0.0143(13)	0.0269(17)	-0.0009(12)	0.0105(12)	-0.0026(11)
C9	0.0183(15)	0.0131(14)	0.0259(19)	-0.0071(13)	0.0081(14)	-0.0057(12)
C10	0.0114(19)	0.010(3)	0.0143(16)	0.0007(16)	0.0047(14)	-0.0001(14)
C11	0.0114(15)	0.010(3)	0.0121(19)	-0.001(2)	0.0062(13)	0.000(2)
C12	0.0107(12)	0.0121(14)	0.0108(13)	0.0018(11)	0.0027(10)	0.0008(10)
C13	0.0099(12)	0.0154(16)	0.0101(13)	-0.0001(11)	0.0024(9)	0.0006(10)
C14	0.0236(15)	0.0156(17)	0.0119(14)	-0.0041(12)	0.0026(11)	-0.0018(14)

C15	0.0232(15)	0.0145(14)	0.0195(17)	-0.0035(12)	0.0102(13)	0.0003(13)
C16	0.0156(12)	0.0135(13)	0.0092(12)	0.0006(10)	0.0050(10)	-0.0011(10)
C17	0.0099(14)	0.018(2)	0.0118(16)	-0.0002(19)	0.0012(11)	0.0006(18)
C18	0.0230(16)	0.0210(16)	0.0150(14)	0.0057(12)	0.0022(11)	-0.0037(12)
C19	0.0154(14)	0.041(2)	0.0156(15)	0.0022(14)	0.0051(11)	0.0013(13)
C20	0.0150(13)	0.0240(16)	0.0132(14)	0.0023(12)	0.0034(10)	-0.0019(12)
C21	0.0171(15)	0.044(2)	0.0270(19)	-0.0051(16)	-0.0048(13)	-0.0028(14)
C22	0.0178(15)	0.0164(15)	0.0252(17)	0.0048(12)	0.0065(13)	0.0026(12)
C23	0.0316(19)	0.0204(18)	0.040(2)	0.0026(16)	0.0257(18)	-0.0019(15)
C24	0.0163(15)	0.0158(16)	0.031(2)	-0.0032(14)	-0.0013(14)	-0.0036(12)
B1	0.0146(14)	0.0161(15)	0.0133(17)	-0.0039(13)	0.0057(12)	-0.0041(13)
P1A	0.0125(4)	0.0118(4)	0.0186(5)	-0.0006(3)	0.0036(3)	-0.0020(3)
O2A	0.0182(11)	0.0198(11)	0.0307(13)	-0.0019(10)	0.0121(10)	-0.0055(9)
O3A	0.0139(10)	0.0133(10)	0.0220(11)	-0.0016(9)	0.0061(8)	-0.0009(8)
N2A	0.0134(16)	0.0129(16)	0.0086(12)	0.0001(12)	0.0030(12)	-0.0009(11)
N3A	0.0129(13)	0.0138(15)	0.0111(14)	-0.0001(12)	0.0043(10)	-0.0013(11)
N4A	0.0130(11)	0.0134(12)	0.0130(12)	0.0000(9)	0.0051(9)	0.0017(10)
N5A	0.0116(18)	0.0104(12)	0.0129(17)	0.0022(11)	0.0059(12)	0.0030(13)
N6A	0.0151(12)	0.0116(11)	0.0144(13)	-0.0013(10)	0.0075(10)	-0.0018(9)
N8A	0.0177(13)	0.0436(19)	0.0250(16)	0.0028(14)	0.0114(11)	0.0051(13)
C3A	0.021(3)	0.016(2)	0.0074(16)	0.0001(19)	0.0041(16)	-0.0038(17)
C4A	0.0093(12)	0.0185(16)	0.0178(15)	0.0026(13)	0.0025(10)	-0.0011(11)
C5A	0.0111(12)	0.0263(16)	0.0200(15)	0.0061(13)	0.0053(11)	0.0026(11)
C6A	0.0179(14)	0.0244(15)	0.0180(15)	0.0119(12)	0.0136(12)	0.0050(11)
C7A	0.0120(13)	0.0153(14)	0.0222(17)	0.0037(12)	0.0075(12)	0.0034(11)
C8A	0.0179(15)	0.0100(13)	0.0278(19)	0.0019(13)	0.0087(14)	-0.0029(11)

C9A	0.0205(14)	0.0123(13)	0.0204(15)	-0.0025(11)	0.0055(12)	0.0000(11)
C10A	0.0102(19)	0.010(2)	0.0146(17)	0.0002(15)	0.0043(14)	-0.0012(13)
C11A	0.0086(15)	0.013(4)	0.0097(18)	-0.001(2)	0.0045(12)	0.002(2)
C12A	0.0101(12)	0.0104(14)	0.0173(15)	-0.0015(12)	0.0057(10)	-0.0017(10)
C13A	0.0127(12)	0.0068(15)	0.0129(14)	-0.0017(11)	0.0050(10)	-0.0033(11)
C14A	0.0194(13)	0.0105(13)	0.0167(15)	-0.0024(11)	0.0078(11)	-0.0025(11)
C15A	0.0160(13)	0.0105(13)	0.0184(15)	-0.0005(11)	0.0074(11)	-0.0014(11)
C16A	0.0164(13)	0.0223(16)	0.0156(14)	0.0007(12)	0.0080(11)	-0.0008(11)
C17A	0.0171(13)	0.0130(13)	0.0138(14)	0.0001(11)	0.0067(10)	-0.0023(10)
C18A	0.0328(18)	0.0171(15)	0.0258(18)	0.0012(12)	0.0195(15)	0.0047(13)
C19A	0.0290(17)	0.0224(16)	0.0142(15)	-0.0005(13)	0.0016(13)	-0.0090(14)
C20A	0.0151(16)	0.010(2)	0.0131(18)	-0.0007(17)	0.0008(12)	-0.0009(16)
C21A	0.0222(14)	0.0107(13)	0.0257(17)	0.0004(12)	0.0051(12)	-0.0009(11)
C22A	0.0198(16)	0.0122(14)	0.032(2)	0.0013(13)	0.0025(15)	0.0004(12)
C23A	0.033(2)	0.0190(18)	0.044(2)	0.0074(17)	0.0229(18)	-0.0006(15)
C24A	0.0200(17)	0.0189(18)	0.035(2)	-0.0065(15)	-0.0067(16)	0.0002(14)
B1A	0.0159(15)	0.0142(15)	0.0125(15)	-0.0026(12)	0.0057(12)	-0.0013(13)

Table 8. Hydrogen atomic coordinates and isotropic atomic displacement parameters (Å^2) for Harman_SS5_44.

	x/a	y/b	z/c	U(eq)
H1	0.4135	0.2954	0.9491	0.029
H2A	0.4673	0.3379	1.0790	0.029
H2B	0.4805	0.3497	1.0780	0.029
H3	0.3719	0.5218	1.0906	0.024
H4	-0.0874	0.4779	0.7994	0.018
H5	-0.1726	0.5904	0.8793	0.021

H6	-0.0031	0.6663	0.9721	0.02
H7	0.2932	0.6723	0.7486	0.019
H8	0.3401	0.8490	0.8114	0.024
H9	0.3135	0.8211	0.9330	0.022
H10	0.3970	0.3025	0.8255	0.014
H11	0.4417	0.4716	0.8518	0.013
H12	0.4091	0.6088	0.7578	0.013
H13	0.2662	0.5275	0.6703	0.014
H14	0.3388	0.3584	0.6159	0.021
H15	0.3273	0.2437	0.7033	0.022
H18A	0.3105	0.7103	0.6379	0.03
H18B	0.3894	0.7296	0.5852	0.03
H18C	0.4487	0.7053	0.6674	0.03
H19A	0.5578	0.5552	0.6380	0.036
H19B	0.5020	0.5689	0.5543	0.036
H19C	0.4936	0.4564	0.5915	0.036
H21A	0.1005	0.5901	0.4413	0.047
H21B	0.0154	0.6092	0.4904	0.047
H21C	0.0671	0.4925	0.4848	0.047
H22A	0.2232	0.1321	0.8075	0.03
H22B	0.1317	0.0871	0.8465	0.03
H22C	0.2448	0.1494	0.8911	0.03
H23A	0.0828	0.2657	0.9433	0.041
H23B	-0.0144	0.1940	0.8907	0.041
H23C	-0.0274	0.3214	0.8901	0.041
H24A	-0.0619	0.3021	0.7375	0.034
H24B	-0.0402	0.1763	0.7489	0.034
H24C	0.0327	0.2437	0.7066	0.034
H1A	0.2318	0.6590	1.0000	0.017
H3A	0.3420	0.4845	1.0905	0.018
H4A	-0.0878	0.4288	0.7762	0.019
H5A	-0.2067	0.4968	0.8546	0.023
H6A	-0.0643	0.5655	0.9655	0.022
H7A	0.2724	0.7042	0.7740	0.019
H8A	0.2769	0.8632	0.8532	0.022
H9A	0.2293	0.7925	0.9622	0.021
H10A	0.3669	0.2777	0.8330	0.014
H11A	0.4411	0.4420	0.8439	0.012
H12A	0.4177	0.5571	0.7385	0.015

H13A	0.2512	0.4851	0.6640	0.013
H14A	0.2783	0.2932	0.6190	0.018
H15A	0.2776	0.2033	0.7187	0.017
H18D	0.5249	0.4407	0.6092	0.034
H18E	0.4522	0.4391	0.5274	0.034
H18F	0.4352	0.3457	0.5796	0.034
H19D	0.2165	0.4059	0.5242	0.034
H19E	0.2578	0.5082	0.4885	0.034
H19F	0.1810	0.5234	0.5430	0.034
H21D	0.3585	0.8075	0.5930	0.03
H21E	0.4066	0.7816	0.6759	0.03
H21F	0.2738	0.8151	0.6433	0.03
H22D	0.2749	0.1339	0.7931	0.034
H22E	0.1936	0.0739	0.8334	0.034
H22F	0.2959	0.1500	0.8768	0.034
H23D	0.1078	0.2423	0.9276	0.044
H23E	0.0381	0.1489	0.8779	0.044
H23F	-0.0120	0.2683	0.8696	0.044
H24D	-0.0196	0.2769	0.7150	0.041
H24E	-0.0006	0.1524	0.7333	0.041
H24F	0.0815	0.2129	0.6937	0.041
H1B	0.1703	0.6006	1.0063	0.017

Supporting Information for Chapter 5

^{1}H NMR Spectrum of 3

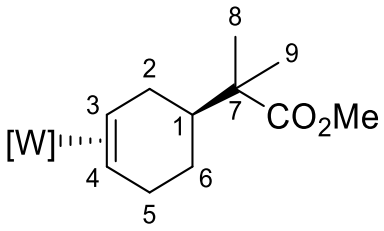

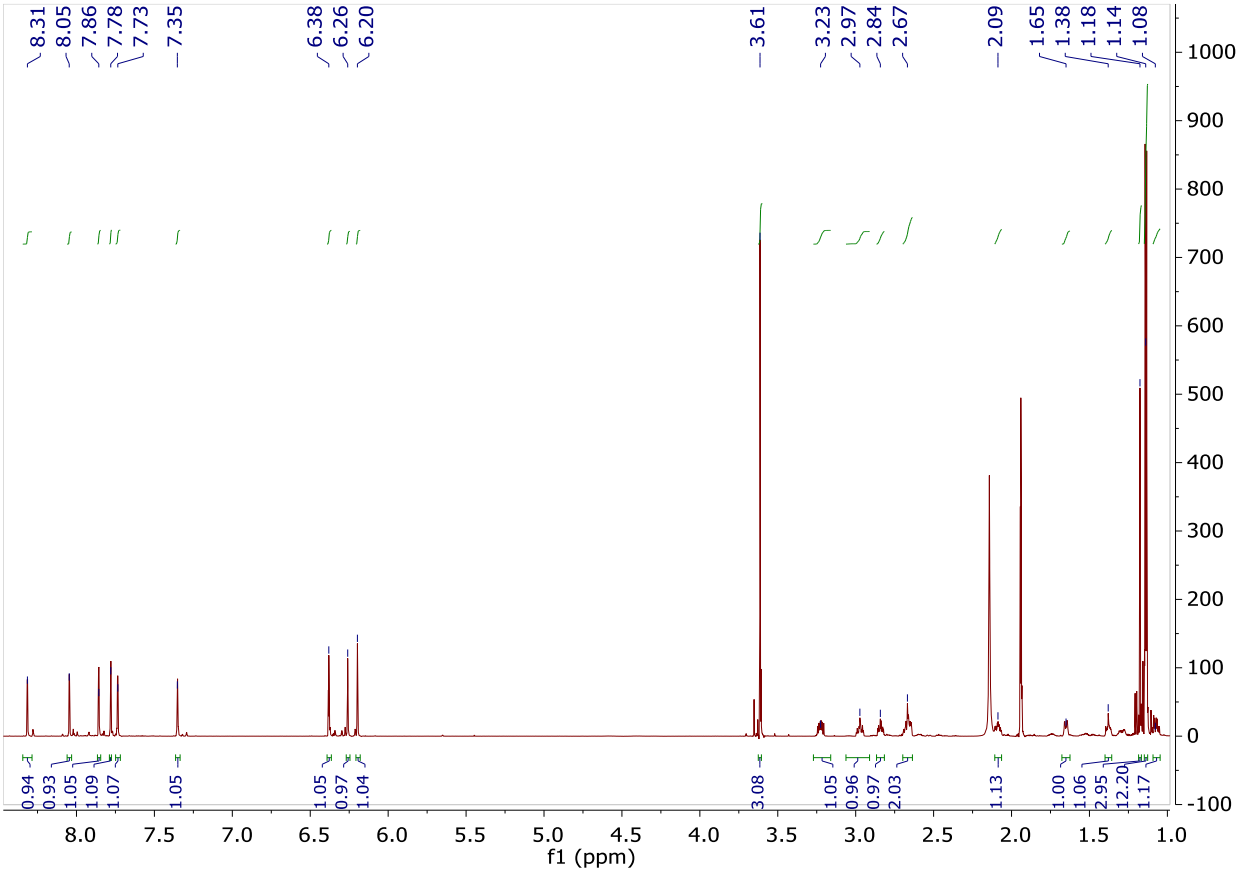

^{13}C {^{1}H} NMR Spectrum of 3

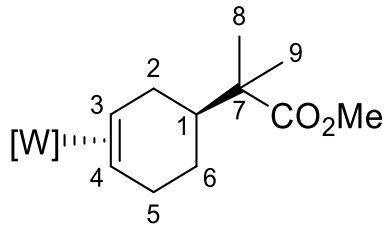

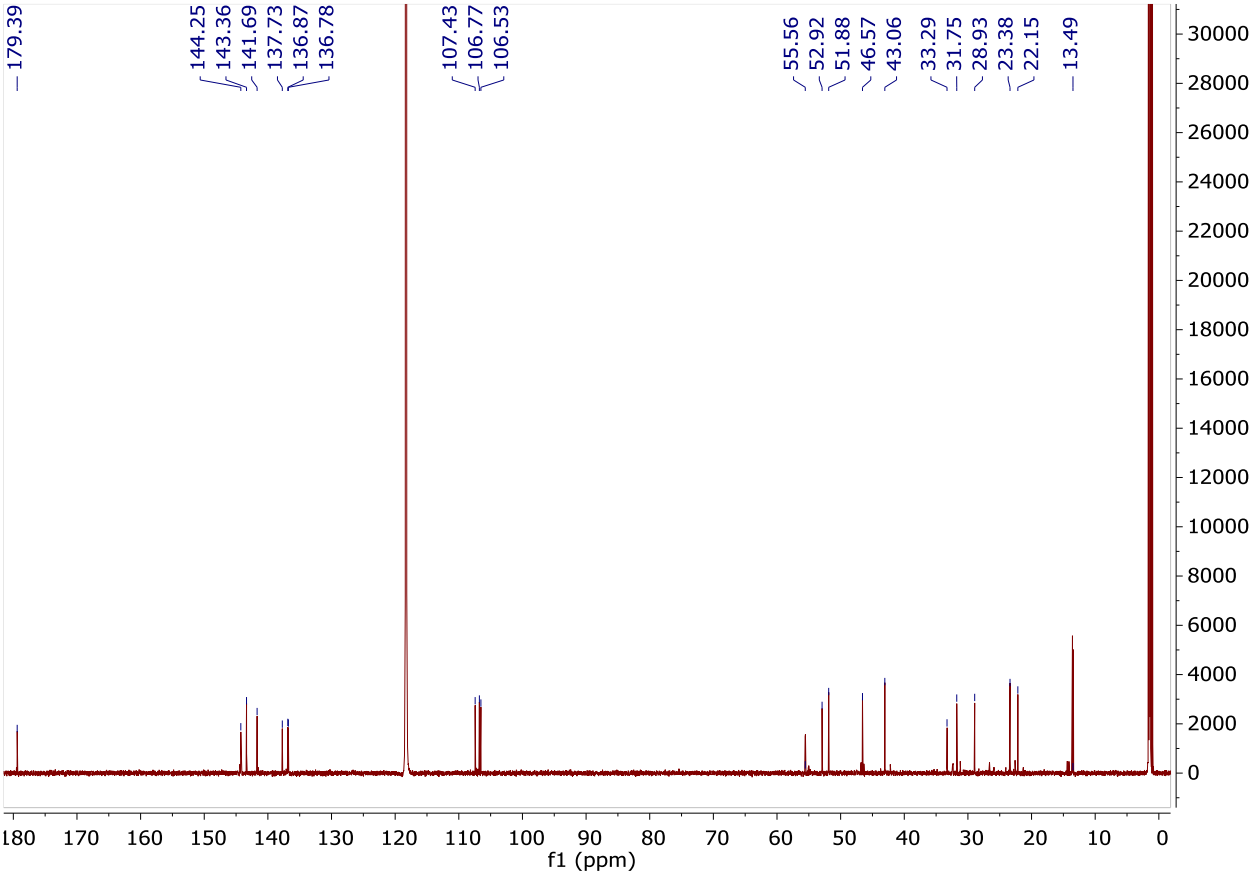

^{1}H NMR Spectrum of 5

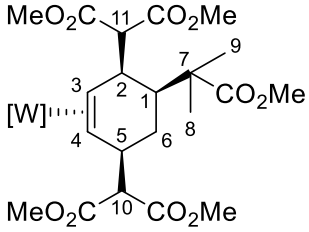

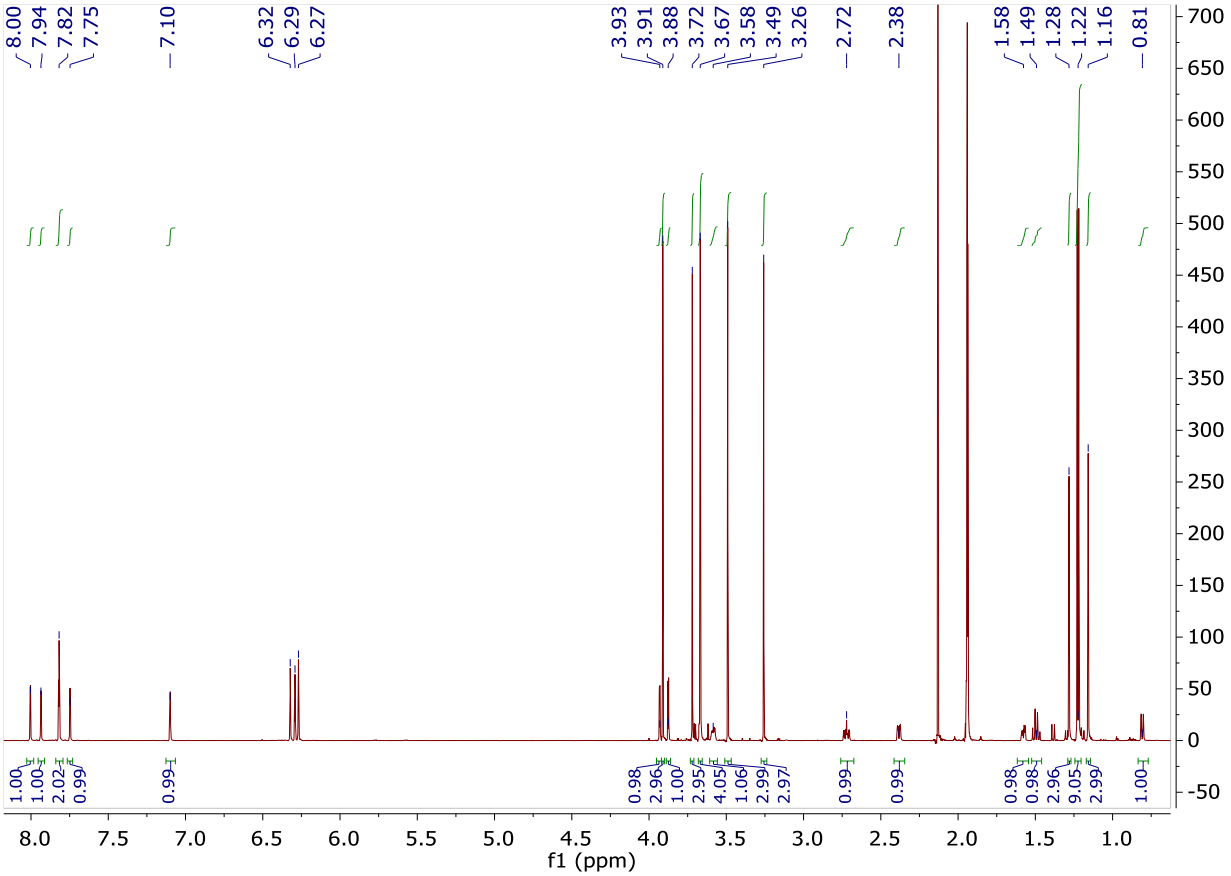

^{13}C {^{1}H} NMR Spectrum of 5

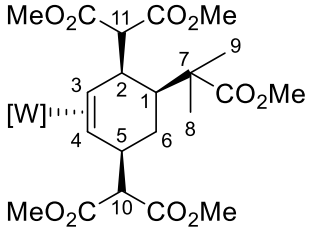

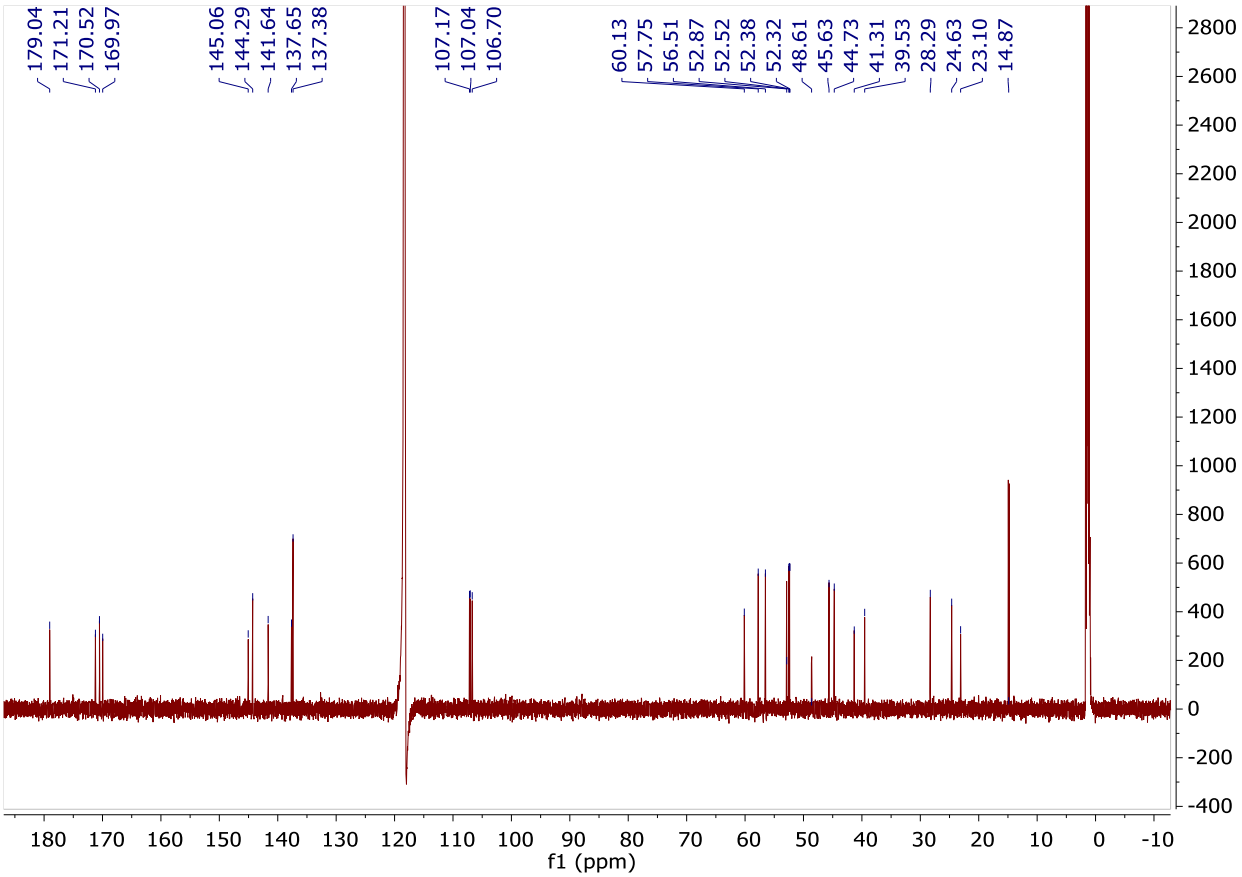

^{1}H NMR Spectrum of 8H

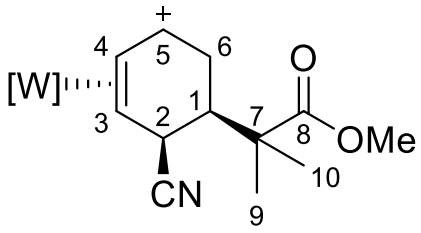

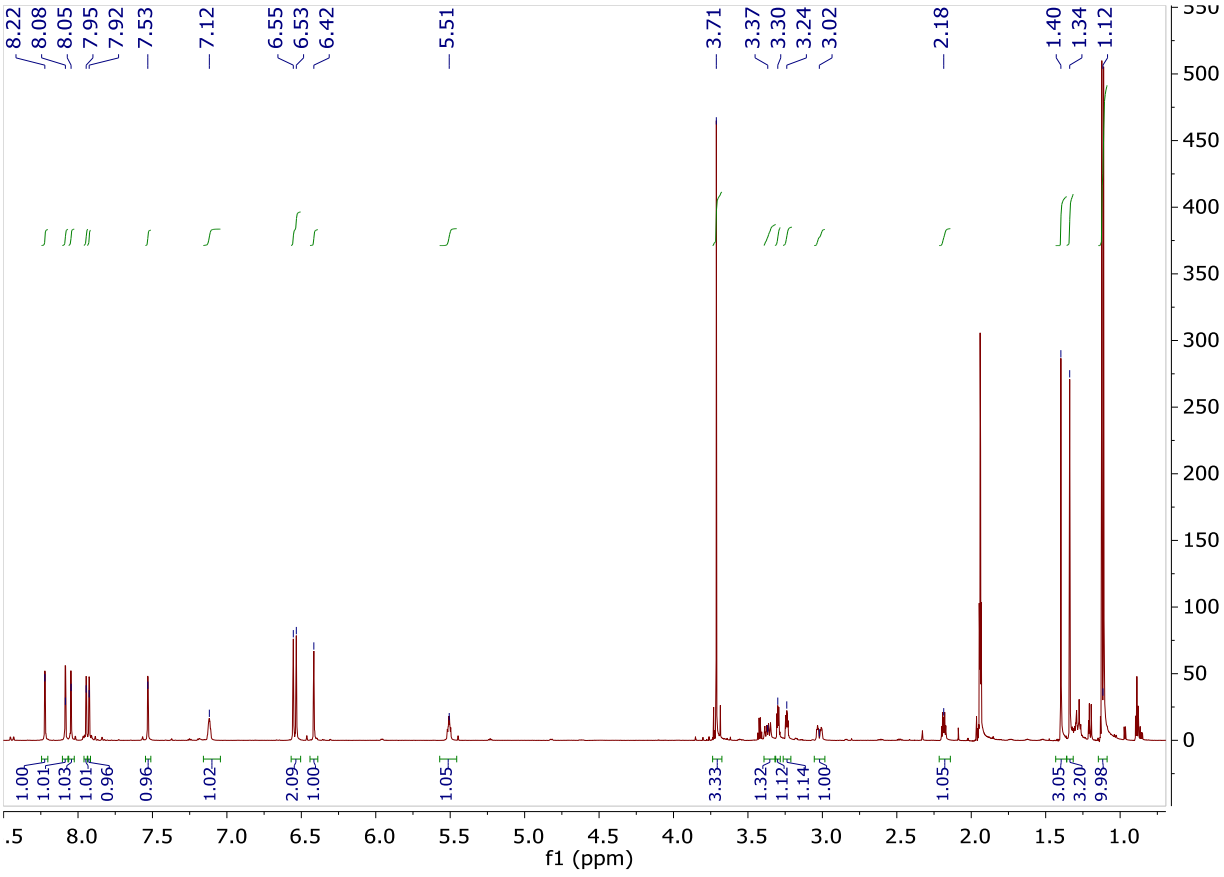

^{13}C {^{1}H} NMR Spectrum of 8H

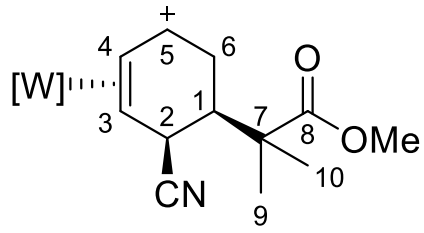

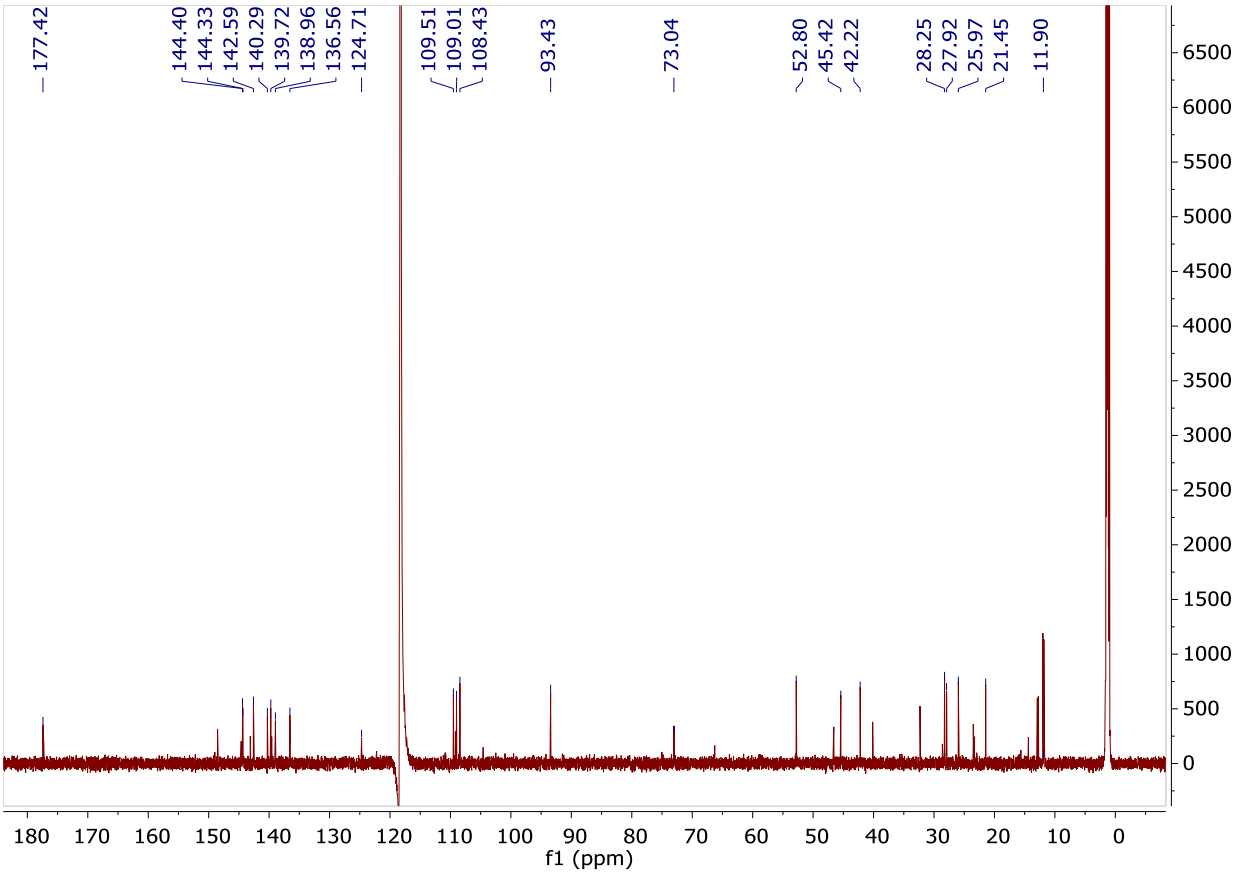

^{1}H NMR Spectrum of 9

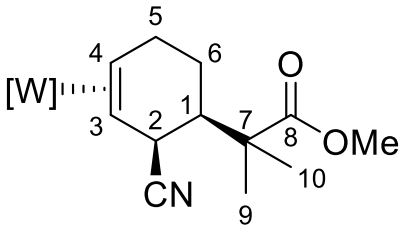

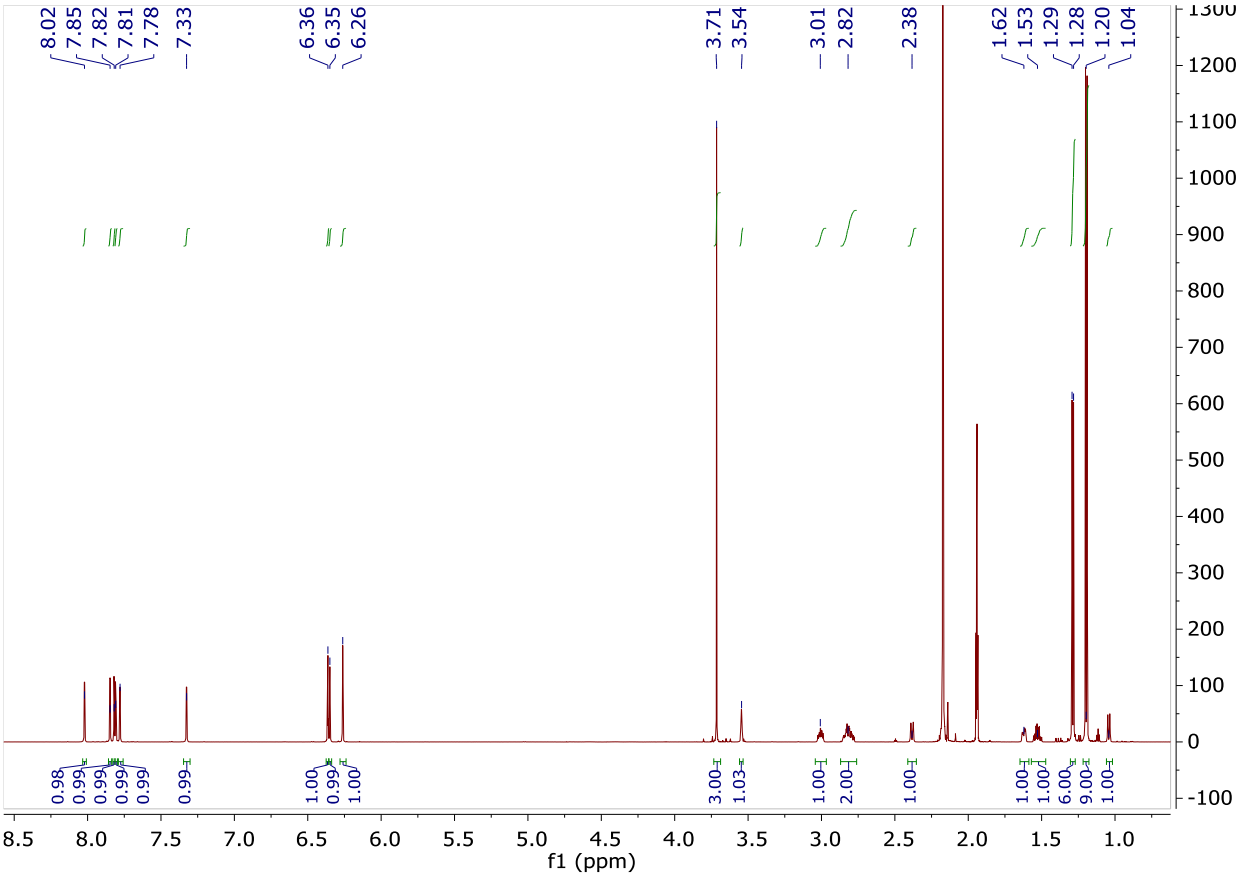

^{13}C {^{1}H} NMR Spectrum of 9

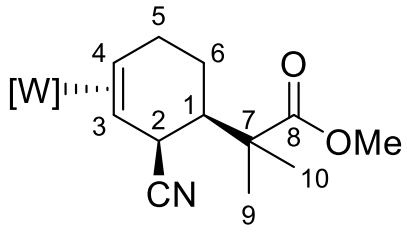

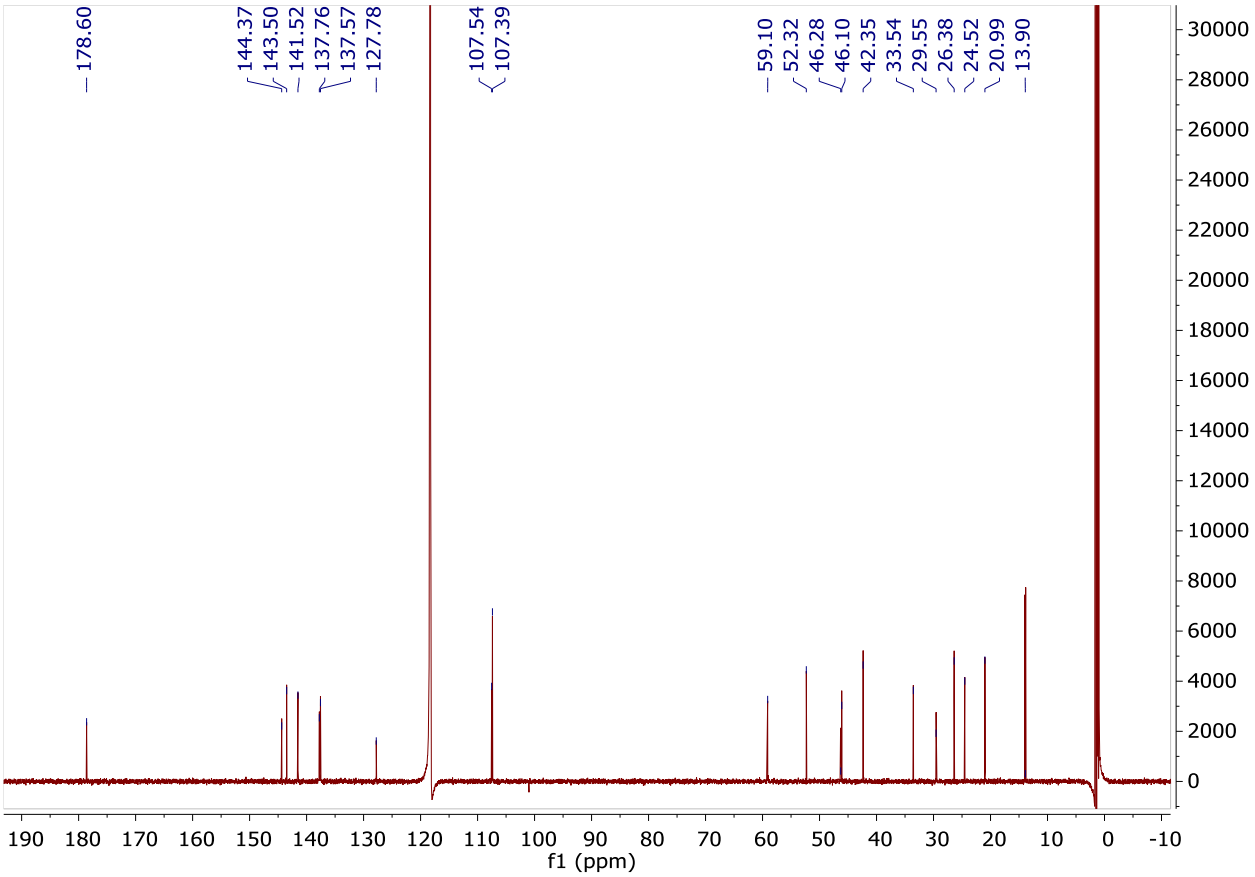

^{1}H NMR Spectrum of 10

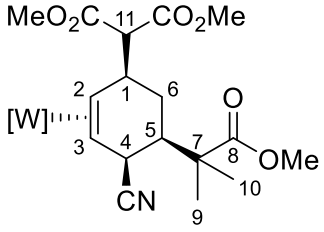

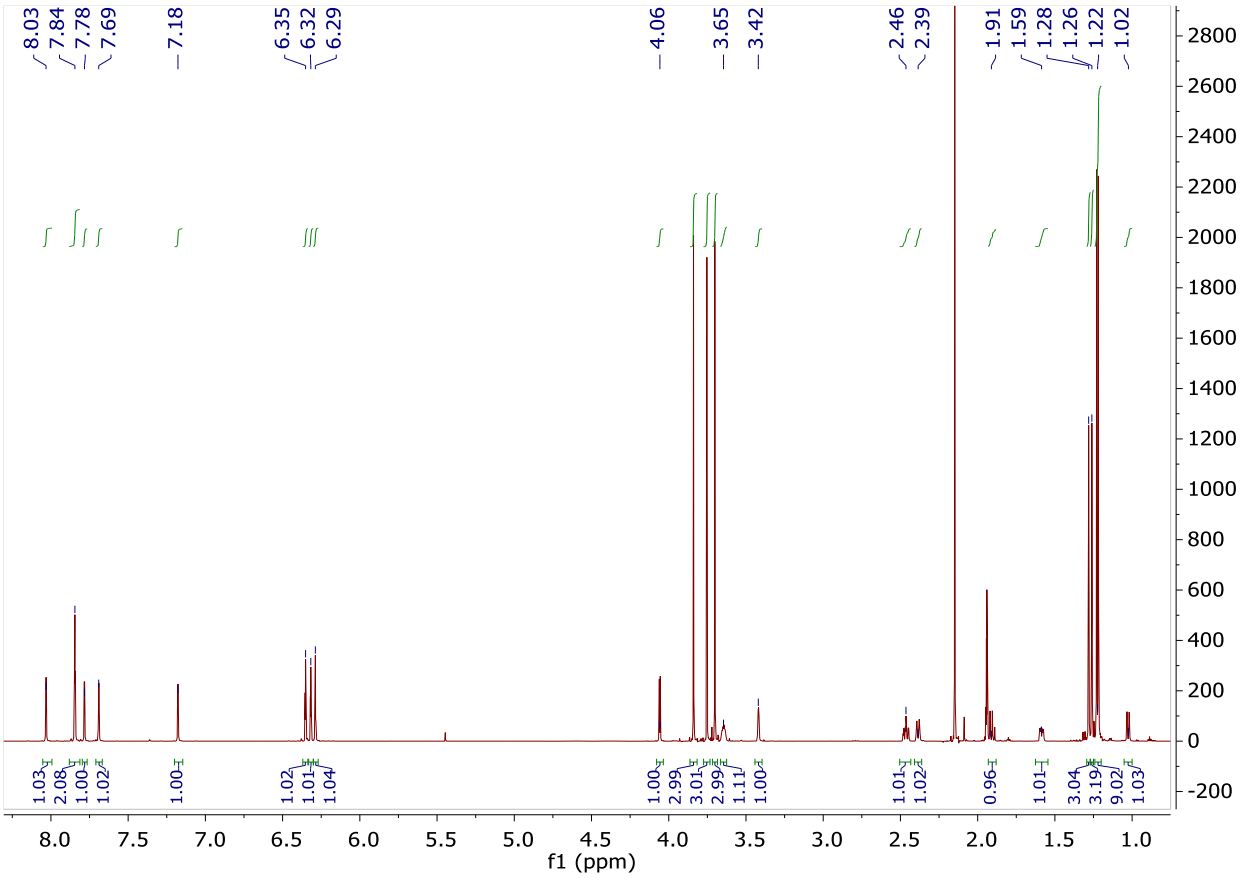

^{13}C {^{1}H} NMR Spectrum of 10

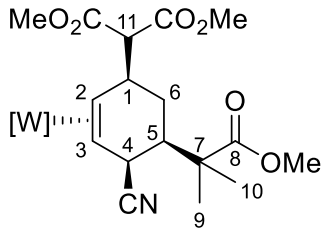

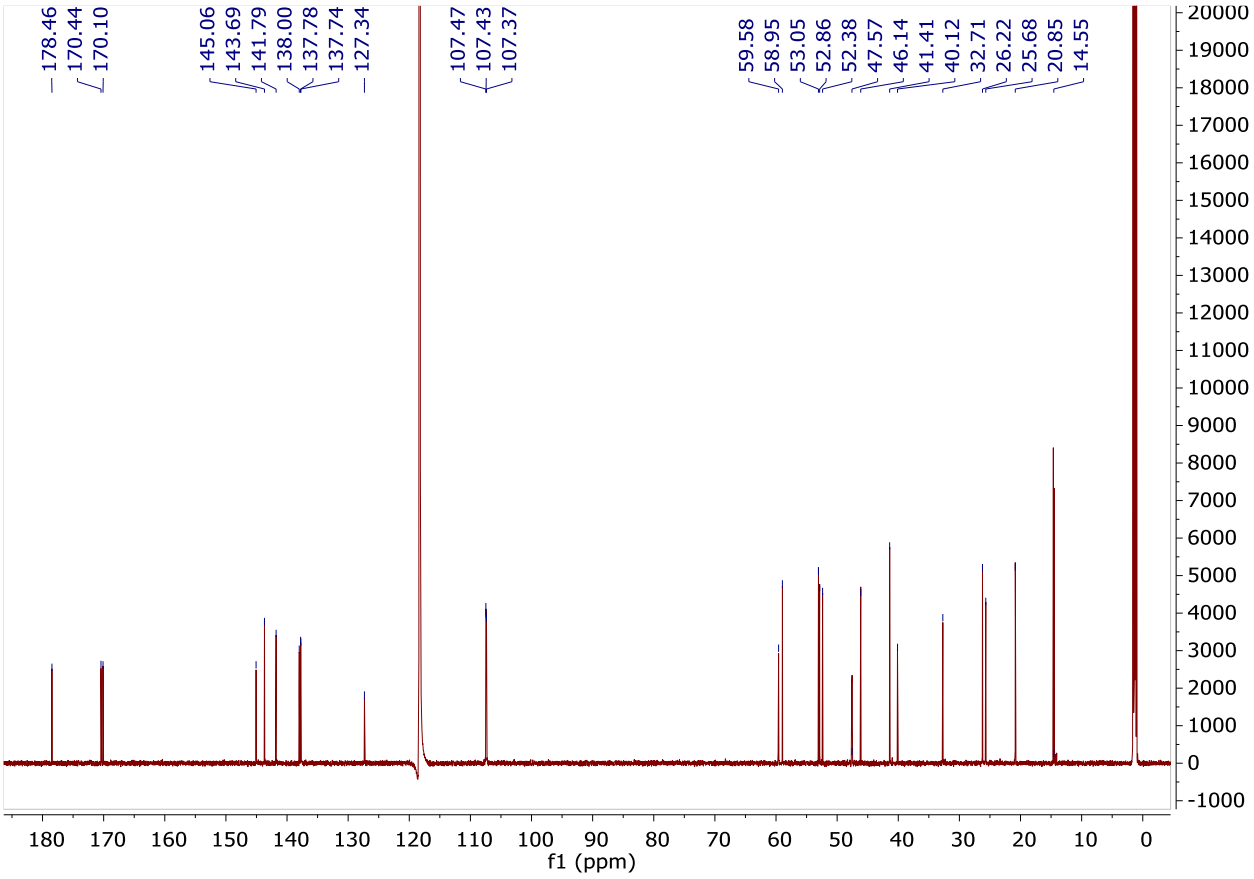

^{1}H NMR Spectrum of 11

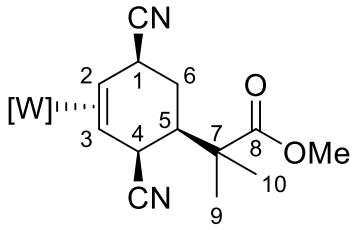

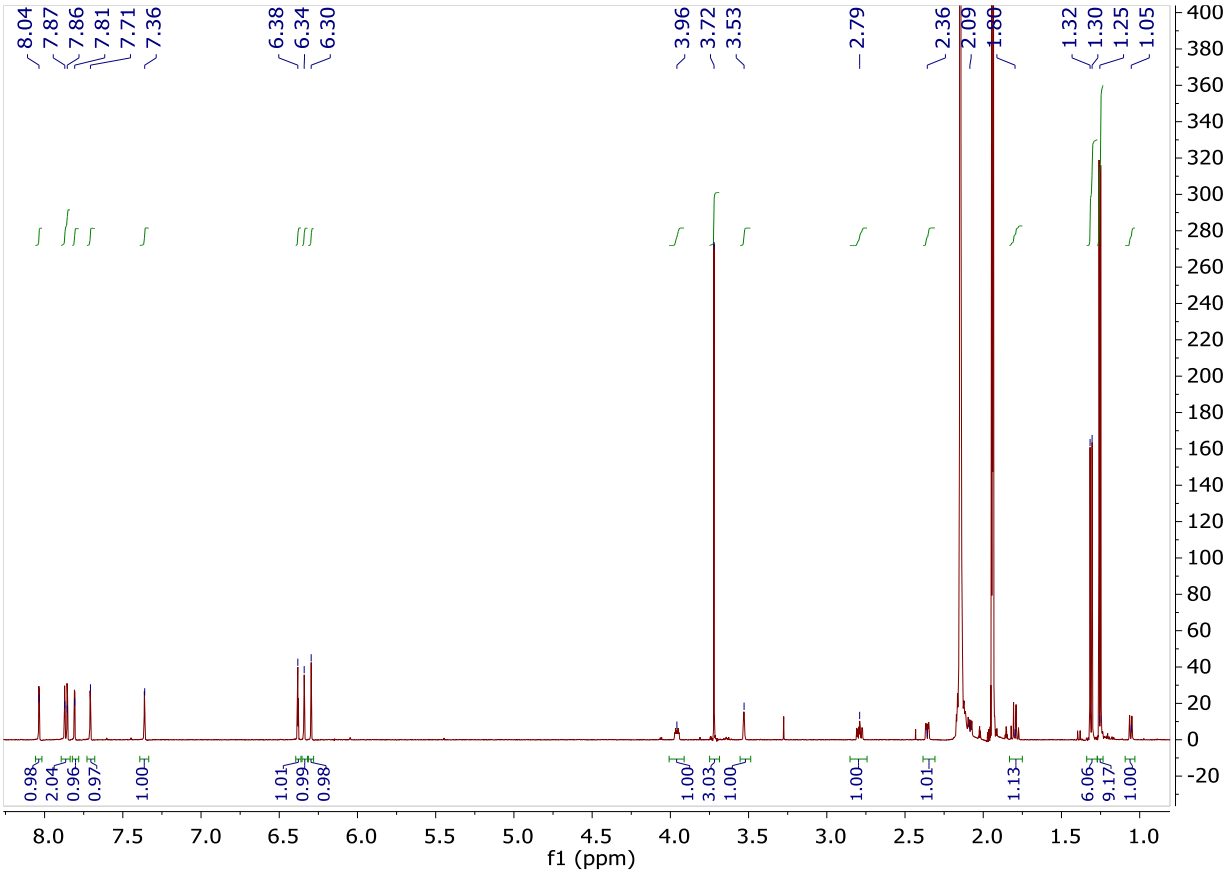

^{13}C {^{1}H} NMR Spectrum of 11

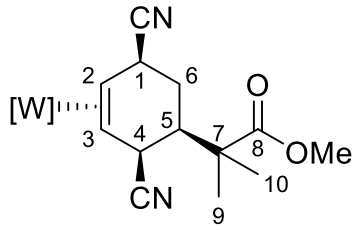

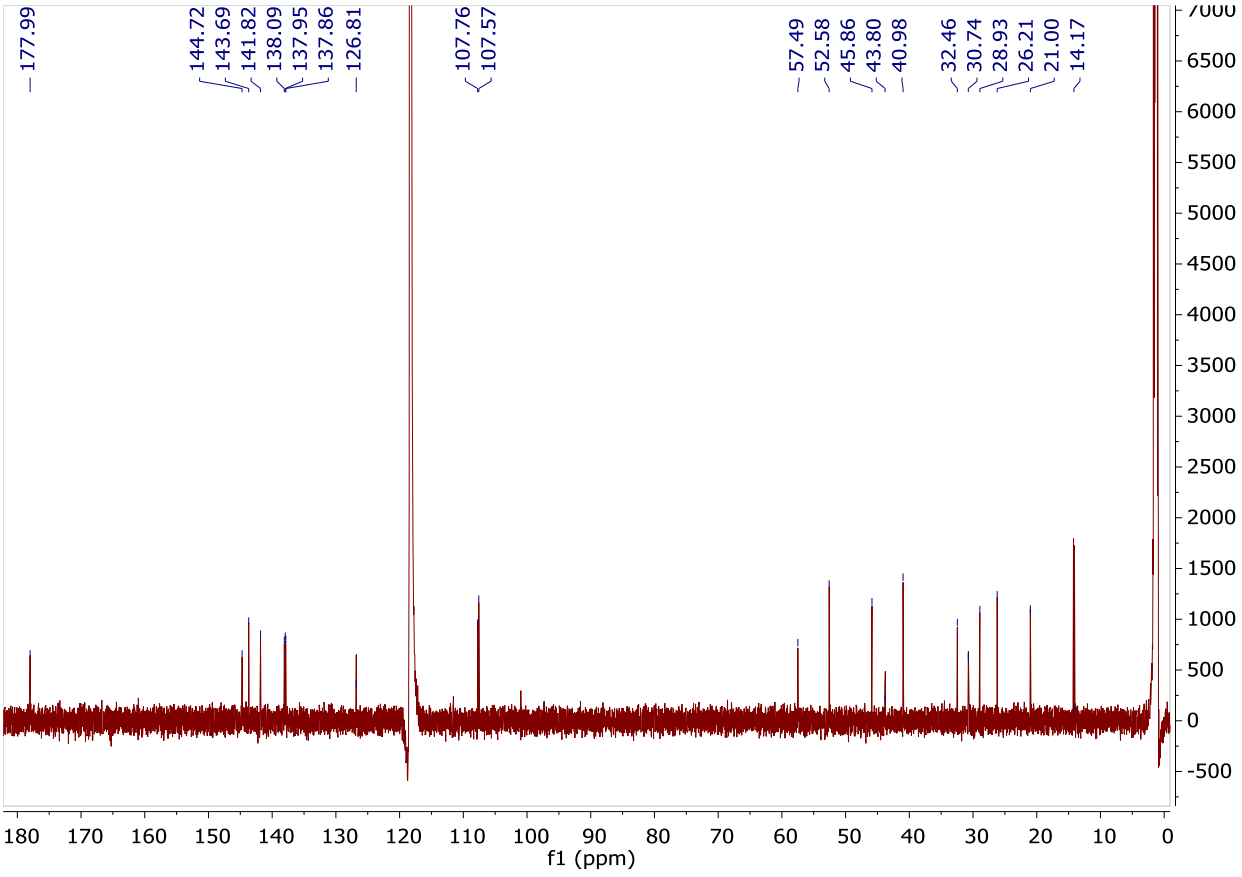

^{1}H NMR Spectrum of 12

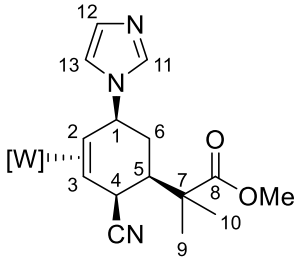

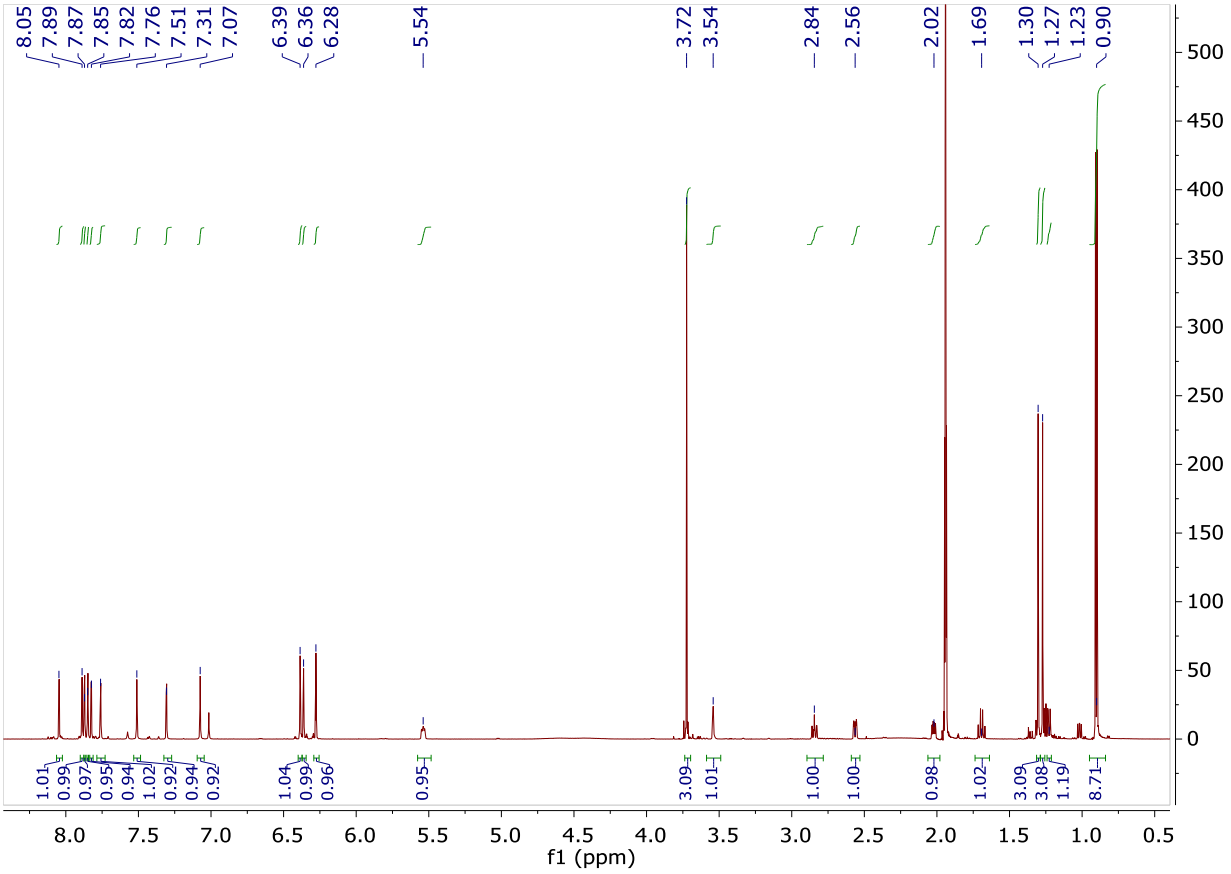

^{13}C {^{1}H} NMR Spectrum of 12

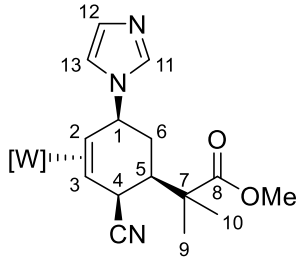

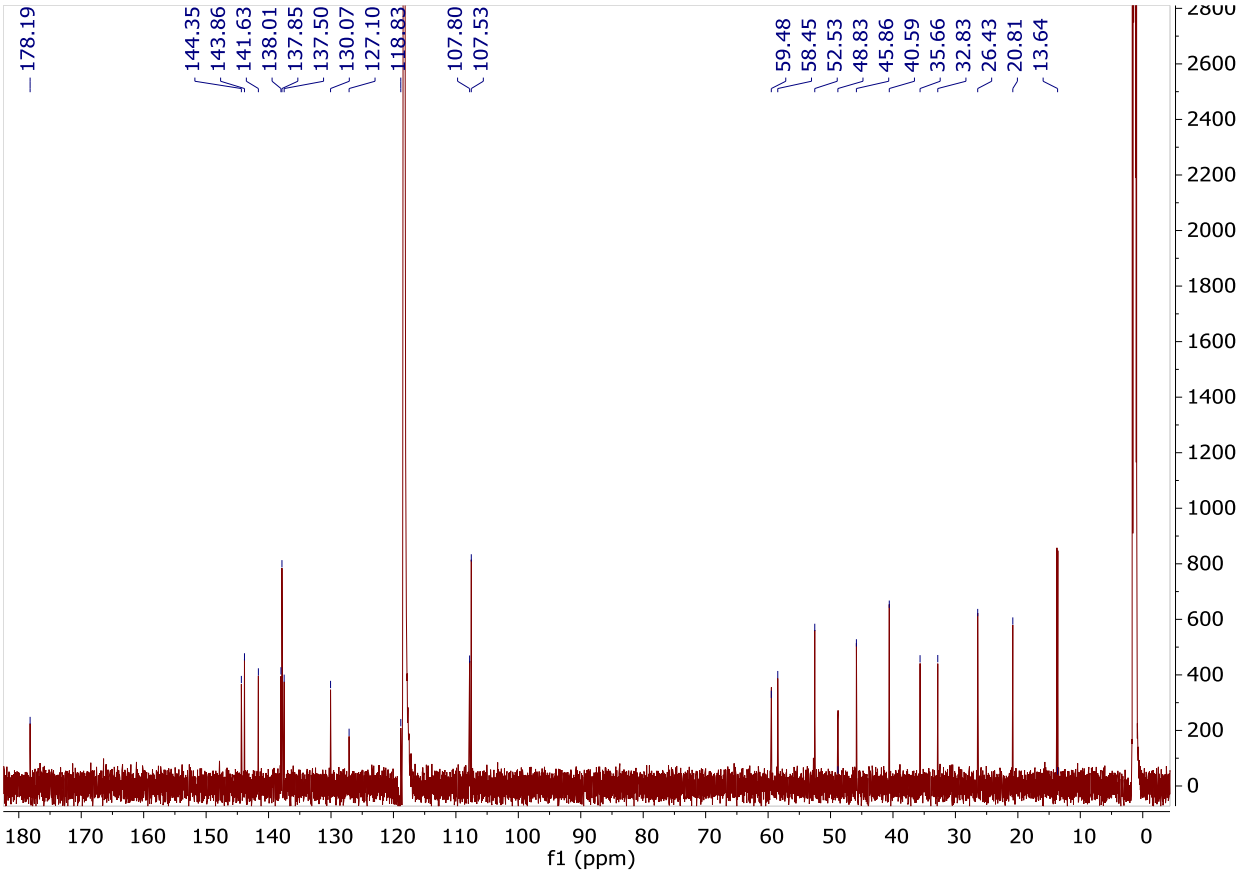

^{1}H NMR Spectrum of 13

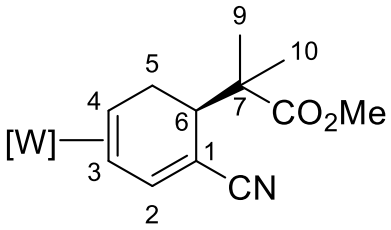

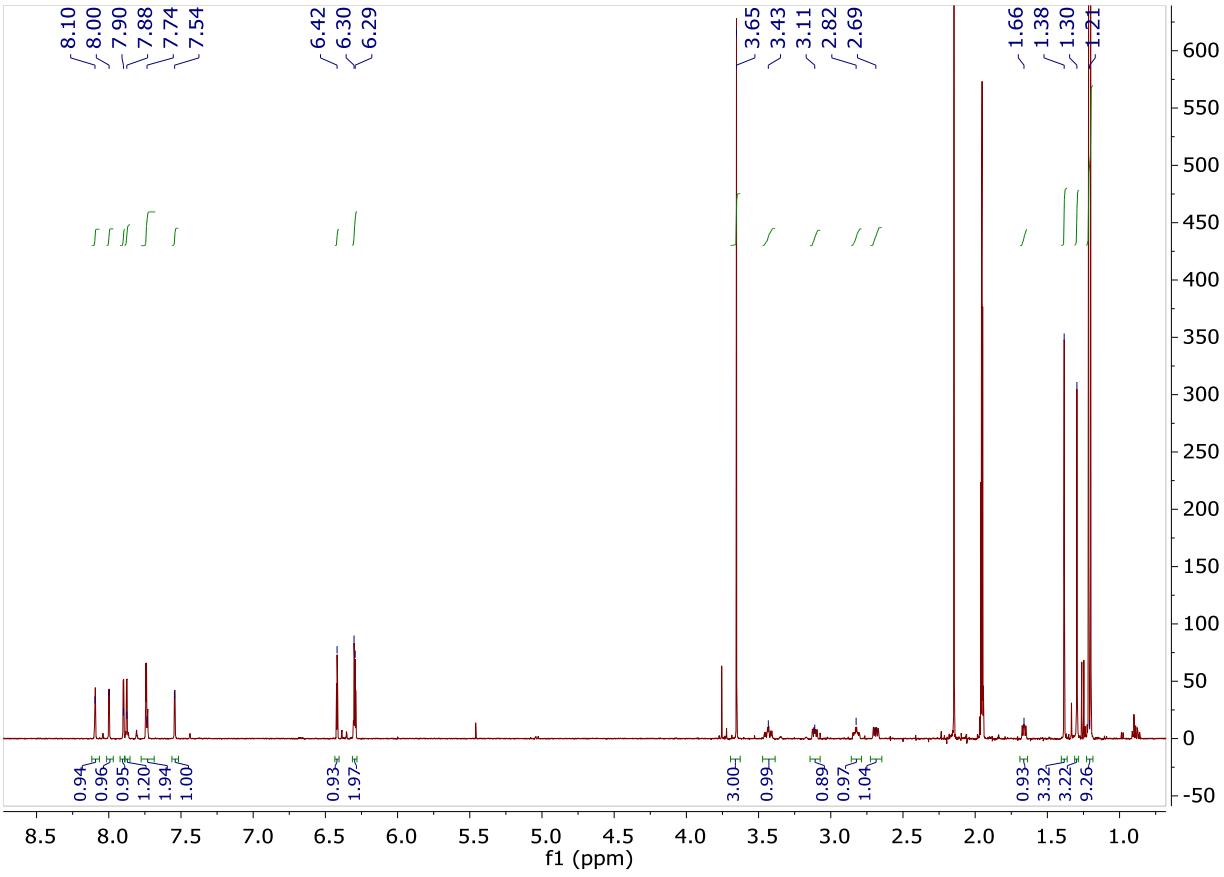

^{1}H NMR Spectrum of 14

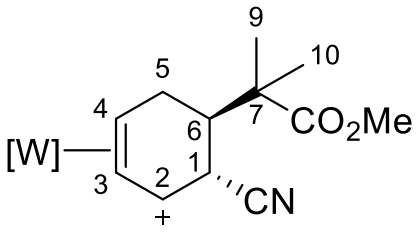

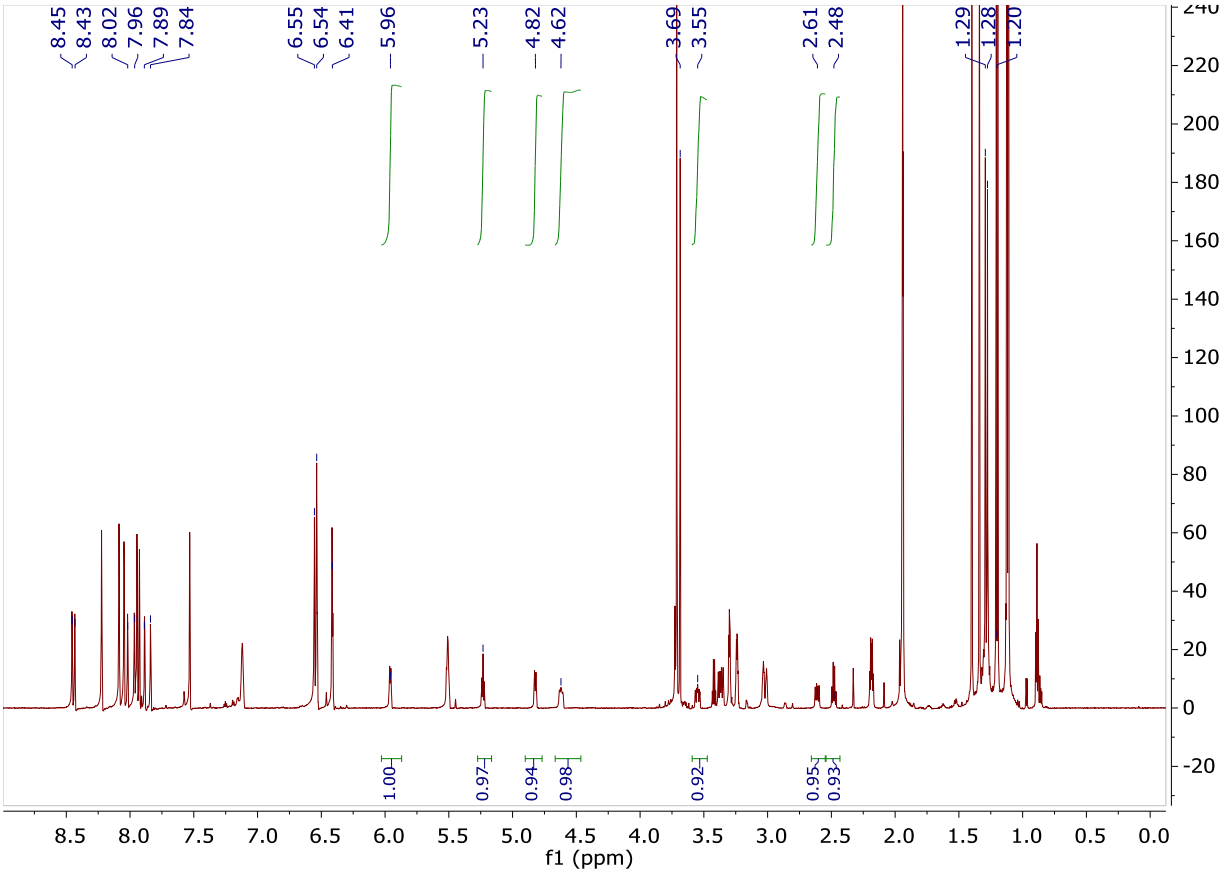

^{13}C {^{1}H} NMR Spectrum of 12

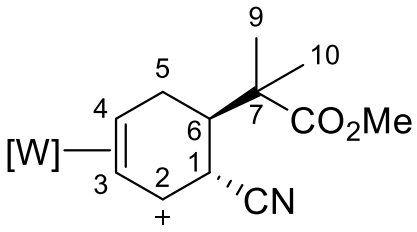

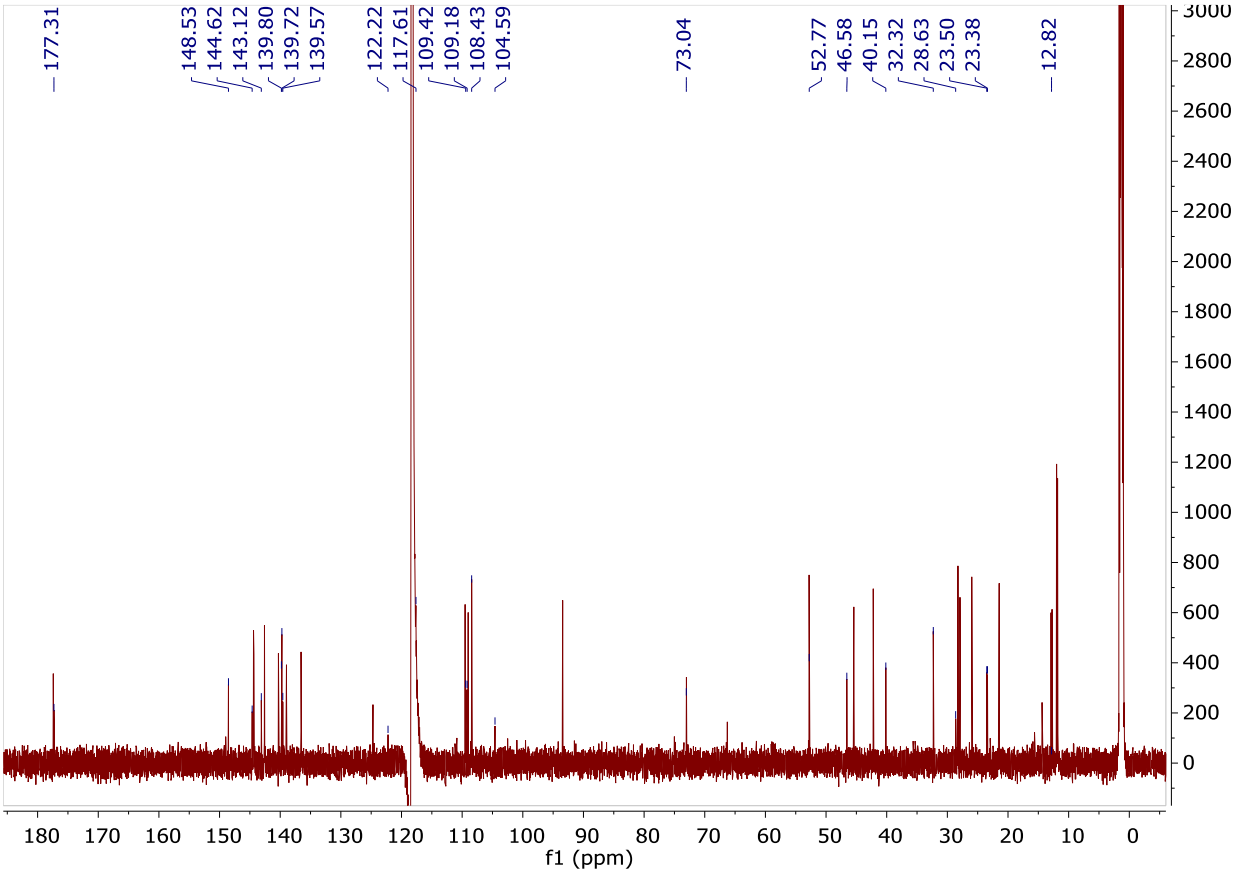

^{1}H NMR Spectrum of 18a and 18b

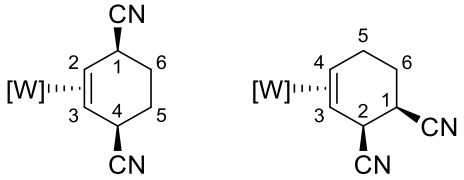

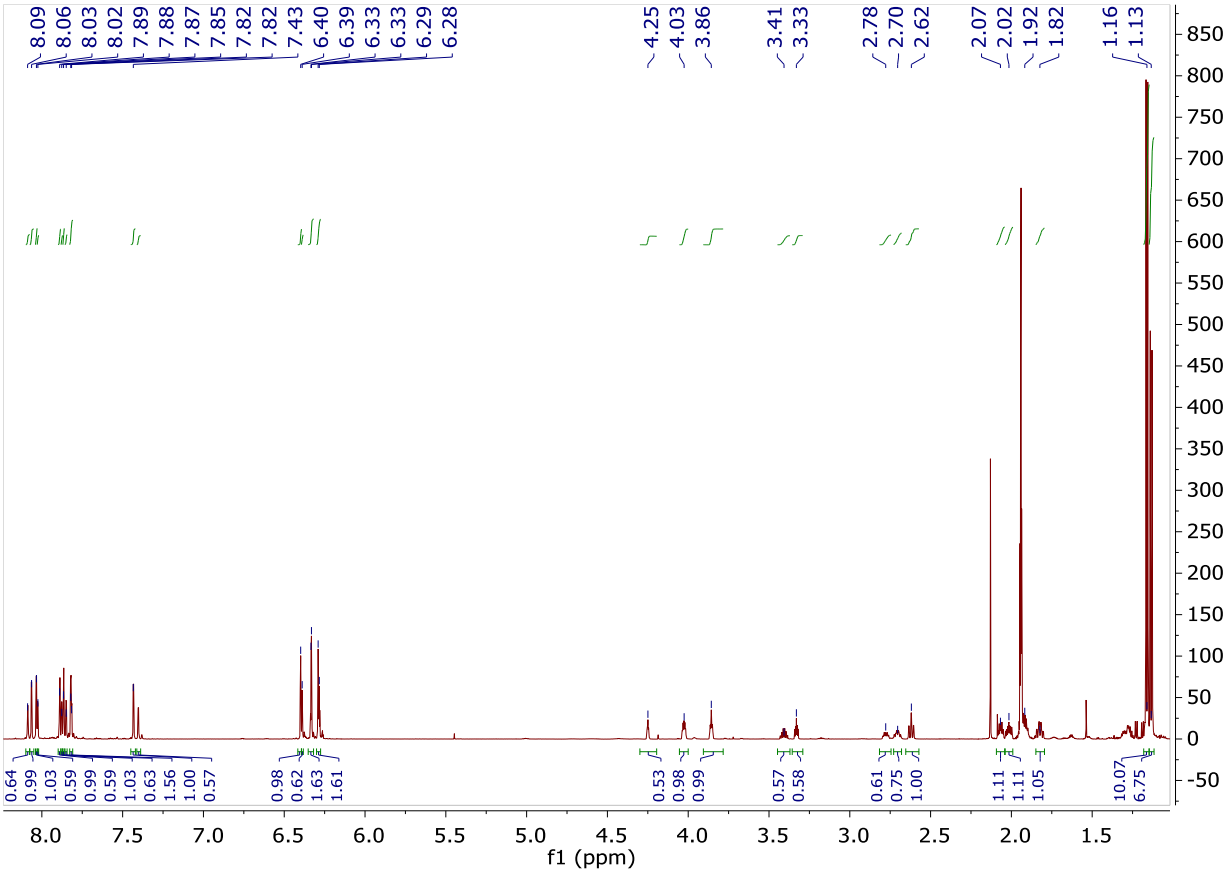

^{13}C {^{1}H} NMR Spectrum of 18a and 18b

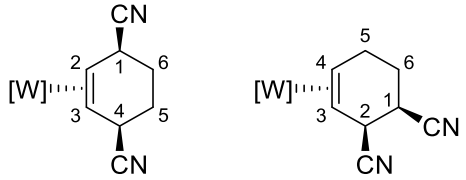

A **B**

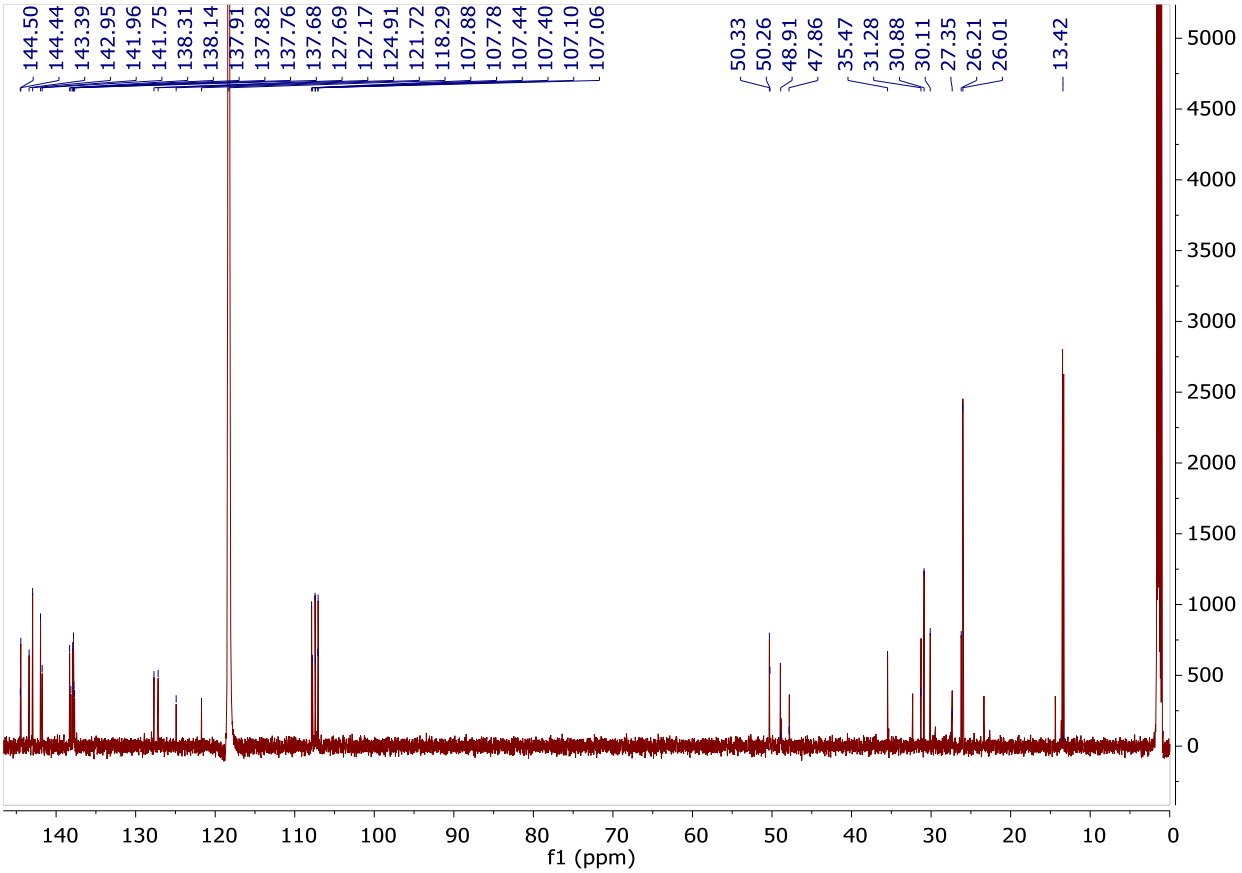

^{1}H NMR Spectrum of 21

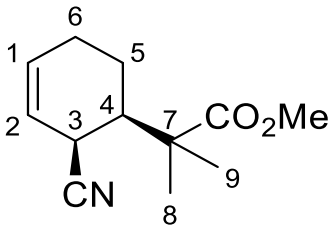

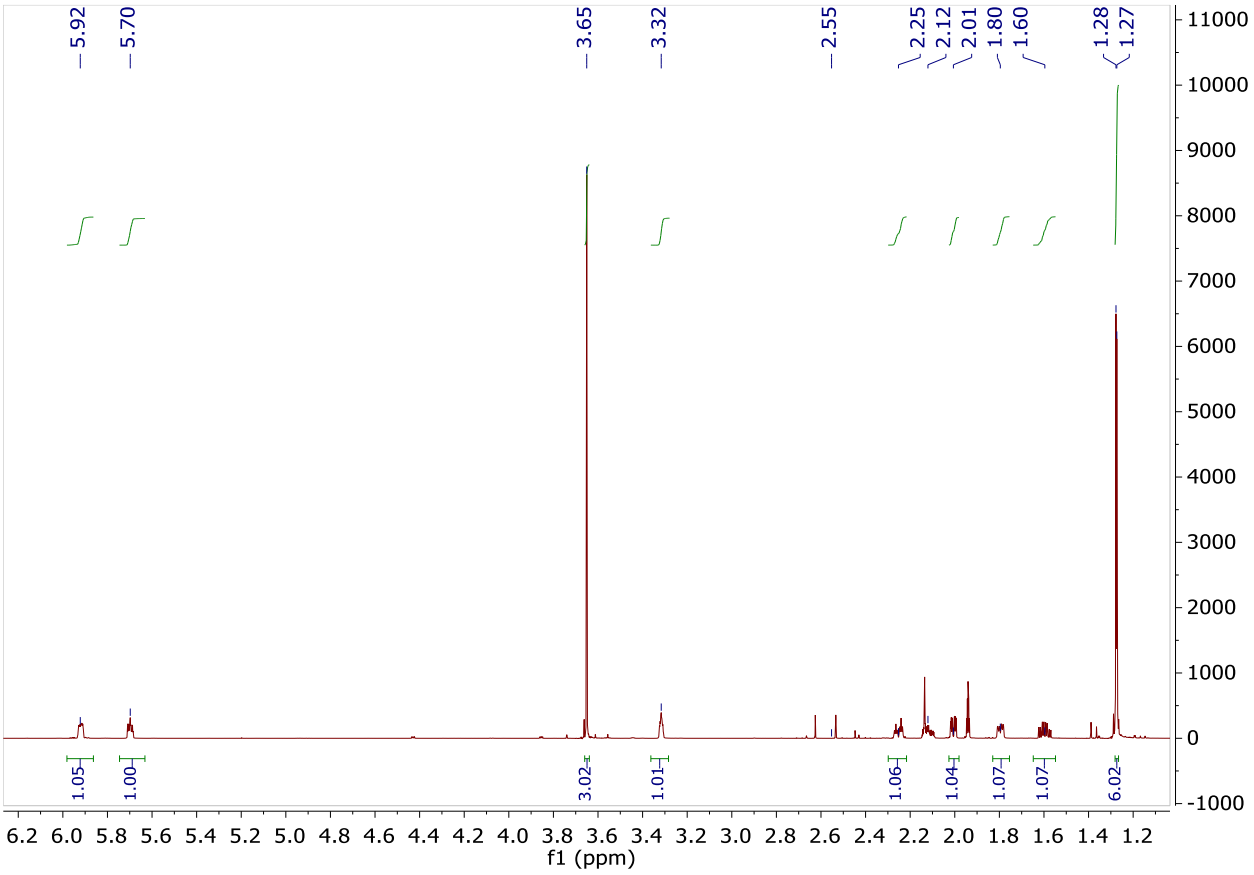

^{13}C {^{1}H} NMR Spectrum of 21

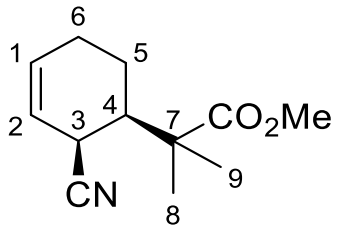

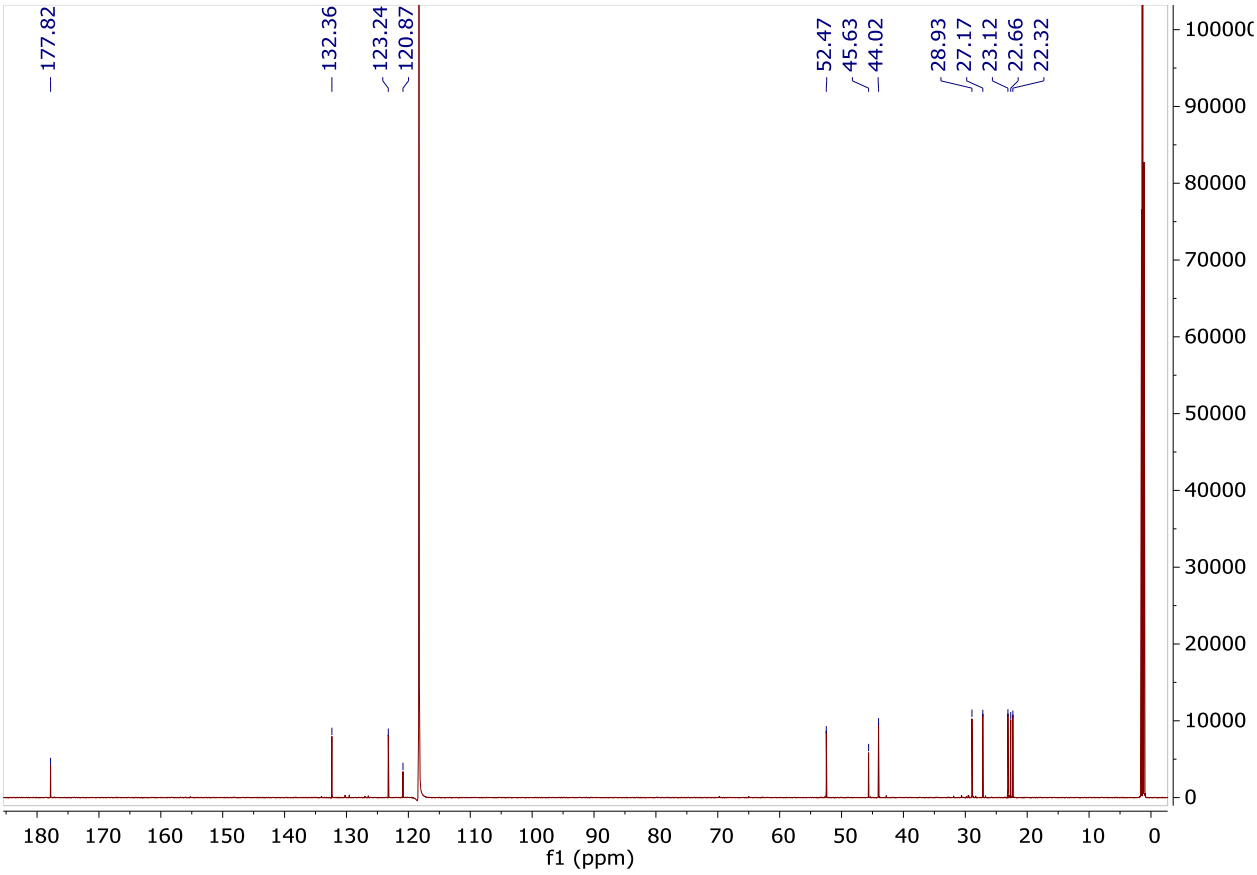

^{1}H NMR Spectrum of 22

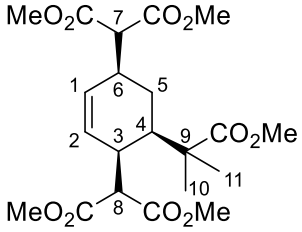

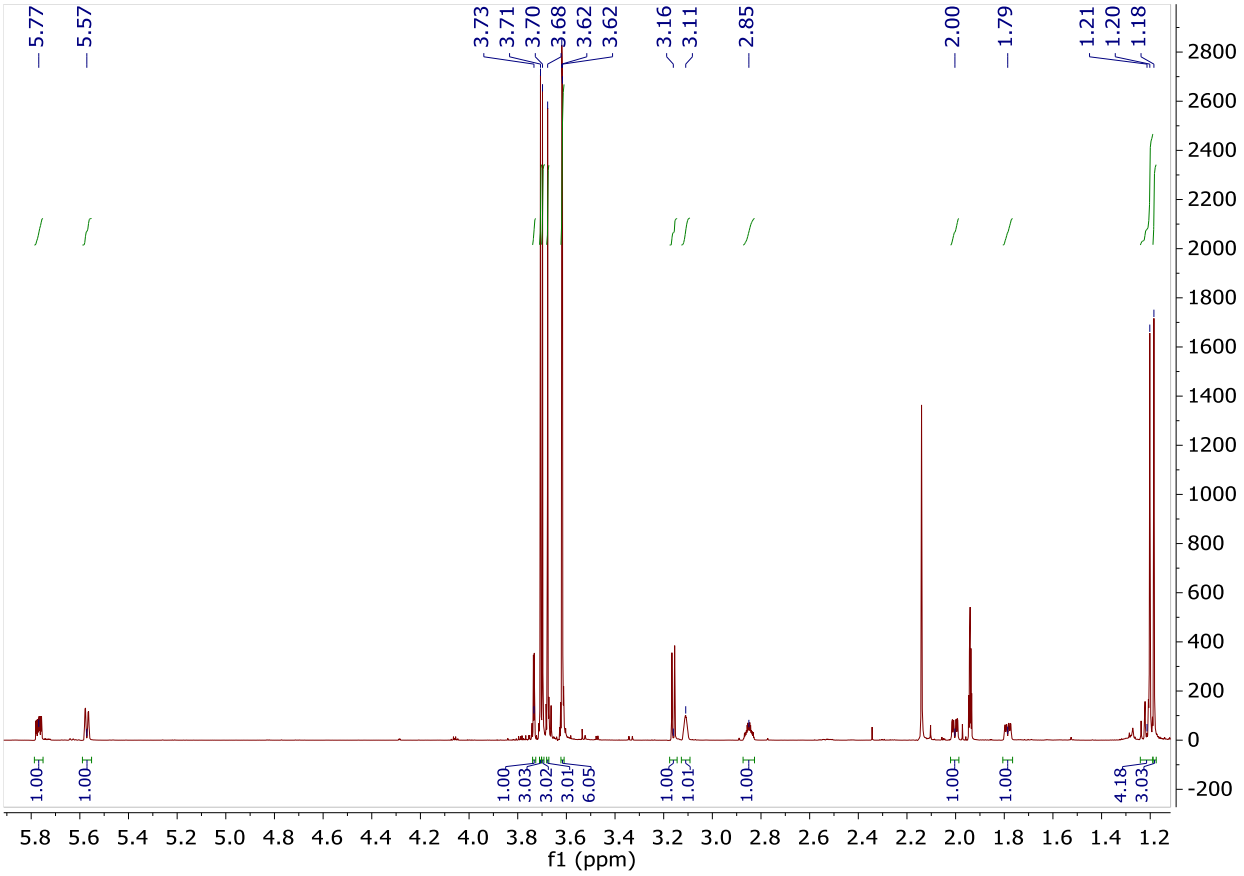

^{13}C {^{1}H} NMR Spectrum of 22

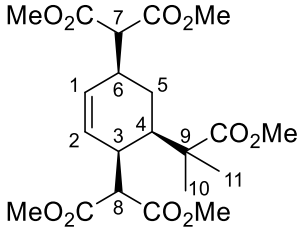

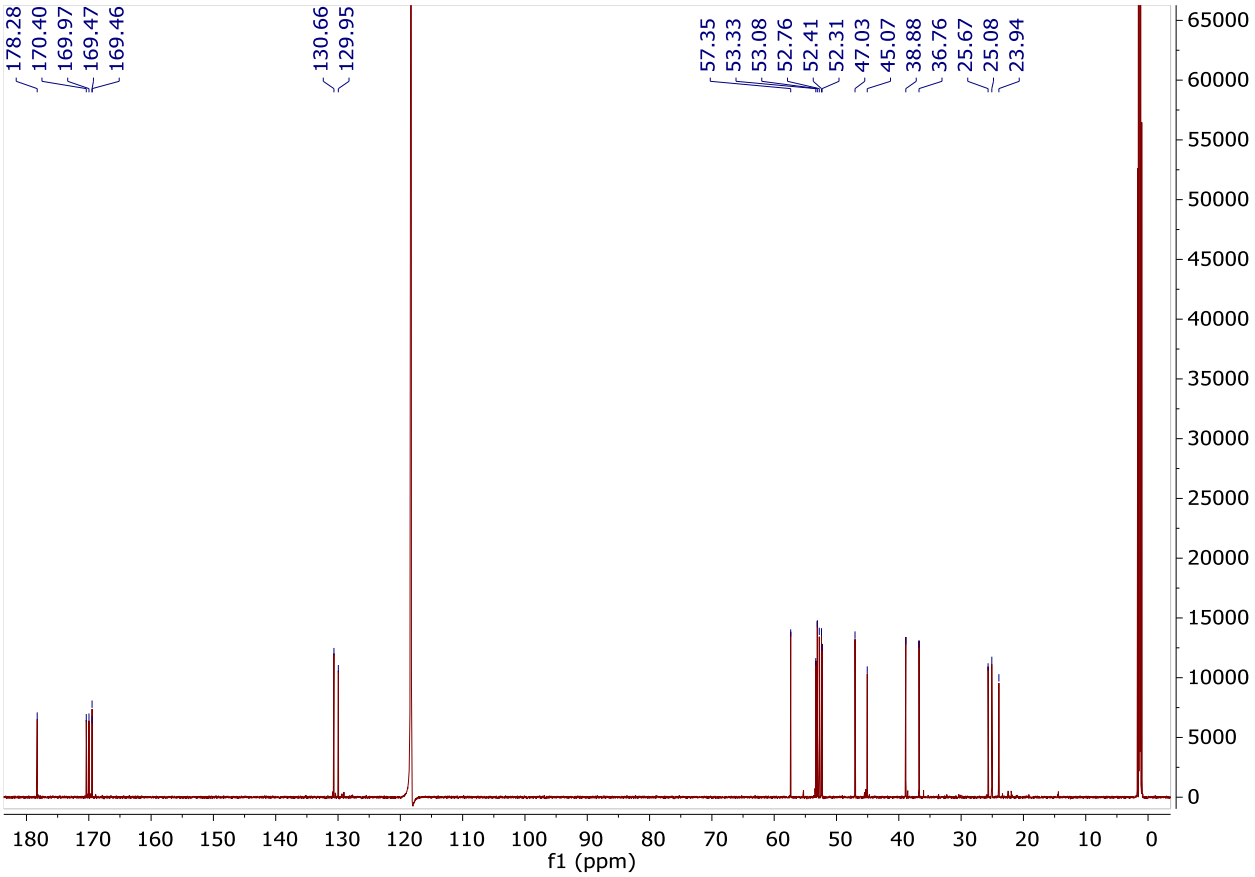

^{1}H NMR Spectrum of 23

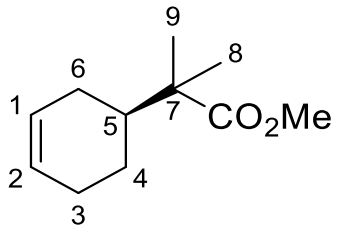

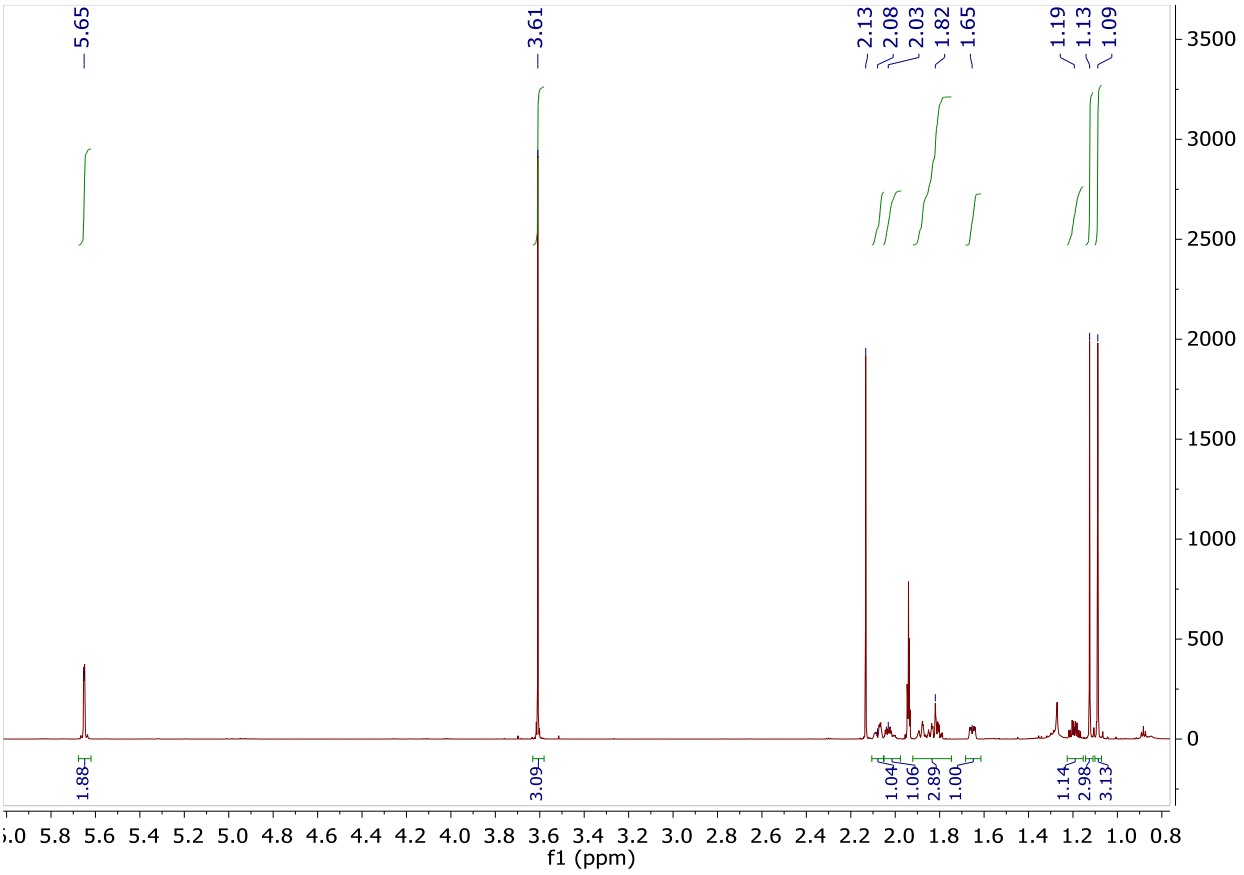

^{13}C {^{1}H} NMR Spectrum of 23

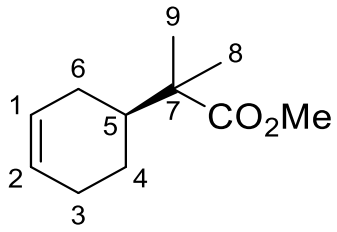

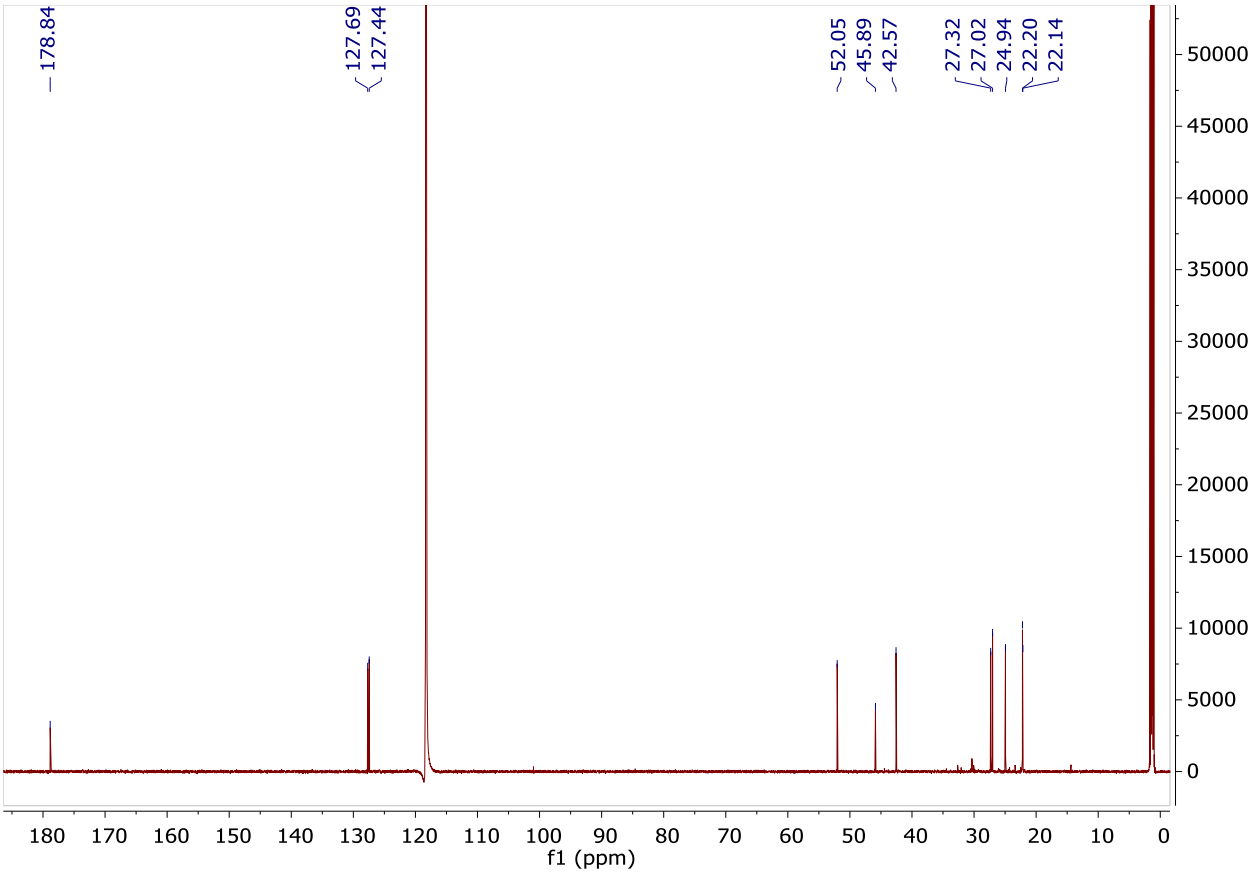

^{1}H NMR Spectrum of 25

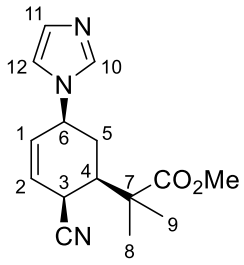

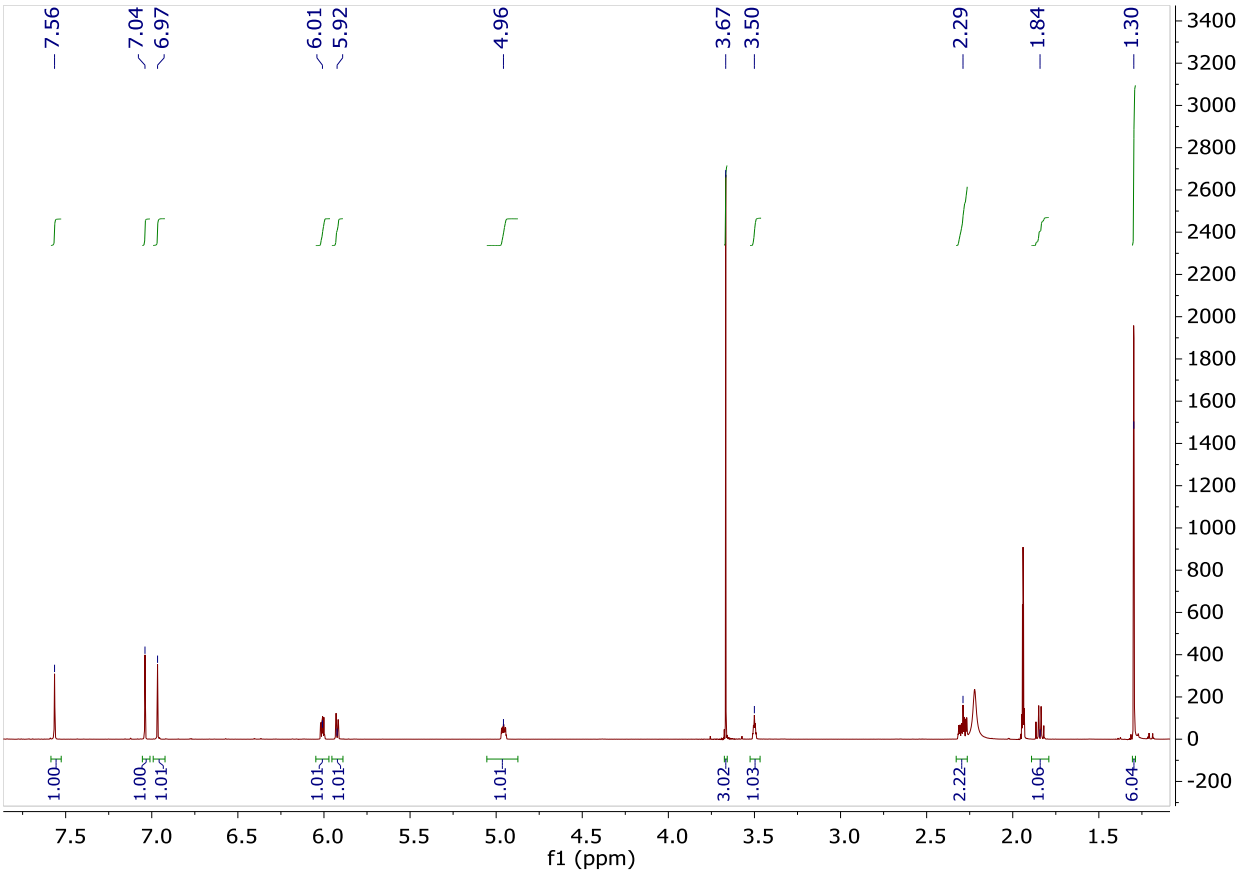

^{13}C {^{1}H} NMR Spectrum of 25

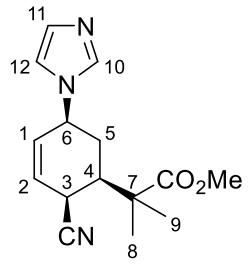

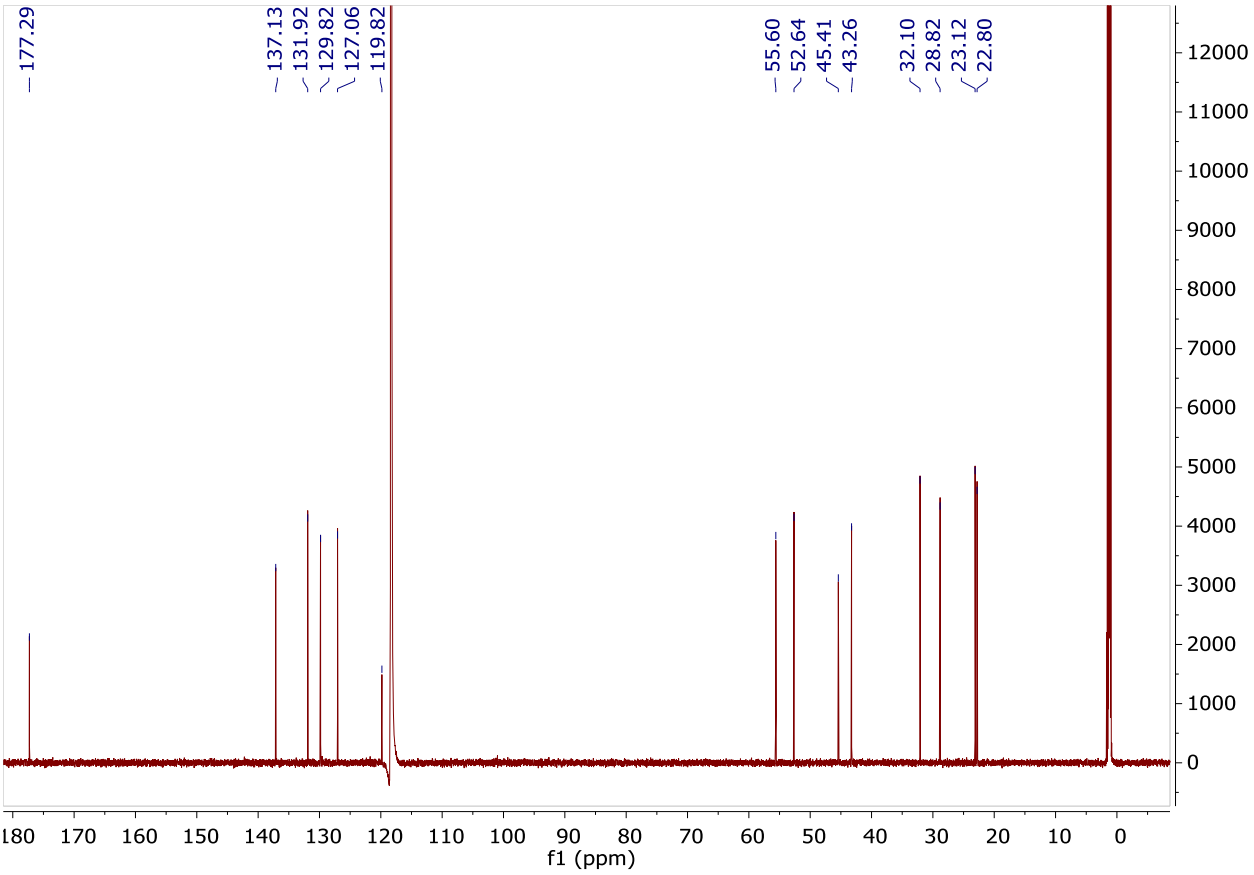

^{1}H NMR Spectrum of 27a and 27b

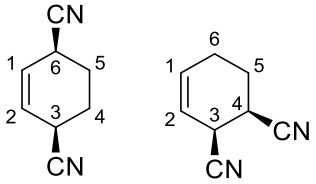

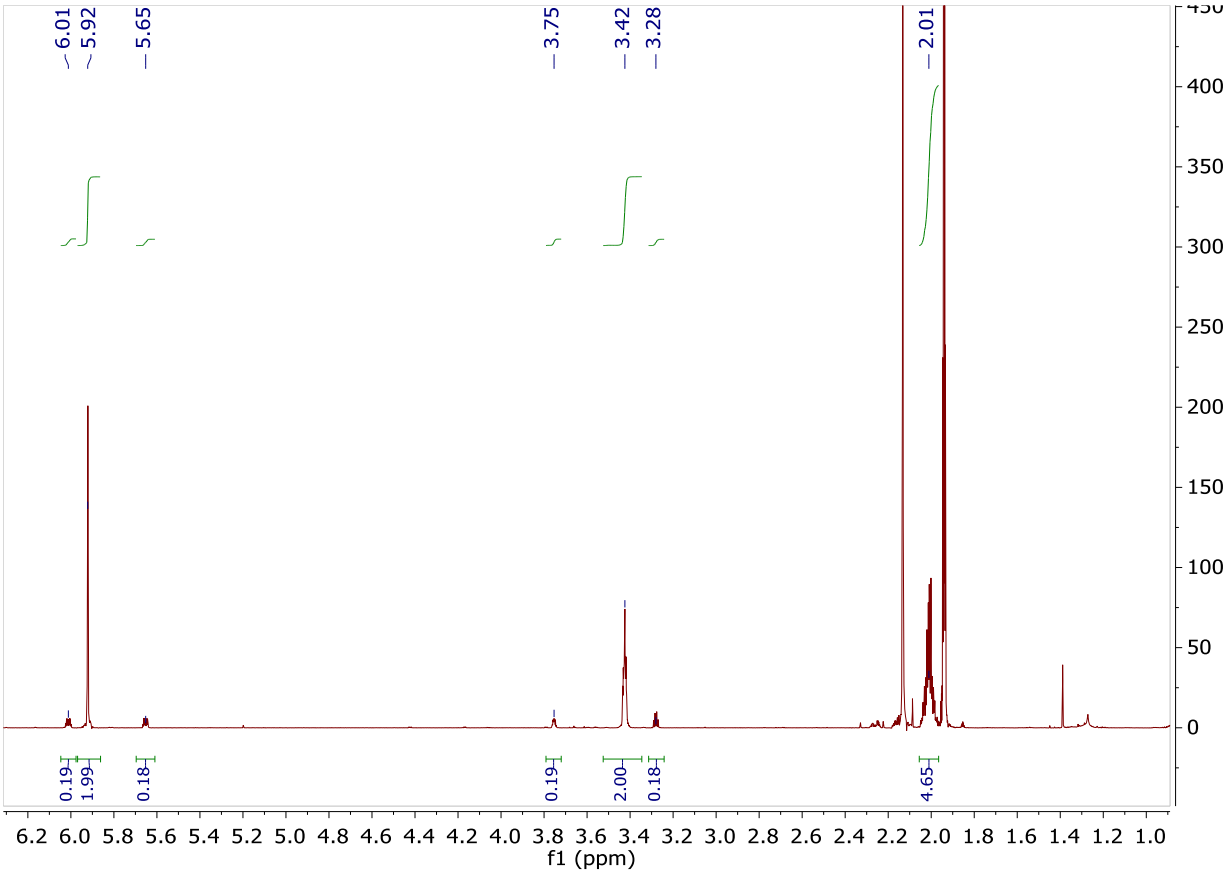

^{13}C {^{1}H} NMR Spectrum of 27a and 27b

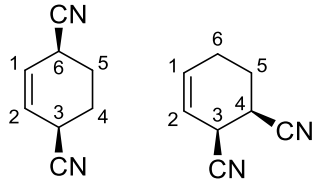

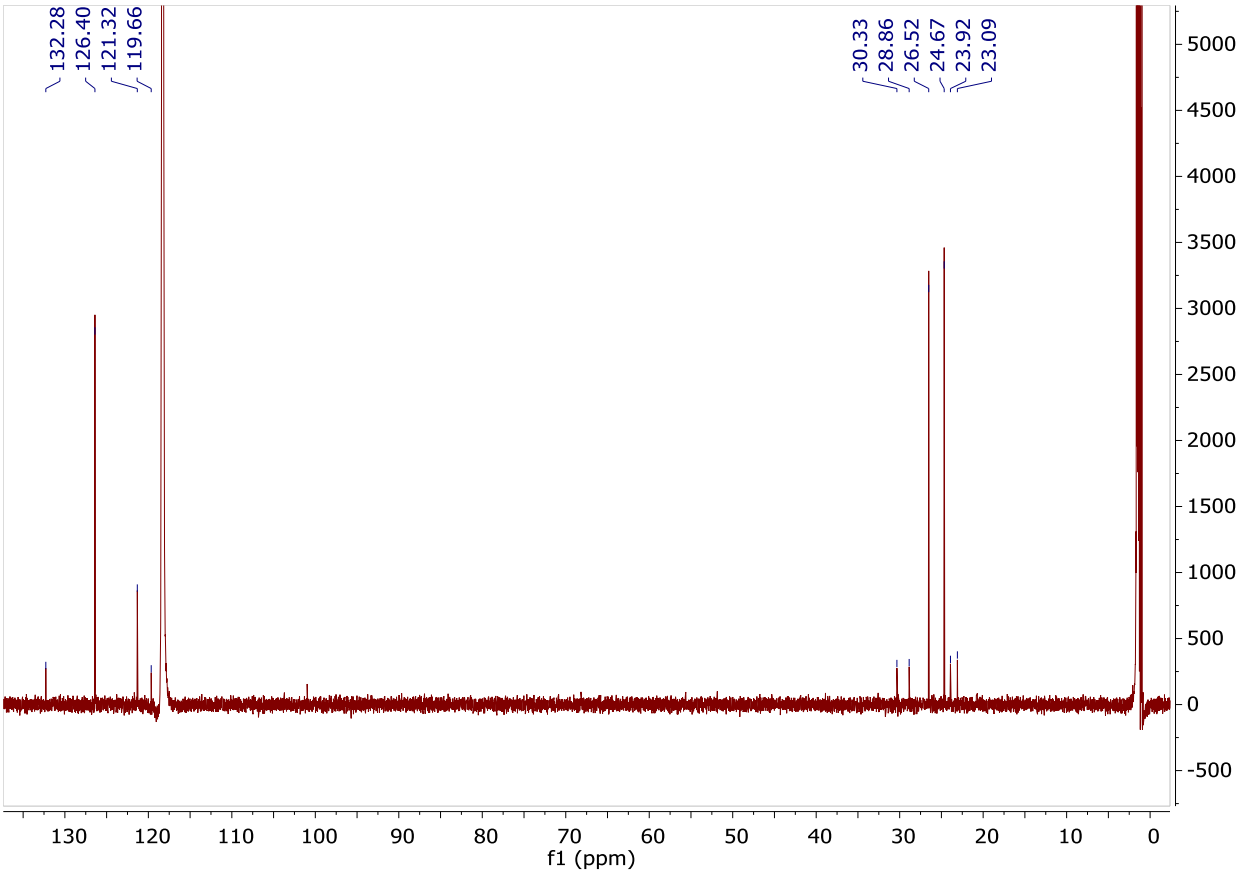

Supporting Crystallographic Data for Chapter 5

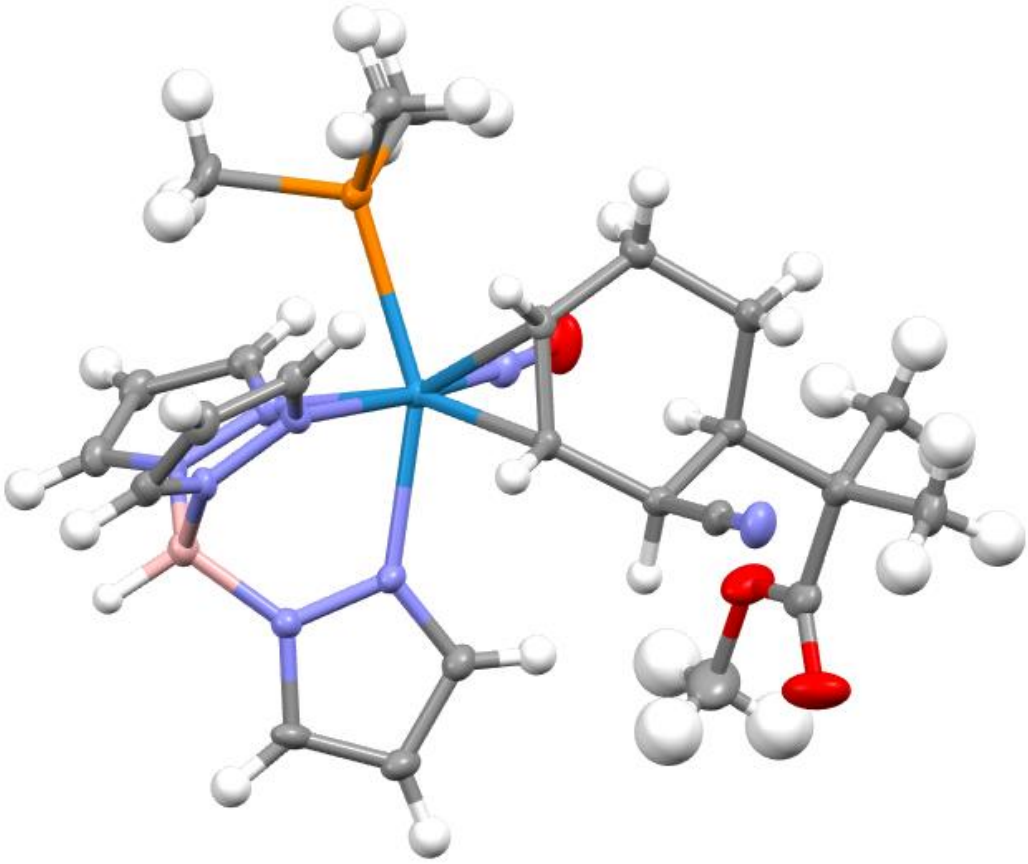

Crystal Structure Report for 47 in Chapter 5

A colorless plate-like specimen of $C_{24}H_{36}BN_8O_3PW$, approximate dimensions 0.054 mm x 0.185 mm x 0.237 mm, was coated with Paratone oil and mounted on a MiTeGen MicroLoop. The X-ray intensity data were measured on a Bruker Kappa APEXII Duo system equipped with a fine-focus sealed tube (Mo K_α, λ = 0.71073 Å) and a graphite monochromator.

The total exposure time was 1.38 hours. The frames were integrated with the Bruker SAINT software package[26] using a narrow-frame algorithm. The integration of the data using a monoclinic unit cell yielded a total of 28679 reflections to a maximum θ angle of 28.32° (0.75 Å resolution), of which 6948 were independent (average redundancy 4.128, completeness = 99.9%, R_{int} = 4.61%, R_{sig} = 4.26%) and 5399 (77.71%) were greater than $2\sigma(F^2)$. The final cell constants of a = 14.4797(10) Å, b = 11.8548(8) Å, c = 16.3796(12) Å, β = 95.918(2)°, volume = 2796.6(3) $Å^3$, are based upon the refinement of the XYZ-centroids of 8451 reflections above 20 σ(I) with 4.959° < 2θ < 56.48°. Data were corrected for absorption effects using the Multi-Scan method (SADABS).[1] The ratio of minimum to maximum apparent

[26] Bruker (2012). *Saint; SADABS; APEX3*. Bruker AXS Inc., Madison, Wisconsin, USA.

transmission was 0.687. The calculated minimum and maximum transmission coefficients (based on crystal size) are 0.4340 and 0.8040.

The structure was solved and refined using the Bruker SHELXTL Software Package[27] within APEX3 [1] and OLEX2,[28] using the space group P $2_1/c$, with Z = 4 for the formula unit, $C_{24}H_{36}BN_8O_3PW$. Non-hydrogen atoms were refined anisotropically. The B-H hydrogen atom was located in the electron density map and refined isotropcially. All other hydrogen atoms were placed in geometrically calculated positions with U_{iso} = 1.2U_{equiv} of the parent atom (U_{iso} = 1.5U_{equiv} for methyl). The final anisotropic full-matrix least-squares refinement on F^2 with 353 variables converged at R1 = 3.04%, for the observed data and wR2 = 7.12% for all data. The goodness-of-fit was 1.051. The largest peak in the final difference electron density synthesis was 1.524 $e^-/Å^3$ and the largest hole was -1.596 $e^-/Å^3$ with an RMS deviation of 0.147 $e^-/Å^3$. On the basis of the final model, the calculated density was 1.687 g/cm^3 and F(000), 1416 e^-.

Table 1. Sample and crystal data for Harman_SS6_304.

Identification code	Harman_SS6_304	
Chemical formula	$C_{24}H_{36}BN_8O_3PW$	
Formula weight	710.24 g/mol	
Temperature	100(2) K	
Wavelength	0.71073 Å	
Crystal size	0.054 x 0.185 x 0.237 mm	
Crystal habit	colorless plate	
Crystal system	monoclinic	
Space group	P $2_1/c$	
Unit cell dimensions	a = 14.4797(10) Å	α = 90°
	b = 11.8548(8) Å	β = 95.918(2)°
	c = 16.3796(12) Å	γ = 90°
Volume	2796.6(3) $Å^3$	
Z	4	
Density (calculated)	1.687 g/cm^3	
Absorption coefficient	4.229 mm^{-1}	
F(000)	1416	

Table 2. Data collection and structure refinement for Harman_SS6_304.

Diffractometer	Bruker Kappa APEXII Duo
Radiation source	fine-focus sealed tube (Mo K_α, λ = 0.71073 Å)
Theta range for data collection	2.12 to 28.32°
Index ranges	-19<=h<=19, -15<=k<=15, -21<=l<=17
Reflections collected	28679

[27] Sheldrick, G. M. (2015). *Acta Cryst.* A**71**, 3-8.
[28] Dolomanov, O. V.; Bourhis, L. J.; Gildea, R. J.; Howard, J. A. K.; Puschmann, H. *J. Appl. Cryst.* (2009). **42**, 339-341.

Independent reflections	6948 [R(int) = 0.0461]	
Coverage of independent reflections	99.9%	
Absorption correction	Multi-Scan	
Max. and min. transmission	0.8040 and 0.4340	
Structure solution technique	direct methods	
Structure solution program	SHELXT 2018/2 (Sheldrick, 2018)	
Refinement method	Full-matrix least-squares on F^2	
Refinement program	SHELXL-2018/3 (Sheldrick, 2018)	
Function minimized	$\Sigma\ w(F_o^2 - F_c^2)^2$	
Data / restraints / parameters	6948 / 0 / 353	
Goodness-of-fit on F^2	1.051	
Δ/σ_{max}	0.001	
Final R indices	5399 data; I>2σ(I)	R1 = 0.0304, wR2 = 0.0607
	all data	R1 = 0.0534, wR2 = 0.0712
Weighting scheme	$w=1/[\sigma^2(F_o^2)+(0.0262P)^2+6.4638P]$ where $P=(F_o^2+2F_c^2)/3$	
Largest diff. peak and hole	1.524 and -1.596 eÅ^{-3}	
R.M.S. deviation from mean	0.147 eÅ^{-3}	

Table 3. Atomic coordinates and equivalent isotropic atomic displacement parameters (Å^2) for Harman_SS6_304.

U(eq) is defined as one third of the trace of the orthogonalized U_{ij} tensor.

	x/a	y/b	z/c	U(eq)
W1	0.28709(2)	0.63942(2)	0.65399(2)	0.01398(5)
P1	0.24018(8)	0.78008(9)	0.54368(6)	0.0180(2)
O1	0.0913(2)	0.6378(3)	0.6987(2)	0.0354(8)
O2	0.1744(3)	0.2077(3)	0.8013(2)	0.0439(10)
O3	0.0995(3)	0.3704(3)	0.80912(19)	0.0380(9)
N1	0.4307(2)	0.6613(3)	0.6163(2)	0.0166(7)
N2	0.5004(2)	0.7056(3)	0.6694(2)	0.0165(7)
N3	0.3159(2)	0.7952(3)	0.7258(2)	0.0177(7)
N4	0.4034(2)	0.8266(3)	0.7555(2)	0.0172(7)
N5	0.3663(2)	0.5792(3)	0.76891(19)	0.0169(7)
N6	0.4467(2)	0.6322(3)	0.79941(19)	0.0169(7)
N7	0.1727(2)	0.6350(3)	0.6824(2)	0.0204(7)

N8	0.3048(3)	0.1883(3)	0.5641(2)	0.0282(9)
C1	0.4700(3)	0.6357(3)	0.5480(2)	0.0186(8)
C2	0.5644(3)	0.6618(4)	0.5568(3)	0.0239(9)
C3	0.5802(3)	0.7061(3)	0.6347(3)	0.0206(9)
C4	0.2595(3)	0.8779(3)	0.7469(2)	0.0188(8)
C5	0.3105(3)	0.9626(3)	0.7894(3)	0.0230(9)
C6	0.4005(3)	0.9269(3)	0.7941(2)	0.0212(9)
C7	0.3512(3)	0.4975(3)	0.8223(2)	0.0203(9)
C8	0.4225(3)	0.4947(3)	0.8868(2)	0.0224(9)
C9	0.4814(3)	0.5810(4)	0.8702(2)	0.0211(9)
C10	0.2542(3)	0.5246(3)	0.5458(2)	0.0152(8)
C11	0.2989(3)	0.4630(3)	0.6154(2)	0.0155(8)
C12	0.2495(3)	0.3603(3)	0.6484(2)	0.0161(7)
C13	0.1434(3)	0.3735(3)	0.6367(2)	0.0175(8)
C14	0.1145(3)	0.3898(3)	0.5444(3)	0.0210(9)
C15	0.1529(3)	0.5021(4)	0.5147(2)	0.0207(9)
C16	0.2796(3)	0.2605(3)	0.6031(3)	0.0201(9)
C17	0.0866(3)	0.2822(4)	0.6789(3)	0.0210(9)
C18	0.9834(3)	0.3211(4)	0.6716(3)	0.0309(11)
C19	0.0910(4)	0.1632(4)	0.6434(3)	0.0312(11)
C20	0.1247(3)	0.2793(4)	0.7686(3)	0.0247(9)
C21	0.1285(5)	0.3749(5)	0.8955(3)	0.0472(15)
C22	0.2490(3)	0.7481(4)	0.4361(2)	0.0226(9)
C23	0.1228(3)	0.8298(4)	0.5431(3)	0.0240(10)
C24	0.3067(3)	0.9102(4)	0.5537(3)	0.0271(10)
B1	0.4822(3)	0.7378(4)	0.7576(3)	0.0189(9)

Table 4. Bond lengths (Å) for Harman_SS6_304.

W1-N7	1.767(4)	W1-C11	2.197(4)
W1-N3	2.206(3)	W1-N5	2.219(3)
W1-N1	2.244(3)	W1-C10	2.247(4)
W1-P1	2.5006(11)	P1-C23	1.797(4)
P1-C24	1.816(4)	P1-C22	1.819(4)
O1-N7	1.236(4)	O2-C20	1.203(5)
O3-C20	1.337(5)	O3-C21	1.435(6)
N1-C1	1.342(5)	N1-N2	1.367(4)
N2-C3	1.339(5)	N2-B1	1.542(6)
N3-C4	1.344(5)	N3-N4	1.361(5)
N4-C6	1.349(5)	N4-B1	1.551(6)

N5-C7	1.338(5)	N5-N6	1.371(4)
N6-C9	1.359(5)	N6-B1	1.540(6)
N8-C16	1.149(5)	C1-C2	1.394(6)
C1-H1	0.95	C2-C3	1.378(6)
C2-H2	0.95	C3-H3	0.95
C4-C5	1.391(6)	C4-H4	0.95
C5-C6	1.366(6)	C5-H5	0.95
C6-H6	0.95	C7-C8	1.399(6)
C7-H7	0.95	C8-C9	1.377(6)
C8-H8	0.95	C9-H9	0.95
C10-C11	1.449(5)	C10-C15	1.525(5)
C10-H10	1.0	C11-C12	1.539(5)
C11-H11	1.0	C12-C16	1.485(6)
C12-C13	1.537(5)	C12-H12	1.0
C13-C14	1.538(5)	C13-C17	1.563(5)
C13-H13	1.0	C14-C15	1.541(6)
C14-H14A	0.99	C14-H14B	0.99
C15-H15A	0.99	C15-H15B	0.99
C17-C20	1.515(6)	C17-C19	1.529(6)
C17-C18	1.557(6)	C18-H18A	0.98
C18-H18B	0.98	C18-H18C	0.98
C19-H19A	0.98	C19-H19B	0.98
C19-H19C	0.98	C21-H21A	0.98
C21-H21B	0.98	C21-H21C	0.98
C22-H22A	0.98	C22-H22B	0.98
C22-H22C	0.98	C23-H23A	0.98
C23-H23B	0.98	C23-H23C	0.98
C24-H24A	0.98	C24-H24B	0.98
C24-H24C	0.98	B1-H1A	1.08(4)

Table 5. Bond angles (°) for Harman_SS6_304.

N7-W1-C11	98.68(15)	N7-W1-N3	90.88(14)
C11-W1-N3	159.11(14)	N7-W1-N5	100.58(14)
C11-W1-N5	83.62(13)	N3-W1-N5	76.36(12)
N7-W1-N1	174.99(14)	C11-W1-N1	85.92(13)
N3-W1-N1	85.41(12)	N5-W1-N1	81.84(12)
N7-W1-C10	93.51(15)	C11-W1-C10	38.04(14)
N3-W1-C10	160.23(13)	N5-W1-C10	121.55(13)
N1-W1-C10	88.89(13)	N7-W1-P1	91.02(11)

C11-W1-P1	116.76(10)	N3-W1-P1	81.35(9)
N5-W1-P1	154.92(9)	N1-W1-P1	85.10(9)
C10-W1-P1	79.31(10)	C23-P1-C24	102.4(2)
C23-P1-C22	103.0(2)	C24-P1-C22	100.1(2)
C23-P1-W1	114.11(15)	C24-P1-W1	113.50(15)
C22-P1-W1	121.30(14)	C20-O3-C21	116.9(4)
C1-N1-N2	105.6(3)	C1-N1-W1	133.5(3)
N2-N1-W1	120.9(2)	C3-N2-N1	110.1(3)
C3-N2-B1	129.4(4)	N1-N2-B1	120.3(3)
C4-N3-N4	106.1(3)	C4-N3-W1	131.4(3)
N4-N3-W1	122.5(2)	C6-N4-N3	109.6(3)
C6-N4-B1	130.3(4)	N3-N4-B1	118.6(3)
C7-N5-N6	106.5(3)	C7-N5-W1	133.0(3)
N6-N5-W1	120.4(2)	C9-N6-N5	109.4(3)
C9-N6-B1	129.1(4)	N5-N6-B1	121.4(3)
O1-N7-W1	175.8(3)	N1-C1-C2	111.0(4)
N1-C1-H1	124.5	C2-C1-H1	124.5
C3-C2-C1	104.4(4)	C3-C2-H2	127.8
C1-C2-H2	127.8	N2-C3-C2	108.9(4)
N2-C3-H3	125.6	C2-C3-H3	125.6
N3-C4-C5	110.5(4)	N3-C4-H4	124.8
C5-C4-H4	124.8	C6-C5-C4	105.0(4)
C6-C5-H5	127.5	C4-C5-H5	127.5
N4-C6-C5	108.9(4)	N4-C6-H6	125.6
C5-C6-H6	125.6	N5-C7-C8	110.6(4)
N5-C7-H7	124.7	C8-C7-H7	124.7
C9-C8-C7	105.0(4)	C9-C8-H8	127.5
C7-C8-H8	127.5	N6-C9-C8	108.5(4)
N6-C9-H9	125.7	C8-C9-H9	125.7
C11-C10-C15	120.8(3)	C11-C10-W1	69.1(2)
C15-C10-W1	119.2(3)	C11-C10-H10	113.6
C15-C10-H10	113.6	W1-C10-H10	113.6
C10-C11-C12	119.2(3)	C10-C11-W1	72.8(2)
C12-C11-W1	126.8(3)	C10-C11-H11	110.9
C12-C11-H11	110.9	W1-C11-H11	110.9
C16-C12-C13	111.1(3)	C16-C12-C11	106.5(3)
C13-C12-C11	111.7(3)	C16-C12-H12	109.2
C13-C12-H12	109.2	C11-C12-H12	109.2
C12-C13-C14	107.6(3)	C12-C13-C17	116.0(3)

C14-C13-C17	114.8(3)	C12-C13-H13	105.8
C14-C13-H13	105.8	C17-C13-H13	105.8
C13-C14-C15	110.4(3)	C13-C14-H14A	109.6
C15-C14-H14A	109.6	C13-C14-H14B	109.6
C15-C14-H14B	109.6	H14A-C14-H14B	108.1
C10-C15-C14	114.3(3)	C10-C15-H15A	108.7
C14-C15-H15A	108.7	C10-C15-H15B	108.7
C14-C15-H15B	108.7	H15A-C15-H15B	107.6
N8-C16-C12	175.3(4)	C20-C17-C19	108.9(4)
C20-C17-C18	109.4(4)	C19-C17-C18	108.7(4)
C20-C17-C13	106.8(3)	C19-C17-C13	115.2(4)
C18-C17-C13	107.7(3)	C17-C18-H18A	109.5
C17-C18-H18B	109.5	H18A-C18-H18B	109.5
C17-C18-H18C	109.5	H18A-C18-H18C	109.5
H18B-C18-H18C	109.5	C17-C19-H19A	109.5
C17-C19-H19B	109.5	H19A-C19-H19B	109.5
C17-C19-H19C	109.5	H19A-C19-H19C	109.5
H19B-C19-H19C	109.5	O2-C20-O3	122.0(4)
O2-C20-C17	126.1(4)	O3-C20-C17	111.9(4)
O3-C21-H21A	109.5	O3-C21-H21B	109.5
H21A-C21-H21B	109.5	O3-C21-H21C	109.5
H21A-C21-H21C	109.5	H21B-C21-H21C	109.5
P1-C22-H22A	109.5	P1-C22-H22B	109.5
H22A-C22-H22B	109.5	P1-C22-H22C	109.5
H22A-C22-H22C	109.5	H22B-C22-H22C	109.5
P1-C23-H23A	109.5	P1-C23-H23B	109.5
H23A-C23-H23B	109.5	P1-C23-H23C	109.5
H23A-C23-H23C	109.5	H23B-C23-H23C	109.5
P1-C24-H24A	109.5	P1-C24-H24B	109.5
H24A-C24-H24B	109.5	P1-C24-H24C	109.5
H24A-C24-H24C	109.5	H24B-C24-H24C	109.5
N6-B1-N2	108.2(3)	N6-B1-N4	106.4(3)
N2-B1-N4	110.1(3)	N6-B1-H1A	111.(2)
N2-B1-H1A	112.(2)	N4-B1-H1A	109.(2)

Table 6. Torsion angles (°) for Harman_SS6_304.

C1-N1-N2-C3	-0.5(4)	W1-N1-N2-C3	177.4(3)
C1-N1-N2-B1	-175.9(3)	W1-N1-N2-B1	2.1(4)
C4-N3-N4-C6	0.0(4)	W1-N3-N4-C6	177.7(3)

C4-N3-N4-B1	167.2(3)	W1-N3-N4-B1	-15.2(4)
C7-N5-N6-C9	1.4(4)	W1-N5-N6-C9	179.3(3)
C7-N5-N6-B1	-175.1(3)	W1-N5-N6-B1	2.8(5)
N2-N1-C1-C2	0.7(4)	W1-N1-C1-C2	-176.9(3)
N1-C1-C2-C3	-0.6(5)	N1-N2-C3-C2	0.1(5)
B1-N2-C3-C2	175.0(4)	C1-C2-C3-N2	0.3(5)
N4-N3-C4-C5	0.4(4)	W1-N3-C4-C5	-176.9(3)
N3-C4-C5-C6	-0.7(5)	N3-N4-C6-C5	-0.5(5)
B1-N4-C6-C5	-165.6(4)	C4-C5-C6-N4	0.7(5)
N6-N5-C7-C8	-1.5(5)	W1-N5-C7-C8	-178.9(3)
N5-C7-C8-C9	1.0(5)	N5-N6-C9-C8	-0.8(5)
B1-N6-C9-C8	175.3(4)	C7-C8-C9-N6	-0.1(5)
C15-C10-C11-C12	10.7(5)	W1-C10-C11-C12	123.1(3)
C15-C10-C11-W1	-112.4(3)	C10-C11-C12-C16	90.0(4)
W1-C11-C12-C16	179.8(3)	C10-C11-C12-C13	-31.5(5)
W1-C11-C12-C13	58.3(4)	C16-C12-C13-C14	-60.7(4)
C11-C12-C13-C14	58.1(4)	C16-C12-C13-C17	69.5(4)
C11-C12-C13-C17	-171.7(3)	C12-C13-C14-C15	-65.7(4)
C17-C13-C14-C15	163.4(3)	C11-C10-C15-C14	-17.4(5)
W1-C10-C15-C14	-99.2(4)	C13-C14-C15-C10	44.9(5)
C12-C13-C17-C20	53.7(5)	C14-C13-C17-C20	-179.6(4)
C12-C13-C17-C19	-67.3(5)	C14-C13-C17-C19	59.3(5)
C12-C13-C17-C18	171.1(3)	C14-C13-C17-C18	-62.2(5)
C21-O3-C20-O2	-4.8(7)	C21-O3-C20-C17	177.6(4)
C19-C17-C20-O2	20.2(6)	C18-C17-C20-O2	138.8(5)
C13-C17-C20-O2	-104.8(5)	C19-C17-C20-O3	-162.4(4)
C18-C17-C20-O3	-43.7(5)	C13-C17-C20-O3	72.7(4)
C9-N6-B1-N2	123.6(4)	N5-N6-B1-N2	-60.7(5)
C9-N6-B1-N4	-118.1(4)	N5-N6-B1-N4	57.6(4)
C3-N2-B1-N6	-117.3(4)	N1-N2-B1-N6	57.1(5)
C3-N2-B1-N4	126.8(4)	N1-N2-B1-N4	-58.8(5)
C6-N4-B1-N6	113.9(4)	N3-N4-B1-N6	-50.1(4)
C6-N4-B1-N2	-129.0(4)	N3-N4-B1-N2	66.9(4)

Table 7. Anisotropic atomic displacement parameters (Å^2) for Harman_SS6_304.

The anisotropic atomic displacement factor exponent takes the form: $-2\pi^2[h^2 a^{*2} U_{11} + \ldots + 2 h k a^* b^* U_{12}]$

	U_{11}	U_{22}	U_{33}	U_{23}	U_{13}	U_{12}
W1	0.01591(8)	0.01105(8)	0.01495(8)	-0.00073(7)	0.00147(5)	-0.00049(7)
P1	0.0220(6)	0.0139(5)	0.0177(5)	0.0000(4)	0.0009(4)	-0.0017(4)
O1	0.0253(17)	0.0305(18)	0.053(2)	-0.0097(17)	0.0192(15)	-0.0015(16)
O2	0.044(2)	0.055(2)	0.0324(19)	0.0113(18)	0.0019(16)	0.022(2)
O3	0.065(3)	0.0269(18)	0.0210(16)	0.0011(14)	-0.0001(16)	0.0027(18)
N1	0.0165(17)	0.0168(17)	0.0162(16)	-0.0007(13)	0.0004(13)	-0.0014(13)
N2	0.0158(17)	0.0132(16)	0.0200(17)	-0.0007(13)	-0.0009(13)	-0.0027(14)
N3	0.0189(18)	0.0135(16)	0.0210(17)	-0.0017(13)	0.0036(14)	-0.0011(14)
N4	0.0168(17)	0.0160(16)	0.0179(17)	-0.0018(13)	-0.0022(13)	-0.0071(14)
N5	0.0223(18)	0.0130(16)	0.0149(16)	0.0011(13)	-0.0001(13)	-0.0028(14)
N6	0.0194(17)	0.0143(16)	0.0163(16)	0.0001(13)	-0.0015(13)	-0.0008(14)
N7	0.0249(18)	0.0159(16)	0.0205(17)	-0.0026(14)	0.0037(14)	-0.0004(16)
N8	0.031(2)	0.0177(18)	0.036(2)	-0.0024(17)	0.0045(17)	-0.0025(17)
C1	0.020(2)	0.0146(18)	0.021(2)	-0.0016(16)	0.0043(15)	0.0014(18)
C2	0.023(2)	0.021(2)	0.029(2)	-0.0014(17)	0.0088(18)	-0.0001(18)
C3	0.018(2)	0.016(2)	0.028(2)	0.0028(17)	0.0007(17)	0.0003(17)
C4	0.024(2)	0.016(2)	0.0168(19)	0.0006(15)	0.0042(16)	0.0015(17)
C5	0.031(3)	0.0141(19)	0.024(2)	-0.0036(16)	0.0063(18)	0.0013(18)
C6	0.028(2)	0.016(2)	0.020(2)	-0.0044(16)	0.0033(17)	-0.0037(18)
C7	0.027(2)	0.016(2)	0.018(2)	-0.0001(16)	0.0037(17)	-0.0020(17)
C8	0.033(3)	0.017(2)	0.017(2)	0.0023(16)	-0.0004(17)	0.0014(18)
C9	0.028(2)	0.018(2)	0.0147(19)	-0.0010(16)	-0.0062(16)	0.0075(19)

	U_{11}	U_{22}	U_{33}	U_{23}	U_{13}	U_{12}
C10	0.020(2)	0.0143(18)	0.0121(18)	-0.0038(14)	0.0037(15)	-0.0014(16)
C11	0.0155(19)	0.0122(18)	0.0186(19)	-0.0005(15)	0.0004(15)	-0.0002(15)
C12	0.0180(18)	0.0139(18)	0.0162(18)	0.0000(16)	0.0002(14)	0.0026(17)
C13	0.0173(19)	0.016(2)	0.0190(19)	0.0034(15)	0.0005(15)	-0.0010(16)
C14	0.020(2)	0.016(2)	0.026(2)	0.0014(16)	-0.0042(17)	-0.0022(16)
C15	0.021(2)	0.020(2)	0.020(2)	-0.0002(16)	-0.0015(16)	0.0011(18)
C16	0.019(2)	0.016(2)	0.025(2)	0.0027(17)	0.0011(17)	-0.0017(17)
C17	0.021(2)	0.019(2)	0.024(2)	0.0048(17)	0.0022(17)	-0.0030(17)
C18	0.020(2)	0.039(3)	0.033(3)	0.011(2)	0.0006(19)	-0.003(2)
C19	0.034(3)	0.025(2)	0.036(3)	-0.0013(19)	0.007(2)	-0.011(2)
C20	0.022(2)	0.026(2)	0.026(2)	0.0067(18)	0.0041(18)	-0.0028(19)
C21	0.074(4)	0.047(3)	0.021(2)	-0.001(2)	0.004(2)	-0.012(3)
C22	0.028(2)	0.020(2)	0.020(2)	0.0012(16)	0.0008(17)	-0.0001(18)
C23	0.027(2)	0.027(2)	0.016(2)	-0.0035(17)	-0.0062(17)	0.0174(19)
C24	0.038(3)	0.017(2)	0.026(2)	0.0019(18)	0.0030(19)	-0.011(2)
B1	0.021(2)	0.015(2)	0.021(2)	-0.0011(18)	-0.0011(18)	-0.0012(19)

Table 8. Hydrogen atomic coordinates and isotropic atomic displacement parameters (Å^2) for Harman_SS6_304.

	x/a	y/b	z/c	U(eq)
H1	0.4378	0.6039	0.5000	0.022
H2	0.6079	0.6513	0.5179	0.029
H3	0.6382	0.7327	0.6598	0.025
H4	0.1939	0.8784	0.7344	0.023
H5	0.2876	1.0306	0.8106	0.028
H6	0.4526	0.9662	0.8202	0.025
H7	0.2992	0.4482	0.8172	0.024
H8	0.4289	0.4443	0.9321	0.027

H9	0.5370	0.6013	0.9028	0.025
H10	0.2950	0.5366	0.5009	0.018
H11	0.3646	0.4442	0.6068	0.019
H12	0.2702	0.3510	0.7082	0.019
H13	0.1298	0.4468	0.6633	0.021
H14A	0.0459	0.3898	0.5341	0.025
H14B	0.1385	0.3265	0.5134	0.025
H15A	0.1467	0.5022	0.4539	0.025
H15B	0.1145	0.5646	0.5327	0.025
H18A	-0.0197	0.4000	0.6890	0.046
H18B	-0.0514	0.2738	0.7067	0.046
H18C	-0.0436	0.3140	0.6145	0.046
H19A	0.0736	0.1658	0.5840	0.047
H19B	0.0479	0.1140	0.6690	0.047
H19C	0.1543	0.1337	0.6544	0.047
H21A	0.1960	0.3652	0.9047	0.071
H21B	0.0979	0.3145	0.9235	0.071
H21C	0.1114	0.4481	0.9173	0.071
H22A	0.2112	0.6816	0.4201	0.034
H22B	0.3140	0.7328	0.4281	0.034
H22C	0.2267	0.8126	0.4023	0.034
H23A	0.1155	0.8677	0.5952	0.036
H23B	0.0800	0.7657	0.5361	0.036
H23C	0.1090	0.8830	0.4977	0.036
H24A	0.2872	0.9599	0.5073	0.041
H24B	0.3729	0.8930	0.5542	0.041
H24C	0.2957	0.9478	0.6051	0.041
H1A	0.544(3)	0.771(3)	0.792(2)	0.014(11)

DFT Calculations for Chapter 5

Allyl Conformations (DFT Calculations ran by Karl Westendorf and Megan Ericson)

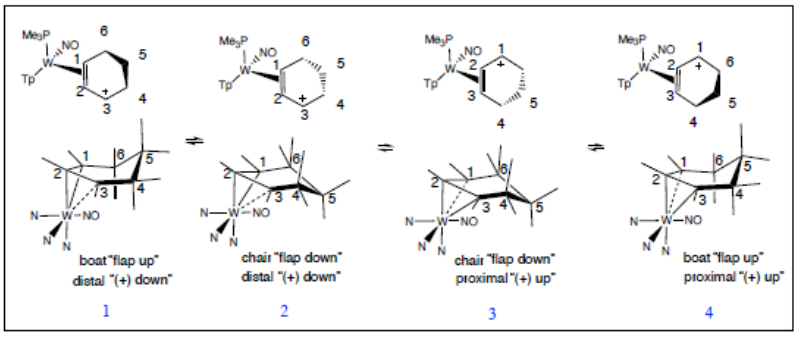

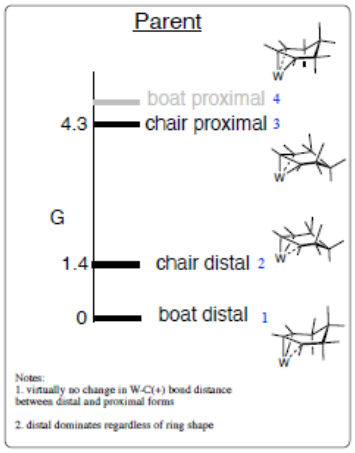

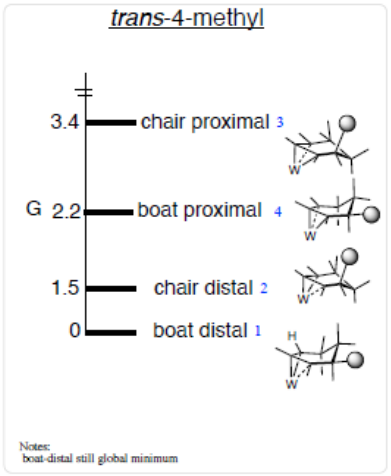

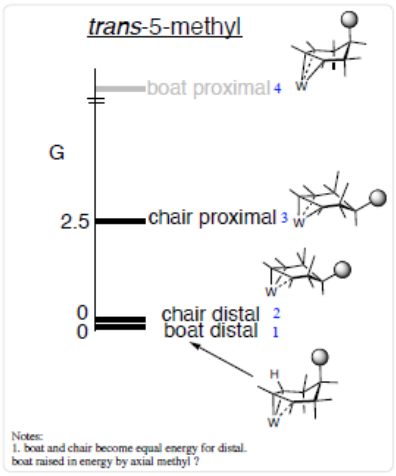

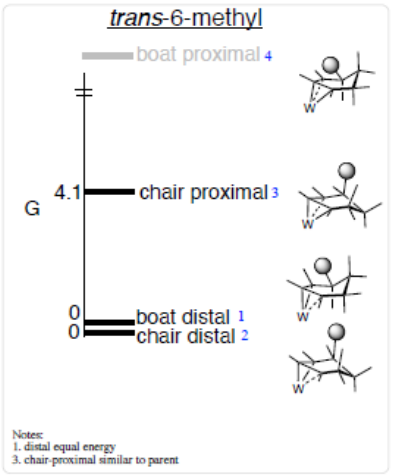

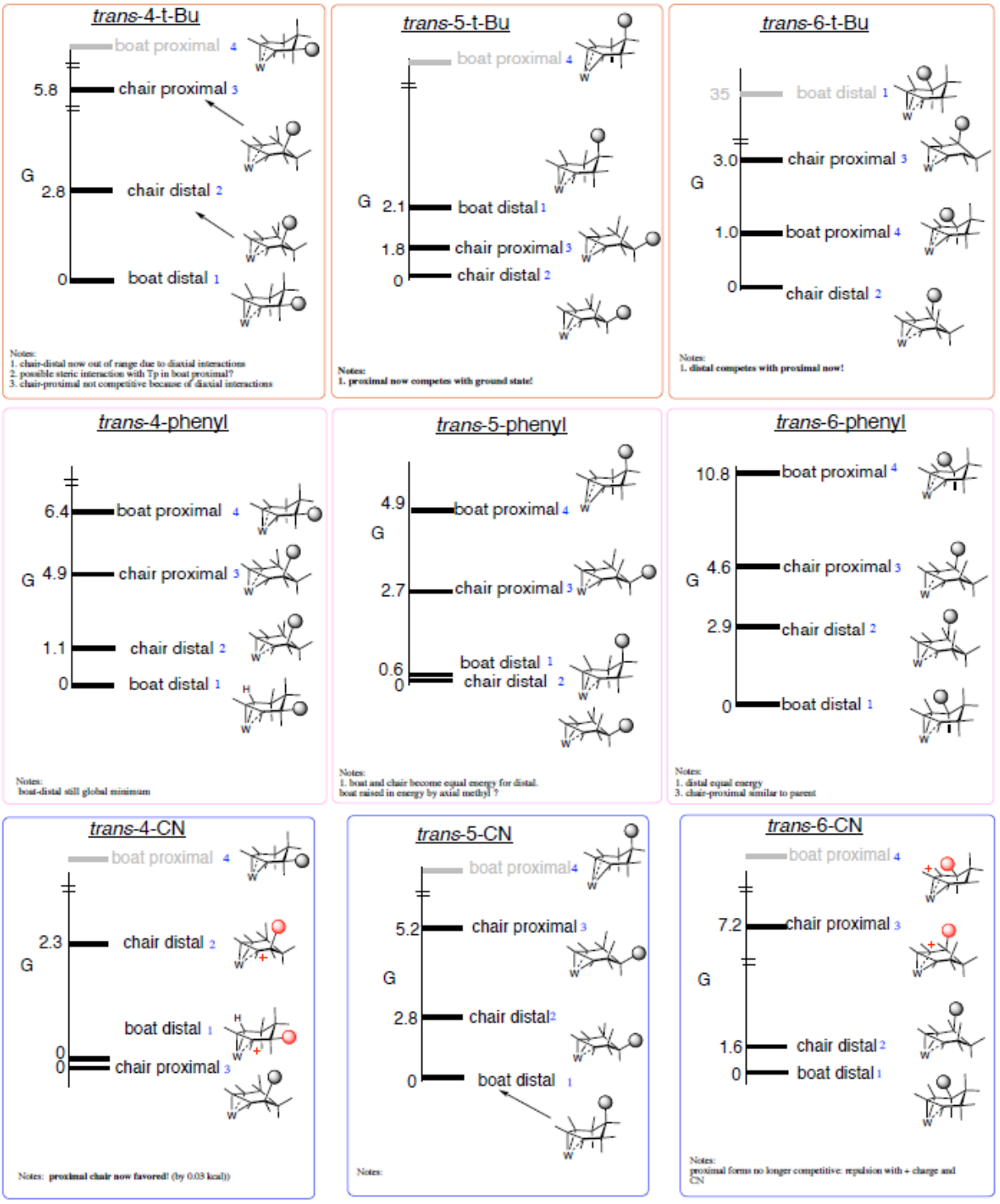
trans-4-t-Bu
boat proximal 4
5.8
chair proximal 3
G
2.8
chair distal 2
0
boat distal 1
Notes:
1. chair-distal now out of range due to diaxial interactions
2. possible steric interaction with Tp in boat proximal?
3. chair-proximal not competitive because of diaxial interactions
trans-5-t-Bu
boat proximal 4
G
2.1
boat distal 1
1.8
chair proximal 3
0
chair distal 2
Notes:
1. proximal now competes with ground state!
trans-6-t-Bu
35
boat distal 1
3.0
chair proximal 3
G
1.0
boat proximal 4
0
chair distal 2
Notes:
1. distal competes with proximal now!
trans-4-phenyl
6.4
boat proximal 4
G
4.9
chair proximal 3
1.1
chair distal 2
0
boat distal 1
Notes:
boat-distal still global minimum
trans-5-phenyl
4.9
boat proximal 4
G
2.7
chair proximal 3
0.6
boat distal 1
0
chair distal 2
Notes:
1. boat and chair become equal energy for distal.
boat raised in energy by axial methyl ?
trans-6-phenyl
10.8
boat proximal 4
4.6
chair proximal 3
G
2.9
chair distal 2
0
boat distal 1
Notes:
1. distal equal energy
3. chair-proximal similar to parent
trans-4-CN
boat proximal 4
2.3
chair distal 2
G
boat distal 1
0
0
chair proximal 3
Notes: proximal chair now favored! (by 0.03 kcal))
trans-5-CN
boat proximal 4
5.2
chair proximal 3
G
2.8
chair distal 2
0
boat distal 1
Notes:
trans-6-CN
boat proximal 4
7.2
chair proximal 3
G
1.6
chair distal 2
0
boat distal 1
Notes:
proximal forms no longer competitive: repulsion with + charge and CN

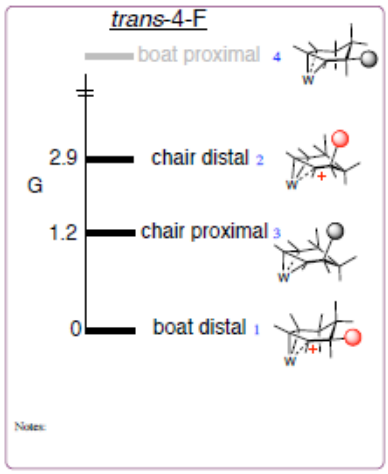
trans-4-F
boat proximal 4
2.9
chair distal 2
G
1.2
chair proximal 3
0
boat distal 1
Notes:

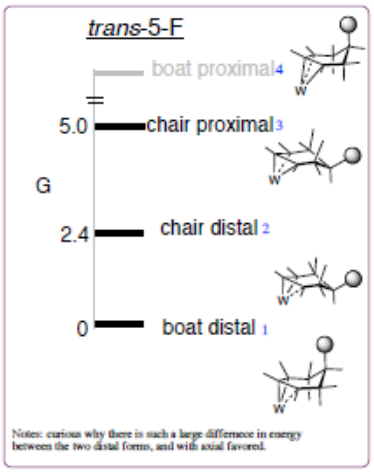
trans-5-F
boat proximal 4
5.0
chair proximal 3
G
2.4
chair distal 2
0
boat distal 1
Notes: curious why there is such a large difference in energy between the two distal forms, and with axial favored.

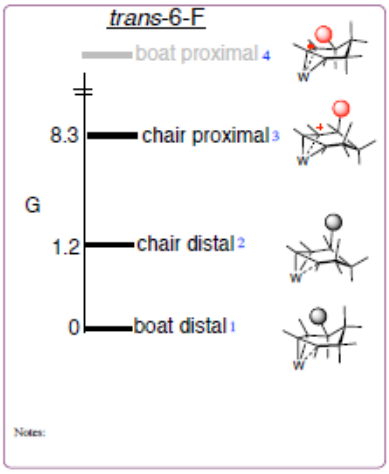
trans-6-F
boat proximal 4
8.3
chair proximal 3
G
1.2
chair distal 2
0
boat distal 1
Notes:

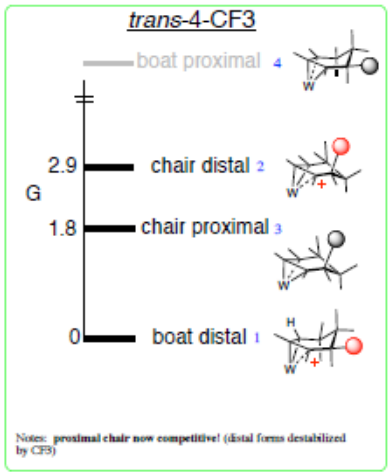
trans-4-CF3
boat proximal 4
2.9
chair distal 2
G
1.8
chair proximal 3
0
boat distal 1
Notes: proximal chair now competitive! (distal forms destabilized by CF3)

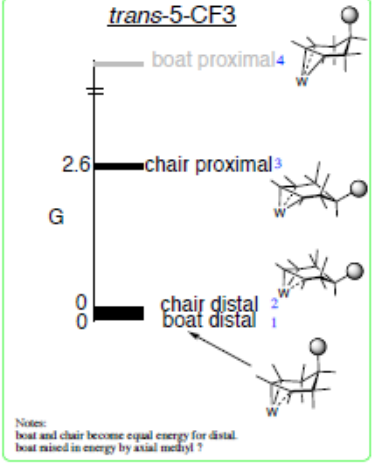
trans-5-CF3
boat proximal 4
2.6
chair proximal 3
G
0
chair distal 2
0
boat distal 1
Notes:
boat and chair become equal energy for distal.
boat raised in energy by axial methyl ?

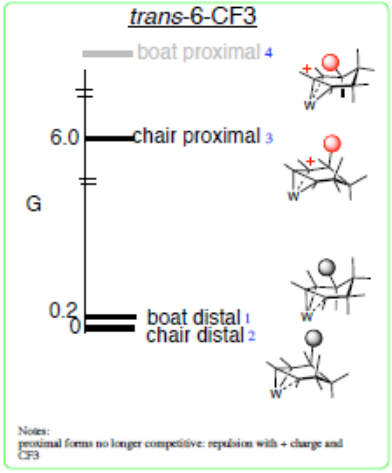
trans-6-CF3
boat proximal 4
6.0
chair proximal 3
G
0.2
boat distal 1
0
chair distal 2
Notes:
proximal forms no longer competitive: repulsion with + charge and CF3

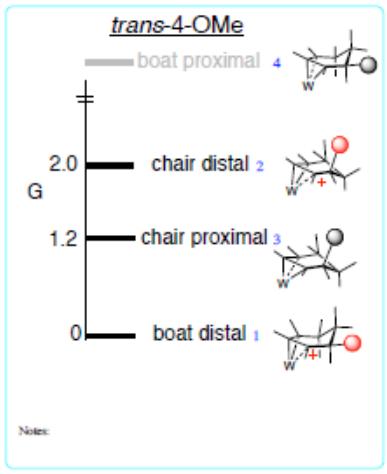
trans-4-OMe
boat proximal 4
2.0
chair distal 2
G
1.2
chair proximal 3
0
boat distal 1
Notes:

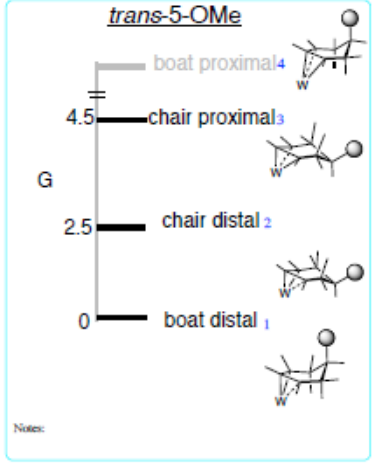
trans-5-OMe
boat proximal 4
4.5
chair proximal 3
G
2.5
chair distal 2
0
boat distal 1
Notes:

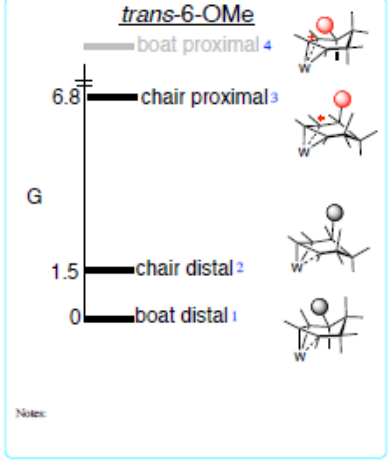
trans-6-OMe
boat proximal 4
6.8
chair proximal 3
G
1.5
chair distal 2
0
boat distal 1
Notes:

DFT Calculations for Scheme 5.1 (4 and 5 are in Chair Conformations)

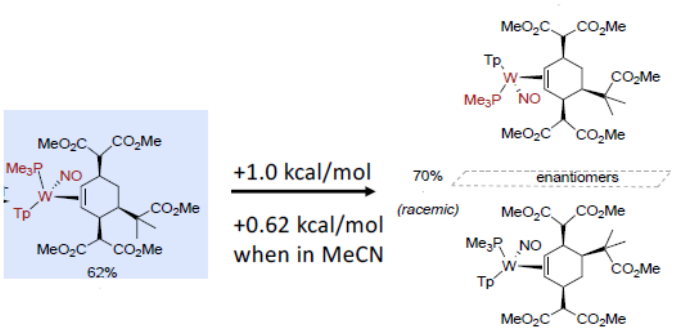

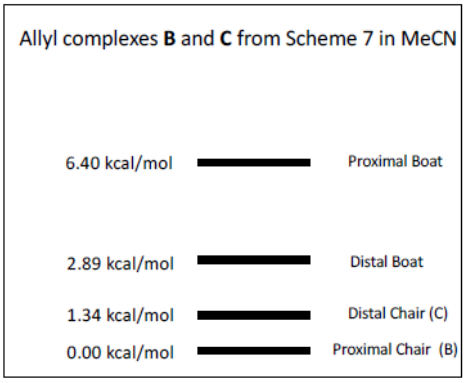

DFT Calculations for Allyl Complexes E and F in MeCN

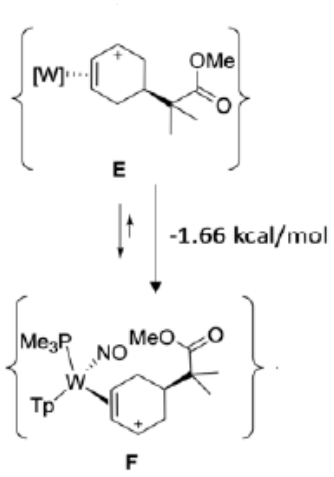

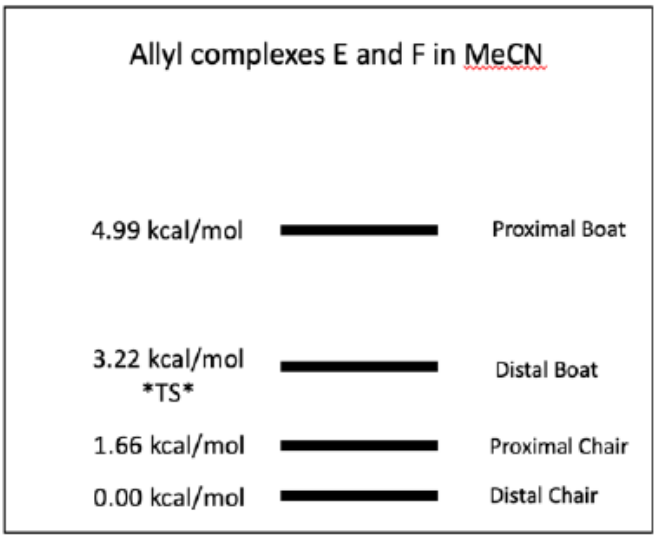

Supporting Information for Chapter 6

^{1}H NMR Spectrum of 3

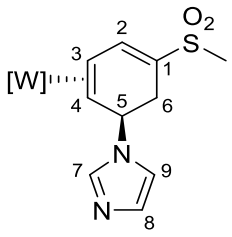

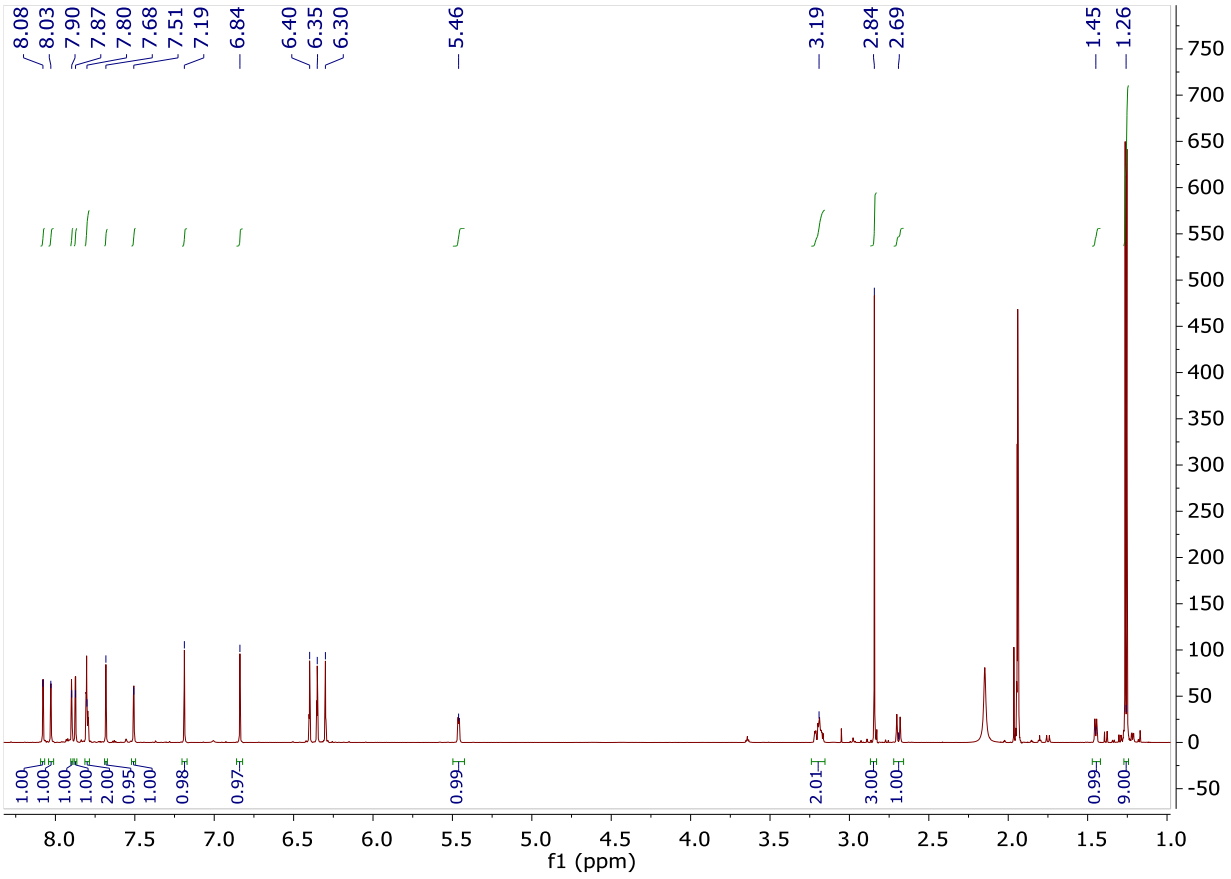

^{13}C {^{1}H} NMR Spectrum of 3

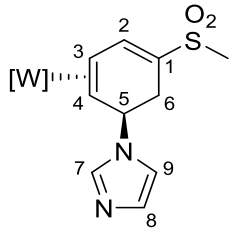

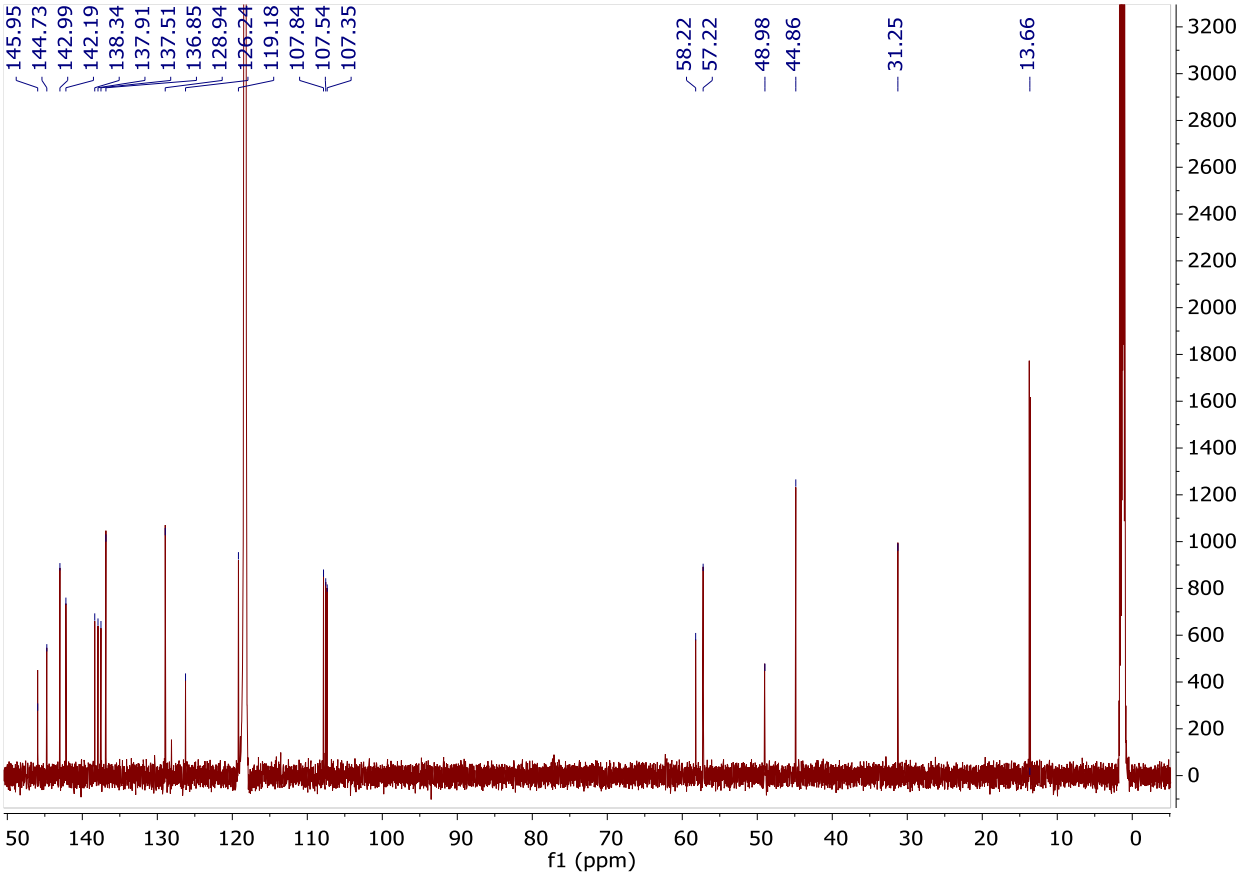

^{1}H NMR Spectrum of 4

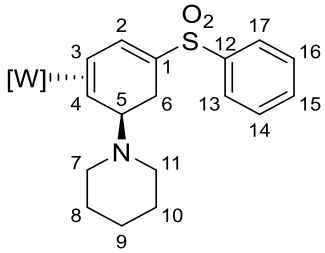

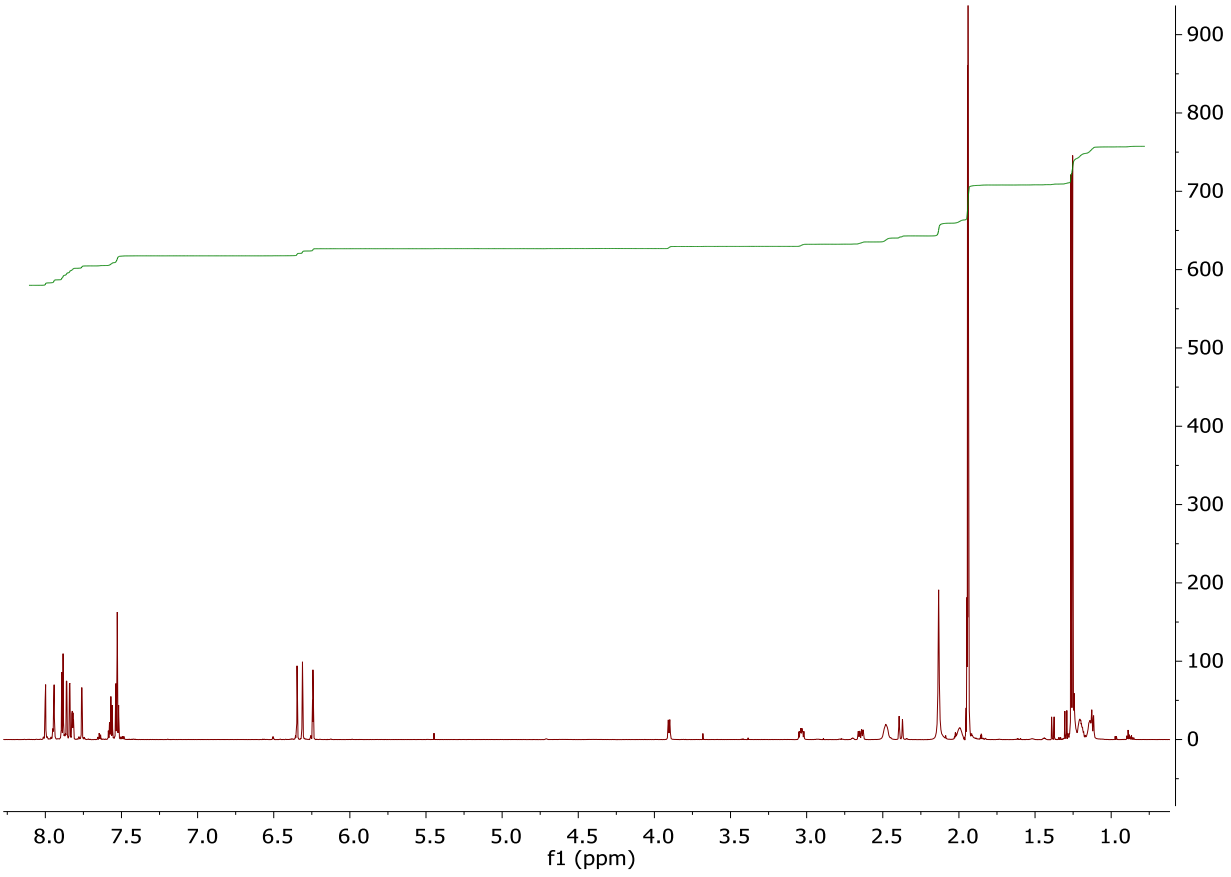

^{13}C {^{1}H} NMR Spectrum of 4

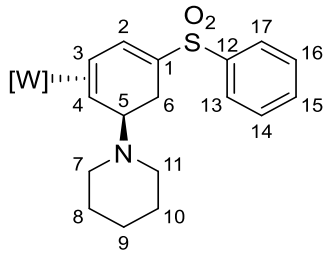

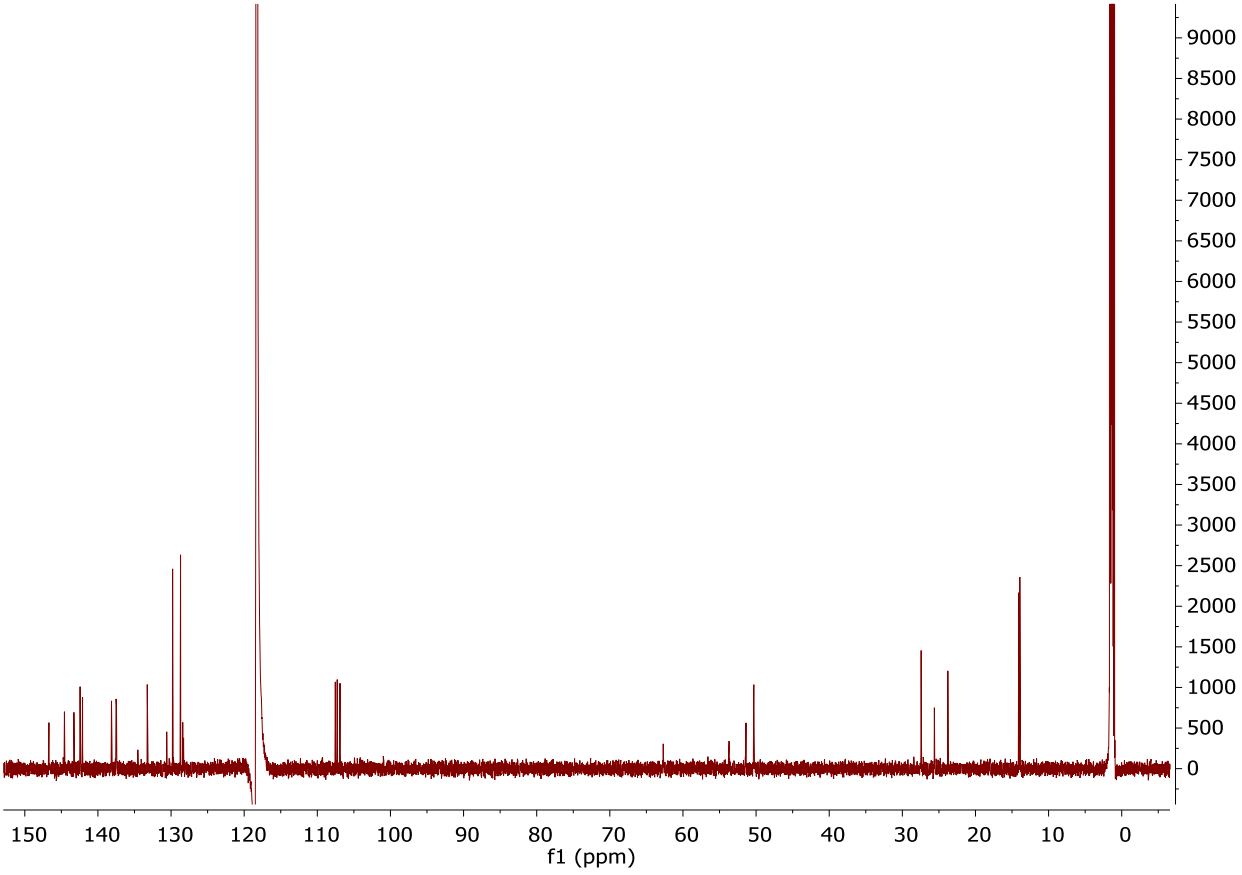

^{1}H NMR Spectrum of 5

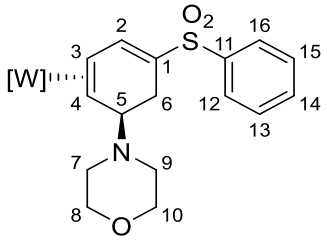

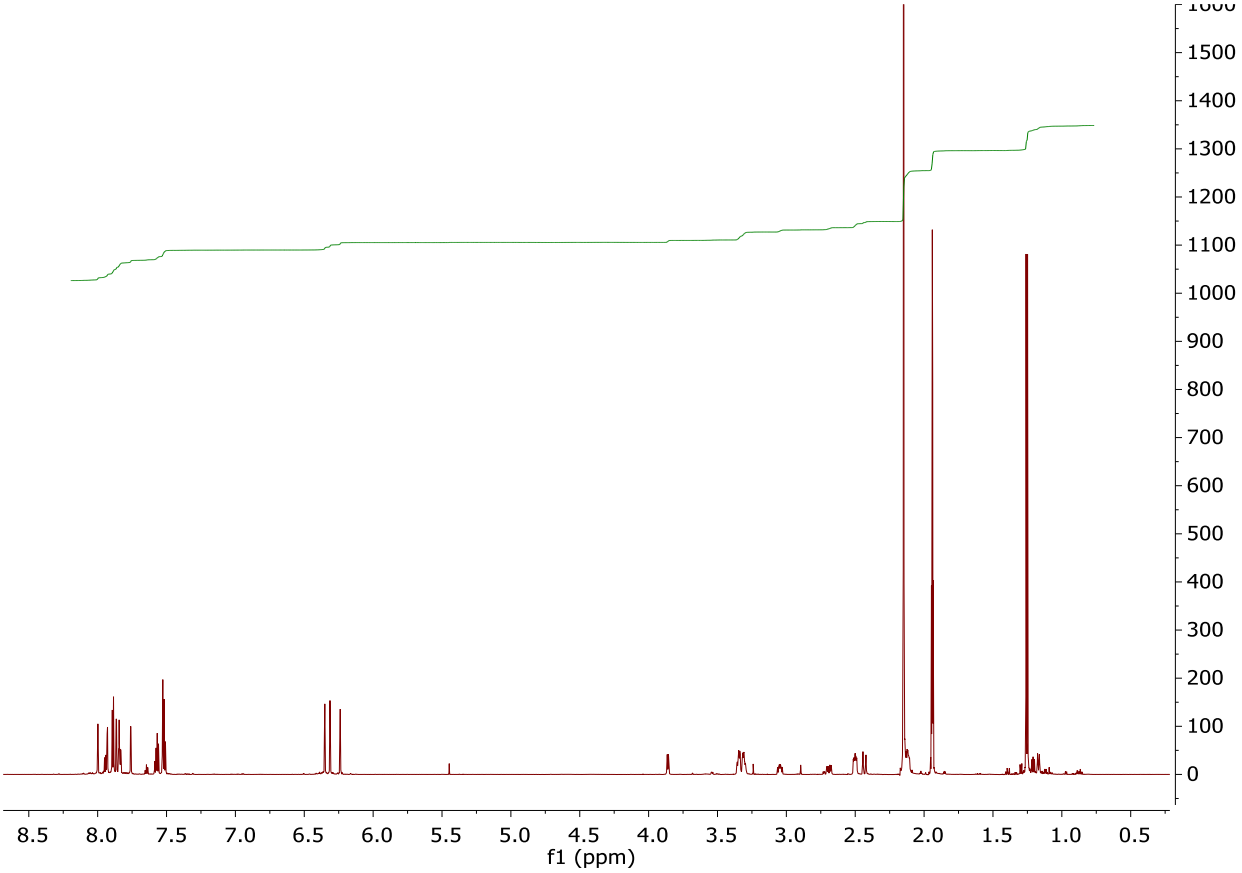

^{13}C {^{1}H} NMR Spectrum of 5

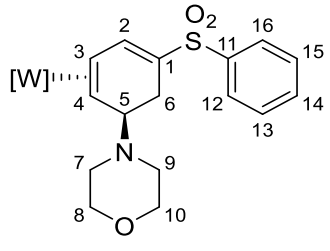

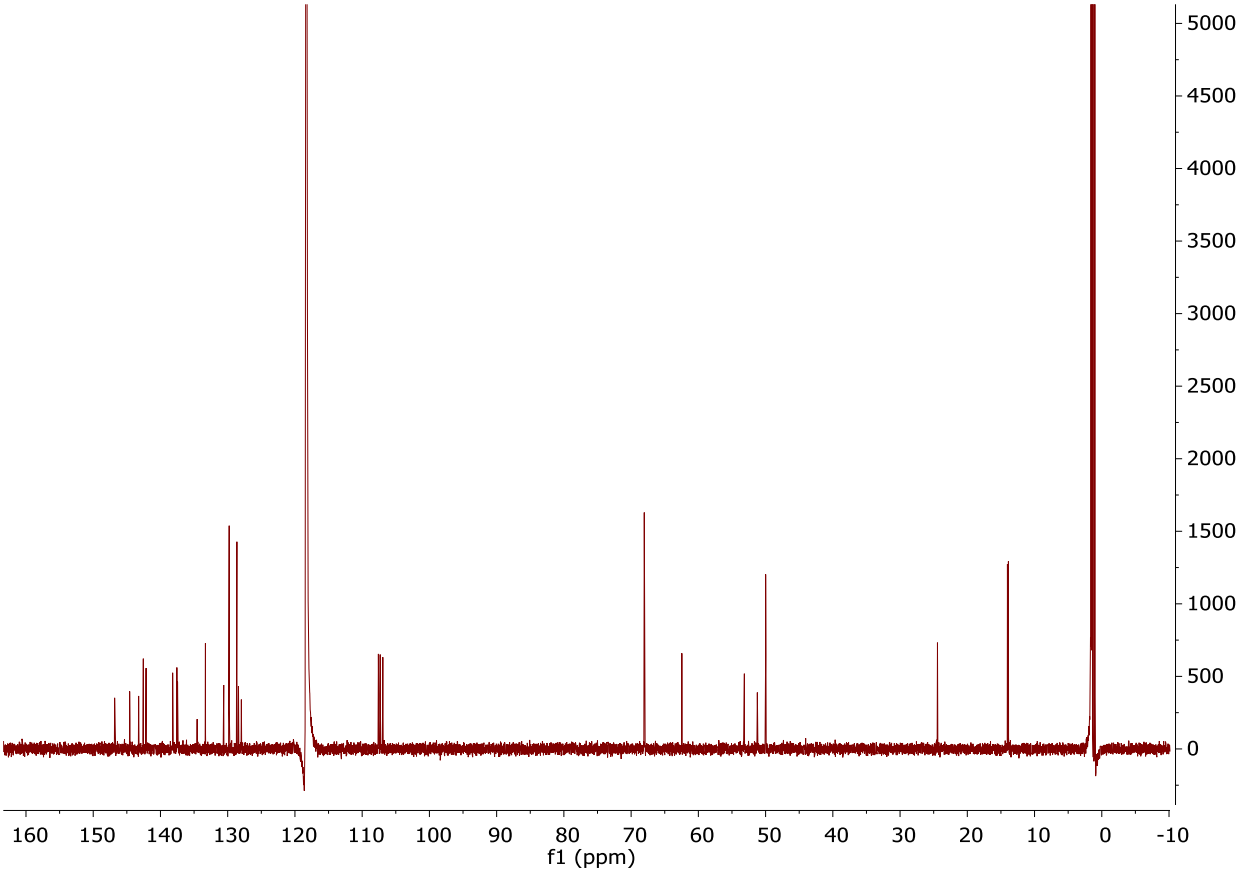

^{1}H NMR Spectrum of 7

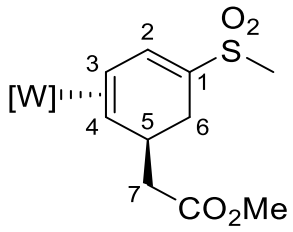

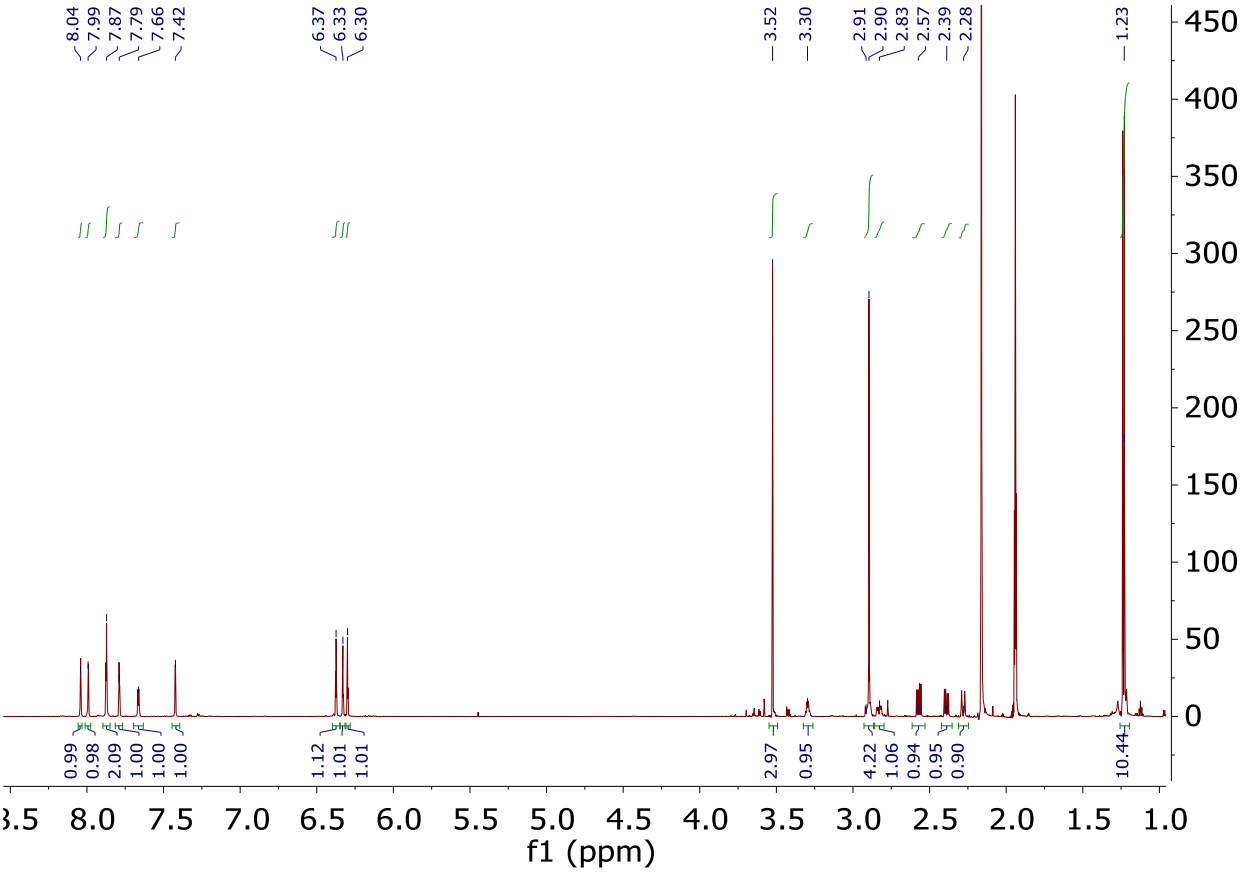

^{13}C {^{1}H} NMR Spectrum of 7

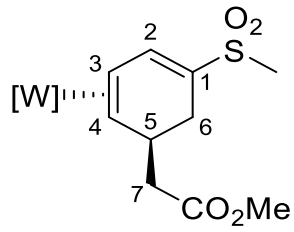

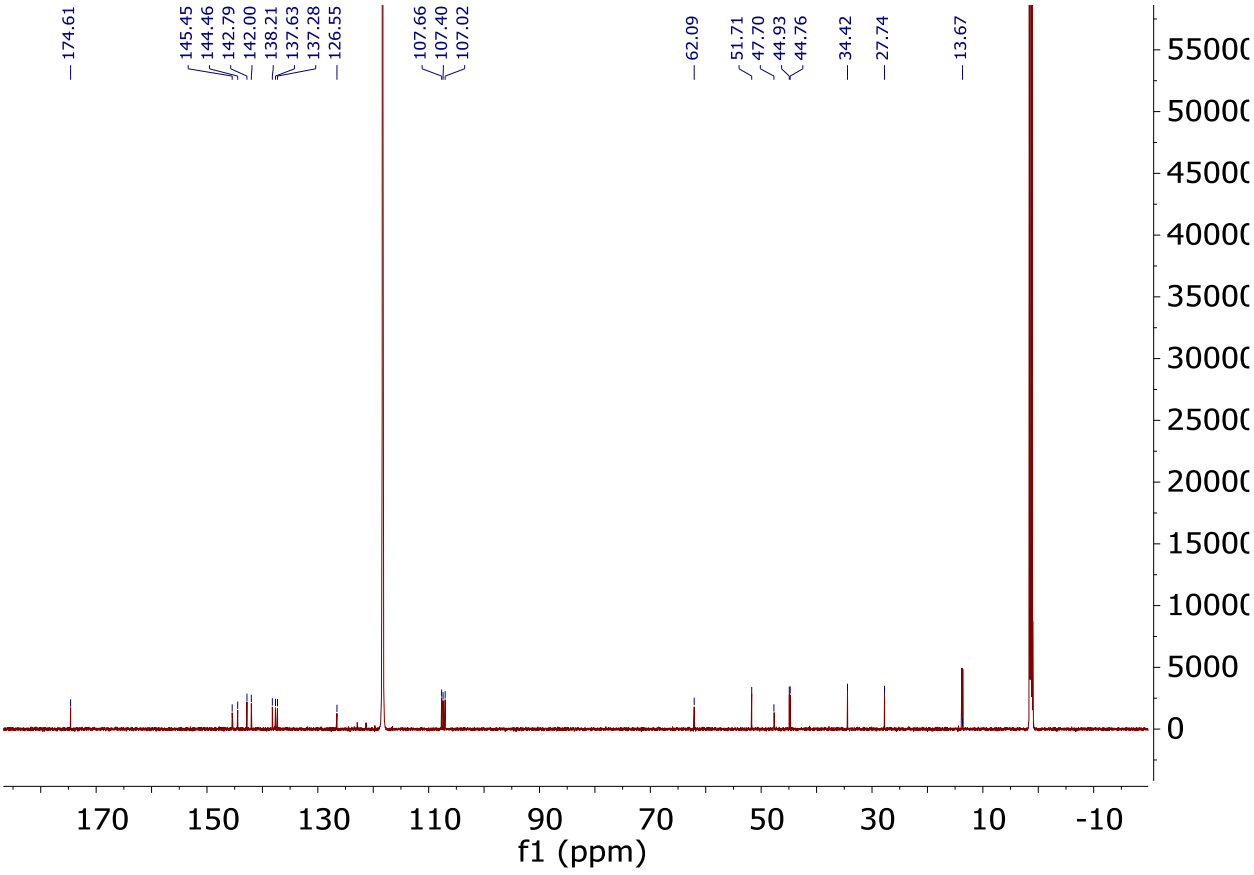

^{1}H NMR Spectrum of 8

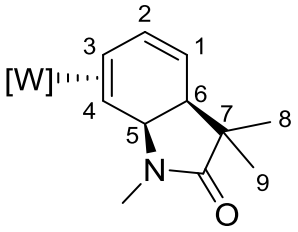

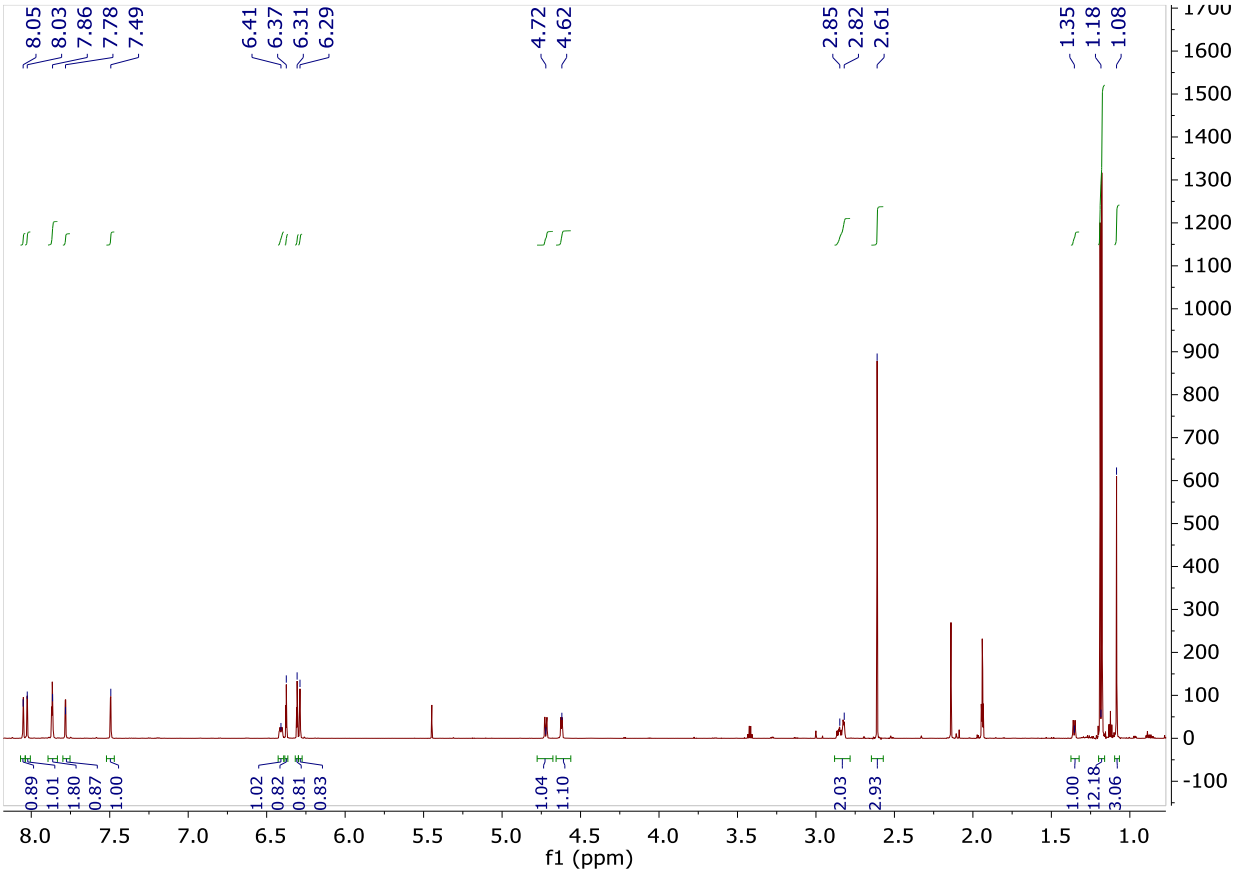

^{1}H NMR Spectrum of 9

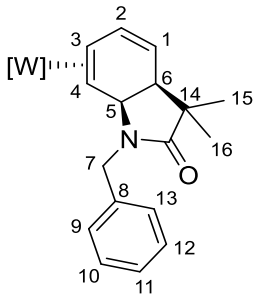

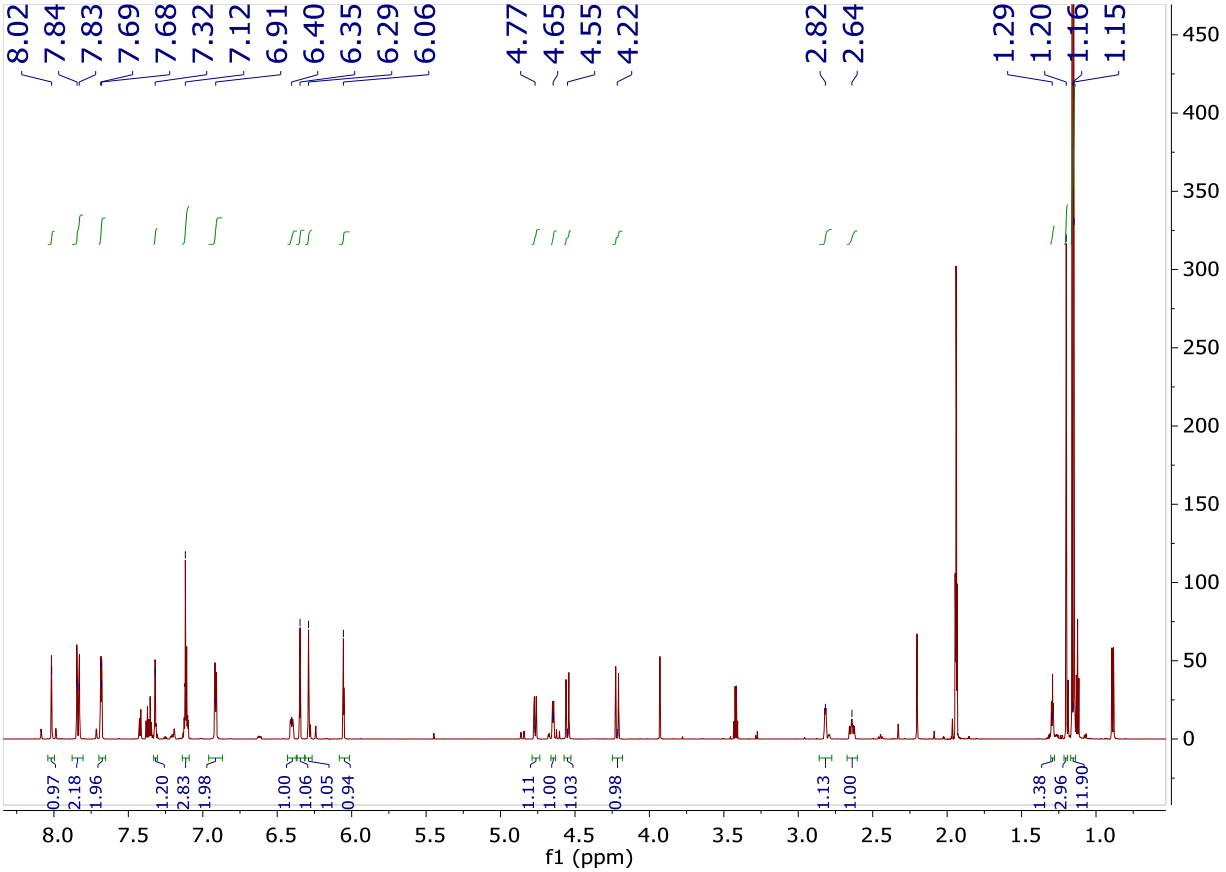

^{13}C {^{1}H} NMR Spectrum of 9

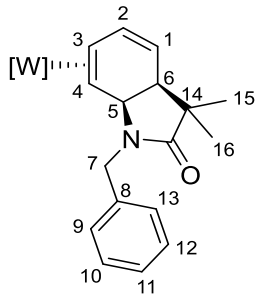

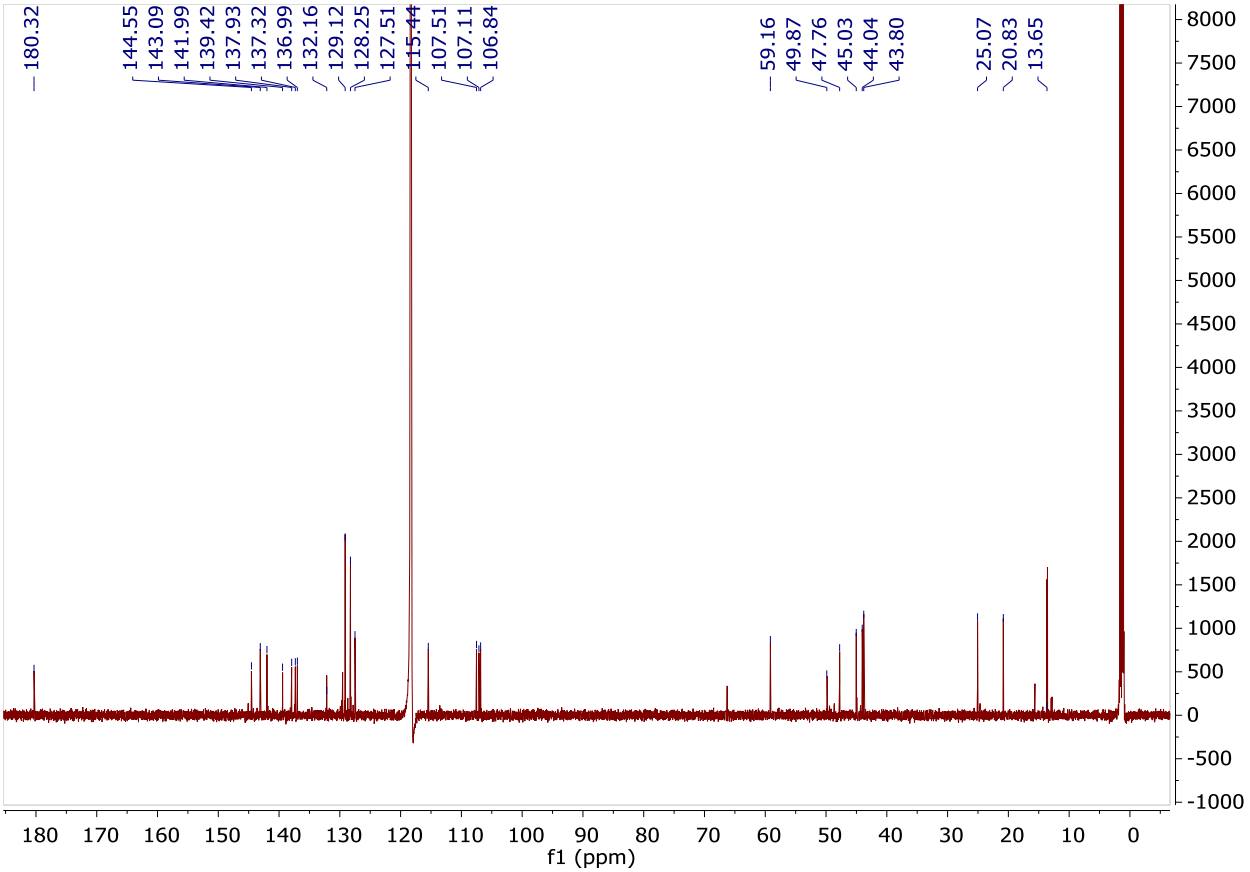

^{1}H NMR Spectrum of 10

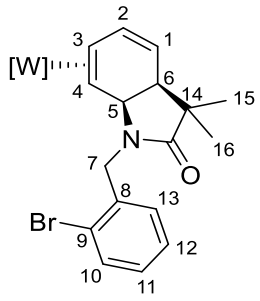

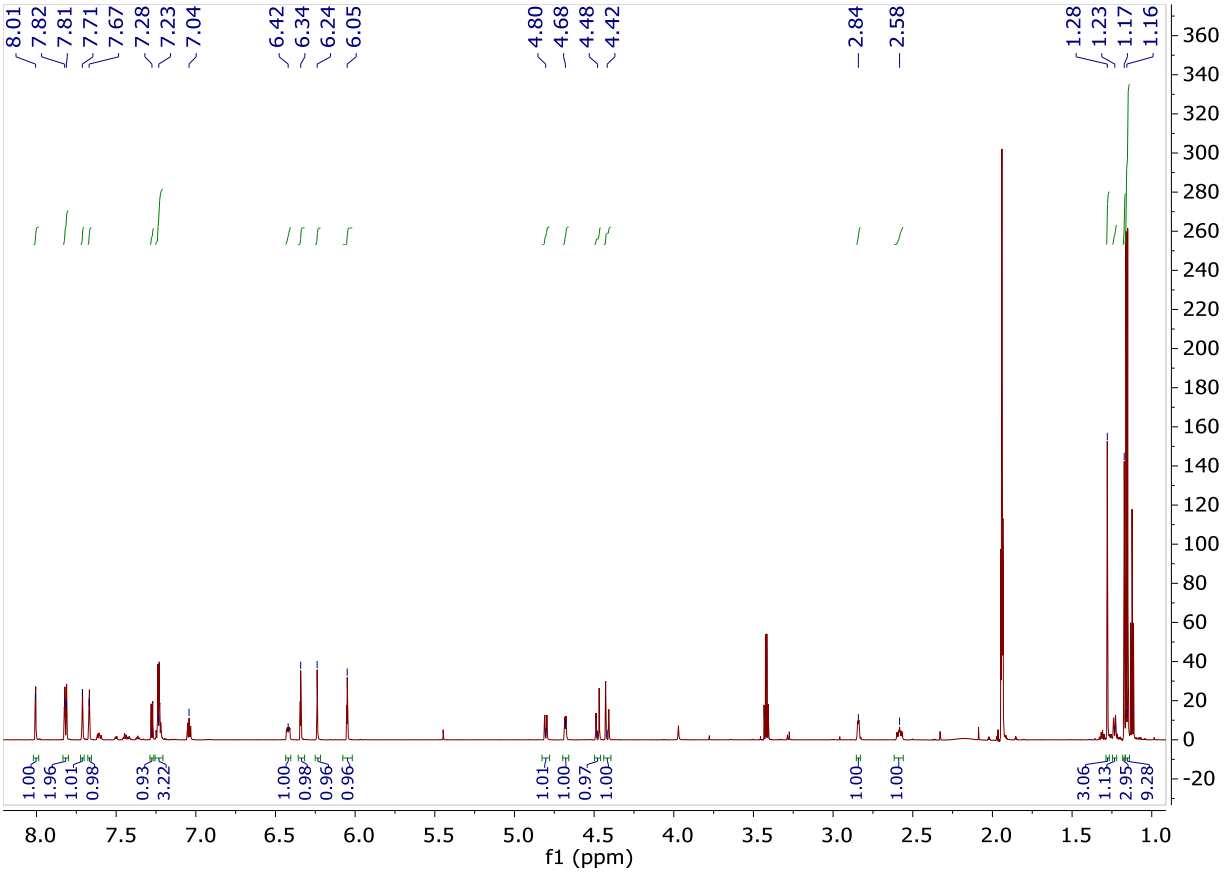

^{13}C {^{1}H} NMR Spectrum of 10

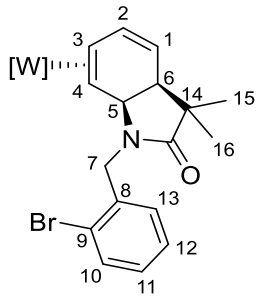

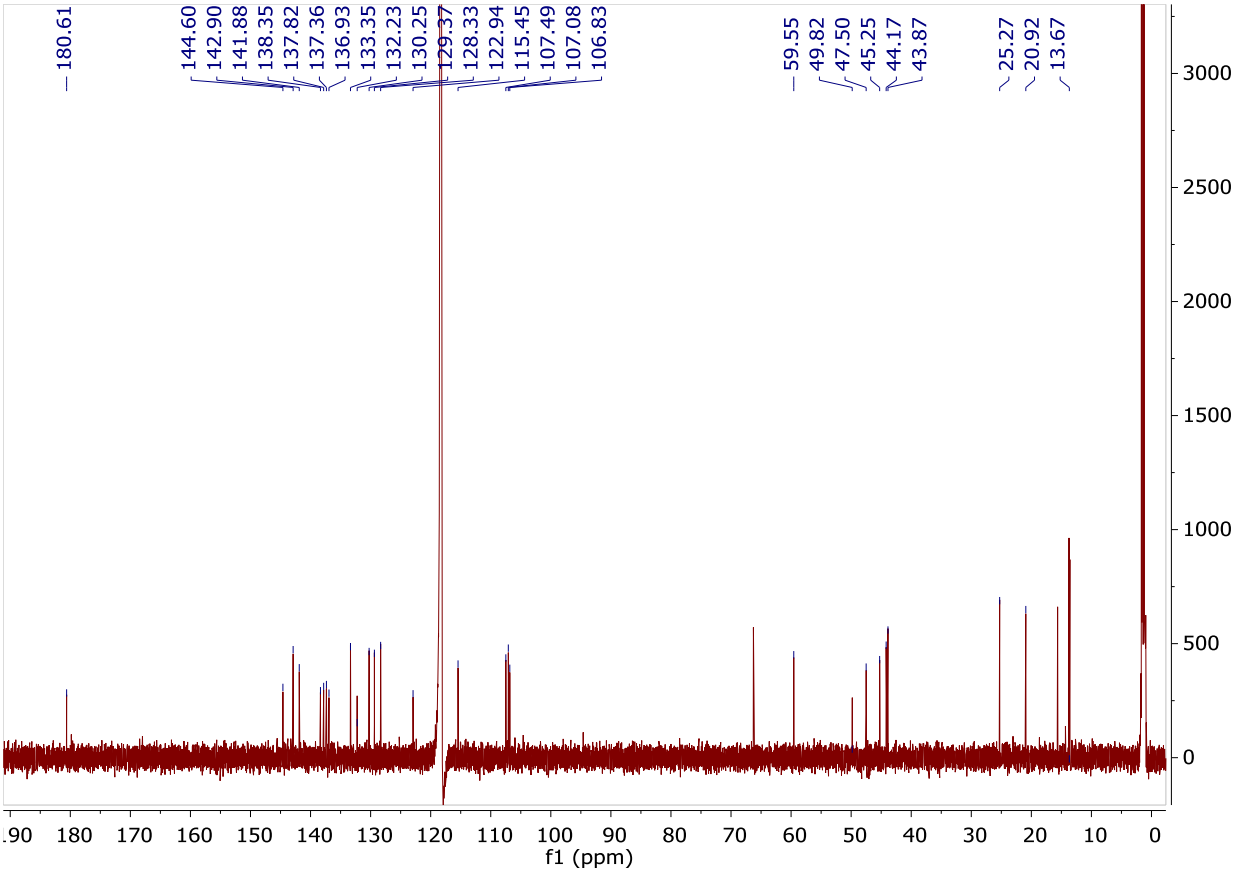

^{1}H NMR Spectrum of 11

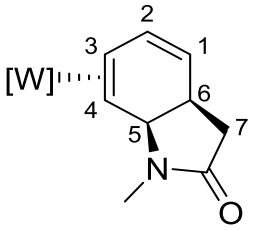

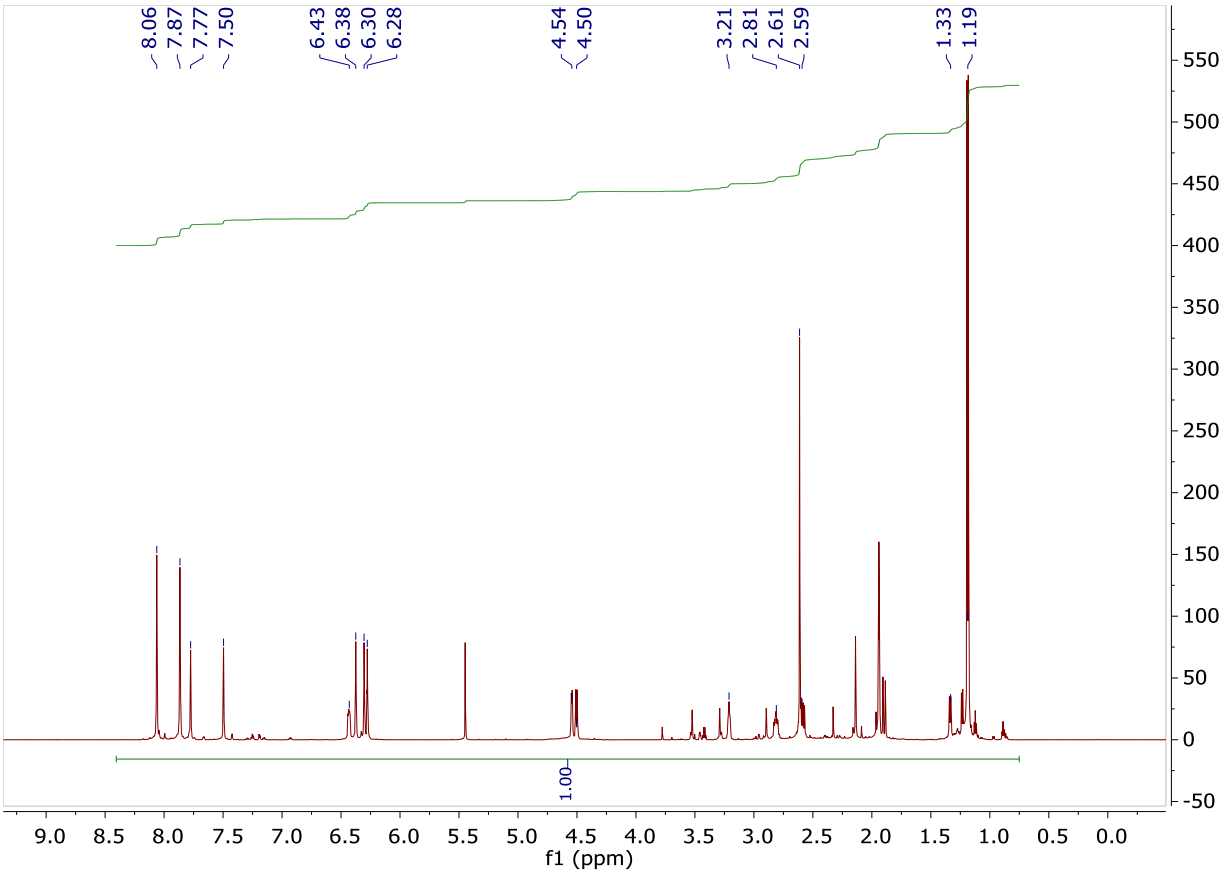

^{13}C {^{1}H} NMR Spectrum of 11

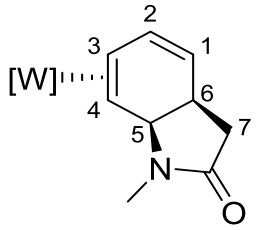

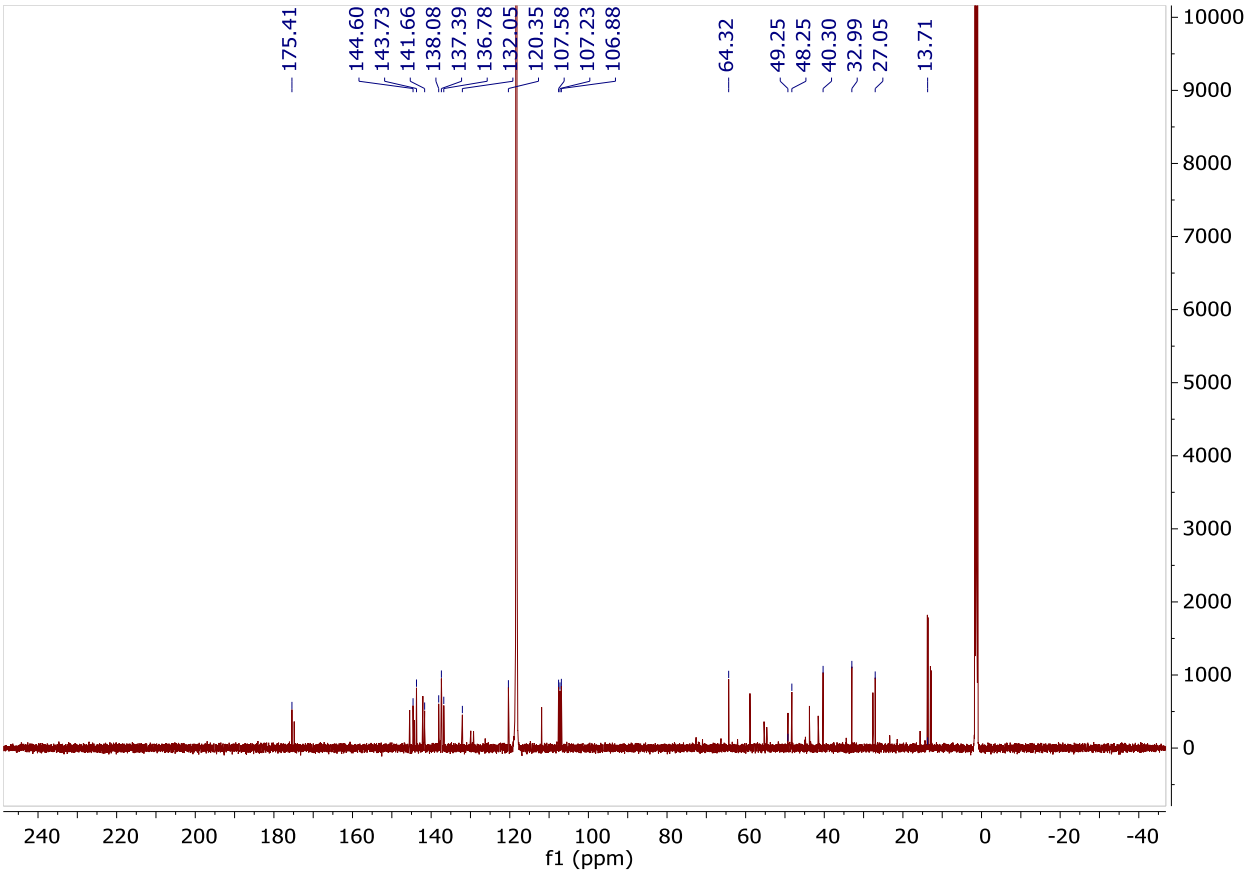

^{1}H NMR Spectrum of 12

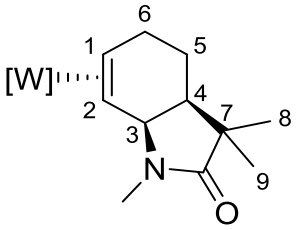

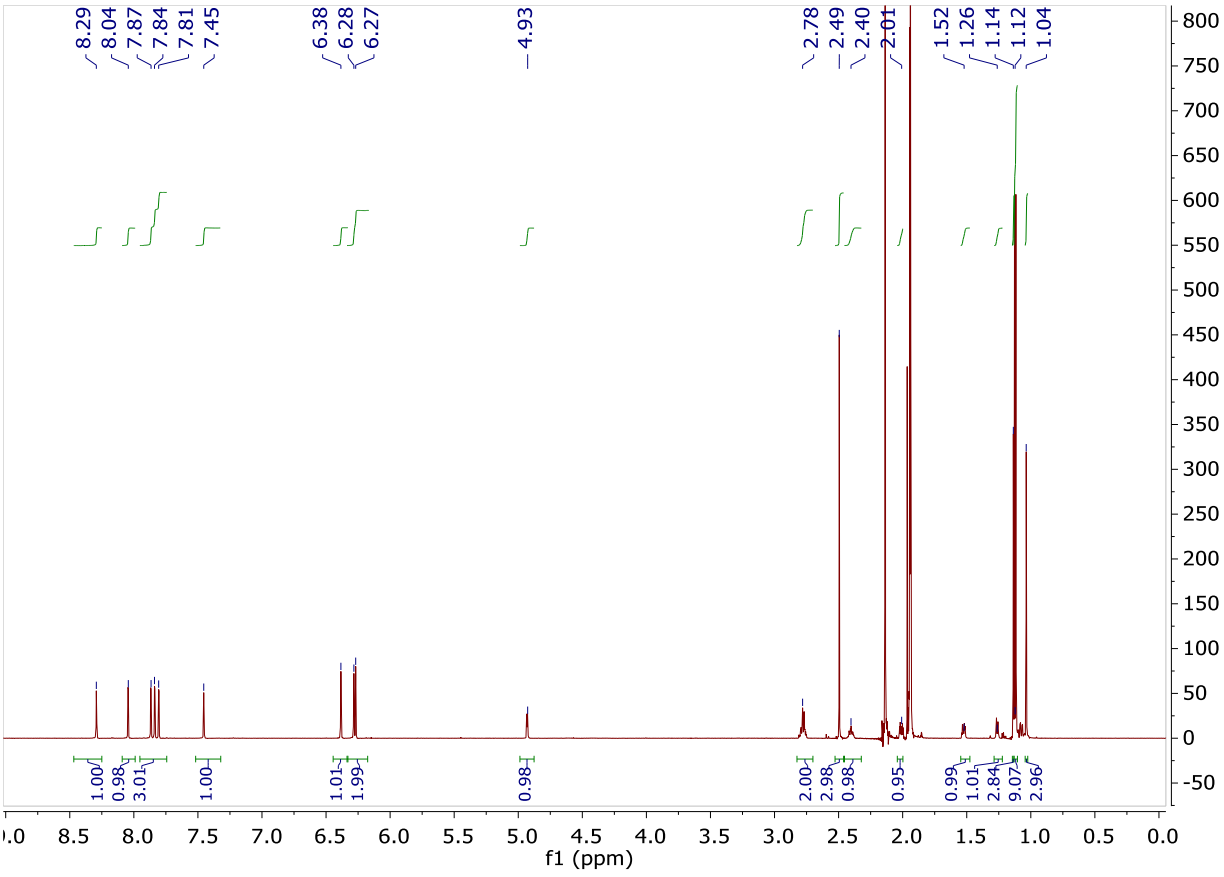

^{1}H NMR Spectrum of 13

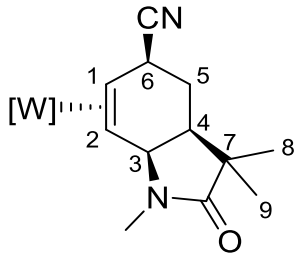

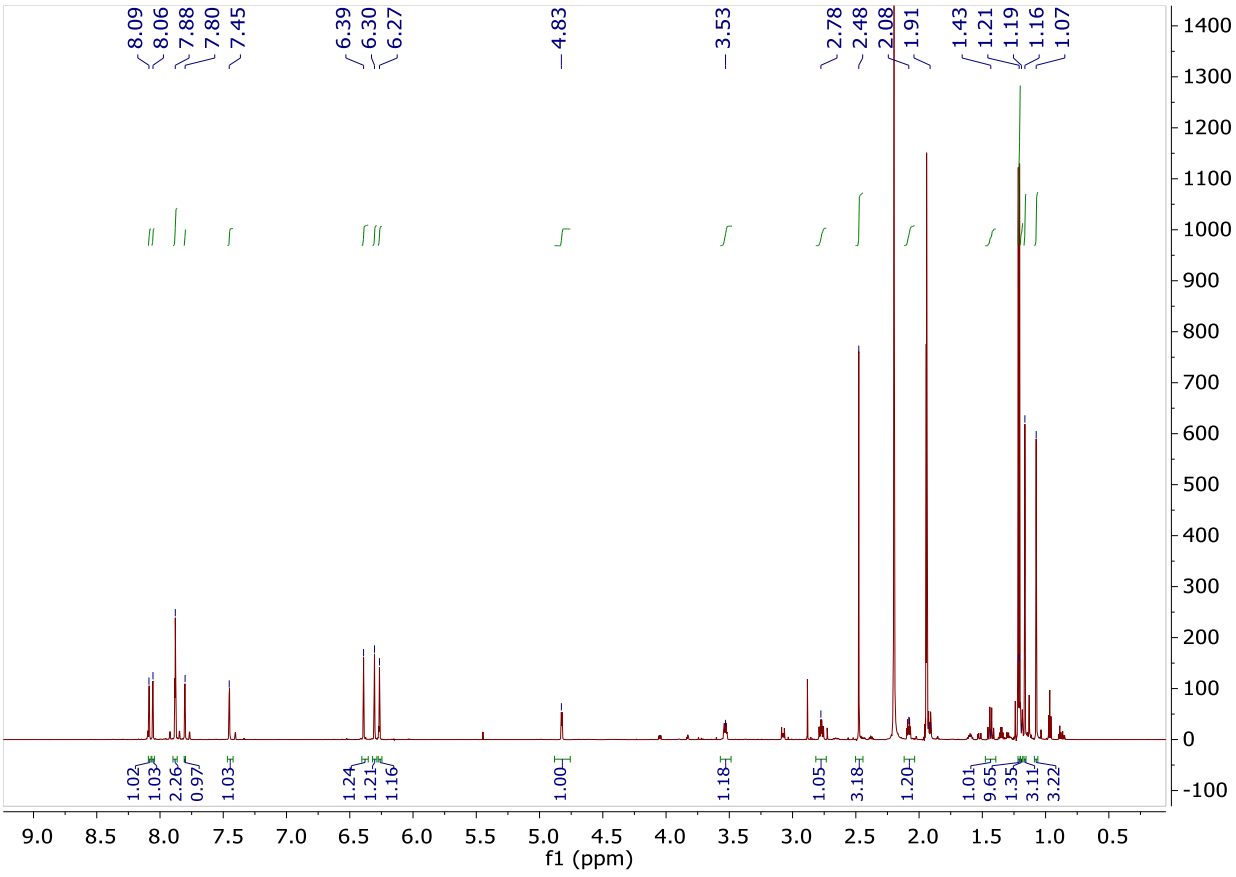

^{1}H NMR Spectrum of 14

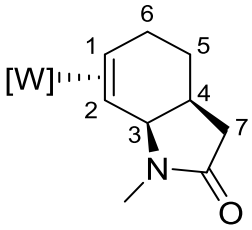

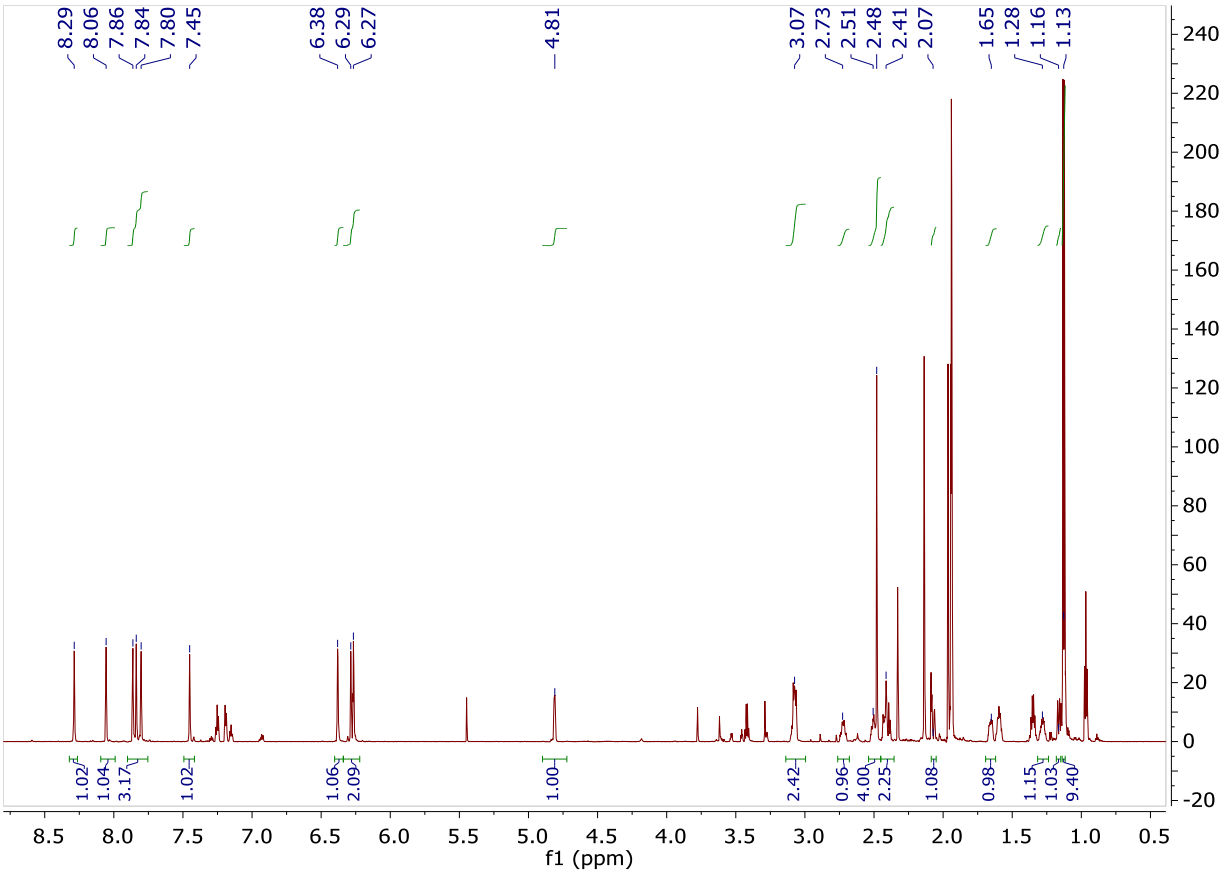

^{13}C {^{1}H} NMR Spectrum of 14

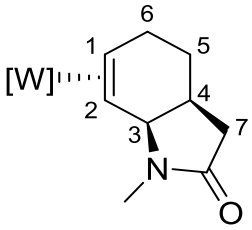

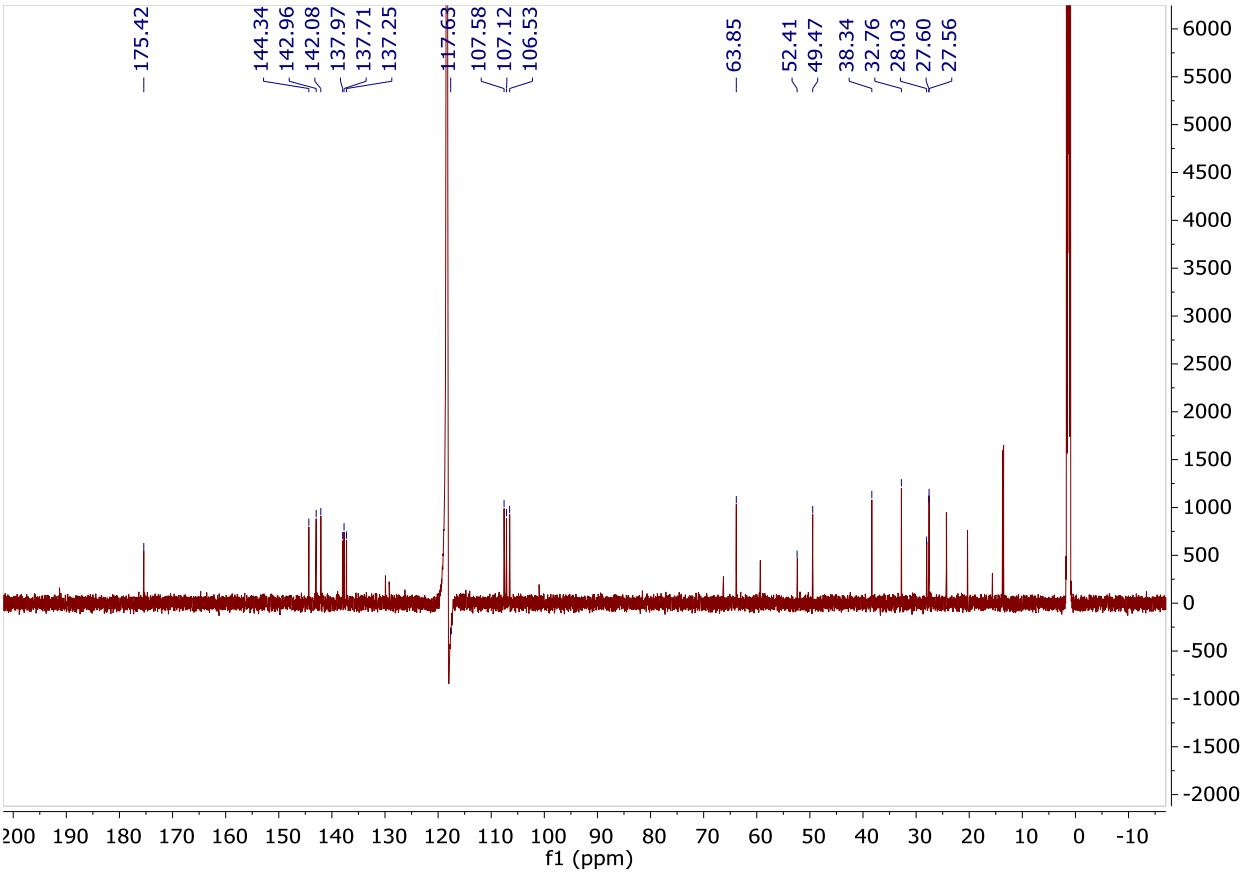

^{1}H NMR Spectrum of 15

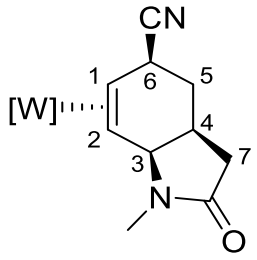

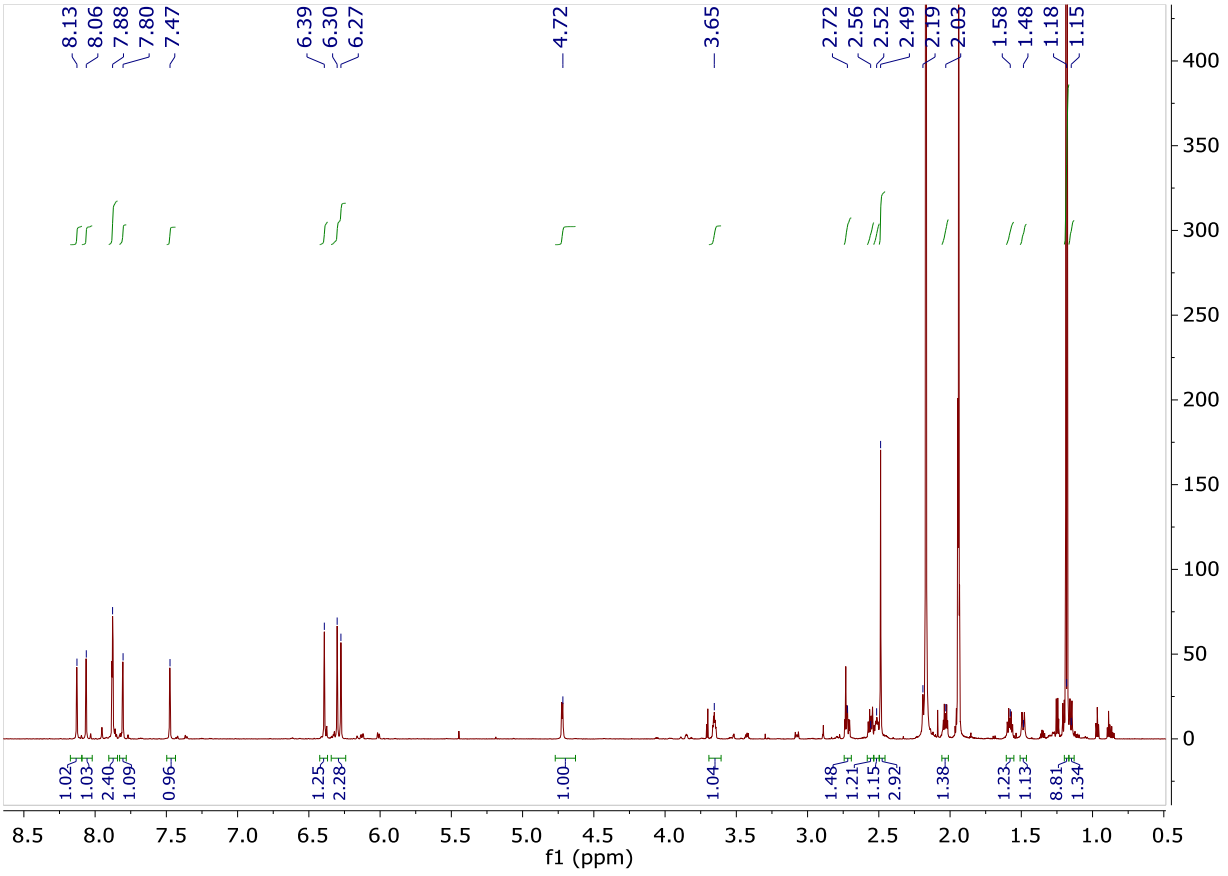

^{13}C {^{1}H} NMR Spectrum of 15